Exploring the Link between Insulin Resistance and Neurodegenerative Disorders and its Possible Mechanism(s)

THESIS

Submitted in partial fulfilment
of the requirements for the degree of
DOCTOR OF PHILOSOPHY

by

SORABH SHARMA

Under the Supervision of
Dr. RAJEEV TALIYAN

BITS Pilani
Pilani | Dubai | Goa | Hyderabad

BIRLA INSTITUTE OF TECHNOLOGY & SCIENCE, PILANI
2017

BIRLA INSTITUTE OF TECHNOLOGY & SCIENCE, PILANI

CERTIFICATE

This is to certify that the thesis entitled **Exploring the Link between Insulin Resistance and Neurodegenerative Disorders and its Possible Mechanism(s)** and submitted by **Sorabh Sharma** ID No **2013PHXF0007P** for award of Ph.D. degree of the Institute embodies original work done by him under my supervision.

Signature (Supervisor):

Name (Supervisor) : **Dr. RAJEEV TALIYAN**

Designation : **Assistant Professor**

Department of Pharmacy, BITS-Pilani

Date:

Table of Contents

Acknowledgments

Foremost, I would like to express my sincere gratitude to my Supervisor **Dr. Rajeev Taliyan, Assistant Professor, Department of Pharmacy, BITS-Pilani** for his continuous guidance for my PhD. His immense knowledge of the subject has always contributed to improve my research. His suggestions have helped me all the time of research and writing of thesis. This thesis becomes possible due to his continuous support, constructive criticism, and the freedom he gave for conducting this work.

I am grateful to **Prof. Souvik Bhattacharyya,** Vice-Chancellor and **Prof. B. N. Jain**, Ex-Vice-Chancellor, BITS Pilani, **Prof. A. K. Sarkar,** Director and **Prof. G. Raghurama**, Former-Director, BITS Pilani, Pilani Campus for permitting me to pursue my research work in the Institute.

I also express my sincere thanks to **Prof. S. K. Verma**, Dean, Academic Research Division (ARD) and **Dr. Hemant R. Jadhav**, Associate Dean, ARD for their motivation, constant support and encouragement. I would also like to thank **Prof. R. Mahesh,** Dean Faculty Affairs, BITS-Pilani, for his guidance throughout the PhD work.

I am highly indebted to my Doctoral approval committee (DAC) members **Dr. Anil Gaikwad,** Head and Assistant Professor, Department of Pharmacy, Pilani Campus and **Dr. Aniruddha Roy** for fruitful discussions and suggestions and sparing their time for evaluation of this thesis. I would also like to acknowledge **Dr. Atish Paul**, Convener, Departmental Research Committee, Assistant Professor, Department of Pharmacy, Pilani Campus who has provided valuable comments during the departmental seminars.

My special thanks to the faculty members **Dr. R. P. Pareek**, **Dr. S Murugesan, Dr. Anil Jindal, Dr. Deepak Chitkara, Dr. Anupama Mittal, Dr. Sunil Dubey, Dr. Gautam Singhvi, Dr. Murli M. Pandey, Mr. Mahaveer Singh, Ms. Archana Kakkar, Dr. Shvetank Bhatt** and **Dr. Priti Jain**, for their encouragement, insightful comments, and suggestions.

I would like to specially thank **Dr. Ankur Jindal, Dr. Arghya, Dr. Emil, Dr. Vibhu, Dr. Garima, Dr. Prashant, Dr. Vadiraj, Dr. Ashok, Mr. Yeshwant, Mr. Satish, Mr. Almesh, Mr. Pankaj and Mr. Subash** for the enormous assistance provided throughout my research

work. I would like to add special thanks to **Dr. Deepali Gupta,** who as a good friend, was always willing to help and gave her best suggestions.

I cherish all the moments spent with my friends and highly talented Research Scholars, **Mr. Pankaj Munjal and Mr. Sanjeev Jakhar**. I thank them for always there for me and making my time memorable in BITS Pilani. I wish them very bright future.

I am extremely lucky to have a great company of research scholars, **Mr. Santosh, Ms. Anuradha, Mr. Vajir, Ms. Nisha, Mr. Saurabh, Mr. Kishan, Mr. Krishna, Mr. Sridhar**, **Ms. Shruti, Ms. Dhanushree, Mr. Ginson, Mr. Samrat, Mr. Sarathlal** and **Ms. Pracheta**. I have learnt a lot from each and everyone. I would also like to thank to Post graduate students, Mr. Sumel, Mr. Karthik, Mr. Mahesh, Ms. Annanya and Mr. Bhanu Chander, who have all worked with me during my PhD journey.

I would like to thank the Central Animal House Staff, especially **Dr. Sushil K Yadav,** (Senior Vet. Incharge), for his continous help and support during my work. He always suggested me the best, academically and personally too. I would also thank the animal house staff **Mr. Vishal**, **Mr. Shyam**, **Mr. Mukesh** and **Mr. Shiv Kumar** for taking care of animals and providing necessary help during experimental work in the lab. My special thanks to **Mr. Goel** and **Mr. Vikas** (members of **Central Purchase Unit**, BITS Pilani) for providing the timely delivery of drugs and chemicals used in this study.

I also thank the non-teaching staff **Mr. Ram Suthar**, **Mr. Puran**, **Mr. Sajjan**, **Mr. Mahender**, **Mr. Naveen**, **Mr Tarachand**, **Mr. Laxman** and all the students of Department of Pharmacy for their valuable help at each stage of the research work. My sincere thanks to all persons whom I miss to acknowledge, who had directly or indirectly helped me to accomplish this task.

I would also like to thank **Department of Pharmacy** and **BITS Pilani University** for giving me an opportunity to carry out my research and providing me the necessary research fellowship during my PhD.

Last but not the least, I would like to thank my family: To my grandparents and to my Dad, **Mr. Dharmpal Sharma** and Mum, **Mrs. Asha Sharma**. I am deeply indebted to all the

pains taken by them to made my dream come true. Thank you both for giving me the confidence and courage to make the choices I have made. I would also thank my parents-in law. My sincere thanks to my loving brother, **Sunil Sharma** and my family members **Mrs. Richa , Mrs. Ritu, Mr. Chetan.** Their constant love and care empowered me to accomplish my thesis and also ignited me to take more challenges in my life. I am also thankful to my loving pets who had always relieved all my stress.

I would like to add special thanks to my beloved wife, **Shalini**, who was always there cheering me up and stood by me through the good and bad times.

I would like to pay homage to those experimental animals who have sacrificed their lives in making my endeavour successful. May GOD grant them eternal peace.

Above all, I owe it all to Almighty God for granting me the wisdom, health and strength to undertake this research task and enabling me to its completion.

Sorabh Sharma

List of Abbreviations

6BIO: 6-bromoindirubin-3′-oxime

6-OHDA: 6-hydroxydopamine

Ach: Acetyl Choline

AchE: Acetyl cholinesterase

AD: Alzheimer's disease

AgRP: Agouti related peptide

ALS: Amyotrophic lateral sclerosis

ApoE4: Apolipoprotein E4

ATP: Adenosine triphosphate

Aβ: Amyloid-β

BACE1: Beta site APP cleaving enzyme 1

BBB: Blood-brain barrier

BDNF: Brain-derived neurotrophic factor

BMI: Body mass index

BSA: Bovine serum albumin

Ca^{2+}: Calcium channels

CBP: CREB binding protein

CDKs: Cyclin-dependent protein kinases

ChEIs: Cholinesterase inhibitors

CNS: Central nervous system

COMT: Catechol-O-methyltransferase

CREB: cAMP Responsive element binding protein

CSF: Cerebrospinal fluid

CTCL: Cutaneous T-cell lymphoma

DAG: Diacylglycerol

DAT: Dopamine transporter

DMSO: Dimethyl Sulphoxide

DNA: Deoxyribonucleic acid

DNPH: 2,4- dinitrophenyhydrazine

DTNB: 5,5'-dithiobis-(2-nitrobenzoic acid)

ELISA: Enzyme Linked Immunosorbate Assay

ER: Endoplasmic reticulum

ERK: Extracellular signal–regulated kinases

FDA: Food and Drug Administration

FFA: Free fatty acid

GABA: γ-aminobutyric acid

GDP: Guanosine Diphosphate

GLP-1: Glucagon-like peptide 1

GLUT2: Glucose transporter 2

Grb: Growth factor receptor-bound

GSK-3β: Glycogen synthase kinase-3β

GTP: Guanosine Triphosphate

H2O2: Hydrogen peroxide

HATs: Histone acetyltransferases

HD: Huntington's disease

HDAC: Histone deacetylases

HDL: High density lipoprotein

HFD: High fat diet

HOMA-IR: Homeostatic model assessment of insulin resistance

ICV: Intracerebroventricular

IDE: Insulin degrading enzyme

IFN-γ: Interferon γ

IGF-1: Insulin like Growth Factor-1

IL-1β: Interleukin- 1β

iNOS: Inducible nitric oxide synthase

IRS: Insulin Receptor Substrate

JNK: c-Jun NH_2-terminal kinase

K_{ATP}: ATP dependent potassium channels

LBs: Lewy bodies

L-DOPA: Levodopa

LiCl: Lithium chloride

LPS: Lipopolysaccaride

LTP: Long-term potentiation

MAO-B: Monoamine oxidase-B

MAP 1: Microtubule associated protein1

MAPK: Mitogen-activated protein kinases

MCP-1: Monocyte chemoattractant protein-1

MDA: Malondialdehyde

MEF2: Myocyte enhancer factor-2

MFB: Medial Forebrain bundle

MPP^+: 1-methyl-4-phenylpyridium

MPTP: 1-methyl-4-phenyl-1,2,3,6-tetrahydropyridine

mTOR: Mammalian Target Of Rapamycin

MWM: Morris water maze

NaCl: Sodium chloride

NAD: Nicotinamide adenine dinucleotide

NBW: Narrow Beam Walk

NET: Norepinephrine transporter

NFTs: Neurofibrillary tangles

NGF: Nerve growth factor

NMDA: N-methyl-D-aspartate

NO: Nitric oxide

NOR: Novel Object Recognition

NPY: Neuropeptide Y

NSC: Neural stem cells

PA: Passive Avoidance task

PD: Parkinson's disease

PDK1: Phosphoinositide-dependent kinase

PEG: Polyethylene glycol).

PHF: Paired helical filament

PI3K: Phosphatidylinositol 3-kinase

PKC: Protein kinase C

PKC: Protein kinase C

POMC: Proopiomelanocortin

PPARs: Peroxisome proliferator-activated receptors

Raf: Rapidly Accelerated Fibrosarcoma

RNA: Ribonucleic acid

RNS: Reactive nitrogen species

ROS: Reactive oxygen species

RR: Rotarod

SAC: Sacrifice

sAD: sporadic AD

SAHA: Suberoylanilide hydroxamic acid

SCFAs: Short chain fatty acids

SLA: Spontaneous locomotor activity

SNpc: Substantia nigra pars compacta

STZ: Streptozotocin

T1DM: Type 1 diabetes Mellitus

T2DM: Type 2 diabetes Mellitus

TBA: Thiobarbituric acid

TC: Total cholesterol

TC: Total Cholesterol

TDZDs: Thiadiazolidinones

TG: Triglycerides

TG: Triglycerides

TH^+: Tyrosine hydroxylase

TLR4: Toll like receptor 4

TNF-α: Tumour necrosis factor-α

TSA: Trichostatin A

VPA: Valproic acid

WHO: World health Organization

ZDF: Zucker Diabetic Fatty rat

α-Syn: α-Synuclein

List of Figures

List of Tables

Abstract

Type 2 diabetes mellitus (T2DM) and other metabolic disorders, are well-recognized epidemiological and clinical risk factors for cardiovascular complications. Recently, studies have also suggested an increased risk for developing dementia of Alzheimer's type in T2DM patients. The risk of T2DM for other neurodegenerative conditions, including Parkinson's disease (PD), has been inconsistently reported. Evidences from animal studies supporting a role of T2DM in neurodegeneration also parallel clinical and epidemiological observations. However, the exact role and mechanisms by which T2DM exacerbate neurodegenerative diseases are still elusive.

In this regard, there are at least several possibilities that are not mutually exclusive. First, neurodegenerative disorders and T2DM share similar pathologies, including protein aggregation, oxidative stress, mitochondrial dysfunction, endoplasmic reticulum (ER) stress and neuro-inflammation. Second, it has been assumed that formation of advanced glycation end products (AGEs) may commonly underlie among T2DM and other age-related disorders, including neurodegenerative diseases. Third, and perhaps the most important factor is the development of insulin resistance syndrome, which is present in T2DM and also impairment of insulin signaling in the brain may be linked to neurodegenerative diseases. In the recent past, numerous studies have demonstrated that insulin resistance increases the risk of developing neurodegenerative diseases including Alzheimer's disease (AD) and PD. During insulin resistance, the insulin receptor signaling may be impaired primarily at the level of insulin receptor substrate (IRS)-1/2. It is predicted that reduced insulin receptor expression in the brain and dysregulated activity of the insulin receptor signaling pathway may lead to increased amyloid-β (Aβ) accumulation. Similar is the case for PD, where impaired insulin receptor signalling has been reported to be associated with α-synuclein alterations.

Increasing evidence indicates that insulin carries out multiple functions in the brain and dysregulation of insulin signaling during insulin resistance condition leads to aberrant activation of serine/threonine kinase, glycogen synthase kinsae-3β (GSK-3β). Numerous studies have reported up-regulation in expression as well as increased activity of GSK-3β in the respective brain regions of AD and PD patients. Moreover, actions of GSK-3β affecting nuclear functions, specifically gene expression, include indirect effects via its regulation of many transcription factors, and more direct effects resulting from the regulation of recently identified epigenetic mechanisms. Among these, histone acetylation/deacetylation has been widely studied and is carried out by opposing activities of two enzymes histone

acetyltransferases (HATs) and histone deacetylases (HDACs). GSK-3β has been reported to interact and phosphorylate several HDACs and HDAC inhibitors have been reported to increase the inhibitory serine-phosphorylation of GSK-3β. Moreover, it has been demonstrated that diabetes can induce changes in HDAC levels in the brain, which, in turn, trigger a detrimental molecular cascade that leads to compromised neuronal structure integrity and synaptic plasticity. Thus, there is a huge possibility that epigenetic mechanisms involving HDACs and GSK3β could be involved in insulin resistance induced neurodegeneration.

Therefore, this work was conducted in adherence to the following major objectives namely, (1) To standardize in-vivo animal models of insulin resistance and neurodegenerative diseases, including AD and PD (2) To examine the association between insulin resistance and neurodegenerative diseases including, AD and PD (3) To explore the epigenetic mechanism(s), primarily histone acetylation/deacetylation, involved in insulin resistance mediated AD and PD pathogenesis (4) To evaluate the effect of GSK-3β and HDAC inhibitors alone/or in combination in AD and PD associated with insulin resistance.

For induction of insulin resistance, the Swiss albino mice were fed with high fat diet (HFD) for 8 weeks. The mice subjected to HFD exhibited characteristic features of insulin resistance as confirmed using homeostatic model assessment of insulin resistance (HOMA-IR) values. These mice also exhibit impaired spatial learning and memory as assessed by battery of behavioural tests including, morris water maze, passive avoidance task and object recognition task. Moreover, increased level of $A\beta_{1-42}$ and p-tau, both of which characterized AD pathology were observed in hippocampus homogenates of HFD fed animals. Also, elevated level of oxidative stress markers (malondialdehyde (MDA), nitrite) and pro-inflammatory cytokine (tumour necrosis factor-α [TNF-α]) and reduced level of antioxidant enzyme (reduced glutathione) was observed in hippocampal homogenates of HFD fed mice as compared to NPD fed mice. Interestingly, we also observed significant increase in GSK3β activity and reduction of global histone H3 acetylation in HFD fed animals. These changes occurred concurrently with reduced cAMP response element binding protein (CREB) and brain derived neurotrophic factor (BDNF) levels.

In contrast, the mice treated with selective GSK3β inhibitors (Indirubin-3'-monoxime and AR-A014418) and pan HDAC inhibitors, Suberoylanilide hydroxamic acid (SAHA) and sodium butyrate, reversed the insulin resistance condition along with significant improvement of cognitive functions as assessed by battery of behavioral tests. Moreover, the mice treated

with GSK3β inhibitors and HDAC inhibitors showed significant reduction in oxidative stress (MDA, nitrite) and pro-inflammatory marker (TNF-α) and ameliorate antioxidant enzyme levels (reduced glutathione) as compared to alone HFD fed mice. In addition, these compounds attenuated the elevated levels of $A\beta_{(1-42)}$ and p-tau in HFD fed animals. Further, treatment with GSK3β and HDAC inhibitors results in significant amelioration of CREB and BDNF levels in HFD fed animals. The neuroprotective effects of these compounds were also confirmed by histopathological analysis, where reduced percentage of damaged neurons in dentate gyrus and CA1 regions was observed. These results clearly indicate an alteration in GSK-3β activity and epigenetic mechanisms regulating gene expression in brain may play a key role in the etiology and progression of neurodegenerative diseases.

In fact, from a therapeutic point of view, HDAC inhibitors have emerged as promising compounds that might help manage neurodegenerative processes. However, the toxicity associated with HDAC inhibitors has limited the clinical data available. In order to reduce side effects while maintaining benefits, one strategy would be to develop isoform-selective HDAC inhibitors. Moreover, since the side effects reported for HDAC inhibitors in humans are dose dependent, the use of lower doses of pan-HDAC inhibitors to reduce their toxicity could represent another solution. In this dissertation work, we tested both these approaches.

In the first approach, to evaluate the therapeutic potential of low dose combination of GSK-3β inhibitor and HDAC inhibitor in cognitive decline associated with HFD induced insulin resistance, we selected Indirubin-3'-monoxime as GSK-3β inhibitor and SAHA as HDAC inhibitor, respectively. Interestingly, we found that low dose combination of these compounds was more effective as compared to either drug alone in ameliorating cognitive decline and attenuating $A\beta_{1-42}$, p-tau, oxidative stress markers, TNF-α levels and GSK3β levels. Further, significant amelioration of reduced histone H3 acetylation, CREB and BDNF levels was observed with low dose combination of these drugs when compared to either drug alone. Moreover, reduced percentage damaged neuronal count in histological studies further elucidates the neuroprotective effect of this low dose combination.

In addition to HFD induced insulin resistance model, we also explored the potential of low dose combination of GSK-3β inhibitor and HDAC inhibitor in brain specific insulin resistance model induced by Intracerebroventricular Streptozotocin (ICV-STZ) administration. For this purpose, we used lithium chloride as GSK-3β inhibitor and valproate as HDAC inhibitor. The low dose combination of both these drugs was found to ameliorate

ICV-STZ induced cognitive decline, oxidative stress, pro-inflammatory marker and GSK-3β level in a synergistic manner. Moreover, the combination of both these drugs improved the CREB, BDNF levels and increased neuronal count in hippocampus of ICV-STZ treated rats, in a synergistic manner as compared with either drug alone.

In second approach, we identify the involvement of class selective HDACs in insulin resistance induced neurodegeneration. For this purpose, we used class selective HDAC inhibitors, Class I inhibitors (HDACi 4b and CI-994), Class II inhibitor (MC-1568) and Class III inhibitor (Sirtinol) were used. We found that Class II selective HDAC inhibitor (MC-1568) was more effective in attenuating cognitive deficits and neuronal loss as compared to Class I or Class III selective inhibitors.

Although some of the clinical reports suggest that insulin resistance could also be a risk factor for PD development, however experimental data is scarce. Thus, in the last part of this work, we evaluated whether insulin resistance is linked to PD pathology or not. For this purpose, we first standardized an animal model which could mimic the co-morbid insulin resistance and PD condition. For development of insulin resistance, we fed the male Wistar rats with HFD for eight weeks, followed by low dose 6-hydroxydopamine (6-OHDA) administration in medial forebrain bundle of rats, a toxin widely used for PD induction in animals. As expected, the 6-OHDA treatment produced nigral dopaminergic degeneration as evidenced by the loss of striatal dopamine level. This dopamine loss was correlated with impaired performance in behavioral tasks such as rotarod, narrow beam walk test and locomotor activity. Interestingly, we found that prior exposure to HFD exacerbated the effects of 6-OHDA on striatal dopamine loss and behavioral observations in rats, indicating that HFD-induced insulin resistance is associated with a reduced capacity of nigral dopaminergic terminals to cope with 6-OHDA-induced neurotoxicity. Thus, insulin resistance may be an important modifiable risk factor for PD.

Further, to our surprise, we found a significant increase in GSK-3β activity and reduced histone H3 acetylation in HFD+6-OHDA treated rats as compared to alone HFD rats. We administered GSK-3β inhibitor (Indirubin-3-monoxime) and HDAC inhibitor (SAHA) in these animals and found that these compounds significantly ameliorate the HFD+6-OHDA induced exacerbated motor deficits, restore dopamine levels, increased CREB and BDNF level.

Altogether, the findings of the present work strongly suggest that insulin resistance may induce epigenetic modifications affecting neuropathological mechanisms in the brain

leading to increased susceptibility to insults associated with neurodegeneration. The molecular mechanisms involved in neurodegenerative processes associated with insulin resistance may include elevated GSK-3β activity, reduced histone H3 acetylation, increased oxidative stress and neuro-inflammation. Moreover, these changes occurred concurrently with reduced CREB and BDNF levels. Based upon our results, we suggest that either a low dose combination of HDAC inhibitor and GSK-3β inhibitor could be used for long term therapy of cognitive deficits related with insulin resistance conditions or isoform specific Class II HDAC inhibitors could be used. In line with these, we also demonstrated the beneficial effects of GSK-3β inhibitors and HDAC inhibitors in ameliorating insulin resistance induced exacerbated PD pathology. Thus, our study for the first time provides an epigenetic explanation for the increased risk of neurodegeneration associated with insulin resistance and also suggests that epigenetic modulation might be used along with GSK3β inhibitors to provide therapeutic effects under such disease conditions.

1.0 Introduction

The insulin resistance syndrome has been proposed to include a set of metabolic characteristics of which glucose intolerance, hypertriglyceridemia, a reduced concentration of high density lipoprotein (HDL) cholesterol, hyperinsulinemia, and central obesity are the predominant components (Reaven, 1988). Although hyperinsulinemia is often found among subjects at risk of macrovascular disease (Pyorala, 1979), not all the features of the insulin resistance syndrome are necessarily expressed in any one individual. Insulin resistance has been reported to play role in many pathophysiological states including Type 2 diabetes Mellitus (T2DM) and obesity. According to World health Organization (WHO), an estimated 422 million adults were living with diabetes in 2014, compared to 108 million in 1980. Over the past decade, diabetes prevalence has risen faster in low- and middle-income countries than in high-income countries. Diabetes alone caused 1.5 million deaths in 2012. Higher-than-optimal blood glucose caused an additional 2.2 million deaths, by increasing the risks of cardiovascular and other diseases (WHO, 2016). Insulin resistance has been widely reported as a risk factor for T2DM. Various studies have suggested that insulin resistance already exists before blood glucose abnormalities in diabetic patients (Groop, 2000; Praveen et al., 2012) and that hyperinsulinemia occurs before impaired glucose tolerance shows several pathophysiological abnormalities.

Insulin is a circulating peptide hormone made of two amino acid chains: one “A” chain of 21 amino acids and one “B” chain of 30 amino acids. The two chains are linked and stabilized by two disulfide bonds, and a third disulphide bond is found within the A chain. Insulin is produced, stored and secreted by β-cells of pancreatic islets of Langerhans. Insulin synthesis is under multifactorial regulations, but glucose is the major physiologic regulator of insulin secretion (Poitout et al., 2006). Insulin content in β-cells is extremely dynamic, so is the regulation of insulin secretion, to match with the subject’s metabolic need. β-cells are capable to sense nutrients concentration, especially glucose, in the blood. This sensing occurs due to a widely developed and irrigated vascular system and the presence of the glucose transporter 2 (GLUT2) and glucokinase, an enzyme that facilitates phosphorylation of glucose to glucose-6-phosphate. After a meal, the high influx of glucose in β-cells via GLUT2 leads to an increase of glycolysis and mitochondrial β-oxidation, resulting in higher adenosine triphosphate (ATP) production. This increase in ATP increases the ATP/ADP ratio leading to the closure of ATP dependent potassium (K_{ATP}) channels, depolarizing the membrane, opening voltage dependent calcium (Ca^{2+}) channels provoking an influx of Ca^{2+} favoring the insulin containing granules exocytosis. Almost all cell types are responsive to

insulin. However, liver, muscle, and adipose tissue are the most sensitive to insulin (Fulop et al., 2003), rendering it the most important anabolic hormone identified to date.

1.1. Insulin receptor and Insulin receptor substrates

1.1.1. Insulin receptor

The insulin structure shows numerous amino acids which are specifically involved in the binding to the insulin receptor. The insulin receptor is a tetrameric glycoprotein localized at the plasma membrane, consisting of two extracellular α-subunits and two transmembrane β-subunits. Two isoforms of the insulin receptor exist, type A and type B (Lee and Pilch, 1994). Insulin receptor type "B" binds insulin with high affinity, whereas Insulin receptor type "A" can bind with insulin or Insulin like Growth Factor-1 (IGF-1) with comparable affinity. Insulin binds to its receptor, found as a dimer on the cell membrane, and provokes its auto-phosphorylation mediated by its intrinsic tyrosine kinase activity. The insulin receptor can also heterodimerize with IGF-1 receptor, modulating the affinity for insulin of IGF-1 (White, 2003). The auto-phosphorylation of 3 tyrosine residues in the regulatory region of the receptor activates its kinase activity (White et al., 1988). On the contrary, the phosphorylation of serine residues decreases the receptor activity and participates in the regulation/control of its activity provoking its internalization. The activated insulin receptor dimer can in turn bind and phosphorylate several other proteins leading to the activation of a signaling cascade controlling numerous processes like cell growth, survival and metabolism.

1.1.2 Insulin Receptor Substrates

The activated Insulin receptor recruits and phosphorylates many substrates like Grb (Growth factor receptor-bound) family adapters, Dock1 (Dedicator of Cytokinesis), Cbl (Casitas B-lineage lymphoma) and APS (adapter protein with Pleckstrin homology and Src homology 2 domains) adaptor protein. The principal activated substrates are: IRS (Insulin Receptor Substrate) and Shc (Src homology/collagen). Activation occurs through a phosphorylation cascade. There are four known specifically-named IRS proteins. IRS-1 and -2 have widely overlapping tissue distribution while IRS-3 and -4 are less well characterised. IRS-1 has 21 potential tyrosine phosphorylation sites, and 30 serine/threonine phosphorylation sites, respectively mostly linked to activation for tyrosines and inhibition/degradations for serines (Draznin, 2006; Pederson et al., 2001). The phosphorylated tyrosines act to transduce insulin action by recruiting downstream proteins (White and Kahn, 1994). Two main signaling pathways originate from this activation. The first one is the PI3K (Phosphatidylinositol 3-kinase) pathway, mediating the effects of insulin on metabolism and cell survival. The second

one is the ERK/MAPK (extracellular signal–regulated kinases/Mitogen-activated protein kinases) pathway, mediating the effects of insulin on mitogenesis and cellular growth.

1.1.3. Insulin Signalling Pathways

1.1.3.1. MAPK pathway: In Mammals, four distinct groups of MAPK exist and regulate gene expression in response to extracellular stimuli. We focused on the MAPK pathway activated by insulin (Fig. 1.1). The activation of IRS1 and its phosphorylation makes it bind with Grb2 through its SH2 (Src Homology 2) domain. Grb2 interacts with SOS (Son of Sevenless) (Baltensperger et al., 1993), which promotes the removal of GDP (Guanosine Diphosphate) from Ras proteins, allowing the binding of GTP (Guanosine Triphosphate) and their activation. The rest of the pathway involves a series of serine/threonine kinases. Ras activates Raf (Rapidly Accelerated Fibrosarcoma) (a MAPKKK), which phosphorylates and activates MEK 1-2 (MAPK/ERK Kinase) (a MAPKK), which phosphorylates and activates MAPK. The pathway regulates cell differentiation, notably by stimulating DNA synthesis, along with cell proliferation (Chang and Karin, 2001).

1.1.3.2. PI3K pathway IRS-1 binds to the adaptor subunit of PI3K, a SH2-domain (Src Homology 2) containing protein, and activates it. PI3K catalytic subunit phosphorylates PIP2 (Phosphatidylinositol (4,5)-diphosphate) leading to the generation of PIP3 (Phosphatidylinositol (3, 4, 5)-trisphosphate). PIP3 recruits and activates PDK1 and 2 (Phosphoinositide-dependent kinase). PI3K activation leads to the activation of AKT/PKB (Protein kinase B), atypical PKC (Protein kinase C) and mTOR (mammalian Target Of Rapamycin). AKT is activated by the phosphorylation of two sites threonine 308 and serine 473, and needs PDK1 (Phosphoinositide-dependent kinase) intervention (Alessi et al., 1997). PDK2 has been linked to the phosphorylation of AKT serine 473, with the intervention of mTOR (Sarbassov et al., 2005). AKT plays a key role in multiple cellular processes such as glucose metabolism, apoptosis, cell proliferation, transcription and regulates several downstream targets by phosphorylation. AKT, and PKC, control the glucose uptake by the cell, by activating AS160 (Akt Substrate of 160 KDa), a Rab GTPases (Ras-related proteins), increasing GLUT-4 translocation at the plasma membrane and consequently glucose uptake (Fig. 1.1). AKT also inhibits Bad (BCL2 associated agonist of cell death) and regulates several metabolic and survival pathways by controlling transcription through the action of transcription factors like SREBP (Sterol regulatory element binding protein) and FOXO (Forkhed box). AKT is further divided into AKT1 and AKT2. AKT1 is involved in cellular survival and protein synthesis. In contrast, AKT2 is an important signalling molecule in the insulin signaling pathway. It is required to induce glucose transport.

A key target of AKT in the glucose metabolism and insulin signalling pathways is Glycogen synthase kinase-3β (GSK-3β), a serine/threonine protein kinase. GSK3β phosphorylates and inhibits glycogen synthase (Rylatt et al., 1980) and thus regulates the glycogen synthesis and ultimately glucose homeostasis. It is now widely accepted that GSK-3β plays an important role in various essential physiological processes, such as development, cell cycle, or apoptosis (Ferkey and Kimelman, 2002). Apart from glycogen synthase, a plethora of different substrates has been identified for GSK3β in all cellular compartments, that is, metabolic proteins (Alessi et al., 1996), cytoskeletal proteins (Hanger et al., 1992), and transcription factors (Hart et al., 1998).

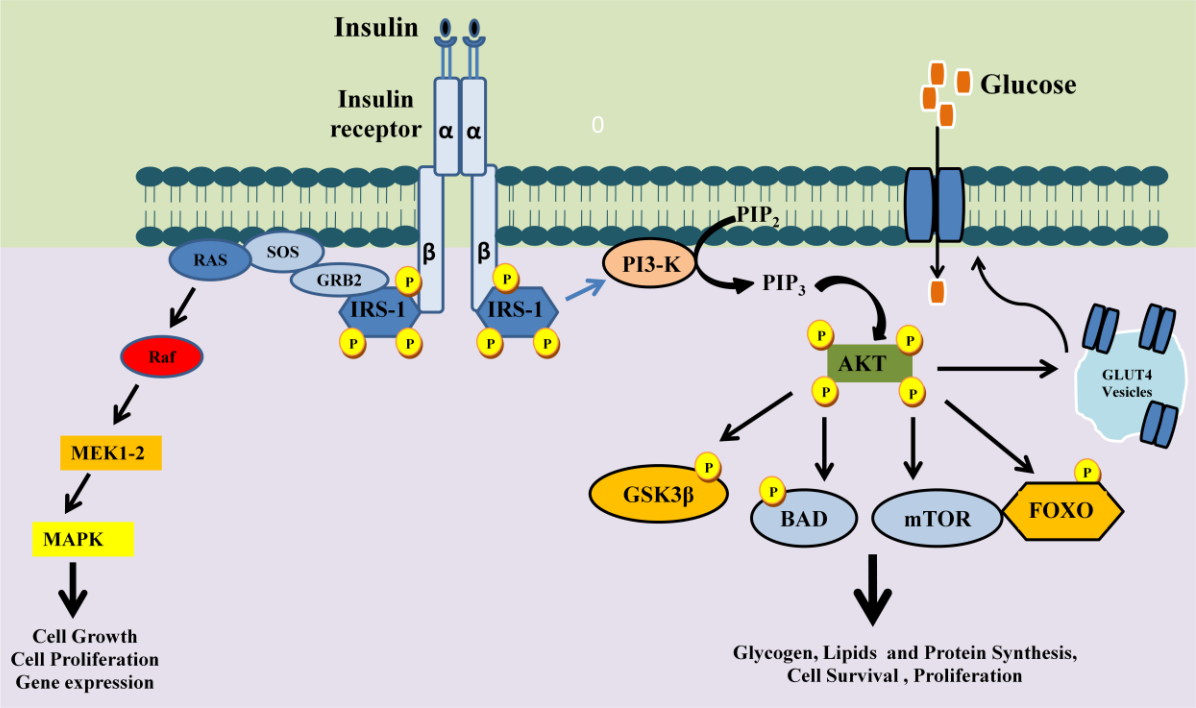

Fig. 1.1 The insulin signaling pathway

The insulin receptor is localized at the plasma membrane. When insulin binds to the receptor, it provokes the receptor dimerization and its auto-phosphorylation by its tyrosine kinases. The auto-phosphorylation of 3 tyrosine residues of the receptor activates its kinase activity recruiting and activating downstream proteins like Grb. The principal substrate is IRS-1 which once activated by tyrosine phosphorylation, activates two pathways, MAPK pathway represented on the left, and PI3K pathway, represented on the right. Activated IRS-1 activates Grb2, interacting with SOS switching GDP for GTP on Ras. Ras activates Raf, activating MEK 1-2, activating MAPK regulating cell growth, proliferation and gene expression. Activated IRS1 activates PI3K which phosphorylates PIP2 into PIP3 that activates PDK1/2 itself activating AKT. AKT activates GSK3β, BAD, mTOR, FOXO, respectively for glycogen metabolism, inhibition of apoptosis and gene transcription.

Recently, factors external to the “classical” insulin pathway have also been reported to contribute to its regulation. Among them, the epigenetic modifications are important ones. The term ‘epigenetics’ is widely used to refer to changes in gene expression that are not

caused by changes in the DNA (Deoxyribonucleic acid) sequence and that involve classical epigenetic mechanisms, namely, DNA methylation and histone modifications (Berger et al., 2009). Among these histone acetylation/deacetylation has been widely studied. Recent reports indicate that histone deacetylase-2 (HDAC2) bind with IRS-1 in liver cells of the db/db mouse (mice commonly used for the investigation of T2DM and screening variety of agents such as insulin mimetic and insulin sensitizers). This binding of HDAC2 with IRS-1 leads to decreased acetylation and reduced insulin receptor-mediated tyrosine phosphorylation of IRS-1 (Kaiser and James, 2004; Sun and Zhou, 2008).

1.1.4. Insulin and Glucose Transporter (GLUT) system

Insulin is the most potent physiological anabolic agent known, promoting the storage and synthesis of lipids, protein, and carbohydrates and inhibiting their breakdown and release into the circulation (Saltiel and Kahn, 2001). The first step by which insulin increases energy storage or utilization involves the regulated transport of glucose into the cell, mediated by the facilitative glucose transporters. There are 14 sugar transporter proteins (GLUT1-GLUT14) encoded in the human genome (Thorens and Mueckler, 2010; Wood and Trayhurn, 2003) that catalyzes hexose transport across cell membranes through an ATP-independent, facilitative diffusion mechanism (Hruz and Mueckler, 2001). Among all Glucose transporters, GLUT2 and GLUT4 are most important ones in glucose homeostasis and are widely studied. GLUT2 is expressed in liver, intestine, kidney and pancreatic islet β-cells, as well as in the central nervous system, in neurons and astrocytes. In pancreatic β-cells, GLUT2 is required for glucose-stimulated insulin secretion (Thorens, 2015). On the other hand, GLUT4 is highly expressed in adipose tissue and skeletal muscle, but these tissues also express a selective cohort of other transporters. GLUT4 displays the unique characteristic of a mostly intracellular disposition in the unstimulated state that is acutely redistributed to the plasma membrane in response to insulin and other stimuli (Bryant et al., 2002; Czech and Corvera, 1999). Transgenic mice expressing high levels of GLUT4 in adipose tissue (Tozzo et al., 1995) or in skeletal muscle (Tsao et al., 2001) are both highly insulin sensitive and glucose tolerant. Conversely, conditional depletion of GLUT4 in either adipose tissue or skeletal muscle causes insulin resistance and a roughly equivalent incidence of diabetic animals (Zisman et al., 2000; Abel et al., 2001). In line with these, it has been reported that the skeletal muscle expression of GLUT4 in T2DM patients is significantly reduced, indicating that such patients have less capability to process glucose (Maier and Gould, 2000).

1.1.5. Insulin degrading enzyme (IDE)

The short half-life of insulin in the human body (4-6 min) prompted the search and discovery of insulin-degrading enzyme (IDE), a 110-kDa metalloprotease that can rapidly degrade insulin into inactive fragments. The ability of IDE to degrade insulin was reported in late 1940's (Mirsky and kahn, 1949). Despite decades of research, the role of IDE in the degradation of insulin, as well as the cellular location of this process, remains controversial (Authier et al., 1996; Hersh, 2006). Recent evidence has strengthened the physiological relevance of this protease. A decrease in insulin degradation and associated hyperinsulinemia was observed in IDE knockout mice (Farris et al., 2003). In addition, reducing the levels of human IDE in HepG2 cell-line cultured cells using silencing RNA (Ribonucleic acid) inhibited insulin degradation by up to 76% (Fawcett et al., 2007). Interestingly, while IDE is an important contributor to insulin homeostasis, insulin also contributes to the maintenance of IDE levels. Treatment of primary hippocampal neurons with insulin resulted in an increase of IDE protein levels by ~25%, possibly through a feedback mechanism (Zhao et al., 2004). Although IDE has greatest affinity for insulin, it has been implicated in the degradation of other amyloidogenic peptides (Farris et al., 2003). IDE has been observed in human cerebrospinal fluid (CSF). Its activity and levels have been found to be decreased in AD brain tissue and is associated with increased Aβ levels (Cook et al., 2003). Additionally, the enzymatic activity of IDE from the homogenates of various rat tissues has been classified in a decreasing order: liver > pancreas > kidney > testis > adrenal gland > spleen > ovary > lung > heart > muscle > brain > fat (Duckworth and Kitabchi, 1974). Importantly, IDE is not the sole enzyme responsible for insulin degradation: cathepsin D has also been shown to participate in the lysosomal degradation of insulin (Authier et al., 2002).

1.2. Peripheral actions of Insulin

1.2.1. Carbohydrate metabolism:

• It increases the rate of glucose transport across the cell membrane in muscle and adipose tissue.

• It increases the rate of glycolysis in muscle and adipose tissue by stimulating hexokinase and 6- phosphofructokinase activity.

• It stimulates the rate of glycogen synthesis in a number of tissues, including muscle, adipose tissue and liver. It also decreases the rate of glycogen breakdown in muscle and liver.

• It inhibits the rate of glycogenolysis and gluconeogenesis in the liver.

1.2.2. Lipid metabolism:

• It decreases the rate of lipolysis in adipose tissue and hence lowers the plasma fatty acid level.

• It stimulates fatty acid and triacylglycerol synthesis in tissues.

• It increases the rate of very-low-density lipoprotein formation in the liver.

• It increases the uptake of triglyceride from the blood into adipose tissue and muscle.

• It decreases the rate of fatty acid oxidation in muscle and liver.

• It increases the rate of cholesterol synthesis in the liver.

1.2.3. Protein metabolism:

• It increases the rate of transport of some amino acids into tissues.

• It increases the rate of protein synthesis in muscle, adipose tissue, liver and other tissues.

• It decreases the rate of protein degradation in muscle (and perhaps other tissues).

• It decreases the rate of urea formation.

These effects of insulin serve to encourage the synthesis of carbohydrates, fats and proteins; therefore, insulin is considered to be an anabolic hormone (Fig. 1.2).

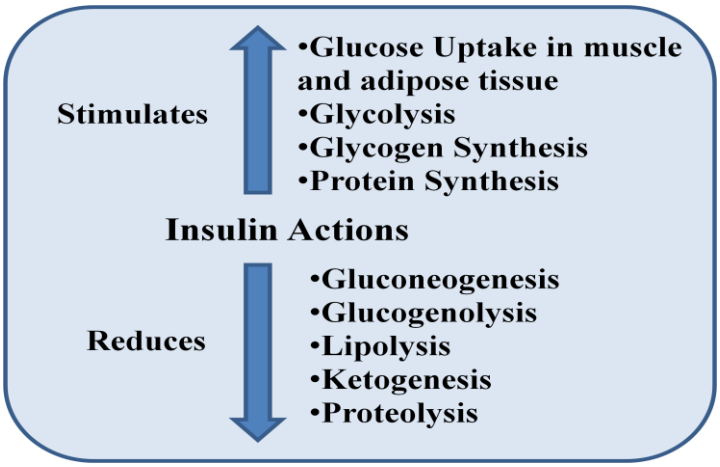

Fig. 1.2 Insulin actions on metabolism

1.3. Central actions of Insulin

Until five decades ago, insulin was considered only as a peripheral hormone, unable to cross the blood-brain barrier (BBB) and to affect the central nervous system (CNS) (Laron, 2009; Erol, 2008; Salkovic-Petrisic and Hoyer, 2007). However, this idea was challenged after the detection of immunoreactive insulin in dog CSF (Margolis and Altszuler, 1967). Insulin levels in the CSF are; 25% of those in the blood and increase proportionally after meals or with peripheral insulin infusion, suggesting that a fraction of plasma insulin is able to cross the BBB via a saturable transport system (Margolis and Altszuler, 1967). De novo insulin

synthesis in brain has been proposed as an alternative source of insulin in CNS. This hypothesis has been supported by the detection of preproinsulin I and II mRNA in rat fetal brain and cultured neurons and also by insulin immunoreactivity in neuronal endoplasmic reticulum, Golgi apparatus, cytoplasm, axon, dendrites and synapses (Schechter et al., 1990; 1996). Although insulin receptors are highly abundant in these brain areas, it remains unclear if insulin is produced locally in the brain or not.

1.3.1. Brain insulin signalling and its action on neuronal function and synaptic plasticity

Insulin and the closely related IGF-1 and IGF-2 mediate their biological effects through two highly related tyrosine kinase receptors—the insulin receptor and the IGF-1 receptor (IGF-1R) (Belfiore et al., 2009). Both, insulin receptor and IGF-1R are differentially expressed throughout the brain. In the mouse brain, the highest expression of the insulin receptors is in the olfactory bulb, followed by the cortex, hippocampus, hypothalamus, and cerebellum, with relatively low levels in the striatum, thalamus, midbrain, and brainstem (Fernandez and Torres-Alemán, 2012; Zhao et al., 2004; Dou et al., 2005).

Insulin has been reported to involve in the regulation of glucose metabolism, food intake, body weight and also affects numerous brain functions through complex insulin/IR signaling pathway (Baker et al., 2011; Zhao and Alkon, 2001; Watson and Craft, 2003). The best-studied effects of insulin signaling in the brain are those regulating food intake and energy expenditure. Woods et al. showed that Intracerebroventricular infusion of insulin in baboons could markedly decrease the food intake and body weight gain (Woods et al., 1979). Insulin administration into the third ventricle in rodents has been shown to decrease food intake by decreasing expression of the orexigenic neuropeptides; neuropeptide Y (NPY) and Agouti related peptide (AgRP), and by increasing the expression of anorexigenic neuropeptides, proopiomelanocortin (POMC) and cocaine- and amphetamine-regulated transcript (CaRT) in the arcuate nucleus, which together result in increased activity of a-melanocyte-stimulating hormone in neurons in the paraventricular nucleus (Schwartz et al., 2000).

Studies have demonstrated that insulin action might also play a role in cognitive function in the brain. Patients with both T1DM and T2DM are at higher risk for behavioural changes and accelerated cognitive decline (Biessels et al., 2008). In humans with either T1DM or T2DM, imaging studies have demonstrated smaller hippocampi, as well as changes in the functional connectivity between regions of the brain (Antenor-Dorsey et al., 2013; den Heijer et al., 2003). All of these point to the possible role of insulin receptor in neuronal

signal transmission. The effects of insulin differ in different neuronal populations. Insulin reduces the activity of AgRP neurons, whereas it increases the activity of dopamine neurons (Konner et al., 2007; Klockener et al., 2011). Insulin also regulates the transmission of N-methyl-D-aspartate (NMDA) receptors in hippocampal neurons through the tyrosine phosphorylation of specific subunits of the NMDA receptors NR2A and NR2B (Christie et al., 1999). Insulin receptor has been shown to regulate type A γ-aminobutyric acid (GABA) receptor activity through both membrane recruitment and protein synthesis in hippocampal neurons, thereby regulating the activity of inhibitory synapses (Wan et al., 1997). Furthermore, insulin can regulate structural plasticity in the brain, including synapse number, dendritic plasticity, and visual circuit function (Chiu et al., 2008), and can induce the expression of PSD95, a scaffold protein that is essential for the formation of the postsynaptic junction (Lee et al., 2005). All of these studies provide molecular mechanisms to support the positive effects of insulin on brain function and behavior. Keeping in mind the vast majority of functions mediated by insulin in the brain, it can be assumed that any alteration in insulin signalling, especially during insulin resistance can severely impact the neuronal activity and possibly results in neurodegeneration.

1.4. Insulin resistance and its possible mechanisms

1.4.1. Insulin resistance: Insulin resistance is an abnormal condition in which cells have a decreased ability to respond to insulin, as a state that a given amount of insulin generates a less-than-expected biological effect. Insulin resistant individuals require higher than normal amounts of insulin (hyperinsulinemia) to maintain normal blood glucose concentrations. The majority of insulin resistant individuals prevent the development of a significant degree of hyperglycemia via compensatory hyperinsulinemia (Reaven, 2003; Sarafidis and Bakris, 2006).

In a vicious cycle, the more insulin will be produced to decrease blood sugar, the more insulin resistance become. Furthermore, the combination of insulin resistance and hyperinsulinemia greatly increases the incidence of closely related abnormalities and clinical diagnoses that make up the insulin resistance syndrome (Reaven, 2005). Broadly, insulin resistance syndrome includes conditions such as obesity (Maitra and Rowland Payne, 2004), glucose intolerance (Wlodarczyk and Strojek, 2008), diabetes (Kawamori, 1996), hypertension (Lee et al. 2012), dyslipidemia (Deedwania 2011), metabolic syndrome (Pinelli et al. 2010), cardiovascular diseases (Reaven 2011) and possibly neurodegenerative diseases (de la Monte 2012a; 2012b; Talbot et al. 2012).

1.4.2. Mechanisms of Insulin Resistance

Insulin resistance in most cases is believed to be manifest at the cellular level via post-receptor defects in insulin signalling. Despite promising findings in experimental animals with respect to a range of insulin signalling defects, their relevance to human insulin resistance is presently unclear. Possible mechanisms include down-regulation, deficiencies or genetic polymorphisms of tyrosine phosphorylation of the insulin receptor, IRS proteins or PIP-3 kinase, or may involve abnormalities of GLUT 4 function (Wheatcroft et al., 2003). Although standard definitions of insulin resistance still define it in terms of the effects of insulin on glucose metabolism, the last decade has seen a shift from the traditional "glucocentric" view of diabetes to an increasingly acknowledged "lipocentric" viewpoint. This hypothesis holds that abnormalities in fatty acid metabolism may result in inappropriate accumulation of lipids in muscle, liver, and β-cells (McGarry, 2002). It is further proposed that ectopic lipid accumulation is involved in the development of insulin resistance in muscle and liver as well as impairing β-cell function (so-called "lipotoxicity") (Unger and Orci, 2000).

Also, excess nutrients, such as abnormally high glucose and fatty acids, promote endoplasmic reticulum (ER) stress, which reduces the ability of β-cell to efficiently secrete insulin, contributing to the increased inflammation, oxidative stress, and elevated circulating nutrients including glucose. Mechanistically, excessive generation of reactive oxygen specis (ROS) can affect DNA, protein, and lipid integrity and consequently lead to cell death. Although it is still difficult to attribute causal effects of oxidative stress and inflammation in relation to each other, both play a significant role and mediate the progression of insulin resistance and T2DM.

1.4.2.1. Insulin resistance and Oxidative stress

Increased oxidative stress appears to be a deleterious factor leading to insulin resistance, β-cell dysfunction, impaired glucose tolerance, and, ultimately, T2DM (Evans et al., 2003; Shah et al., 2007). Chronic oxidative stress is particularly dangerous for β-cells because pancreatic islets are among those tissues that have the lowest levels of antioxidant enzyme expression, and β-cells have high oxidative energy requirements (Shah et al., 2007). In addition, there is considerable evidence that increased free radicals impair glucose-stimulated insulin secretion, decrease the gene expression of key β-cell genes, and induce cell death (Shah et al., 2007; Simmons, 2006). Moreover, impaired β-cell functioning results in an underproduction of insulin, fasting hyperglycemia, and eventually, the development of T2DM (Kahn, 2000).

1.4.2.2. Insulin resistance and Inflammation

Inflammation has been well reported to play an important role in the development of insulin resistance via various cytokines and molecular pathways. For example, the activation of IKKβ/NF-κB signaling might increase the secretion of proinflammatory cytokines such as tumour necrosis factor-α (TNF-α) and interleukin- 1β (IL-1β), which might in turn stimulate IKKβ/NF- κB signaling. Studies of TNF-α in the 1990s first analyzed the relationship between inflammation and insulin resistance (Lee and Lee, 2014). TNF-α is an adipose tissue-derived proinflammatory cytokine that causes insulin resistance by enhancing adipocyte lipolysis and increasing the serine/threonine phosphorylation of IRS-1 (Hotamisligil, 2000). Several signaling pathways, including the IKKβ/NF-κB pathway, are involved in the pathogenesis of insulin resistance (Kahn et al., 2006; Zhou and You, 2014). Moreover, other cytokines such as IL-1β and IL-6 might also increase systemic inflammation and inhibit insulin action in the major insulin-target cells (Hardaway and Podgorski, 2013; Lukic et al., 2014).

1.4.2.3. Insulin resistance and modulation of GSK3β activity

An accumulating body of evidence indicates a role of a distal element of the insulin signaling cascade, the serine/threonine kinase, GSK-3β, in the development of insulin resistance. The expression and activity of GSK-3β plays a number of important roles in mammalian cells, and impacts such diverse cellular processes as glycogen synthesis, glucose transport, protein synthesis, gene transcription, and cell differentiation. While the etiology of skeletal muscle insulin resistance is multifactorial, recent evidence supports a role of elevated GSK-3β as a contributing factor in this pathophysiological state. GSK-3β expression and activity have been found to be significantly elevated in muscle biopsies of T2DM patients (Nikoulina et al., 2001). Moreover, GSK-3β has been reported to be elevated in tissues of insulin-resistant obese rodent models, including high fat diet (HFD) fed mice (Eldar-Finkelman et al., 1999), obese Zucker rats (Dokken et al., 2005), and the Zucker Diabetic Fatty (ZDF) rat, a model of T2DM (Brozinick et al., 2000). Thus, numerous lines of evidence have accumulated linking GSK-3β to the development of insulin resistance. Actions of GSK-3β affecting nuclear functions, specifically gene expression, include indirect effects via its regulation of many transcription factors, and more direct effects resulting from the regulation of recently identified epigenetic mechanisms.

1.4.2.4. Insulin resistance and modulation of epigenetic mechanisms

Although there is no uniform definition of epigenetics, it has been described as heritable changes in gene function that occur without a change in the nucleotide sequence. Epigenetic mechanisms include DNA methylation, histone modifications, and microRNAs. Epigenetic effects may also be affected by the environment, making them potentially important pathogenic mechanisms in complex multifactorial diseases such as T2DM. Many studies have reported the role of epigenetic modifications in the development and pathogenesis of cancer, hypertension, and also insulin resistance and T2DM. Acetylation and deacetylation of histone proteins plays an important role in the epigenetic regulation of transcription in cells. HDACs are enzymes that balance the acetylation activities of histone acetyltransferases in chromatin remodelling. Studies have suggested that HDACs regulate insulin signalling components and also plays an important role in insulin resistance (Kaiser and James, 2004; Sun and Zhou, 2008).

Moreover, DNA methylation has also been reported to play an important role in insulin resistance and T2DM. It was observed that in pancreatic islets of T2DM, candidate genes like IRS-1 are differentially methylated, therefore bringing defects in the signaling pathway. The global increased methylation in β-cells resulted in an impaired glucose-stimulated insulin release (Dayeh et al., 2014). Although the recent research highlights the importance of epigenetic mechanisms in insulin signalling and resistance, however, epigenetic changes associated with T2DM are still poorly understood. During the next few years, it will be a great challenge to dissect the role of histone modifications and DNA methylation in the pathogenesis of the insulin resistance, T2DM and its complications.

1.5. Insulin resistance and associated diseases

1.5.1. Insulin Resistance and T2DM

Insulin resistance was reported to be a characteristic feature of T2DM in the early 1970s (Reaven, 2004). A progressive inability of the β-cells to compensate for the prevailing insulin resistance by sufficient hyperinsulinaemia, indicates the clinical onset of this disorder (Reaven , 2004). Insulin resistance typically occur before the development of diabetes and is commonly found in unaffected first-degree relatives (Hunter and Garvey, 1998). The morbidity of the disorder relates both to the severity of hyperglycaemia and the metabolic consequences of insulin resistance itself. The primary defects in insulin action appear to be in skeletal muscle cells and adipocytes, with impaired GLUT-4 translocation resulting in impaired insulin-mediated glucose transport (Hunter and Garvey, 1998). Compensatory

hyperinsulinaemia develops initially, but the first phase of insulin secretion is lost early in the disorder. Additional environmental and physiological stresses such as pregnancy, weight gain, physical inactivity and medications may worsen the insulin resistance. As the β cells fail to compensate for the prevailing insulin resistance, impaired glucose tolerance and diabetes develops. As glucose levels rise, β-cell function deteriorates further, with diminishing sensitivity to glucose and worsening hyperglycaemia. The pancreatic islet cell mass is reported to be reduced in size in diabetic patients (Nielsen et al., 2001).

1.5.2. Insulin Resistance and Obesity

The relationship between obesity and insulin resistance is seen across all ethnic groups and is evident across the full range of body weights. Large epidemiologic studies reveal that the risk for diabetes, and presumably insulin resistance, rises as body fat content (measured by body mass index [BMI]) increases from the very lean to the very obese, implying that the "dose" of body fat has an effect on insulin sensitivity across a broad range (Colditz et al. 1990). In obese individuals, adipose tissue releases increased amounts of non-esterified fatty acids, glycerol, hormones, proinflammatory cytokines and other factors that are involved in the development of insulin resistance. For example, increased release of TNF-α, IL-6, monocyte chemoattractant protein-1 (MCP-1) and additional products of macrophages and other cells that populate adipose tissue might also have a role in the development of insulin resistance (Wellen and Hotamisligil, 2005; Fain et al., 2004). TNF-α and IL-6 act through classical receptor-mediated processes to stimulate both the c-Jun amino terminal kinase (JNK) and the IκB kinase-β (IKK-β)/nuclear factor-κB (NF-κB) pathways, resulting in upregulation of potential mediators of inflammation that can lead to insulin resistance (Kahn et al., 2006).

1.5.3. Insulin Resistance and Cardiovascular System (CVS) diseases

Insulin resistance is not simply a problem of deficient glucose uptake in response to insulin, but a multifaceted syndrome that increases significantly the risk for cardiovascular disease. In the heart, insulin stimulates glucose uptake and oxidation. Also, it increases fatty acid uptake, it inhibits fatty acid utilization for energy. In diabetes and insulin resistant states, metabolic, structural and functional changes in the heart and vasculature lead to diabetic cardiomyopathy, coronary artery disease and myocardial ischemia, and ultimately heart failure (Fig. 1.3) (Bell, 2003; Gray and Kim, 2011). There are many molecular mechanisms that contribute to the association between insulin resistance and increased cardiovascular

disease. These include the impact of insulin resistance to induce impaired vascular function, which leads to impaired nitric oxide mediated vasorelaxation, which may contribute to hypertension and to increased risk of atherosclerosis (Muniyappa et al., 2008; Molnar et al., 2005; Symons et al., 2009; Zhang et al., 2012). Moreover, genetic manipulation of insulin action in the vasculature increased the risk of atherosclerosis (Rask-Madsen et al., 2012). Insulin resistance via multiple mechanisms may contribute to macrophage accumulation in the vessel wall to increase atherosclerosis and instability of vulnerable plaques (Bornfeldt and Tabas, 2011). Finally, insulin resistance has been shown in many human and animal studies to increase the extent of myocardial injury in the context of myocardial ischemia, which may contribute to the increased risk of heart failure in affected individuals (Abel et al., 2008).

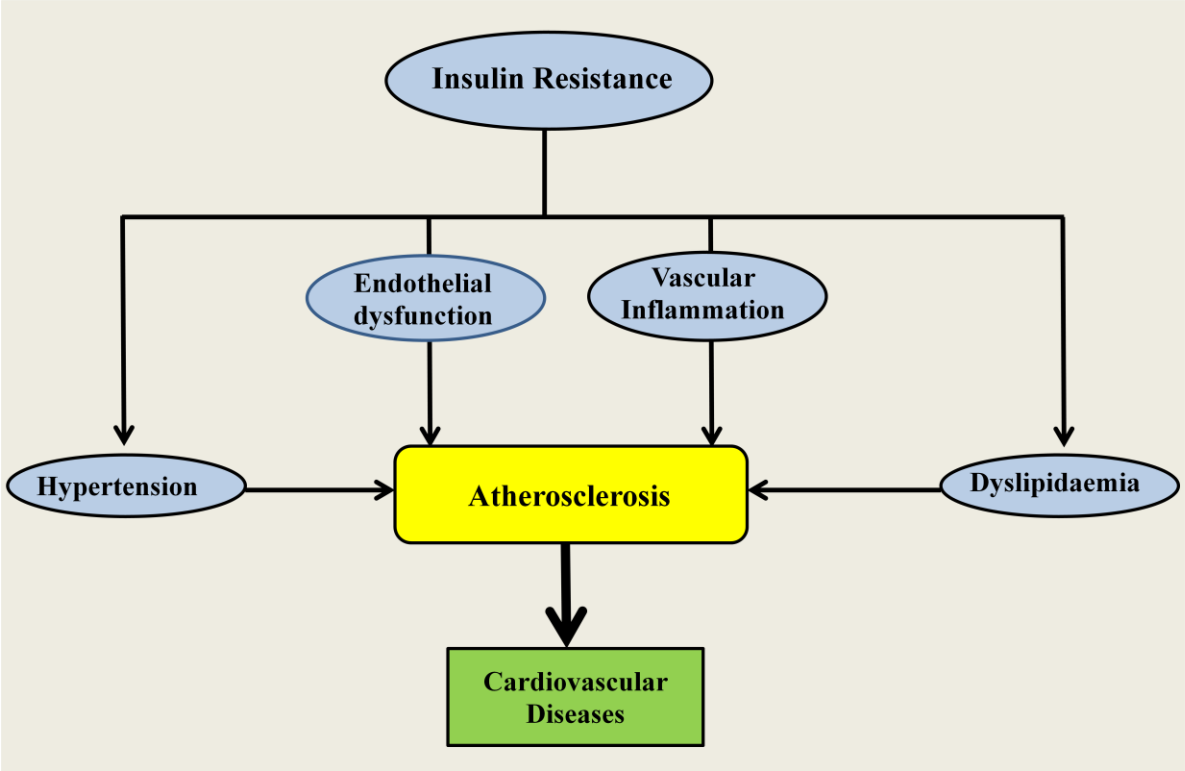

Fig. 1.3 Linkage between Insulin resistance and cardiovascular diseases

1.5.4. Possible Involvement of Insulin resistance in Central Nervous System diseases

The possibility that syndromes associated with insulin resistance in the periphery, such as obesity and T2DM, may also be associated with insulin resistance in the brain, with dysregulation of appetite and body weight, is intriguing (Gerozissis, 2004). A growing body of evidence indicates that alterations in neuronal integrity and function are mediated by abnormal central insulin signaling. The critical role of insulin in normal and abnormal CNS functioning provides the framework for characterizing its role in the pathoetiology,

progression, and treatment of several neuropsychiatric disorders. Recently, insulin resistance has been investigated as one of the mechanisms linking neurological diseases to T2DM and obesity. Insulin resistance might be involve in pathology of various neurological diseases such as depression, anxiety, cerebral ischaemia, Alzheimer's disease (AD), Parkinson's disease (PD) (Pearson et al., 2010; To et al., 2011). Among these diseases, AD and PD are the most prevalent and are one of the biggest global public health and social care challenges. Therefore, we have focused to explore the association of insulin resistance in AD and PD.

There is widening recognition that memory deficit and AD is closely associated with impaired insulin signaling and glucose metabolism in brain, suggesting it to be a brain-specific form of diabetes and so also termed as "type 3 diabetes". AD is a progressive neurodegenerative disease, where dementia symptoms gradually worsen over a number of years. AD accounts for 60 to 80 percent of dementia cases. The symptoms of AD include difficulty remembering recent conversations, names or events along with apathy and depression, impaired communication, confusion, poor judgment, difficulty speaking, swallowing and walking.

During the recent past, a number of studies have shown an association between AD and decreased insulin signaling in the CNS, suggesting that reduced insulin action might play a role in the pathogenesis of this disease (Frolich et al., 1999; Sandyk, 1993). Findings have evidenced that insulin sensitizers (pioglitazone and rosiglitazone) improve cognitive impairment in AD patients and animal model of AD (Araki 2010; To et al. 2011). In line with this possibility, a recent clinical trial of intranasal insulin administration to individuals with AD, decreased the rates of cognitive decline (Claxton et al., 2013). Synaptic loss, a phenotype of AD patients, can also be rescued with insulin treatment of cultured neurons (De Felice et al., 2009). Furthermore, GSK-3β expression is up-regulated in the hippocampus of AD patients (Blalock et al., 2004) and in post-synaptosomal supernatants derived from AD brain (Pei et al., 1997). By contrast, inhibition of GSK-3β attenuates APP processing and inhibits hyperphosphorylated tau-associated neurodegeneration in cell-culture and animal models of AD (Phiel et al., 2003; Noble et al., 2005). Aggregated amyloid-β (Aβ) fibrils and hyperphosphorylation of tau protein causing amyloid plaques and helical neurofibrillary tangles are hallmarks of AD, and these can be ameliorated by insulin signaling (de la Monte, 2012a). Tau hyperphosphorylation might occurs secondary to a decrease in GSK3β phosphorylation. Increased GSK-3β activation might also lead to an elevation in Aβ

production (resulting from a GSK-3β-mediated increase in presenilin 1 activity) (Fig. 1.4). Thus, these reports highlights that GSK3β modulation could play an important role in development of AD pathology

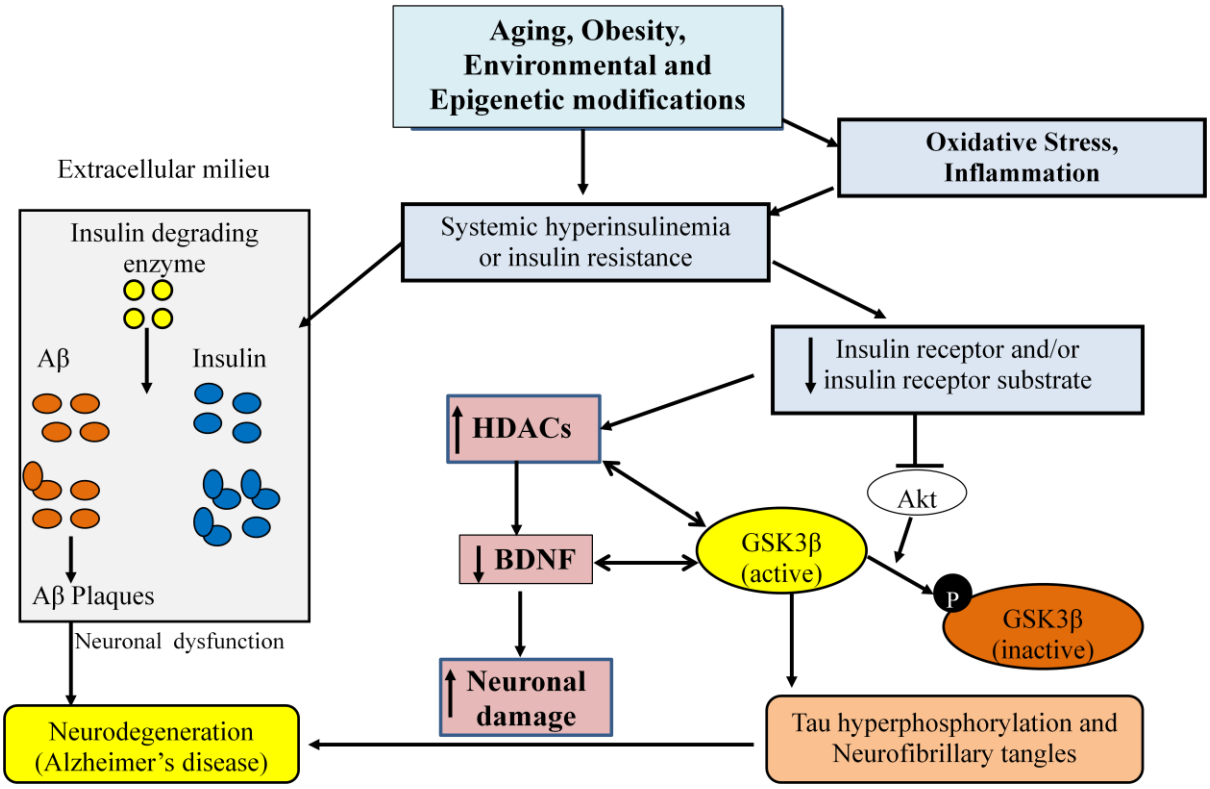

Fig. 1.4 Possible linkage between Insulin resistance and neurodegeneration in AD

Furthermore, actions of GSK-3β affecting nuclear functions, specifically gene expression, include indirect effects via its regulation of many transcription factors, and more direct effects resulting from the regulation of recently identified epigenetic mechanisms. Evidence is particularly strong that GSK-3β contributes to the regulation of histone modifications that play a central role in epigenetics. Among various histone modifications, GSK-3β has been reported to target histone acetylation/deacetylation and phosphorylate several HDACs. As such, a number of recent studies point to the fact that histone acetylation is an essential mechanism for the formation of long-term memories (Levenson and Sweatt, 2005). Further, decreased histone acetylation has been implicated in cognitive dysfunction in mouse models for AD (Ricobaraza et al., 2009). In addition, Bardai and D'Mello proposed that the HDACs exert a strong neurotoxic effect (Bardai and D'Mello, 2011). Moreover, HDAC inhibitors have also been reported to play role in IRS-1 phosphorylation leading to improved insulin sensitivity (Chriett et al., 2016). Thus, targeting HDACs seems to be a

promising therapeutic strategy for treatment of cognitive impairment and AD associated with abnormal GSK3β modulation in insulin resistance.

Recently, the linkage of abnormal insulin signalling has also been reported in PD, the second most common neurodegenerative disease. PD affects approximately 2% of the population over the age of 65 (Zaitone et al., 2012). Selective dopaminergic neuronal degeneration in substantia nigra pars compacta (SNpc) and depletion of dopamine in striatal projections at relatively early stages are the prominent features of PD pathology (Zaitone et al., 2012; Sharma et al., 2013). Neuropathological studies of PD patients have shown that insulin receptors are densely represented on the dopaminergic neurons of the SNpc (Unger et al., 1991) and loss of insulin receptor immunoreactivity and messenger RNA in the SNpc of patients with PD coincides with loss of tyrosine hydroxylase messenger RNA (the rate-limiting enzyme in dopamine synthesis) (Moroo et al., 1994). Clinical evidence has shown a correlation between PD and T2DM, as abnormal glucose tolerance has been reported in >50% of PD patients. Moreover, nigrostriatal dopamine depletion has been associated with impaired insulin signaling in the basal ganglia. Recently, insulin resistance was found to be present in 62 % of PD patients with dementia, of whom 30% were glucose intolerant (Bosco et al., 2012). Furthermore, the onset of diabetes before the onset of PD appears to increase symptom severity in PD patients (Cereda, et al., 2012). Various common mechanisms which might accelerates PD pathology in insulin resistant condition are depicted in Fig.1.5.

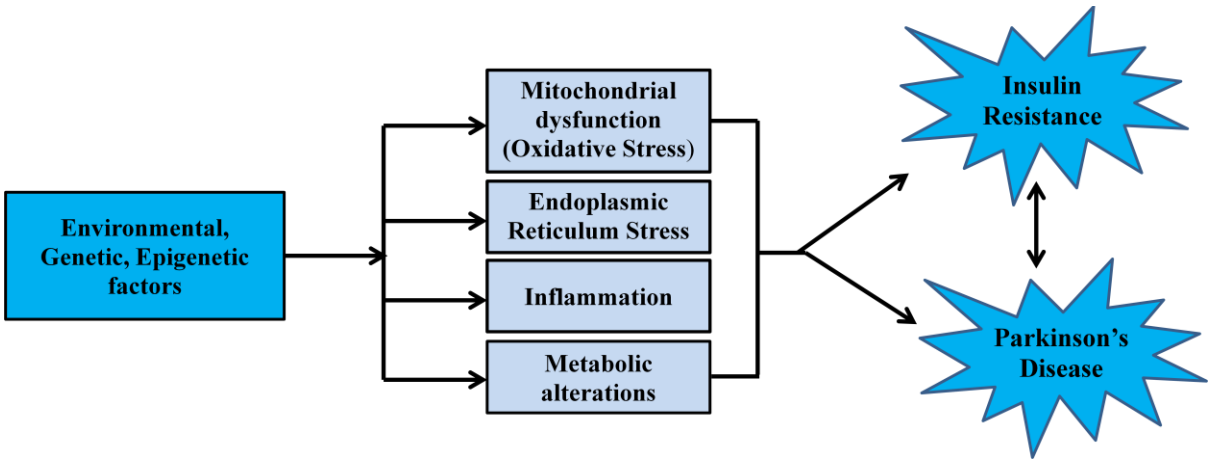

Fig. 1.5 Possible linkage between Insulin resistance and PD

Among other pathways, it is well demonstrated that GSK-3β dysregulation participates in various cellular processes that may eventually promote pathology of neurodegenerative diseases such as PD. Accordingly, it has been recently found that in post-

mortem PD brains, GSK-3β expression is increased in the regions associated with PD pathology (Duka et al., 2009) to such extent that inhibition of GSK-3β is considered as a promising therapeutic approach of PD (Lei et al., 2011). Further, it was observed that both active and inactive forms of GSK-3β are co-localized with α-Synuclein in the halo of Lewy bodies (LBs). More recently studies have highlighted the involvement of epigenetic processes in PD pathology. An imbalance between the acetylation and deacetylation of the histone proteins much in favour of excessive histone deacetylation, has also been reported to occur in PD (Harrison and Dexter, 2013). Keeping in mind the regulatory role of epigenetic mechanisms in insulin signalling, it might be possible that both GSK3β and histone acetylation might be associated with increased risk of PD in insulin resistance condition.

Interestingly, insulin-sensitizing drugs have been shown to be neuroprotective for PD (Randy et al., 2007). For example, chronic administration of rosiglitazone, a commonly prescribed insulin-sensitizing drug that functions by binding to the peroxisome proliferator-activated receptors (PPARs) in fat cells, completely prevented motor and olfactory dysfunctions in Parkinsonism mice (Schintu et al., 2009). Similarly, exendin-4, which treats T2DM by stimulating the glucagon-like peptide 1 (GLP-1) receptor activity, enhances the survival of dopaminergic neurons and improves motor function in MPTP-treated mice (Li et al., 2009). It is thought that anti-diabetic drugs promote neuroprotection by alleviating the effects of inflammation and insulin resistance. These reports suggest the possible involvement of insulin resistance in neurodegeneration. However, the molecular and cellular basis that link insulin resistance with neurodegeneration are yet to be explored.

2.0. Neurodegenerative Diseases

Neurodegeneration is an umbrella term for the progressive loss of structure or function of neurons, including death of neurons. Neurodegenerative diseases comprise one of the major public health concerns in our aging population. The consequences are very significant both in terms of pathology and the cost of caring for patients. The causes of most neurodegenerative diseases remain unknown. Many neurodegenerative diseases including AD, Spinal muscular atrophy, Parkinson's disease (PD), Lewy body disease, Huntington's disease (HD), and amyotrophic lateral sclerosis (ALS) occur as a result of neurodegenerative processes. Such diseases are incurable, resulting in progressive degeneration and/or death of neurons. The proper clinical diagnosis of neurodegenerative diseases is often difficult given the large overlap in signs and symptoms, although in more than 75% of cases the clinical diagnosis is confirmed by postmortem examination (Mok et al., 2004). As research progresses, many similarities appear that relate these diseases to one another on a sub-cellular level. Discovering these similarities offers hope for therapeutic advances that could ameliorate many diseases simultaneously (Armstrong et al., 2005). Recently, insulin resistance and T2DM have been reported as common risk factors that might be involved in various neurodegenerative diseases, including AD and PD. While it is difficult to directly measure insulin resistance in the brain *in vivo*, studies on post-mortem tissue have shown markers of insulin resistance in both AD and PD brains (Takahashi et al., 1996; Steen et al., 2005; Lee et al., 2009; Moloney et al., 2010; Liu et al., 2011).

2.1. Alzheimer's disease (AD)

Dementia is characterized by a decline in memory, language, problem-solving and other cognitive skills that affect a person's ability to perform everyday activities. Dementia is further classified based on etiology. AD is the most common cause of dementia, followed by mixed AD and vascular dementia, Lewy body dementia, and frontotemporal dementia (Nowrangi et al., 2011).

AD is a progressive neurodegenerative disease, where dementia symptoms gradually worsen over a number of years. AD accounts for 60 to 80 % of dementia cases. Although aging is considered as the greatest known risk factor for AD, and the majority of people with AD are 65 and older. However, upto 5 % of people with the disease have early onset AD (also known as younger-onset), which often appears when someone is in their 40s or 50s. Those with AD live an average of eight years after their symptoms become noticeable to

others, but survival can range from 4 to 20 years, depending on age and other health conditions. Although current AD treatments cannot stop it from progressing, they can temporarily slow the worsening of dementia symptoms and improve quality of life for those suffering from this devastating disease.

2.1.1. Epidemiology (http://www.alzheimers.net/resources/alzheimers-statistics/)

Worldwide, nearly 44 million people have AD or a related dementia. Only 1-in-4 people with AD have been diagnosed. The global cost of AD and dementia is estimated to be $605 billion, which is equivalent to 1% of the entire world's gross domestic product. India was ranked among the seven countries with the largest number of people with dementia (1.5 million in 2001) (Ferri et al., 2005). Moreover, according to a report prepared by "Alzheimer's and Related Disorders Society of India" in 2010 the number of people suffering from dementia rises to 3.7 million. An estimated 5.4 million Americans of all ages have AD till 2016. The number of people living with AD above the age of 65 years, is expected to increase thrice from 5.2 million to a projected 13.8 million by 2050 (Hebert et al., 2013).

2.1.2. Symptoms

The early symptoms of AD include difficulty remembering recent conversations, names or events along with apathy and depression. Later symptoms also include impaired communication, disorientation, confusion, poor judgment, behavior changes and, ultimately, difficulty speaking, swallowing and walking.

2.1.3. Pathophysiology

Numerous factors have been shown to effect the development and progression of AD; however, two main hypotheses have been driving much of current drug development. The primary hypothesis, with the most documentation in familial AD research, follows the amyloid pathway. This hypothesis was generated from the pathology of the amyloid precursor protein (APP), which is cleaved by 2 pathways resulting in beta amyloid (Aβ) proteins. The 39-42 amino acid amyloid proteins have been identified as the major component of neuritic (senile) plaques. In the first pathway, APP is cleaved first by β-secretase (or beta site APP cleaving enzyme 1, BACE1) then γ-secretase, producing the $A\beta\text{-}_{42}$ protein (Fig. 2.1). The $A\beta_{42}$ protein readily aggregates into neurotoxic oligomers, which are thought to induce neuronal dysfunction, tau protein phosphorylation, and neurofibrillary tangles (NFTs) formation. In the other pathway, APP is cleaved first by α-secretase then γ-

secretase and does not allow the formation of the $A\beta_{42}$ protein. The discovery that the apolipoprotein E4 (ApoE4) allele (which is associated with increased risk of AD) can lead to increased levels of APP and longer Aβ proteins, including $A\beta_{42}$ protein, provides further support for the amyloid pathway hypothesis.

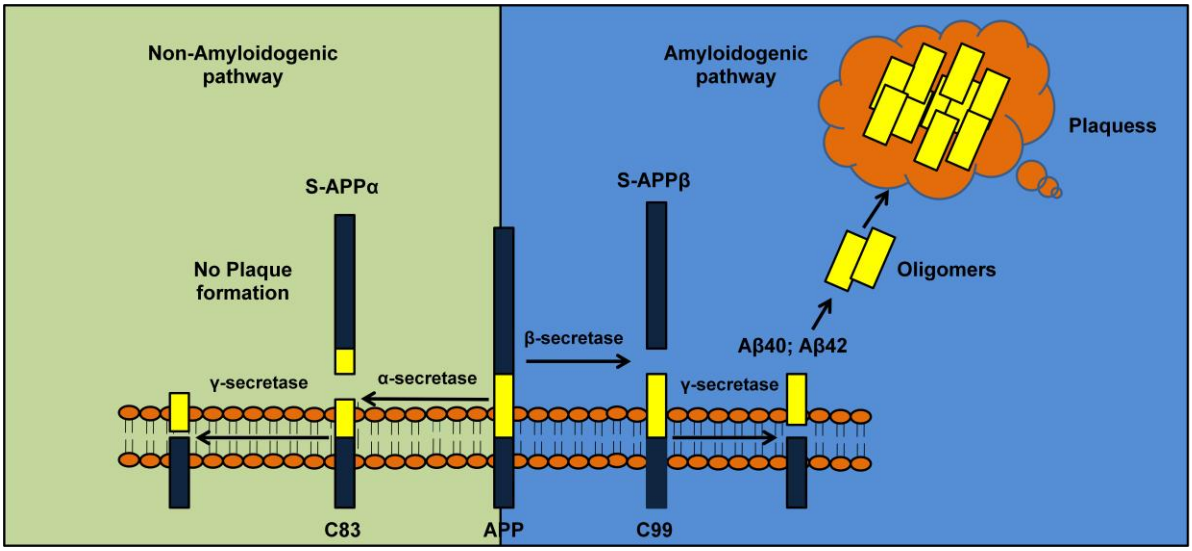

Fig. 2.1 Processing of amyloid precursor protein by amyloidogenic and non-amyloidogenic pathways

The other major hypothesis, that tau protein dysfunction leads to dementia, has generated additional AD drug design. The tau hypothesis states that excessive or abnormal phosphorylation of tau results in the transformation of normal adult tau into PHF-tau (paired helical filament) and NFTs (Fig. 2.2). Tau protein is a highly soluble microtubule-associated protein (MAP). Through its isoforms and phosphorylation, tau protein interacts with tubulin to stabilize microtubule assembly. Hyperphosphorylated tau disassembles microtubules and sequesters normal tau, MAP 1 (microtubule associated protein1), MAP 2 and ubiquitin into tangles of PHFs. This insoluble structure damages cytoplasmic functions and interferes with axonal transport, which can lead to cell death (Mudher and Lovestone, 2002). Thus, pathologically AD is characterized by intracellular neurofibrillary tangles and extracellular amyloidal protein deposits contributing to senile plaques. Although the exact role of plaques and tangles in AD is yet not explored, but most experts believe that they somehow play a critical role in blocking communication among nerve cells and disrupting processes that cells need to survive. It's the destruction and death of nerve cells that causes memory failure, personality changes, problems carrying out daily activities and other symptoms of AD.

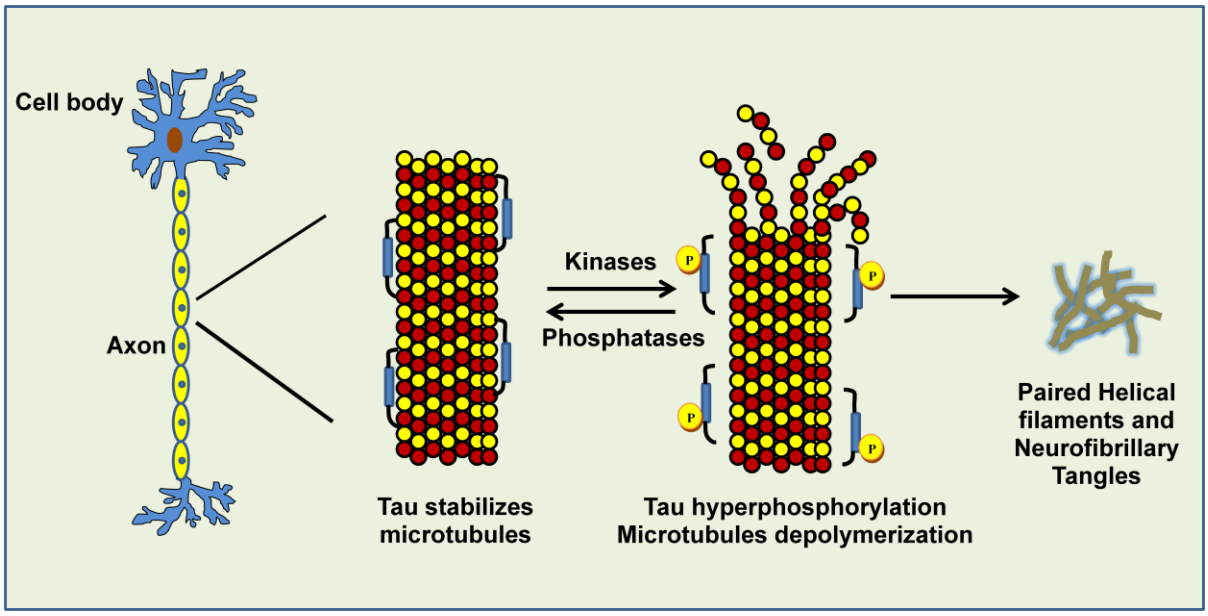

Fig. 2.2 Physiological and Pathological roles of tau leading to microtubule depolymerization

2.1.4. Available Treatments and their drawbacks

Currently, there are no treatments to cure or to prevent or stop disease progression. The only approved therapies for AD are the cholinesterase inhibitors (ChEIs) and an N-methyl-D-aspartate (NMDA) receptor antagonist. Memantine, the only NMDA receptor antagonist, can be used as monotherapy as well as an adjuvant to ChEIs. The ChEIs—donepezil, rivastigmine, galantamine, and tacrine—are indicated for mild-to-moderate AD; only donepezil is approved for the severe stage (Forchetti, 2005). These medications reversibly bind the enzyme acetylcholinesterase, allowing for more available concentrations of acetylcholine, a neurotransmitter associated with thought, learning, memory and other cognitive processes. Although available, tacrine is not recommended because it has a high risk for hepatotoxicity and drug interactions (cytochrome P450), requiring frequent monitoring (Blackard et al., 1998). Although these treatments can bring transient relief of symptoms, they cannot affect the disease course. When more neurons are lost during disease progression, the medications become less effective. Thus new therapeutic strategies such as neuroprotection or neurorestoration are needed to improve the prognosis of neurodegenerative diseases.

In the decade of 2002-2012, 244 drugs for AD were tested in clinical trials registered with clinicaltrials.gov, a National Institutes of Health registry of publicly and privately

funded clinical studies (Cummings et al., 2014). Only one drug (memantine) of the 244 drugs successfully completed clinical trials and went on to receive approval from the FDA. Many factors such as the high cost of drug development, the relatively long time needed to observe whether an investigational treatment affects disease progression, and the structure of the brain, which is protected by the BBB, contribute to the difficulty of developing effective treatments for AD.

2.2. Parkinson's disease (PD)

PD is the second most common neurodegenerative disease following AD. PD is a chronic and progressive movement disorder, meaning that symptoms continue and worsen over time. Selective dopaminergic neuronal degeneration in substantia nigra pars compacta (SNpc) and depletion of dopamine in its striatal projections and of other brain stem neurons in relatively early stages are the prominent feature of PD pathology (Siderowf and Stern, 2003; Zaitone et al., 2012). This neurodegeneration is accompanied by the presence of cytoplasmic (Lewy bodies) and neuritic (Lewy neurites) inclusions in the surviving dopaminergic neurons and other affected regions of the CNS (Wakabayashi et al., 2007; 2013).

2.2.1. Epidemiology of PD

More than 10 million people worldwide are living with PD. Nearly one million people in the US are living with PD. This disease affects approximately 2% of the population over the age of 65 and 4-5% population over the age of 80 years (Kowal et al., 2013). The combined direct and indirect cost of PD, including treatment, social security payments and lost income from inability to work, is estimated to be nearly $25 billion per year in the United States alone. The Parsi community in Mumbai has the world's highest incidences of PD where it affects about 328 out of every 100,000 people despite living in a country, India, with one of the world's lowest incidence of PD (70 out of 100,000) (Gupta and Bala, 2013).

2.2.2. Symptoms of PD

Each person with PD experience different symptoms. For example, many people experience tremor as their primary symptom, while others may not have tremors, but may have problems with balance. Primary motor signs of PD include the following.

- Tremor of the hands, arms, legs, jaw and face
- Bradykinesia or slowness of movement
- Rigidity or stiffness of the limbs and trunk

- Postural instability or impaired balance and coordination

Among motor symptoms and signs, the cardinal ones (bradykinesia, resting tremor, and rigidity) are mainly ascribed to the loss of dopaminergic neurons (Hughes et al., 1992). Those involving posture, balance, and gait are largely secondary to degeneration of nondopaminergic pathways and significantly contribute to impairment and disability in advanced PD patients (Sethi, 2008). Nonmotor features result from multiple neurotransmitter deficiencies in the central and peripheral nervous system (Chaudhuri and Schapira, 2009) and include psychiatric (depression, apathy, hallucinations, and delusions) and autonomic features (constipation, orthostatic hypotension, and urinary and genital disturbances), cognitive impairment (involvement of executive functions, memory, and visuospatial functions up to dementia) (Federico et al., 2015; Varalta et al., 2015), sleep disorders, olfactory dysfunction, and pain (Schrag et al., 2015) that together contribute to worsening the quality of life (QoL) and patient's disability (Chaudhuri and Schapira, 2009). Recent research has also focused to find the possible reason for these non-motor symptoms. Studies suggests that the hallmark feature of PD pathology, the presence of clumps of protein, alpha-synuclein (α-syn), which are also called lewy bodies, are found not only in the mid-brain but also in the brain stem and the olfactory bulb. These areas of the brain correlate to nonmotor functions such as sense of smell and sleep regulation. The presence of lewy bodies in these areas could explain the nonmotor symptoms experienced by some people with PD before any motor sign of the disease appears.

2.2.3. Pathophysiology of PD

The pathophysiology of PD is mainly unknown, although some genetic and environmental factors have been described as contributing factors. It is estimated that approximately 5–10% of cases are caused by inheritable genetic mutations (Dauer and Przedborski, 2003; Samii et al., 2004). The remaining 95% of newly diagnosed PD cases are of idiopathic origin. Although, several hypothesis have been proposed to explain the causes of sporadic cases, however, no unifying mechanisms have yet been discovered. One theory proposes that nigral neurons are selectively vulnerable to environmental contaminants triggering mitochondrial dysfunction (Orth and Schapira, 2002). This theory arose primarily from findings that mitochondrial toxins such as 1-methyl-4-phenylpyridium ions (MPP^+), the active metabolite of the meperidine analog, 1-methyl-4-phenyl-1,2,3,6-tetrahydropyridine (MPTP), and rotenone can induce a parkinsonian condition in humans, non-human primates, and rodents (Schapira, 1994 ; Sherer *et al.*, 2002). Secondly, the proteolytic stress hypothesis ascribes the

loss of nigral neurons in PD to the toxic accumulation of misfolded and aggregated proteins (McNaught and Olanow, 2003). Lastly, the preferential loss of nigral neurons in PD has been attributed to the highly oxidative intracellular environment within dopaminergic neurons (Fig. 2.3) (Lotharius and Brundin, 2002a; Lotharius and Brundin, 2002b; Hald and Lotharius, 2005). Moreover, recent studies have explored the involvement of neuro-inflammatory processes in nigral degeneration. Increased levels of inflammatory mediators along with activated microglia have been observed in striatum region of PD patients. These observations were further supported by a large body of animal studies, which points to a contributory role of inflammation in dopaminergic cell loss. Aging is also an important risk factor, which increases the chances of PD. However, the chemical or genetic trigger(s) that starts the cell death process in dopaminergic neurons is yet to be explored. Understanding the sequence of events that leads to the loss of dopaminergic neurons will help to develop newer therapeutic agents to treat this devastating disease.

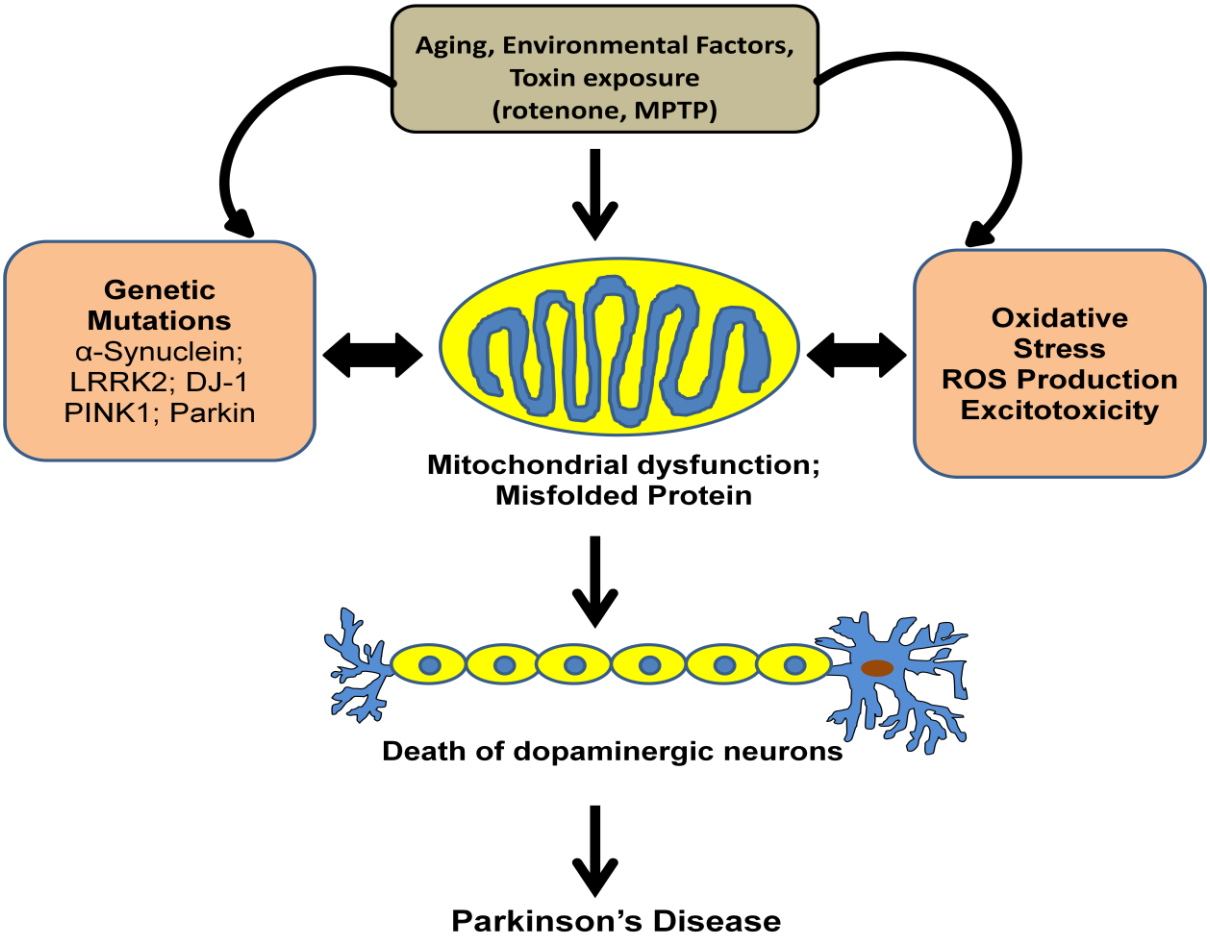

Fig. 2.3 Possible mechanisms of dopaminergic neuronal death in PD

2.2.4. Available Treatments and drawbacks

Currently, pharmacological treatment of motor symptoms of PD depends mainly on the administration of dopaminergic drugs (levodopa (L-DOPA) and dopamine agonists). Moreover, the drugs inhibiting the dopamine metabolism (monoamine oxidase-B (MAO-B) inhibitors and catechol-O-methyltransferase (COMT) inhibitors) are also used to treat PD symptoms. The dopamine replacement therapy in clinical use is only palliative; leading to temporarily limited improvement of clinical symptoms. Further, chronic treatment with dopaminergic drugs either L-DOPA or dopamine agonists have severe side effects such as involuntary movements, termed dyskinesia (Jenner, 2008). Unfortunately, most patients with advanced PD are unsatisfactorily controlled by the usual therapeutic approach. Consequently, new approaches are needed to find disease modifying agents that may delay or stop the neuronal death.

2.2.5. Possible risk factors for AD and PD

The majority of AD and PD cases are ‘sporadic’, which means that there is no clear genetic pathway that causes the onset of the disease. This makes it more difficult to identify which factors trigger the neurodegenerative processes that underlie these diseases. Analysing the effects of known risk factors may therefore be a useful guide to some of the underlying biochemical processes that initially may be responsible for initiating AD or PD. Previous studies have shown that risk factors such as aging, hypertension, diabetes, obesity, environmental toxins exposure, inflammation, head injury and genetic factors might be associated with the risk of developing AD and PD. Growing evidence suggests that among the modifiable risk factors, both AD and PD might be related to a metabolic disease with substantial and progressive derangements in brain glucose utilization and responsiveness to insulin and IGF stimulation (Talbot et al., 2012; Takahashi et al., 1996). Other factors, including impairments in energy metabolism, increased oxidative stress, inflammation, insulin and IGF resistance, and insulin/IGF deficiency in the brain might also be responsible for the development for these diseases. Moreover studies have also suggested a possible association of involvement of T2DM with these neurodegenerative diseases. Of the shared features of AD and T2DM, the one most likely to be an etiological factor is insulin resistance. Several lines of evidence has indicated that insulin and glucose metabolism influence cognitive functions (Luchsinger et al., 2004; Plastino et al., 2010). In addition, an abnormal glucose tolerance was also found to be directly associated with increased risk of AD

development (Ohara et al., 2011). Moreover, altered insulin signalling pathways and increased serine IRS-1 phosphorylation has been observed in AD brains (Talbot et al., 2012).

Studies of PD brain tissues also report similar biochemical changes in insulin signalling components. Early reports suggested that up to 50%-80% of patients with PD have abnormal glucose tolerance (Sandyk, 1993). Moroo and colleagues demonstrate that dysfunction of the insulin/insulin receptor system may precede death of the dopaminergic neurons in the substantia nigra region (Moroo et al., 1994). In addition, increased IRS-2 phosphorylation, a marker of IGF-1-resistance, was found in the basal ganglia of animal model of PD (Morris et al., 2008). Insulin resistance has also been associated with a more severe PD phenotype, accelerated disease progression, and increased risk of PD dementia (Bosco et al., 2012; Cereda et al., 2011; Kotagal et al., 2013). Thus, these reports highlight that insulin resistance might be linked to neurodegeneration observed in AD and PD cases.

2.3. Possible biological mechanisms linking Insulin resistance and neurodegenerative diseases

The various mechanisms that might be involved in insulin resistance induced neurodegeneration and related behavioural abnormalities include:

- Altered brain oxidative-nitrosative stress
- Altered pro-inflammatory cytokines
- Altered neurotrophic factor signalling
- Altered transcriptional regulation
- Altered brain neuronal morphology
- Altered insulin signalling components

2.3.1. Altered brain oxidative-nitrosative stress

The high content of lipids, high requirement for oxygen, and the scarcity of antioxidant defence mechanisms make the brain highly susceptible to oxidative stress. Oxidative stress is well recognised to play a major role in the neurodegenerative process in AD and PD brain. With respect to insulin resistance and the progression to T2DM, continuous overnutrition leads to chronic reactive oxygen species (ROS) and reactive nitrogen species (RNS) production, which promotes oxidative stress in key cells, tissues, and organs (Verdile et al., 2015). Eventually, oxygen and nitric oxide based free radicals damage cell membranes,

DNA, and protein structures, as well as modulating the activity of transcriptional factors through redox chemistry, including NF-κB, leading to chronic inflammation and cell apoptosis (Newsholme et al., 2009). Physiologically, these free radicals are quenched by endogenous antioxidant defense mechanism (antioxidant enzymes such as reduced glutathione, catalase and Superoxide dismutase). However, during insulin resistance, ROS levels overwhelm the antioxidant enzyme capacity and leads to excessive ROS accumulation (Tangvarasittichai et al., 2015). Although every single cell can be potentially damaged by oxidative stress, the reduced capacity of antioxidant defence mechanisms can particularly expose both β-cells and neurons to damage resulting in progression of T2DM and neurodegenerative diseases (Butterfield et al., 2001).

2.3.2. Altered Pro-inflammatory cytokines

Inflammation is part of the body's defence mechanisms against multiple threats, including infections and injury. Both in the brain and in peripheral tissues, unchecked or chronic inflammation becomes deleterious, leading to progressive tissue damage in degenerative diseases. Inflammation plays critical roles in the pathogenesis of metabolic diseases, including T2DM as well as neurological diseases including AD and PD (Ferreira et al., 2014). The association between T2DM, AD and PD has led to the hypothesis that periphery-derived pro-inflammatory molecules could also influence pathogenesis in the CNS. Additional evidence linking systemic inflammation with neurodegeneration comes from epidemiological studies, which show that prolonged use of nonsteroidal anti-inflammatory drugs (NSAIDs) reduces the risk of developing AD (in 't Veld et al., 1998) or PD (Gao et al., 2011) by as much as 50%. Several studies have demonstrated elevated levels of pro-inflammatory cytokines in the AD and PD brain (Rogers et al., 2007; Holmes et al., 2009; McCoy et al., 2006). Moreover, recent studies showed that blood concentrations of several inflammatory mediators, including TNF-α, IL-6, and IL-1β are increased in AD patients (Swardfager et al., 2010; Koziorowski et al., 2012; Dobbs et al., 1999; Brodacki et al., 2008). Interestingly, brain inflammation has recently been proposed to underlie defective neuronal insulin signaling in AD (Bomfim et al., 2012). Several pathological features, including impaired insulin signaling and inflammation, appear to be shared by patients with T2DM, AD and PD. Therefore, it is likely that mechanisms analogous to those that account for peripheral insulin resistance underlie impaired brain insulin signaling and neuronal dysfunction.

2.3.3. Altered neurotrophic factor signalling

Neurotrophic factors are critical controllers of the formation and plasticity of neuronal networks in brain (Castren et al., 2007; Castren and Rantamaki, 2010). Brain-derived neurotrophic factor (BDNF) is a member of the neurotrophin family of growth factors and plays a critical role in activity-dependent neuroplasticity underlying learning and memory in the hippocampus (Egan et al., 2003). BDNF can induce long-term potentiation (LTP) through the activation of signal transduction pathways that plays a key role in neurophysiological basis for learning and memory (Leal et al., 2015). Post mortem studies revealed reduced BDNF mRNA and protein expression in respective brain areas of AD and PD patients (Connor et al., 1997; Howells et al., 2000). Moreover, recent studies suggest that BDNF serum levels are also significantly decreased in neurological diseases such as AD, PD, mild cognitive impairment and HD (Laske et al., 2006; Scalzo et al., 2010; Zhang et al., 2012; Wang et al., 2016). These findings suggest that serum BDNF is a biomarker of neuronal health. Interestingly, BDNF administration has beneficial effects on glucose homeostasis and improves insulin resistance in *db/db* mice (Ono et al., 1997; Tonra et al., 1999; Nakagawa et al., 2000). The role of BDNF in metabolism is supported by studies on BDNF-deficient mice ($Bdnf^{+/-}$), which develop hyperphagia and obesity in early adulthood (Kernie et al., 2000). However, when BDNF is administered to normal mice or rats, it has no effect on blood glucose levels, indicating that BDNF exerts its effects by enhancing insulin sensitivity. Further, BDNF activates several signalling pathways also activated by insulin, including phosphatidylinositol-3 kinase/Akt among others (Cotman, 2005). These reports indicate that BDNF plays a role in glucose metabolism and also suggests that neurotrophins such as BDNF may play pathogenetic roles not only in dementia, AD and PD, but also in T2DM possibly via insulin signalling pathways (Krabbe et al., 2007).

2.3.4. Altered Transcriptional regulation

One of the mechanisms by which insulin regulates transcription is through the phosphorylation and transcriptional activation of cAMP responsive element binding protein (CREB) (Klemm et al., 1998). The insulin signalling pathways mainly, PI3K/Akt signaling pathway has been extensively studied (Du and Montminy, 1998; Brami-Cherrier et al., 2002). CREB is known as one of its downstream effectors, which also regulates the expression of functional proteins associated with learning and memory (Benito and Barco, 2010; Barco and Marie, 2011). CREB undergoes phosphorylation at serine 133 in response to multiple signaling pathways (Shaywitz and Greenberg, 1999; Pugazhenthi et al., 1999). The phosphorylated form of CREB binds to the coactivators, CREB binding protein (CBP) and

p300 resulting in the facilitation of target gene expression (Kwok et al., 1994). In particular, CREB, a transcription factor acts as a mediator of neurotrophin-triggered neuronal differentiation, survival, and plasticity in the brain, and it has been characterized as metabolic sensor modulated by nutrient depletion and fasting hormones (Altarejos and Montminy, 2011; Finkbeiner, 2000). Moreover, CREB activation has also been reported to increase the activities of neurotrophic factors such as BDNF, Nerve growth factor (NGF), neurotrophin-3, neurotrophin-4 etc. which are known to have neuroprotective actions (Delghandi et al., 2005; Merz et al., 2011). In addition, decrease in the levels of CREB-regulated BDNF has been observed in post-mortem brains of AD and PD patients (Phillips et al., 1991; Howells et al., 2000). Thus, these reports suggest a possible link between altered insulin signalling and CREB phosphorylation in neurodegenerative diseases.

2.3.5. Altered brain neuronal morphology

In line with the above neurotrophic factor hypothesis, impairment in brain morphological and structural abnormalities has also been suggested by few histological studies. Studies carried out both *in vitro* and *in vivo* suggest that insulin and IGF-I promote neurogenesis by affecting neural stem cells (NSC) proliferation, differentiation, and survival (Aberg et al., 2003; Brooker et al., 2000; Drago et al., 1991). Moreover, insulin is a crucial trophic factor for nervous system development and maintenance of neurogenic niches. Many brain structures, such as the hippocampus, are extremely sensitive and responsive to changes in glucose homeostasis (Pamidi and Satheesha, 2012; Ramos-Rodriguez et al., 2014). For example, dysfunctional glucose regulation and/or insufficient insulin availability elicits neuronal synaptic reorganization (Magarinos and Mcewen, 2000). Stranahan et al. (2008) reported high fat diet (HFD) induced insulin resistance results in decreased numbers of Golgi-stained dendritic spines, reduced dendrite lengths as well as reduced expression of the presynaptic vesicle marker synaptophysin in hippocampus CA1 region (Stranahan et al., 2008). In line with these, a recent study also demonstrate that hippocampus of mice fed with HFD showed decreased expression of PSD-95, a scaffolding protein enriched in post-synaptic densities, and synaptopodin, an actin-associated protein enriched in spine apparatuses (Arnold et al., 2014). Thus, these studies clearly indicate that insulin resistance and T2DM conditions might severely affects the brain morphology and synaptic plasticity.

2.3.6. Altered insulin signalling components

2.3.6.1. Glycogen Synthase kinase-3β (GSK-3β) in insulin resistance and neurodegenerative diseases

GSK-3 is a cellular serine/ threonine protein kinase (Embi et al., 1980; Rylatt, et al., 1980), belonging to the glycogen synthase kinase family (Embi et al., 1980). GSK-3 was first described as the major regulator of glycogen metabolism, by phosphorylating and thereby inhibiting glycogen synthase (Embi et al., 1980). It is involved in a number of cellular processes, including the division, proliferation, differentiation and adhesion of cells (Kockeritz et al., 2006). Two isoforms of GSK-3 have been identified, namely, GSK-3α and GSK-3β, which although encoded by different genes are similarly regulated (Woodgett, 1990). The GSK-3 isozymes share overall 84% sequence identity, but 98% in the kinase domain indicating similar substrate specificities (Woodgett, 1990). GSK-3α (51 kDa) differs from GSK-3β (47 kDa) in that the former has a glycine-rich extension at the amino-terminal end of the protein (Woodgett, 1990). The activity of GSK-3 is dependent on phosphorylation at specific sites; phosphorylation of Ser 9 of GSK-3β, or Ser 21 of GSK-3α, inhibits activity (Dajani et al., 2001), whereas phosphorylation of Tyr 216 on GSK-3β and Tyr 279 on GSK-3α increases activity (Kockeritz et al., 2006) (Fig.2.4). The alpha isoform regulates longevity-related processes and the beta isoform regulates aging and "shortivity"-related processes. GSK-3α when active negatively regulates at least three pro-aging pathways: mTOR, Wnt and P53. Basically, in normal quiescent cells, GSK-3α restrains aging due to activation of these pathways. GSK-3β on the other hand, plays a role in signaling pathways like those involved in glycogen metabolism. Moreover, GSK-3β, can promote the formation of both beta-amyloid plaques in the brain and tau tangles in nerve cells, the two major hallmarks of AD pathology. Among these isoforms, GSK3β has been widely reported to play role in diabetes, obesity, insulin resistance and possibly in neurodegenerative diseases. Thus, the focus of present work was to explore the role of GSK3β in insulin resistance and neurodegeneration.

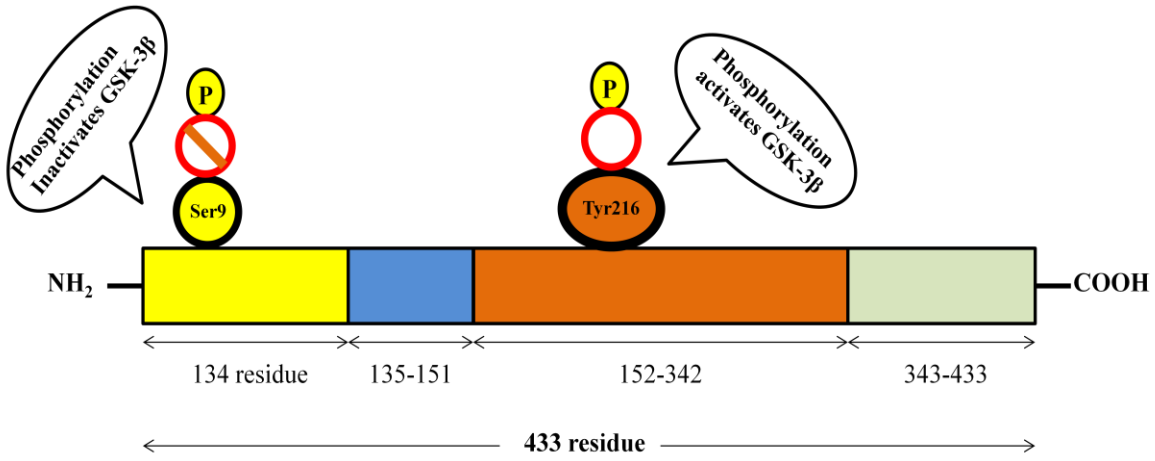

Fig. 2.4.Strand diagram of GSK-3β: It is a 433 residues long protein. The N-terminal (yellow) is made up of 134 residues. Residues 135-151 (blue) act as connecting link between N-terminal domain and a-helical domain (orange). ATP-binding site lies between N-terminal domain and a-helical domain. C-terminal (olive green) is made up of 343-433 residues. Phosphorylation of Serine-9 inactivates the enzyme while the phosphorylation of Tyr216 activates it.

Glycogen Synthase (GS) activity is regulated by allosteric and covalent (phosphorylation/dephosphorylation) mechanisms (Parker et al., 1983; Roach and Larner, 1997; Lawrence and Roach, 1997). Among the various kinases and phosphatases that act on GS, GSK-3β is the most important one (Fig. 2.5). As a downstream signalling pathway, activated protein kinase B/AKT (activated by phosphorylation) phosphorylates and inactivates GSK3β. This means that GSK3β can no longer phosphorylate its substrate, GS. Now, GS, when phosphorylated, is inactive. Hence, as GSK3β is no longer active (as it is phosphorylated) it cannot phosphorylate GS and inactivate it, therefore GS remains un-phosphorylated and therefore active, so it can make glycogen (Eldar-Finkelman et al., 1996; Skurat et al., 1994; Summers et al., 1999; Eldar-Finkelman and Krebs, 1997).

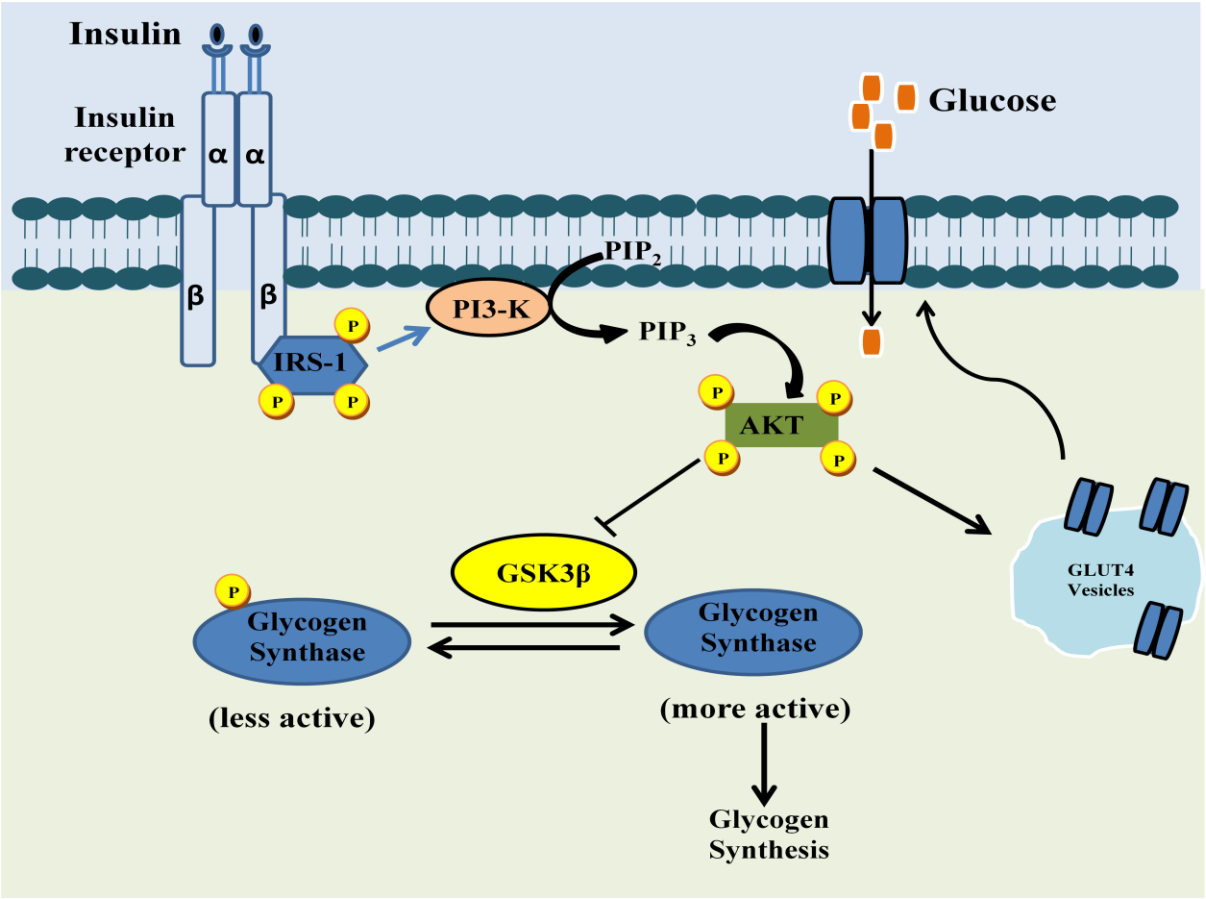

Fig.2.5. Regulation of GSK-3β by insulin signalling pathway

While the etiology of skeletal muscle insulin resistance is multifactorial, recent evidence supports a role of elevated GSK-3β as a contributing factor in this pathophysiological state. Both preclinical and clinical evidences suggest elevated GSK-3β expression and activity in insulin-resistant obese rodent models, such as HFD fed mice (Eldar-Finkelman et al., 1999), obese Zucker rats (Dokken and Henriksen, 2006), and the Zucker Diabetic Fatty (ZDF) rat, a model of T2DM (Brozinick et al., 2000) and in muscle biopsies of T2DM patients (Nikoulina et al., 2000).

The increased insulin sensitivity observed in response to GSK-3β inhibition has been attributed to signaling through IRS-1. Following priming at Ser 336, GSK-3β has been shown to phosphorylate IRS-1 at Ser 332 (Liberman and Eldar-Finkelman, 2005). Serine phosphorylation of IRS-1 is thought to impair tyrosine phosphorylation by the insulin receptor (Eldar-Finkelman and Krebs, 1997), thus attenuating insulin signaling. Moreover, inhibition of GSK-3β using specific inhibitor, CT118637 increased the insulin-stimulated IRS-1 tyrosine phosphorylation in muscle of Zucker diabetic fatty rats (Dokken and Henriksen, 2006).

The effect of GSK-3β overexpression on whole-body glucose tolerance in mice has also been investigated (Pearce et al., 2004). These investigators produced a mouse model that selectively overexpresses the GSK-3β isoform in skeletal muscle by 5-fold. Relative to nontransgenic control mice, male GSK-3β transgenic mice were characterized by increased fat mass, dyslipidemia, decreased muscle protein expression of IRS-1, decreased glycogen synthase activity and glycogen levels in muscle. Moreover, in response to an oral glucose challenge, these mice display an exaggerated glucose response and elevated insulin levels, indicating a decrease in whole-body insulin sensitivity (Pearce et al., 2004). Based upon these reports it could be suggested that elevated GSK-3β expression/activity plays an important role in development of insulin resistance.

2.3.6.1.1. Role of GSK-3β in Alzheimer's disease

Both isoforms of GSK-3 are ubiquitously expressed throughout the brain, with high levels of expression seen in the hippocampus, cerebral cortex, and the Purkinje cells of the cerebellum (Yao et al., 2002). The expression ratio of these isoforms, however, favours GSK-3β (Yao et al., 2002; Lau et al., 1999). Increased GSK-3β activity is believed to participate in sporadic AD (Small and Duff, 2008). However, there is little evidence of increased GSK-3β activity in human AD patients, as it is technically difficult, if not impossible, to measure enzymatic activity in post-mortem brain tissue. Nevertheless, indirect evidence does support the role of GSK-3β in AD. GSK-3β has been shown to co-localize with dystrophic neurites and neurofibrillary tangles (NFTs) in AD patients (Yamaguchi et al., 1996; Imahori and Uchida 1997; Pei et al., 1997). Active GSK-3β appears in neurons with pre-tangle changes (Pei et al., 1999) and there is increased GSK-3β activity in the frontal cortex in AD as evidenced by immuno-blotting for GSK-3β phosphorylated at Tyr 216 (Leroy et al., 2007). Furthermore, GSK-3β expression is up-regulated in the hippocampus of AD patients (Blalock et al., 2004) and in post-synaptosomal supernatants derived from AD brain (Pei et al. 1997). Total GSK-3 expression is also up-regulated in circulating peripheral lymphocytes in both AD and in mild cognitive impairment (Hye et al., 2005). Moreover, it has been demonstrated that a polymorphism in the GSK-3β promoter is associated with increased risk factor for late onset AD (Mateo et al., 2006). Collectively, these findings suggest that GSK-3β activity might be increased in AD, through changes in its phosphorylation state as well as expression levels, although direct evidence for this is still limited at present and some studies find no change in GSK-3β activity (Pei et al., 1997) or reduced GSK-3β activity in AD (Swatton et al., 2004). As such, a mouse model overexpressing GSK-3β in the dentate gyrus was developed (Lucas

et al., 2001) in an attempt to reproduce some of the characteristics of AD patients. Indeed, like patients this mouse model exhibited significant memory impairment (Hernandez et al., 2002).

GSK-3β is one of the main kinases involved in the tau phosphorylation, a process that is crucial to the function of the protein. The normal phosphorylation of tau determines its affinity for microtubule binding (Grundke-Iqbal et al., 1986; Seubert et al., 1995; Harada et al., 1994; Bramblett et al., 1993). On the other hand, pathological hyperphosphorylation of tau affect the axonal transport (Ittner et al., 2011; Moreno et al., 2011). Moreover, presence of hyperphosphorylated tau in dendritic spines impairs synaptic activity (Hoover et al., 2010), and tau phosphorylation by GSK-3β in the hippocampus results in a toxic gain of function (Avila et al., 2010). Also, hyperphosphorylation of tau results in its dissociation from microtubules and subsequent aggregation to form NFTs (Lee et al., 2001; Chun and Johnson, 2007; Engel et al., 2006). Several lines of evidence support a direct functional link between tau phosphorylation and GSK-3. Both isoforms of GSK, GSK-3α and GSK-3β have been reported to phosphorylate tau in various *in vitro* and cell culture models (Hanger et al., 1992; Sperbera et al., 1995; Li and Paudel, 2006). Interestingly tau phosphorylation has been found to be increased in AD postmortem brain, at several sites modified by GSK-3β.

Along with hyperphosphorylation of tau, GSK-3β has also been reported to interfere with the biology of Aβ (Blennow et al., 2006). It has been demonstrated that genetic or pharmacological inhibition of GSK-3β results in reduced Aβ toxicity, amelioration of Aβ-induced behavioral deficits, and rescues neuronal loss in APP-overexpressing mouse models (Rockenstein et al., 2007; Sereno et al., 2009; Decker et al., 2010), thus strongly implicating the role of GSK-3β in Aβ associated toxicity. Decreased GSK-3β activity, with the use of Aβ antibodies has been reported in various invitro and invivo studies, supporting the interaction between Aβ and GSK-3β (Ma et al., 2006). It has also been shown that the activation of GSK-3 by Aβ in primary hippocampal cultures is specific to GSK-3β (Takashima et al., 1998), and that the inhibition of GSK-3β prevents Aβ-induced toxicity to neurons (Takashima et al., 1993; 1996; Hoshi et al., 2003; Aplin et al., 1997; Koh et al., 2008).

2.3.6.1.2. Role of GSK-3β in Parkinson's disease

Earlier, GSK-3β activity was well correlated with AD pathology. However, as soon as it was observed that tau hyperphosphorylation is also involved in PD pathology (Lei et al., 2010; Simon-Sanchez et al., 2009; Edwards et al., 2010), the focus of scientific community shifts to

explore the role of GSK-3β in PD brain, as it is the major kinase involved in tau phosphorylation. As discussed earlier, PD is characterized by misfolded α-synuclein aggregates that accumulate in neuronal inclusion bodies, known as Lewy bodies (LBs). Postmortem studies from PD patients have revealed that GSK-3β, is specifically localised within the halo of Lewy bodies (Nagao and Hayashi, 2009). Moreover, elevated GSK-3β activity was also observed in the striatum of PD patients as compared to controls (Wills et al., 2010). Similar results were observed in mouse models of PD (Duka et al., 2009). Moreover, increased GSK-3β levels have also been reported in peripheral blood lymphocytes in PD patients (Armentero et al., 2011).

Studies have revealed that GSK-3β inhibitors reduces the dopaminergic neuronal death induced by MPTP, indicating the association of GSK-3β with PD pathogenesis (Wang et al., 2007; King et al., 2001). MPTP is a highly lipophilic agent that following systemic injection rapidly crosses the blood–brain barrier. Once inside the brain, MPTP is converted by MAO-B (Monoamine oxidase) into a neurotoxin precursor, MPP+ (1-methyl-4-phenylpyridinium), which causes selective destruction of dopaminergic neurons in the SNpc (Sharma and Deshmukh, 2015). Moreover, it was also observed in the same model that mitochondrial GSK-3β significantly promotes ROS production by inhibiting complex I, which was reversed by GSK-3β inhibitors (King et al., 2008). The potential of GSK-3β inhibitors has also been observed in various cell culture models of PD (Kozikowski et al., 2006; Petit-Paitel et al., 2009; Hongo et al., 2012).

Mechanistically there is evidence to support an interaction between *α*-synuclein and GSK-3β. α-synuclein is a substrate for GSK-3β phosphorylation and may also modulate the activation of GSK-3β (Khandelwal et al., 2010). GSK-3β phosphorylation at Tyr216 (which activates GSK-3β activity) is also abolished in cells lacking *α*-syn and in *α*-syn knockout mice (Duka et al., 2009). GSK-3β inhibition decreases α-syn protein expression and prevents cell death in a cellular model of PD, indicating that inhibition of GSK-3β activity may be neuroprotective to dopaminergic neurons by attenuating the toxicity of α-syn overexpression (Kozikowski et al., 2006). In a recent study by Credle and colleagues using transgenic mice, it was observed that GSK-3β directly phosphorylate α- synuclein at a single site, Ser129, in addition to its known ability to phosphorylate tau. Moreover, α-synuclein and tau together cooperated with one another to increase the magnitude or rate of phosphorylation of the other by GSK-3β (Credle et al., 2015). This study establish a novel upstream role for GSK-3β as

one of several kinases associated with posttranslational modifications of key proteins known to be causal in PD. Taken together, these data strongly implicate GSK-3β in the pathogenesis of PD.

2.3.6.2. Histone acetylation/deacetylation in insulin resistance and neurodegenerative diseases

Epigenetic modulation represents a newly identified mechanism to regulate gene expression or cellular phenotype without the alteration of genome DNA sequences. All of the different cells in the body of one individual have exactly the same genome, that is, exactly the same DNA nucleotide sequence, with only a few exceptions in the reproductive, immune and nervous systems. Thus, in the vast majority of instances, one's liver cells have exactly the same DNA as neurons. However, those two types of cells are clearly vastly different in terms of the gene products that they produce. Some level of mechanism must exist, Waddington reasoned, that is "above" the levels of genes encoded by the DNA sequence, which controls the DNA readout. For this reason, he defined the term *epigenetics* in the early 1940s as "the branch of biology which studies the causal interactions between genes and their products which bring the phenotype into being" (Waddington, 1968).

Within cell nucleus, the fundamental units of chromatin are named nucleosomes. Each nucleosome is formed by 147 DNA base pairs wrapped tightly around an octamer of histone proteins, which is assembled by two copies of each of the four core histones (H2A, H2B, H3 and H4). The linker histone H1 binds to the DNA between the nucleosomal core particles, and their function is to stabilize higher order chromatin structures. Moreover, each histone protein consists of a central globular domain and N-terminal tail that contains multiple sites for potential modifications (Wang et al., 2013). The common epigenetic modulation approaches include DNA methylation, chromatin remodeling, and the gene expression regulation via small noncoding RNAs. Conformational modifications in histone proteins wrapped by the DNA in the nucleosomes may either change or facilitate the availability of the transcriptional machinery to the promoter region of some genes, leading to either gene silencing or activation. One of the most frequently studied histone modifications includes histone acetylation. It is one of several epigenetic mechanisms that control gene expression and is highly dynamic process regulated by two classes of enzyme, histone acetyltransferases (HATs) and HDACs. HAT catalyzes the acetylation of lysine residues in histone tails leading to chromatin relaxation and transcriptional activation; whereas, HDACs

mediates deacetylation resulting in a more condensed chromatin state and transcriptional repression (Waterborg, 2002) (Fig. 2.6).

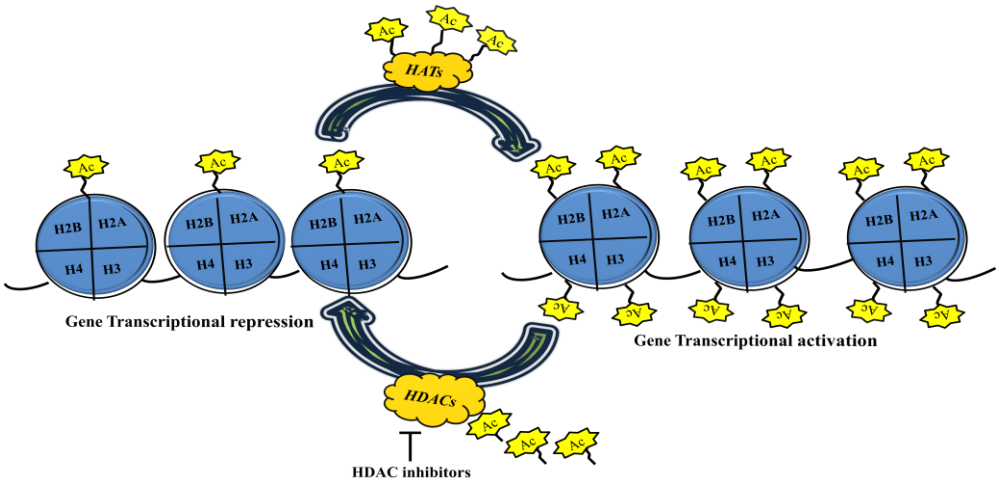

Fig. 2.6 Transcriptional regulation by histone acetyltransferases and HDACs

Briefly, the super family of HDACs consists of at least 18 members that are divided into two main families: 1) the classic HDAC family; and 2) the silent information regulator 2-related protein (sirtuin) family. The classic or zinc-dependent HDACs include class I (HDACs 1, 2, 3, and 8), class IIa (HDACs 4, 5, 7, and 9), class IIb (HDACs 6 and 10), and class IV (HDAC11) (Fig. 2.7). These HDACs are structurally very similar and share a common zinc-dependent catalytic domain. Class I HDACs are primarily nuclear and are expressed ubiquitously. Class II HDAC enzymes generally shuttle between the nucleus and the cytoplasm and are expressed in a cell and tissue-specific manner. Class III (HDAC11) is structurally different from class I and class II HDACs but has been shown to have some properties of both classes. The sirtuin family (class III; zinc-independent) contains seven members (SIRTs 1–7), which are structurally unrelated to classic HDACs. These enzymes have a unique mechanism of action requiring the cofactor NAD^+ for the enzyme activity (de Ruijter et al., 2003; Mottet and Castronovo, 2008).

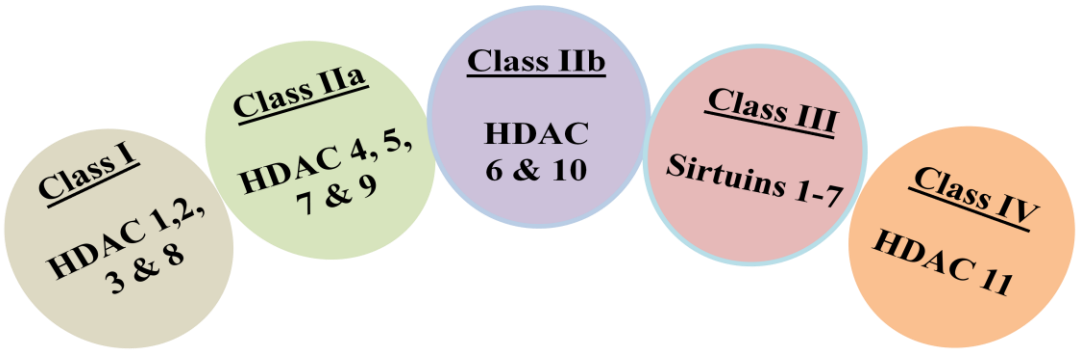

Fig. 2.7 Classification of histone deacetylases

2.3.6.2.1. Role of HDACs in Insulin Resistance

It has been demonstrated that HDACs play a regulatory role in insulin signalling. Recent reports indicate that HDAC2 has been reported to bind with IRS-1 in liver cells of the db/db mouse. These mice have been commonly and extensively used for the investigation of T2DM/diabetic dyslipidaemia and screening variety of agents such as insulin mimetic and insulin sensitizers (Bayley et al., 2016). This binding of HDAC2 with IRS-1 leads to decreased acetylation and reduced insulin receptor-mediated tyrosine phosphorylation of IRS-1. Accordingly, the HDAC inhibitor Trichostatin A (TSA) or gene silencing of HDAC2 enhance acetylation of IRS-1 and partially attenuate insulin resistance (Kaiser and James, 2004; Sun and Zhou, 2008). Similar to HDAC2, the role of HDAC3 isoform has also been explored in insulin resistance and T2DM (Zeng et al., 2014). Sun and colleagues demonstrates that C57BL/6 mice with a liver-specific deletion of HDAC3 have severe hepatosteatosis and increased insulin sensitivity without changes in insulin signalling or body weight (Sun et al., 2012). HDAC3 has also been reported to regulate PPARγ function in adipocytes (Fajas et al., 2002, Guan et al., 2005, Gao et al., 2006). Moreover, Inhibitors of HDAC3 have been suggested to play a role in improving insulin sensitivity and protecting β-cells from cytokine-induced apoptosis (Chou et al., 2012). These reports strongly suggest the potential of HDAC3 inhibition in regulating insulin signalling and improving insulin sensitivity.

Class II HDACs particularly, HDAC 4 and 5 repress transcriptional activity of myocyte enhancer factor-2 (MEF2) and regulate GLUT4 expression by the virtue of their deacetylase activity which makes the chromatin structure compact such that the transcriptional complex does not have access to DNA (McKinsey et al., 2000; Lu et al., 2000; Czubryt et al., 2003). Studies also report that over expression of HDAC5 decreases GLUT4 expression in cardiac tissue. Dissociation of HDAC5 from MEF2 occurs following phosphorylation of HDAC5 on serine 259 and 498 by AMPK. Thus, AMPK regulation of HDAC5 can control GLUT4 gene expression in human skeletal muscle (McGee et al., 2008; Weems and Olsan, 2011).

An important study by Mihaylova and colleagues demonstrated that Class IIa HDACs (HDAC4/5/7) are required for hyperglycemia in diabetic mouse models such as db/db mouse and ob/ob mouse (Mihaylova et al., 2011). Among the various genetic models to study T2DM and obesity related complications, the ob/ob and db/db mice are most widely used models (Betz and Bryan, 2016; Srinivasan and Ramarao, 2007). Mihaylova and co-workers

treated db/db and ob/ob mouse with either scrambled control or HDAC4/5/7 shRNAs and found reduction of class IIa HDAC expression in these diabetic mouse models along with a substantial decrease in fasting blood glucose levels. Moreover, these authors also examined that class IIa HDACs play an important role in regulating hepatic blood glucose in HFD-induced diabetic mouse. They found that the HFD mouse showed a significant reduction of fasting blood glucose levels and improved glucose tolerance when depleted for Class IIa HDACs (Mihaylova et al., 2011). Recently, increased expression of HDAC9 has also been reported in HFD fed mice. However, HDAC9 knockdown completely protected mice from the consequences of HFD feeding, such as hyperglycemia, elevated cholesterol levels, fatty liver disease along with improved glucose tolerance and insulin sensitivity (Chatterjee et al., 2014).

In another study Wang and co-workers demonstrate increased expression of Class II HDACs particularly HDAC5 and HDAC9 in C57BL/6J mouse brains when fed with HFD for 6 months. These mice also developed severe diabetes including increased baseline fasting glucose, and impaired insulin sensitivity and glucose tolerance as compared to the control mice (Wang et al., 2014). All these studies suggest the regulatory role of Class II HDACs in insulin signalling. The alteration in level of these HDACs results in reduced insulin sensitivity and metabolic dysfunction. The results obtained from these preclinical studies are highly encouraging and thus pave the entry HDAC inhibitors into clinical trials for this indication. A Phase IV single blind clinical trial conducted by the University Health Network, Toronto (clinical trial Identifier-NCT00533559) investigated the effect of buphenyl (phenylbutyrate) on fatty acid-induced impairment of glucose-stimulated insulin secretion in healthy males. This small study involving eight patients completed in March 2010 and found that HDAC inhibitor, phenylbutyrate, when administered orally at dose of 7.5gm/day for two weeks provides benefits in humans by ameliorating both insulin resistance and β-cell dysfunction induced by free fatty acids (Xiao et al., 2011). Another clinical trial started in 2008 (clinical trial Identifier-NCT00771901) evaluated the effect of sodium phenylbutyrate in obese (both male and female) subjects in a 4-week randomized controlled study. The clinical study evaluated the effect phenylbutyrate on various parameters related to insulin sensitivity, fatty acid oxidation, ER stress, and inflammation. This study was reported to be completed in 2014, but the results have not yet been disclosed. Thus, there is a rationale to conduct more clinical trials to shed light on the effects of other HDAC inhibitors on insulin secretion and insulin resistance in humans. As these trials proceed, a better understanding of

the potential side effects and dose-limiting toxicities of these drugs will emerge for patients with these conditions.

2.3.6.2.2. Role of HDACs in Neurodegenerative Diseases

In recent years, the epigenetic changes have been well recognized and documented in brain development, plastic changes, as well as different brain diseases. In normal neuronal cells, a tightly regulated balance exists between HAT/HDAC activities to enable finely tuned control of transcription for proper gene expression regulation and maintenance of homeostasis. There is a notion that neuronal cell death occurs and pathologies develop after derangement of HAT/HDAC as histone hypoacetylation and gene repression have been extensively implicated in experimental models of numerous neurodegenerative diseases, including Huntington's disease, Friedreich's ataxia, and spinal muscular atrophy (Herman et al., 2006; Kernochan et al., 2005; Rouaux et al., 2003; Sadri-Vakili et al., 2007). Description of the different classes of HDAC enzymes and their differential localization in brain regions has been provided in Table.2.1.

Table. 2.1 Differential localization of HDAC family members in brain regions

CLASS	Members	Subcellular localization	Localization in brain	References
1	HDAC1	Nucleus	Cortex , Caudate/putamen, Hippocampus, Amygdala, SNpc, SNpr, Locus coeruleus, Corpus callosum, Gray matter, White matter	Didonna and Opal, 2015; Wang et al., 2015; Broide et al., 2007; Lucio-Eterovic et al., 2008 Baltan et al., 2011; Janssen et al., 2010
	HDAC 2	Nucleus	Cortex, Caudate/putamen, Hippocampus, Amygdala, SNpc, SNpr, Locus coeruleus Corpus callosum, Gray matter, White matter	Didonna and Opal, 2015; Wang et al., 2015; Broide et al., 2007; Lucio-Eterovic et al., 2008 Baltan et al., 2011; Janssen et al., 2010
	HDAC 3	Nucleus/Cytosol	Cortex, Caudate/putamen, Hippocampus, Amygdala, SNpc, SNpr, Locus coeruleus Globus palidus,	Didonna and Opal, 2015; Wang et al., 2015; Broide et al., 2007; Lucio-Eterovic et al., 2008 Baltan et al., 2011
	HDAC 8	Nucleus/Cytosol	Hippocampus, Amygdala, Locus coeruleus SNpc	Didonna and Opal, 2015; Wang et al., 2015 Lucio-Eterovic et al., 2008; Hu et al., 2000
IIa	HDAC 4	Nucleus/Cytosol	Cortex, Caudate/putamen, Hippocampus, Amygdala, SNpc, SNpr, Locus coeruleus, Globus palidus	Didonna and Opal, 2015; Wang et al., 2015 Broide et al., 2007; Lucio-Eterovic et al., 2008; Janssen et al., 2010; Grozinger et al., 1999; Bolger and Yao, 2005
	HDAC 5	Nucleus/Cytosol	Cortex, Caudate/putamen, Hippocampus, Amygdala, SNpc, SNpr, Locus coeruleus, Globus palidus	Didonna and Opal, 2015; Wang et al., 2015; Broide et al., 2007; Lucio-Eterovic et al., 2008; Tsankova et al., 2006

	HDAC 7	Nucleus/Cytosol	Cortex, Caudate/putamen, Hippocampus, Amygdala, SNpc, Locus coeruleus, Striatum, Cerebellum	Didonna and Opal, 2015; Wang et al., 2015; Broide et al., 2007; Lucio-Eterovic et al., 2008; Benn et al., 2009
	HDAC 9	Nucleus/Cytosol	Cortex, SNpc, Hippocampus, Amygdala	Didonna and Opal, 2015; Wang et al., 2015; Zhou et al., 2011; Lang et al., 2011
IIb	HDAC 6	Cytosol	Cortex, Caudate/putamen, Hippocampus, ` Amygdala, SNpc, Locus coeruleus, Cerebellum	Didonna and Opal, 2015; Wang et al., 2015; Broide et al., 2007; Lucio-Eterovic et al., 2008; Southwood et al., 2007
	HDAC 10	Nucleus/Cytosol	Cortex, Amygdala, Hippocampus	Kao et al., 2002
III	SIRT 1	Nucleus	Cortex, Hypothalamus, Striatum Hippocampus	Didonna and Opal, 2015; Wang et al., 2015; Sidorova-Darmos et al., 2014
	SIRT2	Cytosol	Cortex, Oligodendrocytes, Hippocampus, olfactory neurons, Cerebellum	Didonna and Opal, 2015; Wang et al., 2015; Sidorova-Darmos et al., 2014
	SIRT3	Mitochondria	Cortex, Hippocampus, Striatum, Spinal cord, Brain stem, Cerebellum	Didonna and Opal, 2015; Wang et al., 2015; Sidorova-Darmos et al., 2014
	SIRT4	Mitochondria	Least expressed member of sirtuin family in brain	Didonna and Opal, 2015; Wang et al., 2015; Sidorova-Darmos et al., 2014
	SIRT5	Mitochondria	Cortex, Hippocampus, Cerebellum Brain stem, Spinal cord, Olfactory bulb	Didonna and Opal, 2015; Wang et al., 2015; Sidorova-Darmos et al., 2014
	SIRT6	Nucleus	Cortex, Hippocampus, Cerebellum, Olfactory bulb	Didonna and Opal, 2015; Wang et al., 2015; Sidorova-Darmos et al., 2014

	SIRT7	Nucleus	Cortex, Hippocampus, Cerebellum	Wang et al., 2015; Sidorova-Darmos et al., 2014
IV	HDAC11	Nucleus	Cortex, Hippocampus, Diencephalon Brain stem, Cerebellum	Didonna and Opal, 2015; Wang et al., 2015; Gao et al., 2002

2.3.6.2.3. Role of HDACs in Alzheimer's Disease

The first reports regarding the relation of histone acetylation and memory formation were found long ago in 1979, when it was found that memory training alters the incorporation of 14C-acetate to histones in different brain regions (Schmitt and Matthies, 1979). Later, studies further highlight the importance of histone acetylation in memory formation and demonstrated by the fact that mice which lack HAT activity show impaired memory function (Alarcon et al., 2004; Wood et al., 2006; Oliveira et al., 2007). It has been demonstrated that histone acetylation/deacetylation is highly regulated and is responsible for long-term potentiation and learning and memory, under normal neuronal conditions. HDACs have been reported to play key roles in synaptic plasticity and learning and memory (Crepaldi and Riccio, 2009; Morrison et al., 2007; Guan et al., 2009). During in vitro studies, it has been observed that HDAC inhibition stimulates the differentiation of embryonic stem cells (Yao et al., 2010) and hippocampal neural progenitor cells (Yu et al., 2009).

Various studies have shown the involvement of specific HDAC isoforms in memory formation and neuronal regeneration. The mice lacking neuronal HDAC1 do not show altered learning ability in the fear conditioning and water maze paradigms (Guan et al., 2009). In contrast, reducing HDAC2 functions was found to facilitate fear extinction learning in mice (Morris et al., 2013). HDAC2 has been shown to negatively regulate memory formation by inhibiting the expression of synaptic plasticity genes (Guan et al., 2009; Graff et al., 2012; Morris et al., 2013). Recently, HDAC2 has also been shown to suppress excitatory and enhance inhibitory synapses in the hippocampus (Hanson et al., 2013).

Mice lacking neuronal HDAC3 show better learning than the corresponding wild type littermates (McQuown et al., 2011). Also, it has been demonstrated that HDAC3 is neurotoxic and that it could possibly mediate the death promoting effects of Glycogen synthase kinase 3 β (GSK-3β) (Bardai and D'Mello, 2011; Bardai et al., 2012). In another study, it was observed that attenuation of long-term potentiation by amyloid-β oligomer could be reversed by specific HDAC3 inhibitor, RGFP966 in rat CA1 pyramidal neurons. These reports further support the hypothesis to target HDACs for ameliorating AD related plasticity impairments (Kumar et al., 2016). The role of HDAC4 in memory formation has also been well explored. It has been demonstrated that deletion of HDAC4 results in improved memory function in *C. elegans* (Wang et al., 2011). In contrast, mice lacking HDAC4 show impaired memory function and synaptic plasticity (Kim et al., 2012; Sando et al., 2012). Moreover, reduced HDAC4 levels have been linked to mental retardation in humans (Williams et al.,

2010). Deletion of HDAC5 does not result in memory impairments in 2-month old mice however, mild memory disturbances were reported in 10-month old HDAC5 knock-out mice (Kim et al., 2012; Agis-Balboa et al., 2013). Conflicting reports regarding the role of HDAC6 have been observed where one study explains that inhibition and deletion of HDAC6 has been shown to promote neurite outgrowth (Rivieccio et al., 2009). In contrast no significant difference in the fear conditioning or water maze paradigm was observed in mice lacking HDAC6 as compared to control (Govindarajan et al., 2013). Thus, it can be proposed that histone acetylation/deacetylation might play an important role in memory formation and synaptic plasticity. Thus, there is considerable evidence that epigenetic regulation is a dynamic and critical mechanism modulating neuronal function.

2.3.6.2.4. Role of HDACs in Parkinson's disease

Despite the lack of insights into the histone modifications in Parkinson's disease (PD) brains, in vitro overexpression studies as well as in vivo α-syn transgenic Drosophila model and mice exposed to herbicide paraquat have revealed that α-syn mediates neurotoxicity in the nucleus by interacting with histones and inhibiting histone acetylation (Goers et al., 2003 ; Kontopoulos et al., 2006). These findings thus garner interest for the exploration of HDAC inhibitors to restore imbalance between HAT/HDACs as potential therapies for PD. Several HDAC inhibitors including suberoylanilide hydroxamic acid (SAHA), trichostatin A (TSA), valproic acid (VPA), and sodium butyrate are shown to be efficacious in cell culture and animal models induced by mitochondrial toxins, including MPP^+, MPTP, rotenone and paraquat (Chen et al., 2012; Kidd and Schneider, 2010; 2011; Monti et al., 2010).

Recently, sodium butyrate, treatment has been reported to reduce the degeneration of dopaminergic neurons in a mutant α-syn drosophila transgenic model of PD. Chronic rotenone exposure results in reduced locomotion and early mortality in drosophila. However, treatment with sodium butyrate-supplemented food rescued the rotenone-induced locomotor impairment and early mortality in flies (St Laurent et al., 2013). Moreover, increased dopamine levels in brains of sodium butyrate treated flies were observed as compared to alone rotenone treated flies. Interestingly it was observed HDAC knockdown mice were resistant to rotenone-induced locomotor impairment and early mortality. Another HDAC inhibitor, Phenylbutyrate has been demonstrated to attenuate motor deficits and reduced α-syn accumulation induced by repeated rotenone administration in C57BL/6 mice (Inden et al., 2007). Similar neuroprotective and dopamine enhancing effects of HDAC inhibitors has

been reported in other neurotoxin models of PD. For example, 6-hyroxydopamine (6-OHDA) administration into the striatum has been widely used as a model to induce PD in rats. The HDAC inhibitor, valproate has been reported to attenuate 6-OHDA induced toxicity in rats and results in sparing of Tyrosine hydroxylase (TH+)-immunoreactivity and elevation of TH^{+} content in SNpc as well as striatum (Monti et al., 2012). Thus, these reports suggest that HDAC inhibition could be of therapeutic importance in restoring behavioral and biochemical abnormalities associated with PD. The details of various preclinical studies using HDAC inhibitors in *in-vitro* and *in-vivo* models of AD and PD, have been listed in Table.2.2.

Table. 2.2. Therapeutic potential of HDAC inhibitors in invivo and invitro models of AD and PD

S.No	Animal model	HDAC inhibitor	Outcome	Reference
1	rTg4510 mouse model	Tubastatin	Reduced total tau levels, increased acetylation of heat shock protein 90.	Selenica et al., 2014
2	Rat CA1 pyramidal neurons	RGFP966	Prevention of Aβ oligomer induced synaptic plasticity.	kumar et al., 2016
3	C57BL/6 Mice	SAHA	Restored spatial memory, increased anti inflammatory action, reinstated epigenetic balance and transcriptional homeostasis.	Benito et al., 2015
4	Tg2576 Mice model	SAHA	Alleviated cognitive deficits in AD, amyloid and tau pathology and increased dendritic spine density on hippocampal neurons.	Cuadlado-Tejedor et al., 2015
5	Fischer 344 Brown Norway F1 hybrid rats	SAHA	Increased number of genes related to neuronal plasticity.	Angila et al., 2015
6	Mice	Sodium butyrate	Significantl ameliorated SIRT-2 induced reduction in cell proliferation and neuroblast differentiation.	Yoo et al., 2015
7	Male Wistar rats	Sodium butyrate	Increased acetylation, memory enhancement in aged rats.	Blank et al., 2015
8	CD-1 BR Strain mice	Trichostatin A	Reduced Lipopolysaccaride (LPS)- induced neuro-inflammation, attenuation of LPS-induced cognitive dysfunction.	Hsing et al., 2015
9	Male spargue Dawley rats	Sodium butyrate	Alleviated hippocampal dependent spatial learning disability in rats, and altered HDAC1/2 mRNA level, histone H4 acetylation in rat hippocampus.	Liu et al., 2015

10	Male C57BL/6 mice	Trichostatin A	Rescued impaired contextual fear memory by promoting histone acetylation and histone acetylation-mediated gene expression.	Zhong et al., 2015
11	Sleep deprivation induced cognitive impairment in rats	Trichostatin A	Increased histone acetylation, increased BDNF levels.	Daun et al., 2016
12	MPTP induced PD model	Phenyl butyrate	Dopaminergic neuronal protection and improved motor functions	Roy et al., 2012
13	MPTP induced PD model	Sodium butyrate, Valproate	Prevented MPP+ mediated cell death, increase in histone acetylation.	Kidd and Schneider, 2010
14	6-OHDA induced PD model	Sodium valproate	Reduced dopaminergic neurons degenation in substantia nigra and dopaminergic terminals in striatum.	Monti et al., 2012
15	6OHDA induced PD model	Sodium butyrate	Prevents 6-OHDA induced motor deficits.	Rane et al., 2012
16	Rotenone induced PD model	Valproate	Prevents alterations in α-syn and attenuates loss of TH+ in SNpc and striatum.	Monti et al., 2010
17	Rotenone induced PD in flies	Sodium butyrate	Elevated dopamine levels, reduced HDAC activity.	St. Laurent et al., 2013
18	Lipopolysaccharide induced neurotoxicity in human fetal brain cell culture	Trichostatin A; Valproate	Reduce expression of cytokines and chemokines in primary human fetal microglial cultures activated by LPS.	Suh et al., 2010
19	Lipopolysaccharide induced neurotoxicity in primary neuron-glia cultures	Valproate	Reduce proinflamatory factors (TNFα, NO, ROS), protection of dopaminergic neurons from LPS toxicity.	Peng et al., 2005

2.4. GSK-3β inhibitors: Classification and selectivity

Much effort has been done in the discovery and development of GSK-3β inhibitors during the last decade. Nowadays, several chemical families have emerged as GSK-3β inhibitors, including great chemical diversity. Some of these GSK-3β inhibitors have synthetic origin but others have been derived directly or indirectly from small molecules of natural origin (Table.2.3). The number of small molecule GSK-3β inhibitors is continuously increasing with most in the early discovery phase. Here, the GSK-3β inhibitors that have been tested in biological systems are mentioned briefly.

2.4.1. Cations as GSK-3β inhibitors

The cation lithium was the first "natural" GSK-3β inhibitor discovered (Klein and Melton, 1996). Lithium is a mood stabilizer long used in treatment of bipolar disorders. Lithium inhibits GSK-3β directly by competition with magnesium ions (Klein and Melton, 1996) and indirectly via enhanced serine phosphorylation and autoregulation (Zhang et al., 2003; Kirshennboim et al., 2004). Other metal ions such as beryllium, zinc, mercury, and copper are potent GSK-3 inhibitors (Ilouz et al., 2002; Ryves et al., 2002).

2.4.2. ATP-competitive GSK-3β inhibitors from natural resources

The dual activity of these inhibitors toward GSK-3β and cyclin-dependent protein kinases (CDKs) is a direct result of their structural similarity within the ATP-binding domain (about 86% sequence similarity). The bis-indole indirubin isolated from the traditional Chinese medicine for treatment of myelocyte leukemia was initially characterized as a CDK inhibitor and then found to be a potent GSK-3β inhibitor (Leclerc et al., 2001). It inhibits both protein kinases within the nanomolar concentration range. The indirubin analog 6-bromoindirubin, isolated from a marine invertebrate, the mollusk known as "Tyrian purple," showed a certain selectivity toward GSK-3β over CDKs (Meijer et al., 2003). Accordingly, a synthetic cell-permeable derivative, 6-bromoindirubin-3′-oxime (6BIO), was developed and was about 16-fold more selective for GSK-3β relative to CDKs (Meijer et al., 2003; Polychronopoulos et al., 2004).

2.4.3. ATP-competitive GSK-3β inhibitors from Organic Synthesis

Among the first synthetic small molecule GSK-3β inhibitors reported were the purine analogs, the aminopyrimidines, developed by Chiron. The potent inhibitors CHIR98014

(CT98014), CHIR98023 (CT98023), CHIR99021 (CT99021) inhibit GSK-3β within the nanomolar concentration range (Ring et al., 2003). Systemic analysis that profiled protein kinase inhibitors also confirmed the high selectivity of CHIRs toward GSK-3β (Bain et al., 2003, 2007). These compounds had been chiefly tested in diabetic models.

The arylindolemaleimides SB-216763 and SB-415286 are highly selective inhibitors developed by GlaxoSmithKline that inhibit GSK-3β within the low nanomolar concentration range (Coghlan et al., 2000). Various studies have demonstrated the neuroprotective effects of SBs against variety of pro-apoptotic conditions including inhibition of the PI3 kinase/Akt survival pathway, trophic deprivation, Aβ toxicity (Hongisto et al., 2008; Hu et al., 2009).

The amino thiazole AR-A014418 developed by AstraZeneca was shown to be a selective inhibitor toward GSK-3β when compared to other protein kinases including CDKs (Bhat et al., 2003). In their initial study, (Bhat et al., 2003) showed that AR-A014418 was neuroprotective in apoptotic conditions induced by inhibition of PI3 kinase and prevented neurodegeneration in hippocampal slices exposed to Aβ peptide.

2.4.4. Non-ATP-competitive GSK-3β inhibitors from Organic Synthesis

There are different chemical families of organic compounds reported in the literature that do not compete with ATP in their GSK-3β inhibitory activity. The first reported family was the small heterocyclic thiadiazolidinones (TDZDs) (Martinez et al., 2002). TDZDs did not show inhibition over various other kinases including PKA, PKC, CK-2, and CDK1/cyclin B. The second family of compounds known as the halomethylketone (HMK) derivatives (Conde et al., 2003) which have been recently described as the first irreversible inhibitors of GSK3β (Perez et al., 2009).

2.4.5. Non-ATP-competitive GSK-3 inhibitors from natural resources

Manzamines are complex β-carboline alkaloids isolated from Indo-Pacific sponges and characterized as having an intricate and novel polycyclic system (Hu et al., 2003). Manzamine A inhibits both GSK-3β and CDK5 and is ineffective towards other kinases (Hamann et al., 2007).

Table 2.3 Classification and Source of GSK-3β inhibitors

Category	GSK-3β inhibitor	Source
Cations	Lithium	Inorganic atom
	Zinc	
	Tungstate	
ATP-competitive GSK-3 inhibitors	Indirubins	Isolated from marine organisms
	6 bromo indirubin	
	Dibromocantherelline	
	Meridianine A	
	Aminopyrimidines CHIR98014; CHIR99021; CHIR98023	Small molecules from organic synthesis programs
	Arylindolemaleimide SB216763; SB415286	
	Thiazoles AR-A014418	
ATP non-competitive GSK-3 inhibitors	**Furanosesquiterpenes** Tricantin; Palinurin	Natural compounds isolated from marine organisms
	Manzamines Manzamine A	
	Thiadiazolidindiones NP00111; TDZD-8	Small molecules from organic synthesis programs
	Halomethylketones HMK-32	

2.5. HDAC inhibitors: classification and selectivity

HDAC inhibitors are a group of compounds that block the activities of HDACs typically by binding to the zinc-containing catalytic domain of HDACs. According to their chemical structure, HDAC inhibitors are classified into four classes, which include hydroxamic acids, short chain fatty acids, benzamides and cyclic peptides.

2.5.1. Hydroxamic acids

The hydroxamate moiety is thought to bind to the zinc ion in the catalytic domain of HDACs and thus inactivating the enzyme (Marks et al., 2004; Villar-Garea et al., 2004). For this reason these compounds are known to inhibit classes of HDACs which share the same zinc dependent catalytic site: classes I and II HDACs only (Fig.2.8). In general drugs within this class of HDACIs are known to have relatively short half-lives, however possess long last effects (Plumb et al., 2003). TSA was the first one of the hydroxamic acids to be characterized as a potent HDAC inhibitor (Yoshida et al., 1990) which was used as the core chemical structure for the design and synthesis of some new compounds of this class. Among them SAHA was the first HDAC inhibitor approved by the U.S. Food and Drug Administration (USFDA) for the treatment of human cutaneous T-cell lymphoma (CTCL) in 2006 (Marks and Breslow, 2007). Both of these HDAC inhibitors crosses the BBB (Chuang et al., 2009), hence highlighting them as targets for neurological conditions such as AD, PD and HD.

2.5.2. Short chain fatty acids (SCFAs)

The three most important drugs within this class are sodium butyrate, sodium-4-phenylbutyrate and valproate. Most of the drugs belonging to this class share HDAC isoform inhibition profiles and inhibit the action of classes I and IIa with most efficacy (Fig. 2.8) (Grayson et al., 2010). Compared with hydroxamic acids, the SCFAs have less potent inhibitory effects, but they can easily cross the BBB due to their smaller molecular weight (Xu et al., 2007). The reason behind their weak potency could be their inability to access the zinc cation in the HDAC active-site pocket, which appears to be pivotal to the deacetylation catalysis (Lu et al., 2003). Due to their high permeability through BBB, these compounds are of particular interest in neuroscience research.

2.5.3. Benzamides

Among the various classes of HDAC inhibitors, benzamides represents a relatively selective class of HDAC inhibitors with a relatively longer half-life. Two most important drugs within this class are currently in clinical trial for cancer: MS-275 and CI-994 (Grayson et al., 2010). Both MS-275 and CI-994 showed higher selectively towards HDAC 1 as compared to other Class I HDACs. Also, Thomas et al. (Thomas et al., 2008) designed and synthesized a series of benzamide type HDAC inhibitors. These compounds are structurally related to the well-known HDAC inhibitor SAHA, but are not hydroxamic acids. Among these, HDACi 4b

(selective for HDAC1 and 3) is currently under preclinical investigations for indications such as HD (Thomas et al., 2008).

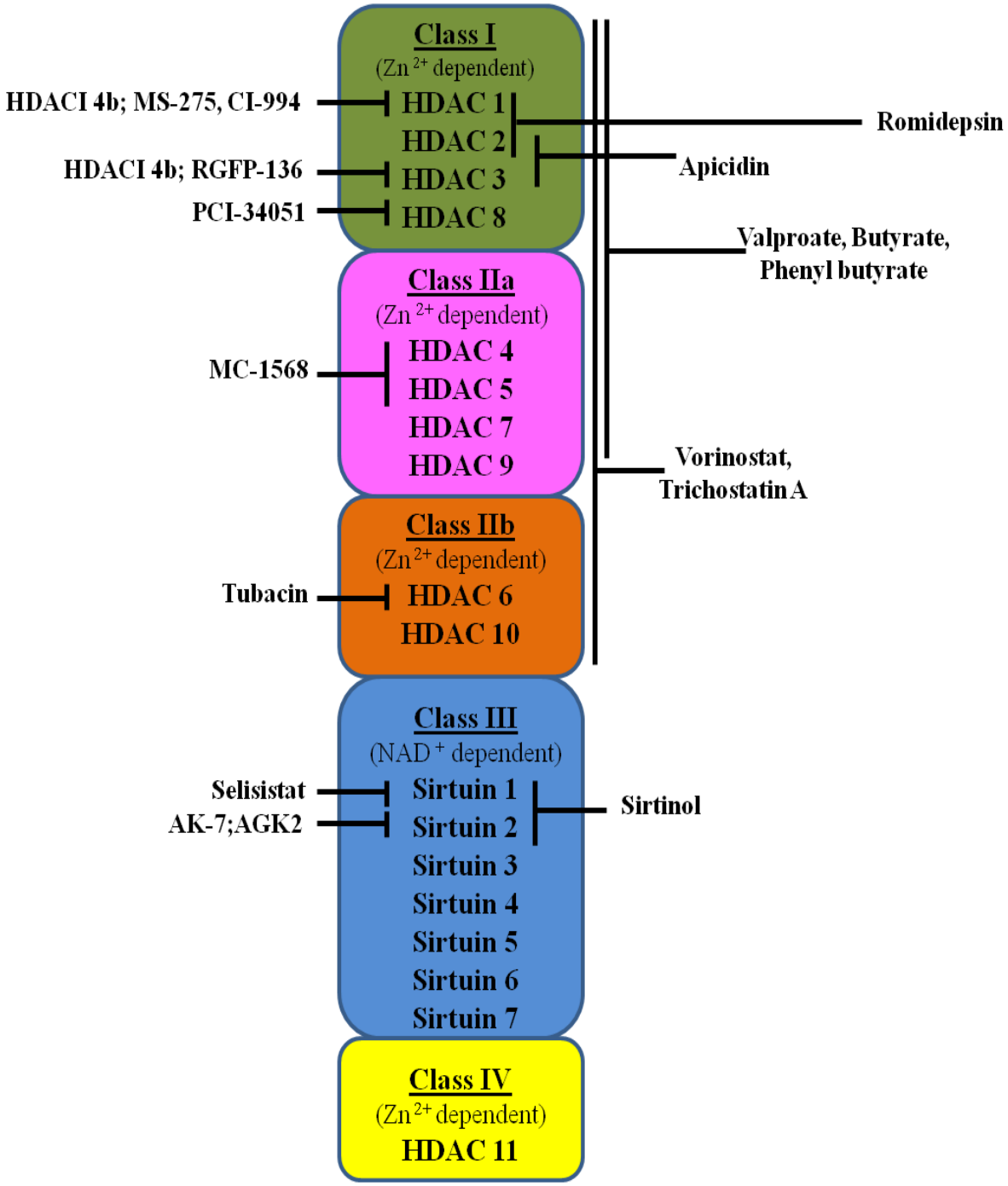

Fig. 2.8 Target selectivity of isoform specific and isoform non-specific HDAC inhibitors

2.5.4. Cyclic peptides

Cyclic peptides are a group of Zn^{2+}-dependent HDAC inhibitors (Furumai et al., 2002). However due to variation in chemical structure among peptides, these HDAC inhibitors are not selective for particular HDAC isoform. The most important members of this class are romidepsin and apicidin. Apicidin has been found to selectivity inhibit HDAC2 and HDAC3 whereas, romidepsin shows potent efficacy for HDAC1 and HDAC2 (Khan et al., 2008). Romidepsin was approved by the USFDA for treatment of cancer in 2009 due to its potency to arrest cell growth (Campas-Moya et al., 2009).

2.5.5. Sirtuin inhibitors

It is important to note that the above described HDAC inhibitors do not affect class III HDACs, the Sirtuins, due to the structural and functional dissimilarity between this class of HDACs and classes I, II and IV. Class III HDACs are Nicotinamide adenine dinucleotide (NAD+)-dependent and therefore they require the binding of an NAD+ molecule in their active site to enable deacetylation (Spange et al., 2009). Therefore, a compound which inhibits the binding of NAD+ to its active site, prevents deacetylation of substrates and thus act as Class III inhibitor. Nicotinamide is one such example, which acts as a competitive inhibitor of all 7 Sirtuin HDACs.

2.6. Experimental model of insulin resistance

There are various types of animal models of insulin resistance, derived either spontaneously or induced by diet, stress, chemicals and their combinations.

2.6.1. High fat diet (HFD) induced insulin resistance

The first description of a HFD to induce obesity by a nutritional intervention was in 1959 (Masek & Fabry, 1959). Subsequent studies have revealed that HFD promote hyperglycemia and whole-body insulin resistance, and numerous researchers have examined their effects on muscle and liver physiology as well as insulin signal transduction. It is generally accepted that HFDs can be used to generate a valid rodent model for the metabolic syndrome with insulin resistance and compromised β-cell function (Oakes et al., 1997; Lingohr et al., 2002). HFD susceptibility, that is, the extent of the metabolic disorder induced by the respective diet, depends more on the specific rodent strain and the dietary regimen employed. For example, C57BL/6J mice develop obesity and insulin resistance similar to Wistar rats, while 129S6 mice (Almind and Kahn, 2004) or A/J mice do not (Surwit et al., 1988). Despite much work, the mechanisms by which HFD induces insulin resistance are still not completely

understood. According to recent literature, it has been proposed that HFD contributes to free fatty acid (FFA) elevation which induces insulin resistance in skeletal muscle. This hypothesis is based on the finding that an increase in plasma FFA results in several metabolites of the FFA re-esterification pathway including long chain Acyl-CoAs and diacylglycerol (DAG) (Itani et al., 2002) (Fig. 2.9). DAG is a potent activator of conventional and novel protein kinase C (PKC) isoforms (Farese, 2000). In human skeletal muscle, elevation of plasma FFA levels has been shown to increase DAG and to activate PKC β2 and δ. PKC, a serine/threonine kinase, has been shown in rodents to cause insulin resistance by decreasing tyrosine phosphorylation of IRS-1/2.

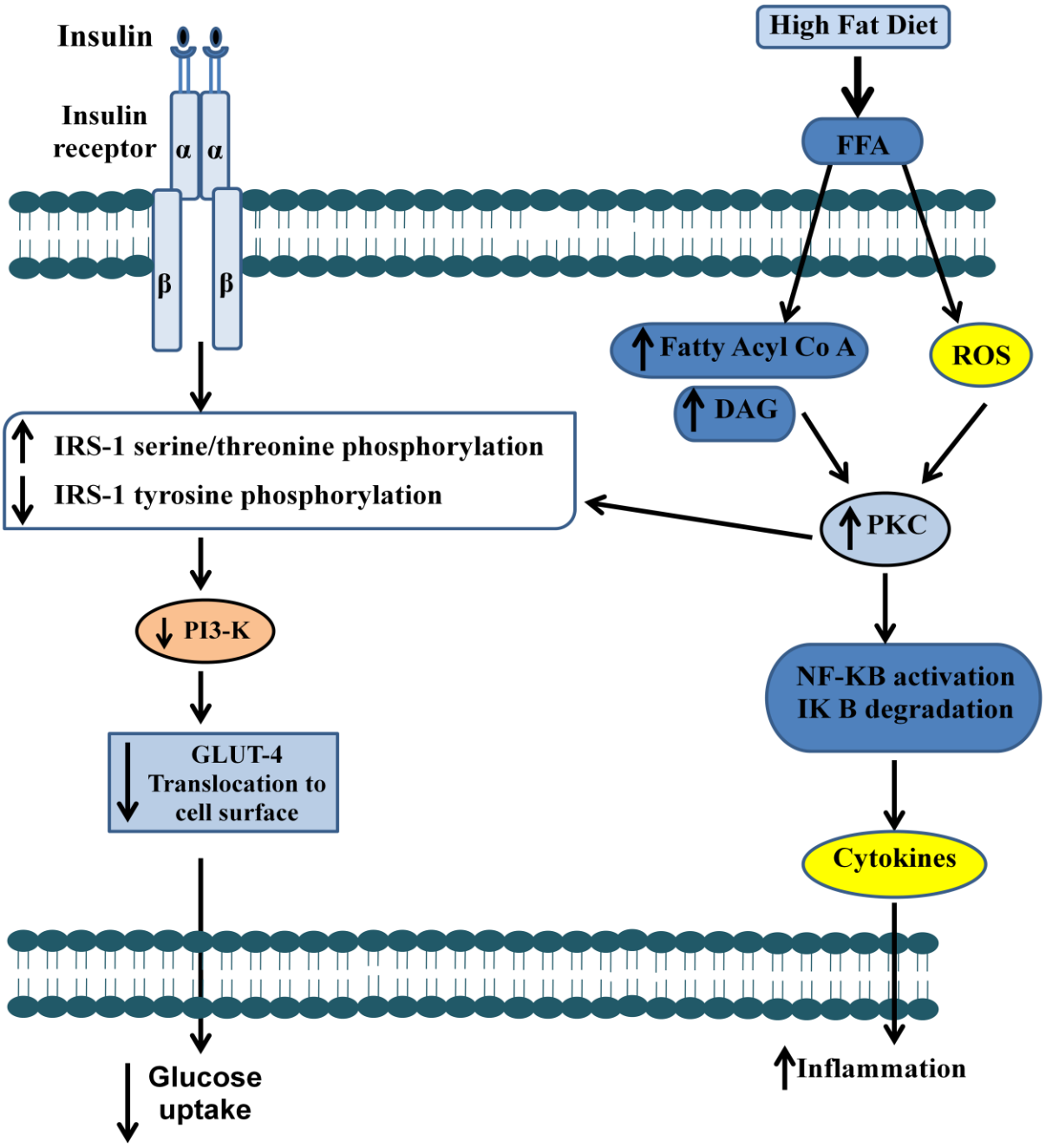

Fig. 2.9 Potential mechanism of FFA on insulin resistance by HFD feeding The key initiating event is an increase in plasma FFA followed by increased uptake of FFA into muscle. This leads to intramyocellular accumulation of fatty acyl-CoA and DAG and activation of PKC (the β II and δ isoforms). It is assumed that activation of PKC interrupts insulin signaling by serine phosphorylation of IRS-1, resulting in a decrease in tyrosine phosphorylation of IRS-1. At the same time, activation of PKC also leads to production of inflammatory and proatherogenic proteins through activation of the IκB-α/NF-κB pathway.

In addition to PKC, several other serine/threonine kinases including IKK-β and c-Jun NH_2-terminal kinase (JNK) can also be activated by acutely raising plasma FFA levels (Boden et al., 2005; Hotamisligil et al., 2005). Exactly, how these kinases are activated by

FFA is not clear but may include FFA mediated generation of ROS (Inoguchi et al., 2000), activation of the Toll like receptor 4 (TLR4) pathway (Shi et al., 2006) or endoplasmic reticulum stress (Hotamisligil, 2005). Once activated, one or several of these serine/threonine kinases can interrupt insulin signaling by decreasing tyrosine phosphorylation of IRS-1/2 (Yu et al., 2002). This inhibits the activity of the IRS/PI3 kinase/Akt pathway which controls most of insulin's metabolic actions including glucose uptake, glycogen synthesis, glycogenolysis and lipolysis (Saltiel and Kahn, 2001).

2.6.1.1. Mechanisms of HFD induced oxidative stress and inflammation

HFD feeding increases the amount of chylomicrons in the intestine. These chylomicrons then enter into the circulation and lead to generation of FFA, which are taken up by the liver (Pessayre et al., 2001). The mitochondrial β-oxidation of FFAs is associated with the conversion of oxidized cofactors (NAD+ and FAD) into reduced cofactors NADH and FADH2 and reoxidized back into NAD+ and FAD by a mitochondrial respiratory chain. During their reoxidation process, NADH and FADH2 transfer their electrons to the complex I of the mitochondrial respiratory chain, where most of these electrons migrate to cytochrome-c oxidase and safely combine with oxygen and protons to form water. However, a fraction of these electrons directly reacts with oxygen to form the superoxide anion radical and other ROS. In contrast, excess intake of fat via HFD, increases mitochondrial β-oxidation of FFAs and leads to an excess electron flow and increased production of ROS. The ROS further react with oxygen to form more and more superoxide anion (Pessayre et al., 2002; Matsuzawa-Nagata et al., 2008) (Fig. 2.10). In addition, lipid peroxidation and ROS can consume endogenous antioxidant enzymes as well (Pessayre et al., 2002). Depletion of these protective substances hamper ROS inactivation and increase lipid peroxidation and ROS-mediated damage (Le et al., 2014). This HFD - induced ROS directed pro-inflammatory state may activate one of the major transcription factor linked with inflammation, NF-κB. Moreover, either this HFD triggers ROS or NF-κB induces the expression of NF-κB-dependent pro-inflammatory agents namely, inducible nitric oxide synthase (iNOS), TNF-α, interferon γ (IFN-γ) (Weisberg et al., 2008). This cause overproduction of nitric oxide (NO) by activated iNOS; in turn increased generation of reactive nitrogen species (RNS) is imminent due to the interaction between superoxides and NO (Rahman et al., 2001). All these interlinked events may explain the reasons for the development of multiple risk factors and chronic disorders on high-fat consumption.

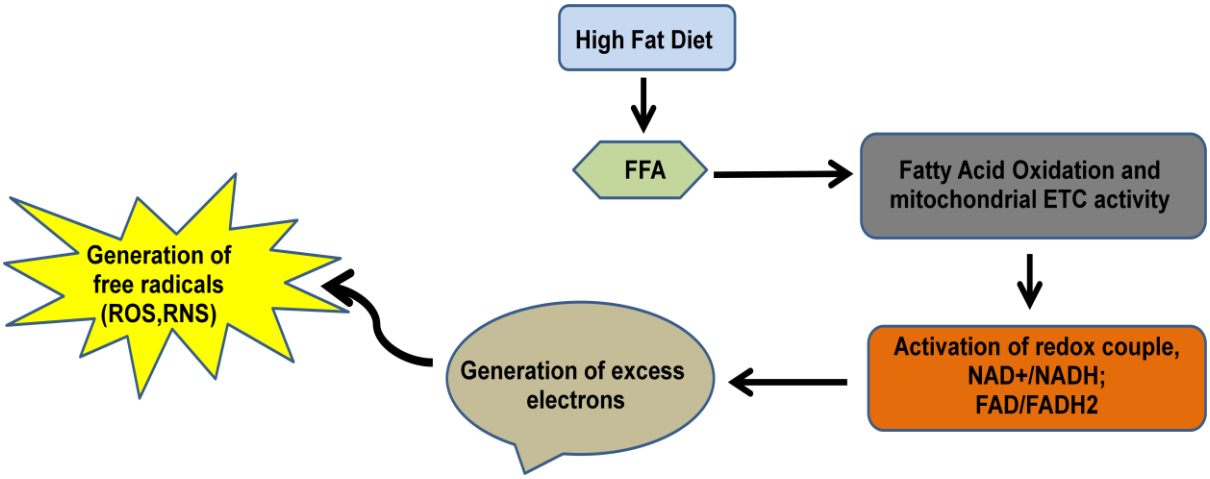

Fig. 2.10 Mechanism involved in HFD induced reactive oxygen species and reactive nitrogen species

A number of studies have found that diets high in saturated fat result in increased body weight and obesity as well as impaired glucose tolerance. For example, Petro et al. showed that mice placed on a 11-week HFD (58% kcal fat) gained significantly more weight and had significantly higher blood glucose levels than those fed on a low fat diet (Petro et al., 2004). A similar study in rats examined the impact of various diets with different quantity and type of fat implemented over 5 weeks. The researchers found that in general, the HFDs significantly increased weight gain, impaired glucose tolerance and increased insulin resistance (Alsaif and Duwaihy, 2004). Moreover, oral ingestion of a high fat emulsion in Wistar rats for a 10 days procudes insulin resistance, along with larger adipocyte and pancreatic islets, increased GLUT2 and α-glucosidase mRNA expression (Ai et al., 2005). Similar reports demonstrate that 4 weeks of HFD feeding results in characteristic features of insulin resistance viz. hyperinsulinemia, mild hyperglycemia, hypertriglyceridemia, hypercholesterimia, glucose intolerance and hypertension (Viswanad et al., 2006; Gaikwad et al., 2007).

An advantage of this model is that it resembles most of the features of the patient with genetic predisposition to develop insulin resistance and T2DM. HFD model represents an important tool for understanding the interplay of western diets and development of insulin resistance, T2DM and obesity. Thus it is widely used to study the insulin sensitizing effects of various synthetic or natural agents.

2.6.2. High fructose diet induced insulin resistance

A number of previous studies reported that high-fructose diet is one of the major contributors for the development of overweight, obesity, insulin resistance, T2DM as well as metabolic syndrome (Elliott et al., 2002; Basciano et al., 2005; Miller et al., 2008; Tapy and Le, 2010). Pooranaperundevi et al. developed an insulin resistance model by feeding 60% (w/w) high fructose diet for 30 days in rats (Pooranaperundevi et al., 2000). Animal studies in Male Syrian Golden hamsters or rats have shown that addition of 60% fructose to solid diets increased plasma insulin, FFAs, and triglyceride concentrations accompanied with decreased hepatic insulin signalling and insulin insensitivity in whole body (Naples et al., 2008; Maithilikarpagaselvi et al., 2016). High-fructose diets have also been associated with hypertension and hyperinsulinemia in fructose-fed animals (Hwang et al., 1987). One hypothesis that has been proposed to explain weight gain in fructose-fed animals is that ingesting fructose-sweetened food raises calorie intake resulting in an over-consumption of energy which is not balanced by energy output, leading to weight gain (Bray et al., 2004). Another hypothesis regarding the relationship between fructose consumption and obesity is based on how fructose is metabolized. Fructose in diet is metabolised by liver and provides carbon atom for glycerol and acyl portions of triglycerides, thus efficiently increasing de novo lipogenesis. This leads to deposition of triacylglycerol in organs like adipose tissue, liver, heart, kidney and muscle thereby increasing body weight. These fat laden tissues than release many inflammatory mediators including TNF-a, IL-6, Cyclo-oxygenase (COX-2), MCP-1 which can activate inflammatory cascade. TNF-a, phosphorylate IRS-1 at serine residue instead of tyrosine thus negatively regulating insulin signalling (Basciano et al., 2005).

2.6.3. The high fat/high carbohydrate diet induced insulin resistance

Recent studies suggest that a diet rich in both fat and sugar has higher risk for development of diabetes as compared to diet rich in fat or sugar (Basu et al., 2013; van Dam et al., 2002). Based upon these reports, efforts were made to combine the HFD with high fructose diet so as to develop suitable model for insulin resistance and T2DM. Although some reports suggest that combination of high-fat and high-fructose diets are usually better than HFD alone (Lozano et al., 2016), it could be better to know, which dietary components are more effective for the development of insulin resistance in animals. To answer this question, Zaman and colleagues conducted a comparative study in rats by feeding either a HFD (65%

calories from fat) or high-fructose diet (65% calorie from fructose) for a period of 10-weeks (Zaman et al. 2011). They observed that 10-week feeding with HFD led to obesity and low insulin sensitivity, whereas rats fed with the high-fructose diet exhibited no change in insulin sensitivity and lipidaemia. Thus, the authors conclude that the HFD had more deleterious response than high-fructose diet to induce obesity and low insulin senstivity in rats (Zaman et al. 2011).

2.6.4. Combination of low dose Streptozotocin and HFD as a model for insulin resistance

Many studies have reported that the rats fed with HFD do not develop frank hyperglycemia or diabetes presumably due to compensatory hyperinsulinemia (Davidson et al., 2011). It is suggested that the HFD might be a better way to initiate the insulin resistance which is one of the important features of T2DM. At the same time, streptozotocin (STZ) is widely used to reproducibly induce both insulin-dependent and noninsulin-dependent diabetes mellitus presently by inducing β cell death through alkylation of DNA (Szkudelski, 2001). Although high-dose STZ severely impairs insulin secretion mimicking T1DM, low-dose STZ has been known to induce a mild impairment of insulin secretion which is similar to the feature of the later stage of T2DM (Reed et al., 2000; Srinivasan et al., 2005). Therefore, investigators have started to develop a rat model by feeding the animal with HFD following low-dose STZ that would closely mimic the natural history of the disease events (from insulin resistance to β cell dysfunction) as well as metabolic characteristics of human T2DM (Reed et al., 2000; Davidson et al., 2011). Studies have reported that low dose of STZ (35 mg/kg, i.p.) administered after 2 weeks HFD feeding, produces characteristics features of insulin resistance such as mild hyperglycemia, hyperinsulinemia, hypertriglyceridemia, hypercholesterolemia and hypertension in male Sprague Dawley rats (Gaikwad et al., 2007; Gaikwad et al., 2010). Also, a high sucrose-fat diet for 8 weeks after low dose STZ (30 mg/kg) in Wistar rats developed obesity, impaired glucose tolerance, decreased IRS-1 protein expression (Liu, 2005)

2.6.5. Stress induced insulin resistance

Psychological stress can lead to insulin resistance in liver and skeletal muscle by interfering with carbohydrate metabolism. Acute insulin resistance was observed in the liver, following acute psychological stress (Electrical foot Shocks, 180 times at an amplitude of 0.3 mA, a

duration of 3–5 s per shock) in adult male C57BL/6 mice (Li et al., 2013). Moreover, Immobilization stress has also been reported to induce insulin resistance. Immobilization stress can be induced by unilateral hindlimb immobilization for 7 days whereas contralateral hindlimb served as control. Immobilization stress has been reported to reduce insulin stimulated tyrosine phosphorylation of IRS-1 and hence cause insulin resistance (Hirose et al., 2000).

2.6.6. Dexamethasone induced insulin resistance

Glucocorticoids belong to a class of steroids intimately involved in regulating glucose homeostasis and lipid metabolism. Glucocorticoids bring about their multiple effects by activating the intracellular glucocorticoid receptor that binds to specific glucocorticoid-responsive elements in the vicinity of regulated genes and subsequently affect their expression (Adcock et al., 2006; Stellato, 2004). Dexamethasone is a synthetic glucocorticoid which has a 50-fold greater affinity for the glucocorticoid receptor relative to cortisol. Clinically, dexamethasone is administered for the suppression of inflammation (Schacke et al., 2002; Czock et al., 2005) and the alleviation of emesis associated with chemotherapy (Maranzano et al., 2005). When administered in excess, dexamethasone induces adverse effects such as muscle catabolism (Prelovsek et al., 2006), hyperphagia (Debons et al., 1986), increased adiposity (Asensio et al., 2004; Korach-André et al., 2005), and increased insulin resistance (Besse et al., 2005; Binnert et al., 2004). In view of these data, dexamethasone has been used to rapidly generate insulin resistance in rodents (Ruzzin et al., 2005); Korach-Andre et al., 2005). The mechanism by which dexamethasone may induce peripheral insulin resistance include inhibition of GLUT4 translocation (Dimitriadis et al., 1997), increased lipoprotein lipase activity in the adipose tissue (Ong et al., 1992), and an impairment of endothelium-dependent vasodilation (Iuchi et al., 2003), which itself is an important determinant of insulin sensitivity. A major advantage of using dexamethasone is that the insulin-resistant state can be generated in a relatively short period of time (Ai et al., 2005). Typically 8–12 wk on a HFD are required for a C57BL/6J male mouse to become obese and mildly hyperglycemic and develop a progressive impairment of glucose tolerance (Surwit et al., 1988). This can be compared with the dexamethasone-aggravated model in which insulin resistance can be generated within a week of dosing. Because the molecular mechanisms by which dexamethasone induces insulin resistance are not yet fully understood, the metabolic characterization of such model is important for drug testing.

2.6.7. Zymosan-induced mice induced insulin resistance

Wang and colleagues used zymosan, a mixture of cell-wall particles from the yeast named *Saccharomyces cerevisiae*, to induce insulin resistance in mice (Wang et al., 2013). Although the authors suggested that this model is better than the high-fructose diet-fed insulin resistance model, however, this model is not sustainable without the zymosan treatment. Hence, it cannot be used as proper animal model of insulin resistance.

2.6.8. Genetic models of insulin resistance

There are numerous genetic models which are being used in preclinical research for evaluating the therapeutic potential of natural or synthetic agents in insulin resistance and T2DM conditions. Below some of the most commonly used genetic models have been explained.

2.6.8.1. Leptin *ob/ob* and Leptin *db/db* mouse

Leptin, a 167-amino acid product of *ob* gene regulates food intake, energy expenditure and maintains energy homeostasis (Cohen et al., 1996). Obese (*ob/ob*) and (*db/db*) mice are autosomal recessive strains with deficits of leptin and its receptor, respectively but both exhibit similar phenotypes of insulin resistance and obesity (Tartaglia et al., 1995; Zhang et al., 1994).

2.6.8.2. Zucker rat

Leptin receptor deficient obese Zucker fatty (*fa/fa*) rat is a model of spontaneous genetic obesity exhibiting mild glucose intolerance, hyperinsulinemia and hyperlipidemia but not hyperglycemia (Oana et al., 2005). These rats develops obesity at an early age due to autosomal recessive (fa) gene (Vogel, 2002).

2.7. Animal model for brain specific insulin resistance and cognitive deficits

2.7.1. Intracerebroventricular-Streptozotocin administration

Streptozotocin (STZ), isolated in the late 1950s from a strain of the soil bacteria *Streptomyces achromogenes*, was patented and initially developed as an antibiotic, later as an anticancer agent. Until now, it is marginally used in the multi-drug therapy of some rare neuroendocrine tumors (Turner et al., 2010), although it is routinely used to induce diabetes in experimental animals. Unlike other nitrosureas which are lipophilic and quickly taken up by cells, STZ due

to hexose substitution is less lipophilic and requires a particular glucose transporter, GLUT2, to cross cellular membranes. Selectivity of STZ toward insulin producing beta cells in pancreas is explained by the presence of GLUT2 in the membranes of vulnerable cells. Acting intracellularly methylnitrosourea moiety of STZ alkylates DNA; cell death, which occurs by necrosis, is the consequence of poly(ADP-ribose)polymerase (PARP) activation with subsequent depletion of NAD^+ and ultimately depletion of ATP stores. Besides insulin-producing pancreatic beta cells, STZ is toxic toward other organs expressing GLUT2 transporter, particularly kidney and liver. Brain is not affected directly, because STZ is not able to penetrate BBB which lacks GLUT2 transporter.

Initial observations led to the hypothesis that the major biochemical perturbation in sporadic AD (sAD) concerns the control over cerebral glucose metabolism, which is subsequent to a signal transduction failure of the cerebral insulin receptor. Later, experiments have shown that application of STZ to the rat lateral ventricles decreased brain glucose utilization, in particular in the frontal and parietal cortex, decreased ATP and, ATP/ADP ratio, and produced several other brain metabolic and behavioral disturbances (Nitsch and Hoyer, 1991). Intracerebroventricular (ICV) administration of drugs are rarely used in the clinic for administering drugs (Cook et al., 2009); more frequently, drugs or selective toxicants are applied to the brain ventricular system of laboratory animals for experimental purpose. In this regard, ICV administration of STZ in rodent's brain has been shown to induce cognitive decline, increased cerebral Aβ deposits, total tau protein, increased oxidative stress, neuroinflammation and other biochemical abnormalities. Thus, it is considered as a valid experimental model of the early pathophysiological changes in AD (Sharma et al., 2010; 2012). Similarly, Deng et al. reported impaired insulin signaling, overactivation of GSK-3β, decreased levels of brain glucose transporters, as well as increased phosphorylation of tau in ICV-STZ administered rats (Deng et al., 2009). These authors further suggested that the key mechanism in the development of disease in the human AD, as well as in the rodent model disease is the development of brain insulin resistance which leads to neurodegeneration via two cooperating pathways, namely decreased PI3K-AKT signaling activity and overactivation of GSK3β, decreased GLUT1/3 expression along with decreased intraneuronal glucose metabolism. Thus, there is widening recognition that memory deficit and sAD is closely associated with impaired insulin signaling and glucose metabolism in brain, suggesting it to be a brain-specific form of diabetes and so also termed as “type 3 diabetes” (Takeda et al., 2011; Talbot et al., 2012). In line, cerebral administration of STZ at sub-dibetogenic doses in animals also results in insulin resistant brain state that share many

features in common with sAD in humans (Shingo et al., 2012). These reports clearly suggest that intracerebral administration of STZ produces most prevalence type of AD.

2.8. Experimental models of Parkinson's disease

Several toxic based models are currently in use in primates and rodents and, interestingly, with the exception of 6-Hydroxydopamine (6-OHDA) and MPTP, these models are actually pesticide based. There are some drawbacks to the use of these models, but this fact does not negate the value of these animal models to study PD pathogenesis. These animal models have opened crucial doors to increase our knowledge base of the events that may lead to the neurodegenerative processes.

2.8.1. 6-OHDA induced model of PD

Since its first description in 1959, 6-OHDA has played a fundamental role in preclinical research on PD. 6-OHDA is a structural analogue of catecholamines (Luthman et al., 1995). Ungerstedt, 1968 first used this neurotoxin in the rats, since that time 6-OHDA has become one of the most widely used neurotoxins for modeling PD in experimental animals. Different 6-OHDA rodent models have been developed in order to obtain a degree of neurodegeneration which replicates the disease pathology to the same extent as seen in human PD. Mice, cats, dogs, and monkeys are all sensitive to 6-OHDA; however it is used much more frequently in rats (Roeling et al., 1995; Valette et al., 1995; Annett et al., 1997). Systemically administered 6-OHDA fails to cross the BBB, so it has to be injected locally using stereotaxic procedures to obtain a unilateral lesion (Betarbet et al., 2002; Ungerstedt, 1968). Usually, there are three sites where 6-OHDA injections were made; into the Medial Forebrain Bundle, the SNpc or the Striatum (Betarbet et al., 2002). One of the most attractive features of the unilateral 6-OHDA model is the fact that each animal can serve as its own control as there is a lesioned and an unlesioned hemisphere. 6-OHDA exhibits a high affinity for catecholaminergic transporters such as the dopamine transporter (DAT) and norepinephrine transporter (NET), (Sachsand and Jonsson, 1975) (Fig. 2.11). Thus it is often used in conjunction with a selective noradrenaline reuptake inhibitor such as desipramine in order to spare the noradrenergic neurons from damage (Martin et al., 1976). When 6-OHDA is infused into the brain, it produces cytotoxic species through both enzymatic and non-enzymatic mechanisms. These mechanisms are intensified by endocellular trace elements such as manganese and iron (Cadet and Brannock, 1998; Choi et al., 1999; Lotharius et al., 1999). Once 6-OHDA is inside the neurons, it accumulates in cytosol and get oxidized by monoamine oxidase (MAO-A) enzyme and generates hydrogen peroxide (H2O2) which is

highly cytotoxic and triggers the production of oxygen radicals. Moreover, 6-OHDA undergoes strong auto-oxidation generating H2O2, ROS and catecholamine quinones which attack endocellular nucleophilic groups (Padiglia et al., 1997; Palumbo et al., 1999). Increase in the levels of ROS and other reactive species result in a rapid depletion of endocellular antioxidant enzymes, in turn leading to an increased metabolic abnormalities and structural damage to the neurons (Blum et al., 2001; Cohen and Werner, 1994).

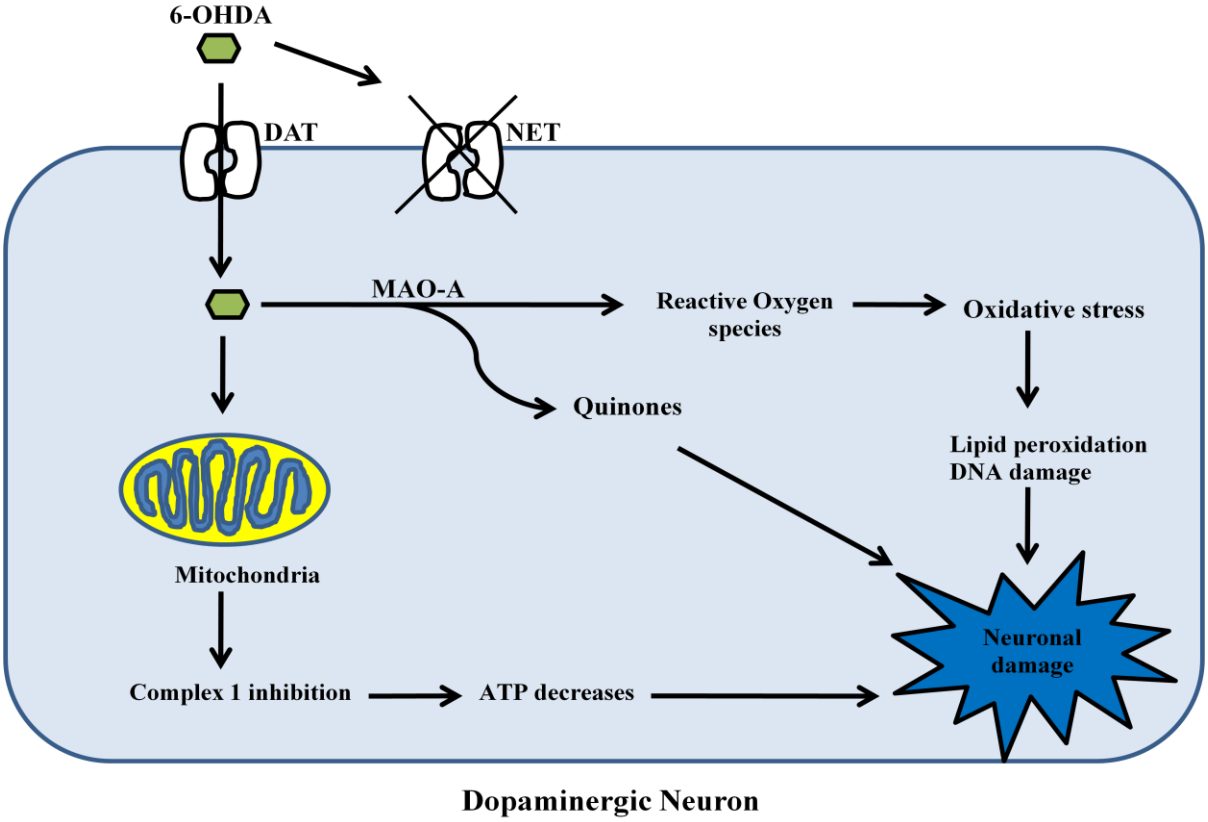

Fig.2.11 Mechanism of Action of 6-OHDA in dopaminergic neuronal death

2.8.2. MPTP induced model of PD

In 1979, MPTP was identified as a strong neurotoxin when young drug addicts developed an idiopathic parkinsonian syndrome. After investigating the etiology of their condition, it was found that MPTP was the neurotoxic contaminant responsible for the parkinsonian effect (Sakai and Gash, 1994). The tragic results of MPTP poisoning in the heroin addicts led to the development of MPTP-induced rodent and nonhuman primate animal models of PD and proved to be extremely valuable (Amalric et al., 1995; Paillé et al., 2007; Langston et al., 1983; Chiueh et al., 1984). Monkeys, humans and many other animal species including nonhuman primates, guinea pigs, mice, rats and cats are susceptible to this neurotoxin (Markey et al., 1984). MPTP can be administered by a variety of regimens, but the most

common and reproducible form is still systemic injection (Kopin and Markey, 1988). The acute regimen consists of multiple systemic administration of MPTP (usually four doses at 2-h intervals per day). The subacute regimen consists of a single systemic administration per day for several consecutive days (usually 5 days) and the chronic regimen through several weeks (Langston and Irwin, 1986). The comparison of these different models indicated clearly that different schedules of administration of MPTP mimic distinct stages of the disease and might induce neuronal death by different mechanisms.

It has been repeatedly demonstrated that MPTP is indeed the gold standard for toxin-based animal model for replicating almost all of the hallmarks of PD. Unfortunately, lacking in this list is the definitive characteristic of PD, Lewy body formation (Haobam et al., 2005; Przedborski et al., 2001). Interestingly, some studies have demonstrated the production of Lewy body-like inclusions after MPTP administration (Meredith et al., 2008; Forno et al., 1993) although these studies have been difficult to replicate.

The mechanism behind the neurotoxic action of MPTP has been the subject of intense investigation and is relatively well understood. MPTP is a lipophilic toxin that, following systemic injection (usually i.p or s.c), rapidly crosses the BBB (Vezoli et al., 2011). Once inside the brain, MPTP is converted by MAO-B (principally in glia) into the intermediary, 1-methyl-4-phenyl-2,3,dihydropyridinium (MPDP+) before its rapid and spontaneous oxidation to the toxic moiety, MPP+ (Bergman et al., 1990). Following its release into the extracellular space, MPP+ is taken up via dopamine transporter (DAT) into dopaminergic neurons where cytoplasmic MPP+ can trigger the production of ROS, which may contribute to its overall neurotoxicity (Guridi et al., 1996) (Fig. 2.12). However, the majority of MPP+ is eventually accumulated within mitochondria and impairs mitochondrial respiration via inhibition of complex I of the electron transport chain (Speciale, 2002). This action impairs the flow of electrons along the respiratory chain, leading to reduced ATP production and the generation of ROS, such as superoxide radicals. The combined effects of lowered cellular ATP and elevated ROS production are most likely responsible for the initiation of cell death-related signalling pathways such as p38 mitogen-activated kinase (Chiba et al., 1984), JNK (Javitch et al., 1985) and bax (Nicklas et al., 1987; Karunakaran et al., 2008), all of which have been demonstrated in vivo following MPTP treatment and may contribute to apoptotic cell death (Saporito et al., 2000; Hassouna et al., 1996).

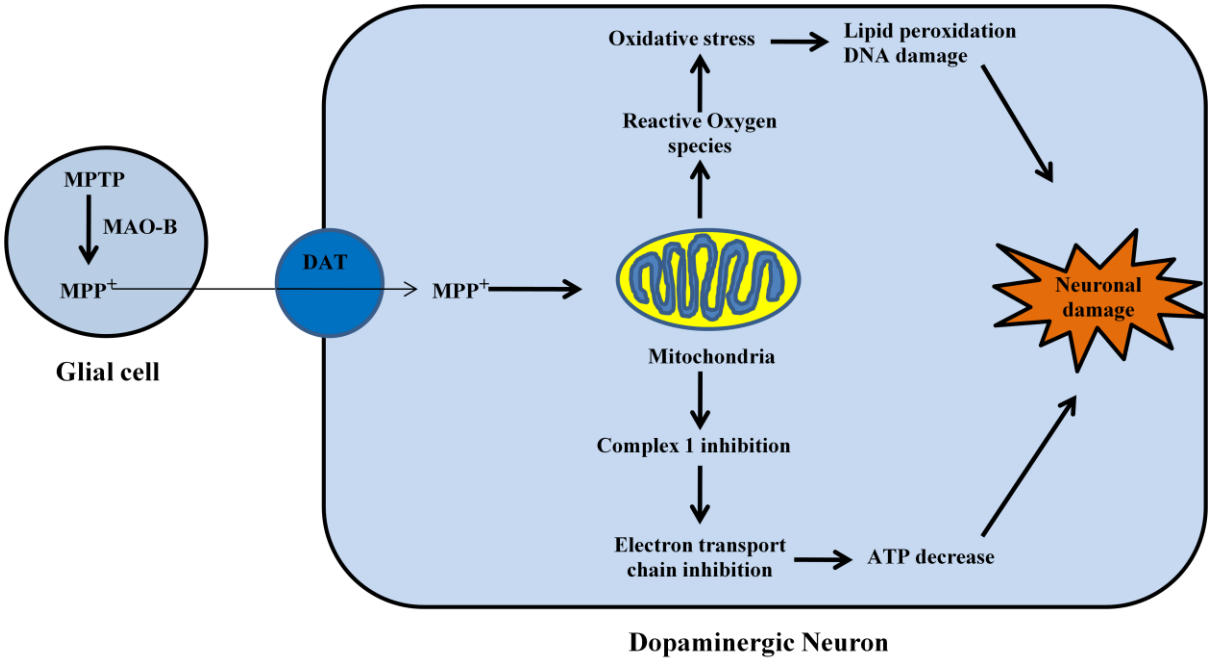

Fig.2.12 Mechanism of action of MPTP in dopaminergic neuronal death

2.8.3. Rotenone induced model of PD

Rotenone is both a herbicide and an insecticide. Its half-life is 3–5 days depending on exposure to sunlight. And, like MPTP, it is highly lipophilic and readily crosses the blood–brain barrier. Rotenone is a strong inhibitor of mitochondrial complex I, which is located at the inner mitochondrial membrane and protrudes into the matrix. It has been demonstrated that the chronic systemic exposure to rotenone, develop many features of PD, including nigrostriatal dopaminergic degeneration (Costello et al., 2009). The apparent beauty of this model is that it results in activation of various pathogenic pathways including: oxidative stress, α-synuclein phosphorylation and aggregation and lewy body pathology etc. (Costello et al., 2009) and also reproduce all the behavioral features seen in the typical form of human PD (Feng et al., 2002).

2.8.4. Paraquat and Maneb induced model of PD

It has been reported that exposure to the herbicide paraquat (1,1′-dimethyl-4,4′-bipyridinium) or the fungicide Maneb (manganese ethylene-bis-dithiocarbamate) have been associated with an increased incidence of PD (Ascherio et al., 2006; Costello et al., 2009). So, it is not surprising that attempts have been made to model PD using these agents. Paraquat enters the brain via the neutral amino acid transporter (Shimizu et al., 2001) before Na+-dependent uptake into cells occurs. Once inside the cells, paraquat lead to both indirect mitochondrial

toxicity via redox cycling and also direct inhibition of complex I (at higher doses) (Miller, 2007). Maneb, on the other hand, preferentially inhibits complex III of the mitochondrial respiratory chain following entry into the brain (Zhang et al., 2005). Paraquat and maneb have been shown to produce enhanced toxicity when combined (Thiruchelvam et al., 2000), possibly as a result of maneb increasing the brain concentration and reducing clearance of paraquat (Barlow et al., 2003). Coupled with the fact that human exposure to one of these pesticides alone is unlikely as they are used in the same geographical regions, this provides a clear rationale for combining their administration in order to produce an animal model of PD.

2.8.5. The genetic models of PD

Although PD was long considered a nongenetic disorder of "sporadic" origin, genetic mutations in PD are rare and represent only about 10% of all PD cases (Dauer and Przedborski, 2003) and, animal models of these mutations (alpha-synuclein and LRRK2, autosomal dominant PD, and PINK1/Parkin and DJ-1, autosomal recessive PD) are important as they represent potential therapeutic targets.

2.9. Gaps in existing research

The prevalence of diabetes worldwide has been projected to be 366 million by 2030 according to the World Health Organization (Wild et al., 2004). The management of typical complications of diabetes has improved significantly in recent decades because of improved glycemic control and additional treatment strategies that target diabetic complications. Therefore, the life span of diabetic patients has considerably lengthened. Although pharmacological interventions have improved their survival from life-threatening complications, silent neurodegenerative pathways over decades contribute to cognitive decline with aging and compromise the quality of life. Although the precise mechanism remains unclear, T2DM can exacerbate neurodegenerative processes. Insulin resistance has emerged as a major molecular link between these diseases. Aging, Obesity and Environmental factors all play an important role in development of insulin resistance. Perhaps, insulin resistance, a proximal cause of T2DM, could also be a risk factor for neurodegenerative diseases, including AD and PD. Impaired insulin signalling pathways might result in elevated GSK-3β activity, however, little is known about the downstream signaling pathways those ultimately leading to neuronal death. It emerges that insulin resistance is multifactorial in nature and its development is dependent on different molecular defects, including direct as well as indirect effects on insulin signalling pathways. Among the indirect effects, epigenetic mechanisms are the recently explored and histone modifications, especially histone acetylation/deacetylation are the main focus of these studies. However, the mechanisms by which these epigenetic mechanisms are involved in neurodegenerative processes are still elusive. Thus, we hypothesized that GSK3β and HDACs could be involved in insulin resistance and exacerbated AD and/or PD pathology associated with insulin resistance (Fig. 2.13).

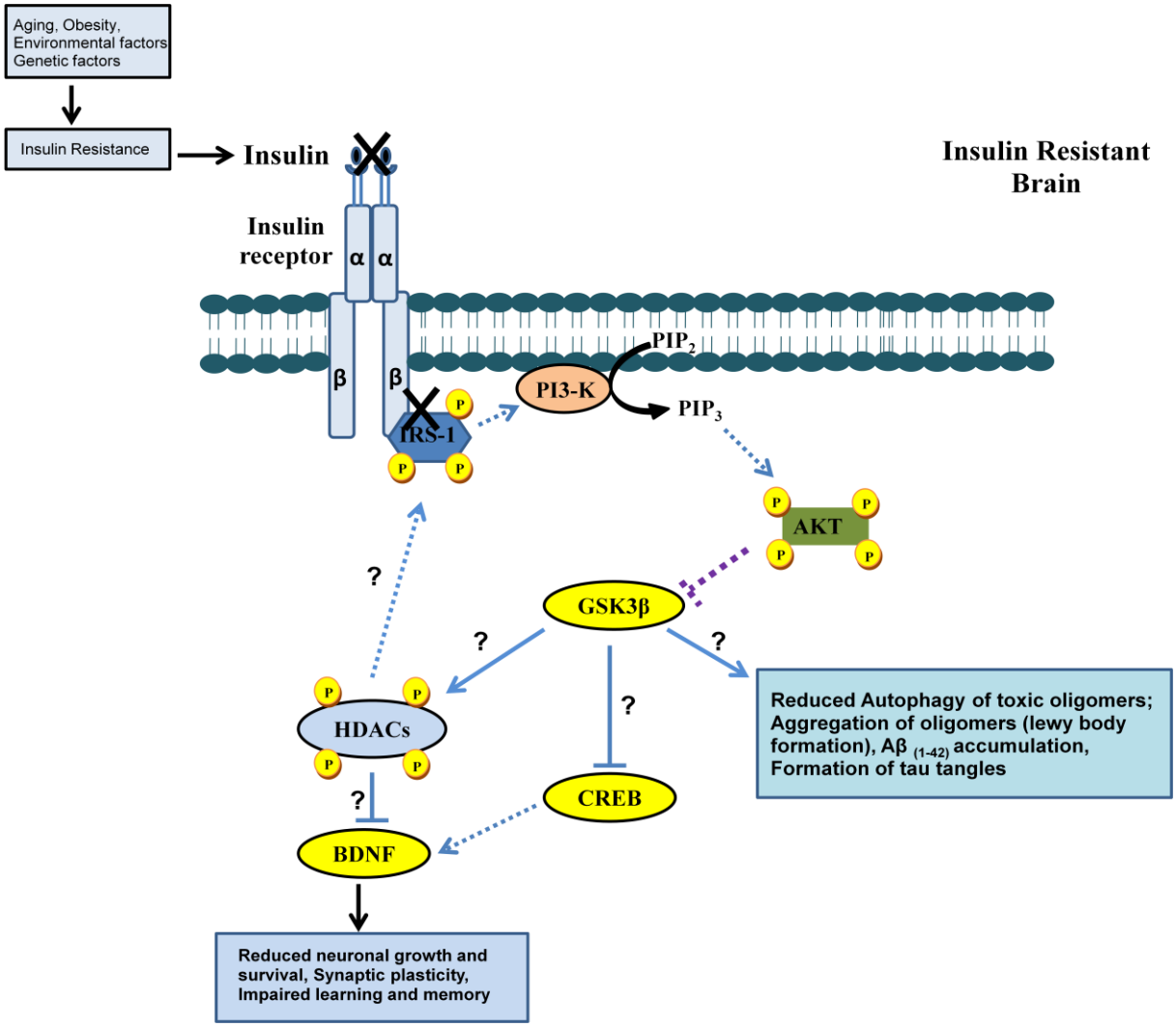

Fig. 2.13 Proposed hypothetical representation for involvement of GSK3β/HDACs in insulin resistance induced neurodegenerative disorders.

3. Objectives and Plan of work

3.1. Objectives of the Proposed Research

1. To standardize animal model for insulin resistance.
2. To study the impact of insulin resistance on central nervous system (CNS) function in relation to cognitive and motor activities.
3. To examine the link and molecular mechanims involved in insulin resistance mediated AD and PD pathology.
4. To explore the epigenetic modifications focusing primarily on histone acetylation in insulin resistance induced AD and PD.
5. To evaluate the effect of GSK-3β and HDAC inhibitors alone/or in combination in AD and PD associated with insulin resistance.

3.2. Plan of work: The work was divided into following phases.

3.2.1. Development of insulin resistance by high fat diet feeding

The primary goal was to standardize an animal model of HFD induced insulin resistance condition. To evaluate the time course of HFD-induced insulin resistance condition, animals were subjected to HFD feeding. Body weight was measured weekly. Serum estimations (insulin, glucose, triglycerides, total cholesterol and HOMA-IR) were performed periodically at an interval of 2 weeks after the initiation of HFD feeding.

3.2.2. Development and Standardization of animal models for insulin resistance induced AD and PD pathology

During this phase animal models for insulin resistance induced AD and PD pathology were developed and standardized. We used two different animal models for insulin resistance induced AD like pathology. In the first model, we fed the mice with HFD to induce insulin resistance mediated cognitive deficit. In the second model, we used intracerebroventricular Streptozotocin administration to induce brain specific insulin resistance condition which results in cognitive deficit and AD like pathology. To develop an animal model for insulin resistance induced PD pathology, we first fed the animals with HFD followed by administration of 6-hydroxydopamine in medial forebrain bundle. The approach here was to determine whether a HFD and the resulting insulin resistance would exacerbate 6-OHDA-induced nigrostriatal dopamine depletion or not.

3.2.3. Selection of GSK3β inhibitors and HDAC inhibitors to ameliorate insulin resistance induced AD and PD pathology

Although a number of GSK3β inhibitors are available for research purposes, however, AR-A014418 and Indirubin-3'-monoxime (IMX) were selected in this study as they offer very high selectivity towards GSK3β in contrast to cyclin dependent kinases (CDKs) and also easily cross the blood brain barrier (BBB) which is a prime requirement for neuroscience studies. AR-A014418 is an ATP-competitive inhibitor of GSK-3β with an IC_{50} = 104 nM. It does not significantly inhibit the closely related CDK2 or CDK5 (Bhat et al., 2003). IMX is a more potent inhibitor of GSK3β with an IC_{50} = 22 nM. It inhibits CDKs, but at very high concentrations, including CDK1/cyclin B (IC_{50} = 180 nM), CDK2/cyclin A (IC_{50} = 500 nM) (LeClerc et al., 2001). Although, Lithium is a non specific GSK3β inhibitor with IC_{50} =

2mM. However, it is used in this study as it is the only GSK3β inhibitor approved by FDA for clinical use (Hagit Eldar-Finkelman and Martinez, 2011).

The HDAC inhibitors used in this study includes: **Pan HDAC inhibitors:** SAHA, Sodium butyrate, Valproate and **Class specific HDAC inhibitors**: CI-994 and HDACi 4b (as Class I HDAC inhibitors), MC-1568 (as Class II HDAC inhibitor). Small molecule HDAC inhibitors hold much promise as pharmacological modifiers of the epigenetic status of the CNS, given their ability to cross the BBB. **SAHA** is a broad-spectrum (class I and II) inhibitor of HDACs with moderate potency (IC_{50} = 100 nM) that is being used to treat T-cell lymphoma (Richon, 2006). Moreover, SAHA is considered as relatively non-toxic to normal cells and was therefore an appropriate choice for our study (Iyer et al. 2010). On the other hand, **Sodium butyrate** inhibits the action of classes I and IIa HDACs. Compared with hydroxamic acids, the short chain fatty acids (SCFAs) such as, sodium butyrate, have less potent inhibitory effects (IC_{50} = 0.80 mM), but they can easily cross the BBB due to their smaller molecular weight (Xu et al., 2007). Due to their high permeability through BBB, these compounds are of particular interest in neuroscience research. Moreover, **Valproate** has been used in this study as an pan HDAC inhibitor (IC_{50} = 400 μM for HDAC1). It can easily cross BBB and has been used primarily to treat epilepsy and bipolar disorder (Cornford et al., 1985; Ziyatdinova et al., 2015).

CI-994 is a selective class I HDAC inhibitor with IC_{50} of 0.9, 0.9, 1.2, and >20 μM for human HDAC 1, 2, 3, and 8, respectively. The brain pharmacokinetics of CI-994 was evaluated in Rhesus monkeys and it was observed that CI-994 has very good potential to cross the BBB (Riva et al., 2000; Moradei et al., 2007). HDAC inhibitor, **4b** (HDACi 4b) has been reported as a selective HDAC1 and HDAC3 inhibitor. HDACi 4b, has also been reported to cross BBB and shown neuroprotective effects in an animal model of HD (Thomas et al, 2008). Therefore, both these compounds were used as Class I selective HDAC inhibitors in this study. Moreover, **MC-1568,** has been reported as a selective class II HDAC inhibitor (Quinti et al., 2010) with IC_{50} of 220 nM and 176-fold class II selectivity and is therefore used in this study. Sirtinol was used as a Class III HDAC inhibitor (or SIRT inhibitor).

3.2.4. Dose response studies

The doses of all drugs were selected on the basis of pilot studies conducted in our laboratory as well as from previous studies as referred in Table. 3.2. Although detailed toxicological study was not done, but the effect of test drugs on locomotor activity was evaluated using

actophotometer (Boissier & Simon, 1965). Briefly, the apparatus consists of a square arena (30 × 30 cm) with walls that are fitted with photocells just above the floor level. The photocells were checked before the beginning of the experiment. The drug/vehicle treated animals were then individually placed in the arena. After a 2 min acclimatization period, the digital locomotor scores were recorded for 10 min in a dimly lit room. All the drugs were administered 30 min prior to testing. The doses at which the drugs does not affect the locomotor activity significantly, were taken further, and investigated for their potential in insulin resistance induced AD and PD pathology.

	SAHA			
Dose (mg/kg)	12.5	25	50	100
Effect on Locomotor activity	NS	NS	NS	S
Drug	**Sodium butyrate**			
Dose (mg/kg)	150	300	600	1200
Effect on Locomotor activity	NS	NS	NS	S
Drug	**Valproate**			
Dose (mg/kg)	200	400	800	1200
Effect on Locomotor activity	NS	NS	NS	S
Drug	**CI-994**			
Dose (mg/kg)	2.5	5		10
Effect on Locomotor activity	NS	NS		S
Drug	**HDACi 4b**			
Dose (mg/kg)	25	50		100
Effect on Locomotor activity	NS	NS		S
Drug	**MC-1568**			
Dose (mg/kg)	1.25	2.5		5
Effect on Locomotor activity	NS	NS		S
Drug	**Sirtinol**			
Dose (mg/kg)	2.5	5		10
Effect on Locomotor activity	NS	NS		S
	Lithium chloride			
Dose (mg/kg)	60	120	240	480
Effect on Locomotor activity	NS	NS	NS	S

Drug	**Indirubin-3-monoxime**			
Dose (mg/kg)	0.1	0.2	0.4	0.8
Effect on Locomotor activity	NS	NS	NS	S
	AR-A014418			
Dose (mg/kg)	1	5	10	20
Effect on Locomotor activity	NS	NS	NS	S

Table 3.1 Dose selection of GSK3β and HDAC inhibitors by locomotor activity
(NS=Non-significant**; S=** Significant difference**)**

3.2.5 Screening of selected GSK-3β inhibitors and HDAC inhibitors in behavioural tasks for insulin resistance induced AD and PD

The selected drug candidates at selected doses were administered to animals and subjected to various neurobehavioral screening assays.

For Cognitive deficit and Alzheimer's disease

1) Morris water maze: Mean escape latency (s)
2) Probe Trial: % time spent in target quadrant (s)
3) Passive avoidance task: Transfer latency
4) Novel object Recognition task: Time spent in exploring objects (s)

For Motor deficit and Parkinson's disease

1) Narrow beam walk test: Time taken to cross the beam (s); No. of foot slips
2) Locomotor activity: Activity counts/ 10 min
3) Rotarod activity: Time to fall (s)
4) Cylinder test: % contralateral contacts

3.2.6 Pharmacological screening to investigate the plausible mechanism(s) of GSK3β inhibitors and HDAC inhibitors in insulin resistance induced AD and PD

To investigate the probable mechanism(s) of action of the selected drug candidates, the following biochemical estimations were carried out.

1) Brain oxidative stress markers: Lipid peroxidation and nitrite levels were estimated in hippocampus or striatal brain homogenates.

2) Brain antioxidant enzyme level: Estimation of anti-oxidant enzyme such as reduced glutathione (GSH) was measured in hippocampus or striatal brain homogenates.

3) Pro-inflammatory marker: TNF-α level was measured in hippocampus or striatal brain homogenates.

4) Pathological Disease hallmarks: Amyloid-β and ptau levels were examined in hippocampus or striatal brain homogenates.

5) Transcriptional activator and Neurotrophic factor level: CREB and BDNF levels were measured in hippocampus or striatal brain homogenates.

6) Neurotransmitter level: Dopamine level was measured in striatum brain homogenate.

7) Molecular targets of drug candidates: GSK3β and global histone H3 acetylation were measured in hippocampus or striatal brain homogenates.

8) Histopathological analysis: Neurodegeneration was observed in various brain regions using histological examination of brain sections.

4. Materials and Methods

4.1. Animals

The experiments were carried out in male Swiss albino mice and male Wistar rats obtained from Central Animal House of Birla Institute of Technology & Science, Pilani, India. The animals were kept in polyacrylic cages and maintained under standard husbandry conditions (room temperature 22±1 °C and relative humidity of 60%) with 12 h light/dark cycle. The animals were fed with either normal pellet diet (NPD) or HFD and filtered water *ad libitum*. On the days of behavioral evaluation, home cages were placed in the testing room 30 minutes before testing to allow habituation. All the behavioral assessments were carried between 09:00 and 17:00 hours. No more than one behavioral test was completed during any single day. All equipment were cleaned between animals. The experimental procedures on animals were in compliance with the Institutional Animal Ethics Committee of BITS, Pilani, Rajasthan (India) protocol numbers IAEC/Res/17/08, IAEC/RES/19/09, IAEC/RES/19/09/Rev-1/21/11.

4.2 Drugs and Chemicals

4.2.1. Drugs

Pan HDAC inhibitors: Suberylanilide hydoraxamic acid (SAHA); Sodium butyrate (NaB); **Class I specific HDAC inhibitor:** CI-994; HDACi 4b, **Class II specific HDAC inhibitor:** MC-1568; **Class III inhibitor**: Sirtinol; **Non selective GSK-3β inhibitor:** Lithium chloride; **Selective GSK-3β inhibitors:** Indirubin-3'-oxime (IMX) and AR-A014418 were purchased from Sigma Aldrich and Cayman Chemicals. Streptozotocin (STZ) and 6-hydroxydopamine (6-OHDA) were purchased friom Sigma Aldrich. Class I HDAC inhibitor (HDACi 4b) was received as an ex-gratia sample form the Scripps Research Institute, USA.

4.2.2. Chemicals

5,5'-dithiobis-(2-nitrobenzoic acid) (DTNB), thiobarbituric acid (TBA), ascorbic acid were purchased from Sigma–Aldrich, USA. Casein and DL-Methionine were procured from CDH, New Delhi, India. Cholesterol was purchased from SD Fine chemicals (Mumbai, India).

4.3. Kits for serum estimations

Glucose (GOD-POD) kit was purchased from Spinreact, Spain. Triglycerides (GPO-PAP), total cholesterol (CHOD-PAP) and HDL-cholesterol (direct enzymatic method) kits were purchased from Coral clinical systems, Goa, India.

4.4. Enzyme Linked Immunosorbate Assay (ELISA) Kits

TNF-α ELISA kit was purchased from Sigma–Aldrich, USA. BDNF ELISA kit was purchased from Boster Biological Tech. Co., LTD, CA, USA. EpiQuik global Histone H3 acetylation assay Kit was purchased from Epigentek, NY. $A\beta_{1-42}$; pTau; CREB; GSK-3β ELISA kits were purchased from Genxbio, China. Rat and mouse Insulin ELISA kits were purchased from Crystal Chem Inc., USA. DNA Fragmentation detection kit was purchased from Merck (Germany). Dopamine ELISA kit was purchased from USCN Co Ltd, USA. All other chemicals used in the study were of analytical grade. Solutions of the drugs and chemicals were always prepared afresh before use.

4.5. Equipments Used

- ✓ Anymaze Video tracking system: Stoelting Co., USA
- ✓ Stereotaxic Instrument: Inco Ambala, India
- ✓ Hamilton syringe
- ✓ Actophotometer: Inco Ambala
- ✓ Rotarod: Inco Ambala
- ✓ Passive Avoidance Task: Inco Ambala
- ✓ Centrifuge: Eppendorf refrigerated centrifuge, 5702-R, Eppendorf AG, Germany
- ✓ Elisa Plate reader: Ark Diagnostic, India
- ✓ Tissue Homogeniser: Kinematica™ Polytron™ Homogenizers, Germany
- ✓ Spectrophotometer: UV-1800 Shimadzu, Japan
- ✓ Digital Microscope: Optika, Microscopes, Italy
- ✓ Deep freeze (-80ºC): OPR-DFC-300CE, Operon Co. Ltd., Korea.

4.6. Screening of GSK-3β inhibitors and HDAC inhibitors in insulin resistance induced AD

4.6.1. Experimental Protocol-1: Animal model for HFD induced insulin resistance and AD pathology

Male Swiss albino mice (20-25g) were allocated into two dietary regimens either NPD or HFD, initially for a period of 8 weeks and continued till the termination of study. Body weight of animals was taken once every week. The composition of HFD was similar to that described by (Srinivasan et al., 2005). Briefly, HFD consists of following ingredients (g/kg): Powdered NPD 365; Lard 310; Casein 250; Cholesterol 10; Vitamin and Mineral mix 60; dl-Methionine 03; Yeast powder 01; Sodium chloride 01.

4.6.1.1. Standardization of HFD induced insulin resistance and cognitive deficits

In order to standardize the animal model for insulin resistance induced cognitive deficits we fed the mice with HFD and evaluate their cognitive performance in morris water maze task. The animals were assigned different groups and were fed with HFD for different time intervals. It was observed that after 8 weeks of HFD feeding, the animals showed significant reduction in escape latency in morris water maze task as compared to NPD fed animals. Moreover, these animals also showed significant neuronal damage in hippocampus regions (dentate gyrus and CA1). From these initial studies, we confirmed the development of cognitive deficit and neuronal death at 8 weeks following HFD feeding and thus, used this model for screening various test drugs.

4.6.1.2. Test compounds screened in HFD induced insulin resistance and cognitive deficit model

Category	Compound	Vehicle	Doses and route of administration	References
Selective GSK3β inhibitor	**Indirubin-3-monoxime**	2.5% v/v DMSO in saline	0.05, 0.1, 0.2 and 0.4 mg/kg; **(i.p.)**	Yadav et al., 2012
	AR-A014418	3% v/v DMSO in saline	1, 5 and 10mg/kg; **(i.p.)**	Wang et al., 2007
Pan HDAC inhibitors	**SAHA**	12.5% v/v DMSO in saline.	12.5, 25, 50 mg/kg; **(i.p.)**	Faraco et al., 2006; Guan et al., 2009
	Sodium butyrate	0.9% w/v NaCl	150, 300, 600 mg/kg; **(i.p.)**	Hu et al., 2014; Sanchis-Segura et al., 2009

Class I HDAC Inhibitors	**CI-994**	10% DMSO, 45% PEG-400, 45% saline	5 mg/kg; **(i.p.)**	Schroeder et al., 2013
	HDACi 4b	10% DMSO 75 % PEG 200	50 mg/kg (**i.p.**)	Jia et al., 2012, 2015
Class II HDAC Inhibitor	**MC-1568**	10% DMSO, 45% PEG-400, 45% saline	2.5 mg/kg (**i.p.**)	Galmozzi et al., 2013
Class III Inhibitor	**Sirtinol**	10% v/v DMSO in saline	5 mg/kg **(i.p.)**	Shalwala et al., 2014

Table. 4.1. Doses and route of administration of HDAC inhibitors and GSK3β inhibitors screened in HFD induced insulin resistance mediated AD model. (Note: **DMSO:** Dimethyl Sulphoxide; **NaCl**: Sodium chloride; **PEG:** Polyethylene glycol).

4.6.1.3. Experimental Schedule: After 8 weeks of diet feeding, mice were randomly divided into different experimental groups and each group comprised of 8-10 animals.

NPD group: Mice in this group received NPD throughout the experiment.

HFD group: Mice in this group received HFD for 8 weeks (56 days) followed by vehicle administration for respective drug once daily for two weeks.

Treatment groups: Mice in these groups received HFD for 8 weeks (56 days) followed by administration of test compounds at various doses mentioned in Table.4.1 once daily for two weeks. The treatment schedule and the interval for estimation of various parameters are presented in Fig. 4.1.

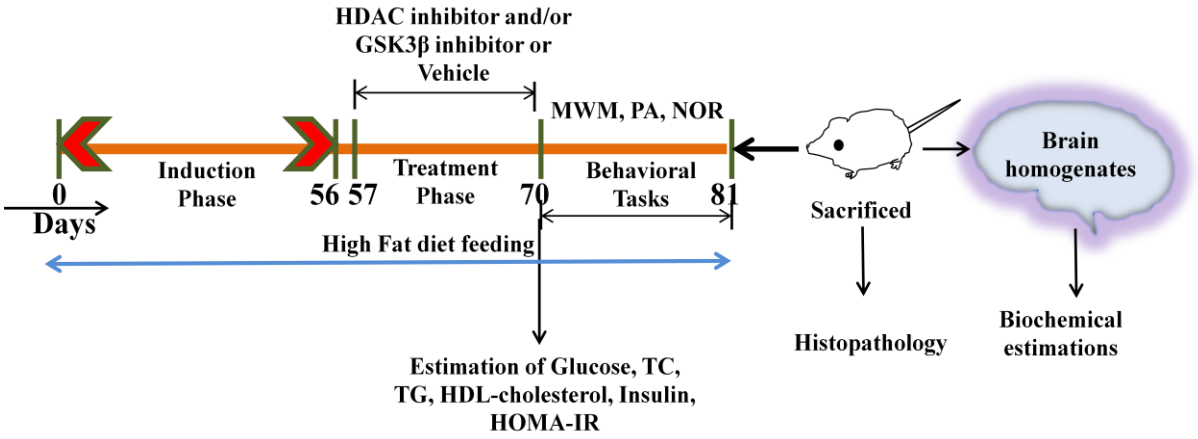

Fig. 4.1 Experimental schedule for GSK3β inhibitors and HDAC inhibitors treatment and the interval for estimation of various parameters in insulin resistance induced cognitive deficits. (Note: **MWM:** Morris water maze; **PA:** Passive Avoidance task; **NOR:** Novel Object Recognition; **TC:** Total cholesterol; **TG:** triglycerides).

4.6.2. Experimental Protocol-2: Animal model for Intracerebroventricular Streptozotocin (ICV-STZ) induced brain specific insulin resistance and AD pathology

4.6.2.1. Administration of ICV-STZ

These experiments were carried out in Wistar rats (200−250 g). The rats were anesthetized with ketamine (80 mg/kg, i.p) and xylazine (5 mg/kg, i.p). The head of the anesthetized rat was placed in position in the stereotaxic apparatus and the skull was exposed by a midline sagittal incision on the scalp. Two holes were drilled through the skull for placement of injection cannulae into the lateral cerebral ventricles using following coordinates: 0.8 mm posterior to bregma; 1.5 mm lateral to sagittal suture; 3.6 mm ventral from the surface of the brain (Paxinos and Watson 1986). A single dose of gentamicin (40 mg/kg, i.p.) was injected following surgery, and a daily application of antiseptic powder (Neosporin®) was done to prevent sepsis. Solutions of the drugs and chemicals were always prepared afresh before use. Drug solution was prepared by dissolving STZ in citrate buffer (pH 4.4) and was administered within 5 min after preparation.

4.6.2.2. Standardization of ICV administration: The ICV administration was confirmed by drilling the skull according to the co-ordinates mentioned in (Paxinos and Watson, 1986). Then, dye solution was infused in ICV region with the help of hamilton syringe. The animals were sacrificed and brain sections were taken after 30 min storage at -20^0 C. The figure clearly shows the accumulation of dye solution in lateral ventricles (Fig.4.2).

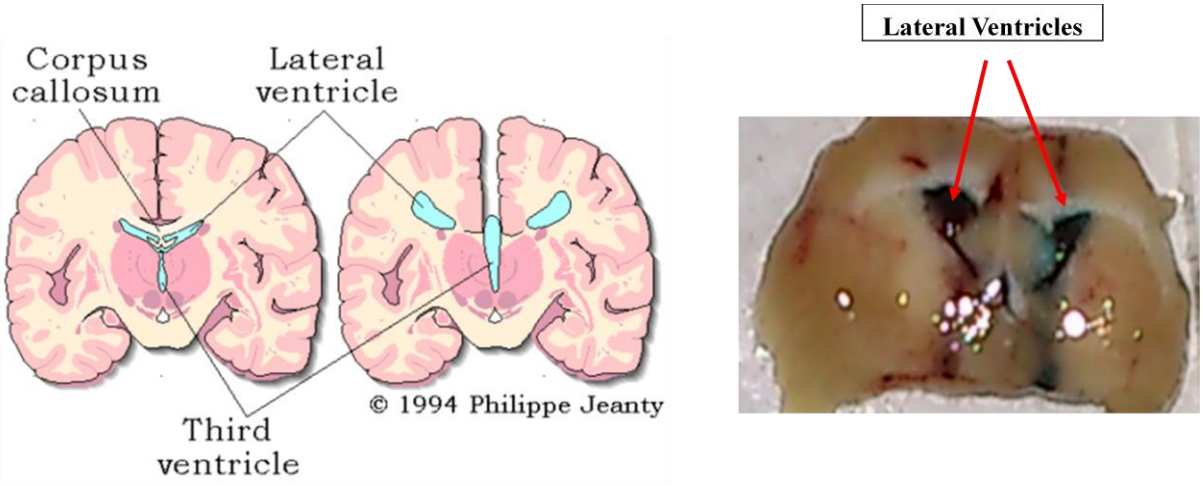

Fig. 4.2 Standardization of intracerebroventricular administration

Fig.4.3 Representative Image of rat fixed in Stereotaxic frame for surgery

4.6.2.3 Compounds screened in ICV-STZ induced brain specific insulin resistance and AD

This model was used to evaluate the effects of low dose combination of GSK3β inhibitor and HDAC inhibitors. For this purpose, we used lithium chloride (LiCl) as GSK-3β inhibitor and valproate as HDAC inhibitor. Although both these drugs are non-selective inhibitors of GSK-3β and HDACs, respectively, but these were selected because these drugs are clinically safe and used for mood disorders. The low doses of LiCl (60 mg/kg) and VPA (200 mg/kg) were selected on the basis of pilot study performed in our laboratory where, we have tested LiCl (60 and 120mg/kg) and VPA (200 and 400mg/kg) and found significant neuroprotection with high doses of these drugs as compared to lower doses. Moreover, the therapeutic doses were selected based upon the earlier reports in which significant antioxidant and neuroprotective properties were demonstrated (Loscher et al., 1989; Dash et al., 2010; Ponce-Lopez et al., 2011; Caberlotto et al., 2013) (Table. 4.2).

Category	Drug	Vehicle	Doses and route	References
Pan HDAC inhibitor	**Valproate**	0.9% w/v NaCl	200 and 400 mg/kg; **(i.p.)**	Loscher et al., 1989; Dash et al., 2010
Non specific GSK3β inhibitor	**Lithium chloride**	0.9% w/v NaCl	60 and 120 mg/kg **(i.p.)**	Ponce-Lopez et al., 2011; Caberlotto et al., 2013

Table.4.2 Doses and route of administration of HDAC inhibitors and GSK3β inhibitors screened in ICV-STZ induced brain specific insulin resistance and AD

4.6.2.4. Experimental schedule Animals were divided into five groups and each group comprised of 8-10 animals. The treatment schedule and the interval for estimation of various parameters are presented in Fig. 4.4.

Group 1: Vehicle Control, (served as double vehicle control), received citrate buffer ICV in a volume of 5 µl in each ventricle on day 1 and 3 as a vehicle for STZ and normal saline (i.p), as a vehicle for LiCl and VPA for 21days.

Group 2: Rats were infused with ICV-STZ (3 mg/kg) dissolved in citrate buffer in a volume of 5 µl in each ventricle on day 1 and 3.

Group 3: Rats received low dose of GSK3β inhibitor, LiCl (60 mg/kg, i.p), 1 hour after the STZ administration starting from day 1 and continued once daily for a period of 21 days.

Group 4: Rats received low dose of HDAC inhibitor, VPA (200 mg/kg, i.p), 1 hour after the STZ administration starting from day 1 and continued once daily for a period of 21 days.

Group 5: Rats received combination of low dose LiCl (60 mg/kg, i.p) and low dose VPA (200 mg/kg, i.p) starting from day 1 and continued once daily for a period of 21 days.

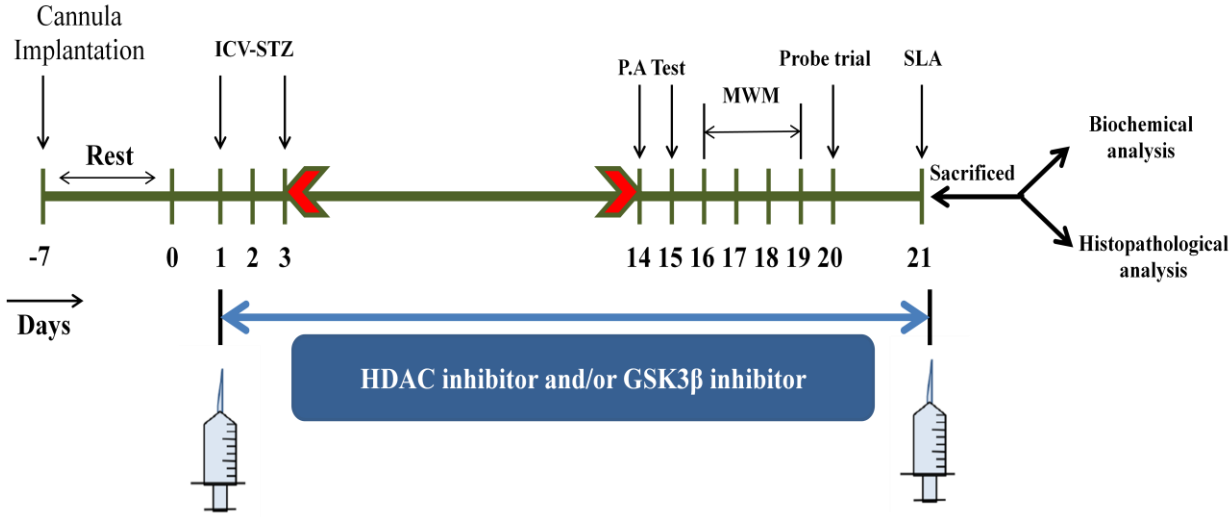

Fig. 4.4 Expermental schedule for treatment and the interval for estimation of various parameters in ICV-STZ induced cognitive deficits. **Day -7** refers to the day of surgery; **ICV-STZ** = Intracerebroventricular Streptozotocin; **MWM** = Morris water maze; **SLA** = Spontaneous locomotor activity; **P.A**= Passive avoidance task.

4.7. Screening of GSK-3β inhibitors and HDAC inhibitors in insulin resistance induced PD pathology

4.7.1. Experimental Protocol-3: Induction and validation of insulin resistance induced PD pathology by HFD feeding and 6-OHDA administration in rats

The experiments were carried out in male Wistar rats (160–200g). All the rats were given training for a period of one week on rotarod and narrow beam walk apparatus. The selection of experimental animals was based on their performance in behavioral tasks during training phase. The rats which fail to cross the narrow beam in 60 s were excluded from study. Similarly, the rats which were not able to hold the rotating rod in rotarod task for a minimum of 30 s were also excluded from study.

4.7.1.1 High fat Diet induced insulin resistance

Initially, the rats were divided into two groups, NPD fed and HFD fed rats. The composition of the HFD was similar to as described by (Srinivasan et al., 2005). The HFD feeding continued till 8 weeks (56 days). The body weight was measured weekly. The fasting serum parameters were measurd 8 weeks (56 days) after diet feeding. (Fig. 4.5)

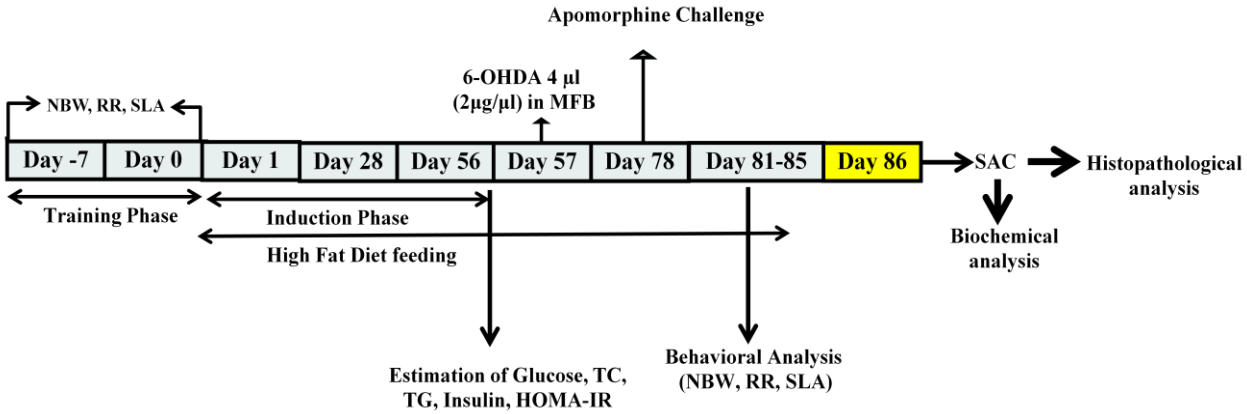

Fig. 4.5 Experimental Schedule for HFD feeding and 6-OHDA administration (Note: **RR:** Rotarod, **SLA:** Spontaneous locomotor activity; **NBW:** Narrow Beam Walk; **TC:** total Cholesterol; **TG:** Triglycerides; **HOMA-IR:** homeostatic model assessment of insulin resistance; **MFB:** Medial Forebrain bundle; **6-OHDA:** 6-hydroxydopamine; **SAC:** Sacrifice).

4.7.1.2. Administration of 6-OHDA into Medial forebrain bundle: 8 weeks after beginning the diet, the rats received a unilateral 6-OHDA lesion in the medial forebrain bundle (MFB). We choose to inject the toxin into the MFB because this approach induces degeneration in striatal terminals before dopaminergic neuron cell death occurs (Saree et al.,

2004). It has been reported that injection of 6-OHDA into the MFB results in a complete loss of dopamine content in the striatum (Fig. 4.6) (Saree et al., 2004).

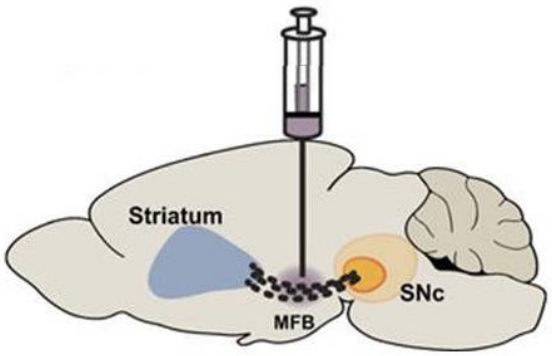

Fig.4.6. Illustration of the site of stereotaxic injection in the MFB: Fig shows dopaminergic fibers connecting the striatum and the SNpc (De Jesus-Cortes et al., 2015)

6-OHDA was dissolved in a solution of 0.02 % w/v ascorbic acid in 0.9% w/v sterile saline preventing heat and light exposure. Briefly, rats were anesthetized using ketamine (80 mg/kg, i.p.) and xylazine (5 mg/kg i.p.) and placed into a stereotaxic frame (Inco, Ambala). Since 6-OHDA damages both dopaminergic and noradrenergic axons in the MFB, we administered desipramine (25 mg/kg i.p.) 30 mins prior to surgical procedure in rats in order to prevent the damage to noradrenergic neurons. A midline saggital incision was made in the scalp and bregma was determined. A dental drill was used to make a hole through the skull. All the rats except vehicle control were infused with 6-OHDA unilaterally into the right MFB using following coordinates: −4.4 mm posterior to bregma; 1.2 mm lateral to sagittal suture and −7.8 mm ventral from the surface of the brain (Paxinos and Watson, 1986). 6-OHDA was injected at a rate of 1 µl/min, and the syringe was left in place for 5 min after injection before being drawn back. Vehicle treated rats received ascorbic acid- saline solution following the same procedures. Immediately after surgery, the rats were injected with gentamicin (5 mg/kg i.p.) and housed individually in polypropylene cages for a week, and then they were re-grouped in their home cages.

4.7.1.3.Apomorphine Challenge: Three weeks (21 days) following 6-OHDA infusion rats were treated with apomorphine (3 mg/kg i.p.) to check rotational behavior response. Apomorphine shows a characteristic contralateral turning behavior when the supersensitive receptors in the lesioned side of the brain are activated and the rats starts showing turning behavior to the contralateral side. The number of contralateral rotations was counted for 30

min. Dopamine deafferentation was considered successful in those animals that made at least 50 contralateral rotations within 20 min of the apomorphine injection.

Experimental Schedule: Following model validation by apomorphine challenge. The selected animals were divided into four groups and behavioral and biochemical estimations were performed.

Group	Treatment
1	NPD + 4 µl vehicle in right MFB
2	NPD + 4 µl 6-OHDA (2 µg/µl) in right MFB
3	HFD + 4 µl vehicle in right MFB
4	HFD + 4 µl 6-OHDA (2 µg/µl) in right MFB

Table 4.3 Experimental groups for studying the effect of HFD feeding and 6-OHDA administartion in rats (**Note:** Vehicle = ascorbic acid-saline solution)

4.7.2. Pharmacological screening of GSK3β inhibitors and HDAC inhibitors in insulin resistance induced PD pathology animal model

The model standardized by above protocol was then used for screening GSK3β inhibitors and HDAC inhibitors. The schedule for treatment phase is in Fig. 4.7.

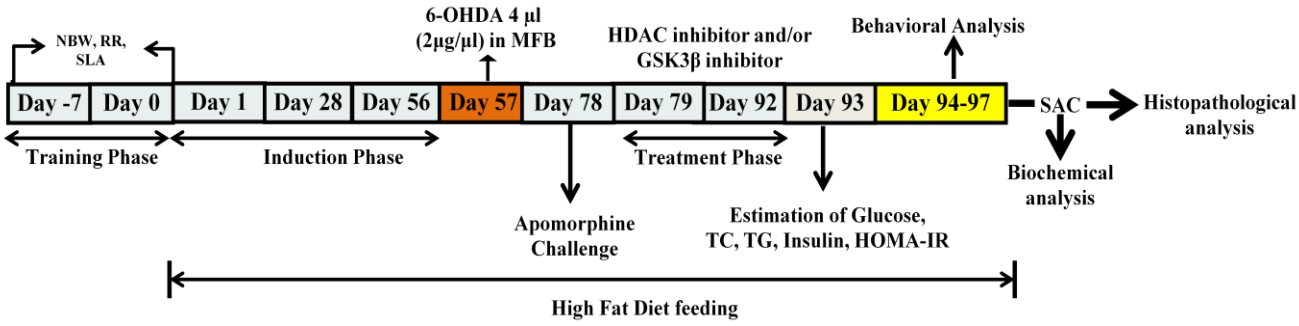

Fig. 4.7 Experimental Schedule for treatment by GSK3β inhibitors and HDAC inhibitors in HFD + 6-OHDA administered rats.
(Note: **RR:** Rotarod, **SLA:** Spontaneous locomotor activity; **NBW:** Narrow Beam Walk; **TC:** total Cholesterol; **TG:** Triglycerides; **HOMA-IR:** homeostatic model assessment of insulin resistance; **MFB:** Medial Forebrain bundle; **6-OHDA:** 6-hydroxydopamine; **SAC:** Sacrifice).

4.7.2.1. Test compounds screened in insulin resistance induced PD pathology

Category	Compound	Vehicle	Doses and route of administration	References
Pan HDAC inhibitors	**SAHA**	12.5% v/v DMSO in saline.	25, 50 mg/kg **(i.p.)**	Faraco et al., 2006; Guan et al., 2009
Non specific GSK3β inhibitor	**Indirubin-3-monoxime**	2.5% v/v DMSO in saline	0.2, 0.4 mg/kg **(i.p.)**	Yadav et al., 2012

Table 4.4 Test Compounds Screened in insulin resistance induced PD pathology

4.8. Blood Collection and serum isolation

Blood was collected using retro-orbital method. Each animal was hand restrained, the neck was gently scuffed and the eye was made to bulge. A glass capillary was inserted. Blood was allowed to flow by capillary action into the eppendorf tube. After collection of required volume, the blood flow was stopped by applying gentle pressure on eye. The tubes were then centrifuged at 4000 rpm, 4°C for 20 min and the serum was separated in another eppendorf tube.

4.9. Serum metabolic parameters

Serum glucose, triglycerides (TGs), total cholesterol (TC) and HDL-cholesterol levels were measured using commercially available kits as per manufacturer's instructions. Serum Insulin was estimated using Ultra sensitive rat/mice insulin ELISA kit (Catalogue no 90060). Insulin sensitivity was estimated using the HOMA-IR (Homeostatic model assessment of insulin resistance) index which is an arithmetic way of deriving indices of peripheral tissue insulin resistance. HOMA-IR was derived using online calculator at https://www.dtu.ox.ac.uk/homacalculator (Akagiri et al., 2008).

4.10. Oral glucose tolerance test (OGTT)

In OGTT, the animals received (20% w/v) glucose solution (2 g/kg) through oral gavage after overnight fasting. Blood glucose level estimation was done from the tail vein using Accu check glucometer at 0, 15, 30, 60 and 120 min after glucose administration (Akagiri et al., 2008).

4.11. Behavioral assessment for cognitive function

4.11.1. Morris water maze (MWM)

Rationale: MWM is one of the most widely used behavioral tests for studying spatial learning and memory. In the MWM task, the animal learns to swim in a water tank, guided by external cues, and find (and climb up to) a submerged platform. Based upon spatial information, the animal learns how to escape to a platform, so this task may be classified as explicit, associative memory with operant-like spatial learning. Rats and mice are natural swimmers, but in this task they just want to get out of the water (Morris, 1984). This simple yet powerful maze design can be used to assay cognitive function, study animal models of neurodegenerative disease, and test potential drug therapies (Bromley-Brits et al., 2011).

Procedure: In our study, MWM consisted of a circular water tank (120 cm diameter, 60 cm height) filled with water (27±1 °C) to a depth of 40 cm and the tank was divided essentially into four equal quadrants such as south-west (SW), south-east (SE), north-east (NE) and north-west (NW) (Fig. 4.8).

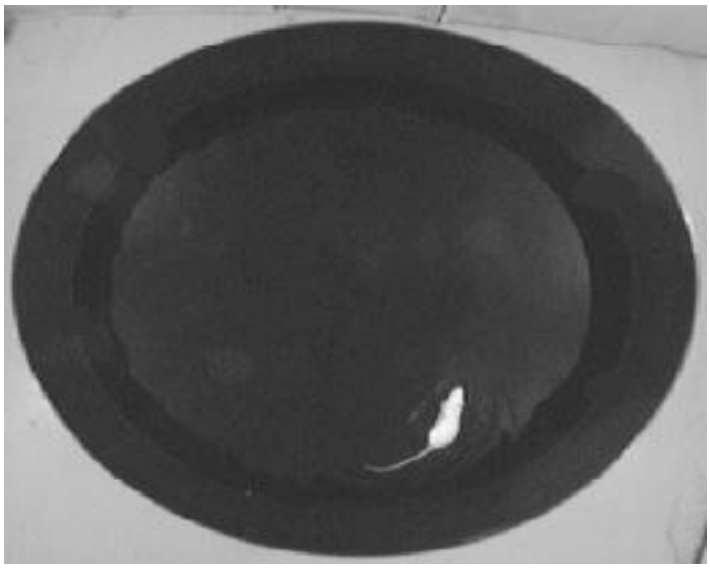

Fig.4.8. The pictorial representation of the Morris Water Maze

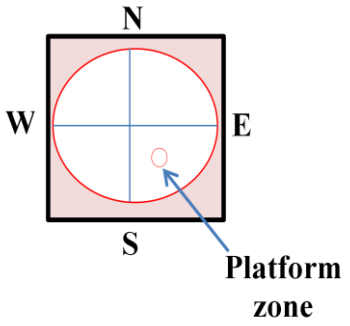

Fig.4.9. Location of various zones in Morris Water Maze

The escape platform (10 cm * 5 cm) was placed 2 cm below the water surface in the middle of one of the randomly selected quadrants of the pool and kept in the same position throughout the entire experiment (south-east for this study) (Fig. 4.9). Before the training started, the animals were allowed to swim freely into the pool for 60 s without platform. Animals received a training session consisting of 4 trials per session (once from each starting point) for 4 days, each trial having a ceiling time of 60 s. After climbing onto the hidden platform, the animals remained there for 30 s before commencement of the next trial. If the animal failed to locate the hidden platform within the maximum time of 60 s, it was gently placed on the platform and allowed to remain there for the same interval of time (Datusalia and Sharma, 2014). The time taken to locate the hidden platform (latency in seconds) was calculated using ANY- maze video tracking system (Stoelting, USA). The various start points used over a period of 4 days during training sessions are listed in Table. 4.5.

Day	**Starting Zone**			
	Trial 1	**Trial 2**	**Trial 3**	**Trial 4**
1	N	W	SW	NE
2	SW	N	NE	W
3	NE	SW	W	N
4	W	NE	N	SW

Table. 4.5. Starting location for various trials in MWM

4.11.2. Probe trial

To assess reference memory at the end of learning, a probe trial was performed. Twenty-four hours after the last navigation trial in MWM, each animal was subjected to a probe trial. Briefly, during the probe trial, the hidden platform was removed and the animal was released from one of the quadrants (NW for this study) and allowed to swim freely for 60 s. The time spent in the target quadrant, where the platform had been located during training session was taken as measures for spatial memory (Datusalia and Sharma, 2014).

4.11.3. Passive avoidance task

Rationale: Passive avoidance involves learning to inhibit a response in order to avoid an aversive stimulus, and the learning (training) session may be one-trial or multi-trial. Since there is punishment to the natural exploratory drive of a rodent with a non-lethal, electric footshock, this is clearly an aversive task.

Procedure: The passive avoidance task was performed as described previously by (Deshmukh et al., 2009). Briefly, the apparatus is divided into two compartments, one illuminated and one dark, both equipped with a shock scrambler grid floor (Fig. 4.10). Both the compartments were separated by a guillotine door.

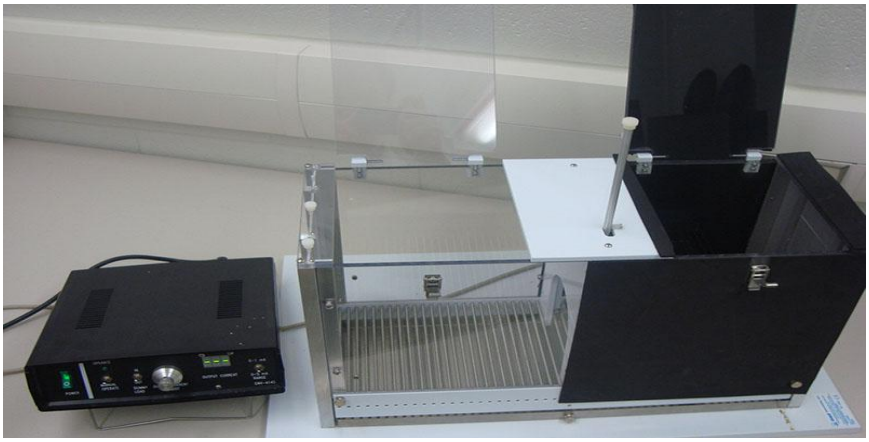

Fig.4.10. The pictorial representation of the Passive Avoidance Apparatus

During the acquisition trial, each animal was placed in the illuminated compartment. After 60 s of habituation a guillotine door separating the lighted and dark chambers was opened and the initial latency to enter the dark chamber was recorded. Animals that had an initial latency period of more than 60 s were excluded from further study. As soon as the animal entered the dark compartment, the door was closed and an electric foot shock (50 V, 0.2 mA, 50 HZ) was delivered through floor grids for 3 s. The animal was then removed from the dark chamber 5 s later and placed back into its home cage. Retention latency was measured 24 h later in the same way as in the acquisition trial, but foot shock was not delivered. The latency time was recorded to a maximum of 300 s. Short latencies indicated poorer retention (Deshmukh et al., 2009). The apparatus was cleaned with dilute (70 % v/v) alcohol and dried between trails.

4.11.4 Novel Object Recognition (NOR) task

Rationale: Recognition is defined as the process by which a subject is aware that a stimulus has been previously experienced. It is strongly dependent on memory, since it requires a series of cognitive operations (such as perception, discrimination, identification and comparisons) that rely on previously known information in order to "match" the observed event against a memory of the previously experienced ones (Quillfeldt, 2010).

Procedure: The NOR task evaluates the rodents ability to recognize a novel object in the environment. The procedure consists of three phases: habituation, familiarization, and test phase. In the habituation phase, each animal was allowed to freely explore the open-field arena in the absence of objects for 5 minutes for 2 consecutive days (Fig.4.11).

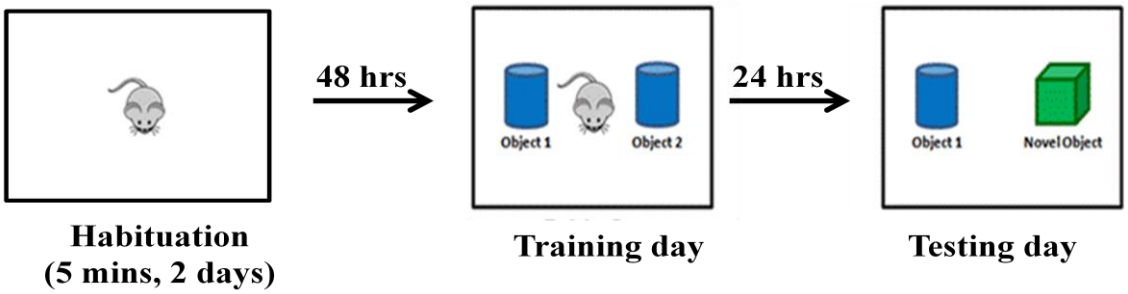

Fig. 4.11. Protocol for Novel Object Recognition task

The animal was then removed from the arena and placed in its home cage. During the familiarization phase, each animal was placed in the open-field arena containing two identical sample objects for 5 minutes. Twenty four hours later during the test phase, the animal was returned to the open-field arena with two objects, one was identical to the sample and the other was novel (Ennaceur 2010). During both the familiarization and the test phase, objects were located in opposite and symmetrical corners of the arena. The time spent by each animal exploring the novel and familiar object was recorded for duration of 5 minutes (Antunes and Biala, 2012).

4.12. Behavioral assessment for motor function

4.12.1. Spontaneous locomotor activity: Locomotor activity was performed as per method described by Kumar and colleagues (Kumar et al., 2015). Each animal was tested for spontaneous locomotor activity over a period of 10 min in a square closed arena (30×30 cm^2) equipped with infrared light sensitive photocells using a digital actophotometer (INCO, India) (Fig. 4.12). The apparatus was cleaned with dilute (70 % v/v) alcohol and dried between trails.

Fig. 4.12. The pictorial representation of the actophotometer

4.12.2. Narrow beam walk test

Rationale: Fine motor coordination and balance can be assessed by the beam walking assay. The goal of this test is for the animal to stay upright and walk across an elevated narrow beam to a safe platform. Performance on the beam is quantified by measuring the time it takes for the animal to transverse the beam and the number of paw slips that occur in the process (Luong et al., 2010).

Procedure: Gait abnormalities and foot slip count was measured by narrow beam walk apparatus as per previous methods (Sharma and Deshmukh, 2015). Briefly, the apparatus consists of a horizontal narrow beam (1 cm×100 cm) suspended 1m above a foam-padded cushion. A home cage painted with black colour was placed at the end of the beam as the finish point. Time taken to cross the beam was measured by stopwatch manually (Fig. 4.13).

Fig.4.13. The pictorial representation of Narrow beam walk test apparatus

During testing, the rats were given 60s to transverse the beam. The latency to cross the beam along with the number of foot slips was recorded. If the rats did not complete the task or if

they fall off the beam or freeze, then they were assigned a maximum latency of 60s to cross the beam and maximum 5 foot slips.

4.12.3. Rotarod activity

Rationale: The rotarod task is more commonly used for motor function assessment in animal models of PD. It is an easily quantifiable test, in which animals try to maintain balance on a rotating rod with a diameter markedly smaller than their body length. Time to fall off the rod is recorded. By adding constant acceleration, task complexity can be increased (Buitrago et al., 2004).

Procedure: Motor coordination was assessed using an automated rotarod apparatus. Rota rod motor training was performed at the beginning of the experiment. The apparatus (Inco, Ambala, India) consists of a metal rod of 4 cm in diameter, 75 cm in length with 6 equally divided sections. Each rat was tested on the rotarod apparatus. Rats had to keep their balance on a rotating rod set at a speed of 15 rpm for a maximum of 300s. The latency to fall from the rod was recorded (Sharma and Deshmukh, 2015).

4.12.4. Cylinder Test

Rationale: The limb-use asymmetry (cylinder) test, which measures weight-bearing forelimb movements during rearing, has been well reported to be a good indicator of nigrostriatal cell loss in unilateral 6-OHDA injected rats and mice (Schallert et al., 2000).

Procedure: In cylinder test, the rats were placed in a glass cylinder (20 cm diameter and 30 cm height) and recorded for 5 minutes. The cylinder was placed next to a mirror in order to visualize limb use movements from all angles. Forelimb asymmetry was assessed by scoring independent, weight-bearing contacts on the cylinder wall of the ipsilateral (ipsi) or contralateral (contra) paw, relative to lesioned hemisphere, as well as movements made by both paws (both). The percentage of ipsilateral and contralateral touches, relative to the total number of touches (ipsi+contra+both = total), was calculated.

4.13. Biochemical parameters

All the biochemical parameters were measured in either hippocampus or striatal homogenate after sacrificing the animals depending upon the study objective.

4.13.1. Hippocampus/Striatum homogenate preparation

Animals were sacrificed by decapitation and brains were removed and rinsed with ice-cold (0.9% w/v Nacl) isotonic saline. The hippocampus (or striatum) region of brains was dissected and then homogenized with ice cold 0.1 M phosphate buffer (pH 7.4) in a volume

10 times (w/v) the weight of tissue. The homogenate was centrifuged at 12,000 g for 15 min (4 °C) and aliquots of supernatant were separated and used for biochemical estimations.

4.13.2. Protein determination

Protein content in brain hippocampus (or striatum) samples was measured by the method of Lowry using bovine serum albumin (BSA) (1 mg/ml) as a standard (Lowry et al. 1951).

4.13.3. Estimation of Reduced Glutathione (GSH) level

The level of GSH in striatal homogenate was estimated according to the method described by Ellman (Ellman, 1959). One ml supernatant was precipitated with 1 ml of 4% sulfosalicylic acid and cold digested at 4 °C for 1 h. The samples were centrifuged at 1200 g for 15 min. To 1 ml of the supernatant, 2.7 ml of phosphate buffer (0.1M, pH 8) and 0.2 ml of 5,5′ dithiobis (2-nitrobenzoic acid) (DTNB) were added. The yellow color that developed was measured immediately at 412 nm using a spectrophotometer. The concentration of glutathione in the supernatant was determined from a standard curve and expressed as µmol per mg protein.

4.13.4. Estimation of Malondialdehyde (MDA) level

The quantitative measurement of MDA–end product of lipid peroxidation was performed according to the method of Wills (Wills, 1966). The amount of MDA was measured after its reaction with thiobarbituric acid at 532 nm using spectrophotometer (Shimadzu, UV-1700). The concentration of MDA was determined from a standard curve and expressed as nmol per mg protein.

4.13.5. Estimation of Nitrite level

The accumulation of nitrite in the supernatant, an indicator of the production of nitric oxide (NO), was determined by a colorimetric assay using Greiss reagent (0.1% N-(1-naphthyl) ethylenediamine dihydrochloride, 1% sulfanilamide and 2.5% phosphoric acid) as described by (Green et al., 1982). Equal volumes of supernatant and Greiss reagent were mixed, the mixture incubated for 10 min at room temperature in the dark and the absorbance was determined at 540 nm spectrophotometricaly. The concentration of nitrite in the supernatant was determined from sodium nitrite standard curve and expressed as µmol/ mg protein.

4.13.6. Estimation of Acetylcholinesterase (AChE) activity

The quantitative measurement of acetylcholinesterase activity in brain was performed according to the method described by Ellman (Ellman et al., 1961). In brief, the assay mixture contained 0.05 ml of supernatant, 3 ml of 0.01 M sodium phosphate buffer (pH 8),

0.10 ml of acetylthiocholine iodide and 0.10 ml of DTNB (Ellman reagent). The change in absorbance was measured immediately at 412 nm spectrophotometrically. Results were expressed as nmol per mg protein.

4.14. Estimation of Pro-inflammatory cytokine TNF-α level

Hippocampus or striatum homogenates were used to estimate the level of pro-inflammatory cytokine (TNF-α) using ELISA kit. The levels of TNF-α was determined according to the manufacturer's instructions (Sigma–Aldrich, USA, Catalog no. RAB0480).

4.15. Estimation of Brain Derived Neurotrophic Factor (BDNF) level

BDNF level was determined in hippocampus (or striatum) homogenates by using a commercially available ELISA kit as per manufacturer's instructions (Boster Biological Tech. Co., LTD, CA, USA, Catalog no. EK0308).

4.16. Estimation of Global histone H3 acetylation level

The level of Global Histone H3 acetylation was estimated by using EpiQuik™ Global Histone H3 Acetylation Assay Kit as per manufacturer's instruction (Catalog no. P-4008). Briefly, the protocol consists of three parts: Nucleic Extraction Preparation, Histone Extraction and Histone H3 Acetylation Detection. First, the nucleic extraction was performed by homogenizing the hippocampus (or striatum) with lysis buffer. Then, the histone proteins were extracted using the extraction buffer. At the end of histone extraction procedure, the protein concentration was measured using lowry's method. After this, the histone proteins were stably spotted on the strip wells. The acetylated histone H3 was recognized with a high-affinity antibody. The amount of acetylated histone H3 was quantified through HRP conjugated secondary antibody-color development system and was proportional to the intensity of color development.

4.17. Estimation of Amyloid-β $_{(1-42)}$ level

Amyloid-β $_{(1-42)}$ level was determined in hippocampus homogenates by using a commercially available ELISA kit as per manufacturer's instructions (YH Bioscience, China, Catalog no. YHB0080Mo).

4.18. Estimation of phosphorylated tau (p-tau) level

p-tau level was determined in hippocampus homogenates by using a commercially available ELISA kit as per manufacturer's instructions (YH Biosearch, China, Catalog no. YHB1501Mo).

4.19. Estimation of CREB level

CREB level was determined in homogenates by using a commercially available ELISA kit as per manufacturer's instructions (YH Biosearch, China, Catalog no. YHB1516Mo).

4.20. Estimation of Dopamine level

Dopamine level was determined in striatum homogenates by using a commercially available ELISA kit as per manufacturer's instructions (USCN life sciences, Houston, USA, Catalog no. CEA851Ge).

4.21. Estimation of Glycogen Synthase Kinase 3 β (GSK3β) level

The measurement of GSK 3β level was performed using a commercially available ELISA kit (YH Biosearch Laboratory, Shanghai, China), according to the manufacturer instructions (Catalog no. YHB0639Mo).

4.22. Assessment of histopathological changes

The brains were rapidly removed and fixed by immersion in 10 % v/v formalin. Subsequently they were embedded in paraffin wax, cut into 5 μm thick sections followed by standard steps of rehydration. These sections were stained with haematoxylin eosin stain (H & E) and further standard steps of dehydration; clearing and coverslipping were performed (Amin et al., 2013). Hippocampus (CA1 and dentate gyrus (DG)) regions as well as striatal regions of brain were examined under bright field illumination using "Optika TCB5" microscope (Optika Research Microscope, Italy) at total magnification of 100X, 400X and 1000X. H&E stained photomicrographs were imported into Image J software (NIH-sponsored public domain image analysis software). Neurons showing degenerating features were counted using the Image J cell counter tool and expressed as the percentage of degenerating neurons.

4.22.1. Standardization of Histological examination of Dentate gyrus and CA1 neurons

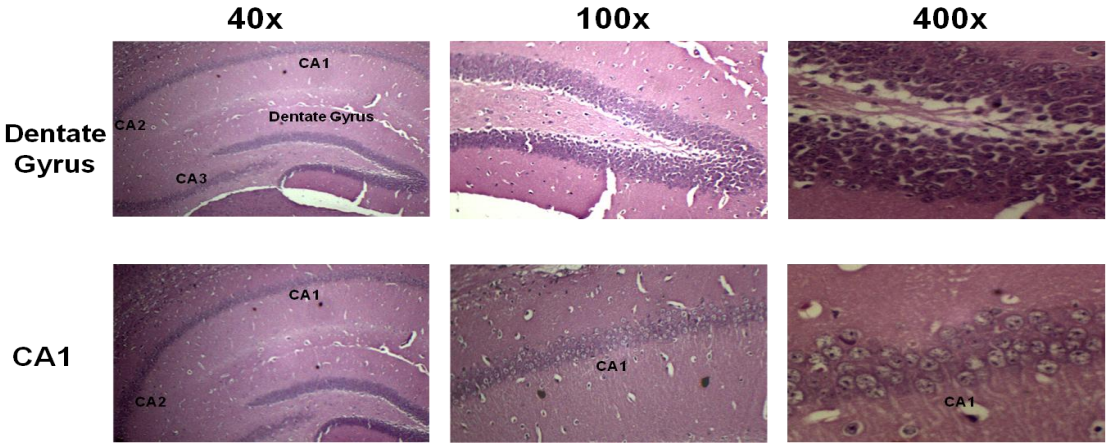

Fig. 4.14. Histological images of dentate gyrus and CA1 neurons stained with Haematoxylin and Eosin stain

4.22.2. Standardization of Histological examination of striatal neurons

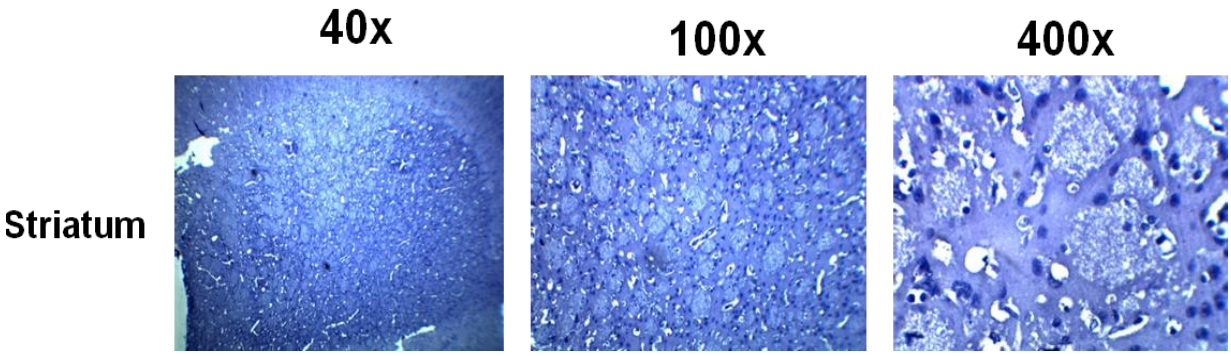

Fig. 4.15. Histological images of striatum neurons stained with Haematoxylin and Eosin stain

4.23. DNA Fragmentation Detections

The evaluation of apoptosis in hippocampal (dentate gyrus and CA1) regions was performed on paraffin-embedded tissues using a QIA33 FragEL DNA Fragmentation Detection Kit, using colorimetric detection and terminal deoxynucleotidyltransferase [TdT] enzyme for a labelling TUNEL assay; Calbiochem/Merck Chemicals, (Darmstadt, Germany). The procedures were performed according to manufacturer's instructions. After labeling and counter stain reactions, the hippocampus regions (CA1 and dentate gyrus) were examined

under bright field illumination using “Optika TCB5” microscope (Optika Research Microscope, Italy) at total magnification of 100X, 400X.

4.24. Statistical Analysis

The results are expressed as mean ± SEM. The behavioral and biochemical parameters were analyzed by one-way analysis of variance (ANOVA) followed by Tukey's post hoc test or two way ANOVA followed by Bonferroni post hoc test using statistical GraphPad Prism software (version 5.0, La Jolla, CA, USA). In case of the object recognition task, unpaired Student's *t*-test was used to analyze the preference for the novel object. $P < 0.05$ was set to be statistically significant.

5.1. Development of HFD induced insulin resistance model

5.1.1 Effect of HFD feeding for different time intervals on body weight, serum glucose and serum insulin

The mice fed with a HFD showed a gradually increased body weight as compared to NPD fed mice (Fig. 5.1a). However, a significant difference in body weight between HFD and NPD fed mice was first evident at 4 weeks after diet feeding ($P < 0.05$). Similarly, increased body weight in HFD mice was observed at 6 weeks ($P < 0.001$) and at 8 weeks ($P < 0.001$) after diet feeding (Fig. 5.1a).

The serum glucose levels were found to be gradually increased in HFD fed mice as compared to NPD fed mice over the entire duration of diet feeding (Fig. 5.1b). Moreover, a statistically significant difference was first evident at 4 weeks after diet feeding ($P < 0.01$). Similarly, increased serum glucose level was also observed at 6 weeks ($P < 0.01$) and 8 weeks after diet feeding ($P < 0.001$).

(a) Body weight **(b) Serum Glucose**

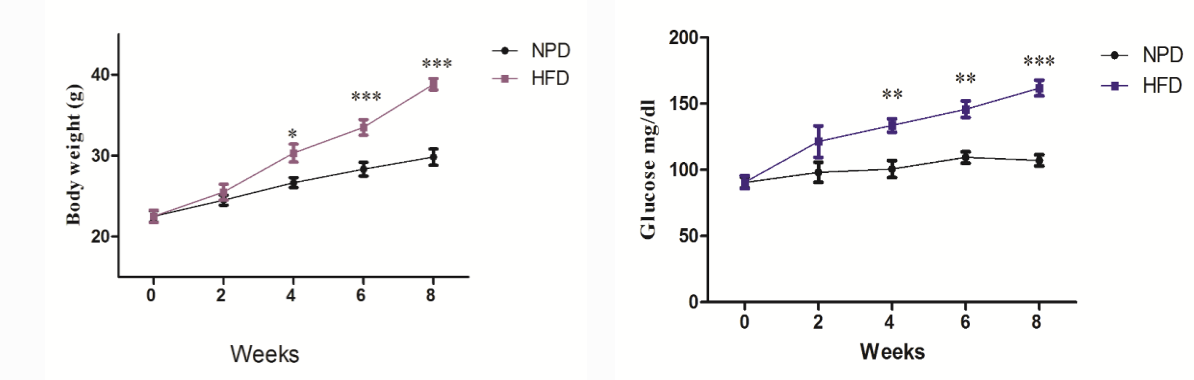

(c) Serum insulin

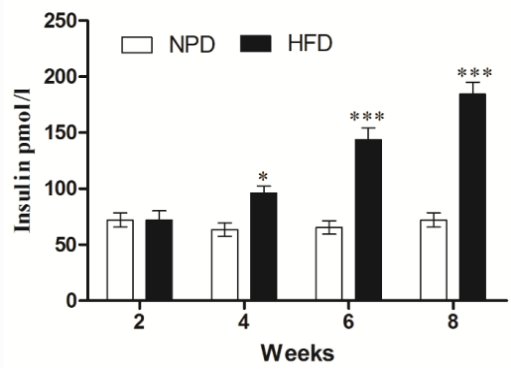

Fig.5.1 Effect of HFD feeding on (a) body weight (*P< 0.05 vs NPD); (***P< 0.001 vs NPD) **(b) serum glucose** (**P< 0.01 vs NPD); (***P< 0.001 vs NPD) **(c) Serum insulin** (*P< 0.05 vs NPD); (***P< 0.001 vs NPD) (n=6).

Serum Insulin level remains unchanged at 2 weeks after HFD feeding but were significantly increased at 4 weeks ($P < 0.05$) and 6 weeks ($P < 0.001$) after HFD feeding. This increased serum insulin level persists even at 8 weeks after diet feeding ($P < 0.001$) (Fig. 5.1c).

5.1.2. Effect of HFD feeding for different time intervals on lipid profile (total cholesterol, triglycerides, LDL-cholesterol)

No significant differene in total cholesterol and triglyceride level was observed in HFD and NPD groups until 2 weeks (Fig. 5.2a, 5.2b). However, HFD feeding results in significant increase in both total cholesterol and triglyceride level as compared with NPD fed mice at 4 weeks after diet feeding ($P < 0.01$). Similarly, increased total cholesterol ($P < 0.001$) and triglyceride level ($P < 0.01$) was observed at 6 weeks and 8 weeks ($P < 0.001$) after diet feeding.

(a) Total Cholesterol **(b) Triglycerides**

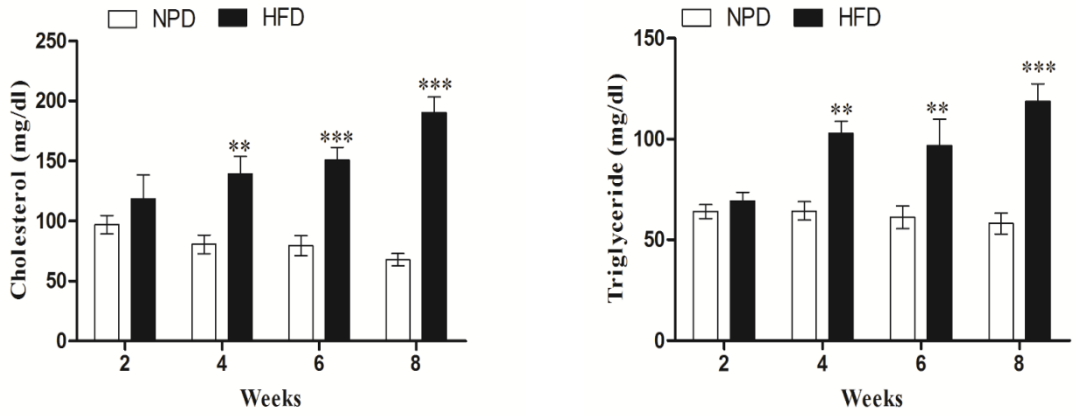

(c) LDL-cholesterol

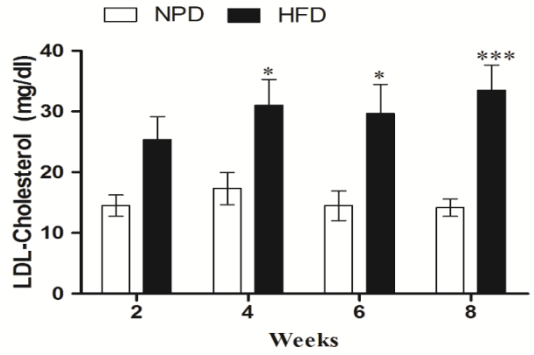

Fig. 5.2 Effect of HFD feeding **(a) serum total cholesterol** (**P< 0.01 vs NPD); (***P < 0.001 vs NPD) **(b) triglyceride** (**P < 0.01 vs NPD); (***P< 0.001 vs NPD) **(c) LDL-cholesterol** (*P< 0.05 vs NPD); (***P < 0.01 vs NPD) (n=6).

Although elevated level of LDL-cholesterol was observed in HFD fed mice at 2 weeks as compared to NPD fed mice, however the results were not statistically significant (Fig. 5.2c).

At 4 weeks after HFD feeding, we observed a significant increase in LDL- cholesterol level as compared to NPD fed mice ($P < 0.05$). Similarly, increased LDL-cholesterol level was observed at 6 weeks ($P < 0.05$) and 8 weeks ($P < 0.001$) after HFD feeding.

5.1.3. Effect of HFD feeding on HOMA-IR level on different time intervals

The changes in circulating glucose and insulin levels induced by HFD were further reflected in a significant increase in the HOMA-IR index, a quantitative measure of insulin resistance. Significant increase in HOMA-IR was first evident at 4 weeks after diet feeding ($P < 0.05$) and further augmented at 6 weeks ($P < 0.001$) and 8 weeks ($P < 0.001$) after HFD feeding as compared to NPD fed mice (Fig. 5.3).

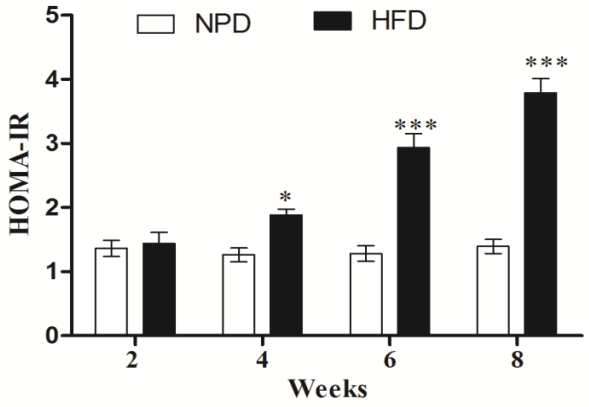

Fig.5.3 Effect of HFD feeding on HOMA-IR levels (*P< 0.05 vs NPD); (***P < 0.01 vs NPD) (n=6).

5.2. Effect of HFD feeding for different time intervals on cognitive and motor activities

5.2.1. Effect of HFD feeding on mean escape latency in morris water maze

2 weeks after the HFD feeding, the mice were subjected to morris water maze (MWM) task. No significant difference was observed in mean escape latency in HFD fed mice as compared to NPD fed mice at any of the test days (Fig. 5.4a).

4 weeks after HFD feeding, no significant difference in mean escape latency was observed between HFD and NPD fed mice during day 1 and day 2 of MWM task. However, significant difference was observed in mean escape latency on day 3 and day 4 between NPD and HFD fed mice ($P < 0.05$). The mice fed with NPD were able to find the hidden platform in lesser time as compare to HFD fed mice (Fig. 5.4b).

(a) 2 Weeks HFD feeding

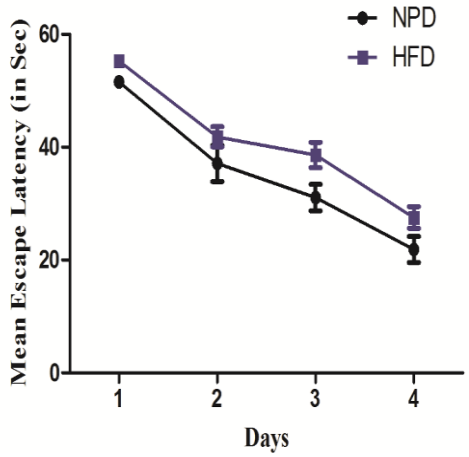

(b) 4 Weeks HFD feeding

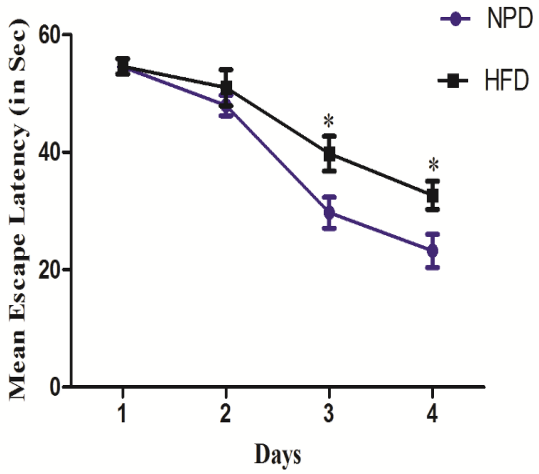

(c) 6 Weeks HFD feeding

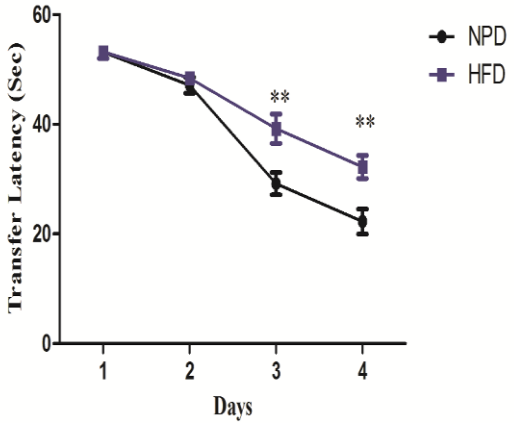

(d) 8 Weeks HFD feeding

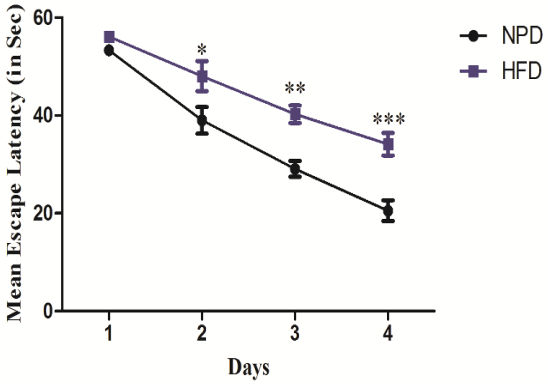

Fig. 5.4 Effect of HFD feeding on mean escape latency in morris water maze on different time intervals (a) 2 weeks after HFD feeding **(b) 4 weeks** after HFD feeding (*P< 0.05 vs NPD) **(c) 6 weeks** after HFD feeding (**P< 0.01 vs NPD) **(d) 8 weeks** after HFD feeding (*P< 0.05 vs NPD); (**P< 0.01 vs NPD); (***P < 0.001 vs NPD) (n=6).

Moreover, it was observed that 6 weeks after diet feeding, the HFD fed mice exhibit no significant difference in mean escape latency as compared with NPD fed mice on day 1 and day 2 (Fig. 5.4c). However, significant difference was observed in mean escape latency on day 3 ($P < 0.01$) and day 4 ($P < 0.01$) between NPD and HFD fed mice.

Similar results were observed after 8 weeks of HFD feeding. Although, no significant difference was observed in performance on day 1 between HFD fed mice and NPD fed mice (Fig. 5.4d). However, a significant difference in mean escape latency was observed on day 2 ($P < 0.05$), day 3 ($P < 0.01$) and day 4 ($P < 0.001$).

5.2.2. Effect of HFD feeding on locomotor activity of animals in actophotometer

No significant effect of HFD feeding was observed on locomotor activity of animals during different time intervals (Fig. 5.5).

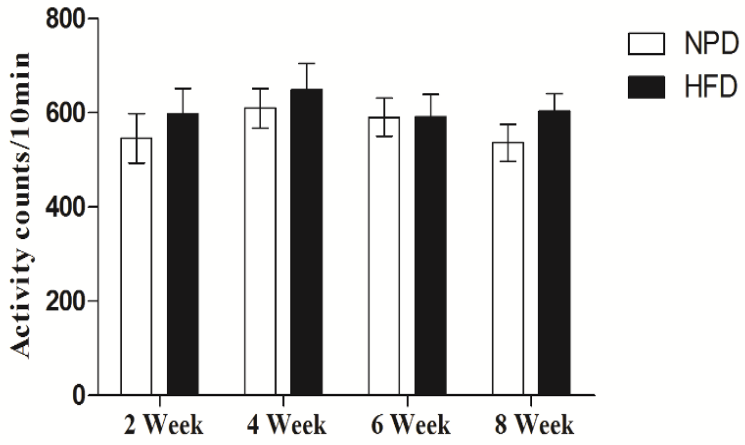

Fig. 5.5 Effect of HFD feeding on spontaneous locomotor activity.

5.3. Effect of NPD and HFD feeding for different time intervals on hippocampus (dentate gyrus and CA1) neurons

Healthy neurons were observed in both DG and CA1 regions of hippocampus after 8 weeks of NPD feeding. These healthy neurons appeared robust in shape, had a spherical or slightly oval nucleus and a single large nucleolus with clear visible cytoplasm as indicated by yellow arrows (Fig. 5.6).

8 weeks NPD feeding

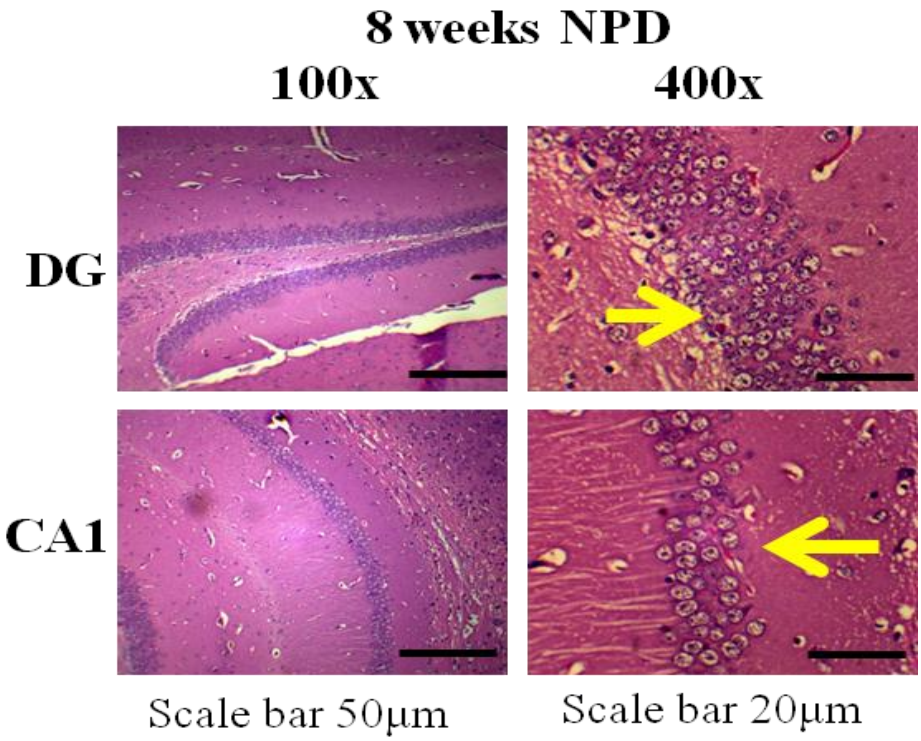

Fig.5.6 Effect of NPD feeding for 8 weeks on dentate gyrus and CA1 region of hippocampus Healthy neurons are indicated by yellow arrows.

Neuronal death was observed in some of the DG neurons after 2 weeks of HFD feeding, as indicated by red arrows (Fig. 5.7a). However, HFD feeding didn't change the integrity of CA1 neurons. The healthy CA1 neurons appeared robust in shape, had a spherical or slightly oval nucleus and a single large nucleolus with clear visible cytoplasm as indicated by yellow arrows. In contrast, 4 weeks after HFD feeding, neuronal death results in marked changes in CA1 in the form of disorganization and cell loss (Fig. 5.7b).

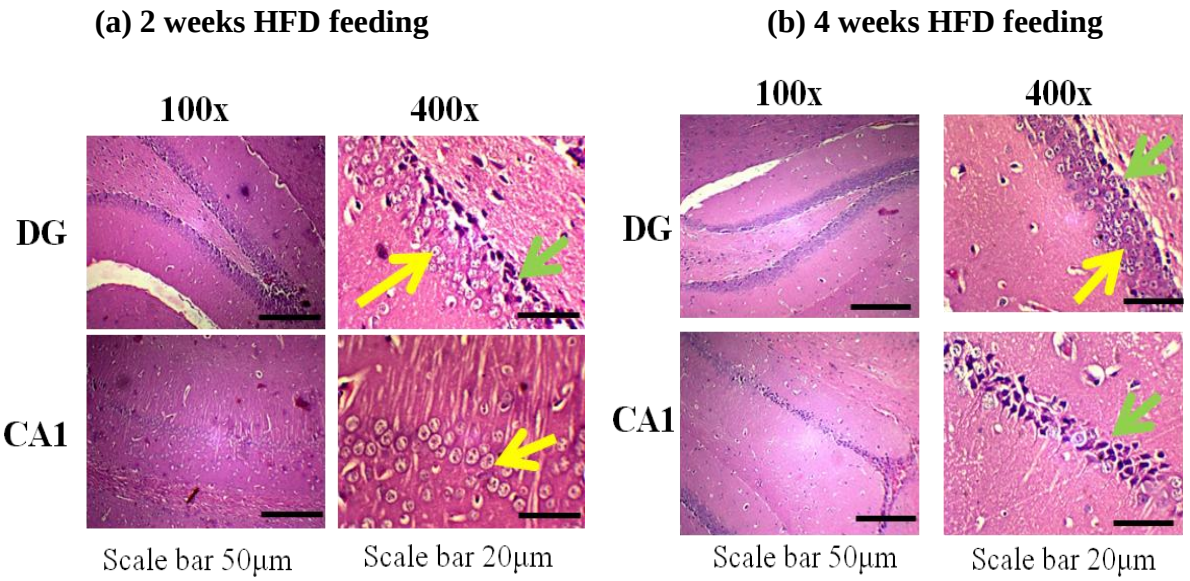

Significant neuronal damage in both DG and CA1 regions was observed at 6 weeks and 8 weeks after HFD feeding (Fig. 5.7c and 5.7d). The neuronal death was characterized by disorganization and cell loss. There was also marked shrinkage in the size of the pyramidal cells with darkened nuclei.

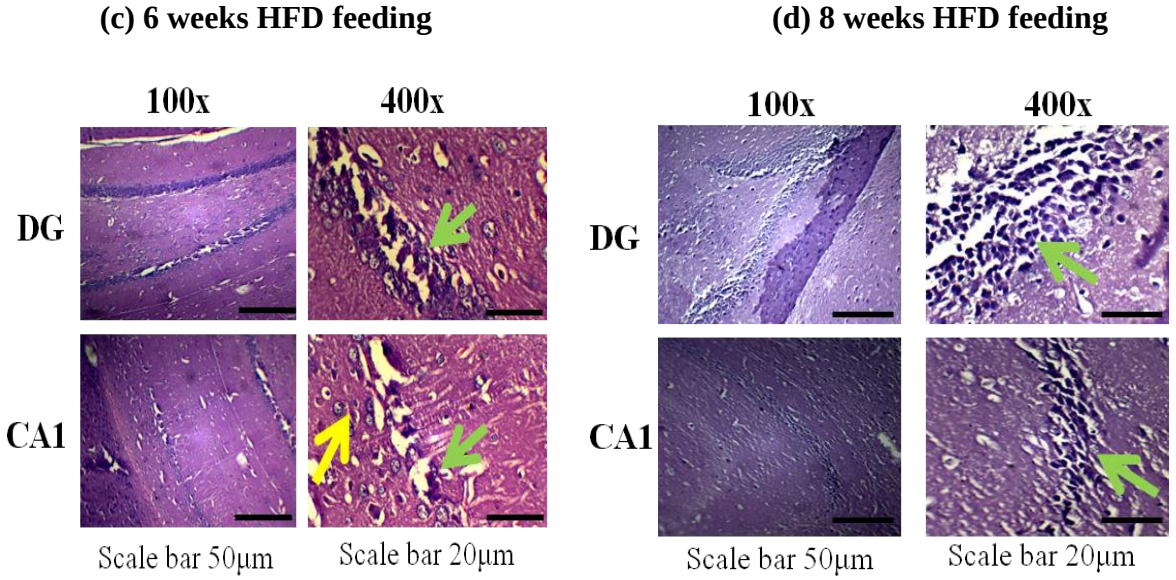

Fig.5.7 Effect of HFD feeding on dentate gyrus and CA1 region of hippocampus (a) 2 weeks HFD feeding (b) 4 weeks HFD feeding (c) 6 Weeks HFD feeding (d) 8 weeks HFD feeding Healthy neurons are indicated by yellow arrows and damaged neurons indicated by red arrows.

5.3.1. Effect of HFD feeding for different time interval on neuronal count in dentate gyrus and CA1 neurons

The neuronal death was evident by increased number of damaged neurons in the DG and CA1 regions of hippocampus at 4 weeks after HFD feeding ($P < 0.01$). Similarly, increased percentage of neuronal damage was observed at 6 weeks ($P < 0.001$) and 8 weeks ($P < 0.001$) after HFD feeding in both DG and CA1 regions as compared to NPD fed mice (Fig.5.8a and 5.8b).

(a) Effect of NPD and HFD feeding on DG neurons

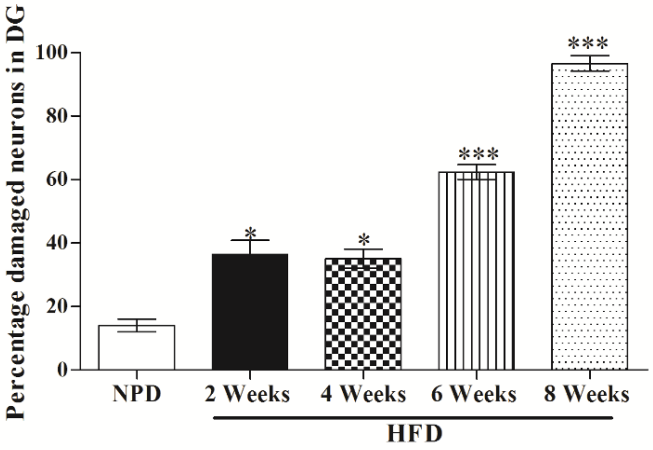

(b) Effect of NPD and HFD feeding on CA1 neurons

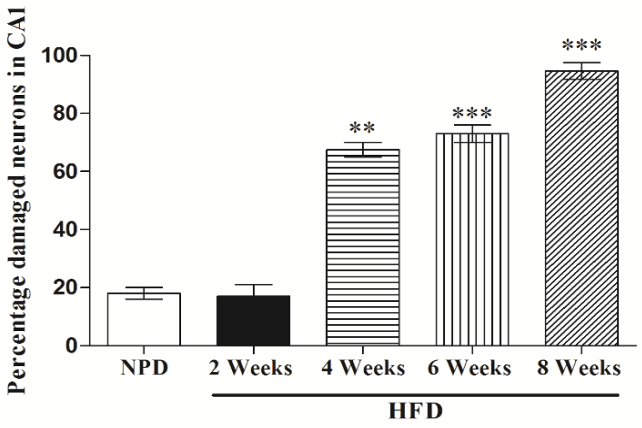

Fig.5.8 Effect of NPD and HFD feeding on neuronal count in (a) dentate gyrus (b) CA1 region Values are indicated as mean ± SEM. (**P< 0.01 vs NPD; ***P <0.001 vs NPD).

5.4. Effect of GSK3β inhibitors on insulin resistance and associated cognitive deficits

5.4.1. Effect of Indirubin-3-monoxime (IMX) on body weight and serum parameters

HFD fed mice gained significantly more weight than the NPD fed mice ($F_{(4,49)}$= 4.41; P < 0.01). In addition, there was a significant increase in serum parameters, characteristic of insulin resistance viz. glucose ($F_{(4,29)}$ =28.72; P < 0.001), Triglycerides (TGs) ($F_{(4,29)}$ = 64.46; P < 0.001), Total cholesterol (TC) ($F_{(4,29)}$ =39.47; P < 0.001) and insulin levels ($F_{(4,29)}$ =38.85; P < 0.001) in HFD fed mice (Table 5.1). Treatment with IMX, reduced the body weight, although not statistically significant at lower doses, but at high dose (0.4 mg/kg) the reduction was statistically significant (P < 0.05). Also, IMX dose dependently attenuated the serum glucose, TGs, TC and insulin levels in HFD fed mice. Moreover, we observed that HFD feeding results in significant increase in HOMA-IR values as compared to NPD fed animals (P < 0.001), indicating insulin resistance condition. In contrast, IMX treatment significantly attenuated HOMA-IR levels as compared to HFD group ($F_{(4,29)}$ =41.76; P < 0.001).

Parameter	**NPD**	**HFD**	**HFD+ IMX (0.1)**	**HFD+IMX (0.2)**	**HFD+ IMX (0.4)**
Body weight (g)	29.90± 4.38	37.6± 4.88[a]	34.8 ± 3.80	34.1 ± 4.67	31.7 ± 4.42[b]
Glucose (mg/dl)	81.17± 9.88	138.0±14.35[a]	129.7±13.44	110.2 ± 7.985[bc]	90.83 ± 8.40[de]
Triglycerides (mg/dl)	53.67± 13.13	201.7±22.23[a]	165.8±19.11[b]	143.7±11.59[c]	113.8 ±17.01[de]
Total Cholesterol (mg/dl)	114.3± 20.56	275.2±29.41[a]	222.3±26.28[b]	174.2± 23.96[cd]	126.7 ± 29.48[ce]
Insulin (pmol/l)	74.25± 5.88	180.8 ± 23.16[a]	150.7 ± 18.79[b]	135.2 ± 17.28[b]	108.0 ± 7.58[cd]
HOMA-IR	1.20 ± 0.17	3.45 ± 0.54[a]	2.88 ± 0.27	2.26 ± 0.27[bc]	1.65 ± 0.32[bd]

Table 5.1 Effect of Indirubin-3'-monoxime treatment on body weight and serum parameters. Values are indicated as mean ± S.D. **Where, Body weight** (^{a}P<0.01 vs NPD; ^{b}P<0.05 vs HFD) (n=10); **Serum Glucose** (^{a}P <0.001 vs NPD; ^{b}P<0.01 vs HFD; ^{c}P<0.05 vs IMX 0.1; ^{d}P< 0.001 vs HFD; ^{e}P<0.05 vs IMX 0.2); (n=6); **Serum Triglycerides** (^{a}P <0.001 vs NPD; ^{b}P<0.05 vs HFD; ^{c}P<0.001 vs IMX 0.1; ^{d}P< 0.001 vs HFD; ^{e}P< 0.05 vs IMX 0.2) (n=6); **Total Cholesterol** (^{a}P <0.001 vs NPD; ^{b}P<0.05 vs HFD; ^{c}P< 0.001 vs HFD; ^{d}P<0.05 vs IMX 0.1; ^{e}P< 0.05 vs IMX 0.2) (n=6); **Insulin** (^{a}P <0.001 vs NPD; ^{b}P<0.05 vs HFD; ^{c}P< 0.001 vs HFD; ^{d}P< 0.05 vs IMX 0.2) (n=6); **HOMA-IR** (^{a}P <0.001 vs NPD; ^{b}P<0.001 vs HFD; ^{c}P<0.05 vs IMX 0.1; ^{d}P<0.05 vs IMX 0.2) (n=6) Note: (IMX= Indirubin-3'-monoxime; NPD= Normal pellet diet; HFD=High fat diet).

5.4.2. Effect of AR-A014418 (AR) on body weight and serum parameters

HFD fed mice gained significantly more weight than the NPD fed mice ($F_{(4,39)}$= 10.87; P < 0.001). In addition, there was a significant increase in serum parameters, characteristic of insulin resistance viz. glucose ($F_{(4,35)}$ =28.49; P<0.001), TGs ($F_{(4,34)}$ = 25.46; P <0.001), TC ($F_{(4,35)}$ =36.38; P < 0.001) and insulin levels ($F_{(4,29)}$ =50.22; P < 0.001) in HFD fed mice (Table 5.2). Treatment with AR-A014418, attenuated the body weight although not statistically significant at low dose (1 mg/kg), but at medium (5mg/kg) and high dose (10 mg/kg), the reduction was statistically significant as compared to alone HFD fed mice. Moreover, AR-A014418 dose dependently attenuated the serum glucose, TGs, TC and insulin levels in HFD fed mice (Table. 5.2). The results showed that HOMA-IR of HFD fed mice were significantly higher than that of NPD fed mice (P < 0.001). AR-A014418 treatment significantly attenuated the HOMA-IR values ($F_{(4,29)}$ = 66.20) as compared to HFD group.

Parameter	NPD	HFD	HFD+ AR (1)	HFD+AR (5)	HFD+ AR (10)
Body weight (g)	30.25± 2.96	38.13± 2.16[a]	36.13± 2.23	33.13.± 3.56[b]	31.88± 2.53[c]
Glucose (mg/dl)	84.01± 12.98	152.8±23.16[a]	146.4±13.64	125.2.±9.45[b]	99.89.±10.75[cd]
Triglycerides (mg/dl)	86.54± 17.81	163.7±22.0[a]	137.6±16.5[b]	127.2.±11.14[c]	95.63.±13.89[de]
Total Cholesterol (mg/dl)	117.4± 16.83	196.3±16. 71[a]	186.5±15.14	158.6± 13.18[bc]	122.6±18.48[bd]
Insulin (pmol/l)	94.07.± 11.8	170.1 ± 13.23[a]	163.9 ± 9.78	137.8.± 10.47[b c]	105.2±13.14[bd]
HOMA-IR	1.68 ± 0.20	3.43 ± 0.28[a]	3.30 ± 0.21	2.72 ± 0.20[bc]	1.98 ± 0.25[bd]

Table 5.2 Effect of AR-A014418 treatment on body weight and serum parameters. Values are indicated as mean ± S.D. **Where, Body weight** ([a]P < 0.001 vs NPD; [b]P< 0.01 vs HFD; [c]P < 0.001 vs HFD) (n=8); **Glucose** ([a]P < 0.001 vs NPD; [b]P < 0.05 vs HFD; [c]P<0.001 vs HFD; [d] P < 0.05 vs AR-5) (n=6-8); **Triglycerides** ([a]P < 0.001 vs NPD; [b]P < 0.05 vs HFD; [c]P < 0.01 vs HFD; [d]P < 0.001 vs HFD; [e] P< 0.05 vs AR-5) (n=6-8); **Total Cholesterol** ([a]P < 0.001 vs NPD; [b]P < 0.001 vs HFD; [c]P < 0.05 vs AR-1; [d]P < 0.01 vs AR-5) (n=6-8); **Insulin** ([a]P < 0.001 vs NPD; [b]P < 0.001 vs HFD; [c]P < 0.01 vs AR-1; [d]P < 0.001 vs AR-5) (n=6); **HOMA-IR** ([a] P < 0.001 vs NPD; [b]P < 0.001 vs HFD; [c]P < 0.01 vs AR-1; [d]P < 0.001 vs AR-5) (n=6).

5.4.3 Effect of GSK3β inhibitors on oral glucose tolerance test (OGTT)

The HFD fed mice showed marked glucose intolerance as assessed by OGTT. Blood glucose levels were found to be significantly higher in HFD fed mice as compared with NPD mice at all the time points after glucose administration (0, 15, 30, 60 and 120 minutes) (Fig 5.9a and 5.9b). Treatment with GSK3β inhibitors**,** IMX and AR-A014418 results in dose dependent improvement in glucose tolerance as significant reduction in blood glucose level was observed at 0, 30, 60 and 120 min after glucose administration ($P < 0.001$) (Fig. 5.9a and 5.9b).

(a) IMX in OGTT **(b) AR-A014418 in OGTT**

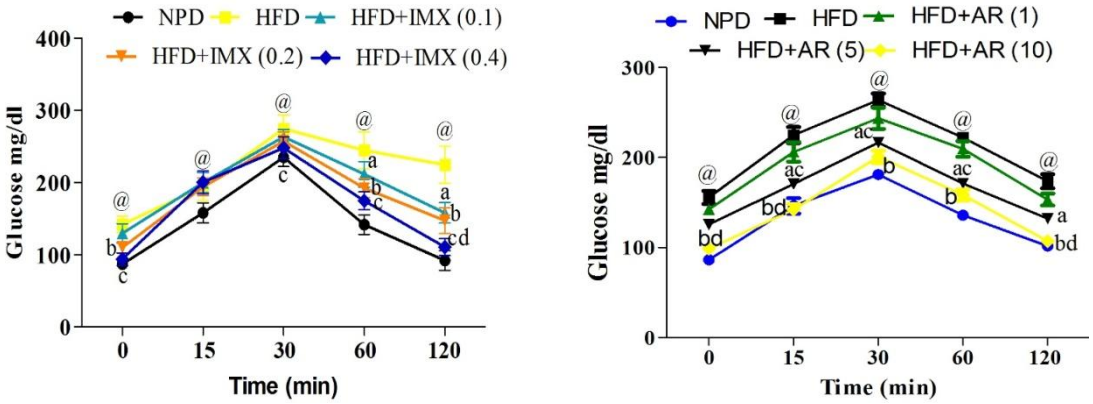

Fig. 5.9 Effect of GSK3β inhibitors on glucose tolerance test. Values are indicated as mean ± SEM. **(a) IMX** ($^{@}P < 0.001$ vs NPD); ($^{a}P < 0.01$, IMX 0.1 mg/kg vs HFD); ($^{b}P < 0.001$, IMX 0.2 mg/kg vs HFD); ($^{c}P < 0.001$, IMX 0.4 mg/kg vs HFD); ($^{d}P < 0.001$ vs IMX 0.2), (n=6) (IMX= Indirubin-3'-monoxime) **(b) AR-A014418** ($^{@}P < 0.001$ vs NPD); ($^{a}P < 0.001$, AR-5mg vs HFD); ($^{b}P < 0.001$, AR-10mg vs HFD); ($^{c}P < 0.05$ AR-1mg vs AR-5mg); ($^{d}P < 0.05$, AR-5mg vs AR-10mg) (n=6) (AR= AR-A014418).

5.4.4 Effect of GSK3β inhibitors on locomotor activity in actophotometer

No significant difference was observed between any of the experimental groups ($P > 0.05$) (Fig. 5.10a and 5.10b), suggesting no effect whatsoever of HFD or GSK3β inhibitors, IMX ($F_{(4,49)} = 0.70$, $P > 0.05$) and AR-A014418 ($F_{(4,29)} = 0.09$, $P > 0.05$), on the locomotion activity of mice.

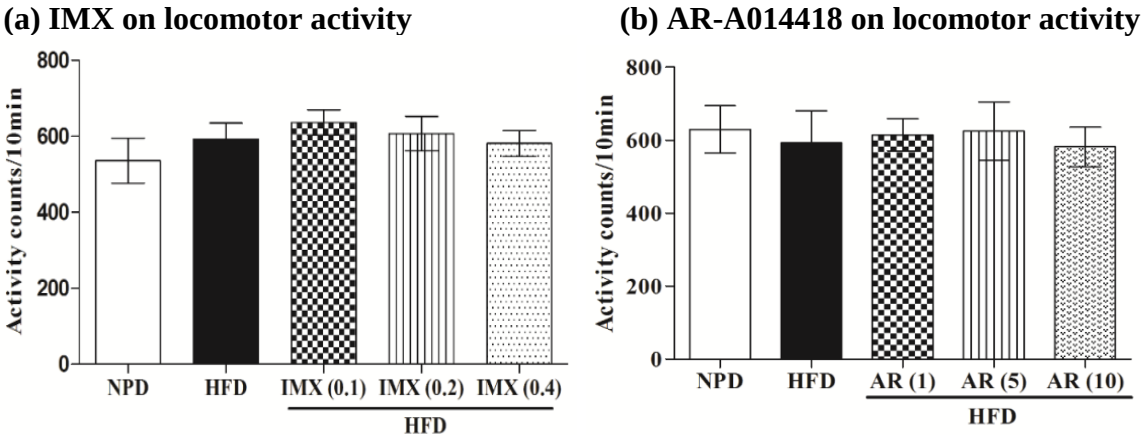

Fig. 5.10 Effect of GSK3β inhibitors on locomotor activity. Values are expressed as mean ± SEM. **(a)** (IMX= Indirubin-3'-monoxime) (n=8-10) **(b)** (AR= AR-A014418) (n=6-8).

5.4.5 Effect of GSK3β inhibitors on mean escape latency in morris water maze

The mean escape latency to find the hidden platform reduced gradually in all the experimental groups during 4 days of training. The mean escape latency was significantly higher ($P < 0.001$) in the HFD fed mice as compared with the NPD fed mice on days 2-4 (Fig. 5.11a) and days 3-4 (Fig. 5.11b), showing poorer learning performance. The increased escape latency in the HFD group was significantly attenuated by IMX treatment at high dose (0.4 mg/kg) on day 3 ($P < 0.01$) and day 4 ($P < 0.001$), however, no significant effect was observed on low (0.1mg/kg) and medium dose (0.2 mg/kg) (Fig. 5.11a). Similar results were observed with AR-A014418 treatment, where the increased escape latency in the HFD group was significantly attenuated by medium dose (5 mg/kg) and high dose (10 mg/kg) on day 3 ($P < 0.01$) and day 4 ($P < 0.001$) (Fig. 5.11b).

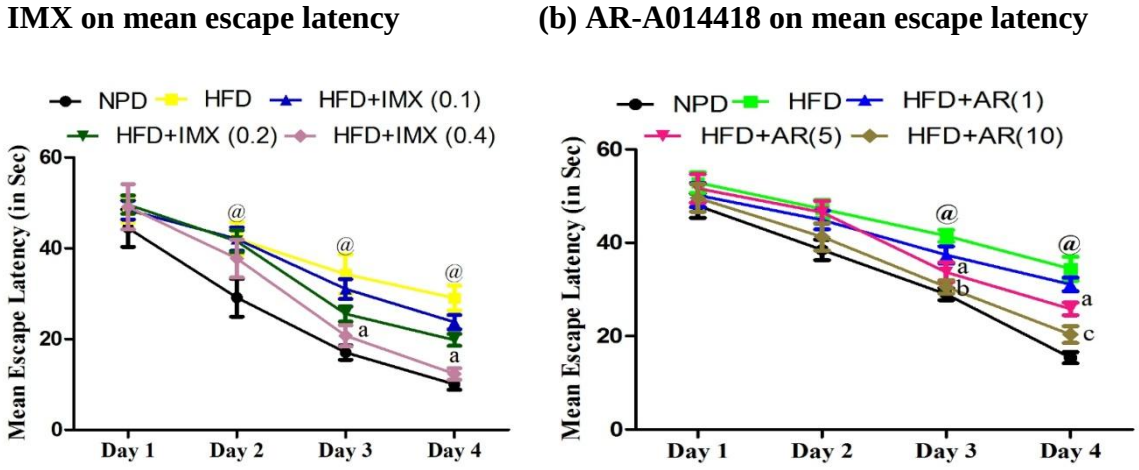

Fig.5.11 Effect of GSK3β inhibitors on mean escape latency. Values are expressed as Mean ± SEM. **(a) IMX** ($^{@}P$ <0.001 vs NPD); (^{a}P <0.001 vs HFD); (n=8-10); (IMX- Indirubin-3'-monoxime) **(b) AR-A014418** ($^{@}P < 0.001$ vs NPD); ($^{a}P < 0.05$ vs HFD); ($^{b}P < 0.01$ vs HFD); ($^{c}P < 0.001$ vs HFD) (n=6-8) (AR= AR-A014418).

5.4.6. Effect of GSK3β inhibitors on probe trial in morris water maze

During the probe trial, HFD fed mice failed to remember the precise location of the platform, spending significantly lesser time in the target quadrant as compared with NPD fed mice ($P < 0.001$, Fig. 5.12a and 5.12b). Whereas, HFD fed mice treated with GSK3β inhibitor, IMX spent significantly more time in the target quadrant indicating improved consolidation of memory ($F_{(4,49)} = 17.01$; $P < 0.001$). Although, this improvement was not significant at lowest dose of IMX (0.1 mg/kg), but at medium (0.2 mg/kg) and high dose (0.4 mg/kg), the effect was statistically significant (Fig. 5.12a). Similarly, the mice treated with AR-A014418 at medium (5mg/kg) and high dose (10 mg/kg), spent more time in the target quadrant as compared with alone HFD fed mice (Fig.5.12b) ($F_{(4,39)} = 7.80$;$P < 0.001$).

(a) IMX in Probe trial **(b) AR-A014418 in Probe trial**

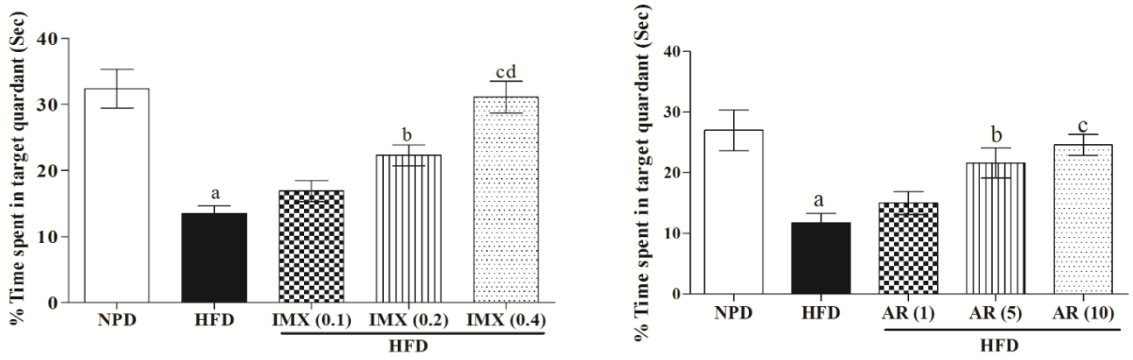

Fig. 5.12 Effect of GSK3β inhibitors on probe trial. Values are expressed as Mean ± SEM. **(a) IMX** ($^{a}P < 0.001$ vs NPD); ($^{b}P < 0.05$ vs HFD); ($^{c}P < 0.001$ vs HFD); ($^{d}P < 0.05$ vs IMX 0.2mg/kg), (n=8-10); (IMX- Indirubin-3'-monoxime) **(b) AR-A014418** ($^{a}P < 0.001$ vs NPD); ($^{b}P < 0.05$ vs HFD); ($^{c}P < 0.01$ vs HFD); (n=8).

5.4.7 Effect of GSK3β inhibitors on passive avoidance task

The initial latency in the acquisition trial did not differ significantly ($P > 0.05$) between all the groups (Fig 5.13a and 5.13b). Twenty-four hours later, the mice were tested again and it was found that the retention latency was significantly decreased in the HFD fed group as compared with NPD fed mice ($P < 0.001$) (Fig. 5.13a and 5.13b). Decreased retention latency in the HFD fed mice was significantly ameliorated by IMX treatment in a dose dependent manner ($F_{(4,49)} = 29.19$; $P < 0.05$) (Fig. 5.13a). Similarly, the mice treated with AR-A014418 at high dose (10 mg/kg), was able to significantly ameliorate the decrease in retention latency in the HFD fed mice ($F_{(4,39)} = 7.72$; $P < 0.05$) (Fig. 5.13b).

(a) Effect of IMX on passive avoidance task

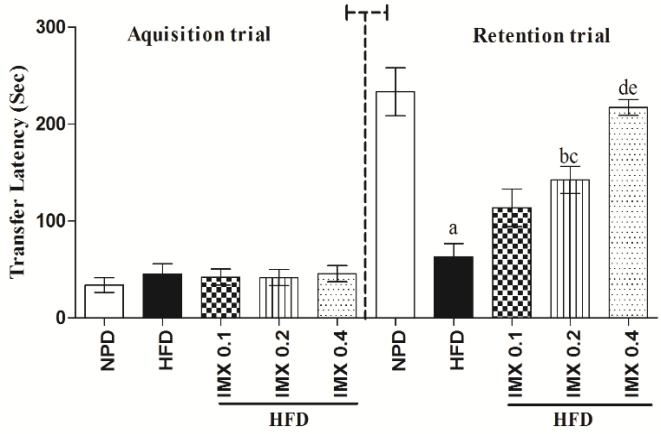

Fig.5.13a Effect of IMX on passive avoidance task. Values are expressed as Mean ± SEM. ([a]*P* < 0.001 vs NPD); ([b]*P* <0.01 vs HFD); ([c]*P* < 0.05 vs IMX 0.1mg/kg); ([d]*P* < 0.001 vs HFD); ([e]P < 0.01 vs IMX 0.2mg/kg), (n= 8-10); (IMX=Indirubin-3'-monoxime).

(b) AR-A014418 on passive avoidance task

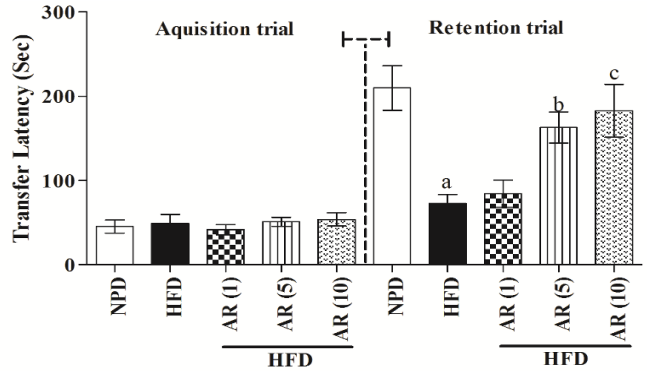

Fig.5.13b Effect of AR-A014418 on passive avoidance task. Values are expressed as Mean ± SEM. ([a]*P* < 0.001 vs NPD); ([b]*P* < 0.05 vs HFD); ([c]*P* < 0.01 vs HFD) (n=6-8) (AR=AR-A014418).

5.4.8 Effect of GSK3β inhibitors on object recognition task (ORT)

In the ORT, during the training session, no significant difference was observed in exploratory preferences among all groups (data not shown). However, during the retention session, the mice fed with NPD spent longer time in exploring the novel object as compared with familiar object (*P* < 0.001) (Fig. 5.14a and 5.14b). However, no significant difference was observed in HFD fed mice group in the time exploring the novel object or familiar object (*P* > 0.05). In addition, treatment with GSK3β inhibitors, IMX and AR-A014418, at low and medium dose failed to produce any significant effect on retention memory. However mice treated with high dose of IMX (0.4mg/kg) and AR-A014418 (10 mg/kg) spent significantly more time exploring the novel object as compared to familiar object (P < 0.01) (Fig. 5.14a and 5.14b).

(a) IMX on ORT **(b) AR-A014418 on ORT**

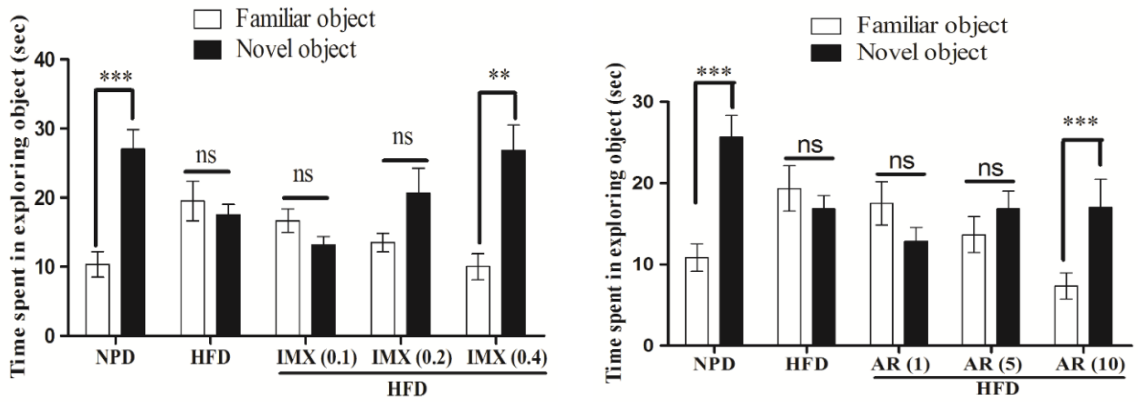

Fig. 5.14 Effect of GSK3β inhibitors on novel object recognition task. (a) IMX (***P < 0.001 vs familiar object); (**P < 0.01 vs familiar object) (n=6) **(b) AR-A014418** (***P < 0.001 vs familiar object) (n= 6). Note (IMX= Indirubin-3-monoxime; AR= AR-A014418; ns: non-significant).

5.4.9. Effect of GSK3β inhibitors on malondialdehyde (MDA) level

Increased level of oxidative stress marker, MDA, was reported in hippocampus homogenates of HFD fed mice as compared to NPD fed mice (P < 0.001) (Fig. 5.15a and 5.15b). In contrast, GSK3β inhibitors, IMX ($F_{(4,29)}$ = 62.35; P < 0.001) and AR-A014418 ($F_{(4,29)}$ = 42.46; P < 0.001) significantly and dose dependently attenuated MDA level in HFD mice.

(a) IMX on MDA level **(b) AR-A014418 on MDA level**

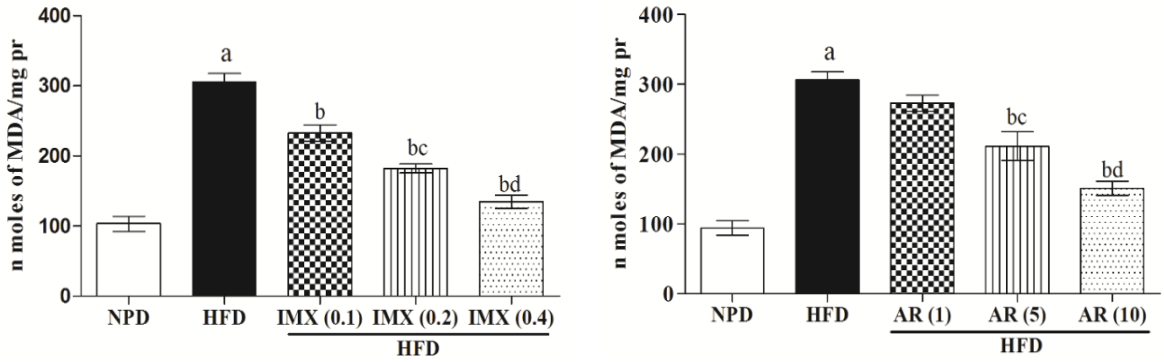

Fig. 5.15 Effect of GSK3β inhibitors on MDA level. Values are expressed as Mean ± SEM. **(a) IMX** (^{a}P < 0.001 vs NPD); (^{b}P < 0.001 vs HFD); (^{c}P < 0.05 vs IMX (0.1mg/kg); (^{d}P < 0.05 vs IMX 0.2 mg/kg), (n=6); (IMX- Indirubin-3'-monoxime). **(b) AR-A014418** (^{a}P < 0.001 vs NPD); (^{b}P < 0.001 vs HFD); (^{c}P < 0.05 vs AR-1mg/kg); (^{d}P < 0.05 vs AR-5mg/kg), (n=6); (AR-A014418).

5.4.10. Effect of GSK3β inhibitors on nitrite levels

HFD feeding results in significantly elevated nitrite levels as compared to NPD fed mice ($P < 0.001$) (Fig.5.16a and 5.16b). However, treatment with GSK3β inhibitors, IMX ($F_{(4,29)}$ = 36.71; $P < 0.001$) (Fig.5.16a) and AR-A014418 ($F_{(4,29)}$ = 30.02; $P < 0.001$) (Fig. 5.16b) significantly and dose dependently attenuated nitrite levels in HFD mice.

(a) IMX on nitrite level **(b) AR-A014418 on nitrite level**

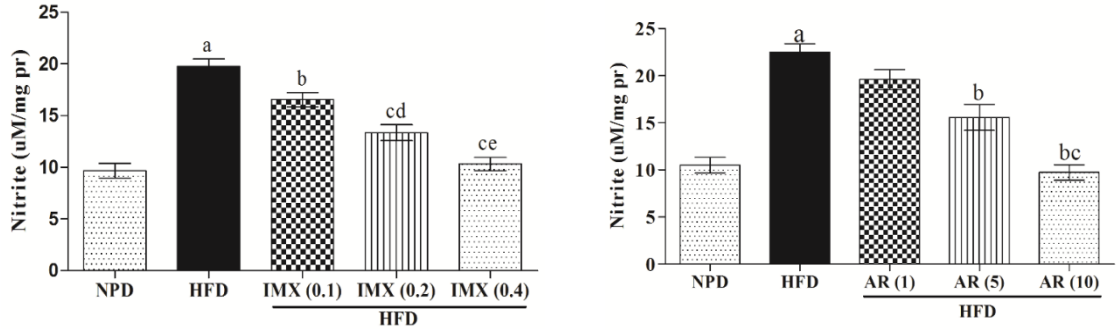

Fig. 5.16 Effect of GSK3β inhibitors on nitrite level. Values are expressed as Mean ± SEM. **(a) IMX** (^{a}P <0.001 vs NPD); ($^{b}P < 0.05$ vs HFD); ($^{c}P < 0.001$ vs HFD; ($^{d}P < 0.05$ vs IMX 0.1mg/kg); ($^{e}P< 0.05$ vs 0.2mg/kg), (n=6); (IMX- Indirubin-3'-monoxime) **(b) AR-A014418** (^{a}P <0.001 vs NPD); ($^{b}P < 0.001$ vs HFD); ($^{c}P < 0.01$ vs AR-5mg/kg), (n=6).

5.4.11. Effect of GSK3β inhibitors on reduced glutathione (GSH) level

Endogenous antioxidant enzyme GSH was found to be reduced in brain homogenates of HFD fed mice as compared to NPD fed mice ($P < 0.001$) (Fig. 5.17a and 5.17b). However, IMX treatment restored GSH level at medium (0.2 mg/kg) and high dose (0.4 mg/kg) in HFD mice ($F_{(4,29)}$ = 24.79; $P < 0.001$) (Fig. 5.17a). Similarly, AR-A014418 treatment at medium (5 mg/kg) and high dose (10mg/kg) was found to significantly restored GSH level in HFD mice ($F_{(4,29)}$ = 14.47; $P < 0.001$) (Fig. 5.17b).

(a) IMX on GSH level **(b) AR-A014418 on GSH level**

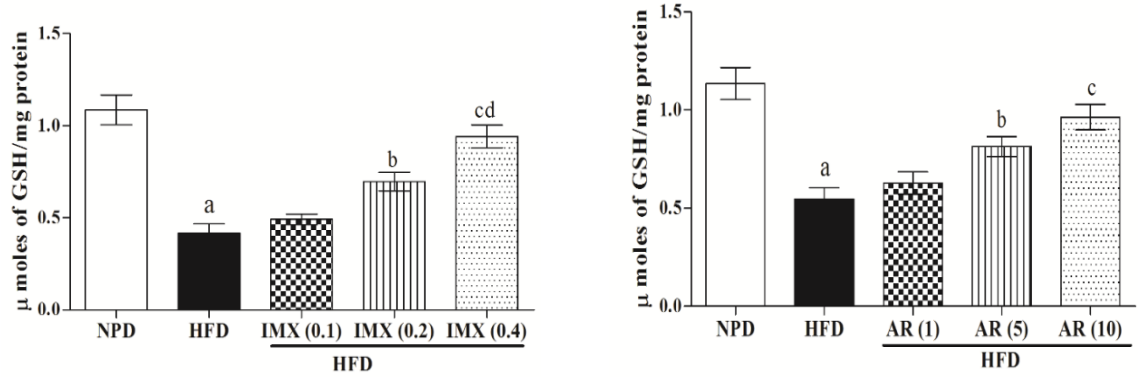

Fig.5.17 Effect of GSK3β inhibitors on reduced glutathione level. Values are expressed as Mean ± SEM. **(a) IMX** (^{a}P <0.001 vs NPD); ($^{b}P < 0.05$ vs HFD); ($^{c}P < 0.001$ vs HFD); ($^{d}P <$ 0.05 vs IMX 0.2mg/kg), (n=6); (IMX- Indirubin-3'-monoxime) **(b) AR-A014418** ($^{a}P < 0.001$ vs NPD); ($^{b}P < 0.05$ vs HFD); ($^{c}P < 0.001$ vs HFD) (n= 6).

5.4.12. Effect of GSK3β inhibitors on Tumour necrosis factor alpha (TNF-α)

The level of TNF-α rose significantly in HFD fed mice as compared to those of NPD fed mice ($P < 0.001$). Treatment with IMX (0.2 mg/kg and 0.4 mg/kg) ($F_{(4,29)} = 13.74$) (Fig. 5.18a) and AR-A014418 (5 mg/kg and 10 mg/kg) ($F_{(4,29)} = 11.89$) (Fig 5.18b); results in significant attenuation of TNF- α level as compared with HFD fed mice ($P < 0.001$).

(a) IMX on TNF-α level **(b) AR-A014418 on TNF-α level**

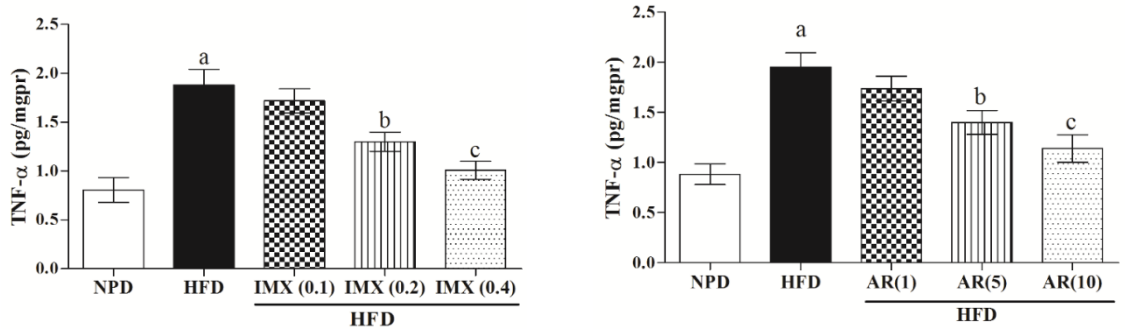

Fig. 5.18 Effect of pan HDAC inhibitors on TNF-α. Values are expressed as Mean ± SEM **(a) IMX** ([a] *P* <0.001 vs NPD); ([b]*P* <0.05 vs HFD) ([c]P < 0.01 vs HFD) **(b) AR-A014418** ([a]P < 0.001 vs NPD); ([b]P < 0.05 vs HFD); ([c]P < 0.01 vs HFD).

5.4.13 Effect of GSK3β inhibitors on phosphorylated tau (ptau) level

HFD feeding results in significant increase in ptau levels as compared with NPD fed mice ($P < 0.001$) (Fig. 5.19a and 5.19b). In contrast, the mice treated with GSK3β inhibitors, IMX ($F_{(4, 29)} = 10.77$; $P < 0.001$) (Fig. 5.19a) and AR-A014418 showed significant reduction in ptau levels in hippocampus homogenates as compared with alone HFD fed mice ($F_{(4,29)} = 14.98$; $P < 0.001$) (Fig. 5.19b).

(a) IMX on pTau **(b) AR-A014418 on pTau**

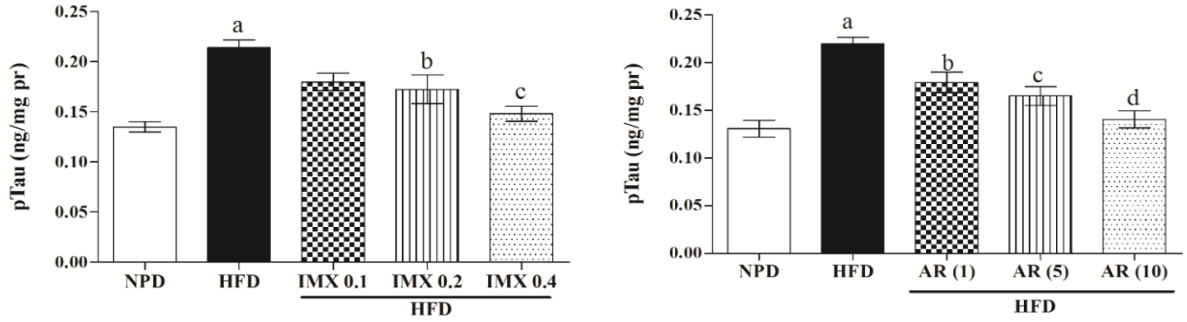

Fig. 5.19 Effect of GSK3β inhibitors on pTau level. Values are expressed as Mean ± SEM. **(a) IMX** ([a]P< 0.001 vs NPD); ([b]P< 0.05 vs HFD); ([c]P< 0.001 vs HFD) (n=6) **(b) AR-A014418** ([a]P< 0.001 vs NPD); ([b]P< 0.05 vs HFD); ([c]P< 0.01 vs HFD); ([d]P< 0.001 vs HFD) (n=6).

5.4.14. Effect of GSK3β inhibitors on Amyloid-β (Aβ $_{1-42}$) level

HFD feeding results in significant increase in Aβ $_{1-42}$ levels as compared with NPD fed mice ($P < 0.001$) (Fig. 5.20a and 5.20b). In contrast, the mice treated with GSK3β inhibitors, IMX ($F_{(4,29)} = 22.42$; $P < 0.001$) (Fig. 5.20a) and AR-A014418 (Fig.5.20b) showed attenuation of Aβ $_{1-42}$ levels in brain homogenates ($F_{(4,29)} = 27.43$; $P < 0.001$).

(a) IMX on Aβ $_{1-42}$ level **(b) AR-A014418 on Aβ $_{1-42}$ level**

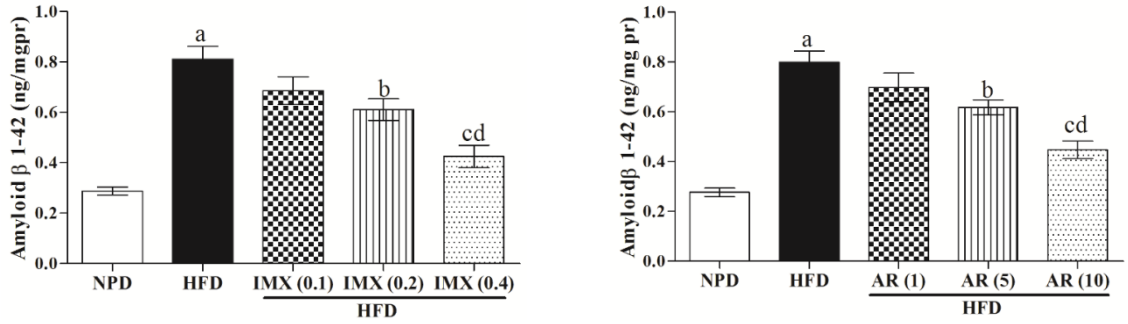

Fig. 5.20 Effect of GSK3β inhibitors on Aβ $_{1-42}$ level. Values are expressed as Mean ± SEM. **(a) IMX** ($^{a}P < 0.001$ vs NPD); ($^{b}P < 0.05$ vs HFD; $^{c}P < 0.001$ vs HFD; ($^{d}P < 0.05$ vs IMX 0.2mg/kg) (n=6). (b) **AR-A014418** ($^{a}P < 0.001$ vs NPD); ($^{b}P < 0.05$ vs HFD); ($^{c}P < 0.001$ vs HFD); ($^{d}P < 0.05$ vs AR-5mg) (n=6).

5.4.15 Effect of GSK3β inhibitors on GSK3β levels

HFD feeding results in significant increase in GSK3β levels as compared with NPD fed mice ($P < 0.001$) (Fig 5.21a and 5.21b). In contrast, treatment with IMX ($F_{(4,29)} = 17.84$; $P < 0.001$) (Fig 5.21a) and AR-A014418 ($F_{(4,29)} = 21.33$; $P < 0.001$) (Fig. 5.21b) showed significant attenuation of GSK3β levels as compared to HFD alone mice.

(a) IMX on GSK3β level **(b) AR-A014418 on GSK3β level**

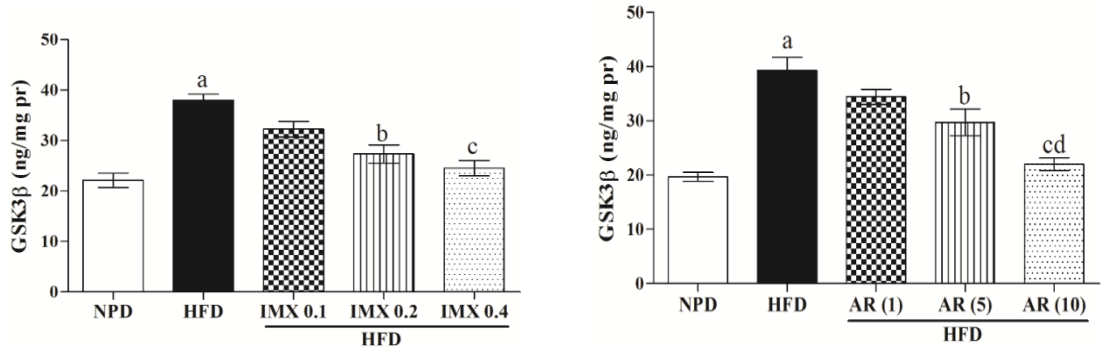

Fig. 5.21 Effect of GSK3β inhibitors on GSK3β level. Values are indicated as Mean ± SEM. **(a) IMX** ($^{a}P< 0.001$ vs NPD); ($^{b}P< 0.001$ vs HFD); ($^{c}P< 0.001$ vs HFD) (n=6). **(b) AR-A014418** ($^{a}P< 0.001$ vs NPD); ($^{b}P< 0.01$ vs HFD; $^{c}P< 0.001$ vs HFD; $^{d}P< 0.05$ vs AR-5mg) (n=6).

5.4.16. Effect of GSK3β inhibitors on brain derived Neurotrophic factor (BDNF)

HFD fed mice showed significant reduction of BDNF level as compared with NPD fed mice ($P < 0.001$) (Fig. 5.22a and 5.22b). Treatment with GSK3β inhibitors, IMX ($F_{(4, 29)} = 25.45$; $P < 0.001$) (Fig. 5.22a) and AR-A014418 (Fig. 5.22b) significantly ameliorate the HFD induced decrease in BDNF level ($F_{(4,24)} = 21.68$; $P < 0.001$).

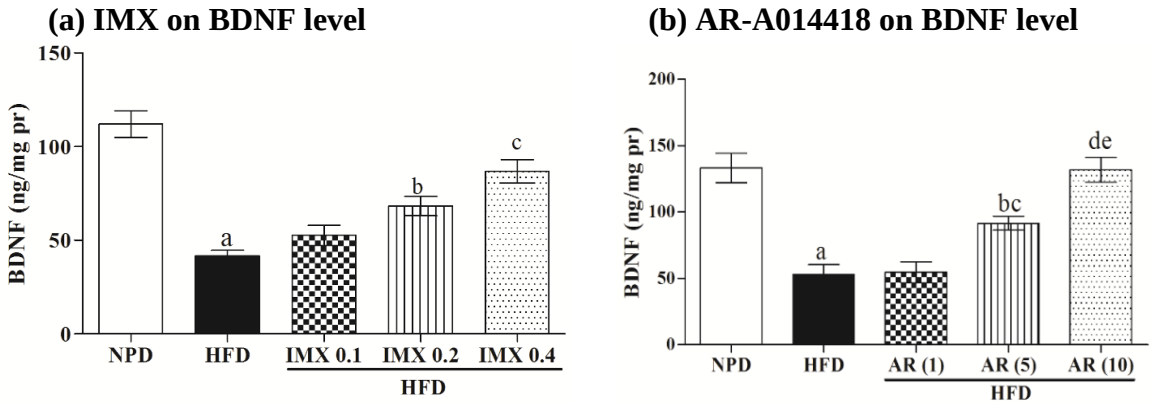

Fig. 5.22 Effect of GSK3β inhibitors on BDNF level. Values are indicated as Mean ± SEM. (a) **IMX** ([a]P< 0.001 vs NPD); ([b]P< 0.05 vs HFD); ([c]P< 0.001 vs HFD) **(b) AR-A014418** ([a]P< 0.001 vs NPD); ([b]P< 0.05 vs HFD); ([c]P< 0.05 vs AR-1mg); ([d]P< 0.001 vs HFD); ([e]P< 0.05 vs AR-5mg).

5.4.17 Effect of GSK3β inhibitors on CREB level

HFD feeding results in significant reduction of CREB levels as compared with NPD fed mice ($P < 0.001$) (Fig 5.23a and 5.23b). In contrast, treatment with GSK3β inhibitors, IMX ($F_{(4,29)} = 9.75$; $P < 0.001$) (Fig 5.23a) and AR-A014418 ($F_{(4,29)} = 27.95$; $P < 0.001$) (Fig. 5.23b) showed significant amelioration of CREB levels as compared to HFD alone mice.

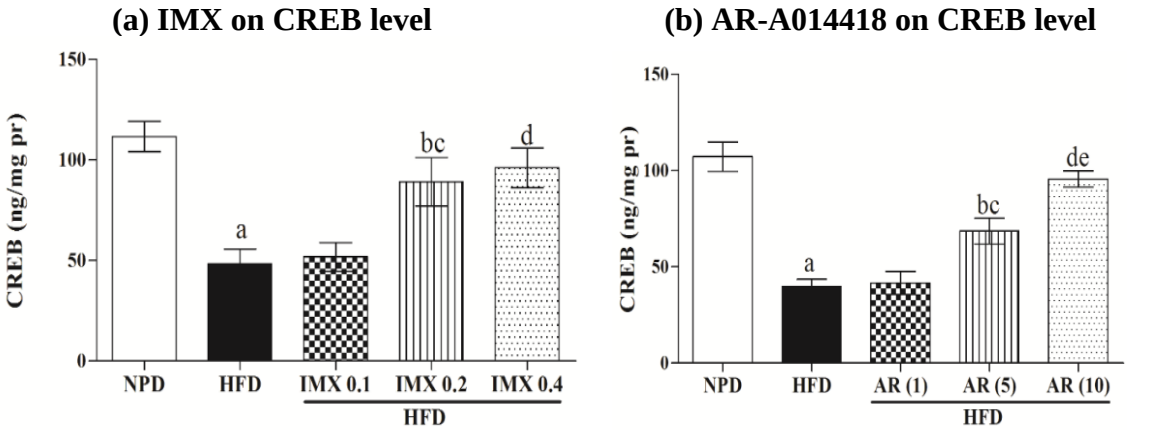

Fig. 5.23 Effect of GSK3β inhibitors on CREB level. Values are indicated as Mean ± SEM. (a) **IMX** ([a]P < 0.001 vs NPD); ([b]P < 0.05 vs HFD; ([c]P < 0.05 vs IMX 0.1); ([d]P < 0.01 vs HFD) (n=6) **(b) AR-A014418** ([a]P< 0.001 vs NPD); ([b]P< 0.05 vs HFD); ([c]P< 0.05 vs AR-1mg/kg); ([d]P< 0.001 vs HFD); ([e]P< 0.05 vs AR-5mg/kg) (n=6).

5.4.18. Effect of IMX on morphological characters of dentate gyrus and CA1 neurons

Along with the cognitive impairments observed in the behavioral paradigms, the HFD feeding also results in significant morphological changes in DG and CA1 region of hippocampus neurons. The H&E stained brain sections showed healthy neurons in DG and CA1 region in the NPD fed mice (Fig. 5.24, Panel A and F, respectively). Healthy neurons appeared robust in shape, had a spherical or slightly oval nucleus and a single large nucleolus with clear visible cytoplasm as indicated by yellow arrows. The HFD feeding results in significant neuronal degeneration in DG and CA1 regions of hippocampus (Fig. 5.24, Panel B and G, respectively). Marked loss of cell bodies and increased pyknotic neurons were observed in DG and CA1 regions in HFD mice. The pyknotic neurons were darkly stained with no nucleus or visible nucleolus and few of the cells were shrunken and sickle shaped in brain sections of HFD fed mice as indicated by red arrows. Treatment with IMX (0.1 and 0.2 mg/kg) (Fig. 5.24, Panel C-D and H-I) attenuated HFD induced cell loss and pyknotic cells I DG and CA1 region. Although, some degenerating cells with morphological changes were still observed at these lower doses. However, there was marked improvement in neuronal density and reduction in pyknotic neurons following IMX treatment at high dose (0.4mg/kg), indicating the dose dependent neuroprotective actions of IMX (Fig. 5.24, Panel E and J).

5.4.18.1. Effect of Indirubin-3-monoxime on DG region

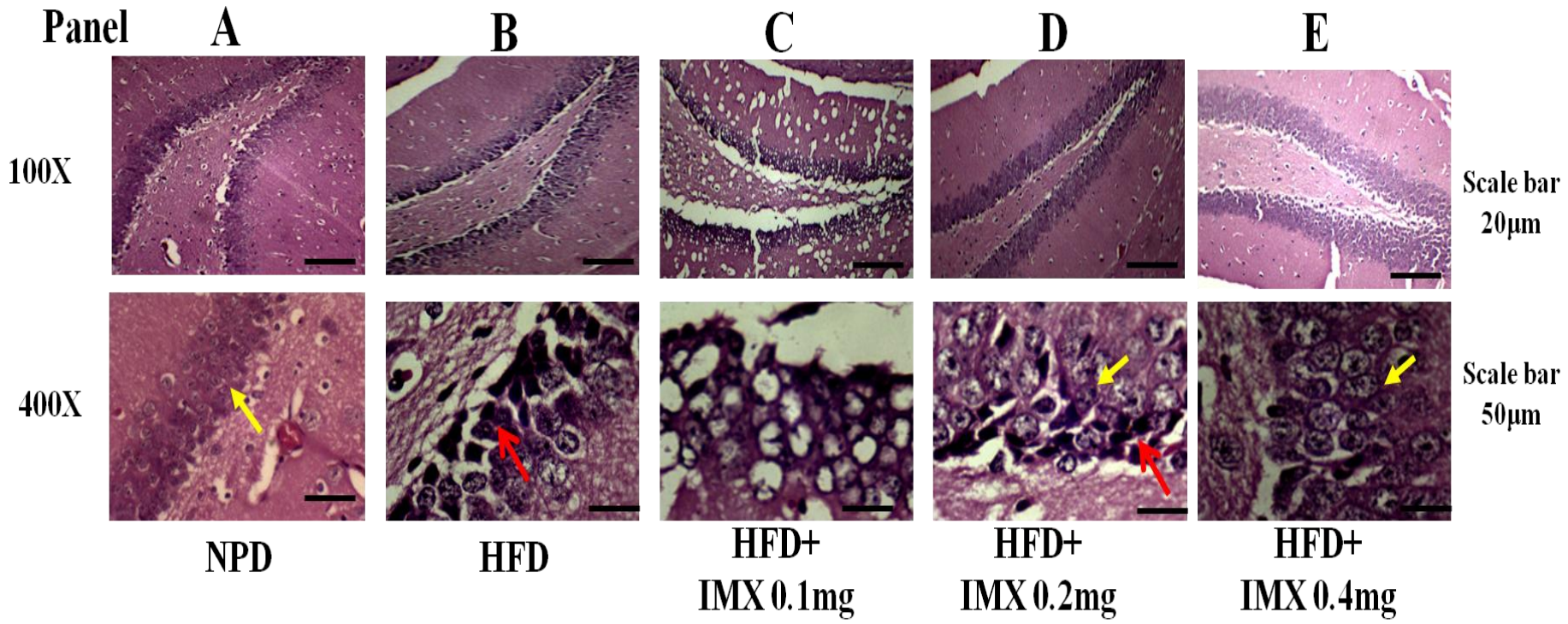

Fig. 5.24(a) Effect of Indirubin-3-monoxime on Dentate gyrus. Figure shows photomicrographs of DG **(Panel A)** normal pellet diet **(Panel B)** High fat diet **(Panel C)** IMX 0.1mg/kg **(Panel D)** IMX 0.2 mg/kg **(Panel E)** IMX 0.4 mg/kg. Yellow arrows indicate normal healthy neurons; Red arrows indicate damaged or sickle shaped pyknotic neurons

5.4.18.2 Effect of Indirubin-3-monoxime on CA1 region

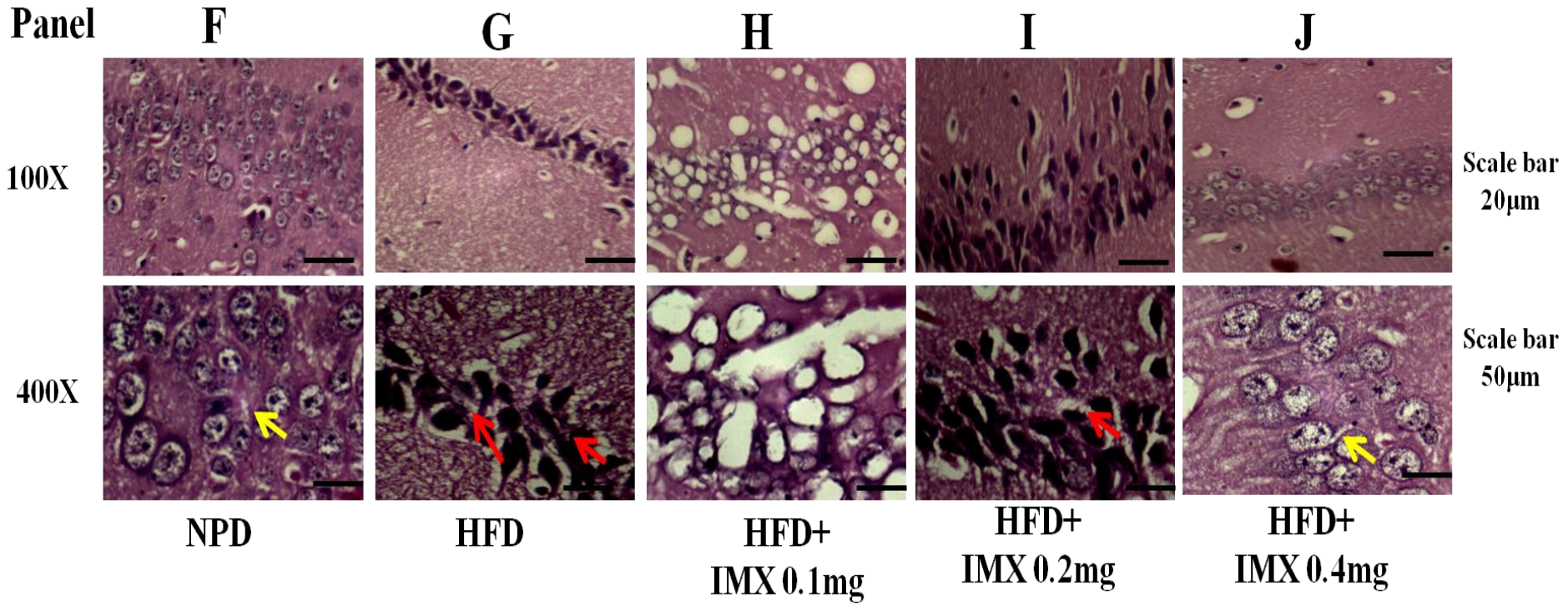

Fig. 5.24 (b) Effect of Indirubin-3-monoxime on CA1 region. Figure shows photomicrographs of CA1 **(Panel F)** normal pellet diet **(Panel G)** High fat diet **(Panel H)** IMX 0.1mg/kg **(Panel I)** IMX 0.2 mg/kg **(Panel J)** IMX 0.4 mg/kg. Yellow arrows indicate normal healthy neurons; Red arrows indicate damaged or sickle shaped pyknotic neurons.

5.4.19. Effect of IMX treatment on neuronal count in dentate gyrus and CA1 regions

The HFD feeding results in a significant increase in the percentage of damaged neurons with altered morphological characters in both DG and CA1 regions ($P < 0.001$) (Fig.5.25a and 5.25b). In contrast, the mice treated with IMX (at high dose, 0.4mg/kg) showed significant neuroprotection as evidenced by reduced percentage damaged neurons in DG and CA1 regions ($P < 0$ .001; Fig. 5.25a and 5..25b).

(a) IMX on % damaged neurons in DG **(b) IMX on % damaged neurons in CA1**

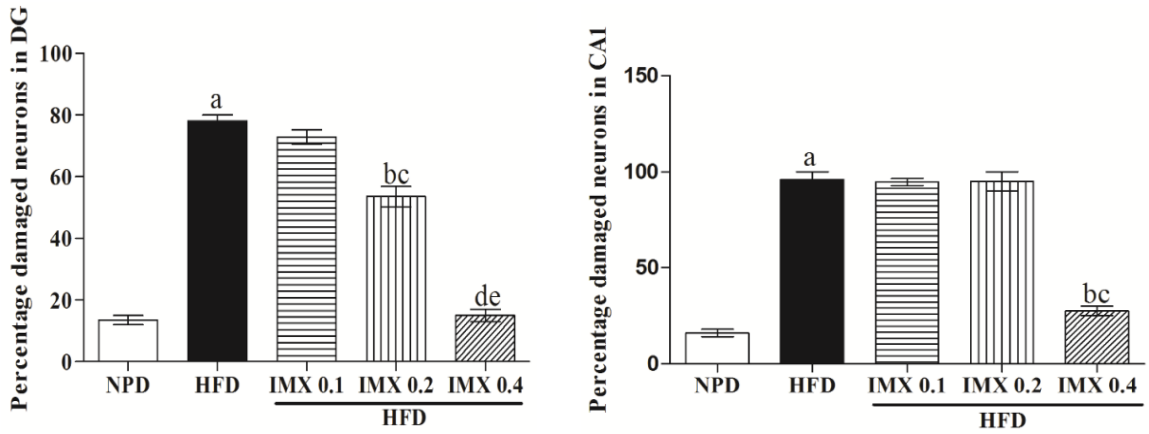

Fig. 5.25 Effect of IMX on DG and CA1 neuronal count. Values are indicated as Mean ± SEM. (a) **DG** ($^{a}P < 0.001$ vs NPD); ($^{b}P < 0.01$ vs HFD); ($^{c}P < 0.05$ vs IMX 0.1); ($^{d}P < 0.001$ vs HFD); ($^{e}P < 0.001$ vs IMX 0.2) (**b) CA1** ($^{a}P < 0.001$ vs NPD); ($^{b}P < 0.001$ vs HFD); ($^{c}P < 0.001$ vs IMX 0.2).

5.4.20. Effect of AR-A014418 on morphological characters of DG and CA1 neurons

Light microscopic results of H&E-stained sections revealed that HFD feeding results in significant morphological changes in neurons of DG and CA1 region of hippocampus. Comparing the hippocampus neurons of HFD fed mice and NPD fed mice, it could be noted that the HFD fed mice showed a significant neuronal damage in DG and CA1 regions of hippocampus (Fig. 5.26, Panel B and G, respectively). Marked loss of cell bodies and increased pyknotic neurons were observed in both DG and CA1 regions in HFD mice. However, the NPD fed mice showed healthy neurons that appeared robust in shape, had a spherical or slightly oval nucleus (Fig. 5.26, Panel A and F, respectively). Treatment with GSK3β inhibitor, AR-A014418 results in significant neuronal protection as evident by healthy neuronal morphological features in DG neurons, when administered at medium (5mg/kg) and high dose (10 mg/kg). Similar, results were observed in CA1 neurons, where the low dose (1mg/kg) was also found to be effective along with medium and high doses in combating neuronal damage (Fig. 5.26, Panel C-E and Panel H-J).

5.4.20.1 Effect of AR-A014418 on Dentate gyrus

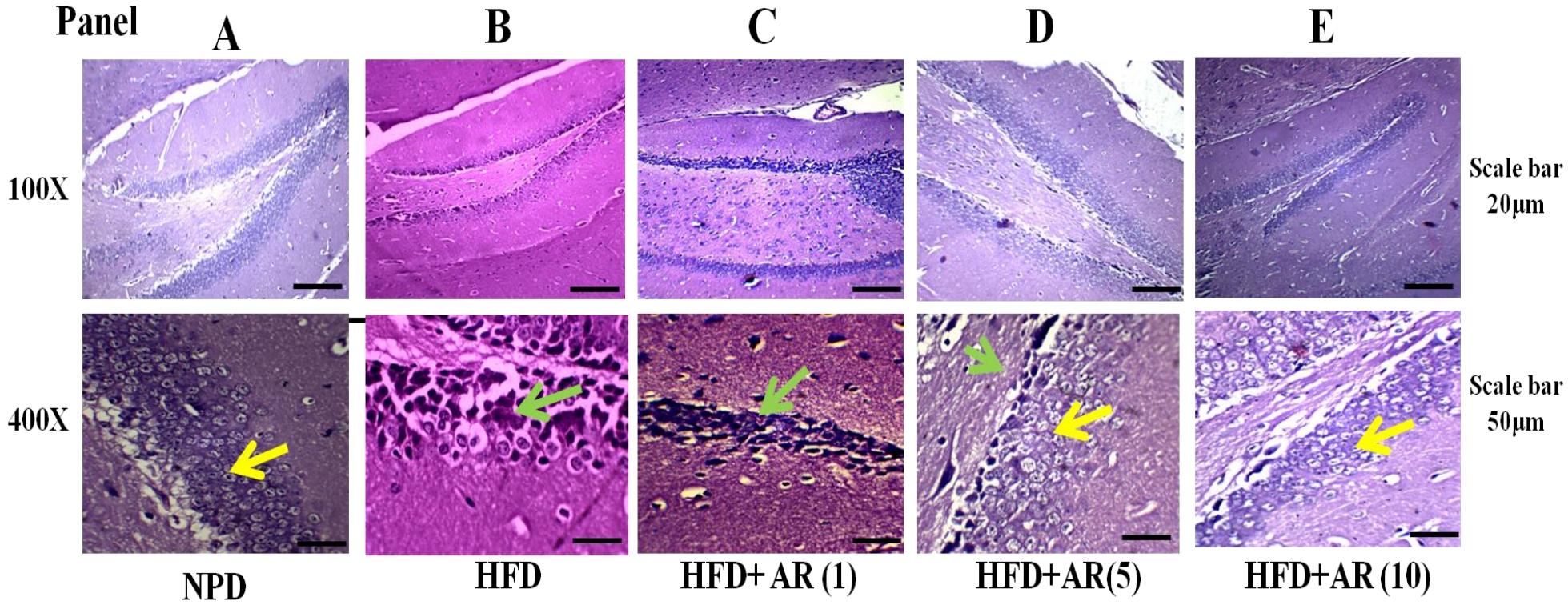

Fig. 5.26 (a) Effect of AR-A014418 on Dentate gyrus. Figure shows photomicrographs of DG **(Panel A)** normal pellet diet **(Panel B)** High fat diet **(Panel C)** AR-A014418 (1mg/kg) **(Panel D)** AR-A014418 (5 mg/kg) **(Panel E)** AR-A014418 (10 mg/kg). Yellow arrows indicate normal healthy neurons; Red arrows indicate damaged or sickle shaped pyknotic neurons

5.4.20.2 Effect of AR-A014418 on CA1 region

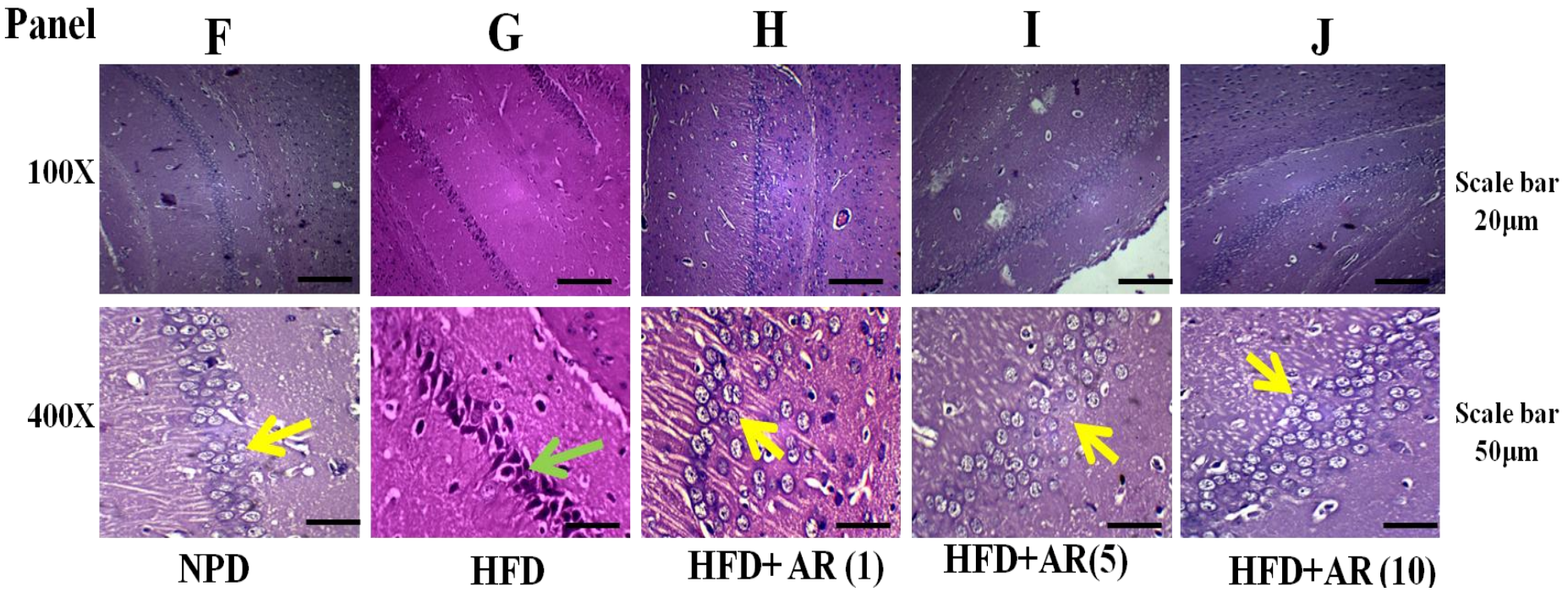

Fig. 5.26 (b) Effect of AR-A014418 on CA1 region. Figure shows photomicrographs of CA1 **(Panel F)** normal pellet diet **(Panel G)** High fat diet **(Panel H)** AR-A014418 (1mg/kg) **(Panel I)** AR-A014418 (5 mg/kg) **(Panel J)** AR-A014418 (10 mg/kg). Yellow arrows indicate normal healthy neurons; Red arrows indicate damaged or sickle shaped pyknotic neurons

5.4.21. Effect of AR-A014418 on hippocampus (DG and CA1) neuronal Count

The HFD feeding results in a significant increase in the percentage of damaged neurons with altered morphological characters in both DG and CA1 regions ($P < 0.001$) (Fig.5.27a and 5.27b). In contrast, the mice treated with AR-A014418 at medium (5mg/kg) and high dose (10mg/kg) showed significant neuroprotection as evidenced by reduced percentage of damaged neurons in DG and CA1 regions ($P < 0.001$; Fig. 5.27a and 5.27b).

(a) AR on % damaged neurons in DG **(b) AR on % damaged neurons in CA1**

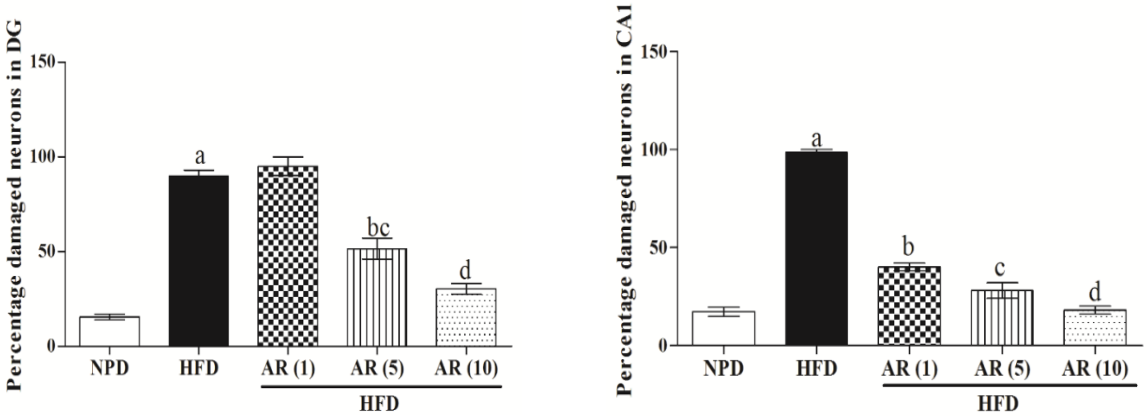

Fig. 5.27 Effect of AR-A014418 on hippocampus neuronal Count (a) DG neurons ($^{a}P < 0.001$ vs NPD; $^{b}P < 0.01$ vs HFD; $^{c}P < 0.01$ vs AR-1mg; $^{d}P < 0.001$ vs HFD) **(b) CA1 neurons** ($^{a}P < 0.001$ vs NPD; $^{b}P < 0.001$ vs HFD; $^{c}P < 0.001$ vs HFD; $^{d}P < 0.001$ vs HFD).

5.5. Effect of pan HDAC inhibitors on insulin resistance and associated cognitive deficits

5.5.1. Effect of Suberoylanilide hydroxamic acid (SAHA) on body weight and serum parameters

Body weight increased significantly in the HFD fed mice as compared to NPD fed mice ($F_{(3, 39)} = 8.23$; $P < 0.001$) (Table.5.3). The HFD feeding also results in significant increase in serum glucose ($F_{(3, 23)} = 23.78$; $P < 0.001$), and serum insulin ($F_{(3, 23)} = 26.95$; $P < 0.001$) levels as compared with NPD feeding, indicating hyperglycemic and hyperinsulinemic condition. Treatment with HDAC inhibitor, SAHA (50 mg/kg), attenuated the increase in body weight (Table.5.3). Also, SAHA significantly lowered the serum glucose and insulin levels. The serum TG ($F_{(3,23)} = 19.35$; $P < 0.001$) and TC ($F_{(3,23)} = 17.90$; $P < 0.001$) concentrations of HFD fed mice were significantly greater than those fed with the NPD (Table.5.3). The HFD fed mice also showed reduction in HDL- cholesterol levels ($F_{(3, 23)} = 6.72$; $P < 0.01$) as compared with NPD fed mice. SAHA administration results in dose dependent reduction of TG and TC levels and further ameliorates HDL-cholesterol in HFD fed mice. The results of HOMA-IR of HFD fed mice were significantly higher than that of NPD fed mice ($P < 0.001$); indicating insulin resistance in peripheral tissues. SAHA treatment significantly decreased HOMA-IR levels as compared to HFD group ($F_{(3,23)} = 32.21$; $P < 0.001$). This data suggests that SAHA treatment significantly ameliorate insulin resistance condition in mice.

Parameter	NPD	HFD	HFD+ SAHA (25)	HFD+SAHA (50)
Body weight (g)	32.2± 0.92	40.10 ± 1.53[a]	36.3 ± 1.31	34.3 ± 0.74[b]
Glucose (mg/dl)	93.2± 4.54	147.8 ± 5.44[a]	130.3 ± 5.03	111.7 ± 4.21[b]
Triglycerides (mg/dl)	45.0± 5.53	141.8 ± 15.32[a]	118.2± 8.71	75.5± 6.72[bc]
Total Cholesterol (mg/dl)	103.8± 9.5	210.0 ± 12.4[a]	181.5± 8.6	137.5± 13.13[bc]
HDL-Cholesterol (mg/dl)	51.7± 4.25	32.33 ± 3.75[a]	35.83 ± 2.28	47.83 ± 3.72[b]
Insulin (pmol/l)	72.0 ± 6.35	184.3 ± 10.8[a]	155.7 ± 10.48	115.8 ± 9.33[bc]
HOMA-IR	1.34 ± 0.28	3.71 ± 0.52[a]	3.08 ± 0.53	2.23 ± 0.39[bc]

Table 5.3 Effect of SAHA treatment on Body weight ([a]P < 0.001 vs NPD); ([b]P < 0.01 vs HFD); **Glucose** ([a]P < 0.001 vs NPD); ([b]P < 0.001 vs HFD); **Triglyceride** ([a]P < 0.001 vs NPD); ([b]P <0.001 vs HFD) ([c]P < 0.05 vs SAHA 25); **Total Cholesterol** ([a]P < 0.001 vs NPD); ([b]P < 0.001 vs HFD); ([c]P < 0.05 vs SAHA 25); **HDL-cholesterol** ([a]P < 0.01 vs NPD); ([b]P < 0.05 vs HFD); **Insulin** ([a]P < 0.001 vs NPD); ([b]P < 0.001 vs HFD) ([c]P < 0.05 vs SAHA 25); **HOMA-IR** ([a]P < 0.001 vs NPD); ([b]P < 0.001 vs HFD) ([c]P < 0.05 vs SAHA 25).

5.5.2. Effect of Sodium butyrate (NaB) on body weight and serum parameters

Body weight increased significantly in the HFD fed mice as compared to NPD fed mice ($F_{(4, 39)} = 8.19$; $P < 0.001$) (Table5.4). The HFD feeding also results in significant increase in serum glucose ($F_{(4,29)} = 16.65$; $P < 0.001$), and serum insulin ($F_{(4,29)} = 30.71$; $P < 0.001$) levels as compared with NPD feeding, indicating hyperglycemic and hyperinsulinemic condition. Treatment with NaB at lower dose (150 mg/kg) did not produce significant change in body weight (Table.5.4). However, NaB at (300mg/kg and 600mg/kg) was able to attenuated the increase in body weight. Also, NaB at these doses significantly lowered the serum glucose and insulin levels.

The serum TG ($F_{(4,29)}$ = 50.44; P < 0.001) and TC ($F_{(4, 29)}$ = 25.92; P < 0.001) concentrations of HFD fed mice were significantly greater than those fed with the NPD. NaB administration results in dose dependent reduction of TG levels and further attenuate Total cholesterol levels at medium and high doses. The results of HOMA-IR of HFD fed mice were significantly higher than that of NPD fed mice (P < 0.001); indicating insulin resistance in peripheral tissues. NaB treatment significantly decreased HOMA-IR levels as compared to HFD group ($F_{(4, 29)}$= 38.29; P < 0.001) (Table.5.4). This data suggests that NaB treatment significantly ameliorate insulin resistance condition in mice.

Parameter	**NPD**	**HFD**	**HFD + NaB 150**	**HFD + NaB 300**	**HFD+ NaB 600**
Body weight (g)	30.25.± 3.19	39.38± 3.96[a]	36.38 ± 4.68	33.25 ± 2.65[b]	31.0 ± 4.0[c]
Glucose (mg/dl)	92.71± 10.92	146.6±10.39[a]	125.8 ± 13.15[b]	115.7 ± 10.07[c]	110.5 ±14.52[d]
Triglycerides (mg/dl)	61.67.± 14.45	206.5±20.2[a]	160.2 ± 20.5[b]	138.3±23.59[c]	89.50 ± 18.83[cd]
Total Cholesterol (mg/dl)	107.8± 24.29	231.7 ± 25.6[a]	192.2 ± 22.16[b]	163.2 ± 16.07[c]	144.2 ± 23.75[c]
Insulin (pmol/l)	63.83 ± 9.78	181.3 ± 23.64[a]	164.0 ± 23.07	145.8 ± 20.84[b]	111.7 ± 22.45[c]
HOMA-IR	1.20 ± 0.21	3.65 ± 0.44[a]	3.21±0.43	2.81±0.34[b]	2.15±0.42[cd]

Table 5.4 Effect of NaB treatment on body weight ([a]P < 0.001 vs NPD); ([b]P < 0.05 vs HFD); ([c]P < 0.001 vs HFD); **Glucose (**[a]P < 0.001 vs NPD); ([b]P < 0.05 vs HFD); ([c]P < 0.01 vs HFD); ([d]P < 0.001 vs HFD); **Triglycerides** ([a]P < 0.001 vs NPD); ([b]P < 0.01 vs HFD); ([c]P < 0.001 vs HFD); ([d]P < 0.01 vs NaB 300); **Total Cholesterol** ([a]P < 0.001 vs NPD); ([b]P < 0.05 vs HFD); ([c]P < 0.001 vs HFD); **Insulin (**[a]P < 0.001 vs NPD); ([b]P < 0.05 vs HFD); ([c]P < 0.001 vs HFD); **HOMA-IR** ([a]P < 0.001 vs NPD); ([b]P < 0.01 vs HFD) ([c]P < 0.001 vs HFD) ([d]P < 0.05 vs NaB 300).

5.5.3. Effect of pan HDAC inhibitors on Oral glucose tolerance test (OGTT)

During OGTT, the mice fed with HFD showed marked glucose intolerance. Blood glucose levels peaked 30 minutes after glucose challenge and were found to be significantly higher in HFD fed mice as compared with NPD fed mice at all measured time points (Fig. 5.28a and 5.28b). Treatment with pan HDAC inhibitors, SAHA and NaB improved glucose tolerance in HFD fed mice and showed significant reduction in plasma glucose levels at various time intervals ($P < 0.001$) (Fig. 5.28a and 5.28b).

(a) SAHA on OGTT **(b) NaB on OGTT**

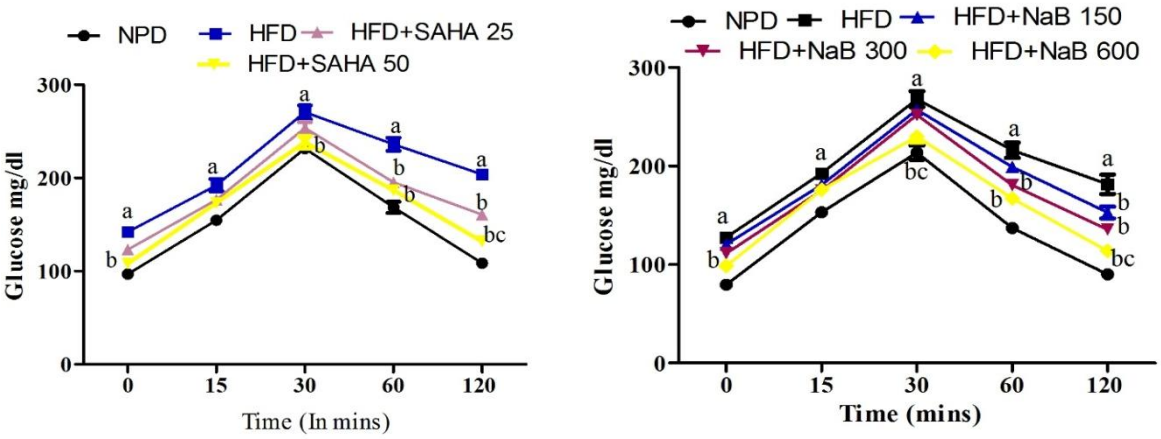

Fig.5.28 Effect of pan HDAC inhibitors on OGTT. Values are expressed as mean ± SEM **(a) SAHA** ($^{a}P < 0.001$ vs NPD); ($^{b}P < 0.001$ vs HFD); ($^{c}P < 0.001$ vs SAHA 25 mg/kg) **(b) Sodium butyrate** ($^{a}P < 0.001$ vs NPD); ($^{b}P < 0.001$ vs HFD); ($^{c}P < 0.05$ vs NaB 300).

5.5.4. Effect of pan HDAC inhibitors on locomotor activity

The spontaneous locomotor activity was performed to rule out the possibility of effect of impaired locomotion on performance of mice in cognitive parameters. No significant difference was observed between any of the groups ($P > 0.05$), suggesting no effect whatsoever of HFD or HDAC inhibitors, SAHA ($F_{(3, 39)} = 0.96$) (Fig. 5.29a) and NaB ($F_{(3, 39)} = 0.45$) (Fig. 5.29b), on locomotor activity at tested doses.

(a) SAHA on locomotor activity **(b) NaB on locomotor activity**

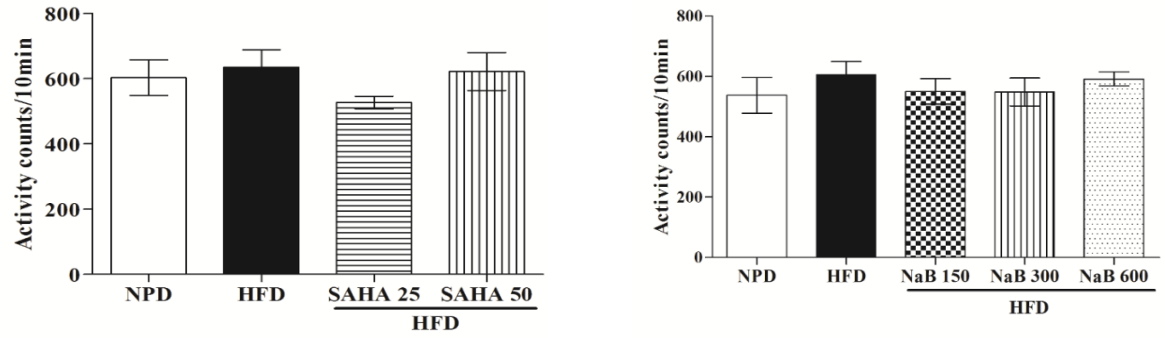

Fig. 5.29 Effect of pan HDAC inhibitors on spontaneous locomotor activity. Values are expressed as mean ± SEM **(a)** SAHA (n=8-10) **(b)** Sodium butyrate (n=8).

5.5.5. Effect of pan HDAC inhibitors on mean escape latency in morris water maze

There was significant effect of treatment and time on the performance of mice in the spatial learning task in MWM ($P < 0.001$) (Fig. 5.30a and 5.30b). The mice fed with HFD took significantly longer time to find the hidden platform as compared with NPD fed mice (Fig. 5.30a and 5.30b). Treatment with HDAC inhibitors, SAHA (50 mg/kg) and NaB (300 and 600 mg/kg) attenuated the mean escape latency in the HFD fed mice on day 3 and day 4, indicating improved memory performance. Fig. 5.30c shows track record with respect to escape latency of one representative animal from each group in MWM acquisition trials.

(a) SAHA on mean escape latency **(b) NaB on mean escape latency**

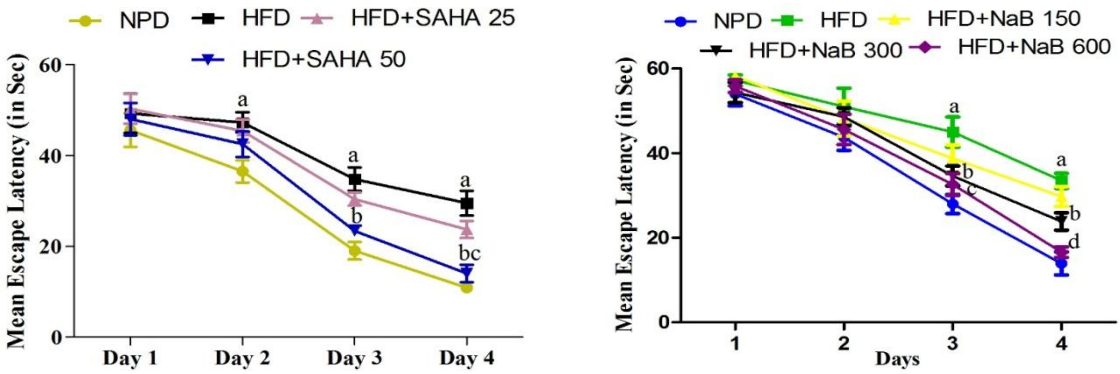

Fig. 5.30 Effect of pan HDAC inhibitors on mean escape latency in MWM. Values are expressed as mean ± SEM **(a) SAHA** (^{a}P <0.001 vs NPD); (^{b}P <0.001 vs HFD); ($^{c}P < 0.05$ vs SAHA 25 mg/kg) **(b) Sodium butyrate** ($^{a}P < 0.001$ vs NPD);($^{b}P < 0.05$ vs HFD); ($^{c}P < 0.01$ vs HFD); ($^{d}P < 0.001$ vs HFD) (n=8).

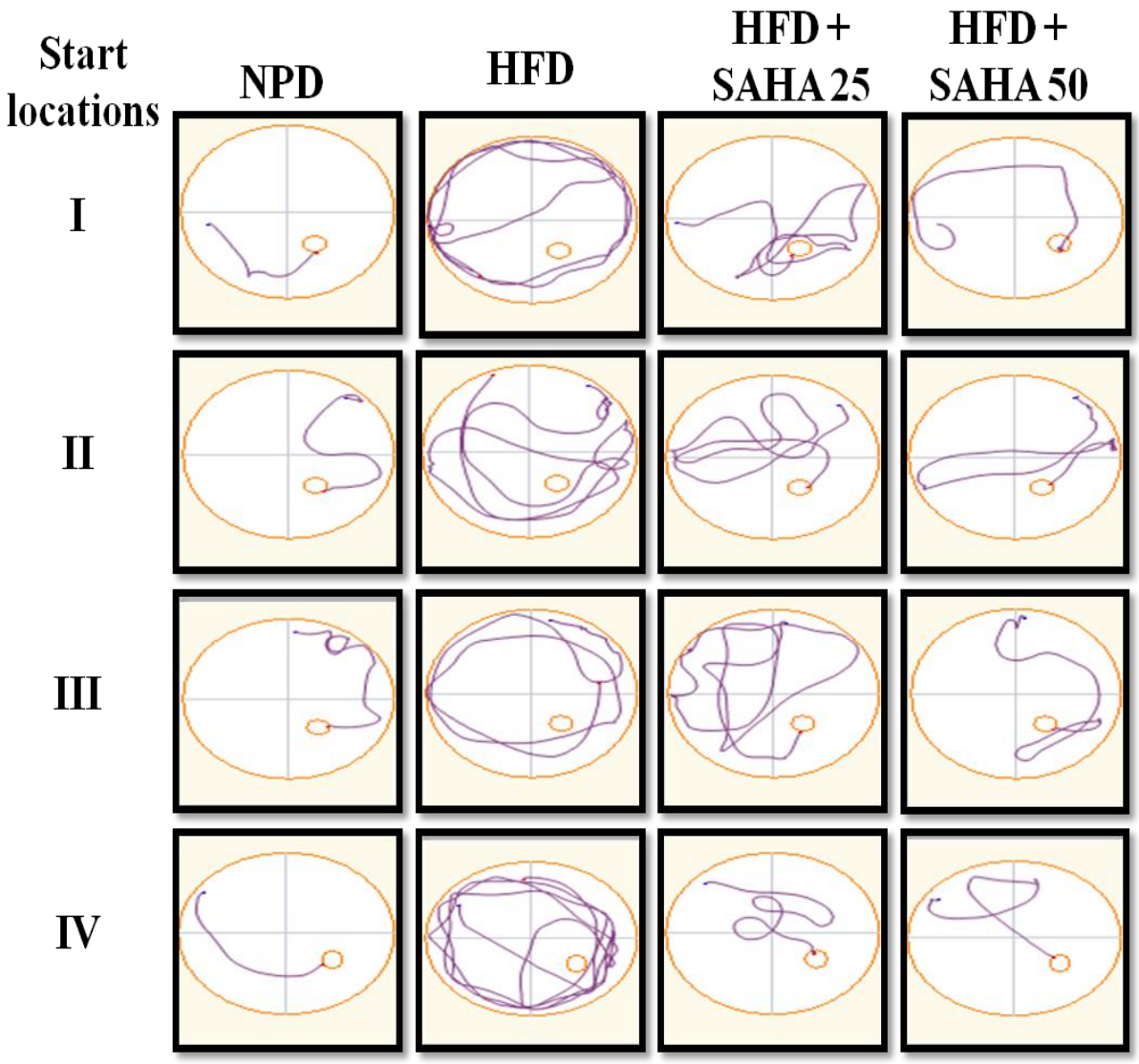

Fig. 5.30c Representative images showing tracking record of mice of different groups to find the hidden platform from various start locations in MWM.

5.5.6. Effect of pan HDAC inhibitors on time spent in target quadrant in the probe trial

During the probe trial, with the platform removed, HFD fed mice did not show a preference for the target quadrant, whereas the NPD fed mice spent significantly more time in the target quadrant. Moreover, the mice treated with HDAC inhibitors, SAHA ($F_{(3, 39)} = 13.46$; $P < 0.01$) (Fig. 5.31a) and NaB ($F_{(4, 39)} = 8.07$; $P < 0.01$) (Fig. 5.31b) spent significantly more time in target quadrant as compared with HFD alone fed mice. Fig. 5.31c shows track record of time spent in the target quadrant of one representative animal from each group in MWM probe trial with platform removed.

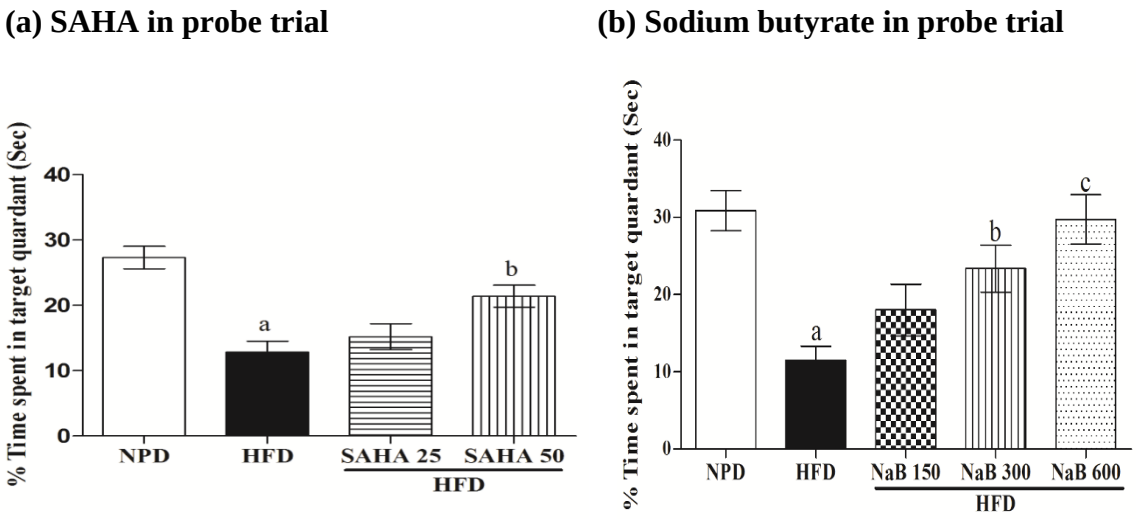

Fig. 5.31 Effect of pan HDAC inhibitors on time spent in target quadrant. Values are expressed as mean ± SEM **(a) SAHA** (^{a} *P* <0.001 vs NPD); (^{b}*P* <0.01 vs HFD) **(b) Sodium butyrate** (^{a}P <0.001 vs NPD); (^{b}P < 0.05 vs HFD); (^{c}P < 0.001 vs HFD).

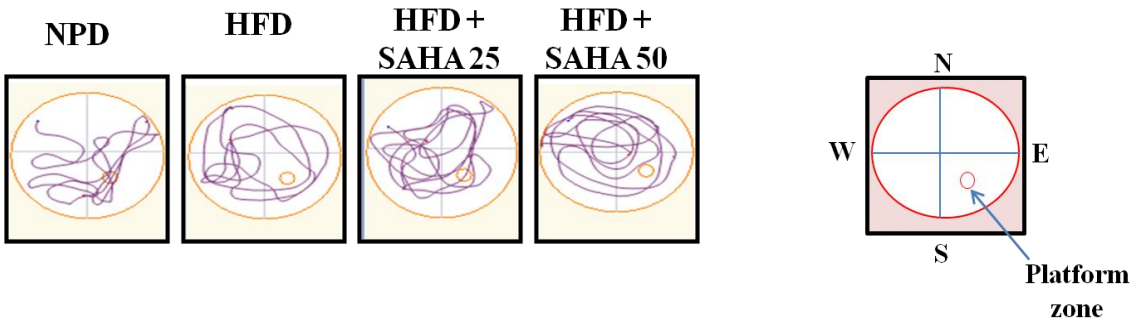

Fig.5.31c Representative images showing tracking record with respect to time spent in target quadrant of one representative animal from each group in MWM retention trial.

5.5.7. Effect of pan HDAC inhibitors on Passive avoidance task

Mice were next tested in passive avoidance task. The latency in the acquisition trial did not differ significantly (P > 0.05) between all the experimental groups (Fig. 5.32a and 5.32b). Twenty four hours after the acquisition trial, the mice were again tested and it was found that the retention latency was significantly decreased in the HFD fed group as compared with NPD fed group (P < 0.001) (Fig. 5.32a and 5.32b). Decreased retention latency in the HFD fed mice was significantly and dose dependently ameliorated by SAHA **(**$F_{(3, 39)}$ = 16.81; P < 0.01) (Fig. 5.32a) and NaB treatment ($F_{(4, 39)}$ =23.73; P < 0.01) (Fig. 5.32b), indicating improved retention of memory.

(a) SAHA on Passive avoidance task

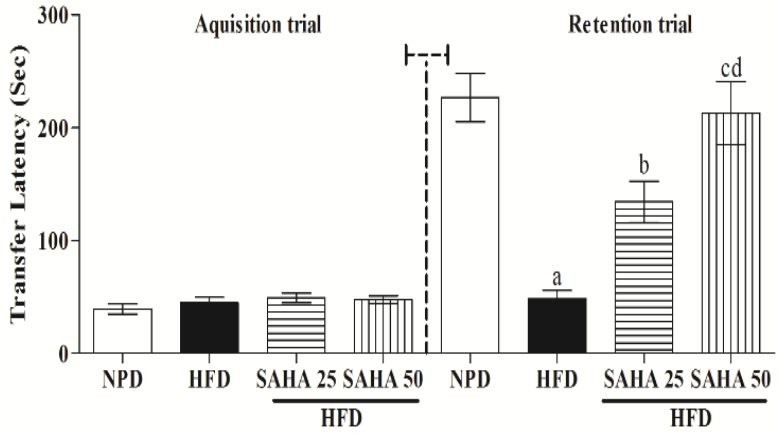

Fig. 5.32 (a) Effect of SAHA treatment on Passive avoidance task.Values are expressed as mean ± SEM ([a] P <0.001 vs NPD); ([b]P <0.05 vs HFD); ([c]P < 0.001 vs HFD); ([d]P < 0.05 vs SAHA 25 mg/kg).

(b) Sodium butyrate on Passive avoidance task

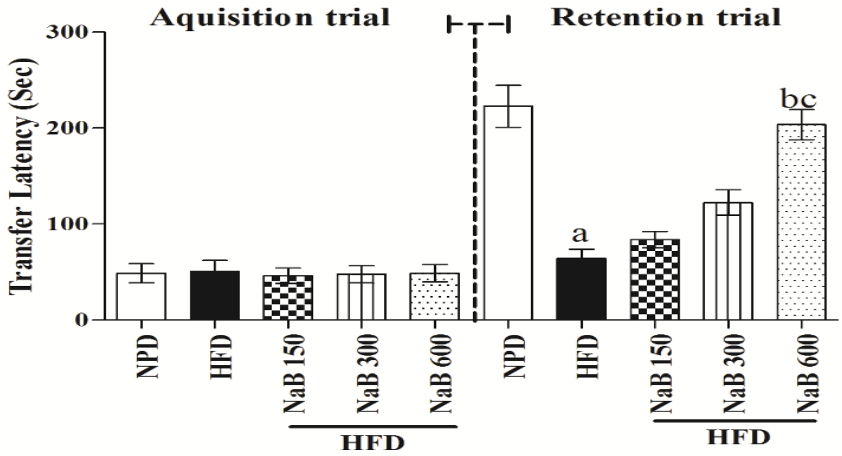

Fig.5.32 (b) Effect of Sodium butyrate treatment on Passive avoidance task. Values are expressed as mean ± SEM ([a]P< 0.001 vs NPD); ([b]P< 0.001 vs HFD); ([c]P< 0.01 vs NaB 300).

5.5.8. Effect of pan HDAC inhibitors on Object recognition task (ORT)

In the ORT, during the training session, no significant difference was observed in exploratory preferences among all groups (data not shown). However, during the retention session, the mice fed with NPD spent longer time in exploring the novel object as compared with familiar object ($P < 0.001$) (Fig 5.33a and 5.33b). No such significant difference was observed in HFD fed mice ($P > 0.05$) (Fig. 5.33a and 5.33b). Treatment with HDAC inhibitors, SAHA (25 and 50mg/kg) and NaB (300 and 600 mg/kg), significantly attenuated the memory

deficits and these mice spent more time exploring the novel object as compared to familiar object (P < 0.001).

(a) SAHA in Novel ORT **(b) NaB in ORT task**

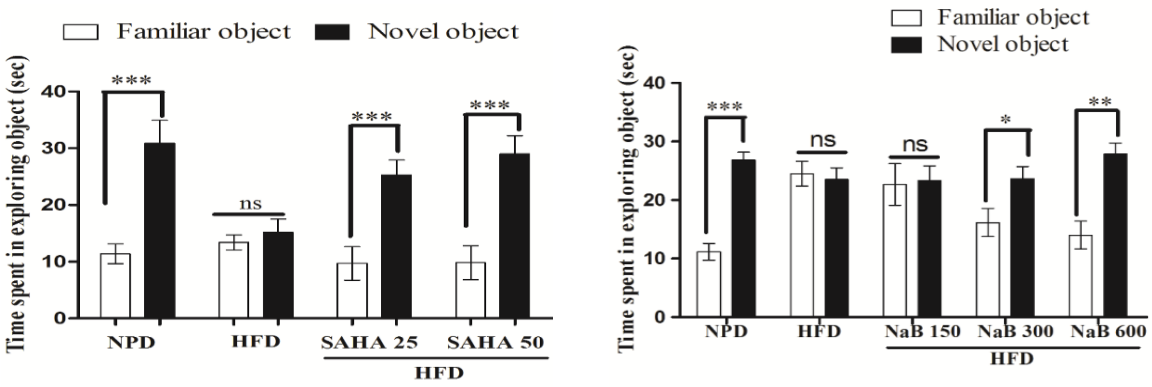

Fig. 5.33 (a) Effect of pan HDAC inhibitors on Object recognition task (a) SAHA (***P < 0.001 vs familiar object) **(b) NaB** (***P < 0.001 vs familiar object); (*P < 0.05 vs familiar object); (**P < 0 .01 vs familiar object).

5.5.9. Effect of pan HDAC inhibitors on TNF-α level

The level of TNF-α rose significantly in HFD fed mice as compared to those of NPD fed mice (P < 0.001). Treatment with SAHA (50 mg/kg) ($F_{(3, 23)} = 14.00$) (Fig. 5.34a) and NaB (300 mg/kg and 600 mg/kg) ($F_{(4,29)} = 10.24$) (Fig 5.34b); results in significant attenuation of TNF- α level as compared with HFD fed mice (P < 0.001).

(a) SAHA on TNF-α level **(b) NaB on TNF-α level**

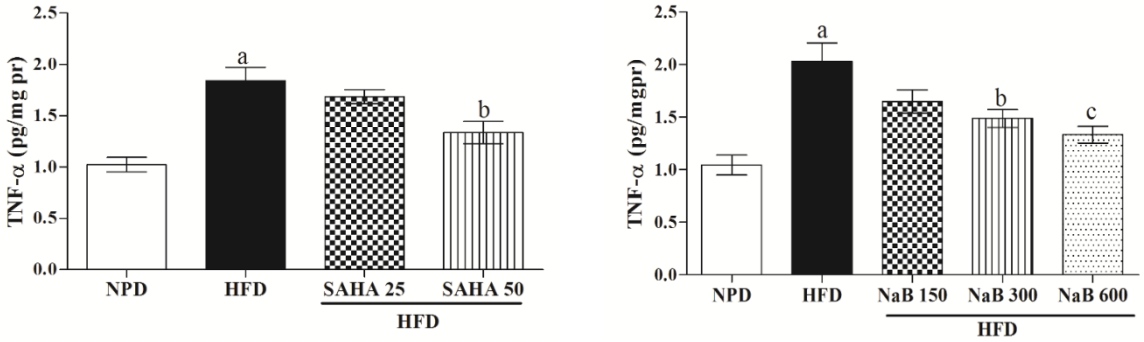

Fig. 5.34 Effect of pan HDAC inhibitors on TNF-α. Values are expressed as mean ± SEM **(a) SAHA** ([a] P <0.001 vs NPD); ([b]P <0.01 vs HFD) **(b) Sodium butyrate** ([a]P < 0.001 vs NPD); ([b]P < 0.05 vs HFD); ([c]P < 0.01 vs HFD).

5.5.10 Effect of pan HDAC inhibitors on malondialdehyde (MDA) level

Elevated level of MDA was reported in brain homogenates of HFD fed mice as compared with NPD fed mice ($P < 0.001$) (Fig. 5.35a and 5.35b). Treatment with HDAC inhibitor, SAHA ($F_{(3,23)}$=33.07; $P < 0.001$) (Fig. 5.35a) and NaB ($F_{(4,29)}$= 23.53; $P < 0.001$) (Fig. 5.35b) significantly and dose dependently attenuated MDA level as compared to HFD alone mice.

(a) SAHA on MDA level **(b) NaB on MDA level**

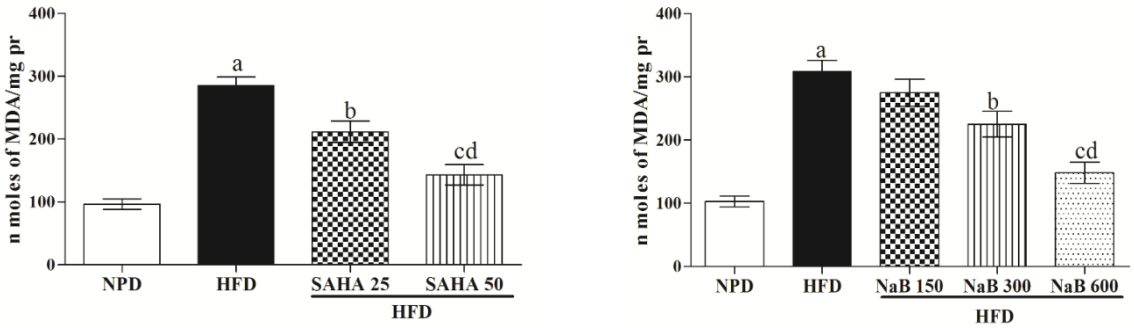

Fig. 5.35 Effect of pan HDAC inhibitors on MDA level. Values are expressed as mean ± SEM **(a) SAHA** ([a]P <0.001 vs NPD); ([b]P <0.01 vs HFD); ([c]P <0.001 vs HFD); ([d]P < 0.05 vs SAHA 25 mg/kg) **(b) NaB** ([a]P <0.001 vs NPD); ([b]P <0.05 vs HFD); ([c]P <0.001 vs HFD); ([d]P < 0.05 vs NaB 300 mg/kg).

5.5.11 Effect of pan HDAC inhibitors on nitrite level

HFD feeding results in significant increased nitrite levels as compared to NPD fed mice ($P < 0.001$) (Fig. 5.36a and 5.36b). However, the mice treated with HDAC inhibitors, SAHA ($F_{(3,23)}$ = 20.78; $P < 0.001$) (Fig. 5.36a) and NaB ($F_{(4,29)}$ = 36.95; $P < 0.001$) (Fig. 5.36b) showed significant and dose dependent reduction in nitrite level in brain homogenates as compared to HFD alone fed mice.

(a) SAHA on Nitrite level **(b) Sodium butyrate on Nitrite level**

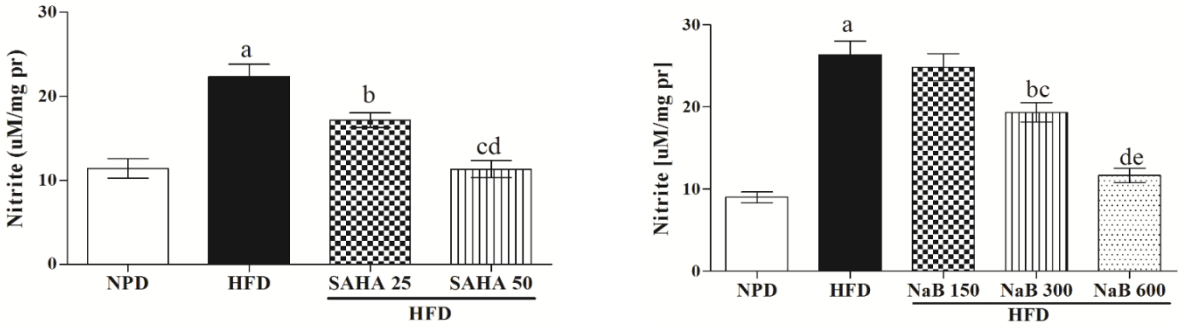

Fig. 5.36 Effect of pan HDAC inhibitors on nitrite level. Values are expressed as mean ± SEM **(a) SAHA** ([a]*P* <0.001 vs NPD); ([b]*P* <0.05 vs HFD); ([c]*P* < 0.001 vs HFD); ([d]P< 0.01 vs SAHA 25). **(b) Sodium butyrate** ([a]P < 0.001 vs NPD); ([b]P < 0.01 vs HFD); ([c]P < 0.05 vs NaB 150 mg/kg); ([d]P < 0.001 vs HFD); ([e]P < 0.01 vs NaB 300).

5.5.12. Effect of pan HDAC inhibitors on reduced glutathione (GSH) level

The level of antioxidant enzyme GSH, was found to be significantly reduced in brain homogenates of HFD fed mice as compared with NPD fed mice ($P < 0.001$) (Fig. 5.37a and 5.37b). However, treatment with HDAC inhibitors, SAHA at high dose (50 mg/kg) ($F_{(3,23)} = 10.29$; $P < 0.001$) (Fig. 5.37a) and NaB at medium (300 mg/kg) and high doses (600 mg/kg) ($F_{(4,29)} = 32.21$; $P < 0.001$) (Fig. 5.37b), restored GSH level in HFD mice.

(a) SAHA on GSH level **(b) Sodium butyrate on GSH level**

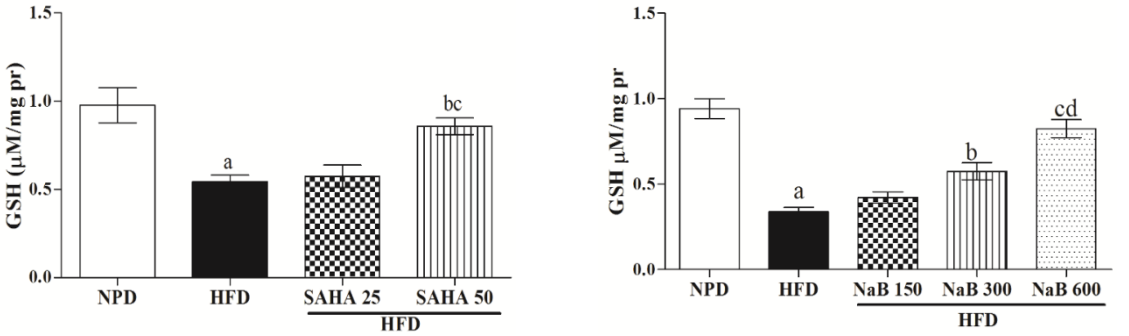

Fig.5.37 Effect of pan HDAC inhibitors on reduced glutathione. Values are expressed as mean ± SEM **(a) SAHA** ($^{a}P < 0.001$ vs NPD); ($^{b}P < 0.05$ vs HFD); ($^{c}P < 0.05$ vs SAHA 25) **(b) Sodium butyrate** ($^{a}P < 0.001$ vs NPD); ($^{b}P < 0.01$ vs HFD); ($^{c}P < 0.001$ vs HFD); ($^{d}P < 0.01$ vs NaB 300).

5.5.13. Effect of pan HDAC inhibitors on ptau level

HFD feeding results in significant increase in ptau levels as compared with NPD fed mice ($P < 0.001$) (Fig. 5.38a and 5.38b). In contrast, the mice treated with HDAC inhibitors, SAHA ($F_{(3,23)} = 10.36$; $P < 0.001$) (Fig. 5.38a) and NaB ($F_{(4,29)} = 7.34$; $P < 0.001$) (Fig. 5.38b) showed significant attenuation of ptau levels in hippocampus homogenates as compared with alone HFD fed mice.

(a) SAHA on ptau level **(b) Sodium butyrate on ptau level**

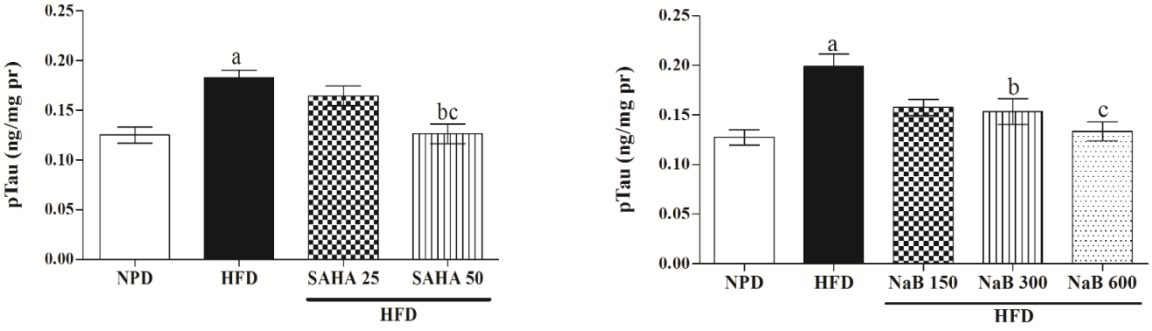

Fig. 5.38 Effect of pan HDAC inhibitors on ptau level. Values are indicated as Mean ± SEM. **(a) SAHA** ($^{a}P < 0.001$ vs NPD); ($^{b}P < 0.01$ vs HFD); ($^{c}P < 0.05$ vs SAHA 25) **(b) Sodium butyrate** ($^{a}P < 0.001$ vs NPD); ($^{b}P < 0.05$ vs HFD); ($^{c}P < 0.01$ vs HFD).

5.5.14. Effect of pan HDAC inhibitors on Aβ level

HFD feeding results in significant increase in Aβ $_{1-42}$ levels as compared with NPD fed mice ($P < 0.001$) (Fig. 5.39a and 5.39b). In contrast, the mice treated with HDAC inhibitors, SAHA ($F_{(3,23)}= 21.40$; $P < 0.001$) (Fig. 5.39a) and NaB ($F_{(4,29)} = 26.10$; $P < 0.001$) (Fig.5.39b) showed attenuation of Aβ $_{1-42}$ levels in hippocampus homogenates.

(a) SAHA on Aβ level **(b) NaB on Aβ level**

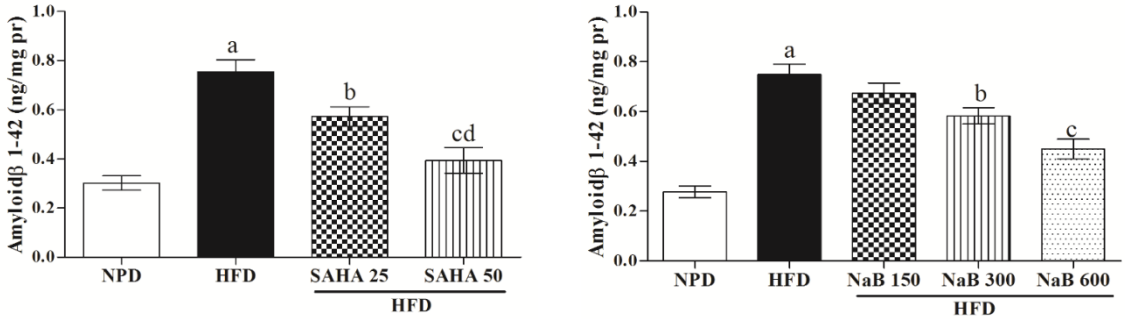

Fig. 5.39 Effect of pan HDAC inhibitors on Aβ level (a) SAHA Values are indicated as Mean ± SEM. ([a]P< 0.001 vs NPD); ([b]P< 0.05 vs HFD); ([c]P <0.001 vs HFD); ([d]P < 0.05 vs SAHA 25) **(b) Sodium butyrate** ([a]P< 0.001 vs NPD); ([b]P< 0.05 vs HFD); ([c]P <0.001 vs HFD).

5.5.15. Effect of pan HDAC inhibitors on histone H3 acetylation level

The level of global histone H3 acetylation was found to be reduced in HFD fed mice as compared with NPD fed mice ($P < 0.001$) (Fig. 5.40a and 5.40b). Treatment with HDAC inhibitor, SAHA significantly ameliorated the histone H3 acetylation levels ($F_{(3, 23)} =36.99$; $P < 0.001$) (Fig. 5.40a). Moreover, sodium butyrate at medium and high dose (300 mg/kg and 600mg/kg), significantly and dose dependently ameliorated the global H3 acetylation levels in HFD mice ($F_{(4,29)}= 17.66$; $P < 0.001$) (Fig. 5.40b).

(a) SAHA on histone H3 acetylation **(b) NaB on histone H3 acetylation**

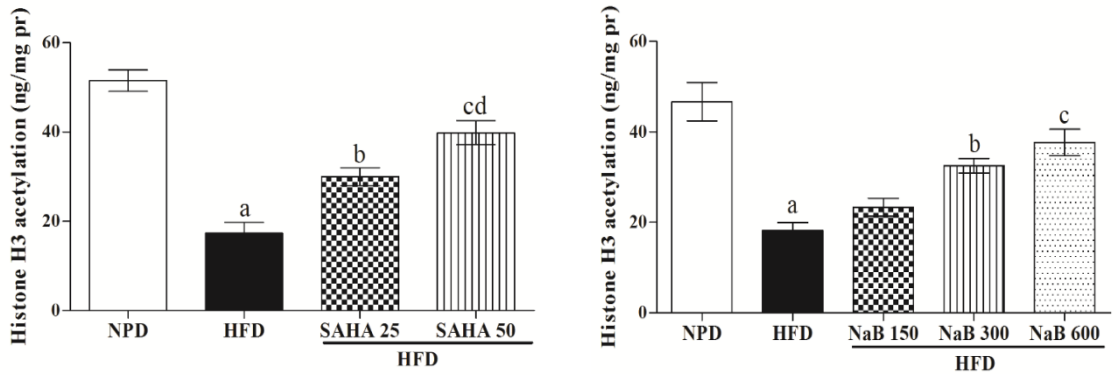

Fig. 5.40 Effect of pan HDAC inhibitors on Global Histone H3 acetylation. Values are expressed as mean ± SEM **(a) SAHA** ([a] P <0.001 vs NPD); ([b]P < 0.01 vs HFD); ([c]P <0.001 vs HFD); ([d]P< 0.05 vs SAHA 25) **(b) sodium butyrate** ([a]P <0.001 vs NPD); ([b]P <0.01 vs HFD); ([c]P < 0.001 vs HFD).

5.5.16. Effect of pan HDAC inhibitors on BDNF level

The BDNF levels were found to be significantly reduced in HFD fed mice as compared with NPD fed mice ($P < 0.001$) (Fig. 5.41a and 5.41b). However, SAHA at higher dose (50 mg/kg), significantly enhanced the BDNF levels in HFD fed mice ($F_{(3, 23)} = 11.55$; $P < 0.01$) (Fig 5.41a). Moreover, NaB dose dependently enhanced the BDNF levels in HFD fed mice ($F_{(4,29)} = 44.81$; $P < 0.001$) (Fig. 5.41b).

(a) SAHA on BDNF level **(b) Sodium butyrate on BDNF level**

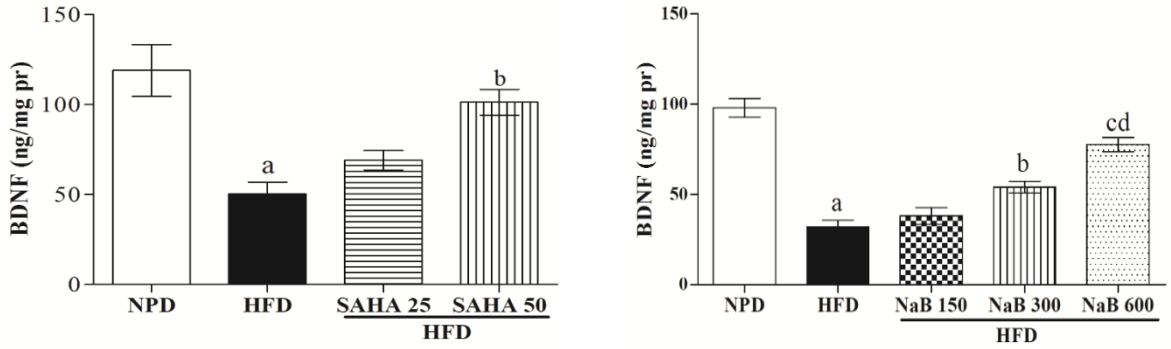

Fig. 5.41 Effect of pan HDAC inhibitors on BDNF level. Values are expressed as mean ± SEM (**a) SAHA** ([a] P <0.001 vs NPD); ([b]P <0.01 vs HFD). **(b) Sodium butyrate** ([a]P <0.001 vs NPD); ([b]P <0.01 vs HFD); ([c]P < 0.001 vs HFD); ([d]P< 0.01 vs NaB 300 mg/kg).

5.5.17. Effect of pan HDAC inhibitors on CREB level

HFD feeding results in significant reduction of CREB level as compared to NPD fed mice (P < 0.01) (Fig. 5.42a and 5.42b). In contrast, treatment with HDAC inhibitors, SAHA at high dose (50 mg/kg) ($F_{(3,23)} = 7.81$; P < 0.01) (Fig. 5.42a) and NaB at medium and high dose (300 mg/kg and 600 mg/kg, respectively) ($F_{(4,29)} = 10.83$; P < 0.001) (Fig. 5.42b), significantly ameliorate the CREB level in HFD mice.

(a) SAHA on CREB level **(b) Sodium butyrate on CREB level**

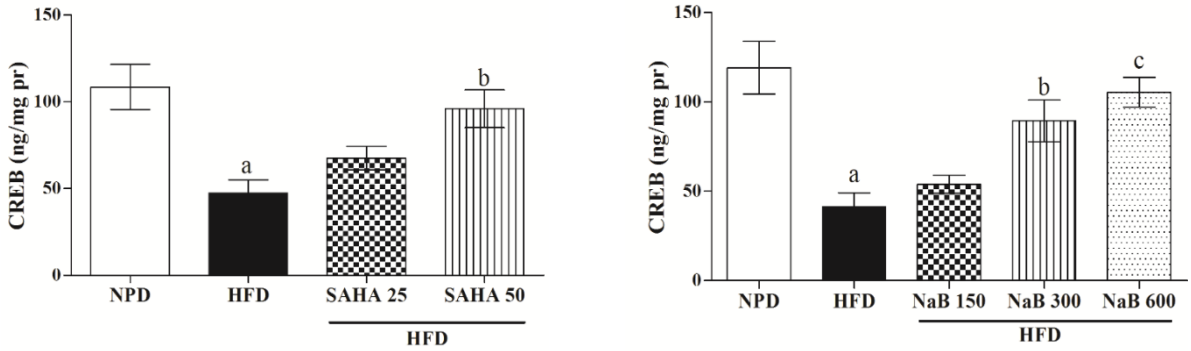

Fig. 5.42 Effect of pan HDAC inhibitors on CREB level. Values are expressed as mean ± SEM **(a) SAHA (**[a]P < 0.01 vs NPD); ([b]P < 0.01 vs HFD) **(b) Sodium butyrate** ([a]P < 0.001 vs NPD); ([b]P < 0.05 vs HFD); ([c]P < 0.01 vs HFD).

5.5.18. Effect of SAHA on Dentate gyrus and CA1 neurons of hippocampus

Light microscopic results of H&E-stained sections showed healthy neurons in DG and CA1 region of hippocampus in NPD fed mice (Fig. 5.43 Panel A; Fig. 5.44 Panel A). Healthy neurons appeared robust in shape, had a spherical or slightly oval nucleus and a single large nucleolus with clear visible cytoplasm as indicated by yellow arrows. However, the HFD fed mice showed marked changes in DG and CA1 in the form of disorganization and cell loss (Fig. 5.43 Panel B; 5.44 Panel B) as indicated by red arrows. There was also marked shrinkage in the size of the pyramidal cells with darkened nuclei. Treatment with SAHA, results in significant improvement in the form of preservation of pyramidal cells and markedly decreased apoptosis. Moreover, there was marked improvement in neuronal density and reduction in pyknotic neurons in DG and CA1 regions following SAHA treatment (Fig. 5.43 Panel C, D and Fig. 5.44 Panel C,D).

5.5.18. 1 Effect of SAHA on Dentate gyrus neurons of hippocampus

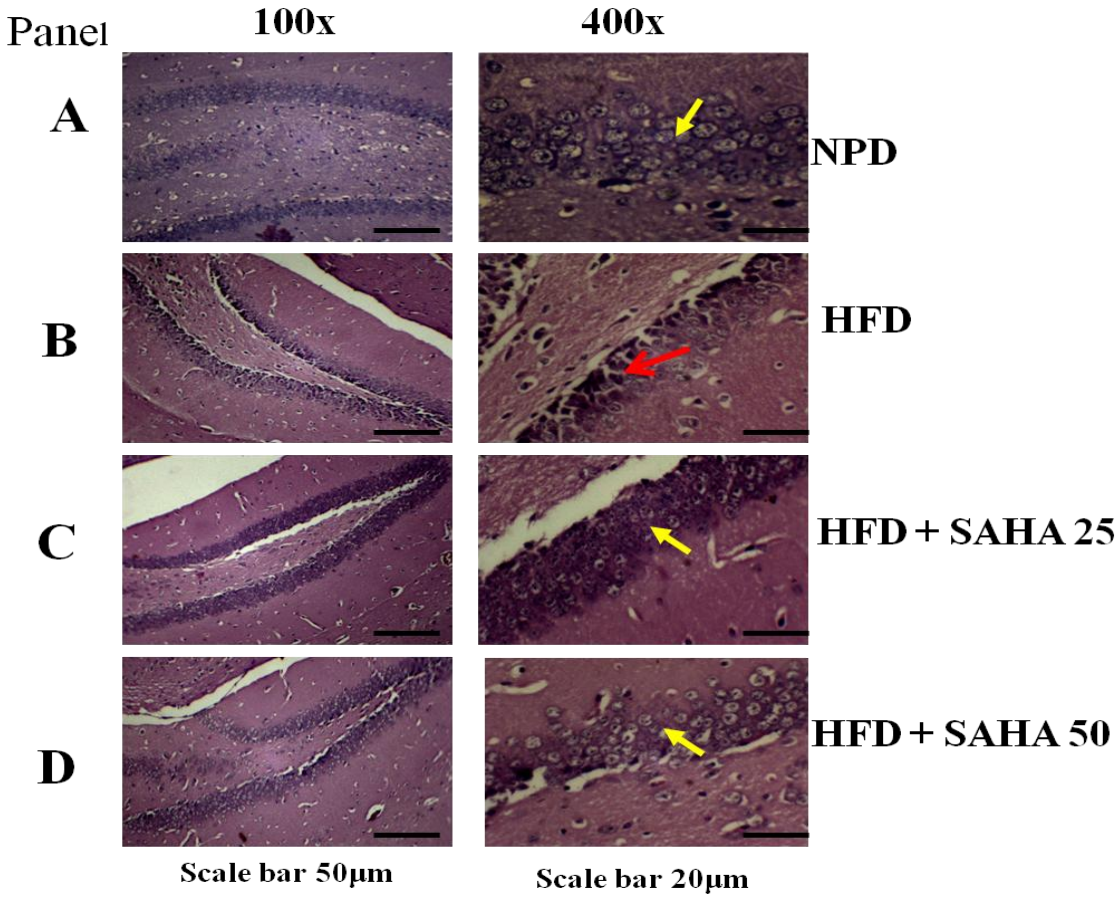

Fig. 5.43 shows photomicrographs of Dentate gyrus (DG) of **(Panel A)** normal pellet diet **(Panel B)** High fat diet **(Panel C)** SAHA 25mg/kg **(Panel D)** SAHA 50mg/kg. Yellow arrows indicate normal healthy neurons; Red arrows indicate damaged or sickle shaped pyknotic neurons

5.5.18.2 Effect of SAHA on CA1 neurons of hippocampus

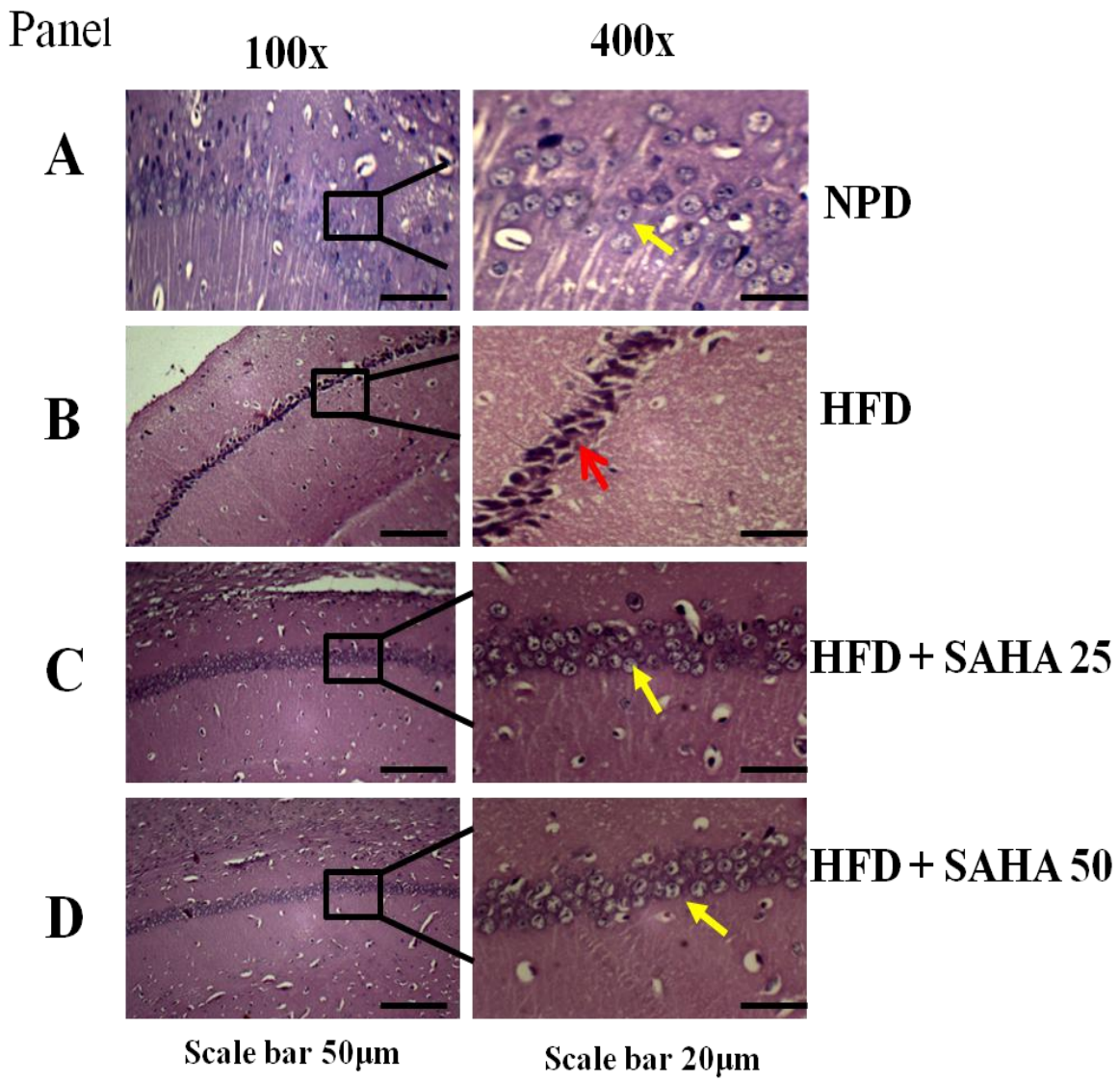

Fig. 5.44 Effect of SAHA on CA1 shows photomicrographs of CA1 **(Panel A)** normal pellet diet **(Panel B)** High fat diet **(Panel C)** SAHA 25mg/kg **(Panel D)** SAHA 50mg/kg. Yellow arrows indicate normal healthy neurons; Red arrows indicate damaged or sickle shaped pyknotic neurons

5.5.19. Effect of SAHA treatment on neuronal count in dentate gyrus and CA1 regions

The HFD feeding results in significant increase in the percentage of damaged neurons with altered morphological characters in both DG and CA1 regions ($P < 0.001$) (Fig.5.45a and 5.45b). In contrast, the mice treated with SAHA showed significant neuroprotection as evidenced by reduced percentage damaged neurons in DG and CA1 regions ($P < 0.001$; Fig. 5.45a and 5.45b).

(a) SAHA on % damaged neurons in DG **(b) SAHA on % damaged neurons in CA1**

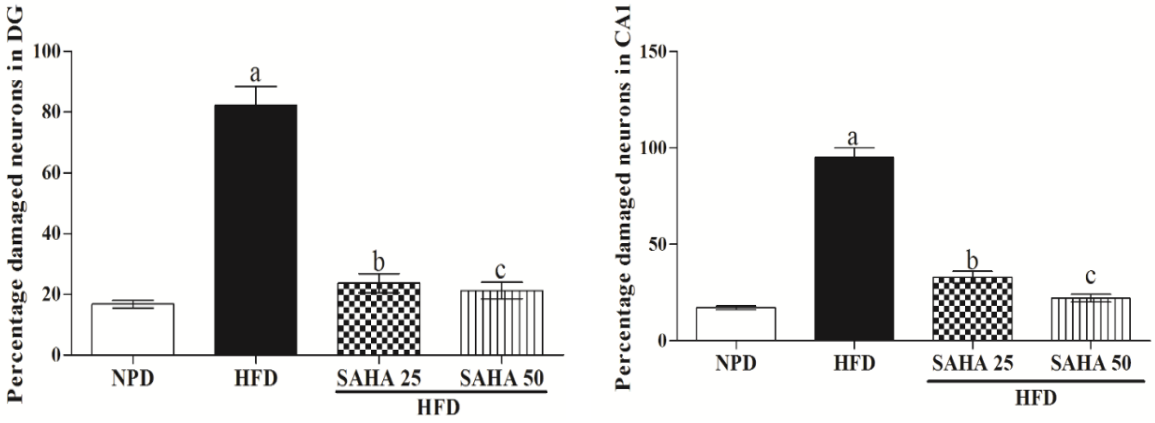

Fig. 5.45 Effect of SAHA on neuronal count (a) DG neurons ($^{a}P < 0.001$ vs NPD; $^{b}P < 0.01$ vs HFD; $^{c}P < 0.01$ vs HFD) **(b) CA1 neurons** ($^{a}P < 0.001$ vs NPD; $^{b}P < 0.001$ vs HFD; $^{c}P < 0.001$ vs HFD).

5.5.20 Effect of sodium butyrate on dentate gyrus and CA1 region of hipppocampus

Light microscopic results of H&E-stained sections showed healthy neurons in DG and CA1 region of hippocampus in NPD fed mice (Fig. 5.46 Panel A and Fig. 5.47 Panel A). Healthy neurons appeared robust in shape, had a spherical or slightly oval nucleus and a single large nucleolus with clear visible cytoplasm as indicated by yellow arrows. However, the HFD fed mice showed marked changes in DG and CA1 neurons in the form of disorganization and cell loss as indicated by red arrows (Fig.5.46 Panel B and Fig. 5.47 Panel B). There was also marked shrinkage in the size of the pyramidal cells with darkened nuclei. Treatment with NaB at doses (300 mg/kg and 600mg/kg) caused improvement in the form of preservation of pyramidal cells (Fig.5.46 Panel C-E and Fig. 5.47 Panel C-E, respectively). Moreover, there was marked improvement in neuronal density and reduction in pyknotic neurons following NaB treatment.

5.5.20.1 Effect of sodium butyrate on dentate gyrus neurons

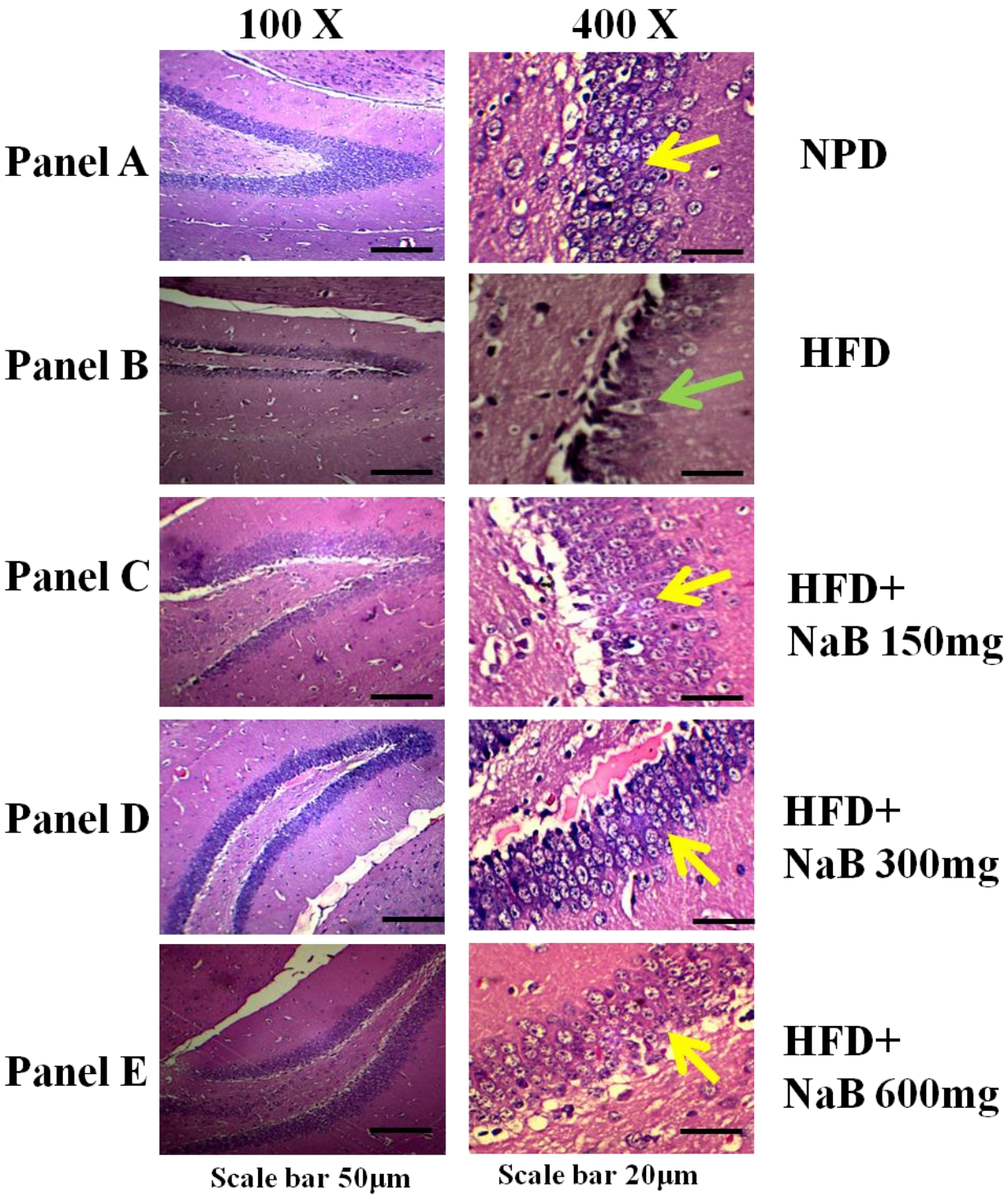

Fig. 5.46 Effect of sodium butyrate on dentate gyrus. Photomicrographs shows Dentate gyrus (DG) neurons of **(Panel A)** normal pellet diet **(Panel B)** High fat diet **(Panel C)** NaB 150 mg/kg **(Panel D)** NaB 300 mg/kg **(Panel E)** NaB 600mg/kg. Yellow arrows indicate normal healthy neurons; Red arrows indicate damaged or sickle shaped pyknotic neurons.

5.5.20.2 Effect of sodium butyrate on CA1 neurons

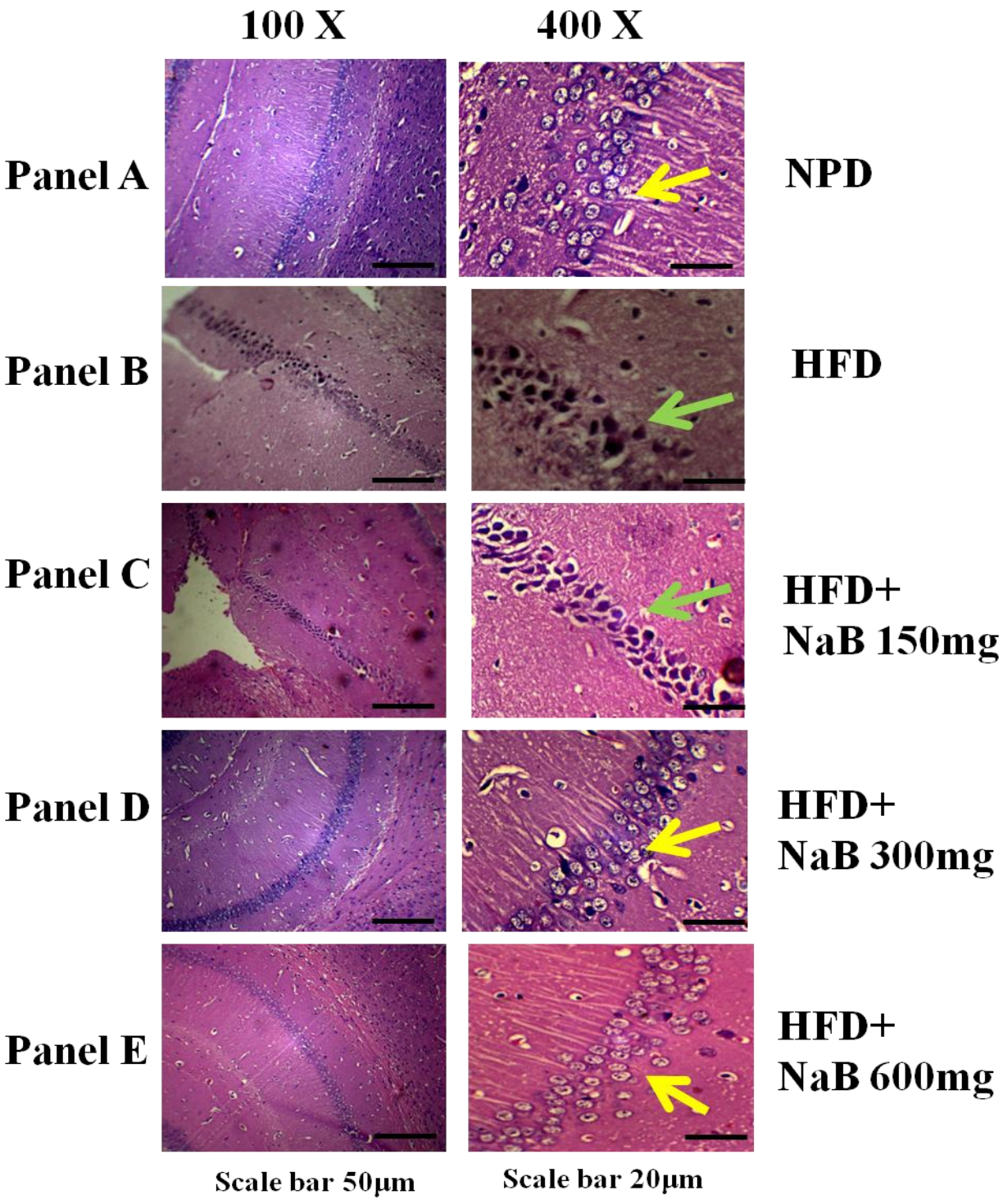

Fig. 5.47 shows photomicrographs of CA1 (Panel A) normal pellet diet **(Panel B)** High fat diet **(Panel C)** NaB 150mg/kg **(Panel D)** NaB 300mg/kg **(Panel E)** NaB 600mg/kg. Yellow arrows indicate normal healthy neurons; Red arrows indicate damaged or sickle shaped pyknotic neurons.

5.5.21. Effect of Sodium butyrate treatment on neuronal count in DG and CA1 neurons

The HFD feeding results in significant increase in the percentage of damaged neurons with altered morphological characters in both DG and CA1 regions ($P < 0.001$) (Fig.5.48 and 5.48). In contrast, the mice treated with NaB showed significant neuroprotection as evidenced by reduced percentage damaged neurons in DG and CA1 regions ($P < 0.001$; Fig. 5.48 and 5.48).

(a) NaB on % damaged neurons in DG **(b) NaB on % damaged neurons in CA1**

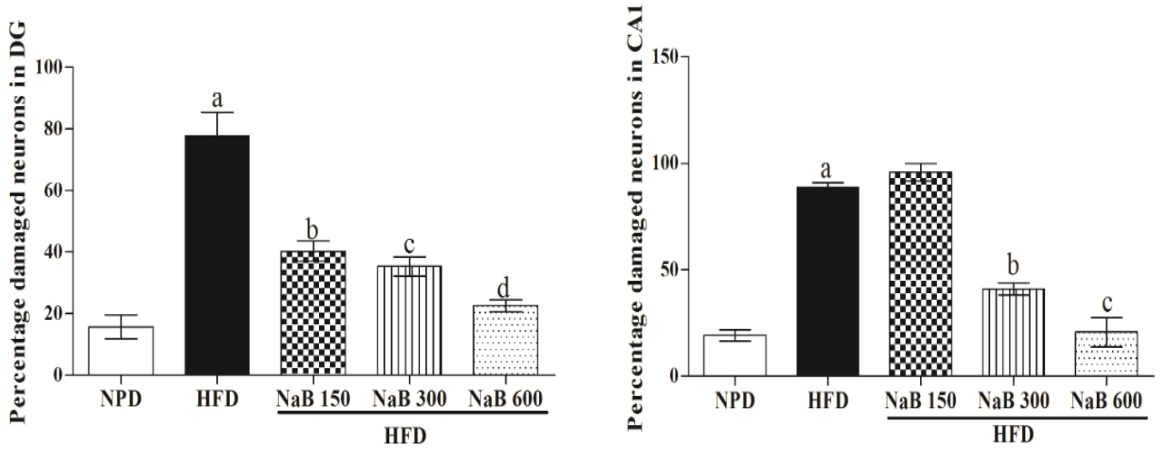

Fig. 5.48 Effect of NaB treatment on neuronal count in (a) DG neurons ($^{a}P < 0.001$ vs NPD; $^{b}P<0.01$ vs HFD; $^{c}P< 0.01$ vs HFD; $^{d}P<0.01$ vs HFD) **(b) CA1 neurons** ($^{a}P < 0.001$ vs NPD; $^{b}P < 0.01$ vs HFD; $^{c}P < 0.001$ vs HFD).

5.5.22. Effect of SAHA treatment on apoptotic cell death in hippocampus

DNA fragmentation study reveals increased apoptotic neuronal death in hippocampus regions (DG and CA1) of HFD fed mice as compared to NPD fed mice (Fig. 5.49 Panel A and Panel B). However, SAHA administration results in significant attenuation of apoptotic cell death in DG and CA1 regions of hippocampus in HFD fed mice (Fig. 5.49 Panel C).

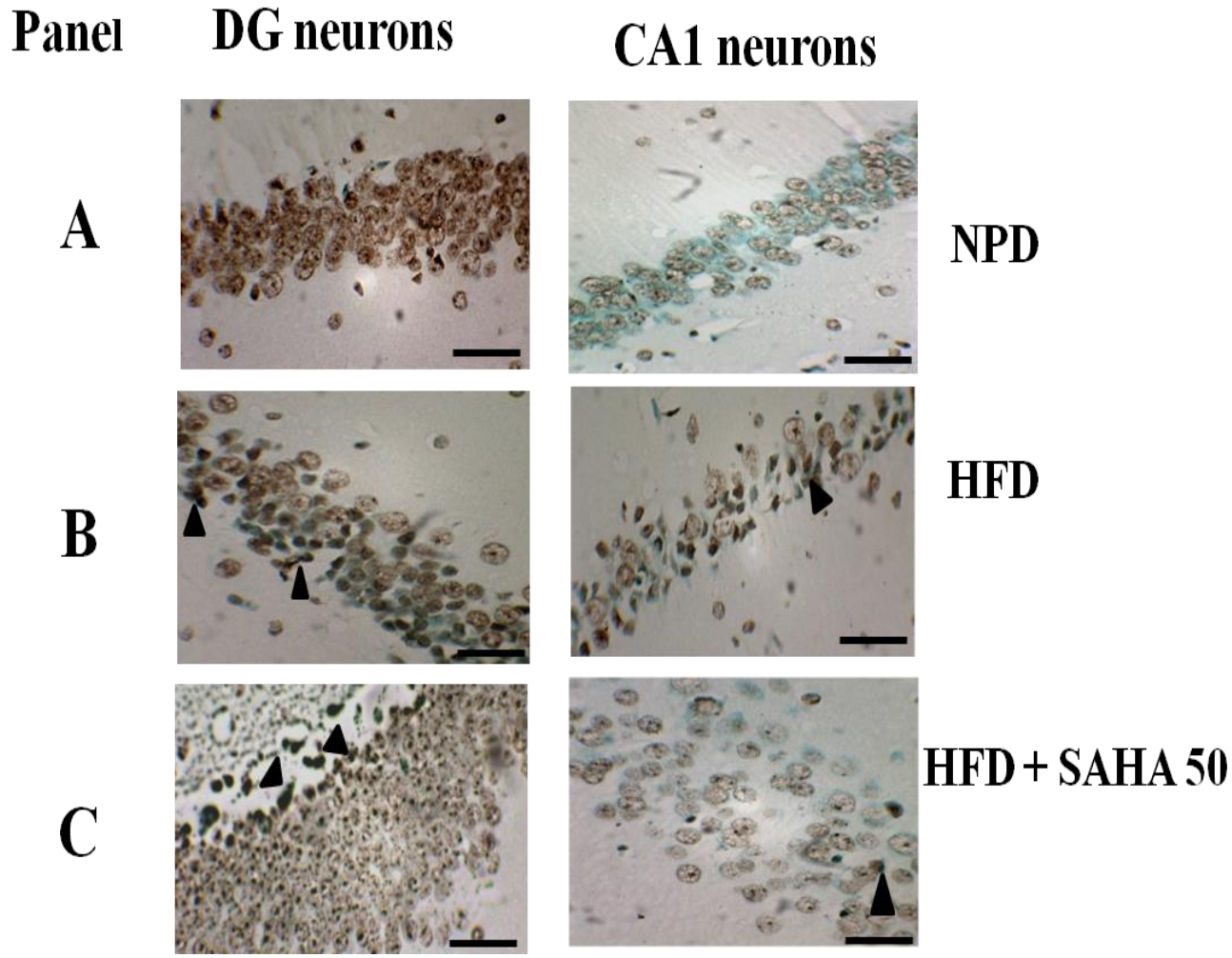

Fig. 5.49 Effect of SAHA treatment on apoptotic cell death in hippocampus: DNA fragmentation (TUNEL) assay: Photomicrographs (400X) shows dentate gyrus (DG) and CA1 regions of hippocampus after TUNEL staining. (Panel A) shows DG and CA1 region of NPD fed mice, (Panel B) shows DG and CA1 of HFD fed mice (Panel C) shows DG and CA1 regions of SAHA (50mg/kg) treated animals, respectively. Black arrowheads show apoptotic cells (**Scale bar 20µm).**

5.5.23. Effect of HFD feeding and SAHA treatment on fat deposition in mice

HFD feeding increases visceral, perirenal as well as liver fat as compared to NPD fed mice. SAHA treatment combat the increased visceral, perirenal and liver fat in HFD fed mice.

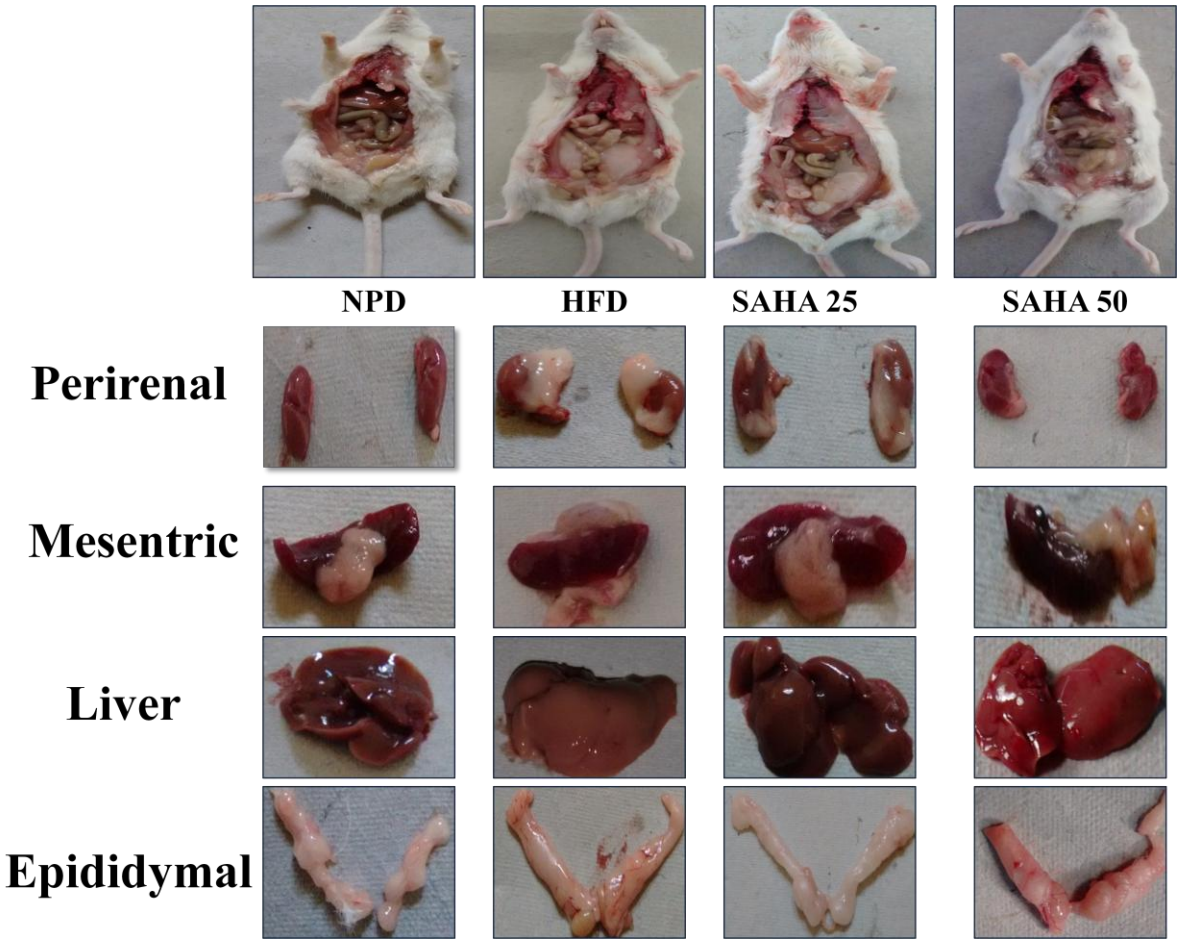

Fig.5.50 Representative images of visceral white adipose tissue and liver of mice.

5.6. Effect of low dose combination of IMX and SAHA on insulin resistance and associated cognitive deficits

5.6.1. Effect of low dose of IMX and SAHA alone and in combination on body weight and serum parameters

HFD fed mice gained significantly more weight than the NPD fed mice ($F_{(4,39)} = 8.54$; $P < 0.01$). In addition, there was a significant increase in serum parameters, characteristic of insulin resistance viz. glucose ($F_{(4,29)} = 14.14$; $P < 0.001$), TGs ($F_{(4,29)} = 56.55$; $P < 0.001$), TC ($F_{(4,29)} = 49.58$; $P < 0.001$) and insulin levels ($F_{(4,29)} = 34.85$; $P < 0.001$) in HFD fed mice (Table 5.5). No significant differences were observed in any of these parameters in mice that received either low dose of IMX (0.05 mg/kg) or SAHA (12.5 mg/kg). In contrast, the mice those received combined treatment of IMX and SAHA showed significant attenuation of body weight, serum glucose, TGs, TC and insulin levels. Further, we observed significant attenuation of HOMA-IR values in mice treated with combination of these drugs as compared to HFD fed mice ($F_{(4,29)} = 37.63$; $P < 0.001$) (Table.5.5).

Parameter	**NPD**	**HFD**	**HFD +IMX**	**HFD + SAHA**	**HFD+ IMX+SAHA**
Body Weight (g)	30.25 ± 4.03	38.88 ± 4.58[a]	38.13 ± 3.36	37.25 ± 3.06	32.75 ± 2.87[bc]
Glucose (mg/dl)	93.83±9.58	136.7±12.93[a]	129.2±8.99	125.2±7.68	104.8±16.77[bcd]
Insulin (pmol/l)	74.00 ± 9.32	166.3 ± 21.27[a]	157.5 ± 18.24	148.2 ± 17.94	113.2 ± 7.52[bcd]
Triglycerides (mg/dl)	60.00±11.95	183.0±24.13[a]	171.0±18.32	183.2±13.70	124.8±15.42[bcd]
Total Cholesterol (mg/dl)	114.7±18.72	250.0±13.45[a]	233.0±24.32	223.0±24.99	146.2±19.56[bcd]
HOMA-IR	1.39 ± 0.17	3.32 ± 0.44[a]	3.12 ± 0.37	2.92 ± 0.36	2.15 ± 0.11[bcd]

Table 5.5 Effect of low dose of IMX and SAHA alone and in combination on body weight and serum parameters. Values are indicated as mean ± S.D. Where, Body weight (^{a}P<0.001 vs NPD; ^{b}P<0.05 vs HFD; ^{c}P< 0.05 vs IMX) (n=8); **Serum Glucose** (^{a}*P* <0.001 vs NPD; ^{b}P<0.001 vs HFD; ^{c}P< 0.05 vs IMX; ^{d}P< 0.05 vs SAHA) (n=6); **Serum Triglycerides** (^{a}*P* <0.001 vs NPD; ^{b}P<0.001 vs HFD; ^{c}P < 0.001 vs IMX; ^{d}P < 0.001 vs SAHA) (n=6); **Total Cholesterol** (^{a}*P* <0.001 vs NPD; ^{b}P<0.001 vs HFD; ^{c}P < 0.001 vs IMX; ^{d}P < 0.001 vs SAHA) (n=6); **Insulin** (^{a}*P* <0.001 vs NPD; ^{b}P<0.001 vs HFD; ^{c}P < 0.001 vs IMX; ^{d}P < 0.01 vs SAHA) (n=6); **HOMA-IR** (^{a}*P* <0.001 vs NPD; ^{b}P<0.001 vs HFD; ^{c}P < 0.001 vs IMX; ^{d}P < 0.01 vs SAHA) (n=6) **Note**: (**IMX=** Indirubin-3'-monoxime (0.05mg/kg); **SAHA=** Suberoylanilide hydroxamic acid (12.5 mg/kg); **NPD**= Normal pellet diet; **HFD**=High fat diet).

5.6.2. Effect of low dose of IMX and SAHA alone and in combination on oral glucose tolerance test (OGTT)

The HFD fed mice showed marked glucose intolerance as assessed by OGTT. Blood glucose levels were found to be significantly higher in HFD fed mice as compared with NPD mice at 0, 15, 30, 60 and 120 minutes after oral glucose administration (Fig 5.51). Treatment with either GSK3β inhibitor, IMX or HDAC inhibitor, SAHA alone were ineffective in improving glucose tolerance at tested low doses. However, a combination of both these drugs, results in significant improvement in glucose tolerance as reduction in blood glucose level was observed at 60 and 120 min after glucose administration as compared to HFD fed mice (P < 0.001) (Fig. 5.51).

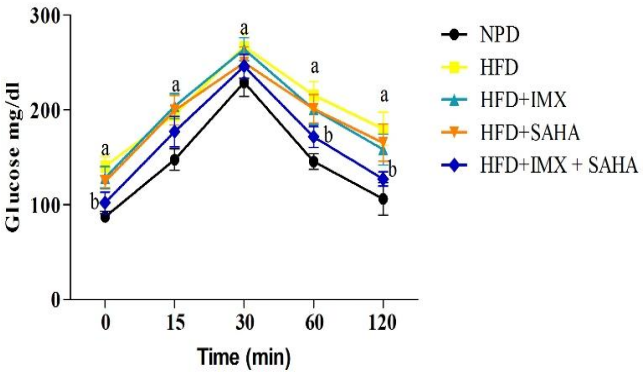

Fig. 5.51 Effect of low dose of IMX and SAHA alone and in combination on oral glucose tolerance test. Values are expressed as mean ± SEM (n=6) (^{a}P< 0.001 vs NPD); (^{b}P< 0.001 vs HFD). **Note**: (**IMX=** Indirubin-3'-monoxime (0.05mg/kg); **SAHA=** Suberoylanilide hydroxamic acid (12.5 mg/kg).

5.6.3. Effect of low dose of IMX and SAHA alone and in combination on locomotor activity

No significant difference was observed between any of the groups (P > 0.05) suggesting no effect whatsoever of HFD or IMX or SAHA alone and in combination on the locomotor activity of animals ($F_{(4,39)}$ = 0.44) (Fig. 5.52).

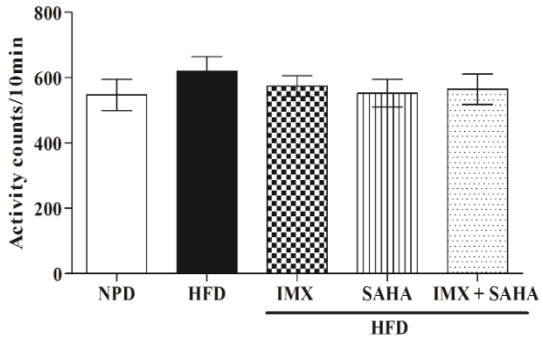

Fig.5.52 Effect of low dose of IMX and SAHA alone and in combination on locomotor activity. Values are expressed as mean ± SEM (n=8). **Note**: (**IMX=** Indirubin-3'-monoxime (0.05mg/kg); **SAHA=** Suberoylanilide hydroxamic acid (12.5 mg/kg).

5.6.4. Effect of low dose of IMX and SAHA alone and in combination on mean escape latency in morris water maze

The mean escape latency to find the hidden platform reduced gradually in all the experimental groups during 4 days of training. The mean escape latency was significantly higher in the HFD fed mice as compared with the NPD fed mice on days 2-4 (Fig. 5.53), showing poorer learning performance. The increased escape latency in the HFD group was significantly attenuated by combined treatment with IMX and SAHA on day 3 ($P < 0.01$) and day 4 ($P < 0.001$) (Fig. 5.53). However, no significant effect was observed in mice treated with either drug alone.

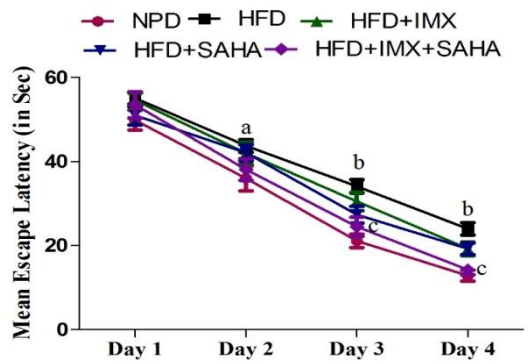

Fig.5.53 Effect of low dose of IMX and SAHA alone and in combination on mean escape latency in MWM. Values are expressed as mean ± SEM (n=8). (^{a}P <0.05 vs NPD); (^{b}P <0.01 vs NPD); (^{c}P < 0.01 vs HFD). **Note**: (**IMX=** Indirubin-3'-monoxime (0.05mg/kg); **SAHA=** Suberoylanilide hydroxamic acid (12.5 mg/kg).

5.6.5. Effect of low dose of IMX and SAHA alone and in combination on probe trial in morris water maze

During the probe trial, HFD fed mice failed to remember the precise location of the platform, spending significantly lesser time in the target quadrant as compared with NPD fed mice ($P < 0.001$, Fig. 5.54). Whereas, HFD fed mice treated with combination of low dose of IMX and SAHA spent significantly more time in the target quadrant indicating improved consolidation of memory ($F_{(4,39)} = 12.50$; $P < 0.01$). However, no significant effect of IMX or SAHA treatment was observed when administered alone (Fig. 5.54).

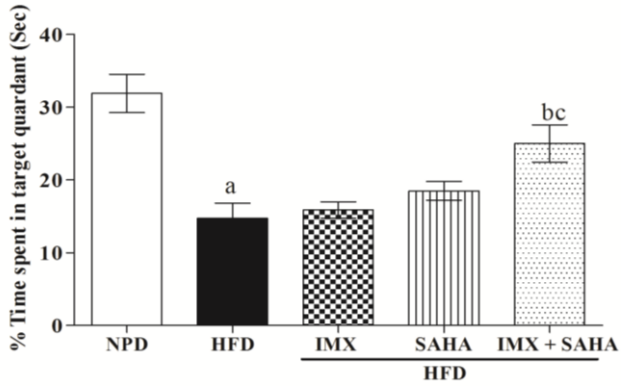

Fig.5.54 Effect of low dose of IMX and SAHA alone and in combination on probe trial in MWM Values are expressed as mean ± SEM (n=8) (**[a]*P* <0.001 vs NPD); ([b]*P* <0.01 vs HFD); ([c]P < 0.05 vs IMX). Note**: (**IMX=** Indirubin-3'-monoxime (0.05mg/kg); **SAHA=** Suberoylanilide hydroxamic acid (12.5 mg/kg).

5.6.6. Effect of low dose of IMX and SAHA alone and in combination on passive avoidance task

The initial latency in the acquisition trial did not differ significantly (P > 0.05) between all the groups (Fig 5.55). Twenty-four hours later, the mice were tested again and it was found that the retention latency was significantly decreased in the HFD fed group as compared with NPD fed mice (P < 0.01) (Fig. 5.55). Decreased retention latency in the HFD fed mice was significantly ameliorated by low dose combination of IMX and SAHA ($F_{(4,39)}$ = 5.79; P < 0.01) (Fig. 5.55).

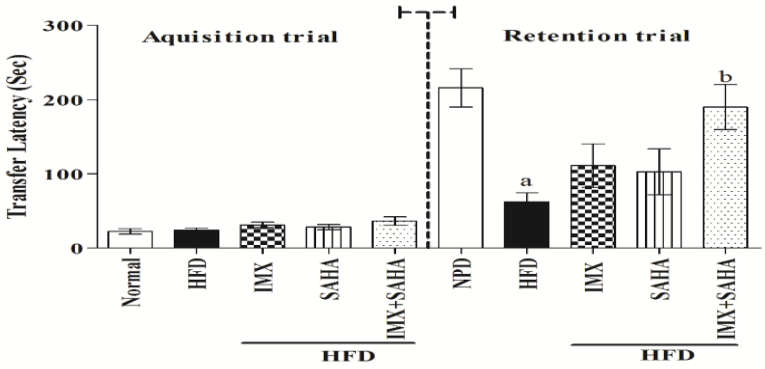

Fig.5.55 Effect of low dose of IMX and SAHA alone and in combination on Passive avoidance task. Values are expressed as mean ± SEM (n=8) ([a]*P* < 0.01 vs NPD); ([b]*P* <0.05 vs HFD). **Note**: (**IMX=**Indirubin-3'-monoxime (0.05mg/kg); **SAHA=**Suberoylanilide hydroxamic acid (12.5 mg/kg).

5.6.7. Effect of low dose of IMX and SAHA alone and in combination on ptau level

HFD feeding results in significant increase in ptau levels as compared with NPD fed mice (P < 0.001) (Fig. 5.56). In contrast, the mice treated with combination of IMX and SAHA, showed significant attenuation of ptau levels in hippocampus homogenates as compared with HFD group or either drug alone treated groups ($F_{(4,29)}$ = 18.12; P < 0.001) (Fig. 5.56).

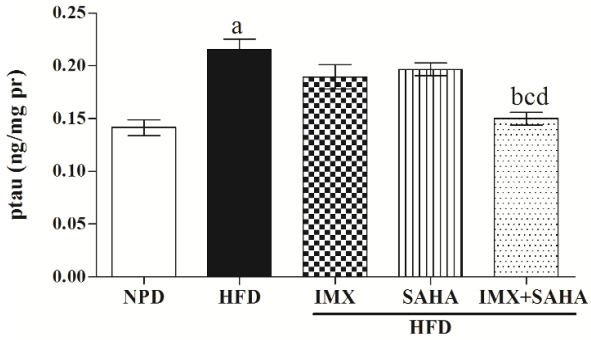

Fig.5.56 Effect of low dose of IMX and SAHA alone and in combination on ptau level. Values are expressed as mean ± SEM (n=6) ([a]P <0.001 vs NPD); ([b]P <0.001 vs HFD) ([c]P<0.05 vs IMX); ([d]P<0.001 vs SAHA) **Note**: (**IMX=** Indirubin-3'-monoxime (0.05mg/kg); **SAHA=** Suberoylanilide hydroxamic acid (12.5 mg/kg).

5.6.8. Effect of low dose of IMX and SAHA alone and in combination on Aβ $_{1-42}$ level

HFD feeding results in significant increase in Aβ $_{1-42}$ levels as compared with NPD fed mice (P < 0.001) (Fig. 5.57). No significant effect was observed on Aβ $_{1-42}$ level in HFD mice when treated with low dose of either GSK3β inhibitor, IMX or HDAC inhibitor, SAHA. In contrast, marked decrease in Aβ$_{1-42}$ level was observed in the mice that received the combination therapy as compared to HFD group and either drug alone treated groups ($F_{(4,29)}$ = 29.66, P < 0.001; Fig. 5.57).

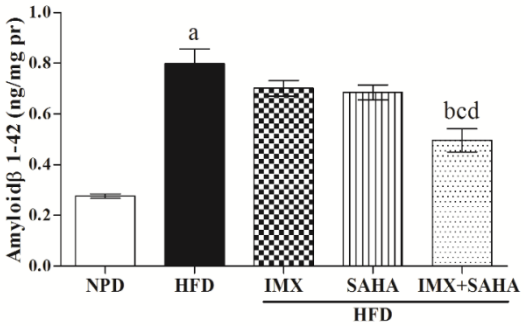

Fig.5.57 Effect of low dose of IMX and SAHA alone and in combination on (Aβ $_{1-42}$) level. Values are expressed as mean ± SEM (n=6) ([a]P <0.001 vs NPD); ([b]P <0.001 vs HFD) ([c]P<0.01 vs IMX); ([d]P<0.05 vs SAHA)**.** **Note**: (**IMX=** Indirubin-3'-monoxime (0.05mg/kg); **SAHA=** Suberoylanilide hydroxamic acid (12.5 mg/kg).

5.6.9. Effect of low dose of IMX and SAHA alone and in combination on histone H3 acetylation level

The level of global histone H3 acetylation was found to be significantly reduced in HFD fed mice as compared with NPD fed mice (P < 0.001) (Fig.5.58). Treatment with either IMX or SAHA alone failed to produce significant effects on histone H3 acetylation levels. However, combined treatment of these drugs results in significant amelioration of histone H3 acetylation levels as compared to alone HFD fed mice or either drug alone treated mice ($F_{(4, 29)}$ =15.25; *P* < 0.001) (Fig. 5.58).

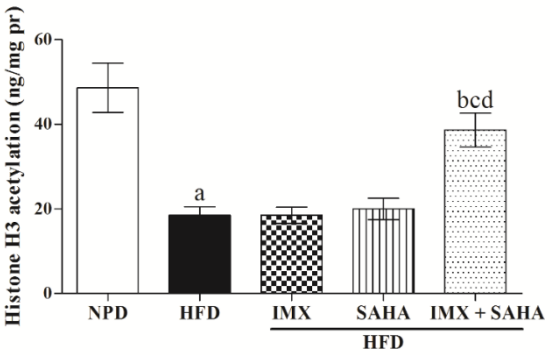

Fig.5.58 Effect of low dose of IMX and SAHA alone and in combination on histone H3 acetylation level. Values are expressed as mean ± SEM (n=6) **(^{a}P <0.001 vs NPD);(^{b}P <0.01 vs HFD); (^{c}P<0.01 vs IMX); (^{d}P<0.01 vs SAHA) Note**: (**IMX=** Indirubin-3'-monoxime (0.05mg/kg); **SAHA=** Suberoylanilide hydroxamic acid (12.5 mg/kg).

5.6.10. Effect of low dose of IMX and SAHA alone and in combination on CREB level

HFD feeding results in significant reduction of CREB levels as compared with NPD fed mice ($P < 0.01$) (Fig 5.59). In contrast, treatment with low dose combination of IMX and SAHA ($F_{(4,29)} = 8.64$; $P < 0.01$) (Fig 5.59) showed significant amelioration of CREB levels as compared to HFD or either drug alone treated mice.

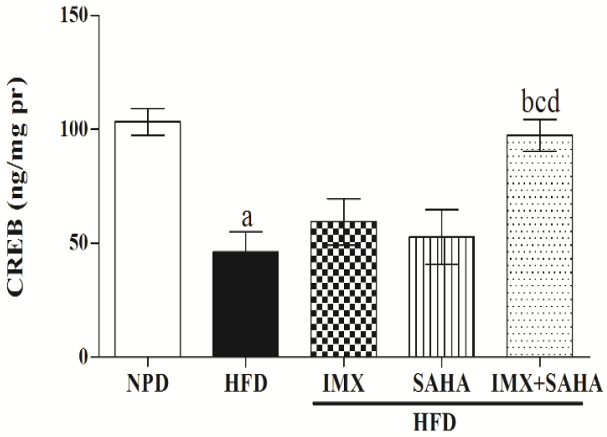

Fig.5.59 Effect of low dose of IMX and SAHA alone and in combination on CREB level. Values are expressed as mean ± SEM (n=6) (^{a}P <0.01 vs NPD);(^{b}P <0.01 vs HFD); (^{c}P<0.05 vs IMX); (^{d}P<0.05 vs SAHA) **Note**: (**IMX=** Indirubin-3'-monoxime (0.05mg/kg); **SAHA=** Suberoylanilide hydroxamic acid (12.5 mg/kg).

5.6.11. Effect of low dose of IMX and SAHA alone and in combination on BDNF level

HFD fed mice showed significant reduction of BDNF level as compared with NPD fed mice ($P < 0.001$) (Fig. 5.60). Treatment with either GSK3β inhibitor, IMX or HDAC inhibitor, SAHA failed to produce any significant effect on BDNF level. In contrast, the mice treated with low dose combination of these drugs showed significant amelioration of BDNF level in hippocampus homogenates as compared to alone HFD group or IMX treated mice ($F_{(4, 29)} = 20.49$; $P < 0.001$) (Fig. 5.60).

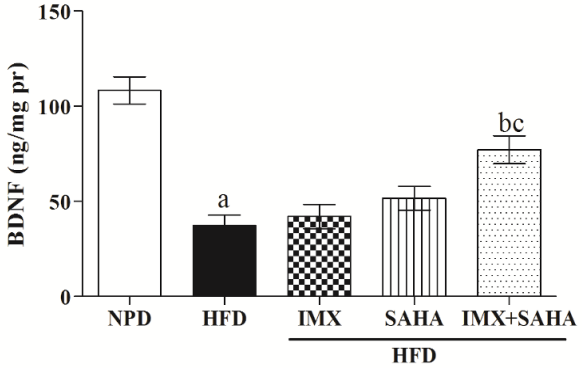

Fig.5.60 Effect of low dose of IMX and SAHA alone and in combination on BDNF level Values are expressed as mean ± SEM (n=6) **([a]*P* <0.001 vs NPD);([b]*P* <0.01 vs HFD); ([c]P<0.01 vs IMX).** (**IMX=** Indirubin-3'-monoxime (0.05mg/kg); **SAHA=** Suberoylanilide hydroxamic acid (12.5 mg/kg).

5.6.12. Effect of low dose of IMX and SAHA alone and in combination on malondialdehyde (MDA) level

Elevated level of MDA was reported in hippocampus homogenates of HFD fed mice as compared with NPD fed mice ($P < 0.001$) (Fig. 5.61). Treatment with low dose combination of IMX and SAHA significantly attenuated MDA level as compared to HFD alone or either drug alone treated mice ($F_{(4,29)}=35.40$; $P < 0.001$) (Fig. 5.61).

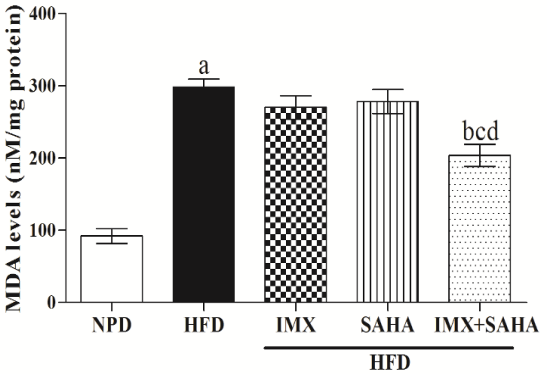

Fig.5.61 Effect of low dose of IMX and SAHA alone and in combination on MDA level. Values are expressed as mean ± SEM (n=6) ([a]P < 0.001 vs NPD); ([b]P < 0.001 vs HFD); ([c]P < 0.05 vs IMX) ([d]P < 0.01 vs SAHA). (**IMX=** Indirubin-3'-monoxime (0.05mg/kg); **SAHA=** Suberoylanilide hydroxamic acid (12.5 mg/kg).

5.6.13 Effect of low dose of IMX and SAHA alone and in combination on nitrite level

HFD feeding results in significant increased nitrite levels as compared to NPD fed mice ($P < 0.001$) (Fig. 5.62). However, the mice treated with low dose combination of IMX and SAHA significantly attenuated nitrite level as compared to HFD alone or either drug alone treated mice ($F_{(4,29)} = 32.58$; $P < 0.001$) (Fig. 5.62).

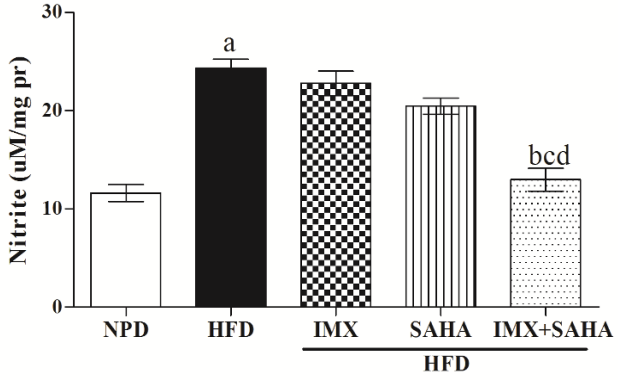

Fig.5.62 Effect of low dose of IMX and SAHA alone and in combination on nitrite level. Values are expressed as mean ± SEM (n=6) ([a]P < 0.001 vs NPD); ([b]P < 0.001 vs HFD); ([c]P < 0.001 vs IMX) ([d]P < 0.001 vs SAHA). (**IMX=** Indirubin-3'-monoxime (0.05mg/kg); **SAHA=** Suberoylanilide hydroxamic acid (12.5 mg/kg).

5.6.14. Effect of low dose of IMX and SAHA alone and in combination on reduced glutathione (GSH) level

The level of antioxidant enzyme GSH, was found to be significantly reduced in hippocampus homogenates of HFD fed mice as compared with NPD fed mice (P < 0.001) (Fig. 5.63). However, treatment with low dose combination of IMX and SAHA ameliorated the GSH level ($F_{(4,29)} = 31.44$; P < 0.001) (Fig. 5.63), as compared to HFD alone or either drug alone treated mice.

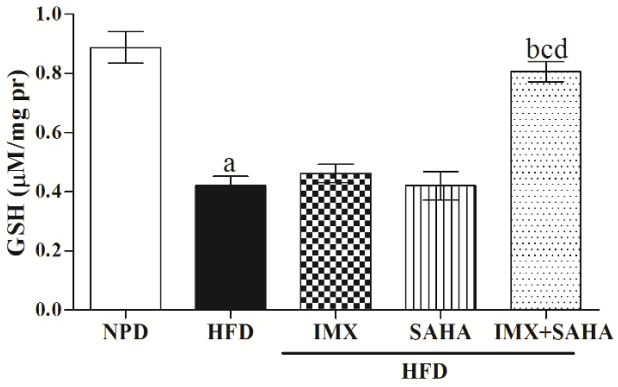

Fig.5.63 Effect of low dose of IMX and SAHA alone and in combination on reduced glutathione level Values are expressed as mean ± SEM (n=6) ([a]*P* <0.001 vs NPD); ([b]*P* <0.001 vs HFD); ([c]P<0.01 vs IMX); ([d]P<0.001 vs SAHA) (**IMX=** Indirubin-3'-monoxime (0.05mg/kg); **SAHA=** Suberoylanilide hydroxamic acid (12.5 mg/kg).

5.6.15 Effect of low dose of IMX and SAHA alone and in combination on Tumour necrosis factor-α (TNF-α) level

The level of TNF-α rose significantly in HFD fed mice as compared to those of NPD fed mice (P < 0.001). Treatment with low dose combination of IMX and SAHA results in significant attenuation of TNF- α level as compared to HFD mice or either drug alone treated mice ($F_{(4,24)} = 16.14$; P < 0.001) (Fig. 5.64).

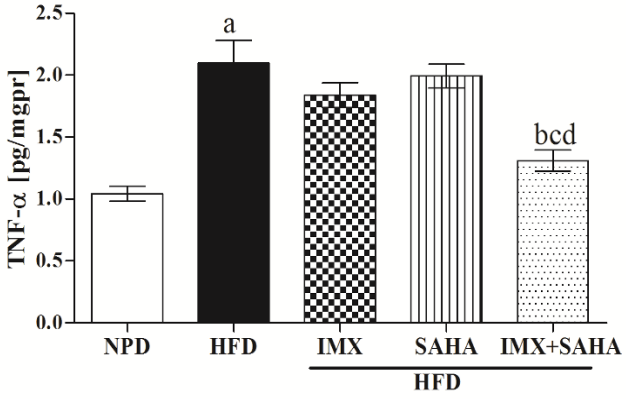

Fig.5.64 Effect of low dose of IMX and SAHA alone and in combination on TNF-α level. Values are expressed as mean ± SEM (n=6) ($^{a}P < 0.001$ vs NPD);($^{b}P < 0.001$ vs HFD); ($^{c}P < 0.05$ vs IMX) ($^{d}P < 0.001$ vs SAHA) (**IMX=** Indirubin-3'-monoxime (0.05mg/kg); **SAHA=** Suberoylanilide hydroxamic acid (12.5 mg/kg).

5.6.16 Effect of low dose of IMX and SAHA alone and in combination on GSK3β levels

HFD feeding results in significant increase in GSK3β levels as compared with NPD fed mice ($P < 0.001$) (Fig 5.65). In contrast, treatment with low dose combination of IMX and SAHA showed significant attenuation of GSK3β levels as compared to HFD alone or either drug alone treated mice ($F_{(4,29)}=21.17$); $P < 0.001$) (Fig 5.65).

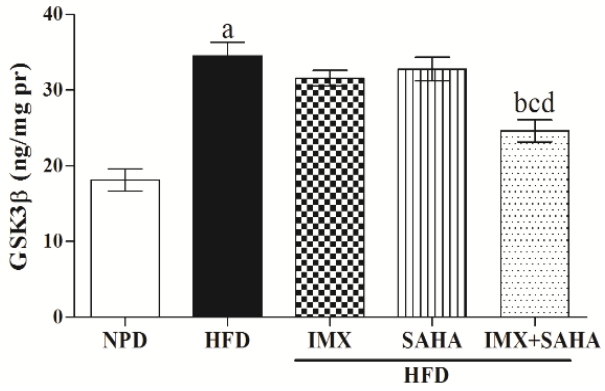

Fig.5.65 Effect of low dose of IMX and SAHA alone and in combination on GSK-3β level. Values are expressed as mean ± SEM (n=6) ($^{a}P < 0.001$ vs NPD);($^{b}P < 0.001$ vs HFD); ($^{c}P < 0.05$ vs IMX) ($^{d}P < 0.01$ vs SAHA) (**IMX=** Indirubin-3'-monoxime (0.05mg/kg); **SAHA=** Suberoylanilide hydroxamic acid (12.5 mg/kg).

5.6.17. Effect of low dose of IMX and SAHA alone and in combination on morphological characters of dentate gyrus and CA1 neurons

Along with the cognitive impairments observed in the behavioral paradigms, the HFD feeding also results in significant morphological changes in DG and CA1 region of hippocampus neurons. The H&E stained brain sections showed healthy neurons in DG and CA1 region in the NPD fed mice (Fig. 5.66, Panel A and F, respectively). Healthy neurons appeared robust in shape, had a spherical or slightly oval nucleus and a single large nucleolus with clear visible cytoplasm as indicated by yellow arrows. The HFD feeding results in significant neuronal degeneration in DG and CA1 regions of hippocampus (Fig. 5.66, Panel B and G, respectively). Marked loss of cell bodies and increased pyknotic neurons were

observed in DG and CA1 regions in HFD mice. Treatment with low dose of IMX or SAHA failed to exert any neuroprotective effects on the neuronal morphology (Fig. 5.66 Panel C-D and Panel H-I, respectively). In contrast, there was marked improvement in neuronal density and reduction in pyknotic neurons following combined treatment with low dose of IMX and SAHA, indicating the neuroprotective actions of this combination treatment (Fig. 5.66, Panel E and J).

5.6.17.1 Effect of low dose of IMX and SAHA on Dentate gyrus neurons

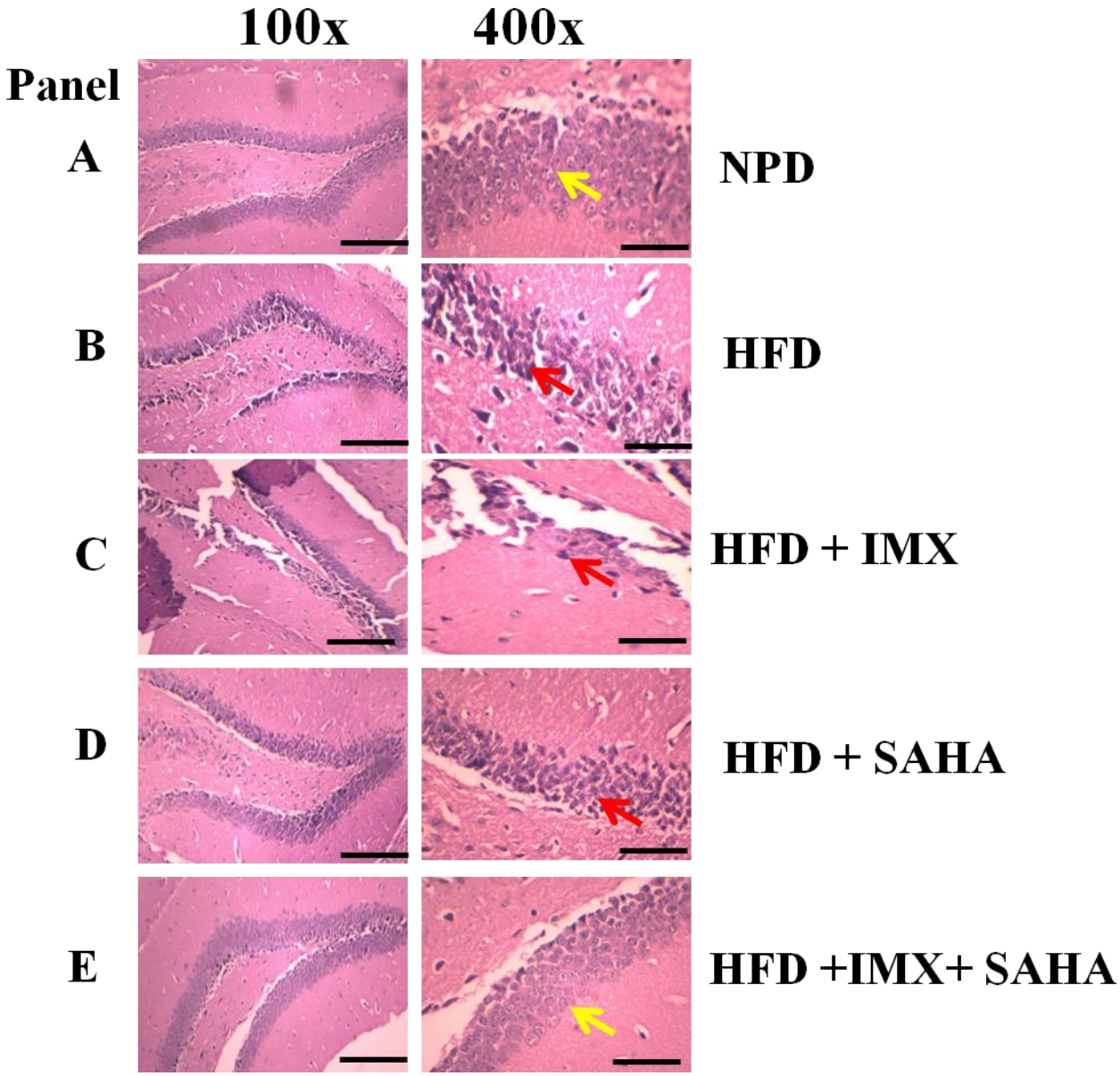

Fig. 5.66a Effect of low dose IMX or SAHA alone or in combination on Dentate gyrus Figure shows photomicrographs of DG **(Panel A)** Normal pellet diet **(Panel B)** High fat diet **(Panel C)** Low dose IMX (0.05mg/kg) **(Panel D)** low dose SAHA (12.5 mg/kg) **(Panel E)** combination of IMX and SAHA. Yellow arrows indicate normal healthy neurons; Red arrows indicate damaged or sickle shaped pyknotic neurons.

5.6.17.2 Effect of low dose of IMX and SAHA on CA1 neurons

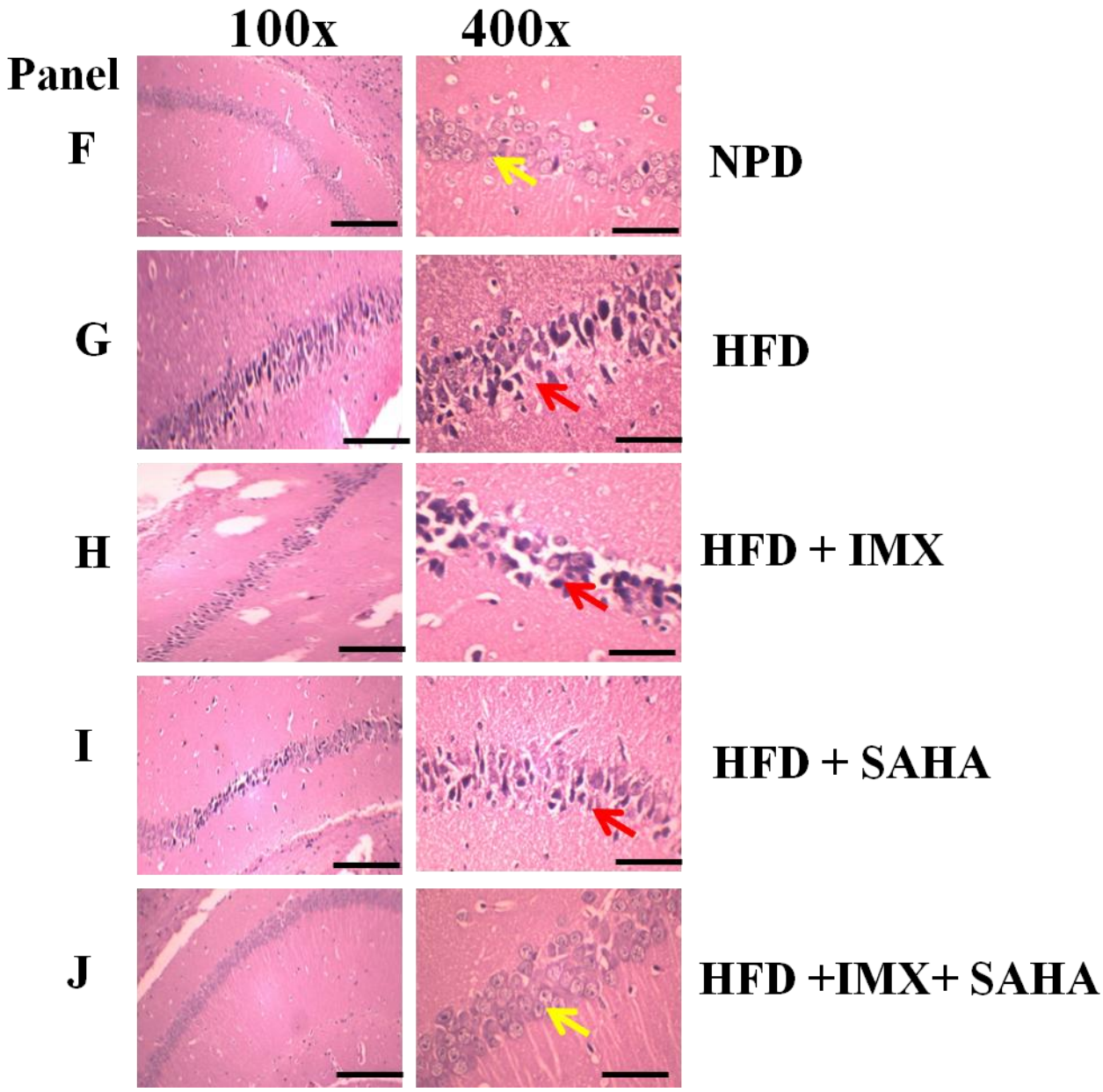

Fig. 5.66 (b) Effect of low dose IMX or SAHA alone or in combination on CA1 region Figure shows photomicrographs of CA1 **(Panel F)** normal pellet diet **(Panel G)** High fat diet **(Panel H)** Low dose IMX (0.05mg/kg) **(Panel I)** Low dose SAHA (12.5 mg/kg) **(Panel J)** Combination of IMX and SAHA. Yellow arrows indicate normal healthy neurons; Red arrows indicate damaged or sickle shaped pyknotic neurons

5.6.18 Effect of low dose IMX or SAHA alone or in combination on hippocampus (DG and CA1) neuronal Count

The HFD feeding results in a significant increase in the percentage of damaged neurons with altered morphological characters in both DG and CA1 regions ($P < 0.001$) (Fig.5.67a and 5.67b). The mice treated with low dose of either IMX or SAHA were failed to attenuate the neuronal damage caused by HFD feeding. In contrast, the mice treated with low dose combination of IMX and SAHA showed significant neuroprotection as evidenced by reduced percentage of damaged neurons in DG and CA1 regions ($P < 0.001$; Fig. 5.67a and 5.67b).

(a) Effect of IMX and SAHA alone or in combination on % damaged neurons in DG

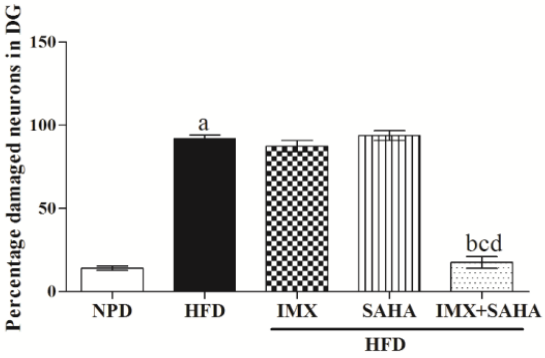

(b) Effect of IMX and SAHA alone or in combination on % damaged neurons in CA1

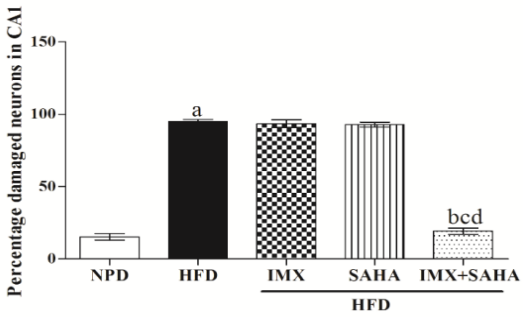

Fig. 5.67 Effect of IMX and SAHA alone or in combination on hippocampus (DG and CA1) neuronal Count

(a) DG neurons ($^{a}P < 0.001$ vs NPD; $^{b}P < 0.001$ vs HFD; $^{c}P < 0.001$ vs IMX; $^{d}P < 0.001$ vs SAHA) **(b) CA1 neurons** ($^{a}P < 0.001$ vs NPD; $^{b}P < 0.001$ vs HFD; $^{c}P < 0.001$ vs IMX; $^{d}P < 0.001$ vs SAHA).

5.7. Effect of combination of LiCl and VPA on ICV-STZ induced cognitive deficits

5.7.1. Effect of Lithium chloride and Valproate alone and in combination on passive avoidance task

The initial latency in the acquisition trial did not differ significantly ($P > 0.05$) between all the experimental groups on day 14. On day 15, the retention latency was significantly ($P < 0.001$) decreased in the ICV-STZ group as compared with the vehicle treated group (Fig. 5.68). Decreased retention latency in the ICV-STZ rats was attenuated by LiCl treatment, indicating improved retention of memory. However, no improvement was observed with VPA alone treatment. Moreover, the effect of combination of these drugs on retention memory was higher than that of alone drugs ($F_{(4,39)} = 49.74$; $P < 0.001$).

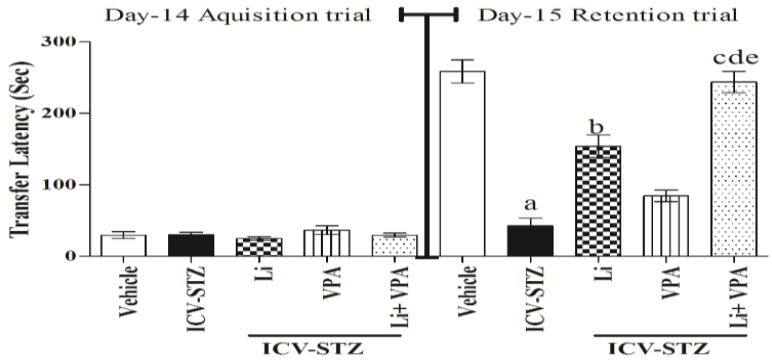

Fig.5.68 Effect of Lithium chloride and Valproate alone and in combination in passive avoidance task. Values are expressed as mean ± SEM (n=8). (^{a}P <0.001 vs Vehicle); (^{b}P < 0.001 Li vs ICV-STZ); (^{c}P < 0.001 vs Li+VPA vs ICV-STZ); (^{d}P < 0.001; Li+VPA vs Li); (^{e}P < 0.001; Li+VPA vs Li) (Li= Lithium chloride; VPA= Valproate).

5.7.2. Effect of Lithium chloride and Valproate alone and in combination on Morris water maze task

The mean escape latency decreased gradually in all the groups during 4 days of training in the MWM test. The mean escape latency was significantly ($P < 0.001$) higher in the ICV-STZ group as compared with the vehicle treated group, showing a poorer learning performance on days 17-19. The increased escape latency in the ICV STZ group was attenuated by treatment with both LiCl and VPA alone on day 18 and 19. Moreover, when administered together, the effect of combination of these drugs on escape latency was higher as compared to either drug alone on day 18 and 19 ($P < 0.01$) (Fig.5.69a). Fig. 5.69 (b- f) shows tracking record with the respect of escape latency of one representative animal from each group in MWM acquisition trials.

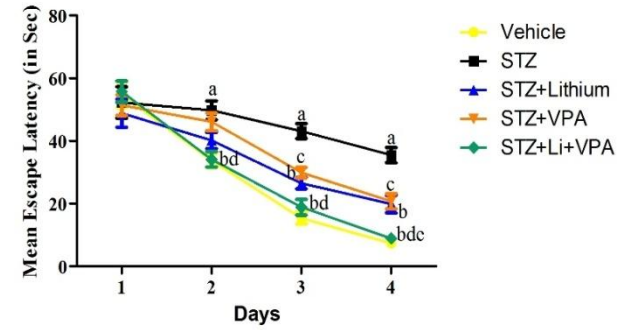

Fig.5.69a Effect of Lithium chloride and Valproate alone and in combination on Morris water maze task. Values are expressed as mean ± SEM ([a]P < 0.001 vs Vehicle); ([b]P< 0.001 vs STZ); ([c]P< 0.01 vs STZ); ([d]P< 0.05 vs VPA); ([e]P< 0.05 vs Li).

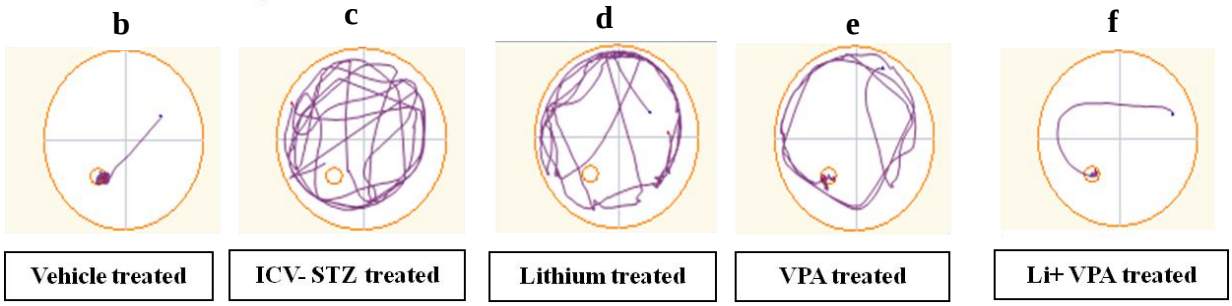

Fig. 5.69 (b-f) Representative images showing tracking record of a rat of individual group on mean transfer latency to find the hidden platform in MWM.

5.7.3 Effect of Lithium chloride and Valproate alone and in combination in Probe trial

In the probe trial, with the platform removed, STZ injected rats failed to remember the precise location of the platform, spending significantly less time in the target quadrant as compared with vehicle treated animals **(**P < 0.001, Fig.5.70a). Whereas, STZ rats treated with LiCl but not VPA were able to identify the precise location of the target quadrant. Moreover, the combination group spent significantly higher time in the target quadrant as compared to either drug alone, which indicates improved consolidation of memory ($F_{(4, 39)}$ = 68.02, P < 0.001). Fig.5.70 (b-f) shows tracking record of time spent in the target quadrant of one representative animal from each group in MWM probe trial with platform removed.

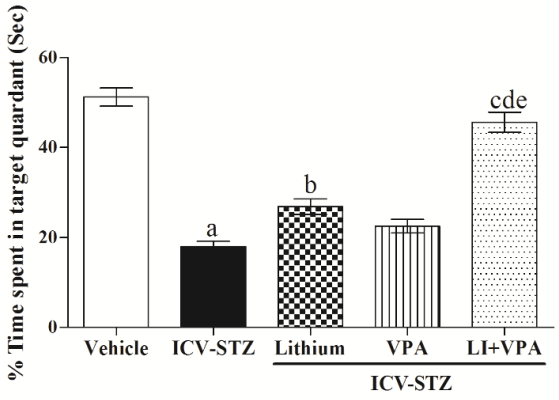

Fig.5.70a Effect of Lithium chloride and Valproate alone and in combination on probe trial. Values are expressed as mean ± SEM (n=8). ([a]P < 0.001 vs Vehicle); ([b]P < 0.05 vs STZ); ([c]P < 0.001 vs STZ); ([d]P < 0.001 vs Li); ([e]P < 0.001 vs VPA).

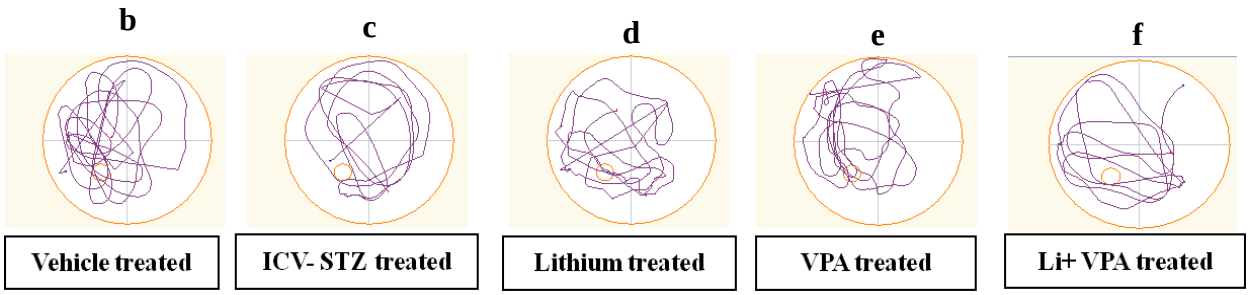

Fig. 5.70 (b-f) Representative images showing tracking record of a rat of individual group on time spent in target quadrant of probe trial in MWM task.

5.7.4. Effect of Lithium chloride and Valproate alone and in combination on spontaneous locomotor activity

The spontaneous locomotor activity on day 21 did not differ significantly among all the groups, ($P > 0.05$) ($F_{(4, 39)} = 2.12$) (Fig. 5.71), indicating no effect whatsoever of STZ, LiCl and VPA either alone/or in combination on locomotor activity of animals.

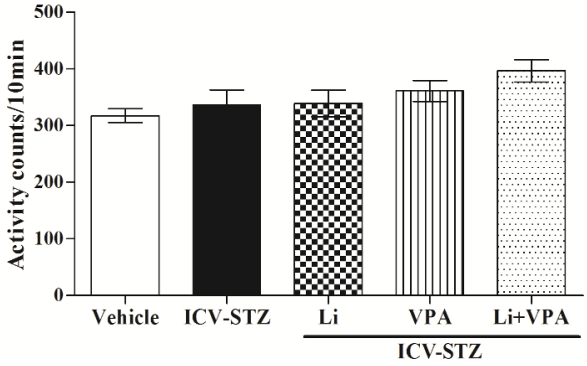

Fig.5.71 Effect of Lithium chloride and Valproate alone and in combination on spontaneous locomotor activity. Values are expressed as mean ± SEM (n=8). The spontaneous locomotor activity on day 21 did not differ significantly ($P > 0.05$) among all the groups. Li= Lithium chloride ; VPA= Valproate.

5.7.5. Effect of Lithium chloride and Valproate alone and in combination on AChE activity

The activity of AChE was increased significantly in brain homogenate of ICV-STZ infused rats compared with those of vehicle treated group ($P < 0.001$) (Fig. 5.72). LiCl decreased STZ induced elevation in AChE activity; whereas no significant difference was observed between STZ and VPA treated groups. However, when administered together, the combination of both drugs significantly attenuated AChE activity as compared with either drug alone treatment ($F_{(4,29)} = 39.05$) ($P < 0.01$).

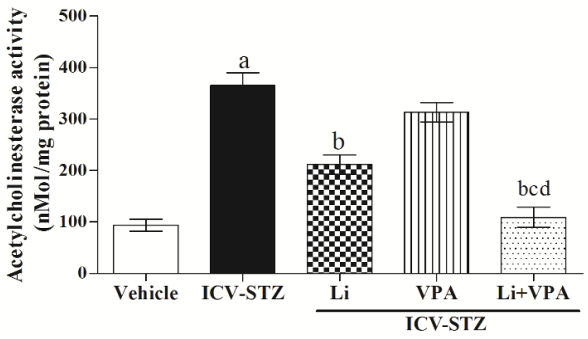

Fig.5.72 Effect of Lithium chloride and Valproate alone and in combination on acetylcholinesterase activity. Values are expressed as mean ± SEM (n=6). ([a]P< 0.001 vs Vehicle); ([b]P< 0.001 vs STZ); ([c]P< 0.01 vs Li); ([d]P< 0.001 vs VPA).

5.7.6 Effect of Lithium and Valproate alone and in combination on GSK-3β level

The levels of GSK3β were found to be significantly increased in STZ treated rats as compared to vehicle treated animals (P < 0.001). Whereas, chronic treatment of STZ injected rats with LiCl was able to attenuate the STZ induced elevation of GSK3β level (*P* < 0.05). However, VPA treatment didn't produce any significant difference on GSK3β level. In addition, the combination of both drugs produced synergistic attenuation of the elevated GSK-3β levels as compared to either drug alone treated rats ($F_{(4,29)}$ = 21.36, P < 0.001) (Fig. 5.73).

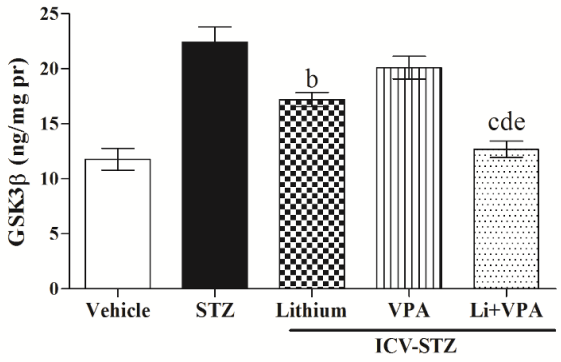

Fig.5.73. Effect of Lithium chloride and Valproate alone and in combination on GSK3β levels. Values are expressed as mean ± SEM (n=6) ([a]P < 0.001 vs Vehicle); ([b]P< 0.01 vs STZ); ([c]P< 0.001 vs STZ); ([d]P< 0.05 vs Li); ([e]P< 0.001 vs VPA) (Li=Lithium chloride; VPA= Valproate).

5.7.7. Effect of Lithium and Valproate alone and in combination on BDNF level

The levels of BDNF were found to be significantly decreased in STZ infused rats as compared to vehicle treated animals (P < 0.01). Whereas, chronic treatment of STZ injected rats with LiCl (P < 0.01) or VPA (P < 0.05) was able to significantly ameliorate the STZ induced decrease in levels of BDNF. Moreover, the low dose combination of both drugs results in more consistent amelioration of decreased BDNF levels as compared to either drug alone treated rats ($F_{(4,29)}$ = 59.12, P < 0.01) (Fig. 5.74).

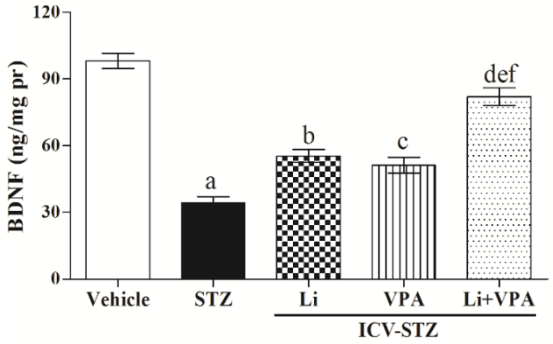

Fig.5.74 Effect of Lithium chloride and Valproate alone and in combination on BDNF level. Values are expressed as mean ± SEM (n=6) ([a]P < 0.001 vs Vehicle); ([b]P < 0.01 vs STZ); ([c]P < 0.05 vs STZ); ([d]P < 0.001 vs STZ); ([e]P < 0.001 vs Li); ([f]P < 0.001 vs VPA).

5.7.8. Effect of Lithium chloride and Valproate alone and in combination on brain MDA, nitrite and GSH levels

The level of MDA rose significantly in STZ treated rats as compared to those of vehicle treated rats (*P* < 0.001). LiCl, but not VPA treatment decreased the elevation in MDA level as compared with those of STZ- injected rats. However, combination of VPA and LiCl results in significant decrease in elevated MDA levels, indicating synergistic potential of these two drugs ($F_{(4, 29)}$= 41.29, *P* < 0.001) (Table.5.6). The level of nitrite rose significantly in STZ treated rats as compared to those of vehicle treated group (*P* <0.001). LiCl but not VPA, results in attenuation of STZ induced nitrite level. Moreover, the combination of both drugs results in significant attenuation of nitrite levels as compared with alone treated groups (P < 0.05) ($F_{(4, 29)}$= 62.49) (Table.5.6). The level of GSH was found to be significantly depleted in STZ injected rats as compared to vehicle treated rats (P < 0.001). Whereas, chronic treatment of STZ injected rats with low dose of LiCl (P < 0.001) or VPA (P < 0.05) was able to restore the GSH levels. Moreover, the combination of both drugs produced more consistent restoration of GSH levels as compared to either drug alone treated rats ($F_{(4, 29)}$=26.07, P < 0.001) (Table.5.6).

Groups	Biochemical Parameters		
	MDA (nMol/ mg protein)	**Nitrite** (µMol/ mg protein)	**GSH** (µMol / mg protein)
Vehicle	71.0 ± 27.60	6.21 ± 1.06	1.57 ± 0.39
STZ	295.0 ± 52.06[a]	16.53 ± 0.99[a]	0.24 ± 0.11[a]
Li	185.0 ± 33.91[b]	11.83 ± 1.56[b]	0.95 ± 0.19[b]
VPA	239.2 ± 35.70	14.67 ± 1.63	0.77 ± 0.14[c]
Li + VPA	101.5 ± 20.54[bcd]	9.25 ± 0.96[bcd]	1.42 ± 0.31[cde]

Table.5.6 Effect of Lithium chloride and Valproate alone and in combination of both drugs on oxidative stress markers. Values are expressed as mean ± S.D. (n=6). **MDA** (^{a}P < 0.001 vs Vehicle); (^{b}P <0.001 vs STZ); (^{c}P< 0.01 vs Li); (^{d}P < 0.001 vs VPA); **Nitrite** (^{a}P < 0.001 vs Vehicle); (^{b}P < 0.001 vs STZ); (^{c}P < 0.05 vs Li); (^{d}P< 0.001 vs VPA); **GSH** (^{a}P< 0.001 vs Vehicle); (^{b}P < 0.001 vs STZ); (^{c}P< 0.01 vs STZ); (^{d}P< 0.05 vs Li); (^{e}P< 0.01 vs VPA).

5.7.9. Effect of Lithium chloride and Valproate alone and in combination on ptau level

ICV-STZ administration results in significant elevation of ptau level as compared to vehicle treated animals (P < 0.01) (Fig. 5.75). Treatment with either LiCl or VPA failed to produce significant effect on ptau levels. In contrast, the combination of both these drugs was able to significantly attenuate the ptau level in ICV-STZ rats ($F_{(4,29)}$ = 14.87; P < 0.001) (Fig. 5.75).

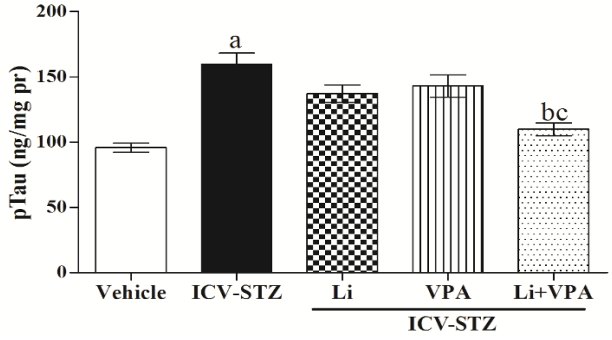

Fig.5.75 Effect of Lithium chloride and Valproate alone and in combination on ptau level. Values are expressed as mean ± SEM (n=6) (^{a}P <0.001 vs Vehicle); (^{b}P <0.001 vs ICV-STZ) ;(^{c}P<0.05 vs VPA).

5.7.10 Effect of Lithium chloride and Valproate alone and in combination on Amyloid-β (Aβ $_{1-42}$) level

ICV-STZ administration results in significant elevation of $A\beta_{1-42}$ level as compared to vehicle treated animals (P < 0.01) (Fig. 5.76). Treatment with either LiCl or VPA didn't show any significant effect on Aβ $_{1-42}$ level. However, the combination of both these drugs was able to significantly attenuate the Aβ $_{1-42}$ level in ICV-STZ rats ($F_{(4,29)}$ = 29.23; P < 0.001) (Fig. 5.76).

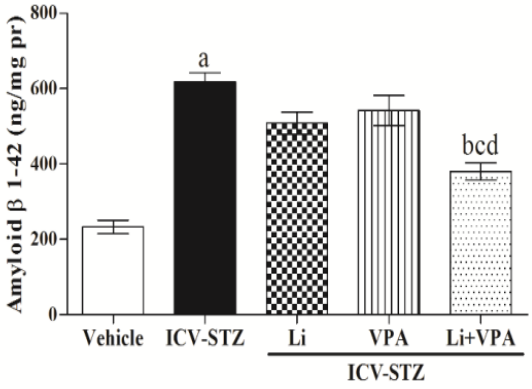

Fig.5.76 Effect of Lithium chloride and Valproate alone and in combination on Aβ level. Values are expressed as mean ± SEM (n=6) ([a]P < 0.001 vs Vehicle); ([b]P < 0.001 vs ICV-STZ); ([c]P < 0.05 vs Li); ([d]P < 0.01 vs VPA).

5.7.11. Effect of Lithium chloride and Valproate alone and in combination on histone H3 acetylation level

The level of global histone H3 acetylation was found to be significantly reduced in ICV-STZ administered rats as compared with vehicle treated rats (P < 0.001) (Fig.5.77). Treatment with VPA but not LiCl, produced significant amelioration of histone H3 acetylation level. However, combined treatment of both these drugs results in more persistent amelioration of histone H3 acetylation levels as compared to ICV-STZ or LiCl alone treated rats ($F_{(4, 29)}$ =15.73; *P* < 0.001) (Fig. 5.77).

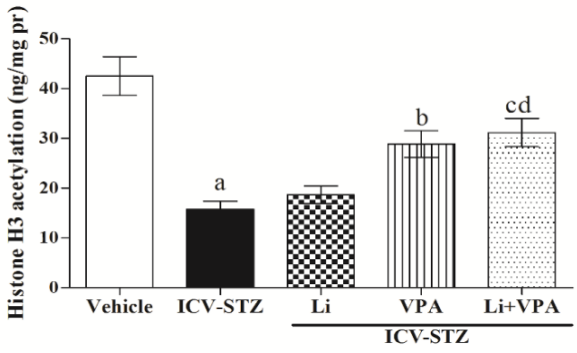

Fig.5.77 Effect of Lithium chloride and Valproate alone and in combination on histone H3 acetylation level. Values are expressed as mean ± SEM (n=6) ([a]*P* <0.001 vs Vehicle); ([b]*P* <0.05 vs ICV-STZ); ([c]P<0.01 vs ICV-STZ); ([d]P<0.05 vs Li).

5.7.12. Effect of Lithium chloride and Valproate alone and in combination on CREB level

ICV-STZ administration results in significant reduction of CREB levels as compared with vehicle treated rats (P < 0.01) (Fig 5.78). In contrast, treatment with combination of LiCl and VPA ($F_{(4,29)}$ = 26.60; P < 0.01) (Fig 5.78) showed significant amelioration of CREB levels as compared to ICV-STZ or either drug alone treated mice.

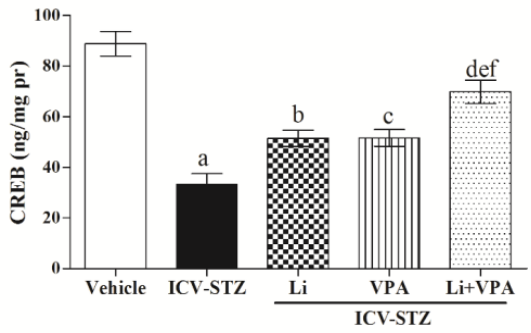

Fig.5.78 Effect of Lithium chloride and Valproate alone and in combination on CREB level. Values are expressed as mean ± SEM (n=6) ([a]*P* <0.001 vs Vehicle); ([b]*P* <0.05; Li vs ICV-STZ);([c]P<0.05; VPA vs ICV-STZ); ([d]P<0.05; Li+VPA vs ICV-STZ); ([e]P<0.05; Li+VPA vs Li); ([f]P<0.05; Li+VPA vs VPA).

5.7.13. Effect of Lithium and Valproate alone and in combination on hippocampal DG and CA3 neurons

The H&E stained brain (dentate gyrus and CA3 of hippocampus) sections showed healthy neurons in vehicle treated animals (Fig. 5.79 Panel A and Fig.5.79 Panel F). Healthy neurons were robust in shape and had a pale and spherical or slightly oval nucleus and a single large nucleolus with clear visible cytoplasm. Treatment with LiCl and VPA in combination showed healthy neurons in dentate gyrus and CA3 of hippocampus (Fig. 5.79 Panel E and Fig 5.79 Panel J). Almost similar morphology and neuronal density in dentate gyrus and hippocampal CA3 regions were observed in vehicle and combination treated groups. Neuronal degeneration may present a range of neurodegenerative morphologies. In this study, pyknotic neurons were darkly stained with no nucleus or visible nucleolus, and few of the cells were shrunken and sickle shaped in brain sections of ICV-STZ rats. The microscopic pictures from the dentate gyrus and CA3 region of hippocampus of ICV-STZ-treated group showed a marked loss of cell bodies (Fig. 5.79 Panel B and Fig. 5.79 Panel G). Further, STZ administration markedly decreased neuronal density and increased pyknotic neurons. Chronic treatment with LiCl or VPA alone (Fig. 5.79, Panel C & D and Fig.5.79 Panel G & H) attenuated STZ induced cell loss and pyknotic cells but some degenerating cells with changes of morphology were observed in these groups. However, there was marked improvement in neuronal density and reduction in pyknotic neurons following combination of both these drugs, indicating their neuroprotective profile when administered together and is line with behavioral and biochemical effects.

5.7.13.1. Effect of Lithium chloride and Valproate alone and in combination on dentate gyrus region of hippocampus in ICV-STZ treated rats

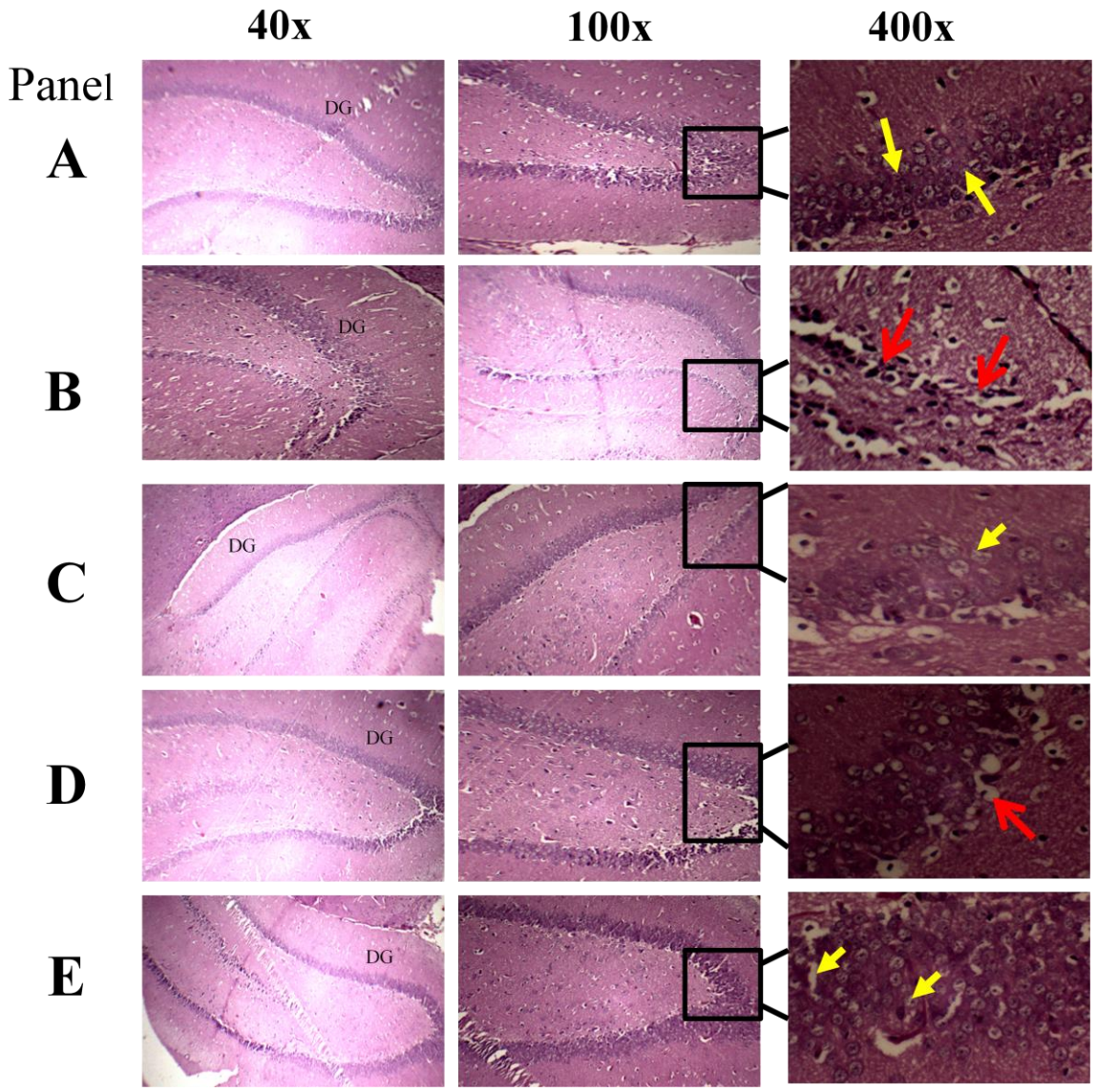

Fig. 5.79a Effect of Lithium chloride and Valproate alone and in combination on dentate gyrus region of hippocampus. **(Panel A)** Vehicle treated **(Panel B)** ICV-STZ administered **(Panel C)** ICV-STZ+ Lithium treated **(Panel D)** ICV-STZ+ Valproate treated **(Panel E)** ICV-STZ+LiCl+VPA treated. Red arrows indicate damaged neurons, Yellow arrows indicate surviving neurons.

5.7.13.2 Effect of Lithium chloride and Valproate alone and in combination on CA3 region of hippocampus in ICV-STZ treated rats

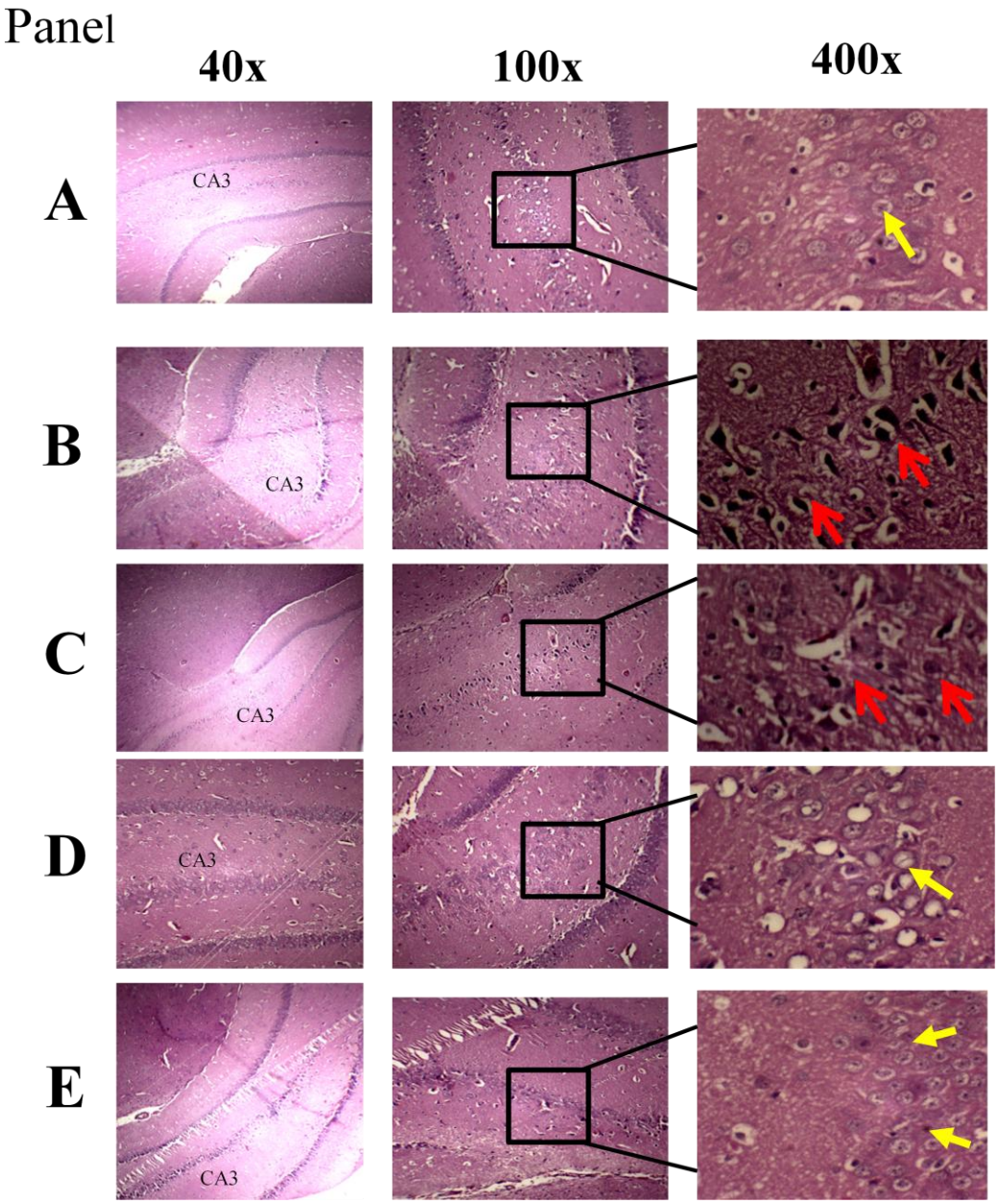

Fig. 5.79b Effect of Lithium chloride and Valproate alone and in combination on CA3 region of hippocampus in ICV-STZ treated rats. (Panel A) Vehicle treated **(Panel B)** ICV-STZ administered **(Panel C)** ICV-STZ+ Lithium treated **(Panel D)** ICV-STZ+ Valproate treated **(Panel E)** ICV-STZ+ LiCl+ VPA treated. Red arrows indicate damaged neurons, Yellow arrows indicate surviving neurons.

5.7.14. Effect of Lithium chloride and Valproate alone and in combination on neuronal count in dentate gyrus and CA3 regions

ICV-STZ administration results in significant increase in the percentage of degenerating neurons with altered morphological characters in both DG and CA3 regions ($P < 0.001$) (Fig. 5.80a and 5.80b). In contrast, the rats treated with both LiCl and VPA in combination results in significant neuroprotection as evidenced by reduced number of degenerating neurons in DG and CA3 regions ($P < 0.001$).

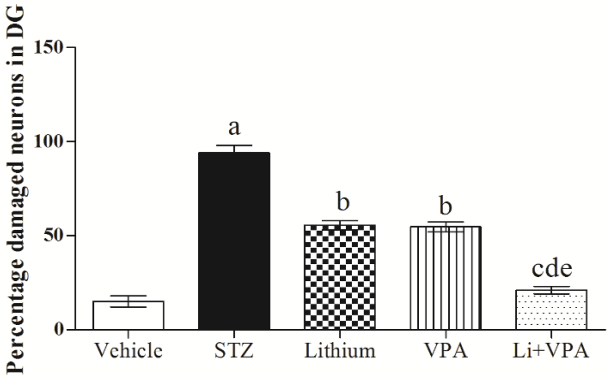

Fig. 5.80a Effect of Lithium chloride and Valproate alone and in combination on neuronal count in dentate gyrus. Values are expressed as mean ± S.D. [a]P<0.001 vs Vehicle; [b]P< 0.01 vs STZ; [c]P< 0.001 vs STZ; [d]P< 0.01 vs Li; [e]P< 0.01 vs VPA.

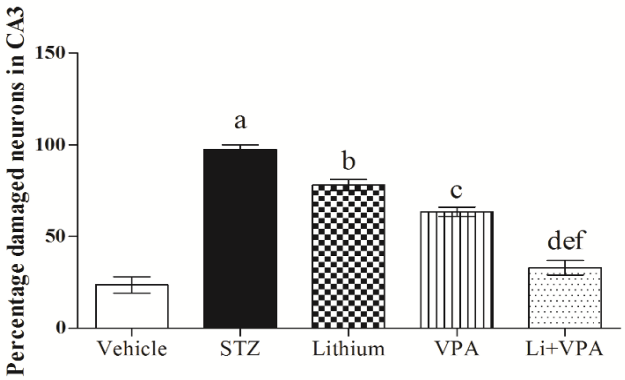

Fig. 5.80b Effect of Lithium chloride and Valproate alone and in combination on neuronal count in CA3 neurons. Values are expressed as mean ± SEM ([a]P< 0.001 vs Vehicle); ([b]P< 0.05 vs Li); ([c]P< 0.01 vs VPA); ([d]P< 0.001 vs STZ); ([e]P< 0.01 vs Li); ([f]P< 0.01 vs VPA).

5.8. Effect of Class specific HDAC inhibitors on insulin resistance and associated cognitive deficits

5.8.1. Effect of Class specific HDAC inhibitors on body weight and serum parameters in HFD fed mice

HFD fed mice gained significantly more weight than the NPD fed mice ($F_{(5,47)}$= 4.99; P < 0.01). In addition, there was a significant increase in serum parameters, characteristic of insulin resistance viz. glucose ($F_{(5,39)}$ =9.95; P < 0.001), TGs ($F_{(5,37)}$ = 5.58; P <0.001), TC ($F_{(5,39)}$ =12.85; P < 0.001) and insulin levels ($F_{(5,35)}$ =8.56; P < 0.001) in HFD fed mice (Table 5.7). Treatment with Class I HDAC inhibitors, (CI-994, HDACi 4b) and Class III inhibitors (Sirtinol) failed to produce significant effect on these parameters. However, treatment with Class II specific HDAC inhibitor, MC-1568, significantly reduced body weight (P < 0.05) as compared to HFD fed mice. Moreover, MC-1568 treatment attenuated the serum glucose, TGs, TC and insulin levels in HFD fed mice. These results indicate the beneficial effects of Class II HDAC inhibitor treatment on insulin resistance state. The results showed that HOMA-IR of HFD fed mice were significantly higher than that of NPD fed mice (P < 0.001). Class I HDAC inhibitors, CI-994 and HDACi 4b failed to produce any significant effect on HOMA-IR level. In contrast, treatment with Class II HDAC inhibitor, MC- 1568, significantly attenuated the HOMA-IR levels as compared to HFD group ($F_{(5,35)}$ =16.18; P < 0.001).

Parameter	NPD	HFD	HDACi 4b	CI-994	MC- 1568	Sirtinol
Body weight (g)	32.0± 0.9	38.00± 1.08^{a}	34.63± 1.03	35.38± 1.14	33.63± 1.16^{b}	36.38 ± 1.05
Glucose (mg/dl)	91.3± 6.6	158.2±9.8^{a}	170.5 ±10.41	156.8±12.03	108.2±8.08^{bcd}	133.7 ± 14.21
TGs (mg/dl)	109.1± 4.51	175.2±11.71^{a}	146.6±9.28	144.5±11.94	127.5±9.85^{b}	151.8 ± 10.63
TC (mg/dl)	102.2± 8.26	183.8±9.0^{a}	155.8±9.94	169.5± 8.4	125.2±9.13^{bcd}	166.7 ± 9.47
Insulin (pmol/l)	93.0 ± 5.3	142.6± 6.67^{a}	136.8± 8.23	138.3± 6.21	107.1±6.24^{bcd}	121.9 ± 7.49
HOMA-IR	1.65± 0.09	2.91± 0.15^{a}	2.89± 0.14	2.90± 0.13	2.05± 0.10^{bcd}	2.42 ±0.13

Table. 5.7. Effect of Class specific HDAC inhibitors on body weight ($^{a}P < 0.01$ vs NPD); ($^{b}P < 0.05$ vs HFD); **Glucose** ($^{a}P < 0.001$ vs NPD); ($^{b}P < 0.05$ vs HFD) ($^{c}P < 0.01$ vs HDACi 4b) ($^{d}P< 0.05$ vs CI-994); **Cholesterol (**$^{a}P < 0.001$ vs NPD); ($^{b}P < 0.001$ vs HFD); ($^{c}P < 0.05$ vs HDACi 4b) ($^{d}P< 0.05$ vs Sirtinol); **Triglycerides**($^{a}P <0.001$ vs NPD); ($^{b}P < 0.05$ vs HFD); **Insulin** ($^{a}P < 0.001$ vs NPD); ($^{b}P < 0.01$ vs HFD) ($^{c}P < 0.05$ vs HDACi 4b) ($^{d}P< 0.05$ vs CI-994); **HOMA IR** ($^{a}P < 0.001$ vs NPD); ($^{b}P < 0.001$ vs HFD); ($^{c}P< 0.01$ vs HDACi 4b); ($^{d}P< 0.01$ vs CI-994)

5.8.2. Effect of Class specific HDAC inhibitors on locomotor activity

No significant difference was observed between any of the groups suggesting no effect whatsoever of HFD or any of the HDAC inhibitors at tested doses on the locomotion activity of animals ($P > 0.05$); ($F_{(5,39)} = 0.44$) (Fig. 5.81).

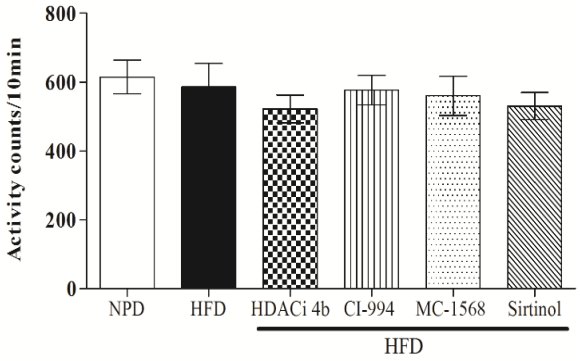

Fig. 5.81 Effect of Class specific HDAC inhibitors on locomotor activity. Values are expressed as mean ± SEM.

5.8.3. Effect of Class specific HDAC inhibitors on mean escape latency in morris water maze

The mean escape latency to reach the target platform reduced gradually in all the groups during 4 days of training (Fig. 5.82). The mean escape latency was significantly ($P < 0.001$) higher in the HFD fed mice as compared with the NPD fed mice on days 2-4, showing poorer learning performance. The increased escape latency in the HFD group was significantly attenuated by MC-1568 on day 3 ($P < 0.05$) and day 4 ($P < 0.01$). However, Class I specific inhibitors, CI-994 and HDACi 4b and Class III inhibitor, sirtinol were not able to attenuate escape latency in HFD fed mice ($P > 0.05$).

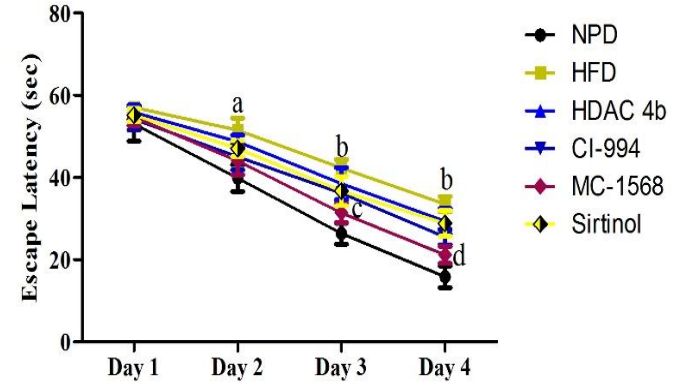

Fig.5.82 Effect of Class specific HDAC inhibitors on mean escape latency. Values are expressed as Mean ± SEM. (^{a}P< 0.01 vs NPD); (^{b}P< 0.001 vs NPD); (^{c} P< 0.05 vs HFD); (^{d}P< 0.01 vs HFD).

5.8.4. Effect of Class specific HDAC inhibitors on probe trial

During the probe trial, HFD fed mice failed to remember the precise location of the platform, spending significantly lesser time in the target quadrant (P < 0.001) (Fig. 5.83). Whereas, HFD fed mice treated with Class II specific HDAC inhibitor, MC 1568, spent significantly more time in the target quadrant indicating improved consolidation of memory [$F_{(5,35)}$ =5.84; P < 0.001]. However, Class I HDAC and Class III inhibitors failed to improve the performance in probe trial.

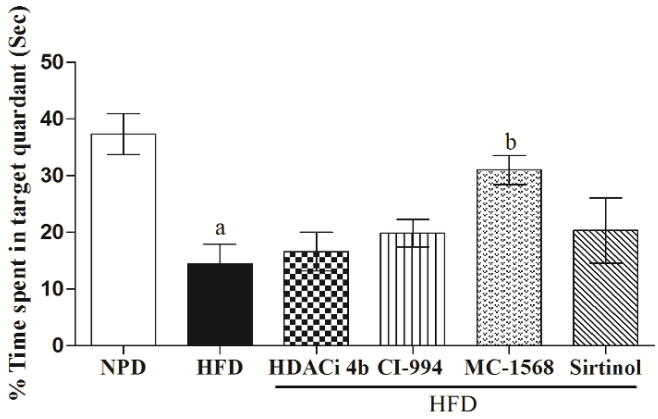

Fig. 5.83 Effect of Class Specific HDAC inhibitors on probe trial. Values are expressed as Mean ± SEM. (^{a}P <0.001 vs NPD); (^{b}P <0.01 vs HFD).

5.8.5. Effect of Class Specific HDAC inhibitors on passive avoidance task

The initial latency in the acquisition trial did not differ significantly (P > 0.05) between all the groups (Fig. 5.84). Twenty-four hours later, the mice were tested again and it was found that the retention latency was significantly decreased in the HFD fed group as compared with NPD fed mice (P < 0.001). Decreased retention latency in the HFD fed mice was significantly attenuated by MC-1568 treatment but not by other HDAC inhibitors ($F_{(5,35)}$ = 10.09; P < 0.001).

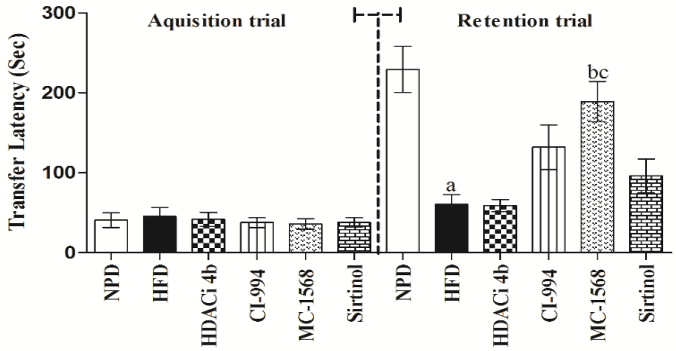

Fig 5.84 Effect of Class specific HDAC inhibitors on passive avoidance task.

Values are expressed as Mean ± SEM. ($^{a}P < 0.001$ vs NPD); ($^{b}P < 0.01$ vs HFD); ($^{c}P < 0.01$ vs HDACi 4b).

5.8.6 Effect of Class specific HDAC inhibitors on ptau level

HFD feeding results in significant increase in ptau levels as compared with NPD fed mice ($P < 0.001$) (Fig. 5.85). No significant changes in ptau level were observed in mice treated with either Class I or Class III inhibitors. In contrast, the mice treated with MC-1568 showed significant reduction in ptau levels in brain homogenates as compared with alone HFD group ($F_{(5,35)} = 5.90$; $P < 0.01$).

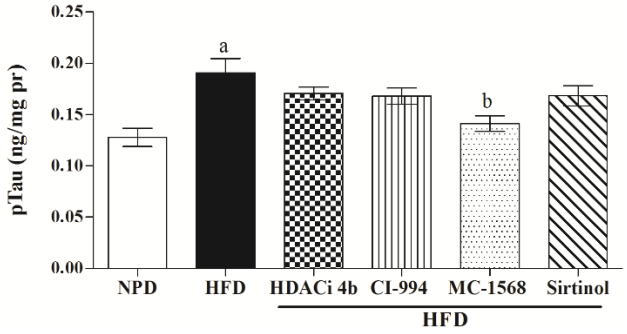

Fig.5.85 Effect of Class specific HDAC inhibitors on ptau level. Values are expressed as Mean ± SEM. ($^{a}P < 0.001$ vs NPD); ($^{b}P < 0.01$ vs HFD).

5.8.7. Effect of Class specific HDAC inhibitors on Amyloid $\beta_{(1-42)}$ level

HFD feeding results in significant increase in $A\beta_{1-42}$ levels as compared with NPD fed mice ($P < 0.001$) (Fig.5.86). The mice treated with Class I HDAC inhibitors, (HDACi 4b and CI-994) or Class III inhibitor (Sirtinol), showed no significant effect on $A\beta_{1-42}$ level as compared with HFD alone group. In contrast, marked decrease in $A\beta_{1-42}$ level was observed in the mice that received Class II HDAC inhibitor, MC-1568 as compared to HFD group ($F_{(5,35)} = 7.51$; $P < 0.01$).

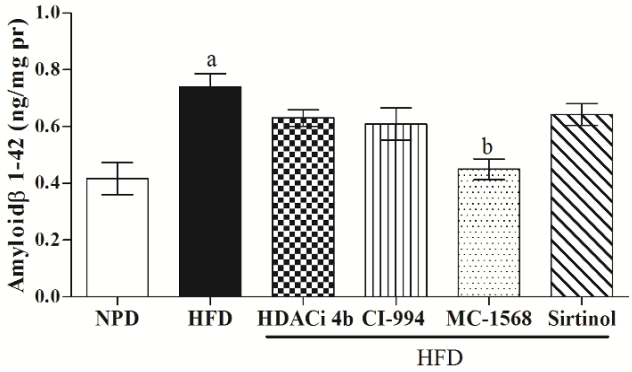

Fig. 5.86 Effect of Class specific HDAC inhibitors on Amyloid $\beta_{(1-42)}$ level. Values are expressed as Mean ± SEM. ($^{a}P< 0.001$ vs NPD); ($^{b}P< 0.01$ vs HFD).

5.8.8. Effect of Class specific HDAC inhibitors on BDNF level

HFD fed mice showed significant reduced of BDNF level as compared with NPD fed mice ($P < 0.001$) (Fig. 5.87). Treatment with MC-1568, significantly ameliorate the HFD induced decrease in BDNF level ($F_{(5,35)} = 9.75$; $P < 0.001$) (Fig. 5.87). However, no significant effect was observed on BDNF levels in mice treated with HDACi 4b, CI-994 or sirtinol.

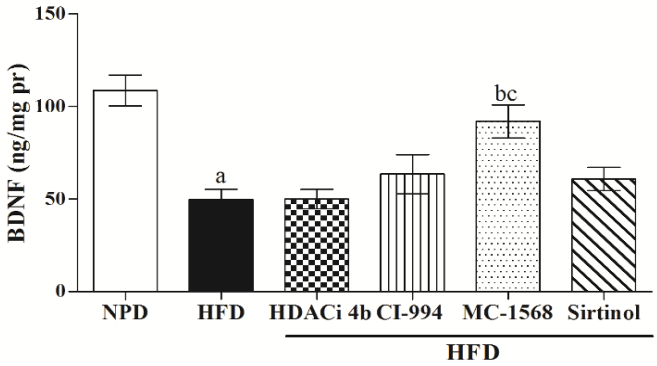

Fig. 5.87. Effect of Class specific HDAC inhibitors on BDNF level. Values are indicated as Mean ± SEM. ($^{a}P< 0.001$ vs NPD); ($^{b}P< 0.01$ vs HFD); ($^{c}P< 0.01$ vs HDACi 4b).

5.8.9. Effect of Class specific HDAC inhibitors on CREB level

HFD fed mice showed significant reduced of CREB level as compared with NPD fed mice ($P < 0.001$) (Fig. 5.88). Treatment with MC-1568, significantly ameliorate the HFD induced decrease in CREB level ($F_{(5,35)} = 7.65$; $P < 0.001$). However, no significant effect was observed on CREB levels in mice treated with either Class I or Class III HDAC inhibitors.

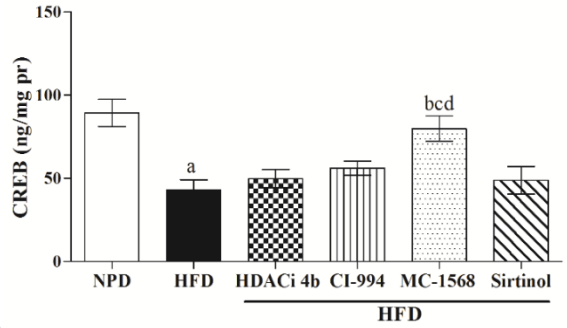

\

Fig. 5.88 Effect of Class specific HDAC inhibitors on CREB level. Values are indicated as Mean ± SEM. (^{a}P< 0.01 vs NPD); (^{b}P< 0.05 vs HFD) (^{c}P<0.05 vs HDACi 4b); (^{d}P<0.05 vs Sirtinol).

5.8.10. Histological photomicrographs of dentate gyrus and CA1 region of brain

Along with the cognitive impairments observed in the behavioral paradigms, the HFD feeding also results in significant morphological changes in DG and CA1 region of hippocampus neurons. The H&E stained brain sections showed healthy neurons in DG and CA1 region in the NPD fed mice (Fig. 5.89 Panel A and Panel G, respectively). Healthy neurons were robust in shape, had a spherical or slightly oval nucleus and a single large nucleolus with clear visible cytoplasm as indicated by yellow arrows. The HFD results in significant neuronal degeneration in CA1 and DG regions of hippocampus (Fig.5.89 Panel B and H). Decreased neuronal density and increased pyknotic neurons were observed in DG and CA1 regions in HFD mice. The pyknotic neurons were darkly stained with no nucleus or visible nucleolus and few of the cells were shrunken and sickle shaped in brain sections of HFD fed mice as indicated by red arrows. The microscopic pictures from the HFD fed mice showed a marked loss of cell bodies. Treatment with Class I HDAC inhibitors (CI-994 and HDACi 4b) and Class III inhibitor (Sirtinol) failed to attenuate HFD induced cell loss and pyknotic cells as degenerating cells with morphological changes were still observed (Fig. 5.89 Panel C, Panel D and Panel F; Fig. 5.89 Panel I, Panel J, Panel L, respectively). However, there was marked improvement in neuronal density and reduction in pyknotic neurons following treatment with Class II HDAC inhibitor, MC-1568 (Fig.5.89 Panel E and K).

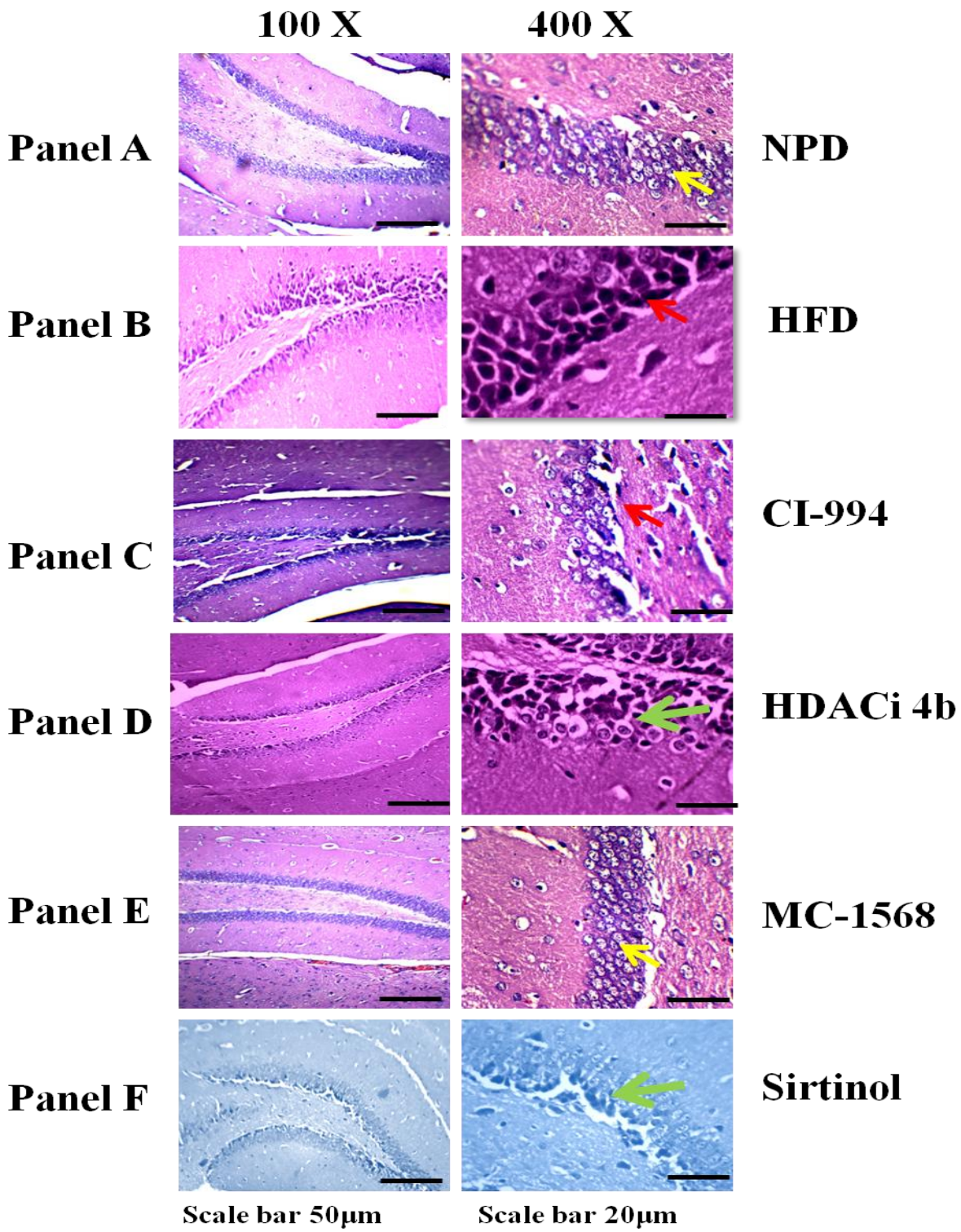

Fig. 5.89 (a) Effect of Class specific HDAC inhibitors on Dentate gyrus neurons. Figure shows photomicrographs of DG Panel A: **normal pellet diet**, Panel B: **High fat diet**, Panel C: **CI-994**, Panel D: **HDACi 4b,** Panel E: **MC-1568**, Panel F: **Sirtinol**. Yellow arrows indicate normal healthy neurons; Red arrows indicate damaged or sickle shaped pyknotic neurons.

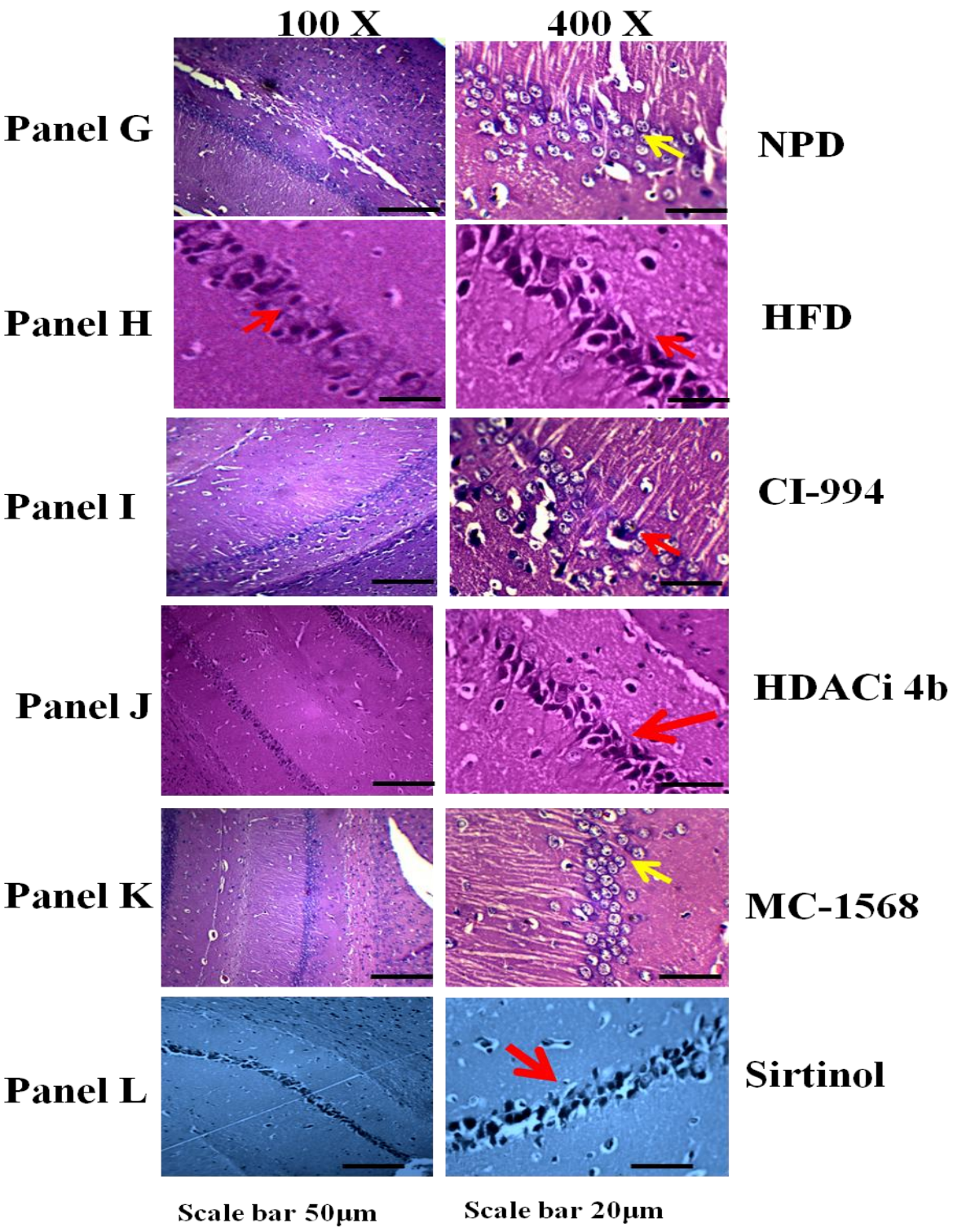

Fig. 5.89 (b) Effect of Effect of Class specific HDAC inhibitors on CA1 neurons. Figure shows photomicrographs of DG **(**Panel G: **normal pellet diet**, Panel H: **High fat diet**, Panel I: **CI-994**, Panel J: **HDACi 4b,** Panel K: **MC-1568**, Panel L: **Sirtinol**. Yellow arrows indicate normal healthy neurons; Red arrows indicate damaged or sickle shaped pyknotic neurons.

5.8.11. Effect of Class specific HDAC inhibitors on hippocampus (DG and CA1) neuronal Count

The HFD feeding results in a significant increase in the percentage of damaged neurons with altered morphological characters in both DG and CA1 regions ($P < 0.001$) (Fig.5.90a and 5.90b). No significant effect was observed on percentage of damaged neurons in mice treated with HDACi 4b, CI-994 and Sirtinol. However, the mice treated with MC-1568 showed significant neuroprotection as evidenced by reduced percentage of damaged neurons in DG and CA1 regions ($P < 0.001$; Fig. 5.90a and 5.90b).

(a) Percentage damaged neurons in DG **(b) Percentage damaged neurons in CA1**

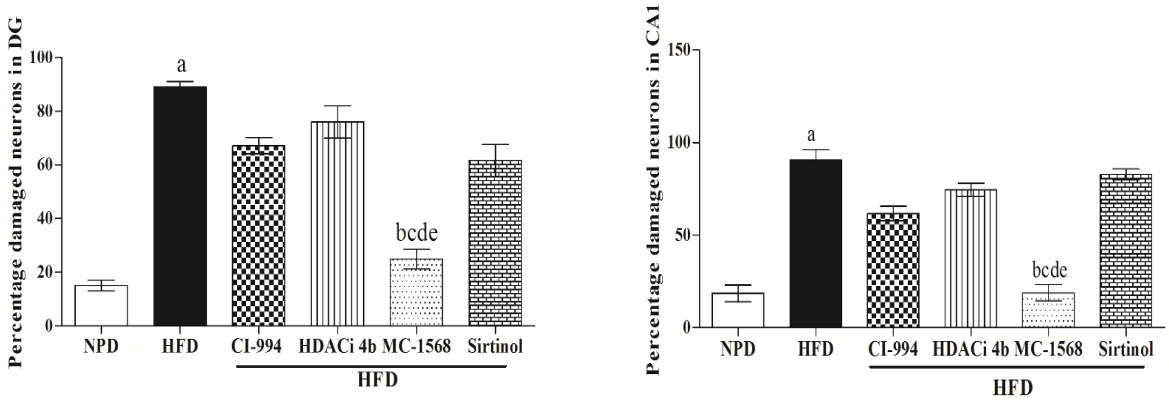

Fig. 5.90 Effect of Class specific HDAC inhibitors on hippocampus (DG and CA1) neuronal Count (a) DG neurons ($^{a}P < 0.001$ vs NPD; $^{b}P < 0.001$ vs HFD; $^{c}P < 0.01$ vs CI-994; $^{d}P < 0.01$ vs HDACi 4b) ($^{e}P < 0.01$ vs Sirtinol) **(b) CA1 neurons** ($^{a}P < 0.001$ vs NPD; $^{b}P < 0.001$ vs HFD; $^{c}P < 0.01$ vs CI-994; $^{d}P < 0.001$ vs HDACi 4b; $^{e}P < 0.01$ vs Sirtinol).

5.9 Effect of insulin resistance on Parkinson's disease pathology

5.9.1. Effect of HFD feeding on serum parameters in rats

HFD fed rats gained significantly more weight than the NPD fed rats after 8 weeks of diet feeding ($P < 0.01$). In addition, there was a significant increase in serum parameters, characteristic of insulin resistance viz. glucose ($P < 0.001$), TGs ($P < 0.001$), TC ($P < 0.001$) and insulin levels ($P < 0.001$) in HFD fed rats (Table 5.8). HOMA-IR values were also significantly higher in HFD rats as compared with NPD fed rats.

Parameter	**NPD**	**HFD**
Body weight (g)	296.3 ± 6.34	317.6 ± 5.79[a]
Glucose (mg/dl)	95.50 ± 3.20	132.6 ± 3.38[a]
Insulin (pmol/l)	84.94 ± 4.29	151.3 ± 8.01[a]
Triglycerides (mg/dl)	75.13 ± 5.77	124.2 ± 8.65[a]
Total Cholesterol (mg/dl)	62.63 ± 5.80	108.4 ± 7.35[a]
HOMA-IR	1.59 ± 0.08	3.01 ± 0.15[a]

Table. 5.8 Effect of HFD feeding on body weight and serum parameters in rats. Where, **Body weight** ([a]$P < 0.05$ vs NPD); **Serum Glucose** ([a]$P < 0.001$ vs NPD); **Serum Triglycerides** ([a]$P < 0.001$ vs NPD); **Total Cholesterol** ([a]$P < 0.001$ vs NPD); **Insulin** ([a]$P < 0.001$ vs NPD); **HOMA-IR** ([a]$P < 0.001$ vs NPD).

5.9.2 Effect of HFD on oral glucose tolerance test

The HFD fed rats showed marked glucose intolerance as assessed by OGTT. Blood glucose levels were found to be significantly higher in HFD fed rats as compared with NPD fed rats at 0, 30, 60 and 120 minutes after oral glucose administration ($P < 0.05$; Fig. 5.91).

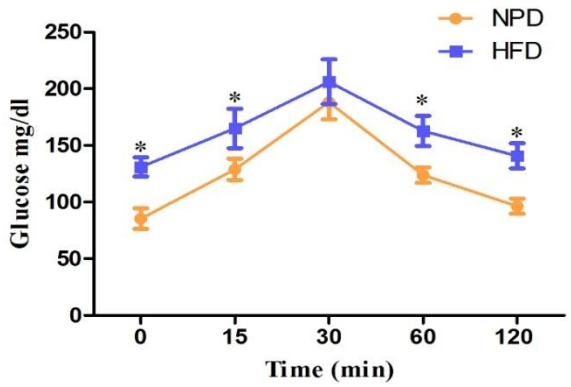

Fig. 5.91 Effect of HFD feeding on Oral glucose tolerance test. Values are indicated as mean ± SEM. (*P< 0.05 vs NPD).

5.9.3. Effect of HFD feeding along with 6-OHDA infusion on Rotarod activity

The rats fed with NPD along with 6-OHDA infusion showed significant reduction in the latency to fall from the rotating rod as compared with alone NPD fed rats (P < 0.001) (Fig. 5.92). Similarly, the rats fed with HFD along with 6-OHDA infusion also showed significant reduction in latency to fall from rotating rod as compared with alone HFD fed rats. Moreover, the reduction in latency in HFD + 6-OHDA rats was significant as compared with NPD + 6-OHDA rats. ($F_{(3,23)} = 33.32$) ($P < 0.001$) (Fig. 5.92).

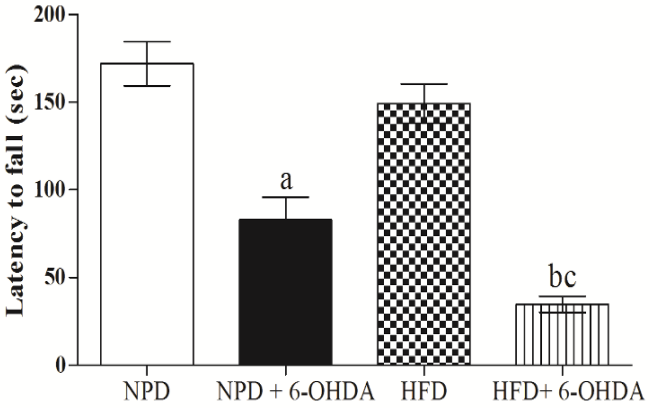

Fig. 5.92 Effect of HFD feeding and 6-OHDA administration on rotarod activity. Values are expressed as mean ± SEM. (^{a}P< 0.001 vs NPD); (^{b}P< 0.001 vs HFD); (^{c}P< 0.05 vs NPD+6-OHDA).

5.9.4. Effect of HFD feeding along with 6-OHDA infusion on spontaneous locomotor activity

The rats fed with NPD along with 6-OHDA infusion showed significant reduction in the locomotor as compared with alone NPD fed rats ($P < 0.001$) (Fig. 5.93). Similarly, the rats fed with HFD along with 6-OHDA infusion also showed significant reduction in locomotor activity as compared with alone HFD fed rats. Moreover, the reduction in latency in HFD + 6-OHDA rats was significant as compared with NPD + 6-OHDA rats. ($F_{(3,23)} = 24.55$) ($P < 0.001$) (Fig. 5.93).

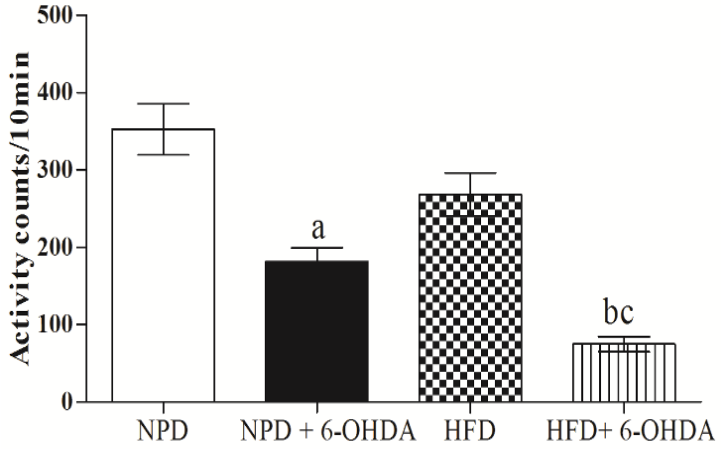

Fig. 5.93 Effect of HFD feeding and 6-OHDA treatment on locomotor activity in rats. ($^{a}P< 0.001$ vs NPD); ($^{b}P< 0.001$ vs HFD); ($^{c}P< 0.05$ vs NPD+6-OHDA).

5.9.5. Effect of HFD feeding along with 6-OHDA infusion on time taken to cross the narrow beam

6-OHDA administration in NPD fed rats results in significant increase in the time taken to cross the beam as compared with alone NPD fed rats ($P < 0.05$) (Fig. 5.94). Similarly, the rats fed with HFD and treated with 6-OHDA took significantly more time to cross narrow beam as compared to alone HFD fed rats. A significant difference in time taken to cross the beam was also observed between HFD+6-OHDA and NPD+6-OHDA treated rats ($F_{(3,23)} = 24.14$; $P < 0.001$) (Fig. 5.94).

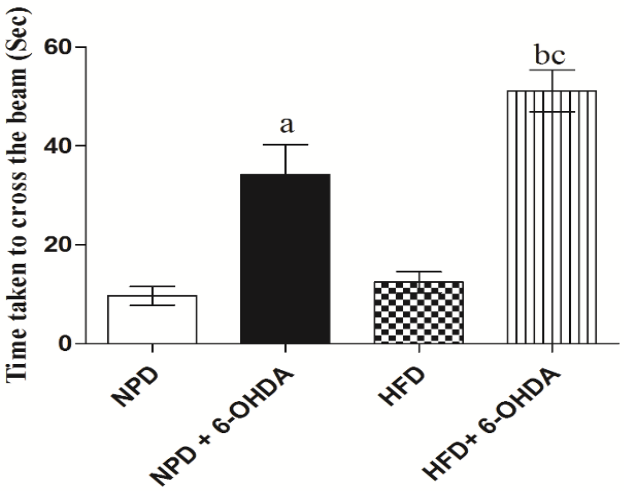

Fig. 5.94 Effect of HFD feeding and 6-OHDA treatment on time taken to cross narrow beam in rats. ([a]P< 0.01 vs NPD); ([b]P< 0.001 vs HFD); ([c]P< 0.05 vs NPD+6-OHDA).

5.9.6 Effect of HFD feeding along with 6-OHDA infusion on number of foot slips during narrow beam task

The rats fed with NPD along with 6-OHDA infusion showed significant increase in number of foot slips as compared with alone NPD fed rats ($P < 0.01$) (Fig. 5.95). Similarly, the rats fed with HFD along with 6-OHDA infusion also showed significant increase in number of foot slips as compared with alone HFD fed rats. Moreover, the increase in number of foot slips HFD + 6-OHDA rats was significant as compared with NPD + 6-OHDA rats ($F_{(3,23)} = 18.19$; $P < 0.001$) (Fig. 5.95).

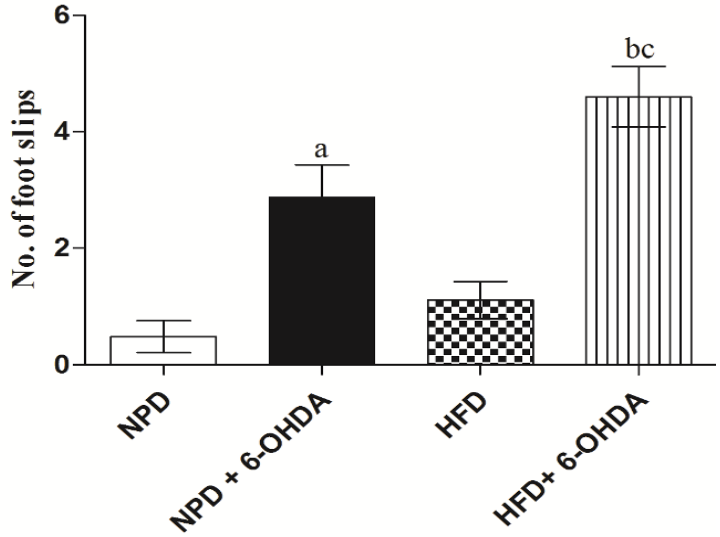

Fig. 5.95 Effect of HFD feeding and 6-OHDA treatment on number of foot slips during narrow beam task. ([a]P< 0.01 vs NPD); ([b]P< 0.001 vs HFD); ([c]P< 0.05 vs NPD+6-OHDA).

5.9.7 Effect of HFD feeding along with 6-OHDA infusion on oxidative stress markers (MDA, nitrite), antioxidant enzyme (GSH) and inflammatory marker (TNF-α) level

HFD feeding results in significant elevation of oxidative stress markers MDA ($F_{(3,23)=}$ 30.99, P< 0.001) and nitrite ($F_{(3,23)=}$ 43.48, P < 0.001) and reduced level of antioxidant enzyme (GSH) ($F_{(3,19)=}$ 21.54, P< 0.01). Also, we found significant increase in TNF- α levels in HFD fed rats ($F_{(3,23)=}$ 35.87, P< 0.01). Infusion of 6-OHDA in HFD fed rats results in significantly higher level of oxidative stress and neuroinflammatory markers as compared to NPD + 6-OHDA treated rats (Table. 5.9).

Groups	**Biochemical Parameters**			
	MDA (nM/ mg pr)	**Nitrite (μM/ mg pr)**	**GSH (μM / mg pr)**	**TNF-α (pg/ mgpr)**
NPD	287.2± 29.86	5.73 ± 0.48	0.58 ± 0.05	31.00 ± 1.48
HFD	415.3± 32.67[a]	7.86 ± 0.53[a]	0.42 ± 0.04[a]	41.17 ± 2.33[a]
NPD + 6-OHDA	503.8± 37.71[b]	11.32 ± 0.58[b]	0.32 ± 0.04[b]	53.33 ± 2.06[b]
HFD + 6-OHDA	711.8± 27.14[cd]	13.63 ± 0.54[cd]	0.16 ± 0.01[cd]	63.67 ± 3.27[cd]

Table. 5.9 Effect of HFD feeding along with 6-OHDA infusion on oxidative stress and neuroinflammatory markers. (a) MDA ([a]P <0.05 vs NPD; [b]P < 0.001 vs NPD; [c]P < 0.001 vs HFD; [d]P< 0.001 vs NPD + 6-OHDA); **(b) Nitrite** ([a]P <0.05 vs NPD; [b]P < 0.001 vs NPD; [c]P < 0.001 vs HFD; [d]P< 0.05 vs NPD + 6-OHDA); **(c) GSH** ([a]P <0.05 vs NPD; [b]P < 0.001 vs NPD; [c]P < 0.001 vs HFD; [d]P< 0.05 vs NPD + 6-OHDA); **(d) TNF-α** ([a]P <0.05 vs NPD; [b]P < 0.001 vs NPD; [c]P < 0.01 vs HFD; [d]P< 0.05 vs NPD + 6-OHDA).

5.9.8.. Effect of HFD feeding along with 6-OHDA infusion on striatal dopamine level

The rats fed with NPD along with 6-OHDA infusion showed significant reduction in the striatal dopamine level as compared with alone NPD fed rats ($P < 0.001$) (Fig. 5.96). Similarly, the rats fed with HFD along with 6-OHDA infusion also showed significant reduction in striatal dopamine level as compared with alone HFD fed rats. Moreover, the reduction in dopamine level in HFD + 6-OHDA rats was significant as compared with NPD + 6-OHDA rats ($F_{(3,19)} = 39.15$) ($P < 0.01$).

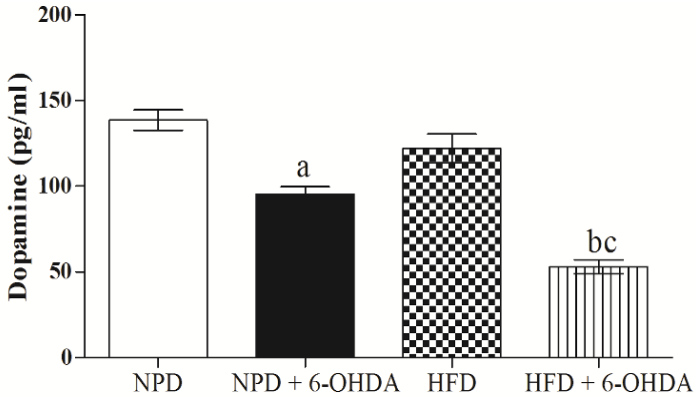

Fig. 5.96 Effect of HFD feeding + 6-OHDA administration on striatal dopamine level. ($^{a}P < 0.001$ vs NPD); ($^{b}P < 0.01$ vs HFD); ($^{c}P < 0.001$ vs NPD+6-OHDA).

5.9.9. Effect of HFD feeding along with 6-OHDA infusion on Histone H3 acetylation level

The global histone H3 acetylation levels were found to be reduced in striatal brain tissue homogenates of NPD+ 6-OHDA treated rats as compared with NPD alone fed rats ($P < 0.05$) (Fig. 5.97). Similarly, reduced level of global Histone H3 acetylation was observed in HFD+ 6-OHDA infused rats as compared with HFD alone fed rats. Moreover, the reduction in histone H3 acetylation was significant as compared with NPD + 6-OHDA rats ($F_{(3, 15)} = 18.66$) ($P < 0.01$) (5.97).

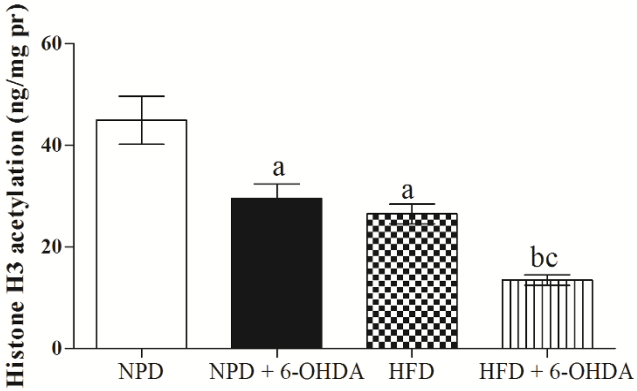

Fig. 5.97 Effect of HFD feeding along with 6-OHDA infusion on Histone H3 acetylation level. Values are expressed as mean ± SEM. ($^{a}P < 0.05$ vs NPD); ($^{b}P < 0.05$ vs HFD); ($^{c}P < 0.05$ vs NPD+6-OHDA).

5.9.10. Effect of HFD feeding along with 6-OHDA infusion on GSK3β level

The GSK3β level was found to be significantly higher in HFD fed rats as compared to NPD fed rats. Moreover, a significant difference was observed in HFD fed 6-OHDA infused rats as compared to NPD fed 6-OHDA infused rats ($F_{(3, 19)} = 8.54$) ($P < 0.01$) (Fig. 5.98).

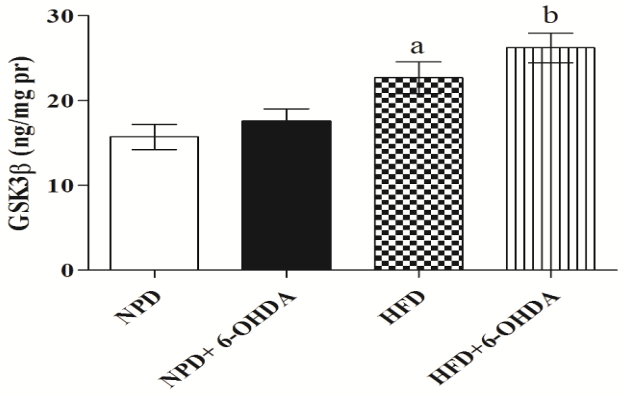

Fig. 5.98 Effect of HFD feeding along with 6-OHDA infusion on on GSK3β level. Values are expressed as mean ± SEM. ($^{a}P < 0.05$ vs NPD); ($^{b}P < 0.01$ vs NPD+6-OHDA).

5.9.11. Effect of HFD feeding along with 6-OHDA infusion on striatal neurons and neuronal count

H&E stained sections of striatum region showed healthy neurons in NPD fed rats (Fig, 5.99a). Healthy neurons appeared robust in shape, had a spherical or slightly oval nucleus and a single large nucleolus with clear visible cytoplasm as indicated by yellow arrows. 6-OHDA treated rats showed significant neuronal damage in striatal region. Moreover, in HFD+6-OHDA infused rats increased pyknotic neurons were observed, as evident by increased percentage of damaged neurons (Fig. 5.99b). The pyknotic neurons were darkly stained and few of the cells were sickle shaped in brain sections of these rats as indicated by red arrows.

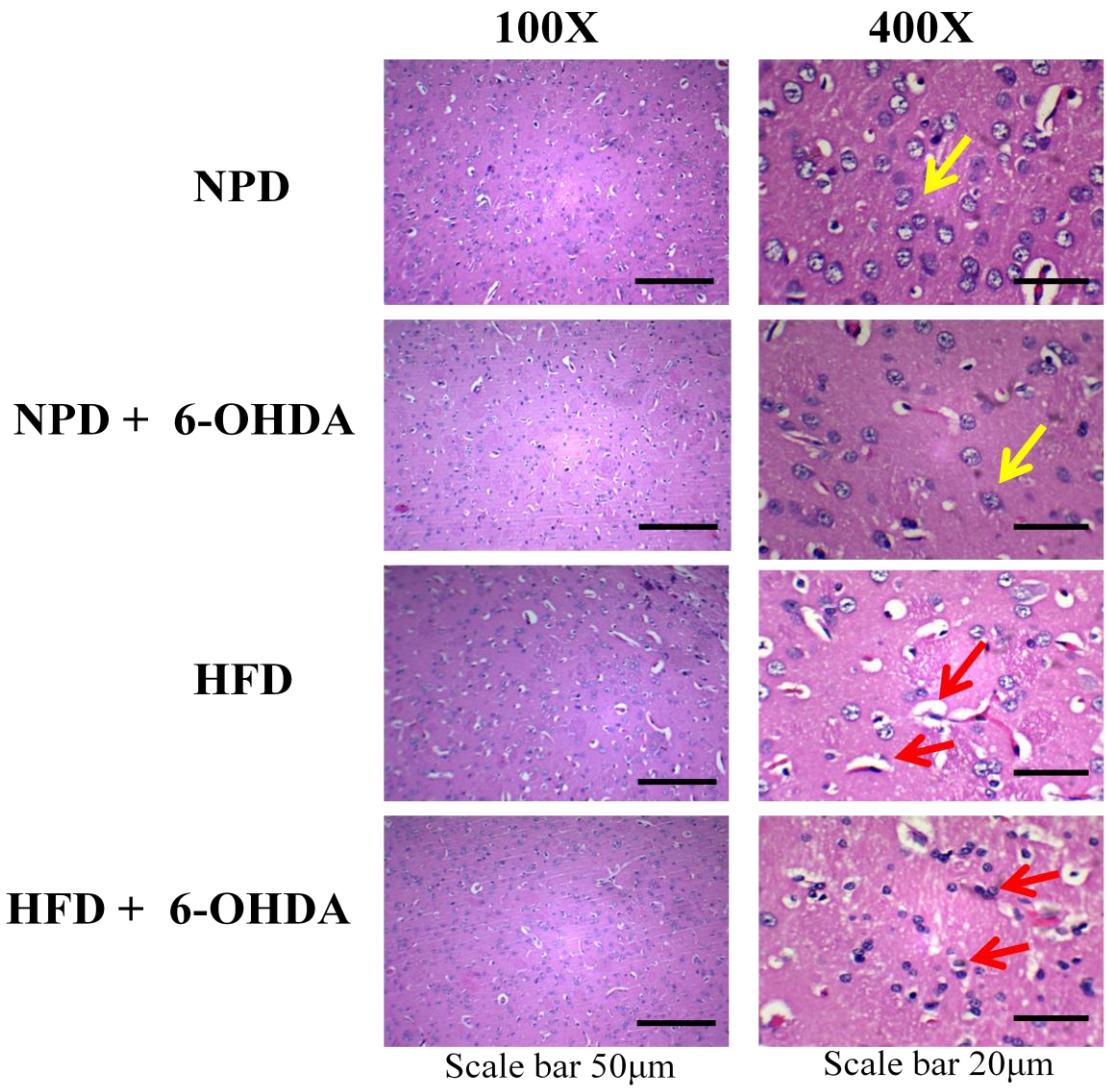

Fig. 5.99a Photomicrographs of Striatal brain region in NPD and HFD rats treated with 6-OHDA. Yellow arrows indicate normal healthy neurons. Red arrows indicate damaged or sickle shaped neurons.

(b) Percentage damaged neurons in Striatum

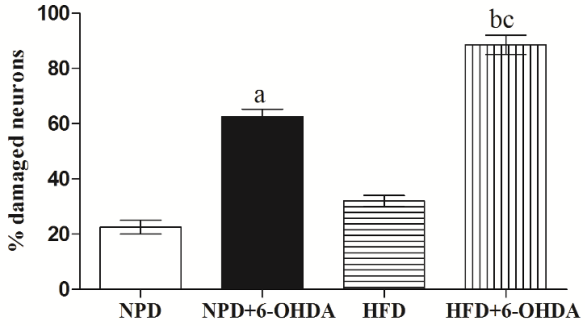

Fig. 5.99b Effect of HFD feeding along with 6-OHDA infusion on striatal neuronal count (^{a}P <0.01 vs NPD; ^{b}P< 0.001 vs HFD; ^{c}P< 0.01 vs NPD+6-OHDA).

5.10. Effect of GSK-3β inhibitor, IMX and HDAC inhibitor, SAHA on insulin resistance induced exacerbated PD pathology

5.10.1. Effect of IMX and SAHA administration on serum parameters in HFD + 6-OHDA administered rats

No significant difference in serum glucose, insulin, triglycerides and total cholesterol was observed in HFD + 6-OHDA administered rats as compared with alone HFD fed rats. In contrast, HDAC inhibitor, SAHA (50 mg/kg) and GSK3β inhibitor IMX (0.4mg/kg) attenuated the level of serum glucose ($F_{(5,35)}= 5.38$; $P < 0.05$), insulin ($F_{(5,35)}= 5.03$; $P < 0.01$), triglycerides ($F_{(5,35)}= 6.17$; $P < 0.05$) and total cholesterol levels ($F_{(5,35)} = 7.47$; $P < 0.05$) in HFD+6-OHDA treated rats (Table 5.10).

Groups	**Glucose** (mg/dl)	**Insulin (pmol/l)**	**TGs (mg/dl)**	**TC (mg/dl)**	**HOMA-IR**
HFD	145.5 ± 19.21	171.1 ± 21.85	108.2 ± 9.446	102.3 ± 12.15	3.43 ± 0.35
HFD+6-OHDA +Vehicle	139.6 ± 16.49	189.5 ± 16.08	111.3 ± 15.07	95. 97 ± 10.96	3.76 ± 0.30
HFD+6-OHDA+ SAHA 25	118.4 ± 15.51	161.4 ± 14.82	96.73 ± 26.58	86.34 ± 13.53	3.12 ± 0.33[a]
HFD+6-OHDA+ SAHA 50	111.8 ± 12.45[a]	146.3 ± 12.45[a]	80.00 ± 18.14[a]	72.51 ± 12.18[a]	2.81 ± 0.28[b]
HFD+6-OHDA+IMX 0.2	125.0 ± 11.80	167.2 ±13.33	83.27 ± 13.30	74.08 ±16.45	3.27 ± 0.30
HFD+6-OHDA+IMX 0.4	112.2 ± 13.38[a]	151.4 ± 20.20	67.35 ± 13.99[b]	65.19 ± 12.23[b]	2.89 ± 0.36[b]

Table. 5.10 Effect of SAHA and IMX administration on serum parameters in HFD + 6-OHDA treated rats. Glucose ($^{a}P < 0.05$ vs HFD + 6-OHDA); **Insulin** ($^{a}P < 0.05$ vs HFD + 6-OHDA); **Triglycerides (**$^{a}P < 0.05$ vs HFD + 6-OHDA); ($^{b}P < 0.01$ vs HFD + 6-OHDA); **Cholesterol** ($^{a}P < 0.05$ vs HFD + 6-OHDA); ($^{b}P < 0.01$ vs HFD + 6-OHDA); HOMA-IR ($^{a}P < 0.05$ vs HFD+6-OHDA), ($^{b}P < 0.001$ vs HFD+6-OHDA).

5.10.2. Effect of IMX and SAHA treatment on rotarod activity in HFD + 6-OHDA administered rats

The HFD+6-OHDA+vehicle administered rats showed significant reduction in latency to fall from rotating rod as compared with alone HFD fed rats (Fig. 5.100). However, treatment with SAHA (50 mg/kg) and IMX (0.4 mg/kg) significantly and dose dependently attenuated HFD+6-OHDA-induced decrease in latency to fall from the rod ($F_{(5,35)} = 16.94$) ($P < 0.001$) (Fig. 5.100).

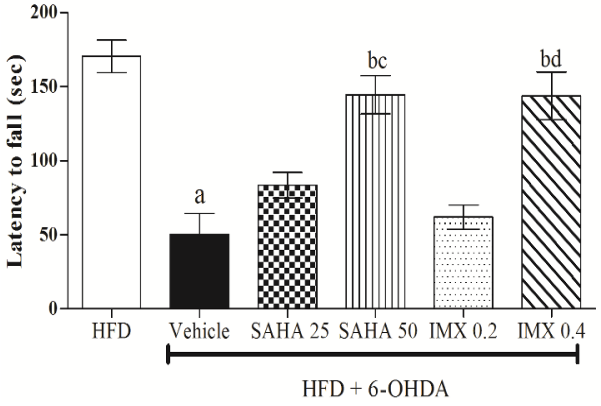

Fig.5.100. Effect of SAHA and IMX treatment on rotarod activity in HFD + 6-OHDA administered rats. Values are expressed as mean ± SEM. ($^{a}P< 0.001$ vs HFD); ($^{b}P< 0.001$ vs HFD+6-OHDA + Vehicle); ($^{c}P < 0.01$ vs SAHA 25); ($^{d}P < 0.05$ vs IMX 0.2).

5.10.3. Effect of SAHA and IMX treatment on locomotor activity in HFD + 6-OHDA administered rats

The HFD + 6-OHDA + vehicle treated rats showed significant reduction in locomotor activity as compared with alone HFD fed rats (5.101). In contrast, SAHA treatment at high dose and IMX treatment at both low and high doses were able to significantly attenuated HFD + 6-OHDA induced decrease in activity counts in rats ($F_{(5, 35)} = 6.45$) ($P < 0.001$) (Fig. 5.101).

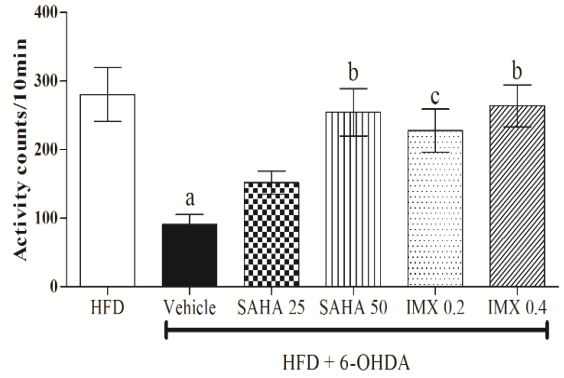

Fig.5.101 Effect of SAHA and IMX on locomotor activity in HFD + 6-OHDA administered rats. Values are expressed as mean ± SEM. ($^{a}P < 0.001$ vs HFD); ($^{b}P < 0.01$ vs HFD+ 6-OHDA+ Vehicle); ($^{c}P < 0.05$ vs HFD+ 6-OHDA+ Vehicle).

5.10.4. Effect of IMX and SAHA treatment on time taken to cross the narrow beam in HFD + 6-OHDA administered rats

HFD + 6-OHDA administration results in significant increase in the time taken to cross the beam as compared with alone HFD fed rats ($P < 0.001$) (Fig. 5.102). In contrast, the rats treated with SAHA (50 mg/kg) and IMX (0.2 and 0.4 mg/kg) took significantly lesser time to cross narrow beam ($F_{(5,35)} = 6.23$) ($P < 0.001$) (Fig.5.102).

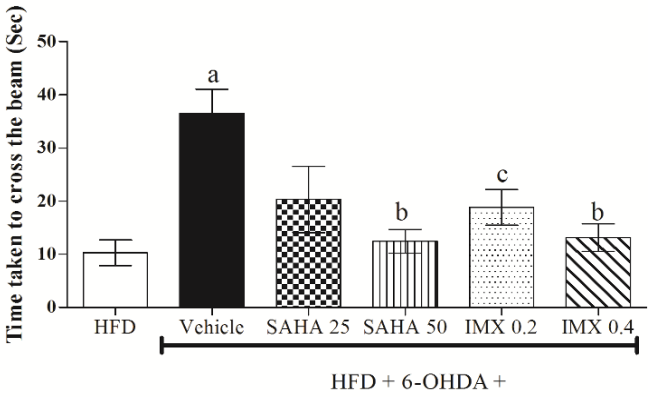

Fig. 5.102 Effect of SAHA and IMX on time taken to cross the narrow beam in HFD + 6-OHDA administered rats. Values are expressed as mean ± SEM. ($^{a}P < 0.001$ vs HFD); ($^{b}P< 0.01$ vs HFD+6-OHDA+Vehicle); ($^{c}P < 0.05$ vs HFD+6-OHDA+Vehicle).

5.10.5. Effect of IMX and SAHA on number of foot slips during narrow beam task in HFD + 6-OHDA administered rats

6-OHDA administration in HFD fed rats results in significant increase in the number of foot slips as compared to alone HFD treated rats ($P < 0.001$) (Fig. 5.103). However, treatment with HDAC inhibitor, SAHA and GSK3β inhibitor, IMX, significantly attenuated the number of foot slip counts in these animals ($F_{(5, 35)} = 4.51$; $P < 0.01$) (Fig.5.103).

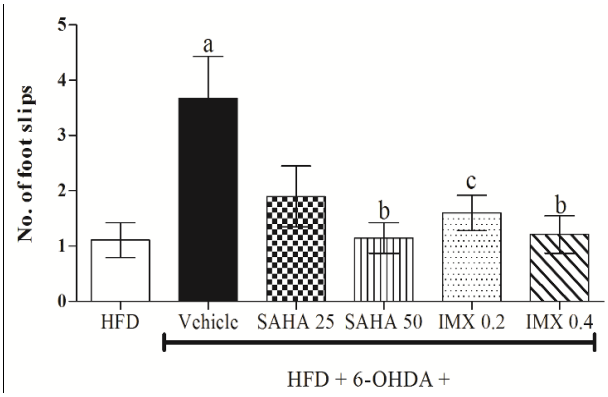

Fig.5.103 Effect of SAHA and IMX on number of foot slips during narrow beam task in HFD + 6-OHDA administered rats. Values are expressed as mean ± SEM ($^{a}P <$ 0.01 vs HFD); ($^{b}P <$ 0.01 vs HFD+6-OHDA+Vehicle); ($^{c}P <$ 0.05 vs HFD+6-OHDA+Vehicle).

5.10.6. Effect of SAHA and IMX on contralateral contacts in cylinder test in HFD + 6-OHDA administered rats

6-OHDA administration in HFD fed rats results in significant reduction in contralateral contacts as compared to alone HFD treated rats ($P < 0.001$) (Fig. 5.104). However, treatment with HDAC inhibitor, SAHA and GSK3β inhibitor, IMX significantly ameliorated the number of contralateral contacts in these animals ($F_{(5,35)} = 10.29$; $P < 0.001$) (Fig. 5.104).

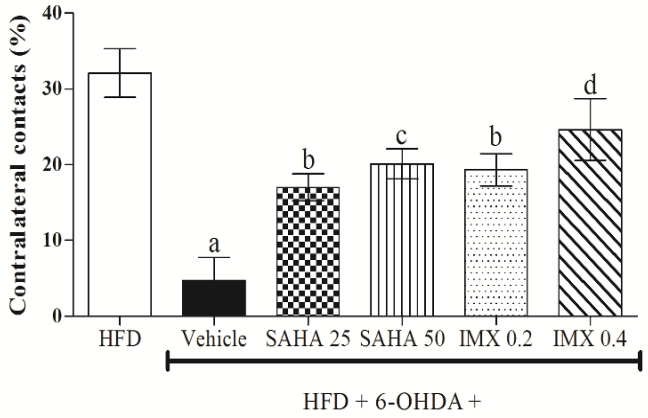

Fig. 5.104 Effect of SAHA and IMX on contralateral contacts in cylinder test in HFD + 6-OHDA administered rats. Values are expressed as mean ± SEM **(**$^{a}P < 0.001$ vs HFD); ($^{b}P < 0.05$ vs HFD+6-OHDA + vehicle); ($^{c}P < 0.01$ vs HFD+6-OHDA + vehicle); ($^{d}P < 0.001$ vs HFD+6-OHDA + vehicle).

5.10.7. Effect of SAHA and IMX treatment on striatal dopamine level in HFD + 6-OHDA administered rats

6-OHDA administration in HFD fed rats results in significant reduction in striatal dopamine level as compared to alone HFD treated rats ($P < 0.001$) (Fig. 5.105). However, treatment with HDAC inhibitor, SAHA and GSK3β inhibitor IMX, significantly improved the striatal dopamine level in these animals ($F_{(5, 29)} = 25.37$; $P < 0.001$) (Fig. 5.105).

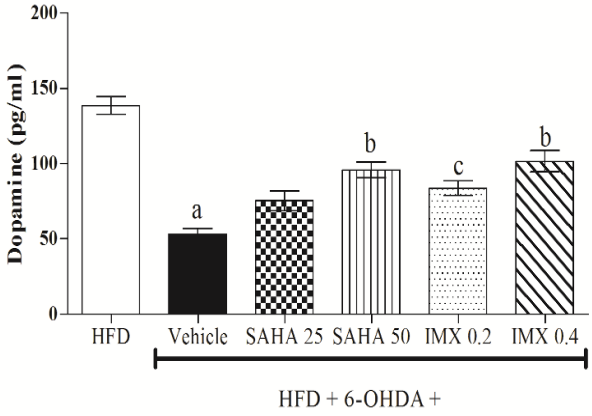

Fig. 5.105 Effect of SAHA and IMX treatment on striatal dopamine level in HFD + 6-OHDA administered rats. Values are expressed as mean ± SEM ($^{a}P < 0.001$ vs HFD); ($^{b}P < 0.05$ vs HFD+6-OHDA+ Vehicle); ($^{c}P < 0.001$ vs HFD+6-OHDA+ Vehicle).

5.10.8. Effect of SAHA and Indirubin-3-monoxime on oxidative stress markers (MDA, nitrite) and antioxidant enzyme (GSH) and inflammatory marker (TNF-α) level in HFD + 6-OHDA administered rats

Groups	Biochemical Parameters			
	MDA (nM/ mg pr)	Nitrite (μM/ mg pr)	GSH (μM / mg pr)	TNFα (pg/mgpr)
HFD	415.0 ± 26.46	7.08 ± 0.23	0.52± 0.04	35.83 ± 2.66
HFD + 6-OHDA	714.0 ± 23.71[a]	13.90 ± 0.49[a]	0.18± 0.01[a]	66.00 ± 3.82[a]
HFD + 6-OHDA+ **SAHA 25**	621.5 ± 29.28	12.68 ± 0.43	0.21± 0.02	56.50 ± 3.49
HFD + 6-OHDA+ **SAHA 50**	547.8 ± 20.59[b]	10.03 ± 0.34[bc]	0.37± 0.01[bc]	45.50 ± 3.40[b]
HFD + 6-OHDA+ **IMX 0.2**	594.5 ± 20.32[c]	12.43 ± 0.38	0.30 ±0.02[d]	50.83 ± 2.29[c]
HFD + 6-OHDA+ **IMX 0.4**	480.2 ± 23.74[de]	9.52 ± 0.36[de]	0.41 ± 0.02[ef]	44.33 ± 3.18[d]

Table.5.11 Effect of SAHA and Indirubin-3-monoxime on oxidative stress and neuroinflammatory markers in HFD + 6-OHDA treated rats. (a) MDA ([a]P <0.001 vs HFD; [b]P < 0.001 vs HFD+6-OHDA; [c]P < 0.05 vs HFD+6-OHDA; [d]P< 0.001 vs HFD + 6-OHDA; eP < 0.05 vs HFD + 6-OHDA+ IMX 0.2); (b) **Nitrite** ([a]P <0.001 vs HFD; [b]P < 0.001 vs HFD+6-OHDA; [b]P < 0.001 vs HFD+6-OHDA; [c]P < 0.001 vs HFD+6-OHDA+ SAHA 25; [d]P < 0.001 vs HFD+6-OHDA; [e]P < 0.001 vs HFD+6-OHDA+ IMX 0.2); (c) **GSH** ([a]P <0.001 vs HFD; [b]P < 0.001 vs HFD+6-OHDA; [c]P < 0.001 vs HFD+6-OHDA+ SAHA25; [d]P < 0.05 vs HFD+6-OHDA; [e]P < 0.001 vs HFD+6-OHDA; [f]P < 0.05 vs HFD+6-OHDA+ IMX 0.2); (d) **TNFα** ([a]P <0.001 vs HFD; [b]P < 0.01 vs HFD+6-OHDA; [c]P < 0.05 vs HFD+6-OHDA; [d]P < 0.001 vs HFD+6-OHDA).

5.10.9 Effect of SAHA treatment on histone H3 acetylation in HFD + 6-OHDA administered rats

6-OHDA administration in HFD fed rats results in significant reduction in global histone H3 acetylation as compared to alone HFD treated rats ($P < 0.001$) (Fig. 5.106). However, treatment with HDAC inhibitor, SAHA (at both 25mg/kg and 50mg/kg) significantly ameliorated the global H3 acetylation in these animals ($F_{(3, 23)} = 17.63$; $P < 0.001$) (Fig. 5.106).

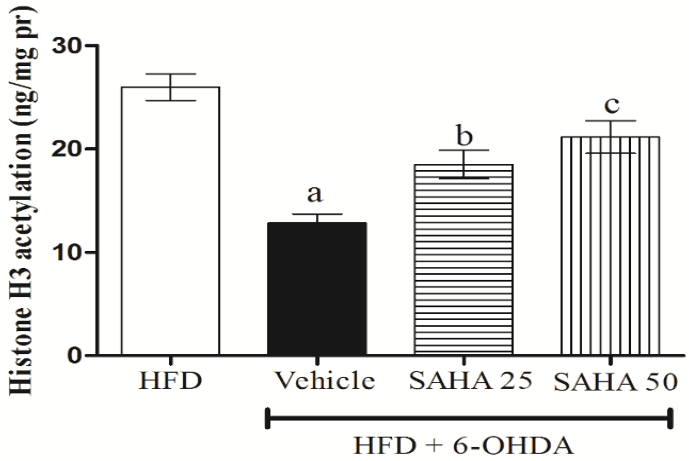

Fig. 5.106 Effect of SAHA treatment on global histone H3 acetylation level in HFD+6-OHDA administered rats. Values are expressed as mean ± SEM ($^{a}P < 0.001$ vs HFD); ($^{b}P < 0.05$ vs HFD+6-OHDA + Vehicle); ($^{c}P < 0.01$ vs HFD+ 6-OHDA+ Vehicle).

5.10.10. Effect of SAHA and IMX treatment on CREB level in HFD + 6-OHDA administered rats

6-OHDA administration in HFD fed rats results in significant reduction in CREB level as compared to alone HFD treated rats ($P < 0.05$) (Fig. 5.107). However, treatment with HDAC inhibitor, SAHA (25 and 50mg/kg) and GSK-3β inhibitor, IMX (0.4 mg/kg) significantly ameliorated CREB level in these animals ($F_{(5, 35)} = 5.38$; $P < 0.001$) (Fig. 5.107).

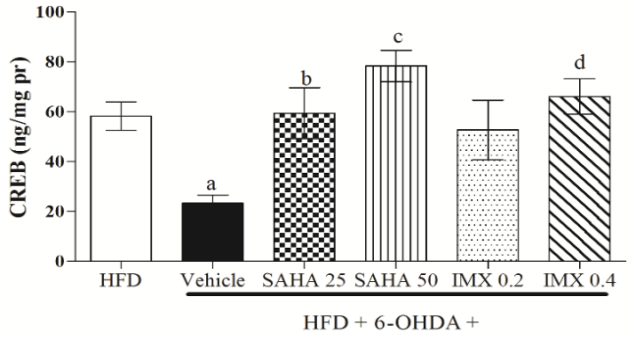

Fig. 5.107 Effect of IMX and SAHA treatment on CREB level in HFD+6-OHDA administered rats. Values are expressed as mean ± SEM ($^{a}P < 0.05$ vs HFD); ($^{b}P < 0.05$ vs HFD+6-OHDA + Vehicle); ($^{c}P < 0.001$ vs HFD+ 6-OHDA+ Vehicle); ($^{d}P < 0.01$ vs HFD+ 6-OHDA+ Vehicle).

5.10.11 Effect of SAHA and IMX treatment on BDNF in HFD + 6-OHDA administered rats

6-OHDA administration in HFD fed rats results in significant reduction in BDNF level as compared to alone HFD treated rats ($P < 0.001$) (Fig. 5.108). However, treatment with

HDAC inhibitor, SAHA (50mg/kg) and GSK-3β inhibitor, IMX (0.4 mg/kg) significantly ameliorated BDNF level in these animals ($F_{(5, 35)} = 11.60$; $P < 0.001$) (Fig. 5.108).

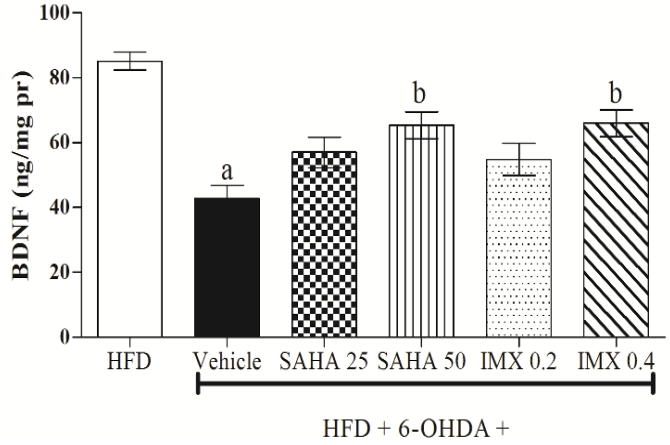

Fig.5.108 Effect of SAHA and IMX treatment on BDNF level in HFD + 6-OHDA administered rats. Values are expressed as mean ± SEM. ($^{a}P < 0.001$ vs HFD); ($^{b}P < 0.01$ vs HFD+6-OHDA + vehicle).

5.10.12. Effect of Indirubin-3-monoxime treatment on GSK3β level in HFD + 6-OHDA administered rats

No significant difference in GSK3β level was observed in HFD + 6-OHDA administered rats as compared with alone HFD fed rats (Fig. 5.109). In contrast, GSK3β inhibitor, IMX (0.4 mg/kg) in HFD+ 6-OHDA administered rats was able to significantly attenuate the levels of GSK3β ($F_{(3, 20)} = 15.76$; $P < 0.01$) (Fig. 5.109).

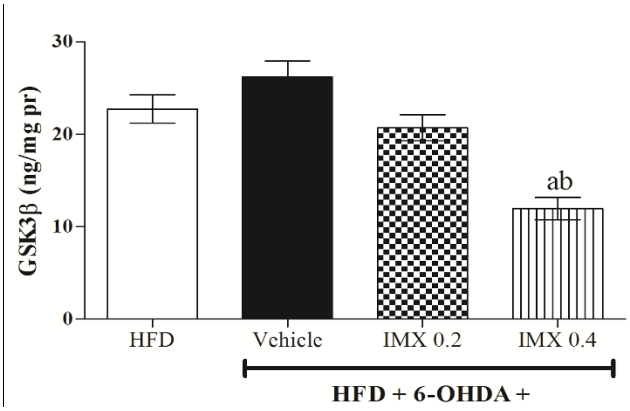

Fig. 5.109 Effect of IMX treatment on GSK3β level in HFD + 6-OHDA administered rats. Values are expressed as mean ± SEM. ($^{a}P < 0.001$ vs HFD+6-OHDA + vehicle); ($^{b}P < 0.01$ vs HFD+6-OHDA+IMX 0.2).

5.10.13. Effect of SAHA and IMX treatment on striatal neurons and neuronal count in HFD + 6-OHDA administered rats

H&E stained sections of striatum region showed healthy and some damaged neurons in HFD fed rats (Fig. 5.110a). Healthy neurons appeared robust in shape, had a spherical or slightly oval nucleus and a single large nucleolus with clear visible cytoplasm as indicated by yellow arrows. Moreover, in HFD + 6-OHDA infused rats there is significant neuronal damage in striatal region as evident by increased percentage of damaged neurons (Fig. 5.110b). The pyknotic neurons were darkly stained and few of the cells were sickle shaped in brain

sections of these rats as indicated by red arrows. Treatment with SAHA (50 mg/kg) and IMX (0.4mg/kg) prevented HFD + 6-OHDA induced neuronal loss and pyknotic neurons and reduction in percentage damaged neurons was observed (Fig. 5.110b)

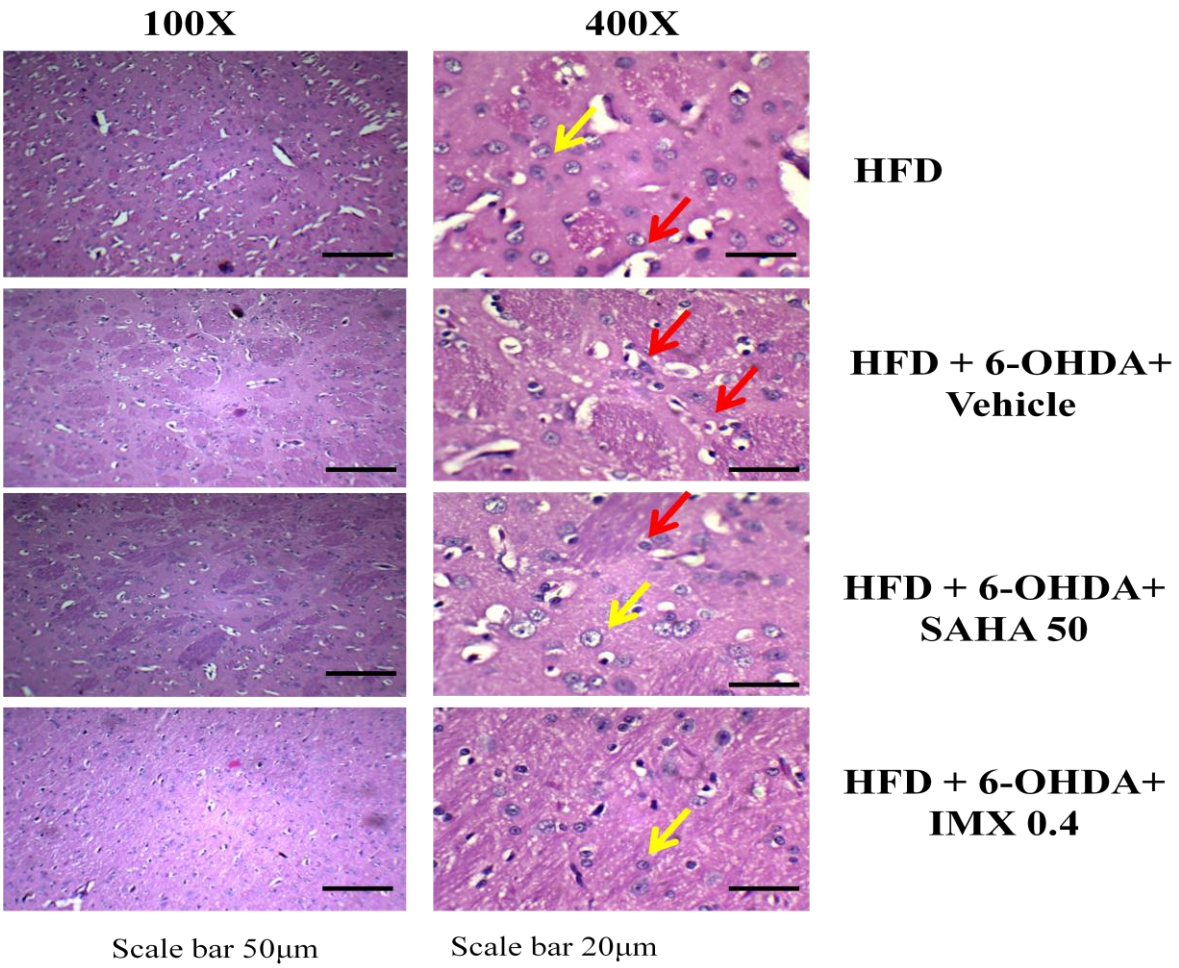

Fig. 5.110a Shows photomicrographs of Striatal brain region of SAHA and IMX treated rats. Yellow arrows indicate normal healthy neurons. Red arrows indicate damaged or sickle shaped neurons.

(b) Percentage damaged neurons in striatum

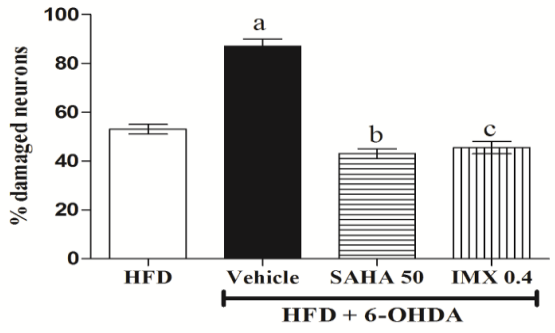

Fig. 5.110b Effect of SAHA and IMX treatment on neuronal count in HFD + 6-OHDA administered rats. Values are expressed as mean ± SEM. (^{a}P < 0.01 vs HFD; ^{b}P< 0.001 vs HFD+6-OHDA + Vehicle); (^{c}P < 0.001 vs HFD+6-OHDA+Vehicle).

6.0 Discussion

In the present study, we have investigated the link factors between insulin resistance and neurodegeneration and explored the beneficial effects of GSK3β and HDAC inhibitors under these conditions. Previously, it has been reported that chronic consumption of diets rich in saturated fats is strongly associated with a variety of related metabolic diseases including obesity, systemic insulin resistance, metabolic syndrome and T2DM (Kraegen et al., 1991; Siri-Tarino et al., 2010). These diseases have reached epidemic proportions and increased co-morbid conditions such as elevated blood pressure, cardiovascular disease and inflammation, which in turn lead to a reduced quality and expectancy of life. Several epidemiologic studies have found that patients with obesity, T2DM and insulin resistance have an increased risk for diverse cognitive and motor impairments, including cognitive decline, mild cognitive impairment, AD and PD (Kivipelto et al., 2005; Whitmer, 2007). Furthermore, epidemiologic studies suggest that diets high in saturated fats are a major risk factor for the development of AD and PD (Eskelinen et al., 2008; Laitinen et al., 2006; Anderson et al., 1999). Although the common link and the exact molecular mechanisms of association between metabolic diseases and neurodegenerative diseases (AD and PD) are still elusive, however, insulin resistance has emerged as an important link factor between these co-morbid conditions. Thus, insulin resistance being the common risk factor involved in various metabolic and neurodegenerative diseases, was the focus of current study. For this purpose, we initially standardize the animal model for insulin resistance by feeding the animals with diet rich in saturated fats and further explored the time course for development of behavioural dysfunctions.

Previous studies have suggested that HFD feeding in rodents (rats and mice) results in insulin resistance condition as early as one week after diet feeding (Winzell & Ahrén, 2004). The induction of insulin resistance, T2DM and obesity by HFD feeding depends upon various factors including the diet composition, type of fat, animal strain used etc. In the present study, we fed male swiss albino mice with HFD containing 58% fat from lard. The level of serum glucose, insulin, triglycerides, total cholesterol and LDL-cholesterol were measured after every 2 weeks interval. We observed that HFD feeding results in significantly increased body weight, serum glucose and insulin level as early as 4 week after diet feeding. These changes in circulating glucose and insulin levels were further reflected in a significant increase in the HOMA-IR index, a quantitative measure of insulin resistance, which appeared at 4 weeks after diet feeding. Interestingly, increased level of serum triglyceride, total cholesterol and

LDL-cholesterol were observed in HFD fed mice as compared to NPD fed mice. Although we observed hyperglycemia and hyperinsulinemia at 4 weeks after diet feeding, however we continued to feed the mice with HFD until we got persistant increase in serum insulin and glucose levels, i.e upto 8 weeks.

Further, we determine the relationship between insulin resistance and neurobehavioral alterations and establish the time course for development of insulin resistance induced cognitive decline. In order to achieve this, the animals fed with HFD were subjected to behavioral tasks to evaluate their cognitive functions and neuronal health. Initially, to examine the effect of HFD feeding on locomotor activity of animals we performed spontaneous locomotor activity test and found no significant effect of HFD feeding on locomotor activity at any time point. Then, we used MWM task to evaluate the cognitive performance of HFD and NPD fed mice. The MWM task is based on the reward principle and is a test of spatial learning and memory in which mice must depend on distal cues to navigate from start locations around the perimeter of a water poll to find a hidden platform. Mice dislike swimming and typically attempt to escape from the water. Eventually, the mice searched for a hidden platform. Both HFD and NPD fed mice were assessed for cognitive functions on different time points (2, 4, 6 and 8 weeks after diet feeding). We found that the mice fed with HFD performed poorly in MWM task. These mice showed higher escape latency than NPD fed mice as early as 4 weeks after diet feeding and their performance worsen over 6 to 8 weeks after diet feeding. Our results are in line with previous studies suggesting that peripheral insulin resistance caused by a HFD feeding decreased cognitive function via the disruption of neuronal insulin signaling (Craft and Watson, 2004; Craft, 2005, 2007; Pratchayasakul et al., 2011; Pipatpiboon et al., 2012).

We further investigated the extent of neuronal injury that could be associated with the cognitive deficits observed in MWM. Thus, we performed histological study to determine the effect of HFD feeding on neuronal health. We specifically selected hippocampus (Dentate gyrus and CA1 region) as it is a highly plastic structure and particularly sensitive to environmental and nutritional stressors (Mills, 2007). Moreover, the consolidation of information from short-term memory to long-term memory is carried out by hippocampus (Pearce, 2001). Although neuronal damage in some of the structures of hippocampus was observed after 4 weeks of diet feeding, however, significant neuronal damage in both DG and CA1 regions of hippocampus was evident after 6 to 8 week of HFD feeding. These structural changes found in the hippocampus may arise from peripheral insulin resistance as well as

alterations in brain insulin signaling. Thus, in our following studies to explore the molecular mechanism(s) involved in insulin resistance induced neurodegeneration, we used 8 weeks of HFD diet feeding as an animal model. Among the insulin signalling pathways, GSK3β, is one of the main downstream effectors. GSK3β phosphorylates and inhibits glycogen synthase (Rylatt et al., 1980) and thus regulates the glycogen synthesis and ultimately glucose homeostasis. Moreover, GSK-3β has been well known to play a leading role in the cascade of events initiated by insulin signalling (Hooper et al., 2008). Therefore, it seems that GSK3β might be involved in insulin resistance condition.

6.1. GSK-3β inhibitors in insulin resistance and associated cognitive decline in mice

6.1.1. GSK-3β inhibitors in insulin resistance and glucose tolerance

GSK-3β expression and activity have been found to be significantly elevated in muscle biopsies of T2DM patients (Nikoulina et al., 2001). Examination of C57B1/6J mice fed with HFD to induce obesity and T2DM, revealed elevated GSK-3β activity in epididymal fat tissue compared to control mice fed a regular chow diet (Eldar-Finkelman et al., 1997). Since GSK-3β is constitutively active in the basal state of cells, its inactivation by insulin is considered important for a normal insulin response and failure to achieve this inactivation may contribute to the pathogenesis of T2DM and in development of insulin resistance condition. We developed insulin resistance condition in mice by feeding them with HFD for 8 weeks (as standardized in our previous study) and found an increased body weight gain, elevated serum glucose, insulin, TGs, TC and LDL-cholesterol levels ($P < 0.001$). The HFD feeding also results in impaired glucose tolerance as assessed by OGTT. Further, we performed HOMA-IR, an index of insulin resistance and found that HFD fed mice showed significant elevation in HOMA-IR levels. These findings are consistent with previous reports suggesting that HFD significantly induced insulin resistance as shown by hyperinsulinemia, and increased HOMA index (Pratchayasakul et al., 2011a,b; Apaijai et al., 2012; Pipatpiboon et al., 2012). By contrast, treatment with GSK-3β inhibitors, IMX and AR-A014418, reduced body weight as compared to HFD fed mice. The reason for selecting both AR-A014418 and IMX was that both these compounds offer higher selectivity towards GSK3β in contrast to CDKs, a kinase which shares 33% amino acid identity with GSK3β or CDK5 (Bhat et al., 2003; Eldar-Finkelman and Martinez, 2011). Moreover, these compounds dose dependently lowered the serum glucose, insulin, TGs and TC levels in HFD fed mice. Further, treatment with IMX and AR-A014418 results in dose dependent improvement in glucose tolerance as

significant reduction in blood glucose was observed 0, 30, 60 and 120 min after glucose administration. The OGTT data indicated that IMX and AR-A014418 improved insulin sensitivity in the HFD group. Moreover, these mice also showed significantly reduced HOMA-IR levels as compared to HFD group. These findings indicate that HFD model used in our study induced insulin resistance condition and the GSK-3β inhibitors attenuated the insulin resistance like condition.

6.1.2 GSK-3β inhibitors and neurobehavioural changes

Numerous studies have reported up-regulation in expression as well as increased activity of GSK-3β in the frontal cortex and hippocampus of AD patients (Leroy et al., 2007; Blalock et al., 2004). Moreover, it has been suggested that over-activity of GSK-3β accounts for memory impairment, tau hyper-phosphorylation and increased Aβ production; all of which are hallmark characteristics of AD (Hooper et al., 2008). Transgenic mice overexpressing GSK-3β in CA1 and dentate gyrus showed impaired spatial memory and long-term potentiation (LTP) (Hernandez et al., 2002). These studies provide strong evidence that GSK3β might be involved in cognitive deficits associated with insulin resistance condition. As it is well known that a single behavior test in animals may not completely cover all the aspects of learning and memory, therefore, we utilized a battery of behavioural parameters (MWM, Novel object recognition (NOR) task, passive avoidance task). MWM has been widely used in rodents since its first introduction in 1984 (Morris, 1984). During MWM task, we observed a significant increase in mean escape latency in HFD group as compared to NPD fed mice. The results obtained clearly indicated cognitive impairment in HFD fed mice, which is in agreement with previous studies (Datusalia and Sharma, 2014; Pathan et al., 2008). In contrast, treatment with GSK3β inhibitors, IMX and AR-A014418 attenuated the mean escape latency in HFD mice. During the probe trial also, HFD fed mice failed to remember the precise location of the platform, spending significantly lesser time in the target quadrant. Whereas, HFD fed mice treated with GSK3β inhibitors, IMX and AR-A014418, spent significantly more time in the target quadrant indicating improved consolidation of memory. In line with our observations, some previous studies have also reported the beneficial effects of GSK3β inhibitors in APP/Presenilin-1 double transgenic mice models of during MWM task (Sereno et al., 2009; Hu et al., 2009).

Behavioral tests that evaluate the ability of recognizing a previously presented stimulus constitute the core of animal models of human amnesia (Baxter 2010). The NOR

task has become a widely used model for the investigation of memory alterations (Goulart et al. 2010; Silvers et al. 2007). Recent studies have demonstrated that HFD feeding in mice impairs the performance in NOR task (Knight et al., 2014). In line with this, we also observed that HFD feeding results in impaired performance during object recognition task. Whereas, the mice treated with GSK3β inhibitors, IMX and AR-A014418 spent more time in exploring the novel object as compared to familiar object. We next performed the passive avoidance task. This task differs from spatial tests such as the MWM based on processing of polymodal sensory information (Baarendse et al. 2008; Burwell et al. 2004; O' gren et al., 2008; McGaugh 2004). During the retention trial in passive avoidance task, it was found that the transfer latency was significantly decreased in the HFD fed group as compared with NPD fed mice. Decreased transfer latency indicates poor retention memory. Treatment with GSK3β inhibitors, IMX and AR-A014418, significantly attenuated the decrease in transfer latency in a dose dependent manner. Moreover, the changes in locomotor activity have been suggested to modulate performance in learning and memory tasks (Deshmukh et al., 2009). However, in present study, no significant difference was observed between any of the groups suggesting no effect whatsoever of HFD and GSK3β inhibitors on the locomotion activity of animals.

6.1.3 GSK-3β and Oxidative stress and Neuroinflammation

An important molecular mechanism that might be involved in insulin resistance induced neurodegeneration is an increase in ROS generation (oxidative stress) and neuroinflammation. It is interesting to note that oxidative stress itself may also be related to GSK-3β activation. For example, oxidative stress induces overactivation of GSK-3β in neuronal cells (Lee et al., 2007), while the inhibition of GSK-3β is involved in the control of oxidative stress in neuronal hippocampal cell lines (Schafer et al., 2004). With respect to the progression of T2DM and insulin resistance, continuous overnutrition leads to chronic ROS and RNS production, this promotes oxidative stress in key cells, tissues, and organs. Eventually, oxygen and nitric oxide based free radicals damage cell membranes, DNA, and protein structures, as well as modulating the activity of transcriptional factors through redox chemistry, including NF-κB, leading to chronic inflammation and cell apoptosis (Newsholme et al., 2009). The hippocampus and neocortex are among the most vulnerable parts of brain that undergo selective damage during oxidative stress conditions. Moreover, hippocampal oxidative stress is strongly linked to cognition dysfunction (de Oliveira et al., 2011; Farr et al., 2008; Stranahan et al., 2011; Evans et al., 2003). Furthermore, increased oxidative stress markers and reduced endogenous antioxidant enzyme level, such as GSH has been reported

in post-mortem AD brains (Padurariu et al., 2010; Pocernich and Butterfield, 2012). In the present study also, we found significantly increased level of oxidative stress markers such as MDA, nitrite and reduction in antioxidant enzyme, GSH level in hippocampus homogenates of HFD fed mice. Treatment with GSK3β inhibitors, IMX and AR-A014418 dose dependently attenuated MDA and nitrite levels and restored GSH level in HFD fed mice. These results are in line with previous studies indicating attenuation of oxidative stress markers as a result of GSK3β inhibition (Koh et al., 2005). Some studies have also reported that HFD fed mice showed activated microglia and astrocytes in the hippocampus and increased mRNA expression of various pro-inflammatory cytokines (Thirumangalakudi et al., 2008; Pistell et al., 2008). In line with these studies, we also found a significant increase in TNF-α level in the hippocampus of HFD fed mice as compared to NPD fed mice. However, the mice treated with IMX and AR-A014418, showed significant and dose dependent attenuation of TNF-α level. The probable mechanism might involve direct inhibition of microglial activation by GSK3β inhibitors. A recent study also suggests that GSK3β inhibitor, IMX, suppressed microglia migration and activation induced by LPS in vitro (Yuskaitis and Jope, 2009). Along with oxidative stress and inflammation, the GSK3β over-activity has also been reported to involve in AD pathology. GSK3β being a major kinase, phosphorylates tau protein and results in formation of NFTs and associated AD pathology.

6.1.4 GSK-3β inhibitors and AD pathology markers

Hyperphosphorylation of tau protein is a characteristic feature of AD pathology. In the AD brain, tau is hyperphosphorylated at more than 38 different sites, which interferes with the affinity of tau-microtubule binding (Aplin et al., 1996) and causes NFT formation. Moreover, the tau pathology in particular, is thought to result from defective insulin signalling which causes an activation of GSK3β, a predominant tau kinase. In line with this, a recent study demonstrated that HF/high cholesterol diet feeding to C57BL/6 mice for 2 months resulted in increased levels of hyperphosphorylated tau in the hippocampus and that the increased presence of phospho-tau correlated with the active form of its kinase i.e., GSK3β and a down-regulation of insulin receptor signaling as indicated by reduced levels of IRS-1 and phospho-Akt (Bhat and Thirumangalakudi, 2013). In our study also, we found that HFD feeding results in significant increase in tau hyperphosphorylation as compared to NPD fed mice. Cdk5, GSK3β and several other kinases, including the MAPK family kinases (e.g. JNK and p38-MAPK), are involved in tau hyperphosphorylation (Churcher, 2006). We therefore hypothesized that IMX and AR-A014418 might be able to attenuate tau

hyperphosphorylation observed in HFD fed mice. Interestingly, we found that treatment with these GSK3β inhibitors showed marked decrease in tau phosphorylation as compared with untreated HFD fed mice. Our results are in line with a previous study demonstrating inhibition of tau phosphorylation as a result of IMX treatment, in vitro (Leclerc et al., 2001).

As it is well known that Aβ peptides play a central role in AD pathogenesis by inducing synaptic loss (Haass and Selkoe, 2007), impairment of LTP, and memory deficits (Weldon et al., 1998), we attempted to examine whether GSK3β inhibitor treatment influences Aβ deposition. Previously, GSK3β has been reported to involve in Aβ accumulation, as aberrant activation of GSK-3β has been shown to modulate APP processing (Aplin et al., 1996; Ryder et al., 2003; Ryder et al., 2004). We focus on $A\beta_{(1-42)}$ rather than other Aβ species because this Aβ form is more prone to aggregate than $A\beta_{(1-40)}$, and the initial Aβ deposition begins with $A\beta_{(1-42)}$ but not with $A\beta_{(1-40)}$. We found that mice fed with HFD exhibited high levels of $A\beta_{(1-42)}$ as compared to NPD fed mice. In contrast, marked decrease in $A\beta_{(1-42)}$ levels was observed in hippocampus of IMX and AR-A014418 treated mice. Our results are in line with previous studies demonstrating that treatment with GSK-3β inhibitors, lithium, or NP12 or silencing of GSK-3 with hairpin RNA constructs, reduced $A\beta_{(1-42)}$ deposition in various AD mouse models (Phiel et al., 2003; Hurtado et al., 2012; Sereno et al., 2009).

To further explore the molecular mechanisms involved in insulin resistance induced cognitive deficits, we focused on the involvement of transcriptional regulators. One of the major transcription factor that may be regulated by GSK-3β is the 43 kDa phosphoprotein cyclic AMP response element binding protein (CREB). CREB is a constitutively expressed nuclear transcription factor that regulates the expression of genes involved in neuronal survival and function (Benito and Barco, 2010; Sakamoto et al., 2011). CREB is essential for the formation and retention of memory in several species (Impey et al., 1998; Frank et al., 1994). Phosphorylation of CREB at serine-133 is required for recruitment of the coactivator CREB-binding protein (CBP) and resulting activation of transcriptional activity (Gonzalez and Montminy, 1989). Moreover, CREB phosphorylation at serine-133 creates a consensus site for phosphorylation by GSK3β at serine-129 (Fiol et al., 1994). Thus, inhibition of GSK3β can facilitate CREB activity (Grimes and Jope, 2001). It has been demonstrated that GSK3β is an inhibitory regulator of CREB. Further, the increased kinase activity of GSK-3β is reported to inhibit CREB-CBP complex formation which is essential for DNA binding of CREB which can be facilitated by lithium (Grimes and Jope, 2001). In the present study, we

found significant reduction in CREB level in brain homogenates of HFD fed mice as compared with NPD fed mice. However, pharmacological inhibition of GSK-3β by IMX and AR-A014418 was found to ameliorate the CREB level. As stated earlier the expression of neurotrophic factor, BDNF is regulated by multiple signaling pathways, including CREB (Shieh et al., 1998). With CREB being regulated by GSK3β, and CREB regulating BDNF, it is intriguing that links have been established between BDNF and GSK3β. Further, it has been proposed that BDNF activation of TrkB (tyrosine kinase) receptors is responsible for activation of the PI3K/Akt pathway followed by GSK3β inhibition (Phillips et al., 1991). The binding of BDNF to TrkB receptor causes many intracellular cascades to be activated, which regulate neuronal development, plasticity and long-term potentiation (Fig.6.1).

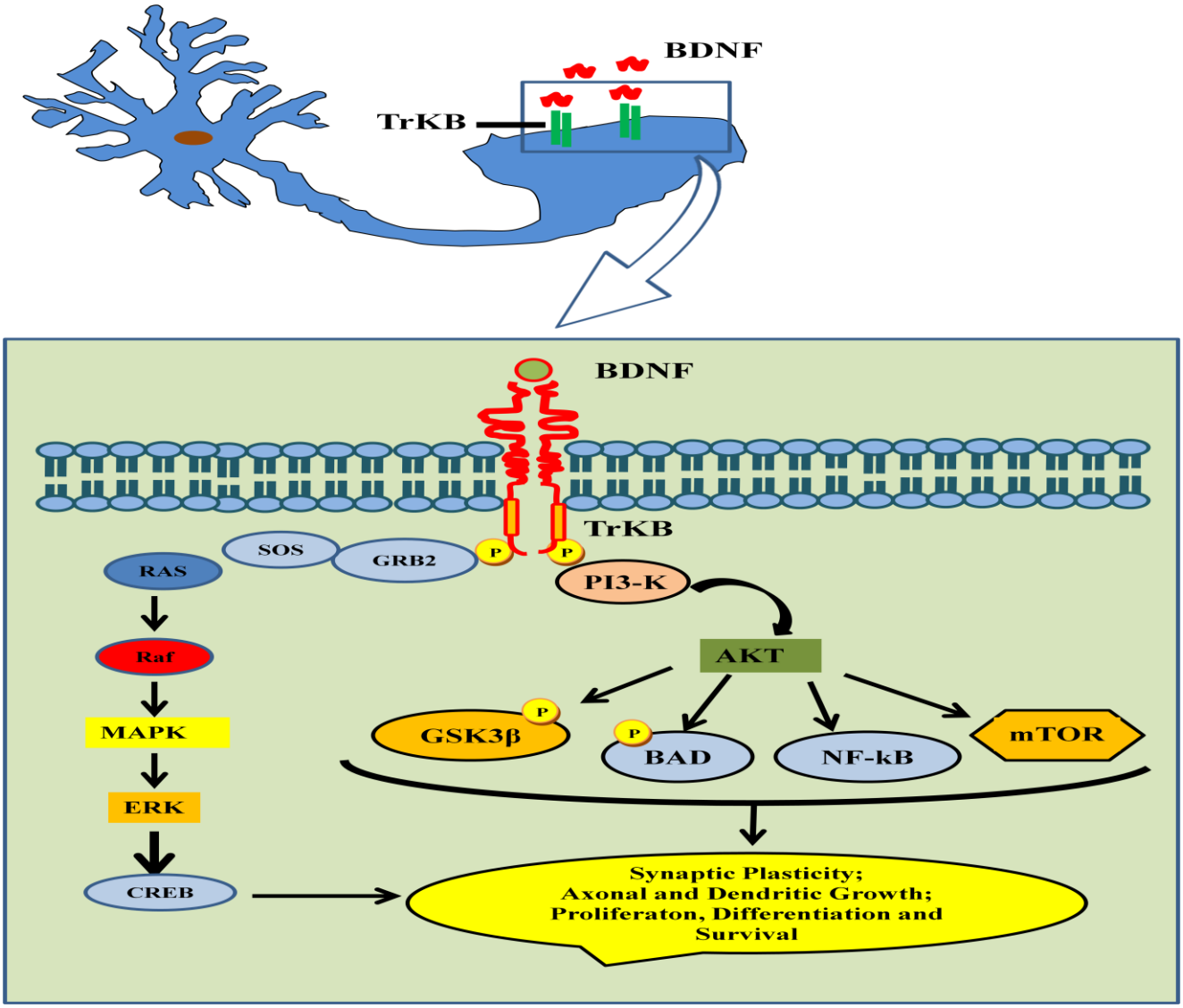

Fig. 6.1 Mechanistic diagram for CREB/BDNF based synaptic plasticity and neuronal survival

Moreover, treatment with GSK3β inhibitors, increased BDNF protein levels in rat brain (Hashimoto et al., 2002; Jacobsen and Mork, 2004; Fukumoto et al., 2001). Although mostly studied for its neuroprotective functions, BDNF administration has also shown beneficial effects on glucose homeostasis and improves insulin resistance in *db/db* mice (Ono et al., 1997; Tonra et al., 1999; Nakagawa et al., 2000; Cotman, 2005). Moreover, the association between GSK3β and BDNF has been well reported in AD such as, reduction in BDNF level has been reported in hippocampal and cortical tissues of AD patients and is associated with increased GSK3β activity (Phillips et al., 1991; Patapoutian and Reichardt, 2001). In the present study, we found reduced BDNF level in HFD fed mice as compared with NPD fed mice. Treatment with GSK3β inhibitors, IMX and AR-A014418, dose dependently ameliorated the HFD induced decrease in BDNF level.

6.1.5 GSK-3β inhibitors and hippocampus neurons

Along with the behavioral and biochemical abnormalities, the HFD feeding also results in significant morphological changes in DG and CA1 region of hippocampus neurons. The histology sections of hippocampus in HFD fed mice showed significant neuronal degeneration in CA1 and DG regions as indicated by increased percentage of damaged neurons in these regions. Decreased neuronal density and increased pyknotic neurons were observed in DG and CA1 regions of HFD mice. As, insulin is considered as a crucial trophic factor for nervous system development and maintenance of neurogenic niches, the impairment of insulin signalling might affects neuronal integrity. Many brain structures, such as the hippocampus, are extremely sensitive and responsive to changes in glucose homeostasis (Pamidi and Satheesha, 2012; Ramos-Rodriguez et al., 2014). Thus, the neuronal damage induced by HFD feeding could be attributed to impaired insulin signalling as a result of insulin resistance. However, treatment with GSK3β inhibitors, IMX and AR-A014418 significantly attenuated the percentage of damaged neurons in DG and CA1 regions of HFD fed mice. This neuroprotective action of GSK3β inhibitors could be a result of increased CREB based BDNF expression.

Based on the aforementioned findings, it can be concluded that GSK3β inhibitors significantly and dose dependently improved the HFD induced cognitive deficit. The observed beneficial effects of IMX and AR-A014418 might be related to their actions on improved glucose tolerance, combating insulin resistance or oxidative stress. Moreover, these neuroprotective and cognitive enhancing actions of GSK3β inhibitors could also be attributed

to increased CREB based transcription and elevated BDNF levels. The possible mechanisms have been illustrated in Fig. 6.2. Thus, it would be safe to conclude that the GSK3β inhibition would be therapeutic in cognitive impairment associated with T2DM and insulin resistance. Despite the long-standing acceptance that GSK-3β plays a key role in promoting neuronal death, little is known about what its substrates are in the context of neurodegeneration. Recent studies have provided significant evidence that GSK3β is directly involved in phosphorylation of HDACs. Thus, to further explore the substrates modulated by GSK3β, we examine the role of HDACs in insulin resistance induced neurodegeneration using HDAC inhibitors.

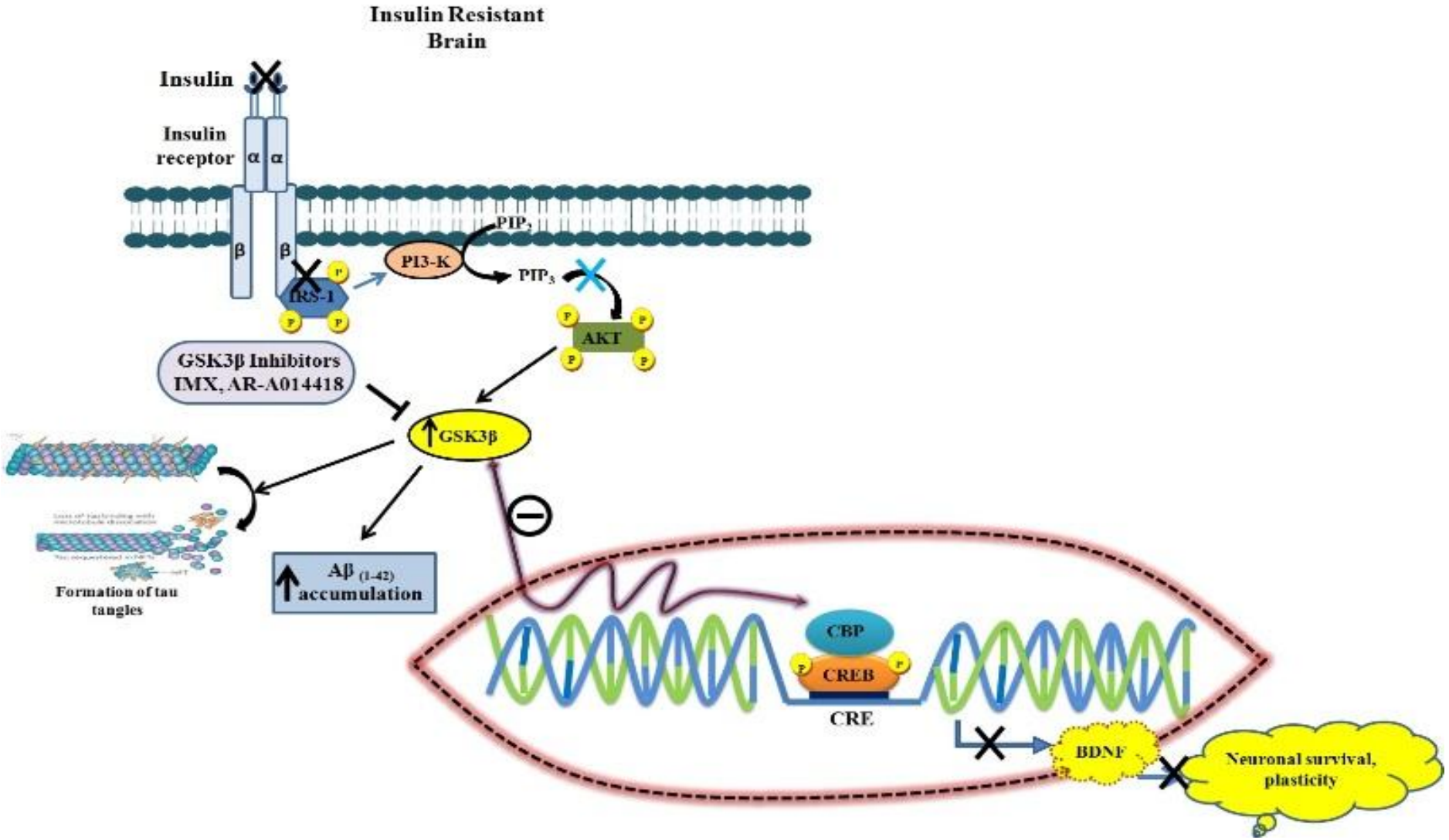

Fig. 6.2 Possible Mechanism of GSK3β inhibitors in ameliorating insulin resistance induced neuronal damage and AD pathology

6.2. HDAC inhibitors in insulin resistance and associated cognitive decline in mice

6.2.1 HDAC inhibitors in insulin resistance and glucose tolerance

During recent years, HDACs have emerged as an important molecular target involved in insulin resistance (Lundh et al., 2015; Henagan et al., 2015; Funato et al., 2011). It has been observed that HDACs play an important role in regulation of glucose and fatty acid metabolism (Jianping, 2013). HDAC inhibitors have been found to reverse insulin resistance and obesity related complications in animal models (Henagan et al., 2015; Gao et al., 2009). Recently, the expression of various HDAC isoforms was found to be elevated in HFD fed mice, which is commonly used model for insulin resistance (Funato et al., 2011). Moreover, the involvement of different classes of HDACs has been studied in insulin resistance and T2DM conditions. It has been demonstrated that insulin receptor activation in peripheral tissues is coupled to signal transduction pathways via the IRS family of adaptor molecules. IRS-1 binds to HDAC2 in liver cells from the *ob*/*ob* mouse, a model of insulin resistance **(**Kaiser et al., 2004). This results in decreased acetylation of IRS-1 and reduced insulin receptor–mediated tyrosine phosphorylation of IRS-1. Consequently, inhibition of HDAC2 with TSA was found to partially restored insulin signaling (Kaiser et al., 2004). Similar to HDAC2, the role of HDAC3 isoform has also been explored in insulin resistance and T2DM (Sun et al., 2012; Zeng et al., 2014). Moreover, in another study, the expression of HDAC9 was also found to be increased as a result of HFD feeding in mice and HDAC9 gene deletion was found to improve the metabolic homeostasis (Chatterjee et al., 2014). These reports clearly provide the evidence that HFD feeding disturbs the homeostasis between HDACs and HATs and further support the rationale of using HDAC inhibitors in insulin resistance conditions. Thus, it seems that HDACs might be involved in insulin resistance and associated neurodegeneration. Therefore, in this study, we evaluated the effect of HDAC inhibitors on insulin resistance induced cognitive deficits.

We used broad spectrum (pan) HDAC inhibitors namely, SAHA and Sodium butyrate. Both of these HDAC inhibitors have been approved by FDA for different interventions. Although widely used for their cytotoxic potential in cancer therapy, the HDAC inhibitors exhibit remarkable property of having cytotoxic selectivity for transformed cells (Bolden et al., 2006). SAHA is a broad-spectrum (class I and II) inhibitor of HDACs and is being used to treat T-cell lymphoma (Richon, 2006). Moreover, SAHA is considered as relatively non-toxic to normal cells (Iyer et al., 2010) and was therefore an appropriate

choice for our study. On the other hand, sodium butyrate inhibits the action of classes I and IIa HDACs. It has been used for several inflammatory bowel conditions, including ulcerative colitis and diversion colitis and found to be relatively non-toxic.

As standardized earlier, we found that the HFD feeding results in increased body weight, hyperglycemia, hyperinsulinemia, impaired glucose tolerance, hypertriglyceridemia, hypercholesterolemia. Treatment with HDAC inhibitors, SAHA and Sodium butyrate significantly and dose dependently attenuated the elevated glucose, triglyceride, cholesterol and restored HDL-cholesterol levels in HFD fed mice. Thus, suggesting the potential of HDAC inhibitors in improving glucose tolerance and improving insulin senstivity. Similar results were obtained by Galmozzi et al. 2013, where they reported improved glucose tolerance along with improved insulin sensitivity in *db/db* diabetic mice model as a result of SAHA administration (Galmozzi et al., 2013). These beneficial effects of HDAC inhibitors might be associated with the increased acetylation of IRS-1 and hence improved insulin receptor–mediated tyrosine phosphorylation of IRS-1.

6.2.2 HDAC inhibitors and neurobehavioural changes

Epigenetic changes, such as histone acetylation regulate chromatin remodeling, are therefore important contributors to the gene regulation involved in neural development and plasticity. HDACs remove acetyl groups, thereby returning the chromatin to its condensed and transcriptionally silent state. Inhibition of HDACs changes the expression of approximately 5–10% of transcribed genes (Scott et al., 2006), suggesting that neuronal plasticity may be improved by preserving histone acetylation following behavioral training. Increased HDAC activity was also correlated with instances of neuronal cell death. In their recent study, Gan and colleagues found that levels of HDAC transcript were trending upward in the dorsal hippocampus and significantly increased in the ventral hippocampus of HFD-fed rats (Gan et al., 2015). Consistent with this, we observed that during the MWM task, the HFD fed mice took significantly longer time to find the hidden platform as compared to NPD fed mice. During the probe trial also, the HFD fed mice spent significantly lesser time in the target quadrant as compared to mice fed with NPD. Treatment with HDAC inhibitors, SAHA (50mg/kg) and sodium butyrate (300 and 600 mg/kg), attenuates the HFD induced cognitive deficit in mice. Moreover, the mice treated with SAHA and sodium butyrate spent significantly higher time in the target quadrant during the probe trial, indicating improved retention of memory.

Similarly, during the retention trial in passive avoidance task, it was observed that the mice fed with HFD tend to enter the dark compartment after few seconds of trial initiation, showing poorer retention memory. In contrast, the mice treated with HDAC inhibitors, SAHA and sodium butyrate, showed dose dependent improvement in retention memory. Moreover, similar results were observed in object recognition task, where the mice treated with HDAC inhibitors spent more time in exploring the novel object as compared to familiar object. Our results are in line with previous studies demonstrating that pan HDAC inhibitors increase LTP and rescue memory deficits in both aged and gene-mutant mice (Peleg et al., 2010; Francis et al., 2009; Morris et al., 2013). However, ours is the first study showing the importance of HDAC inhibition in insulin resistance mediated cognitive decline. The beneficial effects observed in behavioural parameters encourage us to explore the molecular mechanisms that might be underlying these effects. Oxidative stress and neuroinflammation are well characterized to be an underlying mediator of neurodegeneration that is common to CNS disease and injury (Bossy-Wetzel et al., 2004). Thus, we next explored the role of HDAC inhibitors in alleviating oxidative stress and neuroinflammatory markers during insulin resistance condition.

6.2.3 HDAC inhibitors in oxidative stress and neuroinflammation

Previously, it has been demonstrated that the pan-HDAC inhibitors, TSA, Scriptaid and sodium buyrate, can protect against oxidative stress induced death in neurons, in vitro and in permanent and transient focal brain ischemia in rodents (Langley et al., 2008). Furthermore, Nullscript, a structural analog of Scriptaid that lacks HDAC inhibitory activity, showed no protection, suggesting that protection depends on HDAC inhibition and not an off-target effect of the hydroxamic acid moiety. These experiments support a well-established body of literature that targeting HDAC activity might be a valuable strategy for protecting neurons in the CNS (Kazantsev and Thompson, 2008; Langley et al., 2008). In the present study, increased level of oxidative stress markers such as MDA, nitrite and reduction in antioxidant enzyme, GSH level was reported in hippocampus homogenates of HFD fed mice. Treatment with HDAC inhibitors, SAHA and sodium butyrate dose dependently attenuated MDA and nitrite levels and restored GSH level in HFD fed mice.

As mentioned previously that HFD feeding impact CNS homeostasis and induce an inflammatory response. In the present study also, we found that HFD feeding results in significant elevation of TNF-α level in the hippocampus homogenate of mice. However, both

SAHA and sodium butyrate significantly and dose dependently alleviate the TNF- α levels as compared with alone HFD fed mice. The results obtained are in line with previous studies indicating the ability of HDAC inhibitors to reduce cytokines production and mediate their neuroprotective effects in both *in vitro* and *in vivo* models (Choi et al., 2008; Fleiss et al., 2012). Specifically, SAHA has been shown to down-regulate the cellular production of various inflammatory mediators, which are all potentially neurotoxic (Leoni et al., 2002; Mishra et al., 2003). To further explore the molecular mechanisms and effects of HDACs on insulin resistance induced neurodegeneration, we observed the level of AD pathology markers: $A\beta_{(1-42)}$ and p-tau level.

6.2.4. HDAC inhibitors and AD pathology markers

We found that HFD feeding results in significant increased levels of phosphorylated tau and $A\beta_{(1-42)}$ levels as compared to NPD fed animals. However, treatment with HDAC inhibitors, SAHA and sodium butyrate significantly attenuated the level of ptau and $A\beta_{(1-42)}$ in HFD fed mice. Although the exact mechanism for this observation is still not clear, however it has been previously reported that decreases in HDAC6 activity or expression promote tau clearance (Cook et al., 2012), while HDAC6 mutations rescued tau-induced microtubule defects in a Drosophila model of tau pathology (Xiong et al., 2013). As it is well recognized that phosphorylation of tau results in dissociation from tubulin and decreased stabilization of microtubules (Mandelkow and Mandelkow, 2012), we hypothesized that stabilizing microtubules by acetylation using HDAC inhibitors (SAHA, sodium butyrate) might be responsible to counteract the increased ptau levels in the HFD fed mice. Moreover, previous studies have also shown that HDAC inhibitors decreased $A\beta_{(1-42)}$ levels and increased levels of sAPPα, the cleavage product of α-secretase, in primary cortical neurons (Kozikowski et al., 2009). Our results are in line with previous studies demonstrating that administration of HDAC inhibitors results in reduced levels of Aβ in transgenic mouse models of AD (Ricobaraza et al., 2011, 2012; Qing et al., 2008; Govindarajan et al., 2011).

Zhang and colleagues, found that histone H3 acetylation, in particular, H3 K18/K23 acetylation was significantly reduced in temporal lobe of AD patients as compared to control subjects (Zhang et al., 2012). Similar findings were observed in mouse model of AD (Francis et al., 2009; Govindarajan et al., 2011). It has been demonstrated that either reduced HAT activity or increased HDAC activity is associated with impaired memory function in both mice and human AD patients (Wood et al., 2006; Barrett et al., 2011; Ding et al., 2008; Graff

et al., 2012). Previous studies also suggest that HFD feeding in rats or mice results in significant increase of HDAC activity along with reduction of histone acetylation in different brain regions (Gan et al., 2015; Funato et al., 2011). In line with these, we also observed that HFD feeding results in significant reduction of global histone H3 acetylation. However, treatment with SAHA (50 mg/kg) and sodium butyrate (300 mg/kg and 600 mg/kg) results in significant increase in global histone H3 acetylation. HDACs could potentially regulate CREB-dependent transcription via several mechanisms. HDACs could reverse CBP-catalyzed histone acetylation events that mediate transcriptional activation (Valor et al., 2011). Indeed, an HDAC inhibitor failed to enhance cognition in mice with a focal depletion of CBP in the hippocampus (Barrett et al., 2011). Second, HDACs could counteract CBP and the related lysine acetyltransfrease p300 activation by auto-acetylation (Thompson et al., 2004). Also, HDAC-1 and HDAC-8 protein phosphatise-1 complexes have been shown to mediate CREB dephosphorylation (Canettieri et al., 2003; Gao et al., 2009). Also, histone acetylation has been reported to play an important role in BDNF mediated synaptic plasticity (Calfa et al. 2012; Koppel and Timmusk, 2013). Acetylation of histones in BDNF promoters is engaged in learning and memory formation (Bousiges et al., 2013; Bredy et al., 2007; Intlekofer et al., 2013), whereas deacetylation of histone by HDACs negatively regulates BDNF transcription (Guan et al., 2009). In the present study, HFD feeding results in significant reduction of CREB and BDNF level as compared to NPD fed mice. However, treatment with HDAC inhibitors, SAHA and sodium butyrate significantly ameliorated the CREB and BDNF levels (Fig. 6.3). In line with our results, various studies have suggested that HFD feeding points to a decrease in *bdnf* transcription (Wu et al., 2003; Kanoski et al., 2007; Stranahan et al., 2008) and HDAC inhibitors stimulate gene transcription for BDNF (Bredy et al., 2007; Wu et al., 2008; Ishimaru et al., 2010; Boulle et al., 2012; Koppel and Timmusk, 2013; Koppel and Timmusk, 2013; Kim et al., 2009).

6.2.5 HDAC inhibitors and hippocampus neurons

To further confirm the damaging effect of HFD on hippocampal neurons, we performed H and E staining of DG and CA1 regions. The H&E stained sections clearly shows that HFD results in neuronal death in DG and CA1 regions, which is further evidenced by the increased percentage of damaged neurons in these regions. The HFD induced neuronal damage might be associated with the reduced histone acetylation, reduced CREB based BDNF signalling support. In contrast, SAHA and sodium butyrate treated mice showed significant attenuation of neuronal damage as reduced percentage of damaged neurons was

observed in DG and CA1 neurons. The beneficial effects observed might be associated with improved histone H3 acetylation as well as increased BDNF based neuroprotection. Moreover, DNA fragmentation study reveals increased apoptotic neuronal death in hippocampus regions of HFD fed mice as compared to NPD fed mice. However, SAHA administration results in significant amelioration of apoptotic cell death in DG and CA1 regions of hippocampus of HFD fed mice.

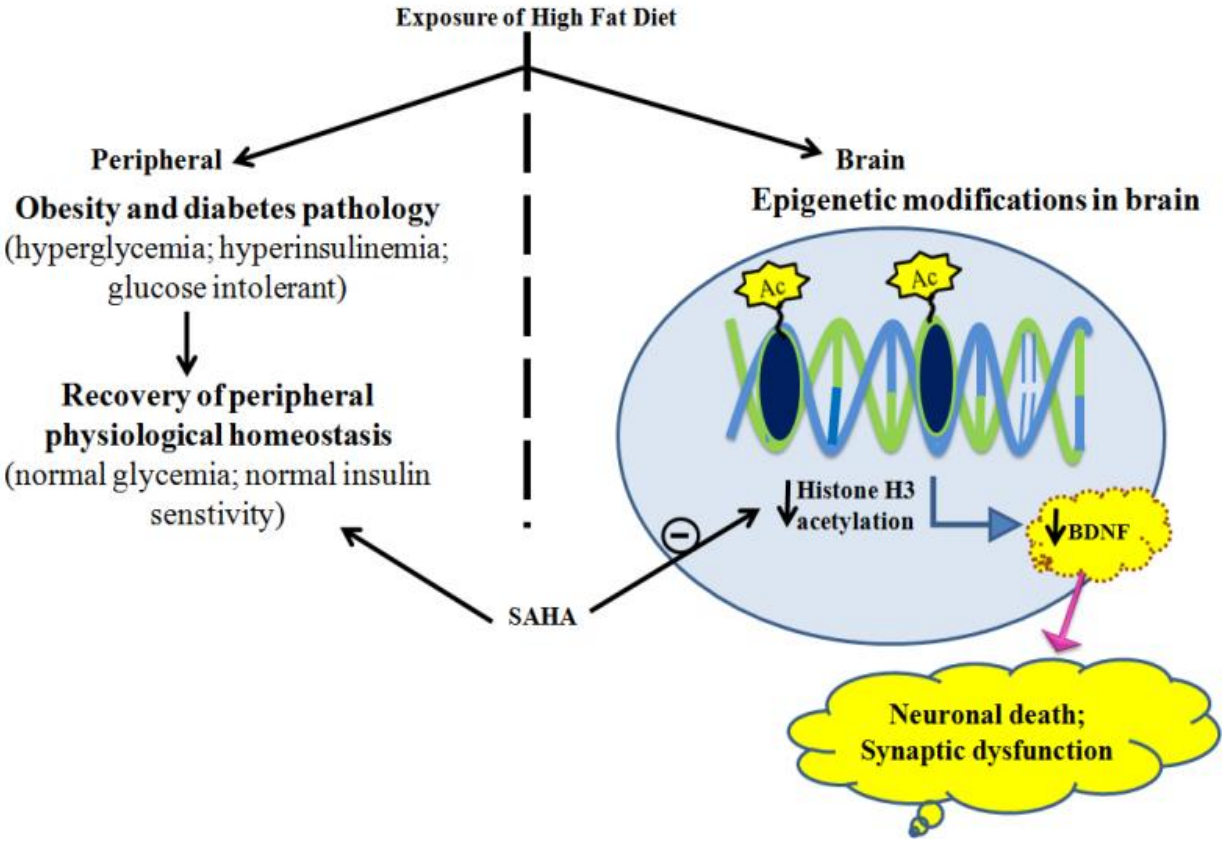

Fig. 6.3 Mechanistic representation of mechanism of HDAC inhibitors in HFD induced cognitive deficits and neuronal death

Taken together, these results data strongly support the idea that increasing histone acetylation via HDAC inhibitors might be a suitable therapeutic strategy to treat memory impairment in insulin resistance condition. The observed beneficial effects of HDAC inhibitors is likely to be mediated, at least in part, by elevated acetylation of histone H3, which concurrently activates transcriptional machinery (CREB levels) and ultimately elevated levels of neurotrophic factor, BDNF. In fact, the use of HDAC inhibitors is tempting because some of the compounds have already been approved for treatment in humans, although for cancer and not AD. However, the toxicity associated with long term use of HDAC inhibitors has limited the clinical data available (Minucci and Pelicci, 2006; Karagiannis and El-Osta, 2007). In order to reduce side effects while maintaining benefits, one strategy would be to develop isoform-selective HDAC inhibitors. Moreover, since the side effects reported for HDAC inhibitors in humans are dose dependent, the use of lower doses of pan-HDAC inhibitors to reduce their toxicity could represent another solution. Thus, we next examine the effect of low dose of HDAC inhibitors in combination with GSK-3β inhibitor in insulin resistance induced cognitive deficit and neurodegeneration. For this purpose, we selected Indirubin-3'-monoxime as GSK-3β inhibitor and SAHA as HDAC inhibitor, respectively.

6.3. Effects of low dose combination of GSK-3β and HDAC inhibitors on insulin resistance induced cognitive deficits and AD like pathology in HFD fed mice

Evidence is particularly strong that GSK-3β contributes to the regulation of histone modifications that play a central role in epigenetics. GSK-3β can directly phosphorylate histone 1.5 (Happel et al., 2009) and promotes histone 3 phosphorylation, although the mechanism was not identified (Gupta et al., 2014). GSK-3β has also been reported to phosphorylate HDAC3, which promotes its toxic activity. Moreover. Inhibition of GSK3β either pharmacologically or caused by expressing a dominant-negative form of the kinase protects against HDAC3-mediated neurotoxicity (Bardai and D'Mello, 2011). Despite the long-standing acceptance that GSK-3β plays a key role in promoting neuronal death, little is known about what its substrates are in the context of neurodegeneration. It has been demonstrated that HDAC3 is directly phosphorylated by GSK3β, suggesting that the neurodegeneration promoting effect of GSK-3β could be mediated through the phosphorylation of HDAC3. An obvious possibility is that GSK3β-mediated phosphorylation stimulates the deacetylase activity of HDAC3, resulting in the deacetylation of specific proteins that regulate neuronal death (Bardai and D'Mello, 2011).

Among other HDACs, GSK-3β has also been reported to phosphorylate HDAC4 (Cernotta et al., 2011). Indirect evidence suggests that GSK-3β may also phosphorylate HDAC6 to regulate its activity (Chen et al., 2010). Conversely, several HDAC inhibitors have been reported to increase the inhibitory serine-phosphorylation of GSK-3β (Wang et al., 2016; Aubry et al., 2009; De Sarno et al., 2002; Kozlovsky et al., 2006; Lamarre and Desrosiers, 2008). These reports suggest a crosstalk between GSK-3β and HDACs. Therefore in this study, we explored the potential of combination of GSK-3β inhibitor, IMX and HDAC inhibitor, SAHA in insulin resistance induced cognitive decline and AD like pathology. This study was conducted by keeping in mind various aspects related with use of HDAC inhibitors. First, despite the history of safe clinical use of broad spectrum HDAC inhibitors, including SAHA, long-term treatment might be associated with dose-dependent side effects in patients (Kwon et al., 2006). Thus, using low doses of these drugs has the potential advantage of reducing side effects. Second, the complexity of pathogenesis in neurodegenerative conditions may require a combination of drugs that target different cell survival pathways. In our previous studies both GSK-3β and HDAC inhibitors alone have shown considerable beneficial effects in neurodegenerative condition associated with insulin resistance. Therefore, in this study we have used the combination of these compounds.

We found that low doses of IMX or SAHA alone were ineffective in reducing insulin resistance condition. In contrast, combined treatment of the same doses of these 2 drugs had significant effect on improving insulin resistance condition in HFD fed mice. Similarly during the behavioural tasks, we found that low doses of IMX or SAHA alone were ineffective in ameliorating HFD induced cognitive deficits. Nevertheless, combined treatment had more profound effects and reduced the mean escape latency during MWM trials and also ameliorates the transfer latency in passive avoidance task. Our results are in line previous studies demonstrating that combined treatment with GSK-3β inhibitors and HDAC inhibitors improves behavioral outcomes in transgenic mouse models of HD (Chiu et al., 2011). It is interesting to note that we found similar beneficial effects in various biochemical parameters as well. We found that IMX or SAHA alone were not effective in ameliorating oxidative stress and neuroinflammation associated with insulin resistance condition. However, combined treatment with these drugs results in significant attenuation of oxidative stress markers (MDA and nitrite), pro-inflammatory cytokine (TNF-α) along with amelioration of antioxidant, GSH levels in HFD fed mice. With regard to AD markers, a reduction in tau phosphorylation and $A\beta_{(1-42)}$ levels were observed in HFD fed mice that received the combination treatment as compared to either drug alone treated HFD mice (Fig.6.4).

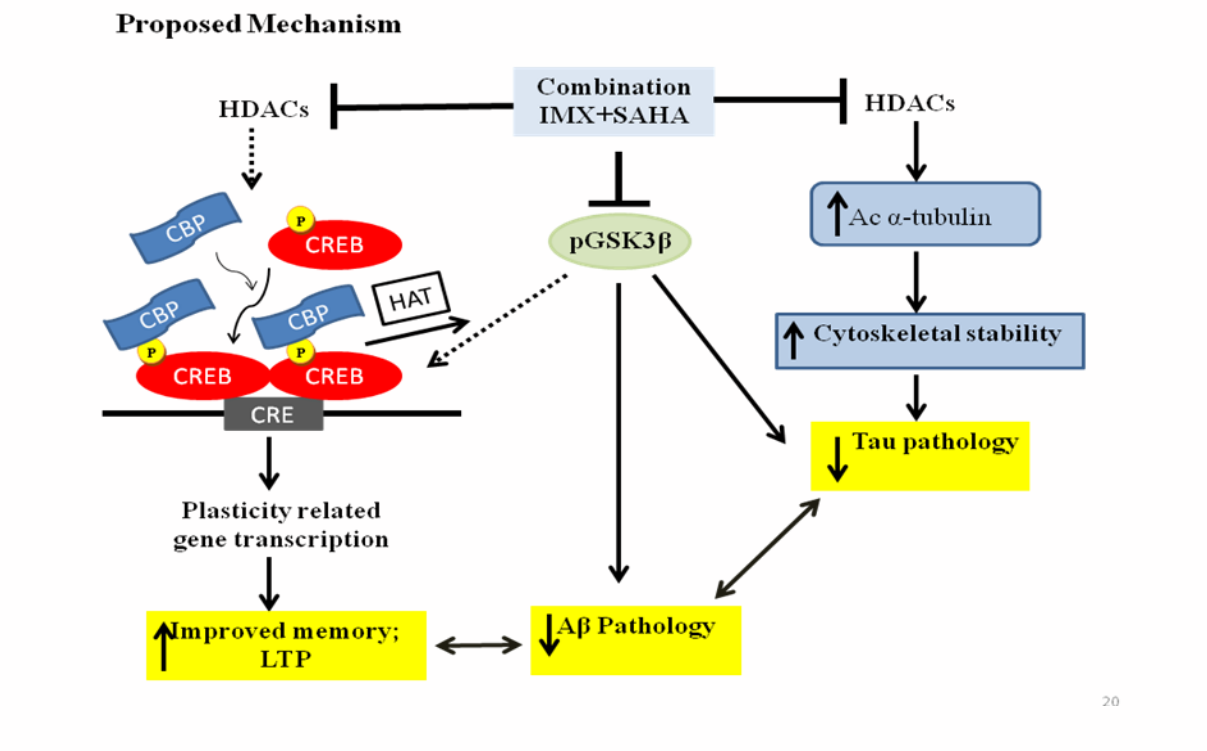

Fig.6.4. Possible mechanism for combined treatment of IMX and SAHA
Note LTP: Long term Potentiation; **Ac:** Acetylation **Aβ:** Amyloid β; **HDACs:** Histone deacetylases; **IMX:** Indirubin-3'-monoxime; **SAHA:** Suberoylanilide hydroxamic acid

The increased GSK-3β inhibition as a result of combined treatment might be involved in reduction of tau phosphorylation in this study. Also, SAHA has been reported to increase α-tubulin acetylation, possibly one of the mechanisms involved in the amelioration of the tau pathology (Ding et al., 2008; Xiong et al., 2013). Evidence is accumulating that α-tubulin acetylation plays a critical role in the clearance of misfolded and aggregated proteins, since it has been shown to influence aggresome formation as a means of cell protection (Boyault et al., 2007a,b). Thus, the inhibitory effect of SAHA on HDAC6 is also likely to be involved in the amelioration of Aβ pathology observed with the combination therapy (Sung et al., 2013; Zhang et al., 2014).

Another interesting finding of this study is the significant increase in histone H3 acetylation as a result of combined treatment with IMX and SAHA as compared to HFD fed mice or either drug alone treated mice. A previous study also found that combined treatment with GSK-3β and HDAC inhibitors results in synergistic increase in histone H3 acetylation and hence neuroprotective effects (Leng et al., 2008). Chromatin remodelling due to changes in histone acetylation induces the transcription of genes that encode proteins, neurotrophic factor (such as BDNF), which are involved in the growth of new synapses and the increase in synaptic strength (Guan et al., 2009; Kazantsev and Thompson, 2008). As discussed earlier, the enhancement of hippocampus-dependent memories by HDAC inhibitors required CREB and its interaction with CBP (Vecsey et al., 2007). Indeed, a novel HDAC inhibitor, crebinostat, enhances memory in mice by facilitating CREB-dependent transcription (Fass et al., 2013). Here, we demonstrate a synergistic effect of SAHA and IMX in the induction of the epigenetic response (increased histone H3 acetylation levels), suggesting that both the pathways affected by these inhibitors may interact at some point. As discussed earlier, GSK-3β inhibitors also produce CREB activation. Altogether, enhanced CREB based BDNF activity could be responsible for restoring cognitive decline and enhancing memory, as observed when the combination of SAHA and IMX was administered in HFD induced cognitive deficit mice.

In summary, the concomitant inhibition of HDAC and GSK-3β shown in this study may reverse insulin resistance induced AD like pathology through different mechanism of action, some of which remain to be explored. Our findings provide evidence that this combination could putatively be used to treat insulin resistance induced cognitive decline and

AD, with the potential advantage of reducing dose dependent side effects of these compounds.

6.4. Effect of low dose combination of Lithium chloride and Valproate on ICV-STZ induced cognitive decline and AD pathology in rats

In addition to HFD induced insulin resistance model, we also explored the potential of low dose combination of GSK-3β inhibitor and HDAC inhibitor in brain specific insulin resistance model induced by Intracerebroventricular Streptozotocin (ICV-STZ) administration in rats. In this study we used, Lithium chloride (LiCl) and Valproic acid (VPA), two well known mood stabilizers that have been reported to act via inhibition of GSK-3β and HDAC, respectively (Gottlicher et al., 2001; Klein and Melton, 1996; Phiel et al., 2001; Ryves et al., 2005). Although both these drugs are non-selective inhibitors of GSK-3β and HDACs, respectively, but these were selected because these drugs are clinically safe and used for mood disorders. LiCl in combination with other mood stabilizers such as VPA has been used to enhance the therapeutic benefits or to treat bipolar patients resistant to single drug therapy. These findings raise the possibility that LiCl and VPA co-treatment may produce stronger or synergistic effects against neuronal cell death in neurodegenerative conditions. Although LiCl and VPA have been tested previously in various models of AD, this is the first combinatorial approach using these mood stabilizers to study their beneficial effects in low doses in ICV-STZ rats. The ICV-STZ administration has been widely used animal model which mimics several hallmarks of sAD (Deshmukh et al., 2009; Khan et al., 2012). AD has been recognized as an insulin-resistant brain state (de la Monte and Wands, 2005) and ICV-STZ administration has been demonstrated to mimic the insulin resistant brain state (Plaschke et al., 2010).

We demonstrated that low dose combination of LiCl and VPA produced synergistic and more consistent neuroprotection against ICV-STZ induced neurotoxicity in rats. ICV-STZ administration in rats exhibit behavioral and biochemical abnormalities similar to those observed in human AD patients (Deshmukh et al., 2009; Khan et al., 2012). In the present study, ICV-STZ administration results in significant deficits in spatial learning and memory. In addition, STZ administration results in increased levels of oxidative-nitrosative stress markers in rat brain homogenates. These observations are in line with earlier reports indicating cognitive deficit and elevated oxidative stress markers after STZ administration (Deshmukh et al., 2009; Khan et al., 2012)

During MWM trials, all the experimental groups showed gradual decrease in escape latency. However, ICV-STZ injected rats took significantly longer time to find the hidden platform as compared to vehicle treated group. In the probe trial also, the ICV-STZ injected rats spent significantly less time in the target quadrant as compared to vehicle treated rats. Similar patterns of cognitive deficit were observed in passive avoidance task wherein, the ICV-STZ injected rats showed decrease in retention latency as compared with vehicle treated rats. Conversely, the pharmacological inhibition of GSK3β and HDAC by LiCl and VPA respectively, attenuated STZ induced cognitive deficit in MWM. Moreover, the rats receiving combination of LiCl and VPA showed more consistent improvement in MWM performance as compared to treatment with either drug alone. Chronic treatment of ICV-STZ infused rats with LiCl alone produce significant improvement in passive avoidance and probe trial tasks. Whereas, VPA alone treatment failed to produce any significant improvement in rats during these behavioural tasks. However, VPA when administered concurrently with LiCl results in higher percentage of time spent in target quadrant in probe trial and increased retention latency in passive avoidance task as compared with either drug alone. Thus, indicating the synergistic potential of these two drugs when administered together. The changes in locomotor activity have been suggested to modulate the learning and memory in passive avoidance and MWM paradigms (Deshmukh et al., 2009; Kumar et al., 2015). However, in the present study, no significant difference in locomotion was observed in any of the experimental groups when assessed by actophotometer. Thus, it rules out any interference in the change of locomotor activity on performance in memory tests by any of the test drugs.

Acetylcholine is the foremost neurotransmitter that plays a key role in learning and memory formation (Miranda et al., 2003). Acetylcholinesterase is the enzyme that hydrolyses ACh in to choline and acetate. Increased levels of AChE have been demonstrated around Aβ - plaques in AD (Mesulam and Moran, 1987) and it has been proposed that AChE may play a role in Aβ- fibrillogenesis (Rees et al., 2003). In the present study, ICV-STZ administration results in increased AChE activity, which is in accordance with earlier studies (Aggarwal et al., 2009; Sharma et al., 2012). Although LiCl partially attenuated AChE activity, however, VPA failed to reduce the elevated level of AChE activity in ICV-STZ treated rats. In contrast, co-treatment of LiCl and VPA significantly attenuated ICV-STZ induced elevation in AChE activity as compared with either drug alone treated rats.

The role of oxidative stress has been well reported in dementia and AD (Mangialasche et al., 2009; Padurariu et al., 2010). In the present study, ICV-STZ administration in rats results in increased levels of oxidative-nitrosative stress markers

(MDA, nitrite) and decreased antioxidant enzyme, GSH level. Our results are in line with previous studies, suggesting the generation of ROS and oxidative stress after ICV-STZ administration (Rai et al., 2012). However, combination of low doses of these compounds attenuated the STZ-induced oxidative-nitrosative burden. Previous studies have also demonstrated the antioxidant potential of LiCl and VPA but at relatively higher doses (Shao et al., 2005; Frey et al., 2006; Cui et al., 2007).

To further explore the molecular mechanisms we assessed the level of GSK3β and histone acetylation in brain homogenates of these animals. We found that ICV-STZ administration results in elevated GSK3β level and reduced histone H3 acetylation level in brain homogenates of these animals. Combined treatment with LiCl and VPA significantly attenuated the GSK-3β level and increased the histone acetylation levels in ICV-STZ treated rats. Previously, VPA has been well reported to enhance the histone H3 acetylation level when administered alone or in combination with LiCl (Chiu et al., 2011; Leng et al., 2008). We also observed significant increase in AD pathology markers, i.e. $A\beta_{(1-42)}$ levels and hyperphosphorylated tau level in brain homogenates of ICV-STZ infused rats as compared to vehicle treated rats. Our results are in line with recent studies that also demonstrated ICV-STZ administration resulted in a significant increase in $A\beta_{(1-42)}$ levels (Chen et al., 2014; Plaschke et al., 2010; Halawany et al., 2017) and hyperphosphorylated tau levels in brain homogenates of rats and mice (Correia et al., 2013; Plaschke et al., 2010). In contrast, treatment with combination of LiCl and VPA resulted in signifcant attenuation of $A\beta_{(1-42)}$ levels and ptau level as compared to ICV-STZ and either drug alone treated rats.

Both GSK-3β and HDAC inhibition has been demonstrated to upregulate the expression of various neuroprotective and/or neurotrophic factors such as heat shock protein-70 (Ren et al., 2004) and BDNF (Chiu et al., 2011). Also, ICV-STZ administration has been reported to associated with decreased expression of BDNF in the hippocampus (Shonesy et al., 2012). We therefore determine the levels of BDNF as well as CREB in ICV-STZ rats. Interestingly, we observed that ICV-STZ administration results in decreased levels of CREB and BDNF as compared to vehicle treated groups. Compared with monotherapy with either LiCl or VPA alone, chronic treatment with both drugs significantly and consistently elevated CREB and BDNF levels. Similar increase in BDNF levels after co-treatment with LiCl and VPA has been observed previously in cortical neuronal cultures and transgenic mice models of HD (Yasuda et al., 2009; Chiu et al., 2011).

In line with biochemical and neurotrophic factor alterations in the present study, histological sections of dentate gyrus and CA3 region of hippocampus in ICV-STZ treated rats showed pyknotic nuclear changes as evident by increased percentage of damaged neurons. The combination of both the drugs results in attenuation of STZ-induced neurotoxicity and was able to attenuate the number of damaged neurons, suggesting their synergistic neuroprotective potential. However, very few neurons were found to be protected when both the drugs were administered alone.

In conclusion, the present results demonstrate that co-administration of LiCl and VPA in low doses produce synergistic effects and improves cognitive deficits. These cognition enhancing actions are likely to be triggered by potentiated inhibition of GSK3β and HDACs respectively, to induce neurotrophic factors such as BDNF, which results in transcriptional activation and hence better neuroprotection (Fig. 6.5). Given that both LiCl and VPA have a long history of safe use in humans and that the devastating symptoms of AD progressively intensify without remission until death. Our data provide a strong rationale for using low dose combination of LiCl and VPA to treat AD patients. Further, exploration of combinational strategy with GSK3β and HDAC inhibitors could result in beneficial actions in AD.

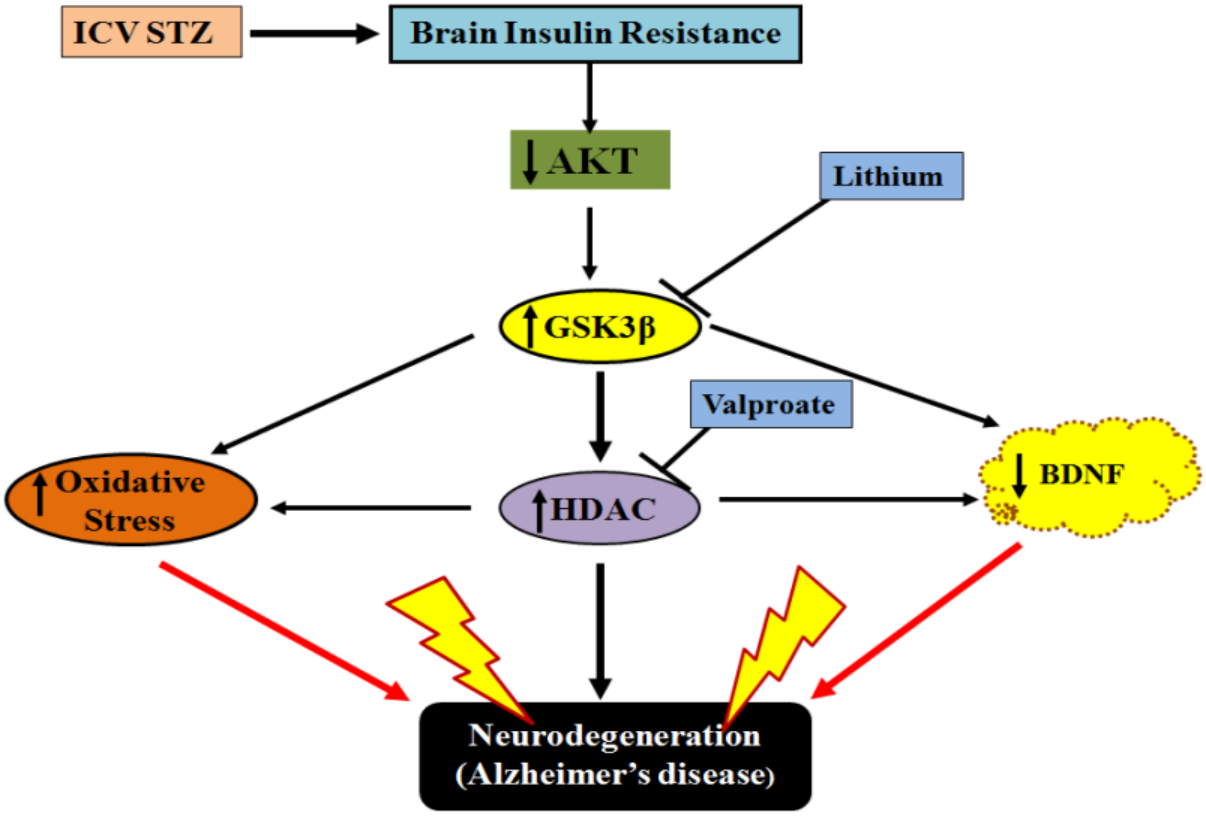

Fig.6.5 Proposed Mechanism of combination of GSK3β inhibitor and HDAC inhibitor in insulin resistance induced cognitive deficits

In our second approach to reduce the toxic effects associated with use of HDAC inhibitors, we explored the class specific HDAC inhibitors involved in insulin resistance induced neurodegeneration. Some HDAC inhibitors, especially pan-inhibitors, indicate serious side effects, such as fatigue, nausea, anorexia, diarrhea, thrombus formation, thrombocytopenia, neutropenia, anemia, hypokalemia, hypophosphatemia, *etc*. which significantly limit their therapeutic applications in patients (Rikiishi, 2011). Therefore, there are dramatic interests and efforts in identifying compounds that have selectivity towards HDAC classes for reducing the side effects and enhancing potential application in different therapeutic areas (Guha, 2015; Micelli and Rastelli, 2015). Targeting individual HDACs with specific inhibitors is an important aim in developing HDAC-related therapeutic strategies, but this has proved challenging due to the highly conserved active site of these enzymes (Kazantsev and Thompson, 2008).

6.5. Class selective HDAC inhibitors in insulin resistance induced neurodegeneration

The aim of this study was to determine which class (class I to III) specific HDAC inhibitors plays the most important role in ameliorating HFD induced insulin resistance and cognitive deficits. For this purpose, we have used, the class I HDAC inhibitors (HDACi 4b and CI-994), class II HDAC inhibitor (MC-1568) and Class III HDAC (SIRT) inhibitor, sirtinol.

This is the first study to report the potential of Class specific HDAC inhibitors. We found that inhibiting Class II HDACs in insulin resistance induced cognitive decline could be of more therapeutic value than Class I and III HDACs. Although, our previous studies with pan HDAC inhibitors, Sodium butyrate and SAHA (which target both Class I and Class II HDACs), showed that these compounds produced protective effects against HFD induced cognitive decline and AD pathology. Surprisingly, class I-specific inhibitors (HDACi 4b and CI-994) and Class III inhibitor (Sirtinol) were not effective in this study.

Initially, to explore the effect of different classes of HDAC inhibitors on insulin resistance, we treated the mice with these agents and observed serum parameters. Interestingly, we found that mice treated with Class II selective HDAC inhibitor, MC-1568, showed a significant reduction of body weight, serum glucose, insulin and HOMA-IR values. On the other hand, there was no significant effect of class I-specific HDAC inhibitors, CI-994 or HDACi 4b or Class III inhibitor, Sirtinol on serum glucose, insulin and HOMA-IR level. Of note, there was also no effect of higher doses of these compounds on these parameters (data not shown). Our results are in line with Mihaylova and co-workers who demonstrated that db/db and ob/ob mouse treated with either scrambled control or HDAC4/5/7 shRNAs results in reduction of class II HDAC expression in these diabetic mouse models along with a

substantial decrease in fasting blood glucose levels (Mihaylova et al., 2011). Moreover, they also examined that the HFD fed mice showed a significant reduction of fasting blood glucose levels and improved glucose tolerance when depleted for Class IIa HDACs. In addition, we found that serum TGs and TC levels were significantly attenuated in animals treated with MC-1568 as compared with HFD fed mice.

To examine the effects of HFD feeding and various classes of HDAC inhibitors on locomotor activity, we performed the actophotometer test. We found no significant change in locomotor activity in any of the experimental groups. Among members in the Class IIa subfamily (Lombardi et al., 2011), HDAC4, 5 and 7 have been identified in the brain (Sando et al., 2012). HDAC7 is abundant in embryonic stage forebrain, whereas HDAC4 and 5 express throughout the later life (Sando et al., 2012). Reports have suggested that HDAC4 is a constitutive negative regulator of memory (Sando et al., 2012). Further, investigations of the expression of HDAC4 in hippocampal tissue of individuals with AD revealed an increase in nuclear HDAC4, and this correlated with severity of the disease (Herrup et al., 2013). Moreover, overexpression of HDAC4 in the adult Drosophila brain also impairs long term memory (Fitzsimons et al., 2013). Thus, these studies clearly indicate that members of Class II HDAC family, especially HDAC4 play an important role in cognitive functions and its overexpression has been found in AD patients. Thus, we were further concerned to study the effects of class specific HDAC inhibitors on behavioural tasks assessing cognitive decline. During the MWM, we observed that the mean escape latency to reach the hidden platform was significantly reduced in HFD fed mice treated with MC-1568 but not with other HDAC inhibitors. During the probe trial also, the mice treated with MC-1568 spent significantly higher time in the target quadrant, indicating improved learning and memory with Class II specific HDAC inhibitors. Also, in passive avoidance task, it was observed that the mice treated with MC-1568 but not CI-994 and HDACi 4b, showed improvement in retention memory. To explore the effect of Class specific inhibitors on AD pathology markers we estimated the levels of $A\beta_{(1-42)}$ and p-tau in hippocampus homogenates. We found that mice treated with MC-1568, but not with HDACi 4b, CI-994 or sirtinol was able to attenuate the level of $A\beta_{(1-42)}$ and p-tau in HFD mice. Our results are in line with a recent study, where it was reported that Class II specific HDAC inhibitors attenuates Aβ production, tau hyperphosphorylation and improved cognitive performance in mouse models of AD (Sung et al., 2013). These authors demonstrated that Class II HDAC inhibitors act by repressing the genes facilitating Aβ production and upregulating Aβ degradation enzymes. Moreover, studies in drosophila also strongly suggest the role of Class II member, HDAC4, in

exacerbating the neurodegenerative phenotype caused by Aβ $_{(1-42)}$ expression (Cao et al., 2008). Further, HDAC inhibitors can confer neuroprotection via the regulation of microtubule stability, which is dependent on post-translational modifications such as acetylation of α-tubulin. Tubulin is another key building block within microtubules that can be acetylated or deacetylated by HDAC6, which belongs to Class II of HDACs. Evidence in patient samples indicates that this regulation is disrupted because of the level of HDAC6 being elevated in the brains of patients with AD, specifically by 52% in the cortex and 91% in the hippocampus, which is the center for learning and memory (Odagiri et al., 2013; Zhang et al., 2013). In addition, levels of acetylated α-tubulin protein are decreased in AD patient brains, suggesting a link between the neurofibrillary tangles characteristic of AD pathology (caused by hyperphosphorylated tau) and the loss of microtubule stability. Recently, a HDAC6 inhibitor, (ACY-738) has been reported to combat AD phenotype in APP/PS1 mice (Majid et al., 2015). Treatment with ACY-738 results in significant reduction of p-tau level, recovery of short-term learning and memory deficits along with reduced insoluble Aβ (1-42) level. Thus, these studies strongly support our results and further indicate the important role of Class II HDAC inhibitors in ameliorating Aβ and ptau related neurotoxicity.

Class II HDACs have also been reported to regulate gene expression through interaction with transcription factors such as MEF2, SRF and CREB (Li et al., 2012; Lu et al., 2000; Miska et al., 1999). HDAC4 has been implicated in regulation of *Bdnf* transcription through suppression of MEF2- and CREB-dependent transcriptional activity in cerebellar neurons (Li et al., 2012). In this regard, previous studies reported that overexpression of HDAC4 and HDAC5 results in downregulation of *Bdnf* promoter IV activity, which was found to reversed by using class II HDAC inhibitor, MC-1568 (Kumar et al., 2005; Koppel & Timmusk, 2013). In the present study also, we found that HFD significantly reduced pCREB and BDNF levels in the hippocampal brain tissues. In contrast, the mice treated with Class II specific HDAC inhibitor, MC-1568 significantly ameliorated the HFD induced reduction in pCREB and BDNF levels. However, the mice treated with CI-994, HDACi 4b or sirtinol didn't showed any significant effect on BDNF or pCREB level. Thus, the observed neuroprotective actions of MC-1568 might be associated with elevated CREB based transcriptional activation of BDNF. Although, the exact mechanisms involved are still elusive, activation of *Bdnf* transcription by MC-1568 suggests that class II selective HDAC inhibitors have potential as therapeutic agents for neurodegenerative diseases (especially AD), associated with synaptic plasticity impairment.

In conclusion, the present study suggests that inhibiting Class II HDACs in insulin resistance induced cognitive decline could be of more therapeutic value than Class I or Class III HDACs. Class IIa enzymes have also been suggested as viable drug targets for various metabolic disorders, including T2DM, owing to their regulation of glucose homeostasis and muscle glucose metabolism (Mihaylova et al., 2011; Raichur et al., 2012). The increased expression of Class II HDACs isoforms especially, HDAC4 and HDAC5, in insulin resistance and T2DM animal models further encourage to study the role of individual HDACs in insulin resistance condition. Further insights from clinical as well as preclinical studies may ultimately pave the way of Class II specific HDAC inhibitors toward possible therapeutics in insulin resistance, T2DM and associated neurodegeneration.

6.6. Insulin resistance and Parkinson's disease

Early reports suggested that up to 50% - 80% of patients with PD have abnormal glucose tolerance when tested (Sandyk, 1993), however data from recent studies suggest the association is more modest with T2DM patients having approximately a 40% increased risk of developing PD (Driver et al., 2008; Hu et al., 2007; Xu et al., 2011). These studies indicate that T2DM is a risk factor for developing PD. Although the exact mechanisms linking PD and T2DM are still elusive, however, insulin resistance and dysregulated insulin signalling might be involved in increased risk for PD. It has been hypothesized that aberrant insulin signalling triggers a stepwise sequence of disruptions of regulatory pathways (including mitochondrial dysfunction, neuroinflammation, increased endoplasmic reticulum stress, abnormal protein aggregation and metabolic abnormalities) which would lead to insulin resistance and diabetes, and might ultimately put an individual at increased risk for PD (De Pablo-Fernandez et al., 2017; Athauda and Foltynie, 2016). Insulin receptors are found in the basal ganglia and substantia nigra and growing evidence suggests insulin plays an essential role regulating neuronal survival and growth, dopaminergic transmission and maintenance of synapses (Bassil et al., 2014). Studies have also shown marked loss of insulin receptor mRNA in the SNpc of patients with PD and increased insulin resistance compared with age matched controls (Duarte et al., 2012; Morris et al., 2014; Takahashi et al., 1996). In addition, increased levels of IRS phosphorylation at serine residues (which deactivates insulin signalling) are also found in the basal ganglia and SNpc (Moroo et al., 1994). Furthermore, it has been shown that these changes may precede the death of dopaminergic neurons (Moroo et al., 1994). In conjunction, there is growing evidence that a process analogous to peripheral insulin resistance occurs in the brains of PD patients, which suggests loss of insulin signalling may contribute to the development of pathological features of PD. In addition to a potential

increased risk for PD, insulin resistance and T2DM have also been suggested as a modifying factor of the disease contributing to more severe motor symptoms requiring higher doses of L-DOPA for symptom control (Cereda et al., 2012), more prominent axial motor symptoms and cognitive impairment (Giuntini et al., 2014). The possibility that PD and diabetes share dysregulated pathways is particularly important as further study of these mechanisms might lead to more effective treatments or disease-modifying therapies for PD and T2DM. These clinical reports suggest that insulin resistance and/or T2DM might be a risk factor for PD development, however experimental data is scarce. Although, it is possible that HFD feeding may make dopaminergic neurons more vulnerable to environmental insults, such as neurotoxins, only few preclinical studies have investigated the effect of a HFD diet on dopaminergic neurodegeneration. Choi and colleagues reported that treatment with neurotoxin, MPTP, produced greater striatal dopamine depletion in HFD-fed mice than in chow-fed controls (Choi et al., 2005). We wanted to further characterize the effect of a HFD on toxin-induced nigrostriatal dopamine depletion using the 6-OHDA rat model of PD. Thus, this study was designed to evaluate whether the insulin resistance condition exacerbates the PD pathology or not in experimental animals.

For this study, we used an animal model which can mimic the conditions of both insulin resistance and PD pathology. The insulin resistance condition was developed by HFD feeding as per earlier protocol. We confirmed the induction of insulin resistance by measuring serum levels of glucose, insulin, TG, TC, HOMA-IR and OGTT. We found significant increase in serum glucose, insulin, TG and TC level in HFD fed rats as compared with NPD fed rats. Moreover, we found that HOMA-IR values were significantly higher in HFD fed rats, indicating development of insulin resistance condition. Also, reduced glucose tolerance was observed in OGTT, where increased glucose levels were found at various different time points in HFD fed rats as compared with NPD fed rats.

After the induction of insulin resistance, the animals were infused with either 6-OHDA or vehicle into medial forebrain bundle (MFB) and were assigned different groups. To determine whether HFD-fed animals were indeed more sensitive to 6-OHDA mediated dopamine depletion, we administered equal amounts of 6-OHDA to HFD-fed, insulin-resistant rats and NPD fed rats. Administration of 6-OHDA is known to produce decrease in the density of TH^+ neurons indicating degeneration of the dopaminergic neurons in the nigrostriatal pathway and causes a decrease in the dopamine levels, an important neurotransmitter involved in the motor functions (Kim et al., 2016). The nigrostriatal dopaminergic pathway consists of the A9 dopaminergic cell groups which are located in the

SNpc. The axons of these neurons extend along the MFB and terminate in the dorsal striatum. 3 weeks after 6-OHDA administration, we performed apomorphine challenge. In the 6-OHDA damaged rats, apomorphine produced durative contralateral rotations. This further confirmed that apomorphine-induced circling behavior was closely associated with the degrees of dopamine denervation which was dependent on the damage extents of the striatum and the SNpc. Therefore, the dopamine depletion induced by the 6-OHDA injection into MFB could be considered to be a valid and successful animal model to investigate the possible pathological mechanisms of PD.

During various motor activity based behavioural tasks (rotarod, actophotometer, narrow beam walk test), we found that rats fed with HFD followed by 6-OHDA infusion performed poorly as compared to rats fed with NPD followed by 6-OHDA infusion. Thus, these results clearly indicate that HFD feeding exacerbates the toxic effects of 6-OHDA. These results were further supported by biochemical estimations, where we found that HFD fed, insulin-resistant rats exhibited enhanced nigrostriatal dopamine depletion following 6-OHDA as compared with NPD fed rats. Our results support an exacerbating role for dietary fat, and consequent insulin resistance, in vulnerability to toxin-induced nigrostriatal dopamine depletion. If 6-OHDA is produced endogenously even in small amounts, the increased vulnerability of dopaminergic neurons in response to HFD-induced insulin resistance could put the nigrostriatal pathway at greater risk of damage during long term HFD feeding. The behavioural data obtained was further supported by histopathological studies, where we observed significant damage in striatal regions of 6-OHDA infused insulin resistant rats as compared with 6-OHDA infused non-insulin resistant or NPD fed rats.

The primary neuropathology of PD is the loss of dopamine neurons within the SNpc and massive depletion of dopamine in the striatum, the terminal region of the SNpc. In this study, we also found that HFD fed 6-OHDA treated rats showed significant reduction in striatal dopamine levels as compared with NPD fed 6-OHDA or NPD fed vehicle treated animals. This loss of dopamine appears to be responsible for the most prominent symptoms of PD. The degree of neurological deficit is related to the loss of striatal dopamine (Hornykiewicz and Kish, 1987). As, dopamine transmission has been implicated in a variety of motor, emotional, and cognitive functions (Hosp and Luft, 2013; Lisman et al., 2011; Perreault et al., 2014), the level of dopamine in striatal homogenates of these animals can be well correlated with the results observed in behavioral parameters.

An important molecular mechanism that might be associated with insulin resistance induced PD pathology is oxidative stress and neuroinflammation. Both these factors have

been well reported to play an important role in disease pathology. In the present study, we found that animals fed with HFD followed by 6-OHDA infusion showed significantly higher level of oxidative stress markers (MDA, nitrite) and reduced antioxidant enzyme, GSH level in striatum homogenates as compared with NPD fed 6-OHDA infused rats. Also, elevated level of proinflammatory cytokine, TNF-α was reported in HFD fed 6-OHDA infused rats as compared to NPD fed 6-OHDA infused rats, suggesting that HFD aggravate neuroinflammation.

Also, there is growing evidence that a process analogous to peripheral insulin resistance occurs in the brains of PD patients. This raises the possibility that defective insulin signalling pathways may contribute to the development of the pathological features of PD, and thereby suggests that insulin signalling pathway may potentially be a novel target for disease modification. Among these, increased expression of GSK-3β has been found in PD patients and in experimental models of PD (Hernandez-Baltazar et al., 2013; Wills et al., 2010). Moreover, Inhibition of GSK-3β has been reported to promote autophagy and halt expression, aggregation of α-synuclein and its subsequent neurotoxic effects in vitro and in vivo (Duka et al., 2009; Yuan et al., 2015). Studies have also shown that insulin signalling can modulate degradation of α-synuclein through activation of IDE (Sharma et al., 2015). Correspondingly, induction of insulin signalling with IGF-1 or reversal of insulin resistance suppresses α-synuclein aggregation and toxicity (Kao, 2009). In a damaging feed forward loop, increased levels of α-synuclein can also inhibit IRS-1, causing increased activation of GSK-3β activity, leading to further deleterious effects (Duka et al., 2009). Based upon these reports, we were interested to study the involvement of GSK3β in PD pathology. Interestingly, we found that insulin resistant 6-OHDA infused rats, showed significantly increased GSK3β level as compared to non-insulin resistant 6-OHDA infused rats. Similarly, other studies also demonstrated increased GSK3β activity in the striatum of 6-OHDA administered rats (Xie et al., 2016). Thus, indicating the possible role of GSK3β in HFD induced exacerbated PD pathology. Moreover, we also demonstrated that insulin resistant rats infused with 6-OHDA showed significant reduction in histone H3 acetylation, further highlighting the role of epigenetic pathways in PD pathology. In conclusion, the key findings of the present study indicates that insulin resistance in 6-OHDA model of PD (i) worsens Parkinsonian motor behavior, (ii) exaggerates striatal dopamine loss and striatal neurodegeneration, (iii) intensifies oxidative stress and neuroinflammation in the nigrostriatal pathway (iv) involves increased GSK3β activity and reduced global histone H3 acetylation.

Based upon these findings, our next objective was to explore the effects of GSK3β inhibitor and HDAC inhibitor in insulin resistance induced exacerbated PD pathology.

6.7. Effect of GSK3β inhibitors and HDAC inhibitors in insulin resistance induced hemiparkinson's model

Our next approach was to explore the molecular mechanisms involved in insulin resistance induced exacerbated PD pathology in 6-OHDA infused rats. For this purpose, the 6-OHDA infused insulin resistance rats were treated with either GSK3β inhibitor, IMX or HDAC inhibitor, SAHA once daily for 14 days. We found that treatment with IMX (0.4 mg/kg) or SAHA (50 mg/kg) significantly attenuated the serum glucose, insulin, TGs and TC level in 6-OHDA infused insulin resistant rats, suggesting that both GSK3β inhibitors and HDAC inhibitors play an important role in ameliorating insulin resistance. Moreover, the association of insulin signalling with brain dopaminergic signalling has been previously explored. Insulin receptors have been reported to localize in the midbrain dopaminergic neurons (Figlewicz et al., 2003) and found to increase dopaminergic transporter activity and enhances the clearance of dopamine from the synapse (Davis et al., 2011). It has been demonstrated that impaired insulin signaling aggravates brain dysfunction related to dopamine homeostasis (Wei et al., 2007; Anthony et al., 2006).

An important factor in the appearance of parkinsonian motor symptoms is the loss of striatal dopamine. As reported in our previous study, HFD fed 6-OHDA infused rats showed impaired performance on various behavioural tasks evaluating locomotion and gait abnormalities. The reduced latency to fall from rotating rod, increase in the time take to cross the narrow beam, reduced contralateral contacts in cylinder test, are indications of reduced motor activity. However, treatment with GSK3β inhibitor, IMX and HDAC inhibitor, SAHA results in improved performance in rotarod and locomotor activity. Moreover, these rats also showed significant reduction in time taken to cross the narrow beam, and number of foot errors. Also, during cylinder test, we reported that rats treated with either GSK3β inhibitor, IMX or HDAC inhibitor, SAHA showed significant increased number of contralateral contacts, suggesting improved activity in 6-OHDA lesioned side of brain.

The relatively small depletion of striatal dopamine is associated with the loss of nigrostriatal dopaminergic neurons in insulin resistant rats. Thus, the observed equivalent Parkinsonian motor symptoms in the insulin resistant rats might be linked with the loss of striatal dopamine. In line with these, we found that treatment with IMX and SAHA significantly ameliorate the reduced dopamine levels in insulin resistant 6-OHDA infused rats.

The generation of free radical-induced oxidative stress is regarded as underlying event in PD pathology (Medeiros et al., 2016). Postmortem studies indicated increased level of oxidative stress markers and down-regulation of antioxidant defense mechanisms in PD brain (Ambani et al., 1975; Pearce et al., 1997). In line with these, we also observed significant increase in level of oxidative stress markers, (MDA and nitrite) and reduction of antioxidant enzyme, GSH in striatal homogenates of insulin resistance 6-OHDA infused rats. However, treatment with GSK3β inhibitor, IMX or HDAC inhibitor, SAHA attenuated the increased oxidative stress markers and ameliorates the antioxidant, GSH level.

Along with oxidative stress, neuroinflammation has also been reported to play an important role in dopaminergic neuronal damage. Post mortem studies have revealed an increased level of pro-inflammatory mediators in the SNpc of PD brains (Imamura et al., 2003). Insulin resistance may induce production of pro-inflammatory cytokines leading to cell death. Simultaneously, inflammation induces mitochondrial dysfunction, driving overproduction of ROS to further exacerbate the inflammatory state and ultimately enhancing neurodegeneration (Dineley et al., 2014). Although various proinflammatory cytokines have been reported to be involved in neurodegenerative processes, however, TNF-α, being the most important factor in both insulin resistance and PD pathology, was evaluated in this study. We found that insulin resistance induced by HFD feeding results in significant elevation of TNF-α level in 6-OHDA infused rats. In contrast, treatment with IMX or SAHA significantly attenuated the level of pro-inflammatory cytokine, TNF-α in insulin resistant 6-OHDA infused rats, suggesting the anti-inflammatory role of these compounds.

Recent studies indicate that cellular stress such as ER stress and oxidative stress can modulate GSK3β activity. Elevated GSK-3β activity has been reported in striatum of PD patients as compared to controls (Wills et al., 2010). An interesting study by Chen and colleagues shows that 6-OHDA induces GSK-3β activity by dephosphorylation (Ser-9) (Chen et al., 2004). Similar results were observed in mouse models of PD (Duka et al., 2009). Moreover, increased GSK-3β levels have also been reported in peripheral blood lymphocytes in PD patients (Armentero et al., 2011). In the present study, we found significant elevation in GSK3β activity in insulin resistant 6-OHDA infused rats. However, treatment with IMX ameliorates the GSK3β activity in striatal regions. This data further support the hypothesis that observed beneficial effects of IMX in behavioural and biochemical estimations occurred via its GSK3β inhibitory activity.

6-OHDA treatment elicits activation of several kinases including ERK kinases (Kulich et al., 20011), GSK3β kinase activity (Chen et al., 2004), and stress-activated kinases

(Choi et al., 2004). As discussed earlier, GSK3β is a negative regulator of CREB activity. CREB as a transcription factor, has been reported to play an important role in neuronal survival, in part by controlling the transcription of neuroprotective genes (Finkbeiner et al., 2000). The promoter regions of the genes for BDNF and the pro-survival protein Bcl-2 contain CREs (Mayr and Montminy, 2001). Thus, activated GSK3β kinase activity as a result of 6-OHDA administration might inhibit the CREB dependent transcription. In our study, we found reduced CREB activity in insulin resistant 6-OHDA infused rats as compared to alone insulin resistant rats. However, treatment with GSK3β inhibitor, IMX and HDAC inhibitor, SAHA attenuate the CREB activity in insulin resistant 6-OHDA infused rats.

The neuroprotective role of BDNF in PD has been well established. Studies have suggested that BDNF can protect nigrostriatal dopaminergic neurons from neurotoxins in rodent and monkey models of PD (Sun et al., 2005). Reduced BDNF mRNA expression in SNpc of PD patients has been reported to contribute directly to the death of nigral dopaminergic neurons and the development of PD (Parain et al., 1999; Porritt et al., 2005; Mogi et al., 1999; Howells et al., 2000). Moreover, BDNF induces striatal neurogenesis in adult rats which were treated with 6-OHDA (Mohapel et al., 2005). In the present study, we found significant reduction of BDNF levels in insulin resistant 6-OHDA lesioned rats as compared to alone insulin resistant rats. However, treatment with GSK3β inhibitor, IMX and HDAC inhibitor, SAHA attenuates the BDNF level in insulin resistant 6-OHDA lesioned rats.

In the present study, we also observed that insulin resistant 6-OHDA infused rats showed significant reduction in global histone H3 acetylation as compared to alone insulin resistant rats. However HDAC inhibitor, SAHA, significantly ameliorate the reduced histone H3 acetylation levels in insulin resistant 6-OHDA infused rats. This increased acetylation might be responsible for increased level of BDNF in striatal homogenates of these rats.

As shown earlier, insulin resistant rats infused with 6-OHDA showed significant neuronal damage in striatal region. In contrast, the rats treated with GSK3β inhibitor, IMX and HDAC inhibitor, SAHA exert significant neuroprotection in insulin resistant 6-OHDA infused rats. The neuroprotective effect of these compounds might be attributed to their BDNF enhancing effects. In line with this, previous studies also indicated that BDNF plays a neuroprotective role in 6-OHDA administered neurotoxicity (Spina et al., 1992; Singh et al., 2006).

In conclusion, we suggest that insulin resistance significantly increased the risk of developing PD. We found that Insulin resistance caused by a HFD exacerbates dopaminergic

degeneration in rats. Moreover, we observed that GSK3β inhibitors and HDAC inhibitors might prove to be highly effective in ameliorating insulin resistance induced PD like pathology. Overall, the role of insulin signaling on dopaminergic neurons in PD, in a background of T2DM-related insulin resistance, should be investigated to further understand the underlying mechanism.

7.0 Summary and Conclusion

In this work, we have addressed various important questions regarding the role of insulin resistance in neurodegenerative diseases. We demonstrate that HFD feeding results in significant loss of cognitive functions as assessed by battery of behavioural tests. Moreover, significant neuronal loss was observed in hippocampal neurons, which is the major area involved in learning and memory. Next, we addressed an important issue regarding the molecular mechanisms involved in insulin resistance induced neurodegeneration. We found increased level of GSK3β in hippocampal homogenates of HFD fed mice. Moreover, increased GSK3β activity was found to be involved in formation of hyperphosphorylation of Tau and Amyloid-β formation. Treating these mice with GSK3β inhibitors, results in significant improvement of cognitive functions along with increased neuronal survival as observed by histological studies. The mice treated with GSK3β inhibitors also showed significant reduction in ptau and Amyloid-β levels. Thus, we conclude that GSK3β inhibitors could be therapeutic in ameliorating cognitive deficits associated with insulin resistance condition.

It is well known that phenotype of animals may be modified by the nutritional modulations through epigenetic mechanisms, meaning dietary exposures can have long-term consequences for growth and health. “Epigenetics” introduced for the first time by Waddington in the early 1940s, has been traditionally referred to a variety of mechanisms that allow heritable changes in gene expression even in the absence of DNA mutation. These reports influenced us to study the effect of HFD feeding on the epigenetic pathways in brain of insulin resistant animals. Among various epigenetic modifications, we choose to work on histone acetylation as it has been among the most widely studied post translational modification. We found that insulin resistance condition results in significant reduction of global histone H3 acetylation in hippocampus. As it has been well reported that histone acetylation results in gene transcription activation, whereas, histone deacetylation results in transcriptional repression. In line with this, we observed that mice fed with HFD have significant reduction in levels of BDNF, which support the survival of existing neurons, and encourage the growth and differentiation of new neurons and synapses. We used broad spectrum HDAC inhibitors such as SAHA, Sodium butyrate and found that these compounds results in attenuation of HFD induced cognitive deficits and neuronal damage. The observed beneficial effects of HDAC inhibitors were likely to be mediated, at least in part, by elevated acetylation of histone H3, which concurrently elevated levels of neurotrophic factor, BDNF.

This study strongly supports the potential of HDAC inhibition as a possible therapeutic strategy to ameliorate cognitive deficits associated with insulin resistance. However, the toxicity associated with HDAC inhibitors has limited the clinical data available. In order to reduce side effects while maintaining cognitive benefits, we used a low dose combination of HDAC inhibitors with GSK3β inhibitors and found that the combination of these drugs exert synergistic neuroprotective effects. Thus, our results suggested that using a low dose combination of HDAC inhibitors along with GSK3β inhibitors, could be one stratergy to reduce the side effects associated with higher dose of HDAC inhibitors. Moreover, in second approach, we used class selective HDAC inhibitors and found that Class II selective HDAC inhibitor (MC-1568) was more effective in attenuating cognitive deficits and neuronal loss as compared to Class I and Class III selective inhibitors.

In conclusion, we suggest that either a low dose combination of HDAC inhibitor and GSK3β inhibitor or Class II selective HDAC inhibitors could be used for long term therapy of cognitive deficits related with insulin resistance conditions.

We also explored that insulin resistance could be a possible risk factor for PD. We standardized an animal model where we combined insulin resistance condition along with dopaminergic neuronal damage induced by 6-hydroxydopamine (6-OHDA), a toxin used widely for PD induction in animals. As expected, the 6-OHDA treatment produced nigral dopaminergic degeneration as evidenced by the loss of striatal dopamine and impaired performance in behavioural tasks. Interestingly, we found that exposure to HFD exacerbated the toxic effects of 6-OHDA on striatal dopamine loss and behavioral observations, indicating that insulin resistance is associated with a reduced capacity of nigral dopaminergic terminals to cope with 6-OHDA-induced neurotoxicity. Since high-fat consumption is common place in our modern society, dietary fat intake may represent an important modifiable risk factor for PD. We further explored the molecular mechanisms responsible for this exacerbated neuronal damage in insulin resistant animals. We found the involvement of GSK3β and reduced histone H3 acetylation might play important role in insulin resistance induced exacerbated PD pathology. Thus, we used GSK3β inhibitor and HDAC inhibitor and observed that these compounds significantly ameliorate the HFD induced motor deficits and restore dopamine levels. This is the first study exploring the molecular mechanisms involved in insulin resistance induced PD condition. Although, we observed significant improvement in behavioral tasks characteristic of PD pathology, however, future studies are warranted to explore the underlying molecular changes during disease pathology.

8.0 Salient findings of this work

- Development of insulin resistance and time course for insulin resistance induced cognitive deficit and neurodegeneration was established.
- Alterations in Insulin Signaling Kinase activity, Neurotrophic factor alterations, Neuronal Oxidative Stress and Neuroinflammation, Amyloid-β and Tau pathology and Morphological changes in discrete brain regions in relevance to neurobiological changes, characteristic of AD in association with insulin resistance were studied.
- Involvement of epigenetic pathways, focusing on HDACs, in insulin resistance induced cognitive deficits and AD was also explored.
- The molecular mechanisms of possible neuroprotective effect of GSK3β inhibitors and HDAC inhibitors were evaluated in insulin resistance induced cognitive decline.
- Different strategies (involving use of low dose and isoform specific HDAC inhibitors) were used to reduce the side effects associated with HDAC inhibitors.
- The relationship of insulin resistance and PD pathology was also studied and we explored the molecular mechanism(s) involved in insulin resistance induced PD symptoms in rats.

8.1 Future Scope of this work

The current research work analyzed the neuroprotective effects of GSK3β inhibitors and HDAC inhibitors in insulin resistance induced neurodegeneration. Based on these findings, utilizing the evidence obtained in this work future research can be performed in following areas:

- Exploring the expression of each isoform of Class II HDACs in brain regions during insulin resistance condition will further open the new avenues.
- Combining low dose combinations of HDAC inhibitors with other drugs already showing potential in these conditions.
- Targeted drug delivery formulations of these combinations can also been performed (This work has already been approved by DST, India).
- Studies investigating safety and toxicity profile of the tested drugs during long term usage.
- Experiments identifying other epigenetic mechanisms such as histone methylation, phosphorylation in insulin resistance condition can be performed.

Such knowledge may yield valuable insight into underlying mechanisms involved in insulin resistance induced cognitive decline, AD and PD, while opening newer opportunities for the treatment of these devastating diseases.

8.2 Limitations of current study

- In the current study, the expression of specific HDAC isoforms has not been evaluated.
- Insulin receptor expression has not been studied during disease condition as radio-labelled experiments are required.
- Detailed toxicity studies for the drug candidates used in the present study were not investigated although obvious untoward effects were detected.

9.0 Bibliography

Abel, ED., Litwin, SE., Sweeney, G., (2008) Cardiac remodeling in obesity. Physiol Rev. 88, 389–419.

Abel, ED., Peroni, O., Kim, JK., Kim,YB., Boss, O., Hadro, E., et al., (2001) Adipose-selective targeting of the GLUT4 gene impairs insulin action in muscle and liver. Nature. 409, 729–733.

Aberg, MAI., Aberg, ND., Palmer, TD., Alborn, AM., Carlsson-Skwirut, C., Bang, P., et al., (2003) IGF-I has a direct proliferative effect in adult hippocampal progenitor cells. Mol Cell Neurosci. 24(1), 23–40.

Adcock, IM., Caramori, G., Ito, K., (2006) New insights into the molecular mechanisms of corticosteroids actions. Curr Drug Targets. 7, 649–660.

Agis-Balboa, RC., Pavelka, Z., Kerimoglu, C., Fischer, A., (2013) Loss of HDAC5 impairs memory function: implications for Alzheimer's disease. J. Alzheimers. Dis. 33, 35–44.

Agrawal, R., Tyagi, E., Shukla, R., Nath, C., (2009) A study of brain insulin receptors, AChE activity and oxidative stress in rat model of ICV STZ induced dementia.Neuropharm. 56, 779-787.

Ai, J., Wang, N., Yang, M., Du, ZM., Zhang, YC., Yang, BF., (2005) Development of Wistar rat model of insulin resistance. World J. Gastroenterol. 11, 3675-3679.

Akagiri, S., Naito, Y., Ichikawa, H., Mizushima, K., Takagi, T., Handa, O., (2008). A Mouse Model of Metabolic Syndrome; Increase in Visceral Adipose Tissue Precedes the Development of Fatty Liver and Insulin Resistance in High-Fat Diet-Fed Male KK/Ta Mice, J Clin Biochem Nutr. 42, 150-157.

Alarcon, JM., Malleret, G., Touzani, K., Vronskaya, S., Ishii, S., Kandel, ER., et al., (2004) Chromatin acetylation, memory, and LTP are impaired in CBP+/- mice: a model for the cognitive deficit in Rubinstein-Taybi syndrome and its amelioration. Neuron. 42, 947–959.

Alessi, DR., Caudwell, FB., Andjelkovic, M., Hemmings, BA., Cohen, P., (1996) Molecular basis for the substrate specificity of protein kinase B; comparison with MAPKAP kinase-1 and p70 S6 kinase. FEBS Lett. 399(3), 333-338.

Alessi, DR., Deak, M., Casamayor, A., Caudwell, FB., Morrice, N., Norman, DG., (1997) 3-Phosphoinositide-dependent protein kinase-1 (PDK1): structural and functional homology with the Drosophila DSTPK61 kinase. Curr Biol. 7(10), 776-789.

Almind, K., Kahn, CR., (2004) Genetic determinants of energy expenditure and insulin resistance in diet-induced obesity in mice. Diabetes. 53, 3274–3285.

Alsaif, MA., Duwaihy, MMS., (2004) Influence of dietary fat quantity and composition on glucose tolerance and insulin sensitivity in rats. Nutr Res. 24, 417–425.

Altarejos, JY., Montminy,M., (2011) CREB and the CRTC coactivators: sensors for hormonal and metabolic signals. Nat Rev Mol Cell Biol. 12 (3) 141- 151.

Amalric, M., Moukhles, H., Nieoullon, A., Daszuta, A., (1995) Complex deficits on reaction time performance following bilateral intrastriatal 6-OHDA infusion in the rat. Eur. J. Neurosci. 7, 972-980.

Ambani, LM., Van Woert, MH., Murphy, S., (1975) Brain peroxidase and catalase in Parkinson disease. Arch Neurol. 32 (2), 114–118.

Amin, SN., Younan, SM., Youssef, MF., Rashed, LA., Mohamady, I., (2013) A histological and functional study on hippocampal formation of normal and diabetic rats. F1000Research, 2.

Angila, SS., Holiger, P., Evelyn, JP., Pul, P., Elin, L., Yongqing, Z., et al., (2015) Experience modulate the effects of histone deacetylase inhibitors on gene and protein expression in the hippocampus: impaired plasticity in aging. J Neurosci. 35 (33), 11729-11742.

Annett, LE., Torres, EM., Clarke, DJ., Ishida, Y., Barker, RA., Ridley, RM., et al., (1997) Survival of nigral grafts within the striatum of marmosets with 6-OHDA lesions depends critically on donor embryo age. Cell Transplant.6 (6), 557–569.

Antenor-Dorsey, JA., Meyer, E., Rutlin, J., Perantie, DC., White, NH., Arbelaez, AM.,et al., (2013) White matter microstructural integrity in youth with type 1 diabetes. Diabetes. 62, 581–589.

Anthony, K., Reed, LJ., Dunn, JT., Bingham, E., Hopkins, D., Marsden, PK., et al., (2006) Attenuation of insulin-evoked responses in brain networks controlling appetite and reward in insulin resistance: the cerebral basis for impaired control of food intake in metabolic syndrome? Diabetes 55, 2986–2992.

Antunes, M., Biala, G., (2012) The novel object recognition memory: neurobiology, test procedure, and its modifications. Cogn Process. 13, 93–110.

Apaijai, N., Pintana, H., Chattipakorn, SC., Chattipakorn, N., (2012) Cardioprotective effects of metformin and vildagliptin in adult rats with insulin resistance induced by a high-fat diet. Endocrinology. 153, 3878–3885.

Aplin, AE., Gibb, GM., Jacobsen, JS., Gallo, JM., Anderton, BH., (1996) In vitro phosphorylation of the cytoplasmic domain of the amyloid precursor protein by glycogen synthase kinase-3beta. J Neurochem. 67, 699–707.

Aplin, AE., Jacobsen, JS., Anderton, BH., Gallo, JM., (1997) Effect of increased glycogen synthase kinase-3 activity upon the maturation of the amyloid precursor protein in transfected cells. NeuroReport. 8(3) 639–643.

Araki, A., (2010) Dementia and insulin resistance in patients with diabetes mellitus. Nihon Rinsho 68, 569–574.

Armentero, MT., Sinforiani, E., Ghezzi, C., Bazzini, E., Levandis, G., Ambrosi, G., et al., (2011) Peripheral expression of key regulatory kinases in Alzheimer's disease and Parkinson's disease. Neurobiol Aging. 32(12), 2142–2151.

Armstrong, RA., Lantos, PL., Cairns, NJ., (2005) Overlap between neurodegenerative disorders. Neuropathology. 25(2), 111-124.

Arnold, SE., Lucki, I., Brookshire, BR., Carlson, GC., Browne, CA., Kazi, H., (2014) High fat diet produces brain insulin resistance, synaptodendritic abnormalities and altered behavior in mice. Neurobiol Dis. 67, 79-87.

Ascherio, A., Chen, H., Weisskopf, MG., O'Reilly, E., McCullough, ML., Calle, EE., et al., (2006) Pesticide exposure and risk for Parkinson's disease. Ann Neurol. 60, 197–203.

Asensio, C., Muzzin, P., Rohner-Jeanrenaud, F., (2004) Role of glucocorticoids in the physiopathology of excessive fat deposition and insulin resistance. Int J Obes Relat Metab Disord. 28(Suppl 4), S45–S52.

Athauda, D., Foltynie, T., (2016) Insulin resistance and Parkinson's disease: a new target for disease modification? Prog Neurobiol.145-146, 98-120.

Aubry, JM., Schwald, M., Ballmann, E., Karege, F., (2009) Early effects of mood stabilizers on the Akt/GSK-3beta signaling pathway and on cell survival and proliferation. Psychopharmacology (Berl) 205, 419–429.

Authier, F., Cameron, PH., Taupin, V., (1996) Association of insulin-degrading enzyme with a 70 kDa cytosolic protein in hepatoma cells. Biochem J. 319, 149-158.

Authier, F., Metioui, M., Fabrega, S., Kouach, M., Briand, G., (2002) Endosomal proteolysis of internalized insulin at the C-terminal region of the B chain by cathepsin D. J Biol Chem. 277, 9437–9446.

Avila, J., Gomez De Barreda, E., Engel, T., Lucas, JJ., Hernández, F., (2010) Tau phosphorylation in hippocampus results in toxic gain-of-function. Biochemical Society Transactions 38(4), 977–980.

Baarendse, PJJ., van Grootheest, G., Jansen, RF., Pieneman, AW., O'gren, SO., Verhage, M., et al., (2008) Differential involvement of the dorsal hippocampus in passive avoidance in C57BL/6J and DBA/2J mice. Hippocampus 18, 11–19.

Bain, J., McLauchlan, H., Elliott, M., Cohen, P., (2003) The specificities of protein kinase inhibitors: an update. Biochem. J. 371, 199–204.

Bain, J., Plater, L., Elliott, M., Shpiro, N., Hastie,CJ., McLauchlan, H., et al., (2007) The selectivity of protein kinase inhibitors: a further update. Biochem. J. 408, 297–315.

Baker, LD., Cross DJ., Minoshima, S, Belongia, D., Watson, GS., Craft, S., (2011) Insulin resistance and Alzheimer-like reductions in regional cerebral glucose metabolism for cognitively normal adults with prediabetes or early type 2 diabetes. Arch Neurol. 68, 51–57.

Baltan, S., Bachleda, A., Morrison, RS., Murphy, SP., (2011) Expression of histone deacetylases in cellular compartments of the mouse brain and the effects of ischemia. Transl Stroke Res. 2, 411-423.

Baltensperger, K., Kozma, LM., Cherniack, AD., Klarlund, JK., Chawla, A., Banerjee, U., (1993) Binding of the Ras activator son of sevenless to insulin receptor substrate-1 signaling complexes. Science. 260(5116), 1950-1952.

Barco, A., Marie, H., (2011) Genetic approaches to investigate the role of CREB in neuronal plasticity and memory. Mol. Neurobiol. 44(3), 330-349.

Bardai, FH., D'Mello, SR., (2011) Selective toxicity by HDAC3 in neurons: regulation by Akt and GSK3β. J Neurosc. 31, 1746–1751.

Bardai, FH., Price, V., Zaayman, M., Wang, L., D'Mello, SR., (2012) Histone deacetylase-1 (HDAC1) is a molecular switch between neuronal survival and death. J Biol Chem. 287, 35444 –35453.

Bardai, FH., Verma, P., Smith, C., Rawat, V., Wang, L., D'Mello, SR., (2013) Disassociation of histone deacetylase-3 from normal huntingtin underlies mutant huntingtin neurotoxicity. J Neurosci. 33, 11833-11838.

Barlow, BK., Thiruchelvam, MJ., Bennice, L., Cory-Slechta, DA., Ballatori, N., Richfield, EK., (2003) Increased synaptosomal dopamine content and brain concentration of paraquat produced by selective dithiocarbamate. J Neurochem. 85, 1075–1086.

Barrett, RM., Malvaez, M., Kramar, E., Matheos, DP., Arrizon, A., Cabrera, SM., et al., (2011) Hippocampal focal knockout of CBP affects specific histone modifications, long-term potentiation, and long-term memory. Neuropsychopharmacology. 36(8), 1545–1556.

Basciano, H., Federico, L., Adeli, K., (2005) Fructose, insulin resistance, and metabolic dyslipidemia. Nutr. Metab. (Lond) 2, 5.

Bassil, F., Fernagut, PO., Bezard, E., Meissner, WG., (2014) Insulin, IGF-1 and GLP-1 signaling in neurodegenerative disorders: targets for disease modification? Prog Neurobiol. 118, 1-18.

Basu, S., Yoffe, P., Hills, N., Lustig, RH., (2013) The relationship of sugar to population-level diabetes prevalence: an econometric analysis of repeated cross-sectional data. PLoS One. 8(2), e57873.

Baxter, MG., (2010) ''I've seen it all before'': explaining age-related impairments in object recognition. Theoretical Comment on Burke et al. (2010). Behav Neurosci. 124, 706–709.

Bayley, JS., Pedersen, TH., Nielsen, OB., (2016) Skeletal muscle dysfunction in the db/db mouse model of type 2 diabetes. Muscle Nerve. 54(3), 460-468.

Belfiore, A., Frasca, F., Pandini, G., Sciacca, L., Vigneri, R., (2009) Insulin receptor isoforms and insulin receptor/insulin-like growth factor receptor hybrids in physiology and disease. Endocr Rev. 30, 586–623.

Bell, DS., (2003) Heart failure: The frequent, forgotten, and often fatal complication of diabetes. Diabetes care. 26, 2433–2441.

Benito, E., Barco, A., (2010) CREB's control of intrinsic and synaptic plasticity: implications for CREB-dependent memory models. Trends Neurosci. 33, 230-240

Benito, E., Barco, A., (2010) CREB's control of intrinsic and synaptic plasticity: implications for CREB-dependent memory models. Trends Neurosci. 33(5), 230-240.

Benito, E., Urbanke, H., Ramachandran, B., Barth, J., Halder, R., Awasthi, A., et al., (2015) HDAC inhibitor-dependent transcriptome and memory reinstatement in cognitive decline models. J Clin Invest. 125(9), 3572-3584.

Benn, CL., Butler, R., Mariner, L., Nixon, J., Moffitt, H., Mielcarek, M., et al., (2009) Genetic knock-down of HDAC7 does not ameliorate disease pathogenesis in the R6/2 mouse model of Huntington's disease. PLoS One. 4(6), e5747.

Berger, SL., Kouzarides, T., Shiekhattar, R., Shilatifard, A., (2009) An operational definition of epigenetics. Genes Dev. 23, 781–783

Bergman, H., Wichmann, T., DeLong, MR., (1990) Reversal of experimental Parkinsonism by lesions of the subthalamic nucleus. Science. 249 (4975), 1436–1438.

Besse, C., Nicod, N., Tappy, L., (2005) Changes in insulin secretion and glucose metabolism induced by dexamethasone in lean and obese females. Obes Res. 13, 306–311.

Betarbet, R., Sherer, TB., Greenamyre, JT., (2002) Animal models of Parkinson's disease. Bioessays. 24, 308–318.

Betz, B., Bryan, RC., (2016) An Update on the Use of Animal Models in Diabetic Nephropathy Research. Curr Diab Rep. 16(2), 18.

Bhat, NR., Thirumangalakudi, L., (2013) Increased tau phosphorylation and impaired brain insulin/IGF signaling in mice fed a high fat/high cholesterol diet. J Alzheimers Dis. 36(4), 781-789.

Bhat, R., Xue, Y., Berg, S., Hellberg, S., Ormo, M., Nilsson, Y., et al., (2003) Structural insights and biological effects of glycogen synthase kinase 3-specific inhibitor AR-A014418. J. Biol. Chem. 278, 45937–45945.

Biessels, GJ., Deary, IJ., Ryan, CM., (2008) Cognition and diabetes: a lifespan perspective. Lancet Neurol. 7, 184–190.

Binnert, C., Ruchat, S., Nicod, N., Tappy, L., (2004) Dexamethasone-induced insulin resistance shows no gender difference in healthy humans. Diabetes Metab. 30, 321–326.

Black, M., Werenicz, A., Velho, LA., Pinto, DF., Fedi, AC., Lopes, MW., et al., (2015) Enhancement of memory consolidation by the histone deacetylase inhibitor sodium butyrate in aged rats. Neurosci Lett. 504, 76-81.

Blackard, WG Jr., Sood, GK., Crowe, DR., Fallon, MB., (1998) Tacrine. A cause of fatal hepatotoxicity? J Clin Gastroenterol. 26 (1), 57-59.

Blalock, EM., Geddes, JW., Chen, KC., Porter, NM., Markesbery, WR., Landfield, PW., et al., (2004) Incipient Alzheimer's disease: microarray correlation analyses reveal major transcriptional and tumor suppressor responses. Proc. Natl. Acad. Sci. USA. 101, 2173–2178.

Blennow, K., de Leon, MJ., Zetterberg, H., (2006) Alzheimer's disease. Lancet. 368 (9533), 387–403.

Blum, D., Torch, S., Lambeng, N., Nissou, M., Benabid, AL., Sadoul, R., et al., (2001) Molecular pathways involved in the neurotoxicity of 6-OHDA, dopamine and MPTP: contribution to the apoptotic theory in Parkinson's disease. Prog. Neurobiol. 65, 135-172.

Boden, G., She, P., Mozzoli, M., Cheung, P., Gumireddy, K., Reddy, P., et al., (2005) Free fatty acids produce insulin resistance and activate the proinflammatory nuclear factor-κB pathway in rat liver. Diabetes. 54, 3458–3465.

Boissier, JR., Simon, P., (1965) Action of caffeine on the spontaneous motility of the mouse. Arch Int Pharmacodyn Ther. 158(1), 212-221.

Bolden, JE., Peart MJ., Johnstone, RW., (2006) Anticancer activities of histone deacetylase inhibitors. Nat Rev Drug Discov. 5, 769–784.

Bolger, TA., Yao, TP., (2005) Intracellular trafficking of histone deacetylase 4 regulates neuronal cell death. J. Neurosci. 25, 9544–9553.

Bomfim, TR., Forny-Germano, L., Sathler, LB., Brito-Moreira, J., Houzel, JC., Decker, H., et al., (2012) An anti-diabetes agent protects the mouse brain from defective insulin signaling caused by Alzheimer's disease-associated Abeta oligomers. J Clin Invest. 122, 1339–1353.

Bornfeldt, KE., Tabas, I., (2011) Insulin resistance, hyperglycemia, and atherosclerosis. Cell metab. 14, 575–585.

Bosco, D., Plastino, M., Cristiano, D., Colica, C., Ermio, C., De Borges, N., (2012) Dementia is associated with Insulin Resistance in patients with Parkinson's disease. J Neurol Sci. 315 (1–2), 39–43.

Bossy-Wetzel, E., Schwarzenbacher, R., Lipton, SA., (2004) Molecular pathways to neurodegeneration. Nat Med. 10, S2–S9.

Boulle, F., van den Hove, DL., Jakob, SB., Rutten, BP., Hamon, M., van Os, J., et al., (2012) Epigenetic regulation of the BDNF gene: implications for psychiatric disorders. Mol Psychiatry. 17, 584 –596.

Bousiges, O., Neidl, R., Majchrzak, M., Muller, MA., Barbelivien, A., Pereira de Vasconcelos, A., et al., (2013). Detection of histone acetylation levels in the dorsal hippocampus reveals early tagging on specific residues of H2B and H4 histones in response to learning. PLoS ONE. 8, e57816.

Boyault, C., Sadoul, K., Pabion, M., Khochbin, S., (2007a) HDAC6, at the crossroads between cytoskeleton and cell signaling by acetylation and ubiquitination. Oncogene. 26, 5468–5476.

Boyault, C., Zhang, Y., Fritah, S., Caron, C., Gilquin, B., Kwon, SH., et al., (2007b) HDAC6 controls major cell response pathways to cytotoxic accumulation of protein aggregates. Genes Dev. 21, 2172–2181.

Bramblett, GT., Goedert, M., Jakes, R., Merrick, SE., Trojanowski, JQ., Lee, VMY., (1993) Abnormal tau phosphorylation at Ser396 in Alzheimer's disease recapitulates development tand contributes to reduced microtubule binding. Neuron. 10(6), 1089–1099.

Brami-Cherrier, K., Valjent, E., Garcia, M., Pages, C., Hipskind, RA., Caboche, J., (2002) Dopamine induces a PI3-kinase-independent activation of Akt in striatal neurons: a new route to cAMP response element-binding protein phosphorylation J. Neurosci. 22, 8911-8921.

Bray, GA., Nielsen, SJ., Popkin, BM., (2004) Consumption of high-fructose corn syrup in beverages may play a role in the epidemic of obesity. Am J Clin Nutr. 79, 537–543.

Bredy, TW., Wu, H., Crego, C., Zellhoefer, J., Sun, YE., Barad, M., (2007) Histone modifications around individual BDNF gene promoters in prefrontal cortex are associated with extinction of conditioned fear. Learn Mem. 14, 268–276.

Brodacki, B., Staszewski, J., Toczyłowska, B., Kozłowska, E., Drela, N., Chalimoniuk, M., et al., (2008) Serum interleukin (IL-2, IL-10, IL-6, IL-4), TNFα, and INFγ concentrations are elevated in patients with atypical and idiopathic parkinsonism. Neurosci. Lett. 441 (2), 158–162.

Broide, RS., Redwine, JM., Aftahi, N., Young, W., Bloom, FE., Winrow, CJ., (2007) Distribution of histone deacetylases 1-11 in the rat brain. J Mol Neurosci. 31, 47-58.

Bromley-Brits, K., Deng, Y., Song, W., (2011) Morris Water Maze Test for Learning and Memory Deficits in Alzheimer's Disease Model Mice. *J. Vis. Exp.* (53), e2920.

Brooker, GJF., Kalloniatis, M., Russo, VC., Murphy, M., Werther, GA., Bartlett, PF., (2000) Endogenous IGF-1 regulates the neuronal differentiation of adult stem cells. J Neurosci Res. 59(3), 332–341.

Brozinick, JT., Misener, EA., Ni, B., Ryder, JW., Dohm, GL., (2000) Impaired insulin signaling through GSK-3 in insulin resistant skeletal muscle (abstract). Diabetes 49 (Suppl. 1), A326.

Bryant, NJ., Govers, R., James, DE., (2002) Regulated transport of the glucose transporter GLUT4. Nat Rev Mol Cell Biol. 3, 267-277.

Buitrago, MM., Schulz, JB., Dichgans, J., Luft, AR., (2004) Short and long-term motor skill learning in an accelerated rotarod training paradigm. Neurobiol Learn Mem. 81(3), 211-216.

Burwell, RD., Saddoris, MP., Bucci, DJ., Wiig, KA., (2004) Corticohippocampal contributions to spatial and contextual learning. J Neurosci. 24, 3826–3236.

Butterfield, DA., Drake, J., Pocernich, C., Castegna, A., (2001) Evidence of oxidative damage in Alzheimer's disease brain: Central role of amyloid β-peptide. Trends in Molecular Medicine. 7, 548–554.

Caberlotto, L., Carboni, L., Zanderigo, F., Andreetta, F., Andreoli, M., Gentile, G., et al., (2013) Differential effects of glycogen synthase kinase 3 (GSK3) inhibition by lithium or selective inhibitors in the central nervous system. Naunyn Schmiedebergs Arch Pharmacol. 386, 893–903.

Cadet, JL., Brannock, C., (1998) Free radicals and the pathobiology of brain dopamine systems. Neurochem. Int. 32,117-131.

Calfa, G., Chapleau, CA., Campbell, S., Inoue, T., Morse, SJ., Lubin, FD., et al., (2012) HDAC activity is required for BDNF to increase quantal neurotransmitter release and dendritic spine density in CA1 pyramidal neurons. Hippocampus. 22, 1493–1500.

Campas-Moya, C., (2009) Romidepsin for the treatment of cutaneous T-cell lymphoma. Drugs Today. (Barc) 45, 787–795.

Canettieri, G., Morantte, I., Guzman, E., Asahara, H., Herzig, S., Anderson, SD., et al., (2003) Attenuation of a phosphorylation-dependent activator by an HDAC-PP1 complex. Nat Struct Biol.10(3), 175–181.

Cao, W., Song, H. J., Gangi, T., Kelkar, A., Antani, I., Garza, D., et al. (2008) Identification of novel genes that modify phenotypes induced by Alzheimer's beta-amyloid overexpression in Drosophila. Genetics, 178, 1457–1471.

Carvelli, L., Moron, JA., Kahlig, KM., Ferrer, JV., Sen, N., Lechleiter, JD et al., (2002) PI 3-kinase regulation of dopamine uptake. J. Neurochem. 81, 859–869.

Castren, E., Rantamaki, T., (2010) The role of BDNF and its receptors in depression and antidepressant drug action: Reactivation of developmental plasticity. Dev Neurobiol. 70, 289–297.

Castrén, E., Voikar, V., Rantamaki, T., (2007) Role of neurotrophic factors in depression. Curr Opin Pharmacol. 7, 18–21.

Cereda, E., Barichella, M., Cassani, E., Caccialanza, R., Pezzoli, G., (2012) Clinical features of Parkinson disease when onset of diabetes came first: a case-control study. Neurology. 78, 1507-1511.

Cereda, E., Barichella, M., Pedrolli, C., Klersy, C., Cassani, E., Caccialanza, R., et al., (2011) Diabetes and rsik of Parkinson's disease: a systematic review and meta-analysis. Diabetes Care. 34 (12), 2614–2623.

Cernotta, N., Clocchiatti, A., Florean, C., Brancolini, C., (2011) Ubiquitin-dependent degradation of HDAC4, a new regulator of random cell motility. Mol Biol Cell. 22, 278–289.

Chang, L., Karin, M., (2001) Mammalian MAP kinase signalling cascades. Nature. 410 (6824), 37-40.

Chatterjee, TK., Basford, JE., Knoll, E., Tong, WS., Blanco, V., Blomkalns, AL., (2014) HDAC9 knockout mice are protected from adipose tissue dysfunction and systemic metabolic disease during high-fat feeding. Diabetes. 63, 176–187.

Chaudhuri, KR., Schapira, AH., (2009) Non-motor symptoms of Parkinson's disease: dopaminergic pathophysiology and treatment. The Lancet Neurology. 8 (5), 464–474.

Chen, G., Bower, KA., Ma, C., Fang, S., Thiele, CJ., Luo, J., (2004) Glycogen synthase kinase 3beta (GSK3beta) mediates 6-hydroxydopamine-induced neuronal death. FASEB J. 18(10), 1162-1164.

Chen, S., Owens, GC., Makarenkova, H., Edelman, DB., (2010) HDAC6 regulates mitochondrial transport in hippocampal neurons. PloS One. 5, e10848.

Chen, SH., Wu, HM., Ossola, B., Schendzielorz, N., Wilson, BC., Chu, CH., et al, (2012) Suberoylanilide hydroxamic acid, a histone deacetylase inhibitor, protects dopaminergic neurons from neurotoxin-induced damage. Br J Pharmacol. 165, 494–505.

Chen, Y., Liang, Z., Tian, Z., Blanchard ,J., Dai, CL., Chalbot, S., (2014) Intracerebroventricular streptozotocin exacerbates Alzheimer-like changes of 3xTg-AD mice. Mol Neurobiol. 49(1), 547-562.

Chiba, K., Trevor, A., Castagnoli, N., (1984) Metabolism of the neurotoxic tertiary amine, MPTP, by brain monoamine oxidase. Biochem. Biophys. Res. Commun. 120, 574–578.

Chiu, CT., Liu, G., Leeds, P., Chuang, DM., (2011) Combined treatment with the mood stabilizers lithium and valproate produces multiple beneficial effects in transgenic mouse models of Huntington's disease. Neuropsychopharmacology. 36, 2406-2421.

Chiu, SL., Chen, CM., Cline, HT., (2008) Insulin receptor signaling regulates synapse number, dendritic plasticity, and circuit function in vivo. Neuron. 58, 708–719.

Chiueh, CC., Markey, SP., Burns, RS., Johannessen, JN., Jacobowitz, DM., Kopin, IJ., (1984) Neurochemical and behavioral effects of 1-methyl-4-phenyl-1,2,3-tetrahydropyridine (MPTP) in rat, guinea pig, and monkey. Psychopharmacol Bull. 20 (3), 548–553.

Choi, JY., Jang, EH., Park, CS., Kang, JH., (2005) Enhanced susceptibility to 1-methyl-4-phenyl-1,2,3,6-tetrahydropyridine neurotoxicity in high-fat diet-induced obesity. Free Radic Biol Med. 38, 806–816.

Choi, WS., Eom, DS., Han, BS., Kim, WK., Han, BH., Choi, EJ., et al., (2004). Phosphorylation of p38 MAPK induced by oxidative stress is linked to activation of both caspase-8- and -9-mediated apoptotic pathways in dopaminergic neurons. J Biol Chem. 279(19), 20451-20460.

Choi, WS.,Yoon, SY., Oh, TH., Choi, EJ., O'Malley, KL., Oh, YJ., (1999) Two distinct mechanisms are involved in 6-hydroxydopamine- and MPP+-induced dopaminergic neuronal cell death: role of caspases, ROS, and JNK. J. Neurosci. Res. 57, 86-94.

Choi, Y., Park, SK., Kim, HM., Kang, JS., Yoon, YD., Han, SB., et al., (2008). Histone deacetylase inhibitor KBH-A42 inhibits cytokine production in RAW 264.7 macrophage cells and in vivo endotoxemia model. Exp Mol Med. 40, 574–581.

Chou, DH., Holson, EB., Wagner, FF., Tang, AJ., Maglathlin, RL., Lewis, TA., (2012) Inhibition of histone deacetylase 3 protects beta cells from cytokine-induced apoptosis. Chem Biol. 19, 669-673.

Chriett S., (2016) Epigenetic regulations by insulin and histone deacetylase inhibitors of the insulin signaling pathway in muscle. Cellular Biology. Universite de Lyon, 1-191.

Christie, JM., Wenthold, RJ., Monaghan, DT., (1999) Insulin causes a transient tyrosine phosphorylation of NR2A and NR2B NMDA receptor subunits in rat hippocampus. J Neurochem. 72, 1523–1528.

Chuang, DM., Leng, Y., Marinova, Z., Kim, HJ., Chiu, CT., (2009) Multiple roles of HDAC inhibition in neurodegenerative conditions. Trends Neurosci. 32, 591–601.

Chun, W., Johnson, GVW., (2007) Activation of glycogen synthase kinase 3β promotes the intermolecular association of tau: the use of fluorescence resonance energy transfer microscopy. J Biol Chem. 282 (32), 23410–23417.

Churcher, I., (2006) Tau therapeutic strategies for the treatment of Alzheimer's disease. Curr. Top. Med. Chem. 6, 579–595.

Claxton, A., Baker, LD., Wilkinson, CW., Trittschuh, EH., Chapman, D., Watson, GS., et al., (2013) Sex and ApoE genotype differences in treatment response to two doses of intranasal insulin in adults with mild cognitive impairment or Alzheimer's disease. J Alzheimers Dis. 35, 789–797.

Coghlan, MP., Culbert, AA., Cross, DA., Corcoran, SL., Yates, JW., Pearce, NJ., et al., (2000) Selective small molecule inhibitors of glycogen synthase kinase-3 modulate glycogen metabolism and gene transcription. Chem. Biol. 7, 793–803.

Cohen, B., Novick, D., Rubinstein, M., (1996) Modulation of insulin activities by leptin. Science. 274, 1185–1188.

Cohen, G., Werner, P., (1994) Free radicals, oxidative stress, and neurodegeneration, In Neurodegenerative Diseases, D.B. Calne, ed. (Philadelphia:W.B.Saunders), 139–161.

Colditz, GA., Willett, WC., Stampfer, MJ., Manson, JE., Hennekens, CH., Arky, RA., et al., (1990) Weight as a risk factor for clinical diabetes in women. Am J Epidemiol. 132, 501–513.

Conde, S., Perez, DI., Martinez, A., Perez, C., Moreno, FJ., (2003) Thienyl and phenyl alphahalomethyl ketones: new inhibitors of glycogen synthase kinase (GSK-3beta) from a library of compound searching. J. Med. Chem. 46, 4631–4633.

Connor, B., Young, D., Yan, Q., Faull, RL., Synek, B., Dragunow, M., (1997) Brain-derived neurotrophic factor is reduced in Alzheimer's disease. Brain Res Mol Brain Res. 49(1-2), 71–81.

Cook, C., Gendron, TF., Scheffel, K., Carlomagno, Y., Dunmore, J., DeTure, M., et al., (2012) Loss of HDAC6, a novel CHIP substrate, alleviates abnormal tau accumulation. Hum Mol Genet. 6, 2936–2945.

Cook, DG., Leverenz, JB., McMillan, PJ., Kulstad, JJ., Ericksen, S., Roth, RA., et al., (2003) Reduced hippocampal insulin-degrading enzyme in late-onset Alzheimer's disease is associated with the apolipoprotein E-epsilon 4 allele. Am J Pathol. 162, 313-319.

Cook, AM., Mieure, KD., Owen, RD., Pesaturo, AB., Hatton, J., (2009) Intracerebroventricular administration of drugs. Pharmacotherapy. 29, 832–845.

Cornford, EM., Diep, CP., Pardridge, WM., (1985) Blood-brain barrier transport of valproic acid. J Neurochem. 44, 1541–1550.

Correia, SC., Santos, RX., Santos, MS., Casadesus, G., Lamanna, JC., Perry, G., (2013) Mitochondrial abnormalities in a streptozotocin-induced rat model of sporadic Alzheimer's disease. Curr Alzheimer Res. 10(4), 406-419.

Costello, S., Cockburn, M., Bronstein, J., Zhang, X., Ritz, B., (2009) Parkinson's disease and residential exposure to maneb and paraquat from agricultural applications in the central valley of California. Am J Epidemiol. 169, 919–992.

Cotman, CW., (2005) The role of neurotrophins in brain aging: a perspective in honor of Regino Perez-Polo. Neurochem Res. 30, 877–881.

Craft, S., (2005) Insulin resistance syndrome and Alzheimer's disease: age- and obesity-related effects on memory, amyloid, and inflammation. Neurobiol Aging.26 (1), 65-69.

Craft, S., Watson, GS., (2004) Insulin and neurodegenerative disease: shared and specific mechanisms. Lancet Neurol. 3(3), 169-178.

Credle, JJ., George, JL., Wills, J., Duka, V., Shah, K., Lee, YC., et al., (2015) GSK-3β dysregulation contributes to parkinson's-like pathophysiology with associated region-specific phosphorylation and accumulation of tau and α-synuclein. Cell Death Differ. 22(5), 838-851.

Crepaldi, L., Riccio, A., (2009) Chromatin learns to behave. Epigenetics. 4(1), 23–26.

Cross, DA., Alessi, DR., Cohen, P., Andjelkovich, M., Hemmings, BA., (1995) Inhibition of glycogen synthase kinase-3 by insulin mediated by protein kinase B. Nature. 378, 785–789.

Cuadrado-Tejedor, M., Garcia-Barroso, C., Sanzhez-Arias, J., Mederos, S., Rabal, O., Ugarte, A., et al., (2015) Concomitant histone deacetylase and phosphodiesterase 5 inhibition synergistically prevents the disruption in synaptic plasticity and it reverses cognitive impairment in a mouse model of Alzheimer's disease. Clin Epigenetics. 7, 108.

Cui, J., Shao, L., Young, LT., Wang, JF., (2007) Role of glutathione in neuroprotective effects of mood stabilizing drugs lithium and valproate. Neuroscience.144, 1447-1453.

Cummings, JL., Morstorf, T., Zhong, K., (2014) Alzheimer's disease drug-development pipeline: Few candidates, frequent failures. Alzheimer Res Therapy. 6, 37.

Czech, MP., Corvera, S., (1999) Signaling mechanisms that regulate glucose transport. J. Biol. Chem. 274, 1865–1868.

Czock, D., Keller, F., Rasche, FM., Haussler, U., (2005) Pharmacokinetics and pharmacodynamics of systematically administered glucocorticoids. Clin Pharmacokinet. 44, 61–98.

Czubryt, MP., McAnally, J., Fishman, GI., Olson, EN., (2003) Regulation of peroxisome proliferator-activated receptor gamma coactivator 1 alpha (PGC-1alpha) and mitochondrial function by MEF2 and HDAC5, Proc Natl Acad Sci USA. 100, 1711–1716.

Dajani, R., Fraser, E., Roe, SM., Young, N., Good, V., Dale, TC., (2001) Crystal structure of glycogen synthase kinase 3 beta: structural basis for phosphate-primed substrate specificity and autoinhibition. Cell. 105(6), 721-732.

Dash, PK., Orsi, SA., Zhang, M., Grill, RJ., Pati, S., Zhao, J., et al., (2010) Valproate administered after traumatic brain injury provides neuroprotection and improves cognitive function in rats. PLoS One. 5(6), e11383.

Datusalia, AK., Sharma, SS., (2014) Amelioration of diabetes-induced cognitive deficits by GSK-3β inhibition is attributed to modulation of neurotransmitters and neuroinflammation. Mol Neurobiol. 50(2), 390-405.

Dauer, W., Przedborski, S., (2003) Parkinson's disease: mechanisms and models. Neuron. 39(6), 889-909.

Davidson, EP., Coppey, LJ., Holmes, A., Dake, B., Yorek, MA., (2011) Effect of treatment of high fat fed/low dose streptozotocin-diabetic rats with Ilepatril on vascular and neural complications. Eur J Pharmacol. 668(3), 497–506.

Davis, JF., Choi, DL., Schurdak, JD., Fitzgerald, MF., Clegg, DJ., Lipton, JW., et al., (2011) Leptin regulates energy balance and motivation through action at distinct neural circuits. Biol. Psychiatry 69, 668–674.

Dayeh, T., Volkov, P., Salo, S., Hall, E., Nilsson, E., Olsson, AH., et al., (2014) Genome-Wide DNA Methylation Analysis of Human Pancreatic Islets from Type 2 Diabetic and Non-Diabetic Donors Identifies Candidate Genes That Influence Insulin Secretion. PLoS Genet. 10(3), e1004160.

De Felice, FG., Vieira, MN., Bomfim, TR., Decker, H., Velasco, PT., Lambert, MP., et al., (2009) Protection of synapses against Alzheimer's-linked toxins: insulin signaling prevents the pathogenic binding of Abeta oligomers. Proc Natl Acad Sci U S A. 106, 1971–1976.

De Jesus-Cortes, H., Miller, AD., Britt, JK., DeMarco, AJ., De Jesus-Cortes, M., Stuebing, E., (2015) Protective efficacy of P7C3-S243 in the 6- hydroxydopamine model of Parkinson's disease. NPJ Parkinsons Dis. 1.

de la Monte, SM., (2012a) Brain insulin resistance and deficiency as therapeutic targets in Alzheimer's disease. Curr Alzheimer Res. 9, 35–66.

de la Monte, SM., (2012b) Therapeutic targets of brain insulin resistance in sporadic Alzheimer's disease. Front Biosci. 4, 1582–1605.

De la Monte, SM., Wands, JR., (2005) Review of insulin and insulin-like growth factor expression, signaling, and malfunction in the central nervous system: relevance to Alzheimer's disease. J Alzheimers Dis. 7, 45–61.

de Oliveira, MR., da Rocha, RF., Stertz, L., Fries, GR., de Oliveira, DL., Kapczinski, F., (2011) Total and mitochondrial nitrosative stress, decreased brain derived neurotrophic factor (BDNF) levels and glutamate uptake, and evidence of endoplasmic reticulum stress in the hippocampusof vitamin A treated rats. Neurochem Res. 36(3), 506-517.

De Pablo-Fernandez, E., Breen, DP., Bouloux, PM., Barker, RA., Foltynie, T., Warner, TT., (2017) Neuroendocrine abnormalities in Parkinson's disease. J Neurol Neurosurg Psychiatry. 88, 176-185.

de Ruijter, AJ., van Gennip, AH., Caron, HN., Kemp, S., Van Kuilenburg, AB., (2003) Histone deacetylases (HDACs): characterization of the classical HDAC family, Biochem. J. 370, 737–749.

De Sarno, P., Li, X., Jope, RS., (2002) Regulation of Akt and glycogen synthase kinase-3 beta phosphorylation by sodium valproate and lithium. Neuropharmacology. 43, 1158–1164.

Debons, AF., Zurek, LD., Tse, CS., Abrahamsens, S., (1986) Central nervous system control of hyperphagia in hypothalamic obesity: dependence on adrenal glucocorticoids. Endocrinology. 118(4), 1678–1681.

Decker, H., Lo, KY., Unger, SM., Ferreira, ST., Silverman, MA., (2010) Amyloid-β peptide oligomers disrupt axonal transport through an NMDA receptor-dependent mechanism that is mediated by glycogen synthase kinase 3β in primary cultured hippocampal neurons. J Neurosci. 30(27) 9166–9171.

Deedwania, P., (2011) Hypertension, dyslipidemia, and insulin resistance in patients with diabetes mellitus or the cardiometabolic syndrome: benefits of vasodilating beta-blockers. J Clin Hypertens (Greenwich) 13(1), 52–59.

Delghandi, MP., Johannessen, M., Moens, U., (2005) The cAMP signalling pathway activates CREB through PKA, p38 and MSK1 in NIH 3T3 cells. Cell. Signal. 17, 1343-1351.

den Heijer, T., Vermeer, SE., van Dijk, EJ., Prins, ND., Koudstaal, PJ., Hofman, A., et al., (2003) Type 2 diabetes and atrophy of medial temporal lobe structures on brain MRI. Diabetologia. 46, 1604– 1610.

Deng, Y., Li, B., Liu, Y., Iqbal, K., Grundke-Iqbal, I., Gong, CX., (2009) Dysregulation of insulin signaling, glucose transporters, O-GlcNAcylation, and phosphorylation of tau and neurofilaments in the brain: Implication for Alzheimer's disease. Am J Pathol. 175, 2089–2098.

Deshmukh, R., Sharma, V., Mehan, S., Sharma, N., Bedi, KL., (2009) Amelioration of intracerebroventricular streptozotocin induced cognitive dysfunction and oxidative stress by vinpocetine - a PDE1 inhibitor. Eur J Pharmacol. 620, 49-56.

Didonna, A., Opal, P., (2015) The promise and perils of HDAC inhibitors in neurodegeneration. Ann Clin Transl Neurol. 2(1), 79–101.

Dimitriadis, G., Leighton, B., Parry-Billings, M., Sasson, S., Young, M., Krause, U., et al., (1997) Effects of glucocorticoid excess on the sensitivity of glucose transport and metabolism to insulin in rat skeletal muscle. Biochem J. 321, 707–712.

Dineley, KT., Jahrling, JB., Denner, L., (2014) Insulin resistance in Alzheimer's disease. Neurobiol. Dis. 72, 92–103.

Ding, H., Dolan, PJ., Johnson, GV., (2008) Histone deacetylase 6 interacts with the microtubule-associated protein tau. J Neurochem. 106, 2119–2130.

Dobbs, RJ., Charlett, A., Purkiss, AG., Dobbs, SM., Weller, C., Peterson, DW., (1999) Association of circulating TNF-α and IL-6 with ageing and parkinsonism. Acta Neurol Scand.100 (1), 34–41.

Dokken, BB., Henriksen, EJ., (2006) Chronic selective glycogen synthase kinase-3 inhibition enhances glucose disposal and muscle insulin action in prediabetic obese Zucker rats. Am J Physiol Endocrinol Metab. 291, E207–213.

Dokken, BB., Sloniger, JA., Henriksen, EJ., (2005) Acute selective glycogen synthase kinase-3 inhibition enhances insulin signaling in prediabetic insulin-resistant rat skeletal muscle. Am. J. Physiol. Endocrinol. Metab. 288, E1188-E1194.

Dou, JT., Chen, M., Dufour, F., Alkon, DL., Zhao, WQ., (2005) Insulin receptor signalling in long term memory consolidation following spatial learning. Learn Mem. 12, 646–655.

Drago, J., Murphy, M., Carroll, SM., Harvey, RP., Bartlett, PF., (1991) Fibroblast growth factor-mediated proliferation of central nervous system precursors depends on endogenous production of insulin-like growth factor I. Proc. Natl. Acad. Sci. U. S. A. 88(6), 2199–2203.

Draznin, B., (2006) Molecular Mechanisms of Insulin Resistance: Serine Phosphorylation of Insulin Receptor Substrate-1 and Increased Expression of p85α. Diabetes. 55 (8) 2392-2397.

Driver, JA., Smith, A., Buring, JE., Gaziano, JM., Kurth, T., Logroscino, G., (2008) Prospective cohort study of type 2 diabetes and the risk of Parkinson's disease. Diabetes Care. 31, 2003–2005.

Du, K., Montminy, M., (1998) CREB is a regulatory target for the protein kinase Akt/PKB. J. Biol. Chem. 273(49), 32377-32379.

Duan, R., Liu, X., Wang, T., Wu, L., Gao, X., Zhang, Z., (2016) Histone Acetylation Regulation in Sleep Deprivation-Induced Spatial Memory Impairment. Neurochem Res. 41(9), 2223-2232.

Duarte, AI., Moreira, PI., Oliveira, CR., (2012) Insulin in central nervous system: more than just a peripheral hormone. J. Aging Res. 384017.

Duckworth, WC., Kitabchi, AE., (1974) Insulin and glucagon degradation by the same enzyme. Diabetes. 23, 536–543.

Duka, T., Duka, V., Joyce, JN., Sidhu, A., (2009) Alpha-Synuclein contributes to GSK-3beta-catalyzed Tau phosphorylation in Parkinson's disease models. FASEB J. 23, 2820–2830.

Edwards,TL., Scott, WK., Almonte, C., Burt, A., Powell, EH., Beecham, GW., et al., (2010) Genome-Wide association study confirms SNPs in SNCA and the MAPT region as common risk factors for parkinson disease. Ann Hum Genet. 74 (2), 97–109.

Egan, MF., Kojima, M., Callicott, JH., Goldberg, TE., Kolachana, BS., Bertolino, A., (2003) The BDNF val66met polymorphism affects activity-dependent secretion of BDNF and human memory and hippocampal function. Cell. 112(2), 257-269.

Eldar-Finkelman, H., Argast, GM., Foord, O., Fischer, EH., Krebs, EG., (1996) Expression and characterization of glycogen synthase kinase-3 mutants and their effect on glycogen synthase activity in intact cells. Proc Natl Acad Sci USA. 93, 10228–10233.

Eldar-Finkelman, H., Krebs, EG., (1997) Phosphorylation of insulin receptor substrate 1 by glycogen synthase kinase 3 impairs insulin action. Proc Natl Acad Sci U S A. 94, 9660–9664.

Eldar-Finkelman, H., Martinez, A., (2011) GSK-3 Inhibitors: Preclinical and Clinical Focus on CNS. Front Mol Neurosci. 4, 32.

Eldar-Finkelman, H., Schreyer, SA., Shinohara, MM., LeBoeuf, RC., Krebs, EG., (1999) Increased glycogen synthase kinase-3 activity in diabetes- and obesity-prone C57BL/6J mice. Diabetes. 48, 1662-1666.

Elliott, SS., Keim, NL., Stem, JS., Teff, K., Havel, PJ., (2002) Fructose, weight gain, and the insulin resistance syndrome. Am. J. Clin. Nutr. 76, 911-922.

Ellman, GL., (1959) Tissue sulfhydryl groups. Arch Biochem Biophys. 82, 70-77.

Ellman, GL., Courtney, KD., Andres, V., Featherstone, RM., (1961) A new and rapid colorimetric determination of acetylcholinesterase activity. Biochem Pharmacol. 7, 88–95.

Embi, N., Rylatt, DB., Cohen, P., (1980). Glycogen synthase kinase-3 from rabbit skeletal muscle. Separation from cyclic-AMP-dependent protein kinase and phosphorylase kinase. Eur. J. Biochem. 107(2), 519–527.

Engel, T., Goni-Oliver, P., Lucas, JJ., Avila, J., Hernandez, F., (2006) Chronic lithium administration to FTDP-17 tau and GSK- 3β overexpressing mice prevents tau hyperphosphorylation and neurofibrillary tangle formation, but pre-formed neurofibrillary tangles do not revert. J Neurochem. 99 (6), 1445–1455.

Erol, A., (2008) An integrated and unifying hypothesis for the metabolic basis of sporadic Alzheimer's disease. J Alzheimers Dis. 13 (3), 241–253.

Evans, JL., Goldfine, ID., Maddux, BA., Grodsky, GM., (2003) Are oxidative stress-activated signaling pathways mediators of insulin resistance and β-cell dysfunction? Diabetes. 52, 1– 8.

Fain, JN., Madan, AK., Hiler, ML., Cheema, P., Bahouth, SW., (2004) Comparison of the release of adipokines by adipose tissue, adipose tissue matrix, and adipocytes from visceral and subcutaneous abdominal adipose tissues of obese humans. Endocrinology 145, 2273–2282.

Fajas, L., Fajas, V., Reiter, R., Reiter, J., Reiter, K., Debril, MB., (2002) The retinoblastoma-histone deacetylase 3 complex inhibits PPAR gamma and adipocyte differentiation. Dev Cell. 3, 903-910.

Faraco, G., Pancani, T., Formentini, L., Mascagni, P., Fossati, G., Leoni, F., (2006) Pharmacological inhibition of histone deacetylases by suberoylanilide hydroxamic acid specifically alters gene expression and reduces ischemic injury in the mouse brain. Mol Pharmacol. 70 (6), 1876-1884.

Farese, R., (2000) Diabetes Mellitus: a Fundamental and Clinical Text. LeRoith D, Taylor SI, Olefsky JM, editors. Philadelphia: Lippincott. 239–251.

Farr, SA., Yamada, KA., Butterfield, DA., Abdul, HM., Xu, L., Miller, NE., (2008) Obesity and hypertriglyceridemia produce cognitive impairment. Endocrinology. 149 (5), 2628-2636.

Farris, W., Mansourian, S., Chang, Y., Lindsley, L., Eckman, EA., Frosch, MP., et al., (2003) Insulin-degrading enzyme regulates the levels of insulin, amyloid beta-protein, and the beta-amyloid precursor protein intracellular domain in vivo. Proc Natl Acad Sci USA. 100, 4162–4167.

Fass, DM., Reis, SA., Ghosh, B., Hennig, KM., Joseph, NF., Zhao, WN., et al., (2013) Crebinostat: a novel cognitive enhancer that inhibits histone deacetylases activity and modulates chromatin-mediated neuroplasticity. Neuropharmacology. 64, 81–96.

Fawcett, J., Permana, PA., Levy, JL., Duckworth , WC., (2007) Regulation of protein degradation by insulin-degrading enzyme: analysis by small interfering RNA-mediated gene silencing. Arch Biochem Biophys. 468, 128–133.

Federico, A., Maier, A., Vianello, G., Mapelli, D., Trentin, M., Zanette, G., et al., (2015) Screening for mild cognitive impairment in Parkinson's disease. Comparison of the Italian versions of three neuropsychological tests. Parkinson's Disease 2015 (681976), 1-10.

Feng, HL., Leng, Y., Ma, CH., Zhang, J., Ren, M., Chuang, DM., (2008) Combined lithium and valproate treatment delays disease onset, reduces neurological deficits and prolongs survival in an amyotrophic lateral sclerosis mouse model. Neurosci. 155, 567-572.

Feng, ZH., Wang, TG., Li, DD., Fung, P., Wilson, BC., Liu, B., et al., (2002) Cyclooxygenase-2- deficient mice are resistant to 1-methyl-4-phenyl-1,2,3,6-tetrahydropyridine-induced damage of dopaminergic neurons in the substantia nigra. Neurosci Lett. 329-354.

Ferkey, DM., Kimelman, D., (2002) Glycogen synthase kinase-3 beta mutagenesis identifies a common binding domain for GBP and Axin. J Biol Chem. 277(18), 16147-16152.

Fernandez, AM., Torres-Aleman, I., (2012) The many faces of insulin-like peptide signalling in the brain. Nat Rev Neurosci. 13, 225–239.

Ferreira, ST., Clarke, JR., Bomfim, TR., De Felice, FG., (2014) Inflammation, defective insulin signaling, and neuronal dysfunction in Alzheimer's disease. Alzheimers Dement. 10, S76-S83.

Ferri, CP., Prince, M., Brayne, C., Brodaty, H., Fratiglioni, L., Ganguli, M., (2005) Global prevalence of dementia: a Delphi consensus study. Lancet. 366 (9503), 2112–2117.

Figlewicz, DP., Evans, SB., Murphy, J., Hoen, M., Baskin, DG., (2003) Expression of receptors for insulin and leptin in the ventral tegmental area/substantia nigra (VTA/SN) of the rat. Brain Res. 964, 107–115.

Finkbeiner, S., (2000) CREB couples neurotrophin signals to survival messages. Neuron. 25(1), 11-14.

Fiol, CJ., Williams, JS., Chou, CH., Wang, QM., Roach, PJ., Andrisani, OM., (1994) A secondary phosphorylation of CREB341 at Ser129 is required for the cAMP-mediated control of gene expression. A role for glycogen synthase kinase-3 in the control of gene expression. J Biol Chem. 269(51), 32187-32193.

Fitzsimons, HL., Schwartz, S., Given, FM., Scott, MJ., (2013). The histone deacetylase HDAC4 regulates long-term memory in Drosophila. PloS One, 8, e83903.

Fleiss, B., Nilsson, MK., Blomgren, K., (2012) Neuroprotection by the histone deacetylase inhibitor trichostatin A in a model of lipopolysaccharide-sensitised neonatal hypoxic-ischaemic brain injury. J Neuroinflammation. 9, 1-15.

Fontan-Lozano, A., Romero-Granados, R., Troncoso, J., Múnera, A., Delgado-García, JM., Carrión, AM., (2008) Histone deacetylases inhibitors improve learning consolidation in young and in KA-induced neurodegeneration and SAMP-8-mutant mice. Mol Cell Neurosci. 39, 193–201.

Forchetti, CM., (2005) Treating patients with moderate to severe Alzheimer's disease: implications of recent pharmacologic studies. Prim Care Companion J Clin Psychiatry. 7(4), 155-161.

Forno, LS., DeLanney, LE., Irwin, I., Langston, JW., (1993) Similarities and differences between MPTP-induced parkinsonsim and Parkinson's disease, Neuropathologic considerations. Adv Neurol. 60, 600–608.

Francis, YI., Fa, M., Ashraf, H., Zhang, H., Staniszewski, A., Latchman, DS., et al., (2009) Dysregulation of histone acetylation in the APP/PS1 mouse model of Alzheimer's disease. J Alzheimers Dis. 18, 131–139.

Frank, DA., Greenberg, ME., (1994) CREB: a mediator of long-term memory from mollusks to mammals. Cell. 79, 5-8.

Frey, BN., Valvassori, SS., Reus, GZ., Martins, MR., Petronilho, FC., Bardini, K., et al., (2006) Effects of lithium and valproate on amphetamine-induced oxidative stress generation in an animal model of mania. J Psychiatry Neurosci.31, 326-332.

Frolich, L., Blum-Degen, D., Riederer, P., Hoyer, S., (1999) A disturbance in the neuronal insulin receptor signal transduction in sporadic Alzheimer's disease. Ann N Y Acad Sci. 893, 290–293.

Fukumoto, T., Morinobu, S., Okamoto, Y., Kagaya, A., Yamawaki, S., (2001) Chronic lithium treatment increases the expression of brain-derived neurotrophic factor in the rat brain. Psychopharmacology (Berl). 158(1), 100-106.

Fulop, T., Larbi, A., Douziech, N., (2003) Insulin receptor and ageing. Pathologie Biologie. 51 (10), 574–580.

Funato, H., Oda, S., Yokofujita, J., Igarashi, H., Kuroda, M., (2011) Fasting and high-fat diet alter histone deacetylase expression in the medial hypothalamus. PLoS One. 6(4), e18950.

Furumai, R., Matsuyama, A., Kobashi, N., Lee, KH., Nishiyama, M., Nakajima, H., et al., (2002) FK228 (Depsipeptide) as a natural prodrug that inhibits class i histone deacetylases. Cancer Res 62, 4916–4921.

Gaikwad, AB., Viswanad, B., Ramarao, P., (2007) PPAR gamma agonists partially restores hyperglycemia induced aggravation of vascular dysfunction to angiotensin II in thoracic aorta isolated from rats with insulin resistance. Pharmacol. Res. 55(5), 400-407

Gaikwad, AB., Gupta, J., Tikoo, K., (2010) Epigenetic changes and alteration of Fbn1 and Col3A1 gene expression under hyperglycaemic and hyperinsulinaemic conditions. Biochem J. 432(2), 333-341.

Galmozzi, A., Mitro, N., Ferrari, A., Gers, E., Gilardi, F., Godio, C., (2013) Inhibition of class I histone deacetylases unveils a mitochondrial signature and enhances oxidative metabolism in skeletal muscle and adipose tissue. Diabetes. 62(3), 732-742.

Gan, L., England, E., Yang, JY., Toulme, N., Ambati, S., Hartzell, DL., et al., (2015) A 72-hour high fat diet increases transcript levels of the neuropeptide galanin in the dorsal hippocampus of the rat. BMC Neurosci. 16, 51.

Gao, J., Siddoway, B., Huang, Q., Xia, H., (2009) Inactivation of CREB mediated gene transcription by HDAC8 bound protein phosphatase. Biochem Biophys Res Commun. 379(1), 1–5.

Gao, L., Cueto, MA., Asselbergs, F., Atadja, P., (2002) Cloning and functional characterization of HDAC11, a novel member of the human histone deacetylase family. J Biol Chem. 277, 25748-25755.

Gao, X., Chen, H., Schwarzschild, MA., Ascherio, A., (2011) Use of ibuprofen and risk of Parkinson disease. Neurology. 76 (10), 863–869.

Gao, Z., He, Q., Peng, B., Peng, PJ., Ye, J., (2006) Regulation of nuclear translocation of HDAC3 by Ikappa Balpha is requirsed for tumor necrosis factor inhibition of peroxisome proliferator-activated receptor gamma function. J Biol Chem. 281, 4540–4547.

Garcia, BG., Wei Y., Moron, JA., Lin, RZ., Javitch, JA., Galli, A., (2005) Akt is essential for insulin modulation of amphetamine-induced human dopamine transporter cell-surface redistribution. Mol. Pharmacol. 68, 102–109.

Gerozissis, K., (2004) Brain insulin and feeding: a bi-directional communication. Eur J Pharmacol. 490, 59–70.

Giuntini, M., Baldacci, F., Del Prete, E., Bonuccelli, U., Ceravolo, R., (2014) Diabetes is associated with postural and cognitive domains in Parkinson's disease. Results from a single-center study. Parkinsonism Relat Disord. 20, 671-672.

Goers, J., Manning-Bog, AB., McCormack, AL., Millett, IS., Doniach, S., Di Monte, DA., et al., (2003) Nuclear localization of alpha-synuclein and its interaction with histones Biochemistry. 42, 8465–8471.

Gonzalez, GA., Montminy, MR., (1989) Cyclic AMP stimulates somatostatin gene transcription by phosphorylation of CREB at serine 133. Cell. 59(4), 675-680.

Gottlicher, M., Minucci, S., Zhu, P., Kramer, OH., Schimpf, A., Giavara, S., et al., (2001) Valproic acid defines a novel class of HDAC inhibitors inducing differentiation of transformed cells. EMBO J. 20, 6969-6978.

Goulart, BK., de Lima, MNM., de Farias, CB., Reolon, GK., Almeida, VR., Quevedo, J., et al., (2010) Ketamine impairs recognition memory consolidation and prevents learning-induced increase in hippocampal brain-derived neurotrophic factor levels. Neuroscience 167, 969–973.

Govindarajan, N., Rao, P., Burkhardt, S., Sananbenesi, F., Schlüter, OM., Bradke, F., et al., (2013) Reducing HDAC6 ameliorates cognitive deficits in a mouse model for Alzheimer's disease. EMBO Mol. Med. 5, 52–63.

Govindarajan, N., Agis-Balboa, RC., Walter, J., Sananbenesi, F., (2011) Sodium butyrate improves memory function in an Alzheimer's disease model when administered at an advanced stage of disease progression. J Alzheimers Dis. 26 (1), 187-197.

Graff, J., Rei, D., Guan, JS., Wang, WY., Seo, J., Hennig, KM., et al., (2012) An epigenetic blockade of cognitive functions in the neurodegenerating brain. Nature. 483, 222–226.

Gray, S., Kim, JK., (2011) New insights into insulin resistance in the diabetic heart. Trends Endocrinol Metab. 22, 394–403.

Grayson, DR., Kundakovic, M., Sharma, RP., (2010) Is there a future for histone deacetylase inhibitors in the pharmacotherapy of psychiatric disorders? Mol Pharmacol. 77, 126–135.

Green, LC., Wagner, DA., Glgowski, J., Skipper, PL., Wishnok, JS., Tannebaum, SR., (1982) Analysis of nitrate, nitrite and [15 N] nitrate in biological fluids. Ann Biochem Exp Med. 126, 131–135.

Grimes, CA., Jope, RS., (2001) CREB DNA binding activity is inhibited by glycogen synthase kinase-3 beta and facilitated by lithium. J Neurochem. 78(6), 1219-1232.

Groop, L., (2000) Pathogenesis of type 2 diabetes: the relative contribution of insulin resistance and impaired insulin secretion. Int J Clin Pract Suppl. 113, 3–13.

Grozinger, CM., Hassig, CA., Schreiber, SL., (1999) Three proteins define a class of human histone deacetylases related to yeast Hda1p. Proc Natl Acad Sci. USA 96, 4868-4873.

Grundke-Iqbal, I., Iqbal, K., Tung, YC., (1986) Abnormal phosphorylation of the microtubule-associated protein τ (tau) in Alzheimer cytoskeletal pathology. Proceedings of the National Academy of Sciences of the United States of America, 83 (13), 44913–44917.

Guan, HP., Ishizuka, T., Chui, PC., Lehrke, M., Lazar, MA., (2005) Corepressors selectively control the transcriptional activity of PPAR gamma in adipocytes. Genes Dev. 19, 453-461.

Guan, JS., Haggarty, SJ., Giacometti, E., Dannenberg, JH., Joseph, N., Gao, J., et al., (2009) HDAC2 negatively regulates memory formation and synaptic plasticity. Nature. 459, 55–60.

Guha, M., (2015) HDAC inhibitors still need a home run, despite recent approval. Nat Rev Drug Discov. 14, 225–226.

Gupta, BM., Bala, A., (2013) Parkinson's disease in India: An analysis of publications output during 2002-2011. International journal of nutrition, pharmacology, neurological diseases. 3(3), 254-262.

Gupta, C., Kaur, J., Tikoo, K., (2014) Regulation of MDA-MB231 cell proliferation by GSK-3β involves epigenetic modifications under high glucose conditions. Exp Cell Res. 324, 75–83.

Guridi, J., Herrero, MT., Luquin, MR., Guillén, J., Ruberg, M., Laguna, J., et al., (1996) Subthalamotomy in parkinsonian monkeys, Behavioural and biochemical analysis. Brain. 119 (5), 1717–1727.

Haass, C., Selkoe, DJ., (2007) Soluble protein oligomers in neurodegeneration: lessons from the Alzheimer's amyloid beta-peptide. Nat Rev Mol Cell Biol. 8(2), 101-112.

Halawany, AME., Sayed, NSE, Abdallah, HM., Dine, RSE., (2017) Protective effects of gingerol on Streptozotocin induced sporadic Alzheimer's disease: emphasison inhibition of β-amyloid, COX-2, alpha , beta - secretases and APH1a. Sci Rep. 7(1), 2902.

Hald, A., Lotharius, J., (2005) Oxidative stress and inflammation in Parkinson's disease: is there a causal link? Exp Neurol. 193(2), 279-290.

Hamann, M., Alonso, D., Martin-Aparicio, E., Fuertes, A., Perez-Puerto, MJ., Castro, A., (2007) Glycogen synthase kinase-3 (GSK-3) inhibitory activity and structure-activity relationship (SAR) studies of the manzamine alkaloids. Potential for Alzheimer's disease. J. Nat. Prod. 70, 1397–1405.

Hanger, DP., Hughes, K., Woodgett, JR., Brion, JP., Anderton, BH., (1992) Glycogen synthase kinase-3 induces Alzheimer's disease-like phosphorylation of tau: generation of paired helical filament epitopes and neuronal localisation of the kinase. Neurosci Lett. 147 (1), 58–62.

Hanson, JE., Deng, L., Hackos, DH., Lo, SC., Lauffer, BE., Steiner, P., et al., (2013) Histone deacetylase 2 cell autonomously suppresses excitatory and enhances inhibitory synaptic function in CA1 pyramidal neurons. J Neurosci. 33, 5924 –5929.

Haobam, R., Sindhu, KM., Chandra, G., Mohanakumar, KP., et al., (2005) Swim-test as a function of motor impairment in MPTP model of Parkinson's disease: a comparative study in two mouse strains. Behav Brain Res. 163, 159–167.

Happel, N., Stoldt, S., Schmidt, B., Doenecke, D., (2009) M phase-specific phosphorylation of histone H1.5 at threonine 10 by GSK-3. J Mol Biol. 386, 339–350.

Harada, A., Oguchi, K., Okabe, S., Kuno, J., Terada, S., Ohshima, T., et al., (1994) Altered microtubule organization in small-calibre axons of mice lacking tau protein. Nature. 369 (6480), 488–491.

Hardaway, AL., Podgorski, I., (2013) IL-1β, RAGE and FABP4: targeting the dynamic trio in metabolic inflammation and related pathologies. Future Med Chem. 5 (10) 1089–1108.

Harrison, IF., Dexter, DT., (2013) Epigenetic targeting of histone deacetylase: therapeutic potential in Parkinson's disease? Pharmacol Ther. 140, 34-52

Hart, MJ., Jiang, X., Kozasa, T., Roscoe, W., Singer, WD., Gilman, AG., (1998) Direct stimulation of the guanine nucleotide exchange activity of p115 RhoGEF by Galpha13. Science. 280(5372), 2112-2124.

Hashimoto, R., Takei, N., Shimazu, K., Christ, L., Lu, B., Chuang, DM., (2002) Lithium induces brain-derived neurotrophic factor and activates TrkB in rodent cortical neurons: an essential step for neuroprotection against glutamate excitotoxicity. Neuropharmacology. 43(7), 1173-1179.

Hassouna, I., Wickert, H., Zimmermann, M., (1996) Increase in bax expression in substantia nigra following 1-methyl-4-phenyl-1,2,3,6-tetrahydropyridine (MPTP) treatment of mice. Neurosci Lett. 204, 85–88.

Hebert, LE., Weuve, J., Scherr, PA., Evans, DA., (2013) Alzheimer disease in the United States (2010-2050) estimated using the 2010 Census. Neurology 80 (19), 1778-1783.

Henagan, TM., Stefanska, B., Fang, Z., Navard, AM., Ye, J., Lenard, NR., et al., (2015) Sodium butyrate epigenetically modulates high-fat diet-induced skeletal muscle

mitochondrial adaptation, obesity and insulin resistance through nucleosome positioning. Br J Pharmacol. 172(11), 2782-2798.

Henry, N., (2000) Ginsberg. Insulin resistance and cardiovascular disease. J Clin Invest. 106(4), 453–458.

Herman, D., Jenssen, K., Burnett, R., Soragni, E., Perlman, SL., Gottesfeld, JM., (2006) Histone deacetylase inhibitors reverse gene silencing in Friedreich's ataxia Nat. Chem. Biol. 2, 551–558.

Hernandez, F., Borrell, J., Guaza, C., Avila, J., Lucas, JJ., (2002) Spatial learning deficit in transgenic mice that conditionally over-express GSK3beta in the brain but do not form tau filaments. J Neurochem. 83(6), 1529–1533.

Hernandez-Baltazar, D., Mendoza-Garrido, ME., Martinez-Fong, D., (2013) Activation of GSK-3β and caspase-3 occurs in Nigral dopamine neurons during the development of apoptosis activated by a striatal injection of 6-hydroxydopamine. PLoS One 8, e70951.

Herrup, K., Li, J., Chen, J., (2013) The role of ATM and DNA damage in neurons: Upstream and downstream connections. DNA Repair. 12, 600–604

Hersh, L., (2006) The insulysin (insulin degrading enzyme) enigma. Cell Mol Life Sci. 63, 2432–2434.

Hirose, M., Kaneki, M., Sugita, H., Yasuhara, S., Martyn, JA., (2000) Immobilization depresses insulin signaling in skeletal muscle. Am J Physiol Endocrinol Metab. 279(6), E1235-1241.

Holmes C, Cunningham, C., Zotova, E., Woolford, J., Dean, C., Kerr, S,, et al., (2009) Systemic inflammation and disease progression in Alzheimer disease. Neurology. 73 (10), 768–774.

Hongisto, V., Vainio, JC., Thompson, R., Courtney, MJ., Coffey, ET., (2008) The Wnt pool of glycogen synthase kinase 3 beta is critical for trophic-deprivation-induced neuronal death. Mol. Cell. Biol. 28, 1515–1527.

Hongo, H., Kihara, T., Kume, T., Izumi, Y., Niidome, T., Sugimoto, H., et al., (2012) Glycogen synthase kinase-3β activation mediates rotenone-induced cytotoxicity with the involvement of microtubule destabilization. Biochem Biophys Res Commun. 426, 94–99.

Hooper, C., Killick, R., Lovestone, S., (2008) The GSK3 hypothesis of Alzheimer's disease, J Neurochem. 104, 1433-1439

Hoover, BR., Reed, MN., Su, J., Penrod, RD., Kotilinek, LA., Grant, MK., et al., (2010) Tau mislocalization to dendritic spines mediates synaptic dysfunction independently of neurodegeneration. Neuron. 68 (6), 1067–1081.

Hornykiewicz, O., Kish, S., (1987) Biochemical pathophysiology of Parkinson's disease. Adv Neurol 45, 19-34.

Hoshi, M., Sato, M., Matsumoto, S., Noguchi, A., Yasutake, K., Yoshida, N., et al., (2003) Spherical aggregates of β-amyloid (amylospheroid) show high neurotoxicity and activate tau protein kinase I/glycogen synthase kinase-3β. Proc Natl Acad Sci U S A. 100 (11), 6370–6375.

Hosp, JA., Luft, AR., (2013) Dopaminergic meso-cortical projections to m1: Role in motor learning and motor cortex plasticity. Front Neurol 4, 145.

Hotamisligil, GS., (2000) Molecular mechanisms of insulin resistance and the role of the adipocyte. Int J Obes Relat Metab Disord. 24(4) S23–S27.

Hotamisligil, GS., (2005) Role of endoplasmic reticulum stress and c-Jun NH2-terminal kinase pathways in inflammation and origin of obesity and diabetes. Diabetes. 54, S73–S78.

Howells, DW., Porritt, MJ., Wong, JY., Batchelor, PE., Kalnins, R., Hughes, AJ., et al., (2000) Reduced BDNF mRNA expression in the Parkinson's disease substantia nigra. Exp Neurol. 166, 127–135.

Hruz, PW., Mueckler, MM., (2001) Structural analysis of the GLUT1 facilitative glucose transporter (review) Mol. Membr. Biol. 18, 183–193.

Hsing, CH., Hung, SK., Chen, YC., Wei, TS., Sun, DP., Wang, JJ., et al., (2015) Histone deacetylase inhibitor trichostatin A ameliorated endotoxin induced neuro-inflammation and cognitive dysfunction. 2015, 163140.

Hu, E., Chen, Z., Fredrickson, T., Zhu, Y., Kirkpatrick, R., Zhang, GF., et al., (2000) Cloning and characterization of a novel human class I histone deacetylase that functions as a transcription repressor. J Biol Chem. 275, 15254-15264.

Hu, G., Jousilahti, P., Bidel, S., Antikainen, R., Tuomilehto, J., (2007) Type 2 diabetes and the risk of Parkinson's disease. Diabetes Care. 30, 842–847.

Hu, JF., Hamann, MT., Hill, R., Kelly, M., (2003) The manzamine alkaloids. Alkaloids Chem. Biol. 60, 207–285.

Hu, S., Begum, AN., Jones, MR., Oh, MS., Beech, WK., Beech, BH., et al., (2009) GSK3 inhibitors show benefits in an Alzheimer's disease (AD) model of neurodegeneration but adverse effects in control animals. Neurobiol. Dis. 33, 193–206.

Hu, X., Zhang, K., Xu, C., Chen, Z., Jiang, H., (2014) Anti-inflammatory effect of sodium butyrate preconditioning during myocardial ischemia/reperfusion. Exp. Ther. Med. 8, 229–232.

Hughes, AJ., Daniel, SE., Kilford, L., Lees, AJ., (1992) Accuracy of clinical diagnosis of idiopathic Parkinson's disease: a clinicopathological study of 100 cases. Journal of Neurology Neurosurgery and Psychiatry, 55 (3), 181–184.

Hunter, SJ., Garvey, WT., (1998) Insulin action and insulin resistance: diseases involving defects in insulin receptors, signal transduction, and the glucose transport effector system. Am J Med. 105, 331–345.

Hurtado, DE., Molina-Porcel, L., Carroll, JC., Macdonald, C., Aboagye, AK., Trojanowski, JQ., (2012) Selectively silencing GSK-3 isoforms reduces plaques and tangles in mouse models of Alzheimer's disease. J. Neurosci. 32, 7392–7402.

Hwang, IS., Ho, H., Hoffman, BB., Reaven, GM., (1987) Fructose-induced insulin resistance and hypertension in rats. Hypertension. 10, 512–516.

Hye, A., Kerr, F., Archer, N., Foy, C., Poppe, M., Brown, RC., et al., (2005) Glycogen synthase kinase-3 is increased in whote cells early in Alzheimer's disease. Neurosci. Lett. 373, 1–4.

Ilouz, R., Kaidanovich, O., Gurwitz, D., Eldar-Finkelman, H., (2002) Inhibition of glycogen synthase kinase-3beta by bivalent zinc ions: insight into the insulin-mimetic action of zinc. Biochem. Biophys. Res. Commun. 295, 102–106

Imahori, K., Uchida, T., (1997) Physiology and pathology of tau protein kinases in relation to Alzheimer's disease. J Biochem. (Tokyo). 121, 179–188.

Imamura, K., Hishikawa, N., Sawada, M., Nagatsu, T., Yoshida, M., Hashizume, Y., (2003) Distribution of major histocompatibility complex class II-positive microglia and cytokine profile of Parkinson's disease brains. Acta Neuropathol. 106, 518–526.

Impey, S., Smith, DM., Obrietan, K., Donahue, R., Wade, C., Storm, DR., (1998) Stimulation of cAMP response element (CRE)-mediated transcription during contextual learning. Nat Neurosci. 1, 595-601.

in 't Veld, BA., Launer, LJ., Hoes, AW., Ott, A., Hofman, A., Breteler, MM., et al., (1998) NSAIDs and incident Alzheimer's disease. The Rotterdam Study. Neurobiol Aging. 19 (6), 607–611.

Inden, M., Kitamura, Y., Takeuchi, H., Yanagida, T., Takata, K., Kobayashi, Y., (2007) Neurodegeneration of mouse nigrostriatal dopaminergic system induced by repeated oral administration of rotenone is prevented by 4-phenylbutyrate, a chemical chaperone. J Neurochem. 101, 1491–1504.

Inoguchi, T., Li, P., Umeda, F., Yu, HY., Kakimoto, M., Imamura, M., et al., (2000) High glucose level and free fatty acid stimulate reactive oxygen species production through protein kinase C-dependent activation of NAD(P)H oxidase in cultured vascular cells. Diabetes. 49(11), 1939–1945.

Intlekofer, KA., Berchtold, NC., Malvaez, M., Carlos, AJ., McQuown, SC., Cunningham, MJ., et al., (2013) Exercise and sodium butyrate transform a subthreshold learning event into long-term memory via a brain- derived neurotrophic factor-dependent mechanism. Neuropsychopharmacology, 38, 2027–2034.

Ishimaru, N., Fukuchi, M., Hirai, A., Chiba, Y., Tamura, T., Takahashi, N., et al., (2010) Differential epigenetic regulation of BDNF and NT-3 genes by trichostatin A and 5-aza-2 -deoxycytidine in Neuro-2a cells. Biochem Biophys Res Commun. 394,173–177.

Itani, SI., Ruderman, NB., Schmieder, F., Boden, G., (2002) Lipid-induced insulin resistance in human muscle is associated with changes in diacylglycerol, protein kinase C, and IκB-α Diabetes. 51(7), 2005–2011.

Ittner, A., Ke, YD., Van Eersel, J., Gladbach, A., Gotz, J., Ittner, LM., (2011) Brief update on different roles of tau in Neurodegeneration. IUBMB Life. 63 (7), 495–502.

Iuchi, T., Akaike, M., Mitsui, T., Ohshima, Y., Azuma, H., Matsumoto, T., (2003) Glucocorticoid excess induces superoxide production in vascular endothelial cells and elicits vascular endothelial dysfunction. Circ Res. 92, 81–87.

Iyer, A., Fenning, A., Lim, J., Le, GT., Reid, RC., Halili, MA., et al., (2010) Antifibrotic activity of an inhibitor of histone deacetylases in DOCA-salt hypertensive rats. Br J Pharmacol. 159 (7), 1408-1417.

Jacobsen, JP., Mork, A., (2004) The effect of escitalopram, desipramine, electroconvulsive seizures and lithium on brain-derived neurotrophic factor mRNA and protein expression in the rat brain and the correlation to 5-HT and 5-HIAA levels. Brain Res. 1024(1-2), 183-192.

Janssen, C., Schmalbach, S., Boeselt, S., Sarlette, A., Dengler, R., Petri, S., et al., (2010) Differential histone deacetylase mRNA expression patterns in amyotrophic lateral sclerosis. J Neuropathol Exp Neurol. 69, 573-581.

Javitch, JA., D'Amato, RJ., Strittmatter, SM., Snyder, SH., (1985) Parkinsonism-inducing neurotoxin, N-methyl-4-phenyl-1,2,3,6-tetrahydropyridine: uptake of the metabolite N-methyl-4-phenylpyridine by dopamine neurons explains selective toxicity. Proc Natl Acad Sci U S A. 82, 2173–2177.

Jenner, P., (2008) Molecular mechanisms of L-DOPA-induced dyskinesia. Nat Rev Neurosci. 9(9), 665-677.

Jia, H., Morris, CD., Williams, RM., Loring, JF., Thomas, EA., (2015) HDAC inhibition imparts beneficial transgenerational effects in Huntington's disease mice via altered DNA and histone methylation. Proc Natl Acad Sci U S A. 112(1), E56-64

Jia, H., Pallos, J., Jacques, V., Lau, A., Tang, B., Cooper, A., (2012) Histone deacetylase (HDAC) inhibitors targeting HDAC3 and HDAC1 ameliorate polyglutamine-elicited phenotypes in model systems of Huntington's disease. Neurobiol Dis. 46(2), 351-361.

Jianping, Y., (2013) Improving Insulin Sensitivity With HDAC Inhibitor. Diabetes 62, 685-687.

Kahn, CR., White, MF., (1988) The insulin receptor and the molecular mechanism of insulin action. J Clin Invest. 82, 1151-1156.

Kahn, SE., Hull, RL., Utzschneider, KM., (2006) Mechanisms linking obesity to insulin resistance and type 2 diabetes. Nature. 444 (7121), 840–846.

Kahn, SE., (2000) The importance of the beta-cell in the pathogenesis of type 2 diabetes mellitus. Am J Med. 108, 2S– 8S.

Kaiser, C., James, SR., (2004) Acetylation of insulin receptor substrate-1 is permissive for tyrosine phosphorylation. BMC Biol 2, 23.

Kanoski, SE., Meisel, RL., Mullins, AJ., Davidson, TL., (2007) The effects of energy-rich diets on discrimination reversal learning and on BDNF in the hippocampus and prefrontal cortex of the rat. Behav Brain Res. 182(1), 57–66.

Kao, HY., Lee, CH., Komarov, A., Han, CC., Evans, RM., (2002) Isolation and characterization of mammalian HDAC10, a novel histone deacetylase. J Biol Chem. 277, 187-193.

Kao, SY., (2009) Rescue of alpha-synuclein cytotoxicity by insulin-like growth factors. Biochem. Biophys. Res. Commun. 385, 434–438.

Karagiannis, TC., El-Osta, A., (2007) Will broad-spectrum histone deacetylase inhibitors be superseded by more specific compounds? Leukemia. 21, 61-65.

Karunakaran, S., Saeed, U., Mishra, M., Valli, RK., Joshi, SD., Meka, DP., et al., (2008) Selective activation of p38 mitogen-activated protein kinase in dopaminergic neurons of substantianigra leads to nuclear translocation of p53 in 1-methyl-4-phenyl 1,2,3,6-tetrahydropyridine-treated mice. J Neurosci. 28, 12500–12509.

Kawamori, R., (1996) Insulin resistance seen in non-insulin dependent diabetes mellitus and hypertension. Hypertens Res. 19, S61–S64.

Kazantsev, AG., Thompson, LM., (2008) Therapeutic application of histone deacetylase inhibitors for central nervous system disorders. Nat Rev Drug Discov. 7(10), 854-868.

Kernie, SG., Liebl, DJ., Parada, LF., (2000) BDNF regulates eating behavior and locomotor activity in mice. EMBO J. 19, 1290–1300.

Kernochan, LE., Russo, ML., Woodling, NS., Huynh, TN., Avila, AM., Fischbeck, KH., et al., (2005) The role of histone acetylation in SMN gene expression Hum. Mol. Genet. 14, 1171–1182.

Khan, MB., Khan, MM., Khan, A., Ahmed, ME., Ishrat, T., Tabassum, R., et al., (2012) Naringenin ameliorates Alzheimer's disease (AD)-type neurodegeneration with cognitive impairment (AD-TNDCI) caused by the intracerebroventricular-streptozotocin in rat model. Neurochem Int. 61, 1081-1093.

Khan, N., Jeffers, M., Kumar, S., Hackett, C., Boldog, F., Khramtsov, N., et al., (2008) Determination of the class and isoform selectivity of small-molecule histone deacetylase inhibitors. Biochem J. 409, 581–589.

Khandelwal, PJ., Dumanis, SB., Feng, LR., Maguire-Zeiss, K., Rebeck, G., et al., (2010) Parkinson related parkin reduces α-synuclein phosphorylation in a gene transfer model. Mol Neurodegener. 5(1), 47.

Kidd, SK., Schneider, JS., (2010) Protection of dopaminergic cells from MPP+-mediated toxicity by histone deacetylase inhibition. Brain Res. 1354, 172-178.

Kidd, SK., Schneider, JS., (2011) Protective effects of valproic acid on the nigrostriatal dopamine system in a 1-methyl-4-phenyl-1,2,3,6-tetrahydropyridine mouse model of Parkinson's disease. Neuroscience. 194, 189–194.

Kim, HD., Jeong, KH., Jung, UJ., Kim, SR., (2016) Myricitrin Ameliorates 6-Hydroxydopamine-Induced Dopaminergic Neuronal Loss in the Substantia Nigra of Mouse Brain. J Med Food. 19(4), 374-382.

Kim, HJ., Leeds, P., Chuang, DM. (2009) The HDAC inhibitor, sodium butyrate, stimulates neurogenesis in the ischemic brain. J. Neurochem 110, 1226–1240.

Kim, MS., Akhtar, MW., Adachi, M., Mahgoub, M., Bassel-Duby, R., Kavalali, ET., et al., (2012) An essential role for histone deacetylase 4 in synaptic plasticity and memory formation. J. Neurosci. 32, 10879–10886.

King, TD., Bijur, GN., Jope, RS., (2001) Caspase-3 activation induced by inhibition of mitochondrial complex I is facilitated by glycogen synthase kinase-3β and attenuated by lithium. Brain Res. 919, 106–114.

King, TD., Clodfelder-Miller, B., Barksdale, KA., Bijur, GN., (2008) Unregulated mitochondrial GSK3beta activity results in NADH: ubiquinone oxidoreductase deficiency. Neurotox Res. 14, 367–382.

Kirshennboim, N., Plotkin, B., Ben Shlomo, S., Kaidanovich-Beilin, O., Eldar-Finkelman, H., (2004). Lithium-mediated phosphorylation of glycogen synthase kinase-3 involves PI3 Kinase-dependent activation of protein kinase Calpha. J. Mol. Neurosci. 24(2), 199–207.

Kivipelto, M., Ngandu, T., Fratiglioni, L., Viitanen, M., Kareholt, I., Winblad, B., et al., (2005) Obesity and vascular risk factors at midlife and the risk of dementia and Alzheimer disease. Arch Neurol.62(10), 1556-1560.

Klein, PS., Melton, DA., (1996) A molecular mechanism for the effect of lithium on development. Proc Natl Acad Sci U S A. 93(16), 8455-8459.

Klemm, DJ., Roesler, WJ., Boras, T., Colton, LA., Felder, K., Reusch, JE., (1998) Insulin stimulates cAMP- response element binding protein activity in HepG2 and 3T3-L1 celllines. J Biol Chem. 273(2), 917-923.

Klockener, T., Hess, S., Belgardt, BF., Paeger, L., Verhagen, LA., Husch, A., (2011) High-fat feeding promotes obesity via insulin receptor/PI3K-dependent inhibition of SF-1 VMH neurons. Nat Neurosci. 14(7), 911-918.

Knight, EM., Martins, IV., Gumusgoz, S., Allan, SM., Lawrence, CB., (2014) High-fat diet-induced memory impairment in triple transgenic Alzheimer's disease (3xTgAD) miceis independent of changes in amyloid and tau pathology. Neurobiol Aging. 35(8), 1821-1832.

Kockeritz, L., Doble, B., Patel, S., Woodgett, JR., (2006). Glycogen synthase kinase-3 – an overview of an over-achieving protein kinase. Curr. Drug Targets 7, 1377–1388.

Koh, SH., Lee, YB., Kim, KS., Kim, HJ., Kim, M., Lee, YJ., et al., Role of GSK-3β activity in motor neuronal cell death induced by G93A or A4V mutant hSOD1 gene, Eur J Neurosci. 22 (2005) 301–309.

Koh, SH., Noh, MY., Kim, SH., (2008) Amyloid-beta-induced neurotoxicity is reduced by inhibition of glycogen synthase kinase-3. Brain Res. 1188, 254–262.

Konner, AC., Brüning, JC., (2012) Selective insulin and leptin resistance in metabolic disorders. Cell Metab. 16(2), 144- 152.

Kontopoulos, E., Parvin, JD., Feany, MB., (2006) Alpha-synuclein acts in the nucleus to inhibit histone acetylation and promote neurotoxicity Hum. Mol. Genet., 15, 3012–3023.

Kopin, J., Markey, SP., (1988) MPTP toxicity: implications for research in Parkinson's disease. Annu Rev Neurosci. 11, 81–96.

Koppel, I., Timmusk, T., (2013) Differential regulation of Bdnf expression in cortical neurons by class-selective histone deacetylase inhibitors. Neuropharmacology 75, 106–115.

Korach-Andree, M., Gao, J., Gounarides, J., Deacon, R., Islam, A., Laurent, D., (2005) Relationship between visceral adiposity and intramyocellular lipid content in two models of insulin resistance. Am J Physiol Endocrinol Metab. 288, E106–E116.

Kotagal, V., Albin, RL., Müller, ML., Koeppe, RA., Frey, KA., Bohnen, NI., (2013) Diabetes is associated with postural instability and gait difficulty in Parkinson disease. Parkinsonism Relat Disord. 19(5), 522–526.

Kowal, SL., Dall, TM., Chakrabarti, R., Storm, MV., Jain, A., (2013) The Current and Projected Economic Burden of Parkinson's Disease in the United States. Movement Disorders. 28 (3), 311-318.

Kozikowski, AP., Chen, Y., Subhasish, T., Lewin, NE., Blumberg, PM., Zhong, Z., et al., (2009) Searching for disease modifiers-PKC activation and HDAC inhibition - a dual drug approach to Alzheimer's disease that decreases Abeta production while blocking oxidative stress. ChemMedChem. 4, 1095–1105.

Kozikowski, AP., Gaisina, IN., Petukhov, PA., Sridhar, J., King, LT., Blond, SY., et al., (2006) Highly potent and specific GSK-3β inhibitors that block tau phosphorylation and decrease α-synuclein protein expression in a cellular model of Parkinson's disease. ChemMedChem. 1 (2), 256–266.

Koziorowski, D., Tomasiuk, R., Szlufik, S., Friedman, A., (2012) Inflammatory cytokines and NT-proCNP in Parkinson's disease patients. Cytokine. 60 (3), 762–766.

Kozlovsky, N., Amar, S., Belmaker, RH., Agam, G., (2006) Psychotropic drugs affect Ser9-phosphorylated GSK-3beta protein levels in rodent frontal cortex. Int J Neuropsychopharmacol. 9, 337–342.

Krabbe, KS., Nielsen, AR., Krogh-Madsen, R., Plomgaard, P., Rasmussen, P., Erikstrup, C., (2007) Brain-derived neurotrophic factor (BDNF) and type 2 diabetes. Diabetologia. 50(2), 431-438.

Kraegen, EW., Clark, PW., Jenkins, AB., Daley, EA., Chisholm, DJ., Storlien, LH., (1991) Development of muscle insulin resistance after liver insulin resistance in high-fat-fed rats. Diabetes. 40(11), 1397-1403.

Kulich, SM., Chu, CT., (2001) Sustained extracellular signal-regulated kinase activation by 6-hydroxydopamine: Implications for Parkinson's disease. J Neurochem. 77, 1058–1066.

Kumar, A., Choi, KH., Renthal, W., Tsankova, NM., Theobald, DE., Truong, HT., et al., (2005). Chromatin remodeling is a key mechanism underlying cocaine induced plasticity in striatum. Neuron. 48, 303–314.

Kumar, A., Sharma, S., Prashar, A., Deshmukh, R., (2015) Effect of licofelone- a dual cox/5-lox inhibitor in intracerebroventricular streptozotocin-induced behavioral and biochemical abnormalities in rats. J Mol Neurosci. 55(3),749-759.

Kumar, K., Thomas, B., Sreedharan, S., (2016) Inhibition of Histone Deacetylase 3 Restores Amyloid-β Oligomer-Induced Plasticity Deficit in Hippocampal CA1 Pyramidal Neurons. J Alzheimers Dis. 51(3), 783-791.

Kwok, RPS., Lundblad, JR., Chrivia, JC., Richards, JP., Bachlinger, HP., Brennan, RG., et al., (1994) Nuclear protein CBP is a coactivator for the transcription factor CREB. Nature. 370, 223-229.

Kwon, P., Hsu, M., Cohen, D., Atadja, P., (2006) HDAC Inhibitors. In: Verdin E. (eds) Histone Deacetylases. Cancer Drug Discovery and Development. Humana Press.

Lamarre, M., Desrosiers, RR., (2008) Up-regulation of protein l-isoaspartyl methyltransferase expression by lithium is mediated by glycogen synthase kinase-3 inactivation and beta-catenin stabilization. Neuropharmacology. 55, 669–676.

Lang, B., Alrahbeni, TM., Clair, DS., Blackwood, DH., (2011) International Schizophrenia Consortium. HDAC9 is implicated in schizophrenia and expressed specifically in post-mitotic neurons but not in adult neural stem cells. Am J Stem Cells.1(1), 31-41.

Langley, B., D'Annibale, MA., Suh, K., Ayoub, I., Tolhurst, A., Bastan, B., et al., (2008) Pulse inhibition of histone deacetylases induces complete resistance to oxidative death in cortical neurons without toxicity and reveals a role for cytoplasmic p21(waf1/cip1) in cell cycle-independent neuroprotection. J Neurosci. 28, 163–176.

Langston, JW., Ballard, P., Tetrud, JW., Irwin, I., (1983) Chronic parkinsonism in humans due to a product of meperidine-analog synthesis. Science. 219 (4587), 979–980.

Langston, JW., Irwin, I., (1986) MPTP: current concepts and controversies. Clin Neuropharmacol. 9 (6), 485–507.

Laron, Z., (2009) Insulin and the brain. Arch Physiol Biochem.115 (2), 112–116.

Laske, C., Stransky, E., Leyhe, T., Eschweiler, GW., Wittorf, A., Richartz, E., et al., (2006) Stage-dependent BDNF serum concentrations in Alzheimer's disease. J Neural Transm. 113, 1217–1224.

Lau, KF., Miller, CCJ., Anderton, BH., Shaw, PC., (1999) Expression analysis of glycogen synthase kinase-3 in human tissues. J Pept Res. 54(1), 85–91.

Lawrence, JC Jr., Roach, PJ., (1997) New insights into the role and mechanism of glycogen synthase activation by insulin. Diabetes. 46, 541–547.

Le, LS., Simard, G., Martinez, MC., Andriantsitohaina, R., (2014) Oxidative stress and metabolic pathologies: From an adipocentric point of view. Oxid Med Cell Longev. 2014, 908539.

Leal, G., Afonso, PM., Salazar,IL., Duarte, CB., (2015) Regulation of hippocampal synaptic plasticity by BDNF Brain Res. 1621, 82–101.

LeClerc, S., Garnier, M., Hoessel, R., Marko, D., Bibb, JA., Snyder, GL., et al., (2001) Indirubins inhibit glycogen synthase kinase-3β and CDK5/P25, two protein kinases involved in abnormal tau phosphorylation in Alzheimer's disease. A property common to most cyclin-dependent kinase inhibitors? J Biol Chem. 276(1), 251-260.

Lee, BC., Lee, J., (2014) Cellular and molecular players in adipose tissue inflammation in the development of obesity-induced insulin resistance. Biochimica et Biophysica Acta-Molecular Basis of Disease. 1842 (3), 446–462.

Lee, CC., Huang, CC., Wu, MY., Hsu, KS., (2005) Insulin stimulates postsynaptic density-95 protein translation via the phosphoinositide 3-kinase-Akt-mammalian target of rapamycin signaling pathway. J Biol Chem. 280, 18543–18550.

Lee, HK., Kumar, P., Fu, Q., Rosen, KM., Querfurth, HW., (2009) The insulin/Akt signaling pathway is targeted by intracellular β-amyloid. Mol Biol Cell. 20, 1533–1544.

Lee, IT., Chiu, YF., Hwu, CM., He, CT., Chiang, FT., Lin, YC., et al., (2012) Central obesity is important but not essential component of the metabolic syndrome for predicting diabetes mellitus in a hypertensive family-based cohort. Results from the Stanford Asia pacific program for hypertension and insulin resistance (SAPPHIRe) Taiwan follow-up study. Cardiovasc Diabetol. 11, 43.

Lee, J., Pilch, PF., (1994) The insulin receptor: structure, function, and signaling. Am J Physiol. 266, C319-C334.

Lee, KY., Koh, SH., Noh, MY., Park, KW., Lee, YJ., Kim, SH., (2007) Glycogen synthase kinase-3*β* activity plays very important roles in determining the fate of oxidative stress-inflicted neuronal cells. Brain Research. 1129(1), 89–99.

Lee, VMY., Goedert, M., Trojanowski, JQ., (2001) Neurodegenerative tauopathies. Annu Rev Neurosci. 4, 1121–1159.

Lei, P., Ayton, S., Bush, AI., Adlard, PA., (2011) GSK-3 in neurodegenerative diseases. Int. J. Alzheimers Dis. 2011, 189246.

Lei, P., Ayton, S., Finkelstein, DI., Adlard, PA., Masters, CL., Bush, AI., (2010) Tau protein: relevance to Parkinson's disease. Int J Biochem Cell Biol. 42 (11), 1775–1778.

Leng, Y., Liang, MH., Ren, M., Marinova, Z., Leeds, P., Chuang, DM., (2008) Synergistic neuroprotective effects of lithium and valproic acid or other histone deacetylase inhibitors in neurons: roles of glycogen synthase kinase-3 inhibition. J Neurosci. 28, 2576–2588.

Leoni, F., Zaliani, A., Bertolini, G., Porro, G., Pagani, P., Pozzi, P., et al., (2002) The antitumor histone deacetylase inhibitor suberoylanilide hydroxamic acid exhibits antiinflammatory properties via suppression of cytokines. Proc Natl Acad Sci USA. 99, 2995–3000.

Leroy, K., Yilmaz, Z., Brion, JP., (2007) Increased level of active GSK-3beta in Alzheimer's disease and accumulation in argyrophilic grains and in neurones at different stages of neurofibrillary degeneration, Neuropathol. Appl. Neurobiol. 33, 43–55.

Levenson, JM., Sweatt, JD., (2005) Epigenetic mechanisms in memory formation. Nat Rev Neurosci. 6(2), 108–118.

Li, J., Chen, J., Ricupero, CL., Hart, RP., Schwartz, MS., Kusnecov, A., et al. (2012). Nuclear accumulation of HDAC4 in ATM deficiency promotes neurodegeneration in ataxia telangiectasia. Nature Medicine. 18, 783–790.

Li, L., Li, X., Zhou, W., Messina, JL., (2013) Acute psychological stress results in the rapid development of insulin resistance. J Endocrinol. 217, 175–184.

Li, T., Paudel, HK., (2006) Glycogen synthase kinase 3β phosphorylates Alzheimer's disease-specific Ser396 of microtubule-associated protein tau by a sequential mechanism. Biochemistry.45 (10), 3125–3133.

Li, Y., Perry, T., Kindy, MS., Harvey, BK., Tweedie, D., Holloway, HW., et al. (2009) GLP-1 receptor stimulation preserves primary cortical and dopaminergic neurons in cellular and rodent models of stroke and Parkinsonism. Proc. Natl. Acad. Sci. U.S.A. 106, 1285–1290.

Liberman, Z., Eldar-Finkelman, H., (2005) Serine 332 phosphorylation of insulin receptor substrate-1 by glycogen synthase kinase-3 attenuates insulin signaling. J. Biol. Chem. 280, 4422-4428.

Lingohr, MK., Buettner, R., Rhodes, CJ., (2002) Pancreatic beta-cell growth and survival – a role in obesity-linked type 2 diabetes? Trends Mol Med. 8, 375–384.

Lisman, J., Grace, AA., Duzel, E., (2011) A neohebbian framework for episodic memory; role of dopamine-dependent late ltp. Trends Neurosci 34, 536–547.

Liu, H., Zhang, JJ., Li, X., (2015) Post-occlusion administration of sodium butyrate attenuates cognitive impairment in a rat model of chronic cerebral hypoperfusion. Pharmacol Biochem Behav. 135, 53-59.

Liu, Q., (2005) Pioglitazone can ameliorate insulin resistance in low-dose streptozotocin and high sucrose-fat diet induced obese rats. Acta Pharmacol Sin. 26, 575–580.

Liu, Y., Liu, F., Grundke-Iqbal, I., Iqbal, K., Gong, CX., (2011) Deficient brain insulin signalling pathway in Alzheimer's disease and diabetes. J Pathol. 225(1), 54-62.

Lombardi, PM., Cole, KE., Dowling, DP., Christianson, DW., (2011) Structure, mechanism, and inhibition of histone deacetylases and related metalloenzymes. Curr Opin Struct Biol. 21(6), 735-743.

Loscher, W., Fisher, JE., Nau, H., Hönack, D., (1989) Valproic acid in amygdala-kindled rats: alterations in anticonvulsant efficacy, adverse effects and drug and metabolite levels in various brain regions during chronic treatment. J Pharmacol Exp Ther. 250, 1067–1078.

Lotharius, J., Brundin, P., (2002a) Impaired dopamine storage resulting from alpha-synuclein mutations may contribute to the pathogenesis of Parkinson's disease. Hum. Mol. Genet. 11 (20), 2395–2407.

Lotharius, J., Brundin, P., (2002b) Pathogenesis of Parkinson's disease: dopamine, vesicles and alpha-synuclein. Nat. Rev. Neurosci. 3(12), 932–942.

Lotharius, J., Dugan, LL., O'Malley, KL., (1999) Distinct mechanisms underlie neurotoxin-mediated cell death in cultured dopaminergic neurons. J. Neurosci. 19(4), 1284-1293.

Lowry, OH., Rosebrough, NJ., Farr, AL., Randall RJ (1951) Protein measurement with the Folin phenol reagent. J Biol Chem. 193, 265-275.

Lozano, I., Van der Werf, R., Bietiger, W., Seyfritz, E., Peronet, C., Pinget, M., (2016) High-fructose and high-fat diet-induced disorders in rats: impact on diabetes risk, hepatic and vascular complications. Nutr Metab (Lond). 13, 15.

Lu, J., McKinsey, TA., Nicol, RL., Olson, EN., (2000) Signal-dependent activation of the MEF2 transcription factor by dissociation from histone deacetylases. Proceedings of the National Academy of Sciences USA. 97, 4070–4075

Lu, J., Nicol, RL., Olson, EN., (2000) Signal-dependent activation of the MEF2 transcription factor by dissociation from histone deacetylases, Proc Natl Acad Sci USA. 97, 4070–4075.

Lu, Q., Yang, YT., Chen, CS., Davis, M., Byrd, JC., Etherton, MR., et al., (2003) Zn2+-chelating motif-tethered short-chain fatty acids as a novel class of histone deacetylase inhibitors. J Med Chem. 47, 467–474.

Lucas, JJ., Hernandez, F., Gomez-Ramos, P., Moran, MA., Hen, R., Avila, J., et al., (2001) Decreased nuclear beta-catenin, tau hyperphosphorylation and neurodegeneration in GSK-3beta conditional transgenic mice. EMBO J. 20, 27-39.

Luchsinger, JA., Tang, MX., Shea, S., Mayeux, R., (2004). Hyperinsulinemia and risk of Alzheimer disease. Neurology. 63, 1187–1192.

Lucio-Eterovic, AK., Cortez, MA., Valera, ET., Motta, FJ., Queiroz, RG., Machado, HR., et al., (2008) Differential expression of 12 histone deacetylase (HDAC) genes in astrocytomas and normal brain tissue: class II and IV are hypoexpressed in glioblastomas. BMC Cancer. 8, 1-10.

Lukic, L., Lalic, NM., Rajkovic, N., Jotic, A., Lalic, K., Milicic, T., et al., (2014) Hypertension in obese type 2 diabetes patients is associated with increases in insulin resistance and IL-6 cytokine levels: potential targets for an efficient preventive intervention. Int J Environ Res Public Health. 11 (4), 3586–3598.

Lundh, M., Galbo, T., Poulsen, SS., Mandrup-Poulsen, T., (2015) Histone deacetylase 3 inhibition improves glycaemia and insulin secretion in obese diabetic rats. Diabetes Obes Metab. 17(7), 703-707.

Luo, S., Liang, Y., Cincotta, AH., (1999) Intracerebroventricular administration of bromocriptine ameliorates the insulin-resistant/glucose-intolerant state in hamsters. Neuroendocrinology 69, 160–166.

Luong, TN., Carlisle, HJ., Southwell, A., Patterson, PH., (2010) Assessment of motor balance and coordination in mice using the balance beam. Journal of visualized experiments: JoVE. 49, 218-228.

Luthman, J., Fredriksson, A., Sundstrom, E., Jonsson, G., Archer, T., (1995) Selective lesion of central dopamine or noradrenaline neuron systems in the neonatal rat:motor behaviour and monoamine alteration satadult stage. Behav. Brain Res. 33, 267–277.

Ma, QL., Lim, GP., Harris-White, ME., Yang, F., Ambegaokar, SS., Ubeda, OJ., et al., (2006) Antibodies against β-amyloid reduce Aβ oligomers, glycogen synthase kinase-3β activation and τ phosphorylation in vivo and in vitro. J Neurosci Res. 83 (3), 374–384.

Magarinos, AM., Mcewen, BS., (2000) Experimental diabetes in rats causes hippocampal dendritic and synaptic reorganization and increased glucocorticoid reactivity to stress Proc. Natl. Acad. Sci. U. S. A. 97, 11056–11061.

Maier, VH, Gould, GW., (2000) Long term insulin treatment of 3T3-L1 adipocytes results in mis-targeting of GLUT4: implications for insulin-stimulated glucose transport. Diabetologia. 43(10), 1273–1281.

Maithilikarpagaselvi, N., Sridhar, MG., Swaminathan, RP., Zachariah, B., (2016) Curcumin prevents inflammatory response, oxidative stress and insulin resistance in high fructose fed male Wistar rats: potential role of serine kinases. Chem Biol Interact. 244, 187–194.

Maitra, SK., Rowland Payne, CM., (2004) The obesity syndrome and acanthosis nigricans. Acanthosis nigricans is a common cosmetic problem providing epidemiological clues to the obesity syndrome, the insulin-resistance syndrome, the thrifty metabolism,

dyslipidaemia, hypertension and diabetes mellitus type II. J Cosmet Dermatol. 3, 202–210.

Majid, T., Griffin, D., Criss, Z., Jarpe, M., Pautler, RG., (2015) Pharmocologic treatment with histone deacetylase 6 inhibitor (ACY-738) recovers Alzheimer's disease phenotype in amyloid precursor protein/presenilin 1 (APP/PS1) mice. Alzheimer's & Dementia: Translational Research & Clinical Interventions 1(3), 170-181

Mandelkow, EM., Mandelkow, E., (2012) Biochemistry and cell biology of tau protein in neurofibrillary degeneration. Cold Spring Harbor Perspect Med. 6, a006247.

Mangialasche, F., Polidori, MC., Monastero, R., Ercolani, S., Camarda, C., Cecchetti, R., (2009) Biomarkers of oxidative and nitrosative damage in Alzheimer's disease and mild cognitive impairment. Aging Res Rev. 8, 285-305.

Maranzano, E., Feyer, P., Molassiotis, A., Rossi, R., Clark-Snow, R., Olver, I., et al., (2005) Evidence-based recommendations for the use of antiemetics in radiotherapy. Radiother Oncol. 76, 227–233.

Margolis, RU., Altszuler, N., (1967) Insulin in the cerebrospinal fluid. Nature. 215, 5108, 1375–1376.

Markesbery, RS., Kamat, PK., Nath, C., Shukla, R., (2012) A study on neuroinflammation and NMDA receptor function in STZ (ICV) induced memory impaired rats. J Neuroimmunol. 254, 1-9.

Markey, SP., Johannessen, JN., Chiueh, CC., Burns, RS., Herkenham, MA., (1984) Intraneuronal generation of a pyridinium metabolite may cause drug-induced Parkinsonism. Nature. 311 (5985), 464–466.

Marks, PA., Breslow, R., (2007) Dimethyl sulfoxide to vorinostat: development of this histone deacetylase inhibitor as an anticancer drug. Nat Biotechnol. 25, 84–90.

Marks, PA., Richon, VM., Miller, T., Kelly, WK., (2004) Histone deacetylase inhibitors. Adv Cancer Res.91, 137–168.

Marlatt, MW., Lucassen, PJ., Perry, G., Smith, MA., Zhu, X., (2008) Alzheimer's disease: cerebrovascular dysfunction, oxidative stress, and advanced clinical therapies.J Alzheimers Dis. 15, 199-210.

Martin, GE., Myers, RD., Newberg, DC., (1976) Catecholamine release by intracerebral perfusion of 6 hydroxydopamine and desipramine. Eur J Pharmacol. 36(2), 299-311.

Martinez, A., Alonso, M., Castro, A., Perez, C., Moreno, FJ., (2002) First non-ATP competitive glycogen synthase kinase 3 beta (GSK-3beta) inhibitors: thiadiazolidinones (TDZD) as potential drugs for the treatment of Alzheimer’s disease. J. Med. Chem. 45, 1292–1299.

Masek, J., Fabry, P., (1959) High-fat diet and the development of obesity in albino rats. Experientia. 15, 444–445.

Mateo, I., Infante, J., Llorca, J., Rodriguez, E., Berciano, J., Combarros, O., (2006) Association between glycogen synthase kinase-3beta genetic polymorphism and late-onset Alzheimer's disease. Dement. Geriatr. Cogn Disord. 21, 228–232.

Matsuzawa-Nagata, N., Takamura, T., Ando, H., Nakamura, S., Kurita, S., Misu, H., et al., (2008) Increased oxidative stress precedes the onset of high-fat diet-induced insulin resistance and obesity. Metabolism. 57(8), 1071-1077.

Mayr, B., Montminy, M., (2001) Transcriptional regulation by the phosphorylation-dependent factor CREB. Nat Rev Mol Cell Biol. (8), 599-609.

McCoy, MK., Martinez, TN., Ruhn, KA., Szymkowski, DE., Smith, CG., Botterman, BR., et al., (2006) Blocking soluble tumor necrosis factor signaling with dominant-negative tumor necrosis factor inhibitor attenuates loss of dopaminergic neurons in models of Parkinson’s disease. J Neurosci. 26 (37), 9365–9375.

McGarry, JD., (2002) Banting lecture 2001: dysregulation of fatty acid metabolism in the etiology of type 2 diabetes. Diabetes. 51, 7–18.

McGaugh, JL., (2004) The amygdala modulates the consolidation of memories of emotionally arousing experiences. Annu Rev Neurosci. 27, 1–28.

McGee, SL., van Denderen, BJ., Howlett, KF., Mollica, J., Schertzer, JD., Kemp, KE., (2008) AMP-activated protein kinase regulates GLUT4 transcription by phosphorylating histone deacetylase 5. Diabetes. 57, 860–867.

McKinsey, TA., Zhang, CL., Lu, J., Olson, EN., (2000) Signal-dependent nuclear export of a histone deacetylase regulates muscle differentiation. Nature. 408, 106-111.

McNaught, KS., Olanow, CW., (2003) Proteolytic stress: a unifying concept for the etiopathogenesis of Parkinson's disease Ann. Neurol. 53, S73–S84.

McQuown, SC., Barrett, RM., Matheos, DP., Post, RJ., Rogge, GA., Alenghat, T., et al., (2011) HDAC3 is a critical negative regulator of long-term memory formation. J. Neurosci. 31, 764–774.

Medeiros, MS., Schumacher-Schuh, A., Cardoso, AM., Bochi, GV., Baldissarelli, J., Kegler, A., et al., (2016) Iron and Oxidative Stress in Parkinson's Disease: An Observational Study of Injury Biomarkers. PLoS One. 11(1), e0146129.

Meijer, L., Skaltsounis, AL., Magiatis, P., Polychronopoulos, P., Knockaert, M., Leost, M., et al., (2003) GSK- 3-selective inhibitors derived from Tyrian purple indirubins. Chem. Biol. 10, 1255–1266.

Meredith, GE., Totterdell, S., Potashkin, JA., Surmeier, DJ., (2008) Modelling PD pathogenesis in mice: advantages of a chronic MPTP protocol. Parkinsonism Relat. Disord. 14 (Suppl 2), 112–115.

Merz, K., Herold, S., Lie, DC., (2011) CREB in adult neurogenesis- master and partner in the development of adult-born neurons? Eur. J. Neurosci. 33, 1078–1086.

Mesulam, MM., Asuncion Moran, M., (1987) Cholinesterases within neurofibrillary tangles related to age and Alzheimer's disease. Ann Neurol. 22, 223-228.

Micelli, C., Rastelli, G., (2015) Histone deacetylases: structural determinants of inhibitor selectivity. Drug Discov Today. 20(6), 718–735.

Mihaylova, MM., Vasquez, DS., Ravnskjaer, K., Denechaud, PD., Yu, RT., Alvarez, JG., (2011) Class IIa histone deacetylases are hormone-activated regulators of FOXO and mammalian glucose homeostasis, Cell. 145, 607–621.

Miller, A., Adeli, K., (2008) Dietary fructose and the metabolic syndrome. Curr. Opin. Gastroenterol. 24, 204-209.

Miller, GW., (2007) Paraquat: the red herring of Parkinson's disease research, Toxicol. Sci. 100, 1–2.

Minucci, S., Pelicci, PG., (2006) Histone deacetylase inhibitors and the promise of epigenetic (and more) treatments for cancer. Nat Rev Cancer. 6, 38-51.

Miranda, MI., Ferreira, G., Ramirez-Lugo, L., Bermudez-Rattoni, F., (2003) Role of cholinergic system on the construction of memories: taste memory encoding. Neurobiol Learn Mem. 80, 211-222.

Mirsky, IA., Broh-Kahn, RH., (1949) The inactivation of insulin by tissue extracts; the distribution and properties of insulin inactivating extracts. Arch Biochem. 20, 1–9.

Mishra, N., Reilly, CM., Brown, DR., Ruiz, P., Gilkeson, GS., (2003) Histone deacetylase inhibitors modulate renal disease in the MRL-lpr/lpr mouse. J Clin Invest. 111, 539–552.

Miska, EA., Karlsson, C., Langley, E., Nielsen, SJ., Pines, J., Kouzarides, T., (1999) HDAC4 deacetylase associates with and represses the MEF2 transcription factor. The EMBO Journal, 18, 5099–5107.

Mogi, M., Togari, A., Kondo, T., Mizuno, Y., Komure, O., Kuno, S., (1999) Brain-derived growth factor and nerve growth factor concentrations are decreased in the substantia nigra in Parkinson's disease. Neurosci Lett. 270 (1), 45–48.

Mohapel, P., Frielingsdorf, H., Haggblad, J., Zachrisson, O., Brundin, P., (2005) Platelet-derived growth factor (PDGF-BB) and brain-derived neurotrophic factor (BDNF) induce striatal neurogenesis in adult rats with 6-hydroxydopamine lesions. Neuroscience, 132(3), 767-776.

Mok, W., Chow, TW., Zheng, L., Mack, WJ., Miller, C., (2004) Clinicopathological concordance of dementia diagnoses by community versus tertiary care clinicians. Am J Alzheimers Dis Other Demen. 19(3), 161–165.

Molnar, J., Yu, S., Mzhavia, N., Pau, C., Chereshnev, I., Dansky, HM., (2005) Diabetes induces endothelial dysfunction but does not increase neointimal formation in high-fat diet fed c57bl/6j mice. Circ Res. 96, 1178–1184.

Moloney, AM., Griffin, RJ., Timmons, S., O'Connor, R., Ravid, R., O'Neill, C., (2010) Defects in IGF-1 receptor, insulin receptor and IRS-1/2 in Alzheimer's disease indicate possible resistance to IGF-1 and insulin signalling. Neurobiol. Aging. 31, 224–243.

Monti, B., Mercatelli, D., Contestabile, A., (2012) Valproic acid neuroprotection in 6-OHDA lesioned rat, a model for parkinson's disease. HOAJ Biology. 1, 1-4

Monti, B., Gatta, V., Piretti, F., Raffaelli, SS., Virgili, M., Contestabile, A., (2010) Valproic acid is neuroprotective in the rotenone rat model of Parkinson's disease: Involvement of α-synuclein. Neurotox Res. 17, 130–141.

Moradei, OM., Mallais, TC., Frechette, S., Paquin, I., Tessier, PE., Leit, SM., (2007) Novel aminophenyl benzamide-type histone deacetylase inhibitors with enhanced potency and selectivity. J Med Chem. 50(23), 5543-5546.

Moreno, H., Choi, S., Yu, E., Brusco, J., Avila, J., Moreira, JE., et al., (2011) Blocking effects of human Tau on squid giant synapse transmission and its prevention by T-817 MA. Front Synaptic Neurosci. 3(3).

Moroo, I., Yamada, T., Makino, H., Tooyama I., McGeer, PL., McGeer, EG., et al., (1994) Loss of insulin receptor immunoreactivity from the substantia nigra pars compacta neurons in Parkinson's disease, Acta Neuropathol. 87, 343-348.

Morris, JK., Vidoni, ED., Perea, RD., Rada, R., Johnson, DK., Lyons, K., et al., (2014) Insulin resistance and gray matter volume in neurodegenerative disease. Neuroscience. 270, 139–147.

Morris, JK., Zhang, H., Gupte, AA., Bomhoff, GL., Stanford, JA., Geiger, PC., (2008) Measures of striatal insulin resistance in a 6-hydroxydopamine model of Parkinson's disease. Brain Res. 1240, 185–195.

Morris, MJ., Mahgoub, M., Na, ES., Pranav, H., Monteggia, LM., (2013) Loss of histone deacetylase 2 improves working memory and accelerates extinction learning. J Neurosci. 33(15), 6401-6411.

Morris, R., (1984) Developments of a water-maze procedure for studying spatial learning in the rat. J Neurosci Methods.11(1), 47-60.

Morrison, BE., Majdzadeh, N., D'Mello, SR., (2007) Histone deacetylases: focus on the nervous system. Cell Mol Life Sci. 64, 2258–2269.

Mottet, D., Castronovo, V., (2008) Histone deacetylases: target enzymes for cancertherapy, Clin. Exp. Metastasis 25, 183–189.

Mudher, M., Lovestone, S., (2002) Alzheimer's disease- do tauists and Baptists finally shake hands? Trends Neurosci. 25, 22–26.

Muniyappa, R., Iantorno, M., Quon, MJ., (2008) An integrated view of insulin resistance and endothelial dysfunction. Endocrinol Metab Clin North Am. 37, 685–711.

Murai, H., Okazaki, M., Kikuchi, A., (1996) Tyrosine dephosphorylation of glycogen synthase kinase-3 is involved in its extracellular signal-dependent inactivation. FEBS Lett. 392, 153–160.

Nagao, M., Hayashi, H., (2009) Glycogen synthase kinase-3beta is associated with Parkinson's disease. Neurosci. Lett. 449 (2), 103–107.

Nakagawa, T., Tsuchida, A., Itakura, Y., Nonomura, T., Ono, M., Hirota, F., et al., (2000) Brain-derived neurotrophic factor regulates glucose metabolism by modulating energy balance in diabetic mice. Diabetes. 49, 436–444.

Naples, M., Federico, LM., Xu, E., Nelken, J., Adeli, K., (2008) Effect of rosuvastatin on insulin sensitivity in an animal model of insulin resistance: evidence for statin-induced hepatic insulin sensitization. Atherosclerosis. 198, 94– 103.

Newsholme, P., Morgan, D., Rebelato, E., Oliveira-Emilio, HC., Procopio, J., Curi, R., et al., (2009) Insights into the critical role of NADPH oxidase(s) in the normal and dysregulated pancreatic beta cell. Diabetologia. 52 (12), 2489–2498.

Nicklas, WJ., Youngster, SK., Kindt, MV., Heikkila, RE., (1987) MPTP, MPP+ and mitochondrial function. Life Sci. 40, 721–729.

Nielsen, JH., Galsgaard, ED., Moldrup, A., Friedrichsen, BN., Billestrup, N., Hansen, JA., et al., (2001) Regulation of beta-cell mass by hormones and growth factors. Diabetes. 50 (Suppl 1), S25–S29.

Nikoulina, SE., Ciaraldi, TP., Carter, L., Mudaliar, S., Park, KS., Henry, RR., et al., (2001) Impaired muscle glycogen synthase in type 2 diabetes is associated with diminished phosphatidylinositol 3-kinase activation. J Clin Endocrinol Metab. 86(9), 4307–4314.

Nikoulina, SE., Ciaraldi, TP., Mudaliar, S., Mohideen, P., Carter, L., Henry, RR., (2000) Potential role of glycogen synthase kinase-3 in skeletal muscle insulin resistance of type 2 diabetes. Diabetes. 49, 263-271.

Nitsch, R., Hoyer, S., (1991) Local action of the diabetogenic drug, streptozotocin, on glucose and energy metabolism in rat brain cortex. Neurosci Lett. 128, 199–202

Noble, W., Planel, E., Zehr, C., Olm, V., Meyerson, J., Suleman, F., et al., (2005) Inhibition of glycogen synthase kinase-3 by lithium correlates with reduced tauopathy and degeneration in vivo. Proc Natl Acad Sci USA. 102, 6990–6995.

Nowrangi, MA., Rao, V., Lyketsos, CG., (2011) Epidemiology, assessment, and treatment of dementia. Psychiatr Clin North Am. 34(2), 275–294.

O¨gren, SO., Eriksson, TM., Elvander-Tottie, E., D'Addario, C., Ekstrom, JC., Svenningsson, P., et al., (2008) The role of 5-HT1A receptors in learning and memory. Behav Brain Res. 195, 54–77.

Oakes, ND., Cooney, GJ., Camilleri, S., Chisholm, DJ., Kraegen, EW., (1997) Mechanisms of liver and muscle insulin resistance induced by chronic high-fat feeding. Diabetes. 46, 1768–1774.

Oana, F., Takeda, H., Hayakawa, K., Matsuzawa, A., Akahane, S., Isaji, M., et al., (2005) Physiological difference between obese (fa/fa) Zucker rats and lean Zucker rats concerning adiponectin. Metabolism. 54, 995–1001.

Odagiri, S., Tanji, K., Mori, F., Miki, Y., Kakita, A., Takahashi, H., et al., (2013) Brain expression level and activity of HDAC6 protein in neurodegenerative dementian. Biochem Biophys Res Commun. 430, 394-399.

Ohara, T., Doi, Y., Ninomiya, T., Hirakawa, Y., Hata, J., Iwaki, T., et al., (2011) Glucose tolerance status and risk of dementia in the community: the Hisayama Study. Neurology 77, 1126–1134.

Oliveira, AM., Wood, MA., McDonough, CB., Abel, T., (2007) Transgenic mice expressing an inhibitory truncated form of p300 exhibit long-term memory deficits. Learn. Mem. 14, 564–572.

Ong, JM., Simsolo, RB., Saffari, B., Kern, PA., (1992) The regulation of lipoprotein lipase gene expression by dexamethasone in isolated rat adipocytes. Endocrinology. 130, 2310–2316.

Ono, M., Ichihara, J., Nonomura, T., Itakura, Y., Taiji, M., Nakayama, C., et al., (1997) Brain-derived neurotrophic factor reduces blood glucose level in obese diabetic mice but not in normal mice. Biochem Biophys Res Commun. 238, 633–637.

Orth, M., Schapira, AH., (2002) Mitochondrial involvement in Parkinson's disease Neurochem. Int. 40, 533–541.

Owens, WA., Sevak, RJ., Galici, R., Chang, X., Javors, MA., Galli, A., et al., (2005) Deficits in dopamine clearance and locomotion in hypoinsulinemic rats unmask novel modulation of dopamine transporters by amphetamine. J. Neurochem. 94, 1402–1410.

Padiglia, A., Medda, R., Lorrai, A., Biggio, G., Sanna, E., Floris, G., (1997) Modulation of 6-hydroxydopamine oxidation byvarious proteins. Biochem. Pharmacol. 53, 1065-1068.

Padurariu, M., Ciobica, A., Hritcu, L., Stoica, B., Bild, W., Stefanescu, C., (2010) Changes of some oxidative stress markers in the serum of patients with mild cognitive impairment and Alzheimer's disease, Neurosci Lett. 469, 6–10.

Paille, V., Henry, V., Lescaudron, L., Brachet, P., Damier, P., (2007) Rat model of Parkinson's disease with bilateral motor abnormalities, reversible with levodopa, and dyskinesias. Mov Disord. 22, 533–539.

Palumbo, A., Napolitano, A., Barone, P., d'Ischia, M., (1999) Nitrite- and peroxide-dependent oxidation pathways of dopamine: 6-nitrodopamine and 6-hydroxydopamine formation as potential contributory mechanisms of oxidative stress- and nitric oxide-induced neurotoxicity in neuronal degeneration. Chem. Res. Toxicol. 12, 1213-1222.

Pamidi, N., Satheesha Nayak, BN., (2012) Effect of streptozotocin induced diabetes on rat hippocampus. Bratisl Lek Listy. 113(10), 583-588.

Pappolla, MA., Chyan, YJ., Omar, RA., Hsiao, K., Perry, G., Smith, MA., et ., (1998) Evidence of oxidative stress and in vivo neurotoxicity of β-amyloid in a transgenic mouse model of Alzheimer's disease: a chronic oxidative paradigm for testing antioxidant therapies in vivo. American Journal of Pathology. 152, 871–877.

Parain, K., Murer, MG., Yan, Q., Faucheux, B., Agid, Y., Hirsch, E., et al., (1999) Reduced expression of brain-derived neurotrophic factor protein in Parkinson's disease substantia nigra. Neuroreport. 1999, 10(3), 557-561.

Parker, PJ., Caudwell, FB., Cohen, P., (1983) Glycogen synthase from rabbit skeletal muscle; effect of insulin on the state of phosphorylation of the seven phosphoserine residues in vivo. Eur. J. Biochem. 130, 227-234.

Patapoutian, A., Reichardt, LF., (2001) Trk receptors: mediators of neurotrophin action. Curr Opin Neurobiol. 11(3), 272-280.

Pathan, AR., Gaikwad, AB., Viswanad, B., Ramarao, P., (2008) Rosiglitazone attenuates the cognitive deficits induced by high fat diet feeding in rats. Eur J Pharmacol. 589(1-3), 176-179.

Paxinos, G., Watson, C., (1986) The rat brain in stereotaxic coordinates (2nd Eds). Academic Press, San Diego.

Pearce, NJ., Arch, JRS., Clapham, JC., Coghlan, MP., Corcoran, SL., Lister, CA., (2004) Development of glucose intolerance in male transgenic mice overexpressing human glycogen synthase kinase-3beta on a muscle-specific promoter. Metabolism 53(10), 1322-1330.

Pearce, RKB., Owen, A., Daniel, S., Jenner, P., Marsden, CD., (1997) Alterations in the distribution of glutathione in the substantia nigra in Parkinson's disease. J Neural Transm.104, 661–677.

Pearson, S., Schmidt, M., Patton, G., Dwyer, T., Blizzard, L., Otahal, P., et al., (2010) Depression and insulin resistance: cross-sectional associations in young adults. Diabetes Care. 33(5), 1128-1133.

Pederson, TM., Kramer, DL., Rondinone, CM., (2001) Serine/threonine phosphorylation of IRS-1 triggers its degradation: possible regulation by tyrosine phosphorylation. Diabetes. 50 (1), 24-31.

Pei, JJ., Braak, E., Braak, H., Grundke-Iqbal, I., Iqbal, K., Winblad, B., (1999) Distribution of active glycogen synthase kinase 3beta (GSK-3beta) in brains staged for Alzheimer disease neurofibrillary changes. J. Neuropathol. Exp. Neurol. 58, 1010–1019.

Pei, JJ., Tanaka, T., Tung, YC., Braak, E., Iqbal, K., Grundke-Iqbal, I., (1997) Distribution, levels, and activity of glycogen synthase kinase-3 in the Alzheimer disease brain. J Neuropathol Exp Neurol. 56, 70–78.

Peleg, S., Sananbenesi, F., Zovoilis, A., Burkhardt, S., Bahari-Javan, S., Agis-Balboa, RC., et al., (2010) Altered histone acetylation is associated with age-dependent memory impairment in mice. Science. 328, 753–756.

Peng, GS., Li, G., Tzeng, NS., Chen, PS., Chuang, DM., Hsu, YD., et al., (2005) Valproate pretreatment protects dopaminergic neurons from LPS-induced neurotoxicity in rat primary midbrain cultures: role of microglia. Brain Res Mol Brain Res. 134(1), 162-169.

Perez, M., Perez, DI., Martinez, A., Castro, A., Gomez, G., Fall, Y., (2009) The first enantioselective synthesis of palinurin. Chem. Commun. (Camb.) 22, 3252–3254.

Perreault, ML., O'Dowd, BF., George, SR., (2014) Dopamine d(1)-d(2) receptor heteromer regulates signaling cascades involved in addiction: Potential relevance to adolescent drug susceptibility. Dev Neurosci. 36, 287–296.

Pessayre, D., Berson, A., Fromenty, B., Mansouri, A., (2001) Mitochondria in steatohepatitis. Semin Liver Dis. 21, 57-69.

Pessayre, D., Mansouri, A., Fromenty, B., (2002) Nonalcoholic steatosis and steatohepatitis. Mitochondrial dysfunction in steatohepatitis. Am J Physiol Gastrointest Liver Physiol. 282(2), G193-199.

Petit-Paitel, A., Brau, F., Cazareth, J., Chabry, J., (2009) Involment of cytosolic and mitochondrial GSK-3beta in mitochondrial dysfunction and neuronal cell death of MPTP/MPP+- treated neurons. PLoS One. 4, e5491.

Petro, AE., Cotter, J., Cooper, DA., Peters, JC., Surwit, SJ., Surwit, RS., (2004) Fat, carbohydrate, and calories in the development of diabetes and obesity in the C57BL/6J mouse. Metabolism. 53, 454–457.

Phiel, CJ., Wilson, CA., Lee, VM., Klein, PS., (2003) GSK-3α regulates production of Alzheimer's disease amyloid-β peptides. Nature. 423, 435–439.

Phillips, HS., Hains, JM., Armanini, M., Laramee, GR., Johnson, SA., Winslow, JW., (1991) BDNF mRNA is decreased in the hippocampus of individuals with Alzheimer's disease. Neuron. 7, 695-702.

Pinelli, NR., Jaber, LA., Brown, MB., Herman, WH., (2010) Serum 25- hydroxy vitamin d and insulin resistance, metabolic syndrome, and glucose intolerance among Arab Americans. Diabetes Care. 33, 1373–1375.

Pipatpiboon, N., Pratchayasakul, W., Chattipakorn, N., Chattipakorn, SC., (2012) PPARγ agonist improves neuronal insulin receptor function in hippocampus and brain mitochondria function in rats with insulin resistance induced by long term high-fat diets. Endocrinology.153(1), 329-338.

Pistell, PJ., Morrison, CD., Gupta, S., Knight, AG., Keller, JN., Ingram, DK., et al., (2010) Cognitive impairment following high fat diet consumption is associated with brain inflammation. J Neuroimmunol. 219, 25–32.

Plaschke, K., Kopitz, J., Siegelin, M., Schliebs, R., Salkovic-Petrisic, M., Riederer, P., et al., (2010) Insulin-resistant brain state after intracerebroventricular streptozotocin injection exacerbates Alzheimer-like changes in Tg2576 AbetaPP-overexpressing mice. J Alzheimers Dis. 19, 691-704.

Plastino, M., Fava, A., Pirritano, D., Cotronei, P., Sacco, N., Sperlì, T., (2010) Effects of insulinic therapy on cognitive impairment in patients with Alzheimer disease and diabetes mellitus type-2. J Neurol Sci. 288(1-2), 112-116.

Plumb, JA., Finn, PW., Williams, RJ., Bandara, MJ., Romero, MR., Watkins, CJ., et al., (2003) Pharmacodynamic response and inhibition of growth of human tumor xenografts by the novel histone deacetylase inhibitor PXD101. Mol Cancer Ther. 2, 721–728.

Pocernich, CB., Butterfield, DA., (2012) Elevation of glutathione as a therapeutic strategy in Alzheimer disease, Biochim Biophys Acta. 1822, 625-630.

Poitout, V., Hagman, D., Stein, R., Artner,I., Robertson, RP., Harmon, JS., (2006) Regulation of the Insulin Gene by Glucose and Fatty Acids. J Nutr. 136(4), 873–876.

Polychronopoulos, P., Magiatis, P., Skaltsounis, AL., Myrianthopoulos, V., Mikros, E., Tarricone, A., et al., (2004) Structural basis for the synthesis of indirubins as potent and selective inhibitors of glycogen synthase kinase-3 and cyclin-dependent kinases. J. Med. Chem. 47, 935–946.

Ponce-Lopez, T., Liy-Salmeron, G., Hong, E., Meneses, A., (2011) Lithium, phenserine, memantine and pioglitazone reversememory deficit and restore phospho-GSK3β decreased in hippocampus in Intracerebroventricular streptozotocin induced memory deficit model. Brain Res. 1426, 73–85.

Pooranaperundevi, M., Sumiyabanu, MS., Viswanathan, P., Sundarapandiyan, R., Anuradha, CV., (2000) Insulin resistance induced by a high-fructose diet potentiates thioacetamide hepatotoxicity. Singapore Med. J. 51, 389-398.

Porritt, MJ., Batchelor, PE., Howells, DW., (2005) Inhibiting BDNF expression by oligonucleotide infusion causes loss of nigral dopaminergic neurons, Exp Neurol, 192(1), 226-234.

Pratchayasakul, W., Kerdphoo, S., Petsophonsakul, P., Pongchaidecha, A., Chattipakorn, N., Chattipakorn, SC., (2011a) Effects of high-fat diet on insulin receptor function in rat hippocampus and the level of neuronal corticosterone. Life Sci. 88(13-14), 619-627.

Pratchayasakul, W., Chattipakorn, N., Chattipakorn, SC., (2011b) Effects of estrogen in preventing neuronal insulin resistance in hippocampus of obese rats are different between genders. Life Sci. 89 (19-20), 702-707.

Praveen, EP., Sahoo, J., Khurana, ML., Kulshreshtha, B., Khadgawat, R., Gupta, N., et al., (2012) Insulin sensitivity and β-cell function in normoglycemic offspring of individuals with type 2 diabetes mellitus: impact of line of inheritance. Indian J Endocrinol Metab. 16 (1), 105–111.

Prelovsek, O., Mars, T., Jevsek, M., Podbregar, M., Grubic, Z., (2006) High dexamethasone concentration prevents stimulatory effects of TNF-α and LPS on IL-6 secretion from the precursors of human muscle regeneration. Am J Physiol Regul Integr Comp Physiol. 291, R1651–R1656.

Przedborski, SV., Jackson-Lewis, Naini, AB., Jakowec, M., Petzinger, G., Miller, R., et al., (2001) The parkinsonian toxin 1-methyl-4-phenyl-1,2,3,6-tetrahydropyridine (MPTP): a technical review of its utility and safety. J Neurochem. 76 (5), 1265–1274.

Pugazhenthi, S., Boras, T., O'Connor, D., Meintzer, MK., Heidenreich, KA., Reusch, JE., (1999) Insulin-like growth factor I-mediated activation of the transcription factor cAMP response element-binding protein in PC12 cells. Involvement of p38 mitogen-activated protein kinase-mediated pathway. J Biol Chem. 274, 2829-2837.

Pyorala, K., (1979) Relationship of glucose tolerance and plasma insulin in the incidence of coronary heart disease: results from two population studies in Finland. Diabetes Care 2, 131-141.

Qing, H., He, G., Ly, PT., Fox, CJ., Staufenbiel, M., Cai, F., et al., (2008) Valproic acid inhibits Abeta production, neuritic plaque formation, and behavioral deficits in Alzheimer's disease mouse models. J Exp Med. 205, 2781–2789.

Quillfeldt, JA., (2010) Behavioral methods to study learning and memory in rats. In: Levy-Anderson, M., Tufik, S., (eds) Animal models as tools in ethical biomedical research. AFIP, Sao Paulo, 227–269.

Quinti, L., Chopra, V., Rotili, D., Valente, S., Amore, A., Franci, G., et al., (2010) Evaluation of histone deacetylases as drug targets in Huntington's disease models. Study of HDACs in brain tissues from R6/2 and CAG140 knock-in HD mouse models and human patients and in a neuronal HD cell model. PLoS Curr. 2.

Rahman, MM., Varghese, Z., Moorhead, JF., (2001) Paradoxical increase in nitric oxide synthase activity in hypercholesterolaemic rats with impaired renal function and decreased activity of nitric oxide. Nephrol Dial Transplant. 16(2), 262-268.

Rai, S., Kamat, PK., Nath, C., Shukla, R., (2012) A study on neuroinflammation and NMDA receptor function in STZ (ICV) induced memory impaired rats.J Neuroimmunol. 254, 1-9.

Raichur, S., Teh, SH., Ohwaki, K., Gaur, V., Long, YC., Hargreaves, M., (2012) Histone deacetylase 5 regulates glucose uptake and insulin action in muscle cells. J Mol Endocrinol. 49(3), 203-211.

Ramos-Rodriguez, JJ., Molina-Gil, S., Ortiz-Barajas, O., Jimenez-Palomares, M., Perdomo, G., Cozar-Castellano, I., et al., (2014) Central Proliferation and Neurogenesis Is Impaired in Type 2 Diabetes and Prediabetes Animal Models. PLoS ONE 9(2), e89229.

Ramos-Rodriguez, JJ., Ortiz-Barajas, O., Gamero-Carrasco, C., de la Rosa, PR., Infante-Garcia, C., Zopeque-Garcia, N., (2014) Prediabetes-induced vascular alterations exacerbate central pathology in APPswe/PS1dE9 mice. Psychoneuroendocrinology. 48, 123-135.

Randy, LH., Guoying, B., (2007) Agonism of Peroxisome Proliferator Receptor-Gamma may have Therapeutic Potential for Neuroinflammation and Parkinson's Disease. Curr Neuropharmacol. 5(1), 35-46.

Rane, P., Shields, J., Heffernan, M., Guo, Y., Akbarian, S., King, JA., et al., (2012) The histone deacetylase inhibitor, sodium butyrate, alleviates cognitive deficits in pre-motor stage PD. Neuropharmacology. 62 (7), 2409–2412.

Rask-Madsen, C., Buonomo, E., Li, Q., Park, K., Clermont, AC., Yerokun, O., et al., (2012) Hyperinsulinemia does not change atherosclerosis development in apolipoprotein e null mice. Arterioscler Thromb Vasc Biol. 32, 1124–1131.

Reaven, G., (2004) The metabolic syndrome or the insulin resistance syndrome? Different names, different concepts, and different goals. Endocrinol Metab Clin North Am. 33, 283–303.

Reaven, GM., (1988) Role of insulin resistance in human disease. Diabetes. 37, 1595-607.

Reaven, GM., (2003) Insulin resistance/compensatory hyperinsulinemia, essential hypertension, and cardiovascular disease. J Clin Endocrinol Metab. 88, 2399–2403.

Reaven, GM., (2005) The insulin resistance syndrome: definition and dietary approaches to treatment. Annu Rev Nutr. 25, 391–406.

Reaven, GM., (2011) Relationships among insulin resistance, type 2 diabetes, essential hypertension, and cardiovascular disease: similarities and differences. J Clin Hypertens (Greenwich). 13, 238–243.

Reed, MJ., Meszaros, K., Entes, LJ., Claypool, MD., Pinkett, JG., Gadbois, TM., et al., (2000) A new rat model of type 2 diabetes: the fat-fed, streptozotocin-treated rat. Metabolism. 49 (11), 1390–1394.

Rees, T., Hammond, PI., Soreq, H., Younkin, S., Brimijoin, S., (2003) Acetylcholinesterase promotes beta-amyloid plaques in cerebral cortex. Neurobiol. Aging. 24, 777–787.

Ren, M., Leng, Y., Jeong, M., Leeds, PR., Chuang, DM., (2004) Valproic acid reduces brain damage induced by transient focal cerebral ischemia in rats: potential roles of histone deacetylase inhibition and heat shock protein induction. J Neurochem. 89, 1358-1367.

Richon, VM., (2006) Cancer biology: mechanism of antitumour action of vorinostat (suberoylanilide hydroxamic acid), a novel histone deacetylase inhibitor. Br J Cancer. 95, S2–S6.

Ricobaraza, A., Cuadrado-Tejedor, M., Garcia-Osta, A., (2011) Long-term phenylbutyrate administration prevents memory deficits in Tg2576 mice by decreasing Abeta. Front Biosci. (Elite) 3, 1375–1384.

Ricobaraza, A., Cuadrado-Tejedor, M., Perez-Mediavilla, A., Frechilla, D., Del Rio, J., Garcia-Osta, A., (2009) Phenylbutyrate ameliorates cognitive deficit and reduces tau pathology in an Alzheimer's disease mouse model. Neuropsychopharmacology. 34,1721–1732.

Ricobaraza, A., Cuadrado-Tejedor, M., Marco, S., Pérez-Otano, I., García-Osta, A., (2012) Phenylbutyrate rescues dendritic spine loss associated with memory deficits in a mouse model of Alzheimer disease. Hippocampus. 22(5), 1040-1050.

Rikiishi, H., (2011) Autophagic and apoptotic effects of HDAC inhibitors on cancer cells. J Biomed Biotechnol. 2011, 830260.

Ring, DB., Johnson, KW., Henriksen, EJ., Nuss, JM., Goff, D., Kinnick, TR., et al., (2003) Selective glycogen synthase kinase 3 inhibitors potentiate insulin activation of glucose transport and utilization in vitro and in vivo. Diabetes 52, 588–595.

Riva, L., Blaney, SM., Dauser, R., Nuchtern, JG., Durfee, J., McGuffey, L., et al., (2000) Pharmacokinetics and cerebrospinal fluid penetration of CI-994 (N-acetyldinaline) in the nonhuman primate. Clin Cancer Res. 6, 994–997.

Rivieccio, MA., Brochier, C., Willis, DE., Walker, BA., D'Annibale, MA., McLaughlin, K., et al., (2009) HDAC6 is a target for protection and regeneration following injury in the nervous system. Proc Natl Acad Sci U S A. 106, 19599 –19604.

Roach, PJ., Larner, J., (1997) Covalent phosphorylation in the regulation of glycogen synthase activity. Mol Cell Biochem. 15, 179–199.

Rockenstein, E., Torrance, M., Adame, A., Mante, M., Bar-on, P., Rose, JB., et al., (2007) Neuroprotective effects of regulators of the glycogen synthase kinase-3β signalling pathway in a transgenic model of Alzheimer's disease are associated with reduced amyloid precursor protein phosphorylation. J Neurosci. 27 (8), 1981–1991.

Roeling, TAP., Docter, GJ., Voorn, P., Melchers, BP., Wolters, EC., Groenewegen, HJ., (1995) Effects of unilateral 6-hydroxydopamine lesions on neuropeptide immunoreactivity in the basal ganglia of the common marmoset, Callithrix jacchus, a quantitative immunohistochemical analysis. J Chem Neuroanat. 9 (3), 155–164.

Rogers, J., Mastroeni, D., Leonard, B., Joyce, J., Grover, A., (2007) Neuroinflammation in Alzheimer's disease and Parkinson's disease: are microglia pathogenic in either disorder? Int Rev Neurobiol. 82, 235-246.

Rouaux, C., Jokic, N., Mbebi, C., Boutillier, S., Loeffler, JP., Boutillier, AL., (2003) Critical loss of CBP/p300 histone acetylase activity by caspase-6 during neurodegeneration, EMBO J. 22(24), 6537-6549.

Roy, A., Ghosh, A., Jana, A., Liu, X., Brahmachari, S., Gendelman, HE., et al., (2012) Sodium phenylbutyrate controls neuroinflammatory and antioxidant activities and

protects dopaminergic neurons in mouse models of Parkinson's disease. PLoS ONE 7(6), e38113.

Ruzzin, J., Wagman, AS., Jensen, J., (2005) Glucocorticoid-induced insulin resistance in skeletal muscles: defects in insulin signalling and the effects of a selective glycogen synthase kinase-3 inhibitor. Diabetologia. 48, 2119–2130.

Ryder, J., Su, Y., Liu, F., Li, B., Zhou, Y., Ni, B., (2003) Divergent roles of GSK3 and CDK5 in APP processing. Biochem Biophys Res Commun. 312, 922–929.

Ryder, J., Su, Y., Ni, B., (2004) Akt/GSK3beta serine/threonine kinases: evidence for a signalling pathway mediated by familial Alzheimer's disease mutations. Cell Signal 16, 187–200.

Rylatt, DB., Aitken, A., Bilham, T., Condon, GD., Embi, N., Cohen, P., (1980) Glycogen synthase from rabbit skeletal muscle. Amino acid sequence at the sites phosphorylated by glycogen synthase kinase-3, and extension of the N-terminal sequence containing the site phosphorylated by phosphorylase kinase. Eur J Biochem. 107(2), 529-537.

Ryves, JW., Dalton, EC., Harwood, AJ., Williams, RS., (2005) GSK-3 activity in neocortical cells is inhibited by lithium but not carbamazepine or valproic acid. Bipolar Disord. 7, 260-265.

Ryves, JW., Dajani, R., Pearl, L., Harwood, AJ., (2002) Glycogen synthase kinase-3 inhibition by lithium and beryllium suggests the presence of two magnesium binding sites. Biochem. Biophys. Res. Commun. 290, 967–972.

Sachsand, G., Jonsson, (1975) Mechanisms of action of 6-hydroxydopamine, Biochem Pharmacol. 24 (1), 1–8.

Sadri-Vakili, G., Bouzou, B., Benn, CL., Kim, MO., Chawla, P., Overland, RP., et al., (2007) Histones associated with downregulated genes are hypo-acetylated in Huntington's disease models. Hum Mol Genet. 16 (11), 1293-1306.

Sakai, K., Gash, DM., (1994) Effect of bilateral 6-OHDA lesions of the substantia nigra on locomotor activity in the rat. Brain Res. 633, 144–150.

Sakamoto, K., Karelina, K., Obrietan, K., (2011) CREB: a multifaceted regulator of neuronal plasticity and protection. J Neurochem. 116(1), 1-9.

Salkovic-Petrisic M., Hoyer, S., (2007) Central insulin resistance as a trigger for sporadic Alzheimer-like pathology: an experimental approach. J Neural Transm Suppl. 72, 217–233.

Saltiel, AR., Kahn, CR., (2001) Insulin signalling and the regulation of glucose and lipid metabolism. Nature. 414 (6865), 799-806.

Samii, A., Nutt, JG., Ransom, BR., (2004) Parkinson's disease. Lancet. 363(9423), 1783-1793.

Sanchis-Segura, C., Lopez-Atalaya, JP., Barco, A., (2009) Selective boosting of transcriptional and behavioral responses to drugs of abuse by histone deacetylase inhibition. Neuropsychopharmacology. 34, 2642–2654.

Sando R, 3rd., Gounko, N., Pieraut, S., Liao, L., Yates, J 3rd., Maximov, A., (2012) HDAC4 governs a transcriptional program essential for synaptic plasticity and memory. Cell. 151(4), 821-834.

Sandyk, R., (1993) The relationship between diabetes mellitus and Parkinson's disease. Int. J. Neurosci. 69, 125–130.

Saporito, MS., Thomas, BA., Scott, RW., (2000) MPTP activates c-Jun NH(2)-terminal kinase (JNK) and its upstream regulatory kinase MKK4 in nigrostriatal neurons in vivo. J Neurochem. 75, 1200–1208.

Sarafidis, PA., Bakris, GL., (2006) Insulin resistance, hyperinsulinemia, and hypertension: an epidemiologic approach. J Cardiometab Syndr. 1, 334–342.

Sarbassov, DD., Ali, SM., Sabatini, DM., (2005) Growing roles for the mTOR pathway. Curr Opin Cell Biol. 17(6), 596-603.

Sarre, S., Yuan, H., Jonker, N., Ven Hemelrijck, A., Ebinger, G., Michotte, Y., (2004) In vivo characterization of somatodendritic release in the substantia nigra of 6-hydroxydopamine-lesioned rats. J Neurochem. 90, 29–39.

Scalzo, P., Kümmer, A., Bretas, TL., Cardoso, F., Teixeira, AL., (2010) Serum levels of brain-derived neurotrophic factor correlate with motor impairment in Parkinson's disease. J. Neurology. 257 (4), 540–545.

Schacke, H., Docke, WD., Asadullah, K., (2002) Mechanisms involved in the side effects of glucocorticoids. Pharmacol. Ther. 96, 23–43.

Schafer, M., Goodenough, S., Moosmann, B., Behl, C., (2004) Inhibition of glycogen synthase kinase 3β is involved in the resistance to oxidative stress in neuronal HT22 cells. Brain Research.1005 (1-2), 84–88.

Schallert, T., Fleming, SM., Leasure, JL., Tillerson, JL., Bland, ST., (2000) CNS plasticity and assessment of forelimb sensorimotor outcome in unilateral rat models of stroke, cortical ablation, parkinsonism and spinal cord injury. Neuropharmacology. 39, 777–787.

Schapira, AH., (1994) Evidence for mitochondrial dysfunction in Parkinson's disease—a critical appraisal Mov. Disord. 9, 125–138.

Schechter, R., Beju, D., Gaffney, T., Schaefer, F, Whetsell, L., (1996) Preproinsulin I and II mRNAs and insulin electron microscopic immunoreaction are present within the rat fetal nervous system. Brain Res. 736 (1-2), 16–27.

Schechter, R., Sadiq, HF., Devaskar,SU., (1990) Insulin and insulin mRNA are detected in neuronal cell cultures maintained in an insulin-free/serum-free medium. J Histochem Cytochem. 38 (6), 829–836.

Schintu, N., Frau L., Ibba M., Caboni P., Garau A., Carboni E., Carta AR., et al. (2009) PPAR-gamma-mediated neuroprotection in a chronic mouse model of Parkinson's disease. Eur J Neurosci. 29, 954–963.

Schmitt, M., Matthies, H., (1979) Biochemical studies on histones of the central nervous system. III. Incorporation of [14C]-acetate into the histones of different rat brain regions during a learning experiment. Acta Biol.Med. Ger. 38, 683–689.

Schrag, A., Sauerbier, A., Chaudhuri, KR., (2015) New clinical trials for nonmotor manifestations of Parkinson's disease. Mov. Disord. 30 (11), 1490–1504.

Schroeder, FA., Chonde, DB., Riley, MM., Moseley, CK., Granda, ML., Wilson, CM., (2013) FDG-PET imaging reveals local brain glucose utilization is altered by class I histone deacetylase inhibitors. Neurosci Lett. 550, 119-124.

Schwartz, MW., Woods, SC, Porte, D Jr., Seeley, RJ., Baskin, DG., (2000) Central nervous system control of food intake. Nature. 404, 661–671.

Scott, GK., Mattie, MD., Berger, CE., Benz, SC., Benz, CC., (2006) Rapid alteration of microRNA levels by histone deacetylase inhibition. Cancer Res. 66(3), 1277-1281.

Selenica, ML., Benner, L., Housley, SB., Manchec, B., Lee, DC., Nash, KR., et al., (2014) Histone deacetylase 6 inhibition improves memory and reduces total tau levels in a mouse model of tau deposition. Alzheimers Res Ther. 6(1), 12.

Sereno, L., Coma, M., Rodrıguez, M., Sanchez-Ferrer, P., Sanchez, MB., Gich, I., et al., (2009) A novel GSK- 3β inhibitor reduces Alzheimer's pathology and rescues neuronal loss in vivo. Neurobiol Dis. 35(3), 359–367.

Sethi, K., (2008) Levodopa unresponsive symptoms in Parkinson disease. Mov. Disord. 23(3), S521– S533.

Seubert, P., Mawal-Dewan, M., Barbour, R., Jakes, R., Goedert, M., Johnson, GV., et al., (1995) Detection of phosphorylated Ser in fetal tau, adult tau, and paired helical filament tau. Journal of Biological Chemistry. 270(32), 18917–18922.

Shah, S., Iqbal, M., Karam, J., Salifu, M., McFarlane, SI., (2007) Oxidative stress, glucose metabolism, and the prevention of type 2 diabetes: pathophysiological insights. Antioxid Redox Signal. 9, 911– 929.

Shalwala, M., Zhu, SG., Das, A., Salloum, FN., Xi, L., Kukreja, RC., (2014) Sirtuin 1 (SIRT1) Activation Mediates Sildenafil Induced Delayed Cardioprotection against Ischemia-Reperfusion Injury in Mice. PLoS ONE 9(1), e86977.

Shao, L., Young, LT., Wang, JF., (2005) Chronic treatment with mood stabilizers lithium and valproate prevents excitotoxicity by inhibiting oxidative stress in rat cerebral cortical cells. Biol Psychiatry. 58, 879-884.

Sharma, N., Deshmukh, R., Bedi, KL., (2010) SP600125, a competitive inhibitor of JNK attenuates streptozotocin induced neurocognitive deficit and oxidative stress in rats. Pharmacol Biochem Behav. 96, 386–394.

Sharma, S., Kumar, K., Deshmukh, R., Sharma, PL., (2013) Phosphodiesterases: Regulators of cyclic nucleotide signals and novel molecular target for movement disorders. Eur J Pharmacol. 714, 486-497.

Sharma, S., Deshmukh, R., (2015) Vinpocetine attenuates MPTP-induced motor deficit and biochemical abnormalities in Wistar rats. Neuroscience. 286C, 393-403.

Sharma, SK., Chorell, E., Steneberg, P., Vernersson-Lindahl, E., Edlund, H., Wittung-Stafshede, P., (2015) Insulin-degrading enzyme prevents α-synuclein fibril formation in a nonproteolytical manner. Sci. Rep. 5, 12531.

Sharma, V., Bala, A., Deshmukh, R., Bedi, KL., Sharma, PL., (2012) Neuroprotective effect of RO-20-1724-a phosphodiesterase 4 inhibitor against intracerebroventricular streptozotocin induced cognitive deficit and oxidative stress in rats. Pharmacol Biochem and Behav. 101, 239–245.

Shaywitz, AJ., Greenberg, ME., (1999) CREB: a stimulus-induced transcription factor activated by a diverse array of extracellular signals. Annu Rev Biochem. 68, 821-861.

Sherer, TB., Betarbet, R., Greenamyre, JT., (2002) Environment, mitochondria, and Parkinson's disease Neuroscientist. 8, 192–197.

Shi, A., Kokoeva, V., Inouye, K., Tzameli, I., Yin, H., Flier, JS., et al., (2006) TLR4 links innate immunity and fatty acid-induced insulin resistance. J Clin Invest. 116, 3015–3025.

Shieh, PB., Hu, SC., Bobb, K., Timmusk, T., Ghosh, A., (1998) Identification of a signaling pathway involved in calcium regulation of BDNF expression. Neuron.20(4), 727-740.

Shimizu, K., Ohtaki, K., Matsubara, K., Aoyama, K., Uezono, T., Saito, O., et al., (2001) Carrier-mediated processes in blood – brain barrier penetration and neural uptake of paraquat. Brain Res. 906, 135–142.

Shingo, AS., Kanabayashi, T., Kito, S., Murase, T., (2013) Intracerebroventricular administration of an insulin analogue recovers STZ induced cognitive decline in rats. Behav Brain Res. 241, 105–111.

Shonesy, BC., Thiruchelvam, K., Parameshwaran, K., Rahman, EA., Karuppagounder, SS., Huggins, KW., et al., (2012) Central insulin resistance and synaptic dysfunction in intracerebroventricular-streptozotocin injected rodents. Neurobiol Aging. 33: 5–18.

Siderowf, A., Stern, M., (2003) Update on Parkinson disease. Ann Intern Med. 138(8), 651-658.

Sidorova-Darmos, E., Wither, RG., Shulyakova, N., Fisher, C., Ratnam, M., Aarts, M., et al., (2014) Differential expression of sirtuin family members in the developing, adult, and aged rat brain. Front Aging Neurosci. 6, 1-20.

Siegel, GJ., Chauhan, NB., (2000) Neurotrophic factors in Alzheimer's and Parkinson's disease brain. Brain Res Brain Res Rev. 33, 199-227.

Silvers, JM., Harrod, SB., Mactutus, CF., Booze, RM., (2007) Automation of the novel object recognition task for use in adolescent rats. J Neurosci Met. 166, 99–103.

Simmons, RA., (2006) Developmental origins of diabetes: the role of oxidative stress. Free Radic Biol Med. 40, 917– 922.

Simon-Sanchez, J., Schulte, C., Bras, JM., Sharma, M., Gibbs, JR., Berg, D., et al., (2009) Genome-wide association study reveals genetic risk underlying Parkinson's disease. Nat. Genet. 41 (12), 1308–1312.

Singh, S., Ahmad, R., Mathur, D., Sagar, RK., Krishana, B., (2006) Neuroprotective effect of BDNF in young and aged 6-OHDA treated rat model of Parkinson disease. Indian J Exp Biol. 44(9), 699-704.

Siri-Tarino, PW., Sun, Q., Hu, FB., Krauss, RM., (2010) Saturated fat, carbohydrate, and cardiovascular disease. Am J Clin Nutr. 91(3), 502-509.

Skurat, AV., Wang, Y., Roach, PJ., (1994) Rabbit skeletal muscle glycogen synthase expressed in COS cells: identification of regulatory phosphorylation sites. J Biol Chem. 269, 25534–22542.

Small, SA., Duff, K., (2008) Linking Abeta and tau in late-onset Alzheimer's disease: a dual pathway hypothesis. Neuron. 60, 534-542.

Southwood, CM., Peppi, M., Dryden, S., Tainsky, MA., Gow, A., (2007) Microtubule deacetylases, SirT2 and HDAC6, in the nervous system. Neurochem Res. 32, 187-195.

Spange, S., Wagner, T., Heinzel, T., Kramer, OH., (2009) Acetylation of non-histone proteinsmodulates cellular signalling at multiple levels. Int J Biochem Cell Biol. 41, 185–198.

Speciale, SG., (2002). MPTP insights into Parkinsonian Neurodegeneration. Neurotoxicol Teratol. 24, 607–620.

Sperbera, BR., Leight, S., Goedert, M., Lee, VM., (1995) Glycogen synthase kinase-3β phosphorylates tau protein at multiple sites in intact cells. Neuroscience Letters. 197 (2), 149–153.

Spina, MB., Squinto, SP., Miller, J., Lindsay, RM., Hyman, C., (1992) Brain-derived neurotrophic factor protects dopamine neurons against 6-hydroxydopamine and N-methyl-4-phenylpyridinium ion toxicity: involvement of the glutathione system. J Neurochem. 59(1), 99-106.

Srinivasan, K., Viswanad, B., Asrat, L., Kaul, CL., Ramarao, P., (2005) Combination of high-fat diet-fed and low-dose streptozotocin-treated rat: a model for type 2 diabetes and pharmacological screening. Pharmacol Res. 52(4), 313-320.

Srinivasan, K., Ramarao, P., (2007) Animal models in type 2 diabetes research: an overview, Indian J Med Res. 125, 451-472.

St Laurent, R., O'Brien, LM., Ahmad, ST., (2013) Sodium butyrate improves locomotor impairment and early mortality in a rotenone-induced Drosophila model of Parkinson's disease. Neuroscience. 246, 382-390.

Steen, E., Terry, BM., Rivera, EJ., Cannon, JL., Neely, TR., Tavares, R., et al., (2005) Impaired insulin and insulin-like growth factor expression and signaling mechanisms in Alzheimer's disease-is this type 3 diabetes? J Alzheimers Dis. 7, 63-80.

Stellato, C., (2004) Post-transcriptional and nongenomic effects of glucocorticoids. Proc Am Thorac Soc. 1, 255–263.

Stranahan, AM., Norman, ED., Lee, K., Cutler, RG., Telljohann, RS., Egan, JM., et al., (2008) Diet-induced insulin resistance impairs hippocampal synaptic plasticity and cognition in middle-aged rats. Hippocampus 18(11),1085–1088.

Stranahan, AM., Cutler, RG., Button, C., Telljohann, R., Mattson, MP., (2011) Diet induced elevations in serum cholesterol are associated with alterations in hippocampa lipi d metabolism and increased oxidative stress. J Neurochem.118(4), 611-615.

Suh, HS., Choi, S., Khattar, P., Choi, N., Lee, SC., (2010) Histone deacetylase inhibitors suppress the expression of inflammatory and innate immune response genes in human microglia and astrocytes. J Neuroimmune Pharmacol. 5 (4), 521–532.

Summers, SA., Kao, AW., Kohn, AD., Backus, GS., Roth, RA., Pessin, JE., et al., (1999) The role of glycogen synthase kinase 3 b in insulin-stimulated glucose metabolism. J Biol Chem. 274, 17934–17940.

Sun, C., Zhou, J., (2008) Trichostatin A improves insulin stimulated glucose utilization and insulin signalling transduction through the repression of HDAC2. Biochem Pharmacol. 76(1), 120–127.

Sun, M., Kong, L., Wang, X., Lu, XG., Gao, Q., Geller, AI., (2005) Comparison of the capability of GDNF, BDNF, or both, to protect nigrostriatal neurons in a rat model of Parkinson's disease, Brain Res. 1052(2),119-129.

Sun, Z., Miller, RA., Patel, RT., Patel, J., Dhir, R., Wang, H., et al., (2012) Hepatic Hdac3 promotes gluconeogenesis by repressing lipid synthesis and sequestration. Nat. Med. 18, 934–942.

Sung, YM., Lee, T., Yoon, H., DiBattista, AM., Song, JM., Sohn, Y., et al., (2013) Mercaptoacetamide based class II HDAC inhibitor lowers Aβ levels and improves learning and memory in a mouse model of Alzheimer's disease. Exp Neurol. 239, 192-201.

Surwit, RS., Kuhn, CM., Cochrane, C., McCubbin, JA., Feinglos, MN., (1988) Diet-induced type II diabetes in C57BL/6J mice. Diabetes. 37, 1163–1167.

Swardfager, W., Lanctot, K., Rothenburg, L., Wong, A., Cappell, J., Herrmann, N., (2010) A meta-analysis of cytokines in Alzheimer's disease. Biol. Psychiatry. 68, 930–941.

Swatton, JE., Sellers, LA., Faull, RLM., Holland, A., Iritani, S., Bahn, S., (2004) Increased MAP kinase activity in Alzheimer's and Down syndrome but not in schizophrenia human brain. Eur. J. Neurosci. 19, 2711–2719.

Symons, JD., McMillin, SL., Riehle, C., Tanner, J., Palionyte, M., Hillas, E., et al., (2009) Contribution of insulin and akt1 signaling to endothelial nitric oxide synthase in the regulation of endothelial function and blood pressure. Circ Res. 104, 1085–1094.

Szkudelski, T., (2001) The mechanism of alloxan and streptozotocin action in B cells of the rat pancreas. Physiological Research. 50 (6), 537–546.

Takahashi, M., Yamada, T., Tooyama, I., Moroo, I., Kimura, H., Yamamoto, T., et al., (1996) Insulin receptor mRNA in the substantia nigra in Parkinson's disease. Neurosci Lett. 204, 201-204.

Takashima, A., Murayama, M., Murayama, O., Kohno, T., Honda, T., Yasutake, K., et al., (1998) Presenilin 1 associates with glycogen synthase kinase-3beta and its substrate tau. Proc. Natl. Acad. Sci USA. 95, 9637–9641.

Takashima, A., Noguchi, K., Michel, G., Mercken, M., Hoshi, M., Ishiguro, K., et al., (1996) Exposure of rat hippocampal neurons to amyloid β peptide (25–35) induces the inactivation of phosphatidyl inositol-3 kinase and the activation of tau protein kinase I/glycogen synthase kinase- 3β. Neurosci Lett. 203(1), 33–36.

Takashima, A., Noguchi, K., Sato, K., Hoshino, T., Imahori, K., (1993) Tau protein kinase I is essential for amyloid β- protein-induced neurotoxicity. Proceedings of the National Academy of Sciences of the United States of America. 90 (16), 7789–7793.

Takeda, S., Sato, N., Rakugi, H., Morishita, R., (2011) Molecular mechanisms linking diabetes mellitus and Alzheimer disease: beta-amyloid peptide, insulin signaling, and neuronal function. Mol. BioSyst. 7, 1822–1827.

Talbot, K., Wang, HY., Kazi, H., Han, LY., Bakshi, KP., Stucky, A., et al., (2012) Demonstrated brain insulin resistance in Alzheimer's disease patients is associated with

IGF-1 resistance, IRS-1 dysregulation, and cognitive decline. J Clin Invest 122, 1316–1338.

Tangvarasittichai, S., (2015) Oxidative stress, insulin resistance, dyslipidemia and type 2 diabetes mellitus. World J Diabetes. 6(3), 456-480.

Tanti, JF., Jager, J., (2009) Cellular mechanisms of insulin resistance: role of stress-regulated serine kinases and insulin receptor substrates (IRS) serine phosphorylation. Curr. Opin. Pharmacol. 9, 753– 762.

Tapy, L., Le, KA., (2010) Metabolic effects of fructose and the worldwide increase in obesity. Physiol. Rev. 90, 23-46.

Tartaglia, LA., Dembski, M., Weng, X., Deng, N., Culpepper, J., Devos, R., et al., (1995) Identification and expression cloning of a leptin receptor, OB-R. Cell. 83, 1263–1271.

Thiruchelvam, M., Brockel, BJ., Richfield, EK., Baggs, RB., Cory-Slechta, DA., (2000) Potentiated and preferential effects of combined paraquat and maneb on nigrostriatal dopamine systems: environmental risk factors for Parkinson's disease. Brain Res. 873, 225–234.

Thirumangalakudi, L., Prakasam, A., Zhang, R., Bimonte-Nelson, H., Sambamurti, K., Kindy, MS., et al., (2008) High cholesterol-induced neuroinflammation and amyloid precursor protein processing correlate with loss of working memory in mice. J Neurochem. 106, 475–485.

Thomas, EA., Coppola, G., Desplats, PA., Tang, B., Soragni, E., Burnett, R., et al., (2008) The HDAC inhibitor 4b ameliorates the disease phenotype and transcriptional abnormalities in Huntington's disease transgenic mice, Proc Natl Acad Sci U S A. 105(40), 15564-15569.

Thompson, PR., Wang, D., Wang, L., Fulco, M., Pediconi, N., Zhang, D., et al., (2004) Regulation of the p300 HAT domain via a novel activation loop. Nat Struct Mol Biol. 11, 308–315.

Thorens, B., (2015) GLUT2, glucose sensing and glucose homeostasis. Diabetologia. 58 (2), 221-232.

Thorens, B., Mueckler, M., (2010) Glucose transporters in the 21st Century. Am J Physiol Endocrinol Metab. 298 (2), E141–E145.

To, AW., Ribe, EM., Chuang, TT., Schroeder, JE., Lovestone, S., (2011) The epsilon3 and epsilon4 alleles of human APOE differentially affect tau phosphorylation in hyperinsulinemic and pioglitazone treated mice. PLoS ONE 6, e16991.

Tonra, JR., Ono, M., Liu, X., Garcia, K., Jackson, C., Yancopoulos, GD., et al., (1999) Brain-derived neurotrophic factor improves blood glucose control and alleviates fasting hyperglycemia in C57BLKS-Lepr(db)/lepr(db) mice. Diabetes. 48, 588–594.

Tozzo, E., Shepherd, PR., Gnudi, L., Kahn, BB., (1995) Transgenic GLUT-4 overexpression in fat enhances glucose metabolism: preferential effect on fatty acid synthesis Am. J. Physiol. 268, E956–E964.

Tsankova, NM., Berton, O., Renthal, W., Kumar, A., Neve, RL., Nestler, EJ., (2006) Sustained hippocampal chromatin regulation in a mouse model of depression and antidepressant action. Nat Neurosci. 9, 519-525.

Tsao, TS., Li, J., Chang, KS., Stenbit, AE., Galuska, D., Anderson, JE., et al., (2001) Metabolic adaptations in skeletal muscle overexpressing GLUT4: effects on muscle and physical activity. FASEB J. 15, 958–969.

Turner, NC., Strauss, SJ., Sarker, D., Gillmore, R., Kirkwood, A., Hackshaw, A., et al., (2010) Chemotherapy with 5-fluorouracil, cisplatin and streptozocin for neuroendocrine tumours. Br J Cancer. 102, 1106–1112.

Unger, JW., Livingston, JN., Moss, AM., (1991) Insulin receptors in the central nervous system: localization, signalling mechanisms and functional aspects. Prog Neurobiol. 36, 343-362.

Unger, RH., Orci, L., (2000) Lipotoxic diseases of nonadipose tissues in obesity. Int J Obes Relat Metab Disord. 24 (suppl 4), S28–S32.

Ungerstedt, (1968) 6-hydroxy-dopamine induced degeneration of central monoamine neurons. Eur J Pharmacol. 5 (1), 107–110.

Valette, H., Deleuze, P., Syrota, A., Delforge, J., Crouzel, C., Fuseau, C., et al., (1995) Canine myocardial beta-adrenergic, muscarinic receptor densities after denervation: a PET study. J Nucl Med. 36 (1), 140–146.

Valor, LM., Pulopulos, MM., Jimenez-Minchan, M., Olivares, R., Lutz, B., Barco, A., (2011) Ablation of CBP in forebrain principal neurons causes modest memory and transcriptional defects and a dramatic reduction of histone acetylation but does not affect cell viability. J Neurosci. 31(5), 1652–1663.

van Dam, RM., Willett, WC., Rimm, EB., Stampfer, MJ., Hu, FB., (2002) Dietary fat and meat intake in relation to risk of type 2 diabetes in men. Diabetes Care. 25(3), 417–424.

Varalta, V., Picelli, A., Fonte, C., Amato, S., Melotti, C., Zatezalo, V., et al., (2015) Relationship between cognitive performance and motor dysfunction in patients with Parkinson's disease: a pilot cross-sectional study. BioMed Research International. 2015 (365959), 1-6.

Vecsey, CG., Hawk, JD., Lattal, KM., Stein, JM., Fabian, SA, Attner, MA., et al., (2007) Histone deacetylase inhibitors enhance memory and synaptic plasticity via CREB:CBP-dependent transcriptional activation. J. Neurosci. 27, 6128–6140.

Verdile, G., Keane, KN., Cruzat, VF., Medic, S., Sabale, M., Rowles, J., et al., (2015) Inflammation and Oxidative Stress:The Molecular Connectivity between Insulin Resistan ce, Obesity, and Alzheimer's Disease. Mediators Inflamm. 2015, 105828.

Vezoli, J., Fifel, K., Leviel, V., Dehay, C., Kennedy, H., Cooper, HM., et al., (2011) Early presymptomatic and long-term changes of rest activity cycles and cognitive behavior in a MPTP-monkey model of Parkinson's disease, PLoS One. 6 (8), e23952.

Villar-Garea, A., Esteller, M., (2004) Histone deacetylase inhibitors: Understanding a new wave of anticancer agents. Int J Cancer. 112, 171–178.

Viswanad, B., Srinivasan, K., Kaul, CL., Ramarao, P., (2006) Effect of tempol on altered angiotensin II and acetylcholine-mediated vascular responses in thoracic aorta isolated from rats with insulin resistance. Pharmacol. Res. 53, 209.

Vogel, HG., (2002) Drug discovery and evaluation: pharmacological assays. Springer Science & Business Media.

Waddington, CH., (1968) Towards a Theoretical Biology. Edinburgh, Scotland: Edinburgh University Press. 218, 525-527.

Wakabayashi, K., Tanji, K., Mori, F., Takahashi, H., (2007) The Lewy body in Parkinson's disease: molecules implicated in the formation and degradation of alpha-synuclein aggregates. Neuropathology. 27, 494-506.

Wakabayashi, K., Tanji, K., Odagiri, S., Miki, Y., Mori, F., Takahashi, H., (2013) The lewy body in Parkinson's disease and related neurodegenerative disorders. Mol Neurobiol. 47, 495-508.

Wan, Q., Xiong, ZG., Man, HY., Ackerley, CA., Braunton, J., Lu, WY., et al., (1997) Recruitment of functional GABA(A) receptors to postsynaptic domains by insulin. Nature. 388, 686–690.

Wang, J., Yu, JT., Tan, MS., Jiang, T., Tan, L., (2013) Epigenetic mechanisms in Alzheimer's disease: implications for pathogenesis and therapy. Ageing Res. Rev. 12, 1024–1041.

Wang, W., Yang, Y., Ying, C., Li, W., Ruan, H., Zhu, X., et al., (2007) Inhibition of glycogen synthase kinase-3β protects dopaminergic neurons from MPTP toxicity. Neuropharmacology. 52(8), 1678–1684.

Wang, WH., Cheng, LC., Pan, FY., Xue, B., Wang, DY., Chen, Z., et al., (2011) Intracellular trafficking of histone deacetylase 4 regulates long-term memory formation. Anat. Rec (Hoboken). 294, 1025–1034.

Wang, Y., Liu, H., Zhang, BS., Soares, JC., Zhang XY., (2016) Low BDNF is associated with cognitive impairments in patients with Parkinson's disease. Parkinsonism Relat Disord. 29, 66-71.

Wang, Z., Leng, Y., Wang, J., Liao, HM., Bergman, J., Leeds, P., (2016) Tubastatin A, an HDAC6 inhibitor, alleviates stroke-induced brain infarction and functional deficits: potential roles of α-tubulin acetylation and FGF-21 up-regulation. Sci Rep. 6, 19626.

Wang, ZY., Wen, QIN., Fan, YI., (2015) Targeting histone deacetylases: perspectives for epigenetic-based therapy in cardio-cerebrovascular disease. J Geriatr Cardiol. 12, 153−164.

Wang, J., Gong, B., Zhao, W., Tang, C., Varghese, M., (2014) Epigenetic mechanisms linking diabetes and synaptic impairments. Diabetes. 63, 645-654.

Waterborg, JH., (2002) Dynamics of histone acetylation in vivo. A function for acetylation turnover? Biochem. Cell Biol. 80, 363–378.

Watson, GS., Craft, S., (2003) The role of insulin resistance in the pathogenesis of Alzheimer's disease: implications for treatment. CNS Drugs. 17, 27–45.

Weems, AL., Olson, EN., (2011) Class II histone deacetylases limit GLUT4 gene expression during adipocyte differentiation, J Biol Chem. 286, 460–468.

Wei, Y., Williams, JM., Dipace, C., Sung, U., Javitch, JA., Galli, A., et al., (2007) Dopamine transporter activity mediates amphetamine-induced inhibition of Akt through a Ca^{2+}/calmodulin-dependent kinase II-dependent mechanism. Mol. Pharmacol. 71, 835–842.

Weisberg, SP., Leibel, R., Tortoriello, DV., (2008) Dietary curcumin significantly improves obesity-associated inflammation and diabetes in mouse models of diabesity. Endocrinology. 149(7), 3549-3558.

Weldon, DT., Rogers, SD., Ghilardi, JR., Finke, MP., Cleary, JP., O'Hare, E., (1998) Fibrillar beta-amyloid induces microglial phagocytosis, expression of inducible nitric oxide synthase, and loss of a select population of neurons in the rat CNS in vivo. J Neurosci. 18(6), 2161-2173.

Wellen, KE., Hotamisligil, GS., (2005) Inflammation, stress, and diabetes. J. Clin. Invest. 115, 1111–1119.

Wheatcroft, SB., Williams, IL., Shah, AM., Kearney, MT., (2003) Pathophysiological implications of insulin resistance on vascular endothelial function. Diabet Med. 20, 255–268.

White, MF., (2003) Insulin signaling in health and disease. Science. 302, 1710-1711

White, MF., Shoelson, SE., Keutmann, H., Kahn, CR., (1988) A cascade of tyrosine autophosphorylation in the beta-subunit activates the phosphotransferase of the insulin receptor. J Biol Chem. 263, 2969 –2980.

White, MF., Kahn, CR., (1994) The insulin signaling system. J Biol Chem. 269(1), 1-4.

Whitmer, RA., (2007) Type 2 diabetes and risk of cognitive impairment and dementia. Curr Neurol Neurosci Rep.7(5), 373-380.

Wild, S., Roglic, G., Green, A., Sicree, R., King, H., (2004) Global prevalence of diabetes: estimates for the year 2000 and projections for 2030. Diabetes Care, 27, 1047–1053.

Williams, SR., Aldred, MA., Der Kaloustian, VM., Halal, F., Gowans, G., McLeod, DR.,et al., (2010) Haplo insufficiency of HDAC4 causes brachydactyly mental retardation

syndrome, with brachydactyly type E, developmental delays, and behavioral problems. Am. J. Hum. Genet. 87(2), 219–228.

Wills, ED., (1996) Mechanism of lipid peroxide formation in animal. Biochem J. 99, 667–676.

Wills, J., Jones, J., Haggerty, T., Duka, V., Joyce, JN., Sidhu, A., (2010) Elevated tauopathy and alpha-synuclein pathology in postmortem Parkinson's disease brains with and without dementia. Exp Neurol. 225 (1), 210–218.

Winzell, MS., Ahrén, B., (2004) The high-fat diet-fed mouse: a model for studying mechanisms and treatment of impaired glucose tolerance and type 2 diabetes. Diabetes.53 (3), 215-219.

Wlodarczyk, A., Strojek, K., (2008) Glucose intolerance, insulin resistance and metabolic syndrome in patients with stable angina pectoris. Obesity predicts coronary atherosclerosis and dysglycemia. Pol Arch Med Wewn. 118, 719–726.

Wood IS., Trayhurn, P., (2003) Glucose transporters (GLUT and SGLT): expanded families of sugar transport proteins Br. J. Nutr. 89, 3–9.

Wood, MA., Attner, MA., Oliveira, AM., Brindle, PK., Abel, T., et al., (2006) A transcription factor-binding domain of the coactivator CBP is essential for long-term memory and the expression of specific target genes. Learn. Mem. 13, 609–617.

Woodgett, JR., (1990) Molecular cloning and expression of glycogen synthase kinase-3/factor A. EMBO J. 9, 2431-2438.

Woods, SC., Lotter, EC., McKay, LD., Porte, D Jr., (1979) Chronic Intracerebroventricular infusion of insulin reduces food intake and body weight of baboons. Nature. 282, 503–505.

Wu, X., Chen, PS., Dallas, S., Wilson, B., Block, ML., Wang, CC., et al., (2008) Histone deacetylase inhibitors up-regulate astrocyte GDNF and BDNF gene transcription and protect dopaminergic neurons. Int. J. Neuropsychopharmacol. 11, 1123–1134.

Xiao, C., Giacca, A., Lewis, GF., (2011) Sodium phenylbutyrate, a drug with known capacity to reduce endoplasmic reticulum stress, partially alleviates lipid-induced insulin resistance and beta-cell dysfunction in humans. Diabetes. 60, 918-924.

Xiong, Y., Zhao, K., Wu, J., Xu, Z., Jin, S., Zhang, YQ., (2013) HDAC6 mutations rescue human tau-induced microtubule defects in Drosophila. Proc Natl Acad Sci U S A. 110(12), 4604-4609.

Xu, Q., Park, Y., Huang, X., Hollenbeck, A., Blair, A., Schatzkin, A., et al., (2011) Diabetes and risk of Parkinson's disease. Diabetes Care. 34, 910–915.

Xu, WS., Parmigiani, RB., Marks, PA., (2007) Histone deacetylase inhibitors: molecular mechanisms of action. Oncogene. 26, 5541–5552.

Yadav, HN., Singh, M., Sharma, PL (2012) Pharmacological inhibition of GSK-3b produces late phase of cardioprotection in hyperlipidemic rat: possible involvement of HSP 72, Mol. Cell. Biochem. 369, 227–233.

Yamaguchi, H., Ishiguro, K., Uchida, T., Takashima, A., Lemere, CA., Imahori, K., (1996) Preferential labeling of Alzheimer neurofibrillary tangles with antisera for tau protein kinase (TPK) I/glycogen synthase kinase-3β and cyclin-dependent kinase 5, a component of TPK II. Acta Neuropathologica. 92 (3) 232–241.

Yao, HB., Shaw, PC., Wong, CC., Wan, DC., (2002) Expression of glycogen synthase kinase-3 isoforms in mouse tissues and their transcription in the brain. J Chem Neuroanat. 23 (4), 291–297.

Yao, X., Zhang, JR., Huang, HR., Dai, LC., Liu, QJ., Zhang, M., et al., (2010) Histone deacetylase inhibitor promotes differentiation of embryonic stem cells into neural cells in adherent monoculture. Chin Med J (Engl). 123, 734–738.

Yasuda, S., Liang, MH., Marinova, Z., Yahyavi, A., Chuang, DM., (2009) The mood stabilizers lithium and valproate selectively activate the promoter IV of brain-derived neurotrophic factor in neurons. Mol Psychiatry. 14, 51-59.

Yoo, DY., Kim, DW., Kim, MJ., Choi, JH., Jung, HY., Nam, SM., et al., (2015) Sodium butyrate, a histone deacetylase inhibitor, ameliorates SirT2 induced memory impairment, reduction of cell proliferation and neuroblast differentiation in the dentate gyrus. Neurol Res. 37 (1), 69-76.

Yoshida, M., Kijima, M., Akita, M., Beppu, T., (1990) Potent and specific inhibition of mammalian histone deacetylase both in vivo and in vitro by trichostatin A. J Biol Chem. 265, 17174–17179.

Yu, C., Chen, Y., Cline, GW., Zhang, D., Zong, H., Wang, Y., et al., (2002) Mechanism by which fatty acids inhibit activation of insulin receptor substrate-1 (IRS-1)-associated phosphatidylinositol 3-kinase activity in muscle. J Biol Chem. 277, 50230–50236.

Yu, IT., Park, JY., Kim, SH., Lee, JS., Kim, YS., Son, H., (2009) Valproic acid promotes neuronal differentiation by induction of proneural factors in association with H4 acetylation. Neuropharmacology. 56, 473–480.

Yuan, YH., Yan, WF., Sun, JD., Huang, JY., Mu, Z., Chen, NH., (2015) The molecular mechanism of rotenone-induced α-synuclein aggregation: emphasizing the role of the calcium/GSK3β pathway. Toxicol. Lett. 233, 163–171.

Yuskaitis, CJ., Jope, RS., (2009) Glycogen synthase kinase-3 regulates microglial migration, inflammation, and inflammation-induced neurotoxicity. Cell Signal. 21(2), 264-273.

Zaitone, SA., Elmatty, DMA., Elshazly, SM., (2012) Piracetam and vinpocetine ameliorate rotenone- induced Parkinsonism in rats. Indian J Pharmacol. 44, 774-779.

Zaman, MQ., Leray, V., Le Blocíh, J., Thorin, C., Ouguerram, K., Nguyen, P., (2011) Lipid profile and insulin sensitivity in rats fed with high-fat or high-fructose diets. Br. J. Nutr. 106, S206-210.

Zeng, Z., Liao, R., Yao, Z., Zhou, W., Ye, P., Zheng, X., et al., (2014) Three single nucleotide variants of the HDAC gene are associated with type 2 diabetes mellitus in a Chinese population: A community-based case-control study. Gene 533, 427–433.

Zhang, J., Fitsanakis, VA., Gu, G., Jing, D., Ao, M., Amarnath, V., et al., (2003) Manganese ethylene-bis-dithiocarbamate and selective dopaminergic neurodegeneration in rat: a link through mitochondrial dysfunction. J Neurochem. 84, 336–346.

Zhang, L., Liu, C., Wu, J., Tao, JJ., Sui, XL., Yao, ZG., et al., (2014) Tubastatin A/ACY-1215 improves cognition in Alzheimer's disease transgenic mice. J Alzheimers Dis. 41(4), 1193–1205.

Zhang, L., Sheng, S., Qin, C., (2013) The role of HDAC6 in Alzheimer's disease. J Alzheimers Dis, 33, 283-295.

Zhang, QJ., Holland, WL., Wilson, L., Tanner, JM., Kearns, D., Cahoon, JM., et al., (2012) Ceramide mediates vascular dysfunction in diet-induced obesity by pp2a-mediated dephosphorylation of the enos-akt complex. Diabetes. 61(7), 1848-1859.

Zhang, XY., Liang, J., Chen, DC., Xiu, MH., Yang, FD., Kosten, TA., (2012) Low BDNF is associated with cognitive impairment in chronic patients with schizophrenia. Psychopharmacology (Berl). 222(2), 277-284.

Zhang, Y., Proenca, R., Maffei, M., Barone, M., Leopold, L., Friedman, JM., (1994) Positional cloning of the mouse obese gene and its human homologue. Nature. 372, 425–432.

Zhang. K., Schrag, M., Crofton, A., Trivedi, R., Vinters, H., Kirsch, W., (2012) Targeted proteomics for quantification of histone acetylation in Alzheimer's disease. Proteomics. 12 (8), 1261-1268.

Zhao, L., Teter, B., Morihara, T., Lim, GP., Ambegaokar, SS., Ubeda, OJ., et al., (2004). Insulin-degrading enzyme as a downstream target of insulin receptor signaling cascade: implications for Alzheimer's disease intervention. J Neurosci. 24, 11120–11126.

Zhao, WQ., Alkon, DL., (2001) Role of insulin and insulin receptor in learning and memory. Mol Cell Endocrinol.177, 125–134.

Zhao, WQ., Chen, H., Quon, MJ., Alkon, DL., (2004) Insulin and the insulin receptor in experimental models of learning and memory. Eur J Pharmacol. 490, 71–81.

Zhong, T., Guo, Q., Zou W., Zhu, X., Song, Z., Sun, B., et al., (2015) Neonatal isoflurane exposure induces neurocognitive impairment and abnormal hippocampalhistone acetylation in mice. PLoS One. 10(4), e0125815.

Zhou, W., Bercury, K., Cummiskey, J., Luong, N., Lebin, J., Freed, CR., (2011) Phenylbutyrate up-regulates the DJ-1 protein and protects neurons in cell culture and in animal models of Parkinson disease. J Biol Chem 286, 14941–14551.

Zhou, X., You, S., (2014) Rosiglitazone inhibits hepatic insulin resistance induced by chronic pancreatitis and IKK-β/NF-κB expression in liver. Pancreas. 43(8), 1291–1298.

Zisman, A., Peroni,OD., Abel, ED., Michael, MD., Mauvais-Jarvis, F., Lowell, BB., et al., (2000) Targeted disruption of the glucose transporter 4 selectively in muscle causes insulin resistance and glucose intolerance Nat. Med. 6, 924–928.

Ziyatdinova, S., Viswanathan, J., Hiltunen, M., Tanila, H., Pitkänen, A., (2015) Reduction of epileptiform activity by valproic acid in a mouse model of Alzheimer's disease is not long-lasting after treatment discontinuation. Epilepsy Res. 112, 43-55.

Publications from thesis work

1. **Sorabh Sharma,** Rajeev Taliyan (2016) Epigenetic modifications by inhibiting histone deacetylases reverse memory impairment in insulin resistance induced cognitive deficit in mice. Neuropharmacology. 105, 285-297.
2. **Sorabh Sharma,** Rajeev Taliyan (2016) Histone deacetylase inhibitors: Future therapeutics for insulin resistance and type 2 diabetes. Pharmacological Research. 113, 320-326.
3. **Sorabh Sharma,** Rajeev Taliyan (2015) Targeting histone deacetylases: A novel approach in Parkinson's Disease. Parkinson's Disease 2015, 303294.
4. **Sorabh Sharma,** Rajeev Taliyan (2015) Synergistic effects of GSK-3β and HDAC inhibitors in Intracerebroventricular Streptozotocin induced cognitive deficits in rats. Naunyn-schmiedeberg's archives of pharmacology 388(3), 337-349.
5. **Sorabh Sharma,** Rajeev Taliyan, Sumel Singh (2015) Beneficial effects of sodium butyrate in 6-OHDA induced neurotoxicity and behavioral abnormalities: Modulation of histone deacetylase activity. Behavioral Brain Research. 291, 306-314.
6. **Sorabh Sharma**, Rajeev Taliyan (2014) Neuroprotective role of Indirubin-3'-monoxime, a GSKβ inhibitor in high fat diet induced cognitive impairment in mice. Biochemical and Biophysical Research Communications. 452(4), 1009-1015.
7. **Sorabh Sharma,** Rajeev Taliyan, Sruthi Ramagiri (2014) Histone deacetylase inhibitor, Trichostatin A, improves learning and memory in high fat diet-induced cognitive deficits in mice. Journal of molecular neuroscience 56(1), 1-11.

Other Publications

8. **Sorabh Sharma,** Rajeev Taliyan (2015) Transcriptional dysregulation in Huntington's disease: The role of histone deacetylases. Pharmacological Research. 100, 157-169.

Conference Presentations (Oral/Poster)

1. **Sorabh Sharma,** Rajeev Taliyan. AR-A014418, a GSK-3β Inhibitor, Attenuates Alzheimer like Pathology in High Fat Diet Induced Cognitive Deficit in Mice. Presented at Alzheimer's Association International Conference (AAIC), held at ExCel London Convention Centre, London, England on July 16-20, 2017.
2. **Sorabh Sharma,** Rajeev Taliyan. Beneficial Effects of Co-administered Lithium Chloride and Valproate in Intracerebroventricular Streptozotocin Induced Behavioral and Biochemical Abnormalities in Rats. Presented at BITS Pilani, Pilani Campus, Rajasthan during March 2-4, 2017.
3. **Sorabh Sharma,** Rajeev Taliyan. Peripheral insulin resistance promotes neurodegeneration through altered histone acetylation activity. Presented at ISN-JNC Flagship School, Alpbach, Austria, September 12th – 18th 2016.
4. **Sorabh Sharma,** Rajeev Taliyan. High fat diet feeding exacerbates the toxic effects of 6-hydroxydopamine in rats: Possible involvement of histone acetylation. Presented at XXI World Congress on Parkinson's disease and related disorders held in Milan, Italy on December 6-9, 2015.
5. **Sorabh Sharma,** Rajeev Taliyan. Histone deacetylase inhibitors improves learning and memory consolidation in high fat diet induced cognitive deficit in mice**.** Presented at IBRO-APRC/ISN-APSN Joint Advanced School held in Daegu, South Korea on September 14-20, 2015
6. **Sorabh Sharma,** Rajeev Taliyan. Sodium butyrate, a histone deacetylase inhibitor, attenuates 6-hydroxydopamine induced hemi-Parkinsonism in rats. Presented at 25th ISN-APSN Biennial Meeting in Cairns, Australia held on 23-27August 2015.
7. **Sorabh Sharma,** Rajeev Taliyan. Neuroprotective role of Indirubin-3'-monoxime, a GSK3β inhibitor in high fat diet induced cognitive impairment in mice. Presented at Basic and Research concepts of depression and cognitive dysfunction. 1st IBRO/APRC CHANDIGARH. NEUROSCIENCE SCHOOL, University Institute of Pharmaceutical Sciences, Panjab University, Chandigarh. November 03-08, 2014.

Biography of Dr. Rajeev Taliyan

Dr. Taliyan is currently working as an Assistant Professor in the Department of Pharmacy, Birla Institute of Technology and Science, Pilani, Pilani-campus, Rajasthan. He has earned his PhD (Pharmacology) under the supervision of Prof. P.L Sharma (Emeritus, Prof. PGIMER) and Late Prof. Manjeet Singh (Ex Head, Dean, Punjabi University) from ISF college of Pharmacy, Punjab Technical University, Punjab. He has been involved in teaching and research for past one decade. He has vast experience in the field of Neuropharmacology, Cardiovascular pharmacology and Drug toxicity. He has been awarded with various research projects from DST, UGC, ICMR and BITS-Pilani. He has also several collaborations and projects with Pharmaceutical Industry such as Etica Clin Pharm Pvt Ltd. He has guided more than 15 students for their post graduation dissertation. He has been awarded with many prestigious awards at international and national level including, Prof. Manjeet Singh Gold medal award at IPSCON-2015; PP Suryakumari Gold medal Award at IPSCON-2014. He has been invited by several Research and Academic institutes for delivering guest lectures including GLA University, Mathura, Rayat Bahra, Ram-Eesh university, Shoolini University. He has published several papers in peer reviewed international and national journals and in conferences of international and national repute. He is life member of Indian Pharmacological Society and British Pharmacological Society, UK.

Biography of Mr. Sorabh Sharma

Mr. Sharma enrolled as a PhD student in August, 2013 under the supervision of Dr. Rajeev Taliyan in the Department of Pharmacy, Birla Institute of Technology and Science, Pilani-campus, Rajasthan. He is the recipient of BITS Pilani Institute PhD Fellowship. His area of interest is to explore the molecular mechanisms involved in insulin resistance induced neurodegenerative diseases. He has obtained his B. Pharmacy and M. Pharmacy with distinction from ISF college of Pharmacy, PTU, Jalandhar. He has been awarded with many prestigious awards including, travel grant to attend AAIC in London (2017) by DST-SERB, ISN travel grant to attend 1st Flagship School held in Austria (2016), Best Poster Award at Chitkara university (2015), PP Suryakumari Gold medal Award at IPSCON (2014). He has published several papers in peer reviewed international journals and delivered presentations in conferences of international and national repute. He is life member of Indian Pharmacological Society and International Society for Neurochemistry.